

**MASS CHANGES DURING HYDROTHERMAL ALTERATION
SILVER QUEEN EPITHERMAL DEPOSIT,
OWEN LAKE, CENTRAL BRITISH COLUMBIA**

by

XIAOLIN CHENG

**B.Eng., The China University of Geosciences (Wuhan), 1982
M.Sc., The China University of Geosciences (Wuhan), 1985**

**A THESIS SUBMITTED IN PARTIAL FULFILLMENT OF
THE REQUIREMENTS FOR THE DEGREE OF
DOCTOR OF PHILOSOPHY**

in

**THE FACULTY OF GRADUATE STUDIES
(Department of Geological Sciences)**

**We accept this thesis as conforming
to the required standard**

THE UNIVERSITY OF BRITISH COLUMBIA

October 1995

© Xiaolin Cheng, 1995

In presenting this thesis in partial fulfilment of the requirements for an advanced degree at the University of British Columbia, I agree that the Library shall make it freely available for reference and study. I further agree that permission for extensive copying of this thesis for scholarly purposes may be granted by the head of my department or by his or her representatives. It is understood that copying or publication of this thesis for financial gain shall not be allowed without my written permission.

(Signature)

Department of Geological Sciences

The University of British Columbia
Vancouver, Canada

Date Oct. 19, 1995

ABSTRACT

A procedure for determining metasomatic norms is developed in this thesis to quantitatively and objectively estimate mineral abundances from lithogeochemical data. The norm calculations use the same principles as do other norms such as CIPW, but the different mineral phases present in alteration systems are used as the normative standard minerals. Another distinctive difference between a metasomatic and a conventional norm is that the calculation procedure proposed for a metasomatic norm does not proceed along such a fixed hierarchical path as in the case of an igneous norm. A particular useful approach to the application of the norm concept to metasomatic rocks is to constrain the calculated normative mineralogy by *a priori* knowledge of existing minerals (i.e. to approximate the mode as closely as possible).

Where an immobile component can be recognized the metasomatic norms for protoliths and altered rocks, as well as the chemical constituents lost or gained, can be further recast into the absolute amounts of minerals and chemical constituents relative to a given mass of parent rock. Known errors within lithogeochemical data studied can be propagated to the final results of all norm calculations. As a result, a chemico-mineralogical model for material exchange, including absolute losses and gains of chemical constituents, normative minerals in extensive units, as well as the corresponding propagated errors, is formulated in this work as follows:

$$\begin{aligned} &\sum \text{Mineral}_{\text{parent rock}} \pm \text{error} + \sum \text{Constituent}_{\text{gained from solution}} \pm \text{error} \\ &= \sum \text{Mineral}_{\text{altered rock}} \pm \text{error} + \sum \text{Constituent}_{\text{lost from wall rock}} \pm \text{error} \end{aligned} \quad (\text{I})$$

Equation I is particularly useful because it is quantitative and easily applied: information that can be obtained from the equation includes the mineralogy of the initial and final rocks, absolute gains and losses of specific chemical constituents as well as the uncertainties on each estimate at a specified confidence level.

The methodology for this approach is a natural extension of the use of Pearce element ratio (PER) diagrams for the study of metasomatic rocks. The metasomatic norm recovers the same quantitative information as do Pearce element ratio diagrams. The common principles are (i) correction for closure, that provides true relative lithogeochemical and mineralogical variations between parent and daughter rocks, and (ii) an effort to explain chemical variability in terms of mineralogical variability. The strategy of a PER diagram is to test whether chemical changes in different rocks can be explained purely by the variation(s) of certain mineral(s), as demonstrated by disposition of the binary plotted points along predefined trends (slopes). Metasomatic norms are displayed more effectively as equations or profiles showing the spatial distributions of normative mineral assemblage, as well as the absolute losses and gains of chemical constituents based on comprehensive mass balance relationships.

The approach described in the first part of this thesis is applied to a hydrothermal alteration study of the Silver Queen mine in central British Columbia. Hydrothermal alteration at the Silver Queen mine was derived from a multiple precursor system. However, local, individual alteration profiles exhibit the attributes of a single precursor system. Six types of hydrothermal alteration at Silver Queen mine have been described: viz. propylitization, sericitization, argillization, silicification, pyritization and carbonatization. In general, the wall rock alteration in the study area is composed of a widespread regional propylitic alteration with superimposed carbonatization. Regional alteration gives way, as the vein is approached, to an outer envelope of sericitic and argillic alteration + carbonatization and an inner envelope of silicification and pyritization + sericitic or argillic alteration + carbonatization. Thus, the sequence of alteration development is (i) widespread regional propylitic alteration, (ii) sericitic and argillic outer envelope, and (iii) silicification and pyritization inner envelope.

Most of the hydrothermally altered samples in alteration envelopes at the Silver Queen mine have gained mass during hydrothermal alteration. In contrast, samples from

the profile of the northern segment of the No. 3 vein have lost mass. Other spatial variations of hydrothermal alteration from the southern segment to the northern segment of the No. 3 vein and from different levels (from 2600-foot level to 2880-foot level) have been recognized. In brief, the wall rock alteration is most intense in the alteration envelope at the central segment of the No. 3 vein and mildest at the northern segment of the No. 3 vein. The total mass change of each altered sample is largely the result of depletion of CaO and Na₂O, and addition of SiO₂, K₂O, H₂O and CO₂.

TABLE OF CONTENTS

Abstract	ii
Table of Contents	v
List of Tables	xiii
Acknowledgement	x
Chapter 1. Background and Objectives	1
1.1. Introduction	1
1.2. Current Quantitative Approaches to the Study of Hydrothermal Alteration	4
1.2.1 The Closure Effect	5
1.2.2 Comparison of Various Techniques Used to Remove the Closure Effect	7
1.3. Two Requirements for Loss and Gain Calculation	10
1.4. Pearce Element Ratios (PER) and Their Application to Hydrothermal Alteration	16
1.5. Additional Problems	23
Chapter 2. Metasomatic Norms: A Method of Norm Calculation Adapted to Hydrothermally Altered Rocks	26
2.1. Introduction	26
2.2. The Principle of Metasomatic Norms	28
2.3. A Set of Standard Normative Minerals for Metasomatic Systems	32
2.4. A Manual Procedure for Metasomatic Norm Calculation	33
2.5. A Quantitative Model of Metasomatic Systems	41
2.6. Case Histories: Application of Metasomatic Norms	43
2.6.1. Sigma Mine, Abitibi, Quebec	43
2.6.2. Erickson Gold Mine, Northern British Columbia	47
2.7. Conclusions	55

Chapter 3. Quality Control/Assessment of Lithogeochemical Data	57
3.1. Introduction	57
3.2. Strategies of Sampling and Sample Preparation	58
3.3. Quality Assessment of Analytical Measurements	
Based on a Small Set of Duplicates	64
3.4. Propagation of Errors in Lithogeochemical Calculations	71
Chapter 4. Geology of the Silver Queen mine, Owen Lake area,	
Central British Columbia	76
4.1. Introduction	76
4.2. Regional Geological Setting	77
4.3. Geology of the Study Area	80
4.4. Lithogeochemical Characters and Two Series of	
Igneous and Volcanic Rocks	92
4.5. Veins: Character and Correlation	96
4.6. Structures and the Interpretations	99
4.7. Summary	106
Chapter 5. Hydrothermal Alteration Associated with Epithermal, Base- and	
Precious-Metal Veins at Silver Queen Mine: Petrographic Variations	108
5.1. Introduction	108
5.2. Petrography of Hydrothermal Alteration Types	109
5.3. The Spatial Zonation of Hydrothermal Alteration	115
5.4. Paragenetic Sequence of Hydrothermal Alteration	125
5.5. Discussion and Conclusions	130
Chapter 6. A Quantitative Evaluation of Hydrothermal Alteration	
at Silver Queen Mine, Central British Columbia	133
6.1. Introduction	133
6.2. Sampling and Sample Preparation	134

6.3. Errors inherent in Lithogeochemical Data	140
6.4. Lithogeochemical Data of Altered Rock and Determination of immobile components	142
6.5. Calculation of Absolute Losses and Gains of Chemical Constituents and their Spatial Variations	144
6.6. Application of PER Diagram to the Interpretation of Hydrothermal Alteration	149
6.7. Application of Metasomatic Norm Methodology	158
6.8. Propagated Error Analysis and Confidence Level of the Quantitative Evaluations	167
6.9. A Comprehensive Model of Hydrothermal Alteration	169
Chapter 7. Conclusions and Recommendations	172
Bibliography	183
Appendix A. Megascopic Description of Altered Sample, Silver Queen Mine	196
Appendix B. Lithogeochemical Duplicate Analyses, Silver Queen Mine	201
Appendix C. Use of "Quattro Pro for DOS 5.0" to Calculate Metasomatic Norms	205
Appendix D. Diagrams of Alteration Evaluation, Silver Queen Mine	246
Appendix E. Tables of Alteration Evaluation, Silver Queen Mine	268

LIST OF TABLES

Table 1-1. A Summary of Quantitative Techniques Devised to Remove the Closure Effect and Evaluate Mass Transfer Process	8
Table 1-2. Eight Possible Cases of PER Diagram	13
Table 2-1. A List of Standard Normative Minerals for Metasomatic Volcanic Rocks Associated with Epithermal Ore Deposits	34
Table 2-2. Variations in Major Element Oxide Concentration (in wt%) in the Profile 2103 across Alteration Envelope Around Tension Vein, Sigma Mine, Quebec	44
Table 2-3. The Calculation Results of Metasomatic Norms (in wt%) in the Profile 2103 across Alteration envelope around Tension Vein, Sigma Mine, Quebec	44
Table 2-4. Summary of Characteristics of Alteration Zones of Enclosing Gold-Bearing Quartz Veins and the McDame Dolomite Vein, Total Erickson Mine	48
Table 2-5. Chemical Analyses of Jennie Vein Alteration Profile, Erickson Gold Mine	50
Table 2-6. Metasomatic Norms of Jennie Vein Alteration Profile, Erickson Gold Mine	50
Table 2-7. Metasomatic Norms Corrected for Closure and Absolute Losses and Gains of Components from Profile 80-88-JH across the Jennie Vein, Erickson Mine, Northern British Columbia	52
Table 3-1. The Classification of Major Variations of Lithogeochemical Data Generated by Different Processes	57
Table 4-1. Table of Formations, Owen Lake Area	83
Table 4-2. Lithogeochemical Data of Various Types of Rock at Owen Lake Area, Central British Columbia	94
Table 5-1. Estimated Modes of Alteration Minerals in Hydrothermally Altered Rock around the No. 3 Vein, Silver Queen Mine, Central British Columbia	120

Table 5-2. Paragenetic Sequence of Mineral Assemblages, Silver Queen Mine	129
Table 6-1. Estimation of Optimal Sample Size by Using Binomial Function	136
Table 6-2. Estimated Optimal Fineness of Subsample by Using Binomial Function	138
Table 6-3. Error of Lithgeochemical Data Estimated by Using Sample Duplicates	141
Table 6-4. Error of Lithgeochemical Data Estimated by Using Measurement Duplicates	141
Table 6-7. Metasomatic Norms Corrected for Closure and Absolute Losses and Gains of Components (in Moles) around the No. 3 Vein, Silver Queen Mine, Owen Lake, Central British Columbia	160
Table 6-8. Metasomatic Norms Corrected for Closure and Absolute Losses and Gains of Components (in Grams) around the No. 3 Vein, Silver Queen Mine, Owen Lake, Central British Columbia	161
Table 6-9. Propagated Errors of Metasomatic Norms Corrected for Closure and Absolute Losses and Gains of Components in Grams at the 68% Confidence Level, the No. 3 Vein, Silver Queen Mine, Central British Columbia	168

ACKNOWLEDGMENTS

In the course of completing my thesis, several individuals and agencies have provided much appreciated assistance, without which the thesis would have been an impossibility.

I am especially indebted to Dr. Alastair J. Sinclair for offering me the opportunity to work on the Owen Lake Project as a Ph. D. graduate student under his supervision, and for his constructive criticism, insights, and extraordinary patience that allowed me to complete this work.

Dr. Gerry Carlson, Dr. Craig Leitch and Dr. Margaret Thomson provided much needed assistance in deciphering the geological story behind the Silver Queen precious- and base-metal vein deposit and greatly supplemented the evolution of this thesis with their own work. My thanks also go out to my coworkers Christopher T. S. Hood, Zophia Radlowski and Asger Bentzen for their suggestions, discussions and assistances.

Pacific Houston Resources Inc. and New Nadina Explorations Ltd. are thanked for allowing access to the Silver Queen workings and for financial assistance in and out of the field. J. Hutter and W. W. Cummings provided helpful discussions on the mine area during my stay at Silver Queen mine.

Dr. L. A. Groat and K. N. Nicholson are thanked for the advice and assistance with the X-ray diffraction operation; Dr. W.K. Fletcher and S. Horsky for the guidance on the XRF analytical measurement. I am also grateful to Dr. T. J. Barrett, Dr. T. H. Brown, Dr. R. L. Chase, Dr. G. M. Dipple, Dr. C.I. Godwin, Dr. J. K. Russell, Dr. C. R. Stanley and Dr. Min Sun for providing instruction and discussion.

This work was supported by Pacific Houston Resources Inc., New Nadina Explorations Ltd. and by a grant from the Natural Science and Engineering Research Council of Canada to Dr. A.J. Sinclair.

1.1. Introduction

Bates and Jackson (1987) define alteration as: " ... any change in the mineralogical composition of a rock brought about by physical or chemical means, especially, by the action of hydrothermal solutions ..." It is one of the most important topics studied by economic geologists because in many hydrothermal ore deposits the changes in composition, mineralogy and/or texture of wall rocks, etc., that enclose the ore deposit are more extensive and more obvious than the ore deposit itself. Hydrothermally altered wall-rock is thus a "fossil" of a hydrothermal system; many parameters of the depositional environment of ore are interpretable from the assemblages of alteration minerals. Consequently, wall-rock hydrothermal alteration has been used widely as a guide during exploration of hydrothermal ore deposits and as a clue to the properties of the hydrothermal solution from which ores precipitated.

However, hydrothermally altered wall rock can be the product of the reaction between wall rock and ore-bearing hydrothermal solution either before, during or after the precipitation of ore minerals from hydrothermal solutions. To understand the relation between ore and associated hydrothermally alteration is a challenging task. Uncertainties can lead to errors or complexities in using wallrock alteration as a guide to exploration of hydrothermal ore deposits if different types of alteration are confused. Appleyard and Guha (1991) review such practical uses of hydrothermal alteration and state:

Wall-rock alteration was generally accorded little significance as an exploration focus. Dunbar (1948), for example, noted with reference to the ores of the Porcupine district that moderate bleaching of the chloritic host rock was considered to be a condition favorable for ore occurrence but such evidence can only be utilized in a very general way. Conversely, he found strong bleaching to be a poor indicator of mineralization and wrote that it cannot be said that the ore

occurs where its effect (that of hydrothermal alteration) is most intense. Since those days, technical improvements have been at the heart of the advancement of the state of knowledge we have seen rather than the appearance of new paradigms. Lithogeochemistry, isotope geochemistry, fluid inclusion studies, statistical applications, and geochemical modeling are all areas where great advances in technique and important observations have been achieved.

In recent years, research into hydrothermal alteration associated with precious-metal ore deposits has accelerated appreciably with increasing interest in understanding water/rock interactions, mass losses and gains, the geometry of alteration zones relative to the associated mineral deposit, and assemblages of alteration minerals. This information leads to the development of comprehensive models of alteration systems and provides a basis for designing mineral exploration guidelines, particularly as they relate to the use of lithogeochemical data and their integration into deposit model definition as an exploration tool.

The general aim of this thesis is to improve quantitative methods of evaluating hydrothermal alteration associated with precious- and base-metal vein deposit in volcanic sequences. This goal will be approached through a particular case study of alteration at the Silver Queen mine, central British Columbia. This study is preceded by a brief review of the current status of the study in the field of quantitative losses/gains to wallrock during hydrothermal alteration.

The basic aims of many alteration studies involve such questions as:

- (1) What are the changes in mineralogical assemblage of the rock during the alteration process?
- (2) What variations in chemical compositions of the rock arise from the alteration process?
- (3) What are the sequences, distribution patterns and spatial extents of alteration?

- (4) What are the conditions of formation of alteration minerals and the properties of hydrothermal solution?
- (5) What are the mechanisms of hydrothermal alteration? and
- (6) What is the relationship between hydrothermal alteration and ore deposition?

To answer such questions commonly involves two complementary approaches, mineralogical and lithogeochemical; both can be directed to the quantitative estimation. The basic tasks of these two approaches as applied to the evaluation of material exchange during hydrothermal alteration are: (i) determination of mineral assemblages of altered and parent rocks, and (ii) calculations of the losses and gains of chemical components as a result of hydrothermal alteration.

The mineralogy of altered rocks has been particularly important as a means of classification, such mineral-dependent terms as phyllic, sericitic, argillic, propylitic, etc., are entrenched in the literature. One reason for this is that a mineral assemblage contains information both about the chemical composition and the formation environment of the rock. Such information contributes to answering question 1 to 3, above, and less significantly to questions 4 to 6. Unfortunately, fine grain size, absence of easily identifiable optical features, and mixtures of non-ideal structures of alteration products can obscure mineralogy and/or make mineral abundances impractical to estimate with confidence. Consequently, the use of a mineralogical approach to study and classification of hydrothermally altered rocks, while essential, is limited.

A lithogeochemical approach to the study of altered rock complements and has some advantages over the mineralogical approach. The large samples commonly used for chemical analysis can be more representative than, say, small areas of a thin section; thus, more accurate and consistent quantitative data can be obtained. A lithogeochemical approach to the study of hydrothermal alteration commonly is directed toward quantifying the loss or gain of each component during the alteration process and thus provide an

objective and quantitative chemical classification scheme. Elliott-Meadows and Appleyard (1991) state:

...the outer limits of alteration can be detected more sensitively by their geochemical signatures than by their mineralogical expression, as can alteration zone boundaries.

Lithogeochemical data provide information on the chemical compositions of rock. Rocks with similar chemical composition will have different mineral assemblages under different physical conditions. Therefore, a simple lithogeochemical analysis can provide definitive answers to question 2, and partial ones to question 3, 5 and 6, above, but can not give any answers to questions 1 and 4.

Mineralogical- and lithogeochemical-based methodologies utilize different types of data. However, the two are related through the compositions and amounts of individual minerals. These two approaches are complementary; many researchers have integrated them in different ways (e.g. Gresens, 1967; Meyer and Hemley, 1967; Giggenbach, 1984; MacLean and Barrett, 1993; Barrett et al., 1993; Madeisky and Stanley, 1993). A review of the various approaches used to quantitatively evaluate hydrothermal alteration is given in the following sections.

1. 2. Current Quantitative Approaches to the Study of Hydrothermal Alteration

The quantitative evaluation of material exchange during hydrothermal alteration relies on lithogeochemical data. With the development of X-ray fluorescence (XRF), atomic absorption spectrometry (AA), inductively coupled plasma-atomic emission spectrometry (ICP) and other advanced analytical techniques, the availability of high-quality, sensitive, precise, and inexpensive analyses for a long list of elements has come about.

It is probably fair to say, however, that the use of these data in exploration has to date been largely limited to empirical procedures including: (i) the identification and

distribution of pathfinder elements (e.g., Descarreaux, 1973; Boyle, 1979; Fyon and Crocket, 1982; Davies et al., 1982; Kishida and Kerrich, 1987), and (ii) the application of a varieties of empirical indices, such as an alteration index ($A.I. = 100 \times (MgO + K_2O)/(Na_2O + K_2O + CaO + MgO)$) proposed by Ishikawa et al. (1976), and many others including $Fe_2O_3/(Fe_2O_3+MgO)$, Al_2O_3/Na_2O , $(Fe_2O_3+MgO)/(Fe_2O_3+MgO+CaO+NaO)$, $K_2O/(Na_2O+K_2O)$, K_2O/Na_2O , MgO/CaO , $Na_2O/(Na_2O + K_2O + CaO)$, $K_2O/(Na_2O + K_2O + CaO)$ and $CaO/(Na_2O + K_2O + CaO)$ (Hashiguchi and Usui, 1975; Spitz and Darling, 1978; Saeki and Date, 1980). A thorough review of these indices has been made by Stanley and Madeisky (1993).

Depletion or enrichment anomalies, especially of silica, alkalis, and some metals, have been regarded as favorable signs in conjunction with the more conventional positive anomalies. In some cases, however, where subjective interpretation procedures have been used, these depletion or enrichment anomalies have been misconstrued as to whether or not they are absolutely depleted/enriched or relatively diluted/concentrated by the enrichment/depletions of other components. For example, silica depletion anomalies have been confused with Al or Mg enrichment effects (Appleyard and Guha, 1991). This confusion of enrichment and/or depletion is a product of the closure effect of lithogeochemical data.

1.2.1. The Closure Effect

In attempting to deal quantitatively with the material exchange during alteration using lithogeochemical data, a common problem arises, the closure effect. In a multicomponents system closure refers to the fact that all components must total 100 percent. Thus, if a single component is changed, say SiO_2 is added, the relative abundance of all other components decrease even though their absolute amounts are unchanged. This is the problem of the closure effect. Lithogeochemical analyses of altered rocks superficially can provide a distorted view of losses and gains of components. The matter

can be evaluated quantitatively as follows. Assume an original, simple system S_o consisting of three components X, Y and Z.

$$S_o = X_o + Y_o + Z_o = 100(\text{gram}) \quad (1-1)$$

(upper case letters are used for weights)

During an alteration process, components change by the absolute amounts dX , dY and dZ respectively. The total change of the system (in grams) will be:

$$dS = dX + dY + dZ \quad (1-2)$$

In practice, the values of $X_o + dX$, $Y_o + dY$ and $Z_o + dZ$ are not accessible directly because chemical analytical data are conventionally presented as percentage, that is,

$$s = x + y + z = 100\% \quad (1-3)$$

(lower case letters are used for percentages)

where x , y and z , the concentrations of components can be further described in the following form:

$$x = 100(X_o + dX) / (S_o + dS) \quad (1-4)$$

$$y = 100(Y_o + dY) / (S_o + dS) \quad (1-5)$$

$$z = 100(Z_o + dZ) / (S_o + dS) \quad (1-6)$$

Equations 1-4 to 1-6 indicate that the difference in the concentration of a particular component between the unaltered parent and the altered product is affected not only by the absolute change of individual component (dX , dY or dZ), but also by the total absolute change of all components (dS).

With regard to the impact of the closure effect on different constituents, Stanley and Madeisky (1993) indicate:

Closure will most affect those constituents that occur in large concentrations in a system and which are added to or removed from the system in an incomplete way. Conversely, it will least affect those elements that have been added to or removed from the system in more complete ways. In essence, the larger the concentration of a constituent in a rock relative to the amount of material transfer that constituent

has undergone, the more closure will obscure our ability to understand the material transfers using the constituent concentrations.

As a result, the closure effect should be removed before a meaningful interpretation of geochemical data proceeds.

1.2.2. Comparison of Various Techniques Used to Remove the Closure Effect

The closure effect has long been recognized and researchers working in related fields have devised various techniques to deal with this problem. The earliest paper dealing with this issue has been traced back almost a hundred years. Geochemists working with weathered rock, calculated losses and gains of constituents by assuming the amount of alumina to have remained constant during the weathering process (e.g., Merrill, 1897; Golditch, 1938; Krauskopf, 1967). Later researchers in the field of metasomatic alteration and igneous fractionation developed their own techniques to remove the closure effect from lithogeochemical data (e.g., Gresens, 1967; Pearce, 1968; Winchester and Floyd, 1977; Floyd and Winchester, 1978; Finlow-Bates and Stumpfl, 1981; Grant, 1986; MacLean and Kranidiotis, 1987, MacLean and Barret, 1993). A summary of their principal contributions is presented in Table 1-1. The formulae of Table 1-1 are presented with standardized symbols to emphasize the degree of similarity of proposals by various authors.

Among these techniques, Gresens' equation (Gresens, 1967) and its modification (Grant, 1986) have been widely used by economic geologists to quantify the losses and gains of constituents during hydrothermal alteration processes (e.g., Babcock, 1973; Appleyard, 1980; Morton and Nebel, 1984; Robert and Brown, 1986; MacLean and Kranidiotis, 1987; Leitch and Day, 1990, Leitch and Lentz, 1994; Marquis et al., 1990; Sketchley and Sinclair, 1987, 1991; MacLean, 1990; Richards et al., 1991; Bernier and MacLean, 1989; Barrett and MacLean, 1991, Barrett et al., 1993).

Table 1-1. A Summary of Quantitative Techniques Devised to Remove the Closure Effect and Evaluate Mass Transfer Process

Study	Year	Formula	Application	Notes
Merrill, G. P.	1897	$dX = \left(\frac{z_p}{z_d}\right)x_d - x_p$	weathering	$z = \text{Al}_2\text{O}_3$ and assumed to be immobile
Gresens, R. L.	1967	$dX = f_v \left(\frac{\rho_d}{\rho_p}\right)x_d - x_p$	metasomatism	f_v can be assumed to be one or determined by assuming one component is immobile so $f_v = \rho_p x_p / \rho_d x_d$.
Pearce, T.H.	1968	$\frac{dX}{z_p} = \frac{x_d}{z_d} - \frac{x_p}{z_p}$	igneous fractionation	x can be a combination of several components, Z is immobile.
Winchester et al. Floyd et al.	1977 1978	$\frac{z_d}{z_p} = \frac{x_d}{x_p}$	metabasalt classification	Both z and x are immobile.
Grant, J. A.	1986	$x_d = \frac{P}{D}(x_p + dX)$	Metasomatic alteration	$P / D = z_d / z_p$
MacLean, W. H.	1993	$dX = \left(\frac{z_p}{z_d}\right)x_d - x_p$	Metasomatic alteration	z = immobile elements such as Zr, Ti, Al, Nb, Y.

Notes: where: P- mass of parent rock;

D- mass of daughter or altered rock;

dX - the mass gains or losses of component x from 100 grams parental rock;

x_p - weight or molar fraction of component x in parent rock;

x_d - weight or molar fraction of component x in daughter or altered rock;

z_p - weight or molar fraction of immobile component z in parent rock;

z_d - weight or molar fraction of immobile component z in daughter or altered rock;

ρ_p - specific gravity of parent rock;

ρ_d - specific gravity of daughter or altered rock; and

f_v - volume factor = v_d / v_p .

Pearce element ratio (PER) diagrams, devised by Pearce (1968) for examining material exchange during the process of fractional crystallization, recently have been extended by Stanley and Madeisky (1994) to metasomatic rocks. PER diagrams have been used in the past to examine chemical variations caused by igneous differentiation (Russell and Stanley 1990). More recent applications are to hydrothermal alteration, in particular, that associated with volcanogenetic massive sulfide deposits (Stanley and Madeisky, 1993). In brief, this method converts the weight units of raw chemical analytical data into molar units, then uses a conserved/immobile element as a reference scale to remove the closure effect, and finally, utilizes various diagrams designed in the light of the stoichiometries of the relevant minerals, to test various causes of the lithogeochemical variations in terms of mineralogical variation(s).

Gresens' equation and Pearce element ratio diagrams are superficially different but they are used to solve similar problems. Cheng and Sinclair (1991), and Stanley and Madeisky (1993) show that these two techniques, although having different starting points, are fundamentally similar in principle — that is, they both remove the closure effect in order to decipher the true chemical variations during alteration. Even though an independent solution exists for Gresens' equation where the volume factor is known and the specific gravities have been measured, in practice, the volume factor can not be estimated except through the use of either an immobile component or an assumption such as constant volume during the hydrothermal alteration process.

The concept of immobile element is defined by Stanley and Madeisky (1993) as *'an element that is neither significantly added nor removed from a rock during metasomatism because of its low solubility in aqueous fluids (the stabilities of aqueous complexes that contain it are significantly lower than the stabilities of minerals that contain it).'*

The procedure of removing the effect of closure by using an immobile component is illustrated as follows. Given that a component Z is immobile (i.e. $dZ = 0$) then we have:

$$z = 100Z_o/(S_o + dS) \quad (1-7)$$

The use of this immobile component to remove the effect of closure involves using the immobile component as a divisor (standard reference) for other components as follows:

$$\frac{x}{z} - \frac{x_o}{z_o} = \frac{100(X_o + dX) / (S_o + dS)}{100Z_o / (S_o + dS)} - \frac{X_o}{Z_o} = \frac{dX}{Z_o} \quad (1-8)$$

The final result dX/Z_o in equation 1-8 can also be treated as the absolute change of element x with the reference unit of conserved or immobile component z_o because $Z_o = z_o$ if the original system is assumed to be 100 gram. Rearranging equation 1-8 produces Grant's version of Gresens' equation:

$$dX = \frac{z}{z_o} x_o - x \quad (1-9)$$

In summary, these various techniques of dealing with closure are all based on the same fundamental principle, an immobile component that allows the calculation of the true variations in rock compositions caused by material exchange. Applications of these techniques rely on a knowledge of either the change in rock volume during hydrothermal alteration (e.g. Robert and Brown, 1986), or the recognition of immobile component(s) in the rocks (e.g. MacLean and Kranidiotis, 1987).

1. 3. Two Requirements for Loss and Gain Calculations

Before applying these quantitative techniques for estimating losses and gains in a metasomatic system, two requirements must be met. First, the available analytical data must be shown to contain immobile components; second, a suite of samples for which loss/gain variations are to be evaluated, must be the alteration products of either: (i) a common parent rock characterized by chemical and mineralogical homogeneity (single precursor system), or (ii) a suite of rocks with determinable pre-alteration chemical composition (multiple precursor system).

In order to examine whether a set of lithogeochemical data meets the first requirement, Nicholls (1988) summarizes three ways of recognizing a conserved element for the study of igneous differentiation:

- (1) The petrologic behavior of the element can be used to select conserved elements. They are usually the incompatible elements.*
- (2) The ratio of two conserved elements will be constant in a comagmatic suite.*
- (3) An element ratio diagram that is not constructed with a set of conserved element in the denominator will have a trend with a near zero intercept.*

The geochemical behavior of elements is helpful to infer which elements might be conserved or immobile, particularly under certain circumstances where they are incompatible with the known mass transfer process. For example, the elements P, K and Ti are commonly thought to be incompatible with the main minerals that crystallize in a basaltic system, such as olivine, pyroxene and plagioclase (Pearce: 1968, 1987; Nicholls, 1988; Russell, 1986; Russell and Nicholls, 1987; Russell and Stanley, 1989, 1990a, 1990b). For hydrothermal alteration the assumption of Zr, Ti and/or Al immobility has been used widely because of the relative insolubilities of these components in hydrothermal solutions. An objective method is needed to test these assumptions.

In practice, ratios of immobile components remain constant regardless of the nature of alteration. This is an objective criterion for the recognition of immobile or conserved elements, and it can be easily proven as follows. Given that both dX and dZ equal to zero (i.e. both X and Z are immobile), then we have equation 1-4 divided by equation 1-6:

$$\frac{x}{z} = \frac{100X_o / (S_o + dS)}{100Z_o / (S_o + dS)} = \frac{X_o}{Z_o} \quad (1-10)$$

Thus, a bivariate plot of two immobile components from altered samples with a common parent will define a linear trend that extends through the origin. The concept of equation 1-10 for determining whether certain elements have been immobile in

metasomatism and hydrothermal alteration has been discussed and applied by Gresens (1967), Babcock (1973), Finlow-Bates and Stumpfl (1981), Grant (1986), Kranidiotis and MacLean (1987), MacLean (1988, 1990), Elliott-Meadows and Appleyard (1991), and MacLean and Barrett (1993). For example, Al, Ti, Zr, Nb, Yb and Lu commonly are shown to be immobile in hydrothermal alteration zones formed in homogeneous volcanic rock units (single precursor systems) at the Phelps Dodge deposit (MacLean and Kranidiotis, 1987), at Atik Lake (Bernier and MacLean, 1989), and at other mines in the Noranda district (Cattalani et al., 1989).

Some problems arise with the application of Nicholls' (1988) third criterion for immobility. First, let us see theoretically how many possible patterns can be present in a PER diagram based on simple ratios. The linear relation for any two points on x/z versus y/z diagram can be described by the following equation:

$$\frac{y}{z} = m \frac{x}{z} + b \quad (1-11)$$

the general form of the slope will be:

$$m = \frac{d(y/z)}{d(x/z)} = \frac{dY/z - ydZ/z^2}{dX/z - xdZ/z^2} = \frac{zdY - ydZ}{zdX - xdZ} \quad (1-12)$$

the general form of intercept will be:

$$b = \frac{y}{z} - m \frac{x}{z} = \frac{y}{z} - \frac{(zdY - ydZ)x}{(zdX - xdZ)z} = \frac{ydX - xdY}{zdX - xdZ} \quad (1-13)$$

If the slope and intercept of each individual pair of points in a data set are equal, then all points will plot as a straight line on a PER diagram. Otherwise, a data set may show a scattered distribution pattern to various extents on a PER diagram. Eight possible cases are summarized in Table 1-2.

According to Table 1-2, we see that Nicholl's third criterion for recognizing immobility is correct only under certain constrained conditions: (i) where elements in both

numerators are conserved (case 5), or (ii) $dY \ll dz$ (case 4), then the intercept (dY/dz) will be close to zero. Other possibilities also exist for a trend going through the origin but with a conserved or immobile component as the denominator. For example, in case 2, where $ydX - xdY = 0$, then its slope $dX/dY = X/Y$ and its intercept is equal to zero. The

Table 1-2. Eight possible cases of PER diagram*

case	dX	dY	dZ	slope	intercept	distributed pattern
1	<>0	<>0	<>0	$\frac{zdY - ydZ}{zdX - xdZ}$	$\frac{ydX - xdY}{zdX - xdZ}$	infinite lines or randomly distributed
2	<>0	<>0	=0	$\frac{dY}{dX}$	$\frac{ydX - xdY}{zdX}$...
3	<>0	=0	<0	$\frac{-ydZ}{zdX - xdZ}$	$\frac{ydX}{zdX - xdZ}$...
4	=0	<>0	<>0	$\frac{zdY - ydZ}{-xdZ}$	$\frac{dY}{dZ}$...
5	=0	=0	<>0	y/x	0	infinite lines through the origin
6	=0	<>0	=0	{x/z = x ₀ /z ₀ }	∞	a line // y/z axis
7	<>0	=0	=0	0	{y/z = y ₀ /z ₀ }	a line // x/z axis
8	=0	=0	=0	undefined	undefined	a point

* After Russell and Stanley, 1990

physical meaning of this example is that components x and y are highly correlated to each other (i.e. both of them may exist in the same mineral phase concerned and have very similar geochemical properties). When this mineral phase is removed from the current system, either depletion by crystal fractionation or by hydrothermal alteration, the contents of these components may change in the same proportion as their initial ratio. As a result, there is also a trend with a near zero intercept on the PER diagram. In addition, an

element ratio diagram that is not constructed with a set of conserved element in the denominator could be randomly distributed rather than having a well defined trend with a near zero intercept, as in cases 1, 3 and 4 according to Table 1-2.

In summary, it is reasonable to infer some possible conserved or immobile components on the basis of understanding the behaviors of these components and the geological processes in which they are involved. Nevertheless, it is risky to accept such assumptions without objective tests. It is efficient and rational to demonstrate immobility in the available data set on the basis of the theorem that the ratios of conserved or immobile components remain constant. Moreover, a re-examination of all possible candidates for immobility is warranted to demonstrate that they are not mineralogically or geochemically compatible with each other during the hydrothermal alteration process.

The concepts of mobile/immobile and compatible/incompatible are used frequently in the literature. These terms share many features in common, but it is necessary to clarify their specific implications in the context of hydrothermal alteration. The concepts of mobile/immobile are used to indicate whether or not a component has mass loss or gain during a hydrothermal alteration process. The terms incompatible and conserved have been used to describe certain elements not involved in a primary differentiation processes. Here the terms compatible/incompatible are used to describe whether or not the geochemical relationship among a particular group of components/elements are sufficiently correlated that they may have mass loss or gain in proportion to their initial ratio during a hydrothermal alteration process. Therefore, a pair of possible immobile components, determined from their constant ratio or highly correlated linear trend passing through the origin of the binary plot, also should be incompatible with each other. To emphasize the point, consider a pair of mobile components such as K and Rb which are also highly compatible with each other and which in a hydrothermal alteration system may display a highly correlated linear trend passing through the origin of the binary plot.

In reality, there is no perfectly constant ratio of a pair of immobile components. The reason for this is that apparent variability in ratios is a combination of geological variation, sampling and analytical error. Theoretically, the immobile component has not been involved in chemical transfer processes so the mass of the immobile component remains constant in a single precursor system. In reality, samples may not have been absolutely identical to each other before hydrothermal alteration in terms of immobile components, but if this inherent geological variation of a component is sufficiently small, this component can be treated as immobile. So immobility is a concept that depends on a high degree of homogeneity in the parent system prior to hydrothermal alteration.

Analytical error is another major source of apparent variation of ratios of immobile constituents. Considering the influence of analytical error, Russell and Stanley (1990a, 1990b) suggest that one could test for immobile/conserved components with a Pearce Element Ratio diagram accompanied by the propagated analytical error. If the dispersion or standard deviation of the ratio of two immobile or conserved candidates is less than or equal to the propagated analytical error, the dispersion can be interpreted to result entirely from analytical error. In such a case, the two candidates may be used as immobile or conserved components. This rule has been used in the study of basalt systems by Russell and Stanley (1989, 1990a, 1990b).

The rule should be used cautiously. If the PER ratio is constructed with one of the components having a large geological variation and the other having poor analytical precision, then the latter component will contribute more to the final propagated error of the ratio, especially where it is used as the denominator of the ratio. As a result, mobility of the former component might be obscured and the plot might lead to the correct conclusion that both numerator and denominator are immobile. Therefore, 'immobile' components of relatively high analytical quality should be accepted in preference to those with poor analytical precision.

The second requirement for the removing of closure from lithogeochemical data can be met conventionally through the careful investigation of field and petrographic relationships in the study area. Rock derivatives altered to various degrees from a common homogeneous parent rock commonly are in close spatial proximity and may show gradational contacts between each other. Primary textural and structural features may remain identifiable in least-altered to more intensely altered derivatives. To examine these types of variations rigorously it is recommended that samples be collected systematically along alteration profiles from the strongly altered rock adjacent to or within a mineralized zone, to the least altered rock far from the ore deposit itself. Such sampling should be done after a careful field investigation of the profile. Even though the altered rocks are of main concern, careful attention should be paid to the least altered or unaltered rocks. They provide important information about the parent rocks that preceded hydrothermal alteration and give insight into the occurrence of single precursor or multiple precursor systems.

For a multiple precursor system, the sequential relationships between different volcanic or intrusive events and their phase variations should be determined as clearly as possible. An efficient way of defining a single precursor system versus a multiple precursor system is to examine lithogeochemical plots, especially those constructed with immobile components such as Zr, Ti and Al_2O_3 (MacLean, 1990). A single precursor system will present a trend that extends through the origin on the plot. The plot pattern for multiple precursor system will be more scattered but generally convergent toward the origin. If the numbers of least altered or unaltered samples collected and analyzed are sufficient, their plots may present a well defined trend either going through or cutting tangentially the region where the altered samples plot, as in the case of a sequence of volcanic precursors related through fractional crystallization from a common magma.

1. 4. Pearce Element Ratios (PER) and their Application to Hydrothermal Alteration

The PER approach to examining metasomatic systems has an advantage over other procedures in not only removing the closure effect of lithogeochemical data but also: (i) explaining the corrected chemical variations in terms of mineralogical variation(s), and (ii) testing for a multiprecursor system (Stanley and Madeisky, 1993). PER diagrams have been widely applied to the interpretation of igneous fractionation (Russell and Nicholls, 1987, Russell and Stanley, 1989, 1990a, 1990b). Commonly, igneous crystal fractionation can be interpreted by the addition or subtraction of one or a few minerals. Thus, a specific PER diagram can be designed to illustrate this crystal fractionation trend according to the known stoichiometries of the relevant mineral phases. For example, the compositional variations of a suite of samples which are subjected only to olivine fractionation must be related to the stoichiometry of olivine $[(\text{Fe}, \text{Mg})_2\text{SiO}_4]$, e.g., one mole Si gain or loss along with two moles of Fe and Mg; thus the appropriate combinations (e.g., axes coefficients) of numerator elements for the axes of PER diagram are $\text{Si}/(\text{conserved element})$ as x-axis and $0.5(\text{Fe}+\text{Mg})/(\text{conserved element})$ as y-axis. Finally, the hypothesis of olivine fractionation can be tested according to whether the plots of data are consistent with the model trend that has a predesigned slope of one on the binary plot $\text{Si}/(\text{conserved element})$ versus $0.5(\text{Fe}+\text{Mg})/(\text{conserved element})$.

Recently, Madeisky and Stanley (1993) applied PER analysis to lithogeochemical data for altered rhyolites collected from the volcanic hosted massive sulfide (VHMS) deposit at Rio Tinto, Spain. Their work revealed that quartz, potassium-feldspar and plagioclase fractionation and crystal sorting contribute to geochemical variations of the unaltered rhyolite. The fractionation trend is clearly shown on a PER diagram constructed with Al/Zr as abscissa and $(2\text{Ca}+\text{Na}+\text{K})/\text{Zr}$ as ordinate. In addition, metasomatism (alkali depletion) disperses data on such a plot, toward the abscissa, away from the fractionation trend on the same PER diagram. Metasomatic additions and losses of elements have been

recognized up to 3 km from the centre of the mineralization system (Cerro Colorado open pit). Madeisky and Stanley (1993) also indicate that the rhyolite directly underlying the mineralization is a highly evolved melt and only the most evolved portions of this rhyolite are metasomatized, suggesting a genetic link between these highly evolved rhyolites and the associated VHMS mineralization.

Recent advances in dealing with metasomatic system have not dealt quantitatively with mineral abundances of both parent and altered rocks. Nor have there been enough efforts to integrate mineralogical variations with chemical exchange in a quantitative way. A specific PER diagram can be used to test the hypotheses that chemical variations are due to variations of particular mineral(s), but the amount of these minerals have not been determined explicitly.

The methodology of designing such a specific PER diagram for the purpose of testing an hypothesis is based on a simple matrix equation (Stanley and Russell, 1990; Stanley and Madeisky, 1993, 1994).

$$C \times A = P \quad (1-14)$$

where C is a phase composition matrix (with minerals down the side and elements across the top), A is an axes coefficient matrix (with elements down the side and axes across the top) and P is a phase displacement matrix (with minerals down the side and axes across the top). The phase composition matrix contains the formulas of minerals whose mass transfer effects are to be considered on the diagram. The axes coefficient matrix contains the coefficients for the linear combinations for each axis of the PER numerator. The phase displacement matrix depicts the displacement that mass transfer due to specific mineral losses or gains will have on each axis.

A number of PER diagrams with known axes coefficients have been designed for specific petrological material transfer hypothesis (e.g., Russell and Stanley, 1990a; Stanley and Madeisky, 1994). They can be used to test real data sets for particular mineralogical variations as explanation of chemical variations. However, in attempting to design a

diagram, without knowing the PER numerator linear combination coefficients, a more difficult set of procedures must be followed. These rely on the fact that a number of constraints, both mineralogical and geometric on the PER diagram being designed, can be assigned. This information allows determination of the entries in the 'phase displacement matrix'. Thus, with knowledge of the mineral formulae, the 'axes coefficient matrix' may be calculated using the approach of Stanley and Madeisky (1993). If C is a square and non-singular matrix, the unique solution for A can be found by:

$$A = C^{-1} \times P \quad (1-15)$$

If C is a non-square matrix but $C^T \times C$ is a non-singular matrix, the possible solution for A can be obtained through:

$$A = (C^T \times C)^{-1} \times C^T \times P \quad (1-16)$$

The following example is used to illustrate the procedure of designing a specific PER diagram, given a host rock of andesite in which feldspar and clinopyroxene are dominant. Propylitic, sericitic, argillic and silicic alterations and carbonatization are thought to be major causes of secondary lithogeochemical variations. Specifically, the replacement of primary feldspar (about 60%) by muscovite or kaolinite and quartz, and the replacement of primary mafic minerals (mainly augite and hornblende, about 5% and 3%, respectively) by epidote, chlorite and carbonates are the major contributors to lithogeochemical variations. Thus a composition matrix (C) could be composed of fourteen mineral phases (anorthite, albite, orthoclase, augite, hornblende, epidote, chamosite, clinocllore, calcite, siderite, magnesite, kaolinite, muscovite and quartz) and seven constituents (Si, Al, K, Na, Ca, Fe and Mg). This composition matrix C is then used as a simplified system to test the hypothesis. The displacement vectors of primary minerals such as anorthite, albite, K-feldspar and augite are defined to have slopes equal to one. The displacement vectors of alteration minerals are designed to have their slopes different from one, such as kaolinite and muscovite have slopes equal to 1/4 and 7/6, respectively, on this specific PER diagram. Then the x-axis and y-axis of this specific PER

diagram can be determined by using equations 1-15 and 1-16. The detailed procedure of this calculation is as follows.

$$\begin{matrix} An \\ Ab \\ Or \\ Aug \\ Qtz \\ Kao \\ Mus \\ Ep \end{matrix} \begin{pmatrix} 2 & 2 & 0 & 1 & 0 & 0 & 0 \\ 3 & 1 & 0 & 0 & 0 & 1 & 0 \\ 3 & 1 & 1 & 0 & 0 & 0 & 0 \\ 2 & 0 & 0 & 1 & 0 & 0.5 & 0.5 \\ 1 & 0 & 0 & 0 & 0 & 0 & 0 \\ 2 & 2 & 0 & 0 & 0 & 0 & 0 \\ 3 & 3 & 1 & 0 & 0 & 0 & 0 \\ 3 & 2 & 0 & 2 & 0 & 1 & 0 \end{pmatrix} \times \begin{pmatrix} x_{Si} & y_{Si} \\ x_{Al} & y_{Al} \\ x_K & y_K \\ x_{Ca} & y_{Ca} \\ x_{Na} & y_{Na} \\ x_{Fe} & y_{Fe} \\ x_{Mg} & y_{Mg} \end{pmatrix} = \begin{pmatrix} 2 & 2 \\ 3 & 3 \\ 3 & 3 \\ 2 & 2 \\ 1 & 0 \\ 2 & 0.5 \\ 3 & 3.5 \\ 3 & 4 \end{pmatrix} \begin{matrix} An \\ Ab \\ Or \\ Aug \\ Qtz \\ Kao \\ Mus \\ Ep \end{matrix} \quad (1-17)$$

$$C \quad \times \quad A \quad = \quad P$$

Multiply the right side matrix (P) of equation 1-17 by the inverse matrix C to produce

$$\begin{pmatrix} x_{Si} & y_{Si} \\ x_{Al} & y_{Al} \\ x_K & y_K \\ x_{Ca} & y_{Ca} \\ x_{Na} & y_{Na} \\ x_{Fe} & y_{Fe} \\ x_{Mg} & y_{Mg} \end{pmatrix} = \begin{pmatrix} 0 & 0 & 0.29 & 0 & 0.43 & 0.29 & -0.29 & 0 \\ 0 & 0 & -0.36 & 0 & -0.29 & 0.14 & 0.36 & 0 \\ 0 & 0 & 0.36 & 0 & -0.71 & -0.14 & 0.64 & 0 \\ 1 & 0 & 0.14 & 0 & -0.29 & -0.86 & -0.14 & 0 \\ 0 & 1 & -0.5 & 0 & -1 & -1 & 0.5 & 0 \\ -2 & 0 & -0.43 & 0 & -0.14 & 0.57 & 0.43 & 1 \\ 0 & 0 & -1 & 2 & -1 & 0 & 1 & -1 \end{pmatrix} \times \begin{pmatrix} 2 & 2 \\ 3 & 3 \\ 3 & 3 \\ 2 & 2 \\ 1 & 0 \\ 2 & 0.5 \\ 3 & 3.5 \\ 3 & 4 \end{pmatrix} = \begin{pmatrix} 1 & 0 \\ 0 & 0.25 \\ 0 & 2.75 \\ 0 & 1.5 \\ 0 & 2.75 \\ 0 & 0.5 \\ 0 & 0.5 \end{pmatrix} \quad (1-18)$$

$$A \quad = \quad (C^T \times C)^{-1} \times C^T \quad \times \quad P \quad = \quad x \quad y$$

The results of this calculation show that this specific PER diagram has a Si/(immobile component) as its x-axis and $[1/4Al + 11/4(Na+K) + 3/2Ca + 1/2(Fe+Mg)]$ /(immobile component) as its y-axis. The physical implications of this PER diagram can be understood through the stoichiometries of relevant minerals. For example, the decrease or increase in molar units of augite can be decomposed into two vectors (i.e., a one mole decrease or increase of both Ca and Fe and/or Mg (along the y-axis) will cause a corresponding two mole decrease or increase of Si (along the x-axis) on this specific PER diagram because of the stoichiometry of augite $[Ca(Fe, Mg)Si_2O_6]$. As a result, the plots of different samples whose lithogeochemical variation is caused by the fractionation of augite only, will display

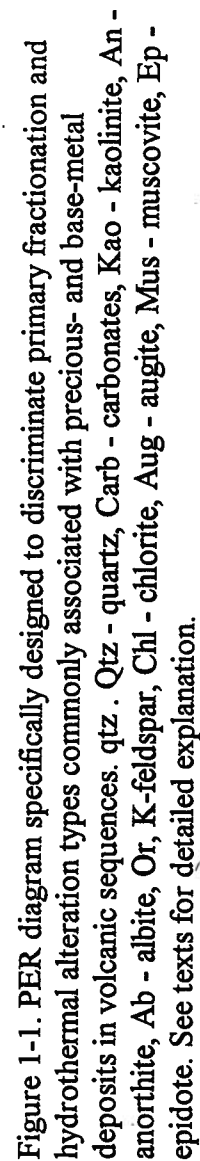
a trend with a slope of one on this particular PER diagram. The vector directions of other relevant mineral phases including hornblende, chlorite (chamosite and clinocllore) and carbonate (calcite, siderite, magnesite) then be projected on this PER diagram by using equation 1-14.

$$\begin{array}{l}
 Fe - Cl \\
 Mg - Cl \\
 Ca \\
 Sd \\
 Ma \\
 Hb
 \end{array}
 \begin{pmatrix}
 3 & 2 & 0 & 0 & 0 & 5 & 0 \\
 3 & 2 & 0 & 0 & 0 & 0 & 5 \\
 0 & 0 & 0 & 1 & 0 & 0 & 0 \\
 0 & 0 & 0 & 0 & 0 & 1 & 0 \\
 0 & 0 & 0 & 0 & 0 & 0 & 1 \\
 7 & 2 & 0 & 1 & 0 & 2 & 2
 \end{pmatrix}
 \times
 \begin{pmatrix}
 1 & 0 \\
 0 & 0.25 \\
 0 & 2.75 \\
 0 & 1.5 \\
 0 & 2.75 \\
 0 & 0.5 \\
 0 & 0.5
 \end{pmatrix}
 =
 \begin{pmatrix}
 3 & 3 \\
 3 & 3 \\
 0 & 1.5 \\
 0 & 0.5 \\
 0 & 0.5 \\
 7 & 4
 \end{pmatrix}
 \quad (1-19)$$

$$C \quad \times \quad A \quad = \quad P$$

The expected mineralogical variation paths on this PER diagram are illustrated in Figure 1 for various hydrothermal products commonly associated with precious- and base-metal vein mineralization in volcanic sequences. A detailed description about this PER diagram is given as follows:

- (1) If all lithogeochemical variations are restricted by mineralogical variations of feldspar, augite and chlorite, then this set of lithogeochemical data will plot along a trend of slope equal to one and an intersection of zero.
- (2) Where quartz exists and has not been involved in mass change, the trend above will be shifted toward the right.
- (3) If the wall rock has suffered propylitic alteration (i.e. augite is replaced by chlorite, and primary feldspars are partially replaced by sericite through the addition of volatile components), the 'loss' of primary minerals can be pictured as moving from the precursor composition (P) to a_1 down along the trend of slope equal to one and the 'addition' of alteration minerals can then be viewed as moving from P to a_2 along the trend of slope equal to one (the replacement of primary mineral and



formations of alteration mineral happen in the meantime, but it is convenient to analyze a metasomatic process as two superimposed processes on this PER diagram). As a result, propylitically altered samples will plot roughly around their primary precursor's position (P) on this diagram.

(4) Where the wall rock has altered into a bleached alteration envelope around the epithermal precious- and base-metal vein, in general, all primary mafic minerals and feldspar are completely replaced by alteration minerals (from P to b_1).

(5) If carbonates and pyritization are the dominant alteration products which replace the primary minerals (i.e. intense carbonatization plus pyritization), samples will plot along a vertical trend shown on the left side of the primary fractionation trend of slope equal to one (from b to c).

(6) If muscovite or sericite is the dominant alteration product (i.e. intense sericitization), samples will plot around a trend of slope equal to $7/6$, which is close to the primary fractionation trend but slightly shifted toward the left (from b to d).

(7) If kaolinite is the dominant alteration product (i.e. intense argillization), samples will plot toward a trend of slope equal to $1/4$ (from b to e).

(8) If quartz is the dominant alteration product (i.e. intense silicification), samples will plot around a trend parallel to x-axis (from b to f).

In brief, some of the alteration types commonly associated with precious- and base-metal vein mineralization in volcanic sequences are expected to be discriminated in a preliminary fashion on the PER diagram of Figure 1 by the relative displacements of altered samples from the primary feldspar and augite fractionation trend (slope = 1).

1. 6. Additional Problems

Mineral assemblages commonly occurring in alteration envelopes or zones can be identified routinely with the aid of various conventional and advanced modern instruments. However, still lacking is an objective and efficient way to assess the

abundances of each alteration mineral with confidence. This arises because hydrothermally altered rock commonly is characterized by a very fine-grained nature and/or intimate intermixing of mineral species. The technique of point counting, useful for medium to coarse grained rocks (especially igneous and metamorphic rocks) is limited in applications to products of hydrothermal alteration. In addition, serious sampling problems commonly arise in using thin sections for quantitative modal analysis.

The losses and gains of chemical components during the hydrothermal alteration process can be calculated with the aid of immobile components. This leads to an appreciation of possible reactions between primary minerals and altered minerals. However, the results of such calculations are not linked routinely in a quantitative way with the mineralogical changes that arise during hydrothermal alteration. To make such quantitative links immobile constituents must be identified and the precursor must be known; such needs are relatively difficult to provide in hydrothermally altered rocks that are products of open systems.

PER diagrams are superior to other quantitative approaches for the evaluation of hydrothermal alteration by not only removing the closure of lithogeochemical data, but also by linking the lithogeochemical variations to the mineralogical variations. However, the PER diagram approach still has some limitations in a quantitative evaluation of hydrothermal alteration. As demonstrated above, the PER diagram can be used to test hypotheses that chemical variations are due to variations of particular mineral(s). But the amount of these minerals can not be determined explicitly when a complicated multivariable system is dealt with because the total displacement on a PER diagram commonly is the sum of the displacements of different minerals. The length and slope of a displacement vector on a PER diagram may be the combination of various displacement vectors (i.e., various types of alteration). Briefly, the ambiguity about the relationship between lithogeochemical variations and mineralogical variations may arise where too many variables are squeezed into a two dimensional space. It is one of the goals of this

thesis to develop the idea of linking the lithogeochemical variations to the mineralogical variations and overcoming this limitation of PER diagrams. The following study consists of two parts: (i) a theoretical documentation about a quantitative approach extended from the PER diagram to hydrothermal alteration systems; and (ii) a detailed, quantitative case history of the alteration system associated with the Silver Queen polymetallic epithermal vein deposit in central British Columbia.

Chapter 2. Metasomatic Norms: A Method of Norm Calculation Adapted to Hydrothermal Altered Rocks

2.1. Introduction

Modeling a hydrothermal system quantitatively using either only mineralogical or only lithogeochemical data limits our knowledge of the system. We commonly limit our quantitative understanding of chemical losses and gains in a system if hydrothermal alteration minerals are the extent of our study. Conversely, if only chemical gains and losses are determined from lithogeochemical data (cf. Gresens, 1967) important mineralogical features are commonly minimized. Clearly, a procedure that takes account of both mineralogy and chemistry of altered rocks is desirable.

Mineralogy and chemistry of rocks are intimately linked through mineral abundances and the compositions of individual minerals. One way of combining mineralogical and lithogeochemical approaches to the study of altered rocks is to compute mineral abundances from the lithogeochemical data. It is easy to calculate an ideal mineral composition or norm. But it is not possible, in general, to calculate modal abundances without additional information because: (i) the minerals so-generated are idealized, or are end members of complex mineral families, and (ii) certain minerals or combinations of minerals are chemically equivalent, for example, $(\text{Fe, Mg})_2\text{SiO}_4 + \text{SiO}_2 = 2(\text{Fe, Mg})\text{SiO}_3$. However, where sufficient mineralogical and chemical controls are available, the norm can be made to approximate closely or even coincide with a mode.

A norm is a '... theoretical mineral composition of a rock expressed in terms of standard mineral molecules that have been determined by specific chemical analysis....' (Margaret, et al., 1972). Norms are used to standardize rock description and classification and to provide insight into some aspects of genesis. The concept, applied widely to igneous rocks, has had limited application to other rock types. Applications to metasomatized rocks

are hindered by the wide range of chemical changes involved and the complexity of many mineral compositions and mineral assemblages.

Various researchers have attempted to derive mineralogical information from lithogeochemical compositions for rocks other than igneous rocks. A particularly informative work by Brown and Skinner (1974) and Capitani and Brown (1987) use thermodynamic constraints and mass balance relations to calculate the weights of the minerals in the equilibrium mineral assemblages. Their results compare remarkably closely with modes. Davis and Ferry (1993) use mass balance relations to calculate the model protolith mineral abundances by assuming that a simple mineral assemblage (including calcite, dolomite/ankerite, quartz, albite, K-feldspar, muscovite and rutile (e.g., Rice, 1977; Ferry, 1985a, 1985b) suffers isochemical metamorphism. MacLean and Barrett (1993) recommend the Niggli-Barth cation normative calculation procedure (Barth, 1962) for metasomatic rocks for the purpose of approximating modes of altered rocks.

The above techniques share the use of mass balance relations between bulk rock composition and mineral abundances. They differ in the method used to select a reasonable mineral assemblage with which to partition the lithogeochemical data. Brown and Skinner (1974) and Capitani and Brown (1987) determine the mineral assemblage based on whether or not the minerals are stable under specific thermodynamic circumstance. Barth (1962), Rice (1977), Ferry (1985a, 1985b), Davis and Ferry (1993), MacLean and Barrett (1993) and many others choose the mineral assemblage according to petrographic observation and/or their experience. An important difference between the 'thermodynamic' and 'petrographic' approaches, above, is in the interpretation of the residuals of constituents. Ideally, there should be a perfect match between the analyzed bulk rock composition and the corresponding estimated normative mineral abundances. In reality, such is not the case. Some norm calculations leave some chemical components unused (residuals), such residuals should be in the range of analytical error. In general, the smaller the residuals are, the better is the quality of mass balance. Brown and Skinner (1974), Capitani and Brown (1987) and

Davis and Ferry (1993) explain residuals as the mass losses or gains of corresponding constituents. The assumption of a stable equilibrium relation in a hydrothermal system is often questionable, whereas petrographic examination can provide the actual mineral assemblage.

Normative approaches originally designed principally for igneous rocks are rigid in their application, and in general, do not accommodate important alteration minerals. In particular, volatile components are essential constituents of many metasomatic rocks but are not involved directly in determining normative minerals either by the CIPW norm or Niggli-Barth norm procedures. A different approach to the determination of norms of hydrothermally altered rocks by combining petrographic and lithogeochemical data warrants investigation.

2.2. The Principle of Metasomatic Norms

A possible approach to the application of the norm concept to metasomatic rocks is to constrain the calculated normative mineralogy by *a priori* knowledge of existing minerals (i.e., to approximate the mode as closely as possible). The methodology for this approach is a natural extension of the use of PER (Pearce element ratio) diagrams for the study of metasomatic rocks (e.g., Stanley and Madeisky, 1993, 1994).

Metasomatic norm calculation uses the same principles as the calculation of CIPW norms (e.g., Cross et al., 1903; Cox et al., 1979; Hughes, 1982; Philpotts, 1990). However, a wide range of possible mineral products is necessary for the determination of metasomatic norms that represent hydrothermal alteration systems. Moreover, the calculation of a metasomatic norm needs to take volatile components into account. Another distinctive difference between a metasomatic and a conventional igneous norm is that the calculation of a metasomatic norm can not proceed along a fixed hierarchical path as is the case of an igneous norm. More flexibility is necessary because of the wide range in both rock and mineral compositions. In some cases, where constrained by known

mineralogy, the calculations must iterate back and forth using various abundance of normative minerals in order to eventually balance or best fit a calculated mineral assemblage with the fixed chemical composition of an altered rock (i.e., to make the chemical masses and the mineral masses balance). In addition, the calculation of a metasomatic norm must take into account possible incompatible mineral pairs in hydrothermal system, for example, kaolinite and feldspar are not stable in the presence of quartz.

The mathematical relationship between lithogeochemical data and metasomatic norms is discussed by Cheng and Sinclair (1994) as follows: a rock mass, P , is comprised of the masses of a set of minerals ($\sum m_j$):

$$P = \sum_{j=1}^p m_j \quad (2-1)$$

For practical purposes, this equation can be extended in terms of the measurable items (in weight units) as follows:

$$P \times \sum_{i=1}^q w_i = \sum_{i=1}^q \sum_{j=1}^p (m_j \times f_{ij}) \quad (2-2)$$

for $i = 1, 2, \dots, q$; and $j = 1, 2, \dots, p$.

where

- q is the number of components analyzed;
- p is the number of involved mineral phases;
- w_i is the weight fraction of component i of the rock sample ($\sum w_i = 1$);
- m_j is the weight percent of mineral j of the rock sample in grams;
- f_{ij} is the weight fraction of component i in mineral phase j ;

The relation between the weight fraction of component i in mineral phase j and corresponding molar amounts can be expressed as follows:

$$f_{ij} = n_{ij} \times \frac{a_i}{b_j} \quad (2-3)$$

for $i = 1, 2, \dots, q$, and $j = 1, 2, \dots, p$, where n_{ij} is the number of moles of component i in mineral phase j , a_i is the molar weight of component i , and b_j is the molar weight of mineral phase j .

The reference weight P can be assigned any value, for example, 100 grams, and equation 2-2 can be converted into molar units as follows:

$$100 \times \sum_{i=1}^q (w_i / a_i) = \sum_{i=1}^q \sum_{j=1}^p ((m_j / b_j) \times n_{ij}) \quad (2-4)$$

In equation 2-4 the weight fraction of each chemical constituent of the rock (w_i) is measurable through whole rock chemical analysis; a_i and b_j hold the constant molar weights for each chemical constituent i and each mineral phase j ; f_{ij} and n_{ij} are either measurable through an analysis of mineral separates or referenced from the standard stoichiometry of corresponding minerals; $\sum m_j$, the remaining unknowns, are to be determined.

Since $1/\sum a_i$ and $1/\sum b_j$ can be converted into a diagonal matrix $[1/a_{ij}]_{pxq}$ and $[1/b_{ij}]_{pxq}$ (for $i \neq j$, $1/a_{ij} = 0$ and $1/b_{ij} = 0$), the relationship can also be expressed in matrix form as:

$$\begin{pmatrix} 1/a_1 & \dots & 0 & \dots & 0 \\ \vdots & \ddots & \vdots & \ddots & \vdots \\ 0 & \dots & 1/a_{ij} & \dots & 0 \\ \vdots & \ddots & \vdots & \ddots & \vdots \\ 0 & \dots & 0 & \dots & 1/a_{qp} \end{pmatrix} \times \begin{pmatrix} w_1 \\ \vdots \\ w_i \\ \vdots \\ w_q \end{pmatrix} =$$

$$\begin{pmatrix} n_{11} & \dots & n_{1j} & \dots & n_{1p} \\ \vdots & \ddots & \vdots & \ddots & \vdots \\ n_{i1} & \dots & n_{ij} & \dots & n_{ip} \\ \vdots & \ddots & \vdots & \ddots & \vdots \\ n_{q1} & \dots & n_{qj} & \dots & n_{qp} \end{pmatrix} \times \begin{pmatrix} 1/b_{11} & \dots & 0 & \dots & 0 \\ \vdots & \ddots & \vdots & \ddots & \vdots \\ 0 & \dots & 1/b_{ij} & \dots & 0 \\ \vdots & \ddots & \vdots & \ddots & \vdots \\ 0 & \dots & 0 & \dots & 1/b_{qp} \end{pmatrix} \times \begin{pmatrix} m_1 \\ \vdots \\ m_j \\ \vdots \\ m_p \end{pmatrix} \quad (2-5)$$

OR

$$A \times W = N \times B \times M \quad (2-6)$$

where $A = [1/a_{ij}]_{p \times q}$ (for $i \neq j$, $1/a_{ij} = 0$), $W = [w_i]_q$, $B = [1/b_{ij}]_{p \times q}$ (for $i \neq j$, $1/b_{ij} = 0$), $N = [n_{ij}]_{p \times q}$ and $M = [m_j]_p$.

Generally, there is a larger number of unknowns than equations in the linear set of equations 2-5 or 2-6. The values q and p are related to the number of analytical items and the number of mineral phases considered, respectively. Usually, the composition of a rock sample is composed of only about a dozen major and minor components (q). In contrast, the mineral phases considered may be over twenty or more (p). Therefore, in general, matrix N is not square. Consequently, this set of linear equations cannot be solved explicitly. Some constraints are needed to reduce the number of independent variable m_j 's through either: (i) thermodynamic calculations (e.g., Brown and Skinner, 1974) to decide what are the stable mineral assemblages, or (ii) observation of the assemblage comprising the rock in question. It is essential that p is equal to or less than q in order that a unique solution is possible.

In some cases the matrix might be singular or overdetermined. These problems may be caused by analytical errors and/or discrepancies between the compositions of real mineral phases of the rock sample and standard normative mineral phases used in matrix N . Thus, such set of linear equations needs to be solved using a fitting procedure, such as minimizing the sum of squares, R^2 (e.g. Wright and Doherty, 1970; Stout and Nicholls, 1977). The principle of the technique is to search for the solution which produces the least R^2 value (R^2_{\min}), where R^2 (sum of squares of residual) is given by:

$$R^2 = \sum_{i=1}^q (w_i/a_i - \sum_{j=1}^p (m_j \times f_{ij}))^2 \quad (2-7)$$

The least squares technique can provide either the best fit solution or the best fit approximations.

In brief, the calculation of metasomatic norms as introduced here rests on the suppositions that lithogeochemical data are of adequate quality, and that the principal

alteration minerals have been identified. Norms determined in the foregoing manner are objective and quantitative. They are representative of the processes being modeled and can closely approximate modes of the altered rocks under study if appropriate constraints are available.

2.3. A Set of Standard Normative Mineral Components for a Metasomatic System

The metasomatic process of wall rock alteration, in most cases, can be described as the additions of volatile components (H_2O , CO_2 , S, etc.) and ionic components (K, Si, etc.) from hydrothermal fluid to wall rock and a corresponding depletion of some ionic components of the wallrock (Na, Ca, Mg etc., extracted from the wall rock and contributed to hydrothermal fluid). This process of chemical exchange can also be described partly in terms of mineral transformations. For example, anhydrous silicates such as olivine, pyroxene and feldspars, alter to (i) phyllosilicates such as chlorite, muscovite, kaolinite, chlorite, (ii) carbonates such as calcite, magnesite, siderite, rhodochrosite, dolomite, ankerite, etc., and, (iii) sulfides such as pyrite. Volatile components clearly are an essential part of a hydrothermal alteration system and cannot be omitted as in the case of CIPW normative calculations.

The selection of a set of standard minerals for metasomatic norm calculation should be based on geological observations. Rock-forming minerals which account for most of the chemical components clearly have priority. In most cases for hydrothermally altered rock systems the major components are composed of: SiO_2 , Al_2O_3 , Fe_2O_3 , FeO , MgO , CaO , Na_2O , K_2O , H_2O and CO_2 . The standard minerals for metasomatic norms must include hydrous phases, carbonates and sulfides as well as anhydrous minerals. Minerals found to be appropriate for metasomatic systems can be classed into nine categories:

- (1) anhydrous mafic silicates such as olivine and pyroxene (Fe, Mg, Ca-silicates);
- (2) anhydrous calc-alkali aluminous silicate such as K-feldspar, albite and anorthite;

- (3) hydrous calc-ferric aluminous silicate such as epidote;
- (4) hydrous mafic aluminous silicate such as chlorite;
- (5) hydrous alkaline aluminous silicate such as muscovite;
- (6) hydrous aluminous silicate such as kaolinite;
- (7) carbonate such as calcite, magnesite, siderite;
- (8) sulfide such as pyrite; and
- (9) oxides such as quartz, magnetite and hematite.

The minor components contained in accessory minerals such as P_2O_5 (apatite), TiO_2 (ilmenite or rutile), are less important to make the masses balance. The abundances of such accessory minerals generally do not exceed a few weight percent; however, in certain cases these normally minor minerals or trace minerals can be relatively abundant and can have strong impact on the norm calculation. For example, S can be dealt with as a minor component in most cases, but if a sample has more than a few weight percent of pyrite then S becomes an important component.

A set of standard normative minerals based on the author's experience in treating metasomatism associated with precious- and base-metal deposits in volcanic sequences is listed in Table 2-1. This list is not exhaustive. It can be extended by the addition of new standard normative mineral(s) or substituted by other identified mineral species in order to meet specific requirements.

2.4. A Manual Procedure of Metasomatic Norm Calculation

Practically, the calculation of metasomatic norms is completed using a computer, but it is essential to understand the conceptual nature of the calculations. A manual procedure has been developed patterned after the CIPW procedure. These calculations must balance the available components (analytical data for an altered rock) with the amounts of a particular group of minerals of known or assumed compositions. By using alteration minerals presented in the altered rock as members of the starting group of

Table 2-1. A List of standard normative mineral components for metasomatic volcanic rocks associated with epithermal ore deposits

Normative mineral	Symbol	Formula	Molecular weight
Fayalite	Fa	Fe ₂ SiO ₄	203.79
Forsterite	Fo	Mg ₂ SiO ₄	140.71
Ferrosilite	Fs	FeSiO ₃	131.94
Enstatite	En	MgSiO ₃	100.4
Wollastonite	Wo	CaSiO ₃	116.17
Rhodonite	Rn	MnSiO ₃	131.03
Orthoclase	Or	KAlSi ₃ O ₈	278.34
Albite	Ab	NaAlSi ₃ O ₈	262.24
Anorthite	An	CaAl ₂ Si ₂ O ₈	278.22
Epidote	Ep	Ca ₂ FeAl ₂ Si ₃ O ₁₂ (OH)	483.24
Chamosite	Fe-Cl	Fe ₅ Al ₂ Si ₃ O ₁₀ (OH) ₈	713.48
Clinocllore	Mg-Cl	Mg ₅ Al ₂ Si ₃ O ₁₀ (OH) ₈	555.78
Muscovite	Mu	KAl ₃ Si ₃ O ₁₀ (OH) ₂	398.3
Paragonite	Pa	NaAl ₃ Si ₃ O ₁₀ (OH) ₂	382.2
Kaolinite	Ka	Al ₂ Si ₂ O ₅ (OH) ₄	258.14
Quartz	Qz	SiO ₂	60.09
Calcite	Ca	CaCO ₃	100.09
Magnesite	Ma	MgCO ₃	84.32
Siderite	Sd	FeCO ₃	115.86
Rhodochrosite	Rc	MnCO ₃	114.95
Pyrite	Py	FeS ₂	119.97
Ilmenite	Im	TiFeO ₃	151.75
Rutile	Ru	TiO ₂	79.9
Hematite	He	Fe ₂ O ₃	159.7
Magnetite	Mt	Fe ₃ O ₄	231.55
Apatite	Ap	Ca ₅ (PO ₄) ₃ (OH)	502.21

standard minerals, a metasomatic norm is expected to approximate the mode of the hydrothermally altered rock. The extent to which this end can be achieved depends on how close the true mineralogy is reflected in the norm and whether appropriate mineral compositions have been used in the calculations. In principle, the calculation scheme is designed to allot cations to various normative minerals and to add in as many anions as required. Hence, the difference in value between calculated cations and the corresponding analyzed cations is generally equal to zero.

To illustrate the procedure of metasomatic norm calculation, equation 2-3 or 2-4 is expanded by using the standard normative minerals listed in Table 3-1 and a set of equations results as follows.

$$w_p = a_p \times 3m_{ap} / b_{ap} \quad (2-8a)$$

$$w_s = a_s \times 2m_{py} / b_{py} \quad (2-8b)$$

$$w_{Ti} = a_{Ti} \times (m_{im}/b_{im} + m_{ru}/b_{ru}) \quad (2-9a)$$

$$w_{Mn} = a_{Mn} \times (m_m/b_m + m_{rc}/b_{rc}) \quad (2-9b)$$

$$w_{Na} = a_{Na} \times (m_{ab}/b_{ab} + m_{pa}/b_{pa}) \quad (2-9c)$$

$$w_K = a_K \times (m_{or}/b_{or} + m_{mu}/b_{mu}) \quad (2-9d)$$

$$w_{Mg} = a_{Mg} \times (2m_{fo}/b_{fo} + m_{en}/b_{en} + 5m_{Mg-Cl}/b_{Mg-Cl} + m_{ma}/b_{ma}) \quad (2-9e)$$

$$w_{Ca} = a_{Ca} \times (m_{wo}/b_{wo} + m_{an}/b_{an} + 2m_{ep}/b_{ep} + m_{ca}/b_{ca} + 5m_{ap}/b_{ap}) \quad (2-9f)$$

$$w_{Fe+3} = a_{Fe+3} \times (m_{ep}/b_{ep} + 2m_{he}/b_{he} + 3m_{ma}/b_{ma}) \quad (2-9g)$$

$$w_{Fe+2} = a_{Fe+2} \times (2m_{fa}/b_{fa} + m_{fe}/b_{fe} + 5m_{Fe-Cl}/b_{Fe-Cl} + m_{sd}/b_{sd} + m_{py}/b_{py} + m_{mt}/b_{mt}) \quad (2-9h)$$

$$w_{Al} = a_{Al} \times (m_{or}/b_{or} + m_{ab}/b_{ab} + 2m_{an}/b_{an} + 2m_{ep}/b_{ep} + 2m_{Fe-Cl}/b_{Fe-Cl} + 2m_{Mg-Cl}/b_{Mg-Cl} + 3m_{mu}/b_{mu} + 3m_{pa}/b_{pa} + 2m_{ka}/b_{ka}) \quad (2-10a)$$

$$w_{Si} = a_{Si} \times (m_{fa}/b_{fa} + m_{fo}/b_{fo} + m_{fe}/b_{fe} + m_{en}/b_{en} + m_{wo}/b_{wo} + m_m/b_m + 3m_{or}/b_{or} + 3m_{ab}/b_{ab} + 2m_{an}/b_{an} + 3m_{ep}/b_{ep} + 3m_{Fe-Cl}/b_{Fe-Cl} + 3m_{Mg-Cl}/b_{Mg-Cl} + 3m_{mu}/b_{mu} + 3m_{pa}/b_{pa} + 2m_{ka}/b_{ka} + m_{qz}/b_{qz}) \quad (2-10b)$$

$$w_{CO3} = a_{CO3} \times (m_{ca}/b_{ca} + m_{ma}/b_{ma} + m_{sd}/b_{sd} + m_{rc}/b_{rc}) \quad (2-11a)$$

$$w_{OH} = a_{OH} \times (m_{ep}/b_{ep} + 8m_{Mg-Cl}/b_{Mg-Cl} + 8m_{rcFe-Cl}/b_{rcFe-Cl} + 2m_{mu}/b_{mu} + 2m_{pa}/b_{pa} + 4m_{ka}/b_{ka} + m_{ap}/b_{ap}) \quad (2-11b)$$

$$w_{Total} = w_{\Sigma minerals} \quad (2-11c)$$

where w represents the weight percent of the certain constituent indicated by subscript, a represents the molar weight value of the constituent denoted by subscript, m is the weight fraction of the mineral indicated by subscript, and b is the molar weight value of the mineral indicated by subscript.

A general procedure to be followed in determining a metasomatic norm has been developed patterned after the procedure used in igneous norm calculation. Significant changes arise in the "metasomatic" procedure mainly due to the necessity of accounting for volatile components. A detailed procedure for establishing a metasomatic norm follows.

1. Recast the oxide weight percentage values to cation amounts, obtained by dividing the weights percent of oxides by their respective molecular weight, multiplying by the number of cations in the oxide formula. For example, if a sample has 12 wt% Al_2O_3 , then

$$\text{Al}^{+3} = (12.00 \times 2) / (26.98 \times 2 + 16 \times 3) = 0.2354$$

2. Use all P (and necessary Ca) to make apatite [$\text{Ca}_5(\text{PO}_4)_3(\text{OH})$]. A unique solution exists for equation 2-8a because apatite is the only mineral in the set of standard normative minerals containing P.
3. Use all S (and necessary Fe) to make pyrite (FeS_2). There is a unique solution for equation 2-8b because pyrite is the only sulfide considered in the current set of standard normative minerals.
4. Use all Ti (and necessary Fe) to make provisional ilmenite (FeTiO_3) and temporarily assign the value of m_{rutile} equal zero (equation 2-9a).
5. Use all Mn to make provisional rhodonite (MnSiO_3) and assign the value of $m_{\text{rhodochrosite}}$ equal zero temporarily (equation 2-9b).
6. Use all Na to make provisional albite ($\text{NaAlSi}_3\text{O}_8$) and let the value of $m_{\text{paragonite}}$ equal zero temporarily (equation 2-9c).
7. All K is provisionally allotted to K-feldspar (KAlSi_3O_8) and the value of $m_{\text{muscovite}}$ is set to zero temporarily (equation 2-9d).
8. There are 3 independent variables in equation 2-9e. Use all Mg to make provisional Mg-end member pyroxene, enstatite (MgSiO_3), and leave the values of other Mg-bearing minerals as zero temporarily.
9. There are five mineral phases in equation 2-9f, the value of m_{apatite} has been calculated previously with equation 2-8a. If the composition of plagioclase is known (i.e., the ratio of Ca:Na in plagioclase can be set) then an appropriate amount of Ca can be allotted provisionally to anorthite ($\text{CaAl}_2\text{Si}_2\text{O}_8$) by assigning all Na to albite. In other words, $m_{\text{anorthite}}$ is dependent on m_{albite} . Finally, use the remaining Ca to make provisional Ca-end member of pyroxene, wollastonite (CaSiO_3) and set the values of m_{epidote} and m_{calcite}

to zero.

10. There are three mineral variables in equation 2-9g; the value of m_{epidote} has been set provisionally in equation 2-9f above. Use all Fe^{+3} and corresponding amount of ferrous iron to make provisional magnetite ($\text{Fe}_2\text{O}_3\text{FeO}$) and leave the values of m_{hematite} to be zero temporally.
11. The values of m_{pyrite} and $m_{\text{magnetite}}$ have been determined by previous equations so there are four items unknown in equation 2-9h. Use the remaining Fe^{+2} to make provisional Fe-end member of pyroxene, ferrosilite (FeSiO_3) and leave the values of the remaining ferrous iron bearing minerals in equation 2-9h at zero.
12. Even though equation 2-10a has 9 items, all of them but $m_{\text{kaolinite}}$ have been determined by previous equations. As a result, the remaining excess Al is used to make provisional kaolinite [$\text{Al}_2\text{Si}_2\text{O}_5(\text{OH})_4$]. However, the rock may already have a deficit of Al^{+3} at this stage. In this eventuality the variable $m_{\text{kaolinite}}$ in equation 2-10a disappears and equation 2-10a becomes a constraint for the previous equations. To eliminate a deficit of Al^{+3} the independent variables of certain minerals containing less Al^{+3} are used to substitute for some or all of the provisional minerals in previous equations.
13. All of the items but m_{quartz} in equation 2-10b have been determined by previous equations. As a result, any excess Si is used to make provisional quartz (SiO_2). Of course, Si^{+4} may already be in deficit at this step, in which case equation 2-10b becomes a constraint for the previous equations. This deficiency can be accounted for by using as independent variables, certain minerals containing less Si^{+4} relative to the provisional minerals estimated in previous equations. For example, convert pyroxene [$(\text{Fe,Mg})_2\text{Si}_2\text{O}_6$] to provisional olivine [$(\text{Fe,Mg})_2\text{SiO}_4$] to the extent necessary to rectify the deficiency.
14. All items in equation 2-11a have been determined by previous equations. Therefore, it is a constraint equation. If the sum of the provisional values on the right side of the equation is not equal to the measured value on the left side, adjustments are required to

make the mass of CO_3^{-2} balance. Usually, the value on the left side is greater than that on right side of the equation at this step because the provisional allotments set the values of all carbonates to be zero. Therefore, more carbonate(s) should be allotted to balance the equation.

15. There are no unknown items in equation 2-11b. As a result, it is another constraint equation. If the sum of the provisional values on the right side of the equation is not equal to the measured value on the left side, adjustments are required to balance the equation. If the measured value on the left side is greater than that on the right side of the equation, the independent variables of minerals containing more hydroxyls are required and provisional amounts of anhydrous mineral must be reduced. Conversely, in other cases it may be necessary to reduce the amounts of hydroxyl-bearing minerals.
16. Equation 2-11c is a general constraint related to the mass balance of O^{-2} . If the two sides of this equation are not balanced, the preceding allotments of standard mineral abundances are somewhere in error.

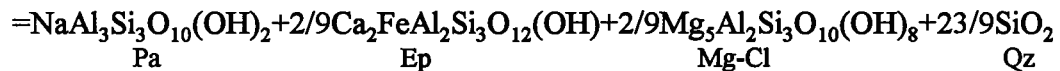
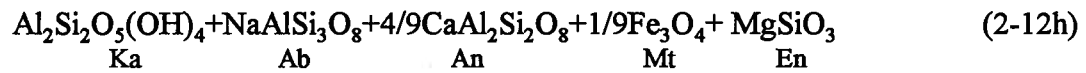
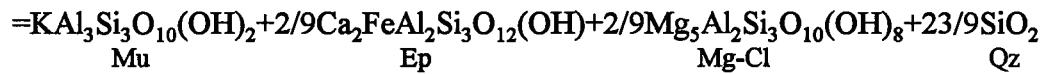
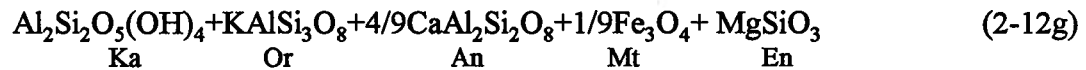
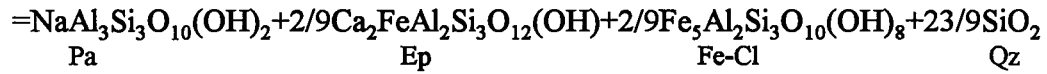
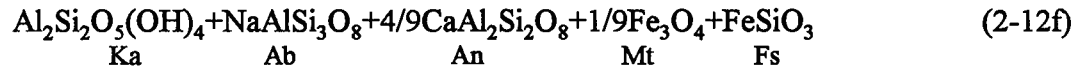
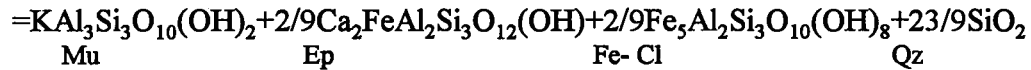
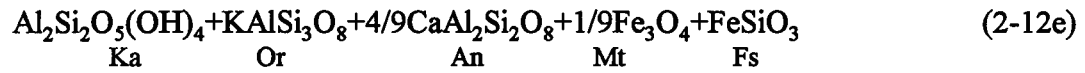
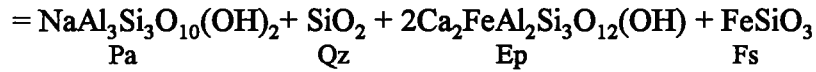
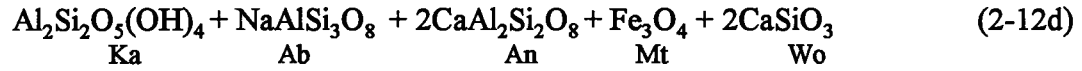
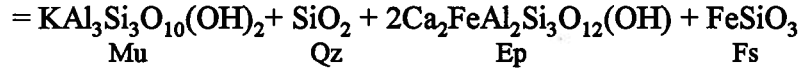
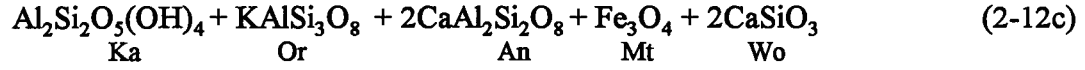
To this point in the calculation, there are two equations with unique solutions (2-8a and 2-8b), eight equations having 14 independent variables in total (2-9a, 2-9b, 2-9c, 2-9d, 2-9e, 2-9f, 2-9g, 2-9h), two equations having single dependent variable (2-10a and 2-10b), and three constraint equations (2-11a, 2-11b and 2-11c). There are more unknowns than available equations so far. More constraints are needed to achieve a satisfactory solution.

17. The first simplification for the calculation of a metasomatic norm is that olivine is not compatible with quartz. In other words, the following reactions move to the right until one of the components on the left side of the reactions is used up.



18. The second simplification is that kaolinite is not compatible with feldspar and

pyroxene under the condition that quartz exists. In other words, the following equilibria proceed to the right until either kaolinite or anhydrous silicates on the left side of the reactions are used up.



This simplification is supported by geological observation and thermodynamic relations.

For example, according to the copper porphyry model, a phyllic or sericitic zone separates a potassic alteration zone from an argillic alteration zone. On $\log(K^+/H^+)$ versus $\log(H_4SiO_4)$ activity-activity diagram, the stable region of K-feldspar is

separated from that of kaolinite by muscovite in the presence of quartz.

19. Some additional practical constraints can be set on a normative calculation. For example, the composition of plagioclase (k) is easily measured, thus, the relation between anorthite and albite can be expressed as follows:

$$k = m_{\text{albite}} / (m_{\text{anorthite}} + m_{\text{albite}}) \quad (2-13)$$

A similar relationship can be applied to the end members of other solid solution minerals. As a result, more constraints can be established. In addition, a set of constraints can be established limiting the values of calculated norms as never less than zero.

In summary, there are 14 independent variables after initial allotments, three constraints related to the mass balance equations of OH^- , CO_3^{-2} and total, and eight constraints derived from two simplifications. In most cases, the bulk chemical composition of the rock studied can be explained by about a dozen minerals within this set of standard normative minerals. The final result is that a particular sample represents a system that is simpler than that initially assumed. In other words, a realistic system generally has substantially less than 14 independent variables. Therefore, a satisfactory solution can commonly be achieved by using the above approach.

A complex system, such as a weakly altered rock in which significant amount of primary minerals coexist with secondary alteration minerals, may have even more independent variables. Therefore, additional constraints are needed. Modern analytical techniques can provide the required knowledge-based constraints.

The general procedural scheme for metasomatic norm calculation has been introduced. The procedure, however, is grossly inefficient for manual calculation. Consequently, a computer-based procedure using Quattro Pro 5.0, a sophisticated and readily available spread sheet program, has been devised to process norm calculations. It can be easily converted to other spread sheet software (Appendix C). The procedure involves the use of a built-in module (the 'Optimizer') in the software. The general

procedures of using Optimizer is to (i) decide the solution destination such as $W_{\text{total}} - W_{\Sigma \text{ mineral}} = 0$, (ii) choose the variables (standard minerals) to be included in the calculation, and (iii) set up the constraints indicated at the end of the forgoing section. Then the Optimizer module can adjust the amounts of the variables and adhere to the constraints to provide a final best fit solution. Unlike other 'black box' types of software, this calculation model is transparent. Users can easily adjust and develop it according to their own purposes.

2.5. A Quantitative Model of Metasomatic Systems

The central goal of this work is to develop the concept of metasomatic norms and to apply the technique. One important outcome is the likelihood that with appropriate petrographic constraints the norm and mode can be made to coincide. With the recognition of an immobile component and a set of lithogeochemical compositions that includes both least altered parent rock (Z_p) and altered daughter rock (Z_d), the metasomatic norms and chemical constituents of an altered rock (x_d) can be further recast into the absolute amounts of minerals and chemical constituents ($x_p + dx$) for a given mass of parent rock (x_p) by using the following equation to remove the closure effect (e.g., Merrill, 1897; Gresens, 1967; Pearce, 1968; Grant, 1986; MacLean and Kranidioties, 1987; MacLean and Barrett, 1993; Cheng and Sinclair, 1991):

$$x_p + dx = \frac{z_p}{z_d} x_d \quad (2-14)$$

Consequently, the contribution of each mineral to the chemical variations of bulk rock, the absolute loss or gain of individual chemical constituents during hydrothermal alteration process can be stated explicitly as follows:

$$\begin{aligned} \Sigma \text{Mineral}_{\text{parent rock}} + \Sigma \text{Constituent}_{\text{gained from solution}} \\ = \Sigma \text{Mineral}_{\text{altered rock}} + \Sigma \text{Constituent}_{\text{lost from wall rock}} \end{aligned} \quad (2-15)$$

where all items have extensive units (e.g. grams). Such an equation is comprehensive, quantitative, and provides an easily understood chemico-mineralogical model; it illustrates and interprets a hydrothermal alteration system in terms of initial and final normative mineral assemblages (corrected for the closure) plus absolute losses and gains of chemical constituents. The model can be applied without the constraints of closed system and equilibrium assemblages.

The value of such a model is that it provides useful, quantitative information about the hydrothermal system. If the altered rock is the product of a simple and unique hydrothermal alteration process, the model may reveal the properties of hydrothermal solutions associated with metasomatic events. In reality, the reaction used may more likely represent the final result of a series of sequential and/or superimposed processes. That is, the model incorporated in the equation is an 'end member' model. Specifically, the model includes starting and ending rock mineralogies that may be evident in the field, as well as documenting gains and losses of specific chemical constituents.

This model is quantitative in the same way as Pearce element ratio diagrams. The common principle is the correction for closure that provides true relative lithogeochemical and mineralogical variations between parent and daughter rocks. The normative approach is a useful supplement to PER analysis; the two procedures have much in common and contain much the same information presented in different ways. The sequence of developing a PER diagram is to:

- (1) remove the closure effect of lithogeochemical data to calculate the absolute chemical changes of elements by using a conserved or immobile element, and
- (2) interpret these absolute chemical variations in terms of specific mineral or mineral assemblage on a binary plot.

In contrast, the technique of metasomatic norm is to:

- (1) allot the chemical analytical data of bulk rock into an assemblage of normative minerals (that in certain cases will approximate the mode), and

- (2) remove the closure effect of the norms and use the difference between norms (modes) of parent and metasomatized rocks and elemental losses and gains to develop a combined chemico-mineralogical model of the metasomatic process.

The strategy of a PER diagram is to test whether chemical changes between two rocks can be explained purely by changes in amounts of one or a few minerals as demonstrated by the distribution of points along predefined trends (slopes). Metasomatic norms are displayed more explicitly as equations (models) or profiles showing the spatial distributions of normative mineral assemblage as well as the absolute losses and gains of chemical constituents based on the comprehensive mass balance relationships.

2.6. Case Histories: Application of Metasomatic Norms

2.6.1. Sigma Mine, Abitibi, Quebec

Mesothermal gold-quartz veins of the Sigma mine are enveloped by well defined, if narrow, wallrock alteration zones (Robert and Brown, 1984, 1986). An outer cryptic alteration zone is succeeded by a visible alteration zone immediately adjacent to the vein. The semiquantitative mineral variations across the alteration envelope are illustrated in Figure 2-1. Unaltered rocks are composed of a greenschist mineral assemblage: albite-chlorite-epidote-white mica-biotite-quartz with minor carbonate and accessory apatite, ilmenite, and pyrite. The cryptic alteration is characterized by the variable replacement of epidote by carbonate; the zone of visible alteration is marked by an abrupt outer transition (2-3 mm wide) parallel to vein margins, a carbonate-white mica outer subzone and a carbonate-albite inner subzone immediately adjacent to the vein. The salient mineralogical feature of visible alteration is the complete destruction of chlorite and biotite originally present in the parent volcanic rocks.

A reassessment of the overall process of hydrothermal alteration at Sigma mine can be made by applying the technique of metasomatic norms using the lithogeochemical data presented in Table 2-2. The results of such a calculation (Table 2-3 and Figure 2-2)

Table 2-2. Variations in major element oxide concentration (in wt%) in the profile 2103 across alteration envelope around tension veins, Sigma mine, Quebec

Sample_id	2103-14	2103-13e	2103-13d	2103-13c	2103-13b	2103-13a
Alteration	u	ch-cb-mi	cb-mi	cb-ab	cb-ab	cb-ab
SiO ₂	61.28	59.19	50.04	49.59	40.75	33.79
Al ₂ O ₃	15.66	16.33	11.73	13.04	10.52	9.22
TiO ₂	0.66	0.7	2.23	1.33	1.27	1.62
FeO	5.39	5.16	1.96	2.89	8.63	12.8
MnO	0.14	0.12	0.27	0.18	0.17	0.17
MgO	2.65	2.56	0.66	0.63	0.62	0.59
CaO	5.03	4.65	14.76	13.42	14.52	14.1
Na ₂ O	4.34	4.12	6.56	7.35	5.38	4.6
K ₂ O	0.67	1.57	0.02	0.03	0.02	0.03
P ₂ O ₅	0.23	0.23	0.54	0.49	0.65	0.78
H ₂ O	1.98	2.05	0.13	0	0	0
CO ₂	2.1	2.94	10.43	9.67	10.76	10.63
S	0.12	0.86	0.8	1.81	6.2	10.31
Total	100.25	100.48	100.13	100.43	99.49	98.64
Density	2.74	2.74	2.71	2.74	2.84	2.98

Profile 2103 is in feldspar porphyry.

Alteration facies: U=unaltered rock, CH-CB-MI=carbonate-chlorite-white mica,

CB-MI = carbonate-white mica, CB-AB=carbonate-albite

nd = not detected

Data source: Robert & Brown 1986.

Table 2-3. The calculation results of metasomatic norms (in wt%) in the profile 2103 across alteration envelope around tension veins, Sigma mine, Quebec

Sample_id	2103-14	2103-13e	2103-13d	2103-13c	2103-13b	2103-13a
Alteration	u	ch-cb-mi	cb-mi	cb-ab	cb-ab	cb-ab
Calcite	0.000	0.133	23.118	21.690	22.769	21.749
Epidote	20.367	18.323	0.000	-0.000	-0.000	-0.000
Ca-pyx*	0.000	0.041	2.270	0.249	0.000	0.000
Anorthite	0.000	0.000	0.000	2.489	4.497	4.401
Mg-carb	3.543	5.355	-0.000	0.000	0.000	1.078
Mg-chl	2.637	0.000	0.300	0.000	0.000	0.008
Mg-pyx	0.000	0.000	1.373	1.569	1.544	0.178
Siderite	0.730	1.611	-0.000	0.000	1.621	0.956
Fe-chl	3.524	0.939	-0.000	0.000	0.000	0.007
Fe-pyx	0.000	0.000	0.000	1.583	0.738	0.000
Muscovite	5.667	13.279	0.169	0.000	0.000	0.003
K-feldspar	0.000	0.000	0.000	0.177	0.118	0.175
Na-mica	3.973	1.254	2.775	0.016	0.000	0.003
Albite	33.999	34.003	53.607	62.185	45.526	38.924
Ilmenite	0.000	0.000	2.246	0.000	0.582	1.375
Rutile	0.660	0.700	1.047	1.330	0.963	0.896
Kaolinite	-0.000	0.300	0.198	0.000	0.000	0.009
Quartz	24.126	21.980	9.618	3.856	6.175	4.901
Mn-carb	0.227	0.194	0.438	0.292	0.275	0.275
Apatite	0.543	0.543	1.274	1.156	1.533	1.840
Pyrite	0.225	1.609	1.497	3.387	11.600	19.290
Hemitite	0.000	0.000	0.000	0.000	0.000	0.000
total	100.220	100.265	99.930	99.978	97.943	96.067

* pyx - pyroxene; carb - carbonate; chl - chlorite.

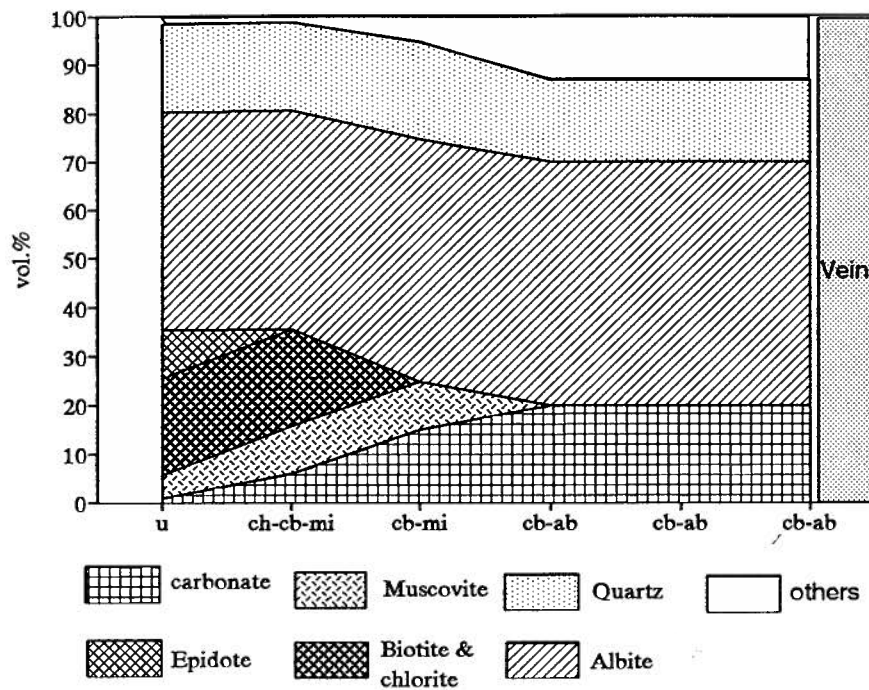


Figure 2-1. A semiquantitative mineral mode profile across the alteration envelope, Sigma mine, Quebec. (After Robert and Brown, 1986)

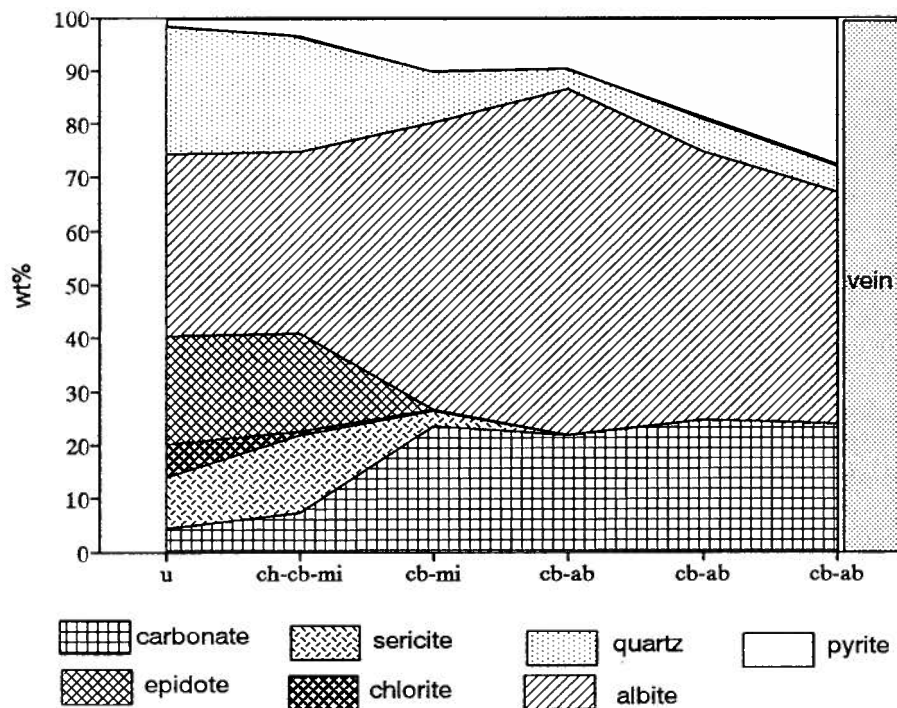


Figure 2-2. A metasomatic norm profile across the alteration envelope, Sigma mine, Quebec.
u = unaltered rock, ch = chlorite, cb = carbonate, mi = white mica, ab = albite

agree qualitatively with the results reported by Robert and Brown (Figure 2-1), but a few quantitative differences arise. One is that the norm profile shows no significant difference between unaltered rock and cryptic alteration zone in contrast to the claim that rocks in the cryptic zone have a marked decrease in epidote (from about 10 % to zero) and carbonate increase (from 1 % to more than 10 %) relative to unaltered rock (Robert and Brown, 1984). Moreover, in all three alteration profiles for which chemical data are published by Robert and Brown (1986) it is clear that the CO₂ content of the cryptic zone is indistinguishable from the CO₂ content of unaltered rock (the contents of CO₂ in unaltered samples versus cryptic altered samples in profile 2103-10, profile 2103-13 and profile 2209-01 are 2.61 versus 2.74, 1.98 versus 2.05 and 0.89 versus 1.08, respectively); this is true for any reasonable level of analytical error.

The second obvious difference between the profiles of published modes and the normative calculations reported here is the existence of abundant pyrite in an inner subzone of visible alteration zone. Even though Robert and Brown (1984) describe the existence of pyrite, they did not estimate its abundance. Up to 10.6 % of S has been measured, equivalent to about 10 wt.% pyrite or other sulfides.

The third difference between the profile of norms and generalized modes is in the estimation of albite abundance. The reported modes indicate no change in the abundance of albite between the unaltered rock and the cryptic alteration zone (about 50 volume % in both) and an obvious increase in the amount of albite in the visible alteration zone (up to 55 %). In contrast, metasomatic norm calculations indicate the presence of about 35 wt.% albite in both the unaltered and cryptic alteration zone, with a marked increase to about 60 wt. % in the outer subzone of the visible alteration zone and a decrease to about 40 % in the inner subzone immediately adjacent to the vein.

The differences noted above emphasize how important quantitative changes can be overlooked where semiquantitative modes are reported. A more objective procedure,

illustrated here by the metasomatic norm calculation, clearly avoids ambiguity in measuring mineralogical changes.

2.6.2. Erickson Gold Mine, Northern British Columbia

The Erickson gold-bearing deposits are quartz veins that cut Mesozoic basalts in the Cassiar area of northern British Columbia (Sketchley and Sinclair, 1991). These veins are surrounded by extensive alteration envelopes (Sketchley and Sinclair, 1987) that can be divided megascopically into 6 distinctive zones (Table 2-4). A semiquantitative cumulative volume percentage of the mode of each mineral is also estimated (Figure 2-3). Quantitative gains and losses during the alteration process have been calculated using Gresens' equation and the assumption that Zr, TiO_2 and Al_2O_3 were immobile (Sketchley and Sinclair, 1987, 1991).

The parent rock at the Erickson mine is noncarbonated basalt that has been regionally metamorphosed to the upper greenschist facies. Sketchley and Sinclair (1991) concluded that the major chemical changes that took place during the development of the carbonate alteration envelope are:

- (i) volatile components increase progressively from unaltered rock toward the vein,
- (ii) K_2O is added throughout an alteration envelope but is most pronounced near the vein,
- (iii) Na_2O is depleted throughout an envelope,
- (iv) SiO_2 is increased throughout an envelope, particularly where a quartz vein is present,
- (v) CaO is depleted in the outer part of an envelope and added to the inner part, and
- (vi) MgO and Fe_2O_3 are depleted throughout an envelope except where quartz veinlets are present (depletion is greater near the vein than in the outer portion of an alteration halo).

They further qualitatively interpreted these variations as follows:

...variations in mineralogy as a function of host-rock composition and losses and gains of components. Minerals noted in the carbonated basalt are ankerite, siderite, quartz, muscovite, kaolinite, titanium oxides, and pyrite. The presence of carbonates, hydrous aluminum silicates, and pyrite implies that the volatile (LOI) include, at least, CO₂, H₂O, and S. An increase in volatile content corresponds to a volume increase.

Table 2-4. Summary of Characteristics of Alteration Zones of Enclosing Gold-Bearing Quartz Veins and the McDame Dolomite Vein, Total Erickson Mine

Zone	Thickness (m)	Occurrence	Color	Mineralogy
B-Noncarbonated basalt		Host	Pale to dark green	pl, chl, act, epi, aug, calc(trace), ti-oxides, \pm py \pm qtz \pm hem \pm mt
2C-outer carbonate	< 1	very common	pale green to buff and pale gray	pl, chl, ank, sid, qtz, ser, ti-oxide, \pm kao \pm dol \pm py \pm carbon \pm calc \pm epi \pm aug \pm act
2B-intermediate carbonate	< 10	very common	buff to pale gray	ank, sid, qtz, ser, ti-oxides \pm kao \pm dol \pm py \pm carbon
2A-inner carbonate	< 4	common	buff to pale gray with minor green mottling	ank, qtz, ser, py, ti-oxides \pm sid \pm carbon \pm arsenopy \pm pl
1B-outer carbon	< 1	uncommon	buff to black	ank, qtz, ser, py, ti-oxides, carbon \pm sid \pm arsenopy
1A-inner carbon	< 3	uncommon	black	ank, qtz, ser, py, ti-oxides, carbon \pm sid \pm arsenopy

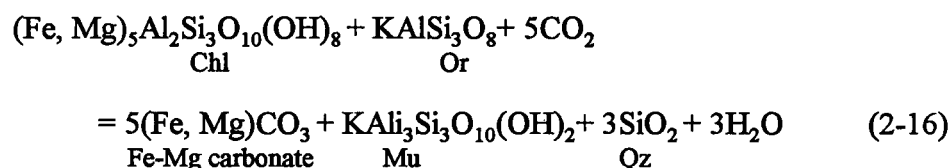
Note: pl-plagioclase, chl-chlorite, act-actinolite, epi-epidote, aug-augite, calc-calcite, py-pyrite, qtz-quartz, hem-hematite, mt-magnetite, ank-ankerite, sid-siderite, ser-sericite, kao-kaolinite, dol-dolomite, arsenopy-arsenopyrite.

Data source: Sketchley and Sinclair (1991)

Even though the chemical data (Sketchley and Sinclair, 1991; listed in Table 2-5) contain LOI rather than measurements of H₂O and CO₂, it is still possible to allot cation to carbonates and hydrous minerals in such a way that the H₂O plus CO₂ comprising LOI can be balanced. Normative calculations of minerals comprising the alteration envelope at Erickson gold mine involve such a partitioning and results are in good agreement with estimated modes (Table 2-6, and compare Figures 2-3 and 2-4). Zone B (unaltered basalt)

has a mineral assemblage consisting of primary minerals such as plagioclase, pyroxene, etc., with a significant amounts of epidote and minor amounts of carbonate, ilmenite and apatite, that is, a greenschist facies assemblage. Zone 2C is characterized by kaolinite and more quartz. Zone 2A is composed of abundant carbonates, sericite, quartz etc.

The distribution pattern of chlorite, the main difference between the normative and modal (petrographic) estimates, may arise due to an underestimation of LOI (particularly CO₂) since there is obvious difference between 100% and the reported analytical total (about 95%). More CO₂ than reported will reduce the abundances of chlorite and K-feldspar and form more carbonate, sericite and quartz according to the following reaction.



This reaction also indicates the importance of accurate measurements of H₂O, CO₂ and S in order to reduce errors that are carried through the calculation of a metasomatic norm. Another possible cause for the difference between the two chlorite profiles may arise from the calculation of sericite abundance. In reality, sericite may not be pure muscovite; instead it may be a non-ideal mixture of, for example, muscovite, paragonite, phlogopite and biotite, etc.

Several pairs of chemical constituents (e.g. Zr, TiO₂, Al₂O₃, total Fe₂O₃) show a linear trend through the origin of a binary plot (Figure 2-5); these pairs of components or elements are incompatible and they are interpreted as having been immobile during the alteration process. Metasomatic normative minerals can be divided by an immobile component/element, such as Zr, to correct for closure (as in the case of PER diagrams) and produce a quantitative model of mineralogical changes during alteration. Figure 2-6 shows the result of such calculation for a 'typical' Erickson alteration profile, by treating the percentage values of components of parent rock as the mass values in grams. It

Table 2-5. Chemical Analyses of Jennie Vein Alteration Profile, Erickson Gold Mine

Sample_id	80-88-JH-	80-88-JH-	80-88-JH-	80-88-JH-	80-88-JH-	80-88-JH-	80-88-JH-	80-88-JH-	80-88-JH-
Alteration	2A	2A	2A	2A	2A	2A	2C	2C	B
(wt %)									
SiO ₂	38.84	38.95	39.55	40.04	41.82	48.19	52.60	46.81	47.90
Al ₂ O ₃	11.40	11.46	12.07	12.06	10.02	15.15	13.43	13.52	14.14
TiO ₂	1.00	1.01	1.02	1.04	0.86	1.40	1.27	1.24	1.32
Fe ₂ O ₃	8.69	8.46	8.93	8.97	8.97	10.61	10.38	10.87	11.33
MnO	0.15	0.15	0.15	0.15	0.18	0.16	0.19	0.17	0.16
MgO	5.87	5.83	5.60	5.61	5.98	5.58	5.83	7.14	7.31
CaO	11.21	11.21	10.40	10.14	10.43	6.23	4.36	11.19	10.40
Na ₂ O	0.30	0.28	0.28	0.29	0.10	0.01	0.01	1.40	2.11
K ₂ O	2.78	2.81	3.12	3.20	2.25	0.17	0.58	0.13	0.11
P ₂ O ₅	0.12	0.11	0.07	0.07	0.07	0.10	0.10	0.10	0.10
LOI	17.28	17.28	15.22	15.22	13.70	7.60	7.44	4.14	2.96
Total	96.77	96.70	95.52	95.89	93.48	94.14	95.15	95.62	96.70
Zr ppm	73.89	73.02	70.75	71.65	64.92	88.68	81.41	83.06	87.58

Data Source: Sketchley, D.A. and Sinclair, A. J. 1991, Econ. Geol. vol. 86, pp. 570-587

Table 2-6. Metasomatic Norms of Jennie Vein Alteration Profile, Erickson Gold Mine

Sample_id	80-88-JH-	80-88-JH-	80-88-JH-	80-88-JH-	80-88-JH-	80-88-JH-	80-88-JH-	80-88-JH-	80-88-JH-
Alteration	2A	2A	2A	2A	2A	2A	2C	2C	B
Carbonate	34.48	34.47	28.73	27.37	23.03	3.40	4.03	5.59	3.44
Epidote	0.00	0.00	0.00	0.00	0.00	18.69	8.74	22.40	18.68
Sericite	21.03	21.63	19.12	18.94	12.42	0.78	4.91	18.37	17.00
Kaolinite	0.00	0.00	0.00	0.00	0.07	15.81	12.09	0.10	0.00
Chlorite	13.49	12.99	18.72	19.81	25.52	27.52	29.78	0.22	0.00
Pyroxene	0.00	0.00	0.00	0.00	0.00	0.00	0.23	31.77	35.87
K-feldspar	4.32	3.91	7.50	8.18	5.48	0.50	0.00	0.00	0.00
Plagioclase	0.00	0.00	0.00	0.00	0.00	0.05	0.09	3.77	12.51
Pyrite	0.00	0.00	0.00	0.00	0.00	0.00	0.00	0.00	0.00
Quartz	22.08	22.35	20.14	20.39	25.17	25.09	32.63	10.81	6.46
others	1.37	1.36	1.31	1.21	1.80	2.30	2.65	2.59	2.74
Total	96.77	96.70	95.52	95.89	93.48	94.14	95.15	95.62	96.70

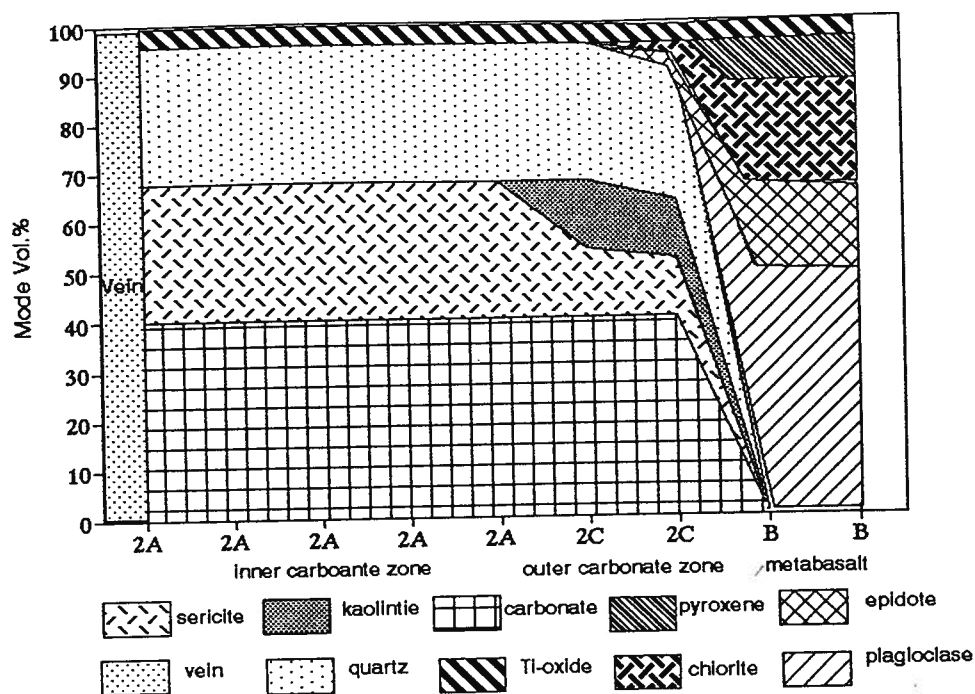


Figure 2-3 Generalized distribution of mineral species throughout carbonate alteration envelopes enclosing gold-bearing veins, white quartz veins and carbon veins. Simplified from Sketchley and Sinclair (1991)

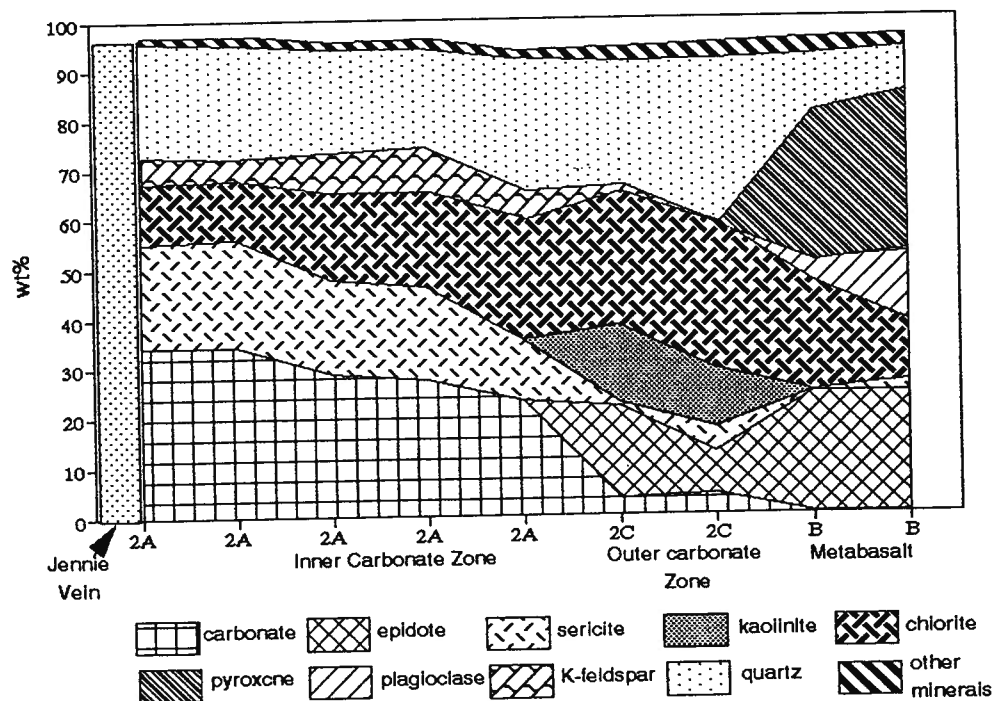


Figure 2-4. Metasomatic norms profile Jennie vein, Erickson gold mine, northern British Columbia

Table 2-7a. Metasomatic norms corrected for closure and absolute losses and gains of components from profile 80-88-JH across the Jennie vein, Erickson mine, northern British Columbia

Sample_id	80-88-JH-1	80-88-JH-1a	80-88-JH-2	80-88-JH-2a	80-88-JH-3	80-88-JH-4	80-88-JH-5	80-88-JH-6	80-88-JH-7
Alteration	2A	2A	2A	2A	2A	2C	2C	B	B
mole									
Calcite	0.234	0.237	0.228	0.219	0.249	0.031	0.040	-0.000	0.000
Mg-carb	0.029	0.033	0.000	0.061	0.034	0.000	0.000	0.000	0.000
Fe-carb	0.128	0.126	0.108	0.052	0.025	0.000	0.000	0.000	0.000
Mn-carb	0.003	0.003	0.003	0.003	0.003	0.002	0.003	0.003	0.002
Mg-chl	0.029	0.028	0.034	0.022	0.033	0.027	0.031	0.037	0.022
Fe-chl	0.000	0.000	0.006	0.017	0.022	0.017	0.021	0.009	0.004
Muscovite	0.052	0.055	0.049	0.047	0.038	0.002	0.013	0.000	0.000
Na-mica	0.011	0.011	0.011	0.011	0.004	0.000	0.000	0.001	0.007
Kaolinite	0.000	0.000	-0.000	0.000	0.000	0.061	0.050	0.000	0.000
quartz	0.435	0.446	0.415	0.415	0.565	0.412	0.584	0.225	0.127
Epidote	0.000	0.000	-0.000	0.000	0.000	0.038	0.019	0.053	0.050
K-spar	0.018	0.017	0.033	0.036	0.027	0.002	0.000	0.003	0.002
Anorthite	0.000	0.000	0.000	0.000	0.000	0.000	0.000	0.014	0.020
Albite	0.000	-0.000	0.000	0.000	0.000	0.000	0.000	0.047	0.061
Ca-pyx	0.000	0.000	0.000	0.000	0.000	0.000	0.001	0.044	0.031
Mg-pyx	0.000	-0.000	0.000	0.000	0.000	0.000	0.000	0.000	0.035
Fe-pyx	0.000	0.000	0.000	0.000	0.000	0.000	0.000	0.015	0.028
ilmenite	0.001	0.001	0.002	0.000	0.015	0.009	0.017	0.016	0.017
rutile	0.013	0.014	0.014	0.016	0.000	0.008	0.000	0.000	0.000
apatite	0.001	0.001	0.000	0.000	0.000	0.000	0.001	0.000	0.000
total	0.954	0.970	0.902	0.900	1.016	0.610	0.781	0.468	0.408
dSiO ₂ *	0.031	0.020	-0.018	-0.017	-0.142	0.005	-0.145	-0.024	0.000
dAl+3	0.012	0.008	-0.016	-0.012	0.012	-0.016	-0.006	-0.002	0.000
dTi+4	0.002	0.001	0.001	0.001	0.002	-0.001	-0.001	0.000	0.000
dFe+2	0.013	0.015	0.003	0.005	-0.010	0.011	0.002	-0.002	0.000
dMn+2	-0.000	-0.000	-0.000	-0.000	-0.001	0.000	-0.001	-0.000	0.000
dMg+2	0.009	0.008	0.009	0.011	-0.019	0.045	0.026	-0.005	0.000
dCa+2	-0.051	-0.054	-0.044	-0.036	-0.065	0.076	0.102	-0.025	0.000
dNa+	0.057	0.057	0.057	0.057	0.064	0.068	0.068	0.020	0.000
dK+	-0.068	-0.069	-0.080	-0.081	-0.062	-0.001	-0.011	-0.001	0.000
dP+5	-0.001	-0.000	0.000	0.000	0.000	0.000	-0.000	-0.000	0.000
Sum O=	-0.015	-0.025	-0.065	-0.048	-0.072	0.139	0.147	-0.026	0.000
dH ₂ O	-0.042	-0.041	-0.084	-0.077	-0.129	-0.182	-0.194	-0.076	0.000
dCO ₂	-0.390	-0.396	-0.336	-0.333	-0.309	-0.031	-0.041	-0.000	0.000
dS	0.000	0.000	0.000	0.000	0.000	0.000	0.000	0.000	0.000
dTotal	-0.444	-0.477	-0.571	-0.531	-0.731	0.111	-0.054	-0.141	0.000
dH ₂ O'	-0.026	-0.017	-0.019	-0.029	-0.057	-0.321	-0.341	-0.051	0.000
dCO ₂ '	-0.360	-0.347	-0.206	-0.237	-0.166	-0.308	-0.334	0.000	0.000
dOH-	0.000	0.000	0.000	0.000	0.000	0.000	0.000	-0.051	0.000
dCO ₃ =	0.000	0.000	0.000	0.000	0.000	0.000	0.000	0.000	0.000
dHCO ₃ -	-0.030	-0.049	-0.129	-0.096	-0.143	0.277	0.294	-0.000	0.000

* prefix d stands for the absolute difference of corresponding constituent between the least altered and altered rocks

Table 2-7b. Metasomatic norms corrected for closure and absolute losses and gains of components from profile 80-88-JH across the Jennie vein, Erickson mine, northern British Columbia

Sample_id	80-88-JH-1	80-88-JH-1a	80-88-JH-2	80-88-JH-2a	80-88-JH-3	80-88-JH-4	80-88-JH-5	80-88-JH-6	80-88-JH-7
Alteration	2A	2A	2A	2A	2A	2C	2C	B	B
gram									
Calcite	23.38	23.69	22.77	21.92	24.89	3.10	4.01	-0.00	0.00
Mg-carb	2.43	2.81	0.00	5.16	2.91	0.00	0.00	0.00	0.00
Fe-carb	14.78	14.56	12.49	6.08	2.87	0.00	0.00	0.00	0.00
Mn-carb	0.29	0.29	0.30	0.30	0.39	0.26	0.33	0.29	0.26
Mg-chl	15.99	15.58	19.12	12.10	18.41	15.20	17.29	20.76	12.31
Fe-chl	0.00	0.00	4.06	12.10	16.01	11.98	14.74	6.26	2.76
Muscovite	20.54	21.80	19.39	18.78	15.09	0.71	5.28	0.00	0.00
Na-mica	4.39	4.14	4.27	4.37	1.66	0.06	0.00	0.38	2.54
Kaolinite	0.00	0.00	-0.00	0.00	0.09	15.62	13.01	0.11	0.10
quartz	26.17	26.81	24.93	24.92	33.95	24.78	35.11	13.52	7.62
Epidote	0.00	0.00	-0.00	0.00	0.00	18.45	9.40	25.48	24.16
K-spar	5.13	4.69	9.28	10.00	7.39	0.49	0.00	0.81	0.65
Anorthite	0.00	0.00	0.00	0.00	0.00	0.01	0.01	3.98	5.68
Albite	0.00	-0.00	0.00	0.00	0.00	0.04	0.09	12.23	16.12
Ca-pyx	0.00	0.00	0.00	0.00	0.00	0.00	0.25	10.24	7.28
Mg-pyx	0.00	-0.00	0.00	0.00	0.00	0.00	0.00	0.00	7.09
Fe-pyx	0.00	0.00	0.00	0.00	0.00	0.00	0.00	4.04	7.40
ilmenite	0.22	0.22	0.33	0.00	2.20	1.38	2.59	2.48	2.51
rutile	1.07	1.10	1.09	1.27	0.00	0.66	0.00	0.00	0.00
apatite	0.34	0.31	0.20	0.20	0.22	0.23	0.25	0.25	0.24
total	114.70	115.98	118.24	117.21	126.11	92.97	102.36	100.82	96.71
dSiO2*	1.86	1.18	-1.06	-1.04	-8.52	0.31	-8.69	-1.46	0.00
dAl+3	0.33	0.21	-0.42	-0.32	0.33	-0.44	-0.16	-0.06	0.00
dTi+4	0.08	0.07	0.03	0.03	0.10	-0.04	-0.03	0.01	0.00
dFe+2	0.72	0.83	0.19	0.26	-0.54	0.60	0.11	-0.09	0.00
dMn+2	-0.01	-0.02	-0.02	-0.02	-0.06	0.00	-0.03	-0.01	0.00
dMg+2	0.21	0.19	0.23	0.27	-0.46	1.09	0.63	-0.13	0.00
dCa+2	-2.06	-2.18	-1.77	-1.43	-2.62	3.04	4.08	-1.00	0.00
dNa+	1.30	1.32	1.31	1.30	1.47	1.56	1.56	0.47	0.00
dK+	-2.64	-2.71	-3.11	-3.16	-2.43	-0.05	-0.43	-0.02	0.00
dP+5	-0.02	-0.01	0.01	0.01	0.00	0.00	-0.00	-0.00	0.00
dH2O	-0.75	-0.74	-1.51	-1.39	-2.32	-3.28	-3.50	-1.37	0.00
dCO2	-17.17	-17.42	-14.77	-14.66	-13.60	-1.36	-1.79	-0.01	0.00
dS	0.00	0.00	0.00	0.00	0.00	0.00	0.00	0.00	0.00
dTotal	-18.39	-19.68	-21.93	-20.91	-29.81	3.64	-5.90	-4.10	0.00
Residual	-0.40	-0.40	-0.40	-0.40	-0.40	-0.09	-0.24	0.02	0.00
dH2O'	-0.48	-0.30	-0.34	-0.52	-1.03	-5.77	-6.14	-0.91	0.00
dCO2'	-15.83	-15.25	-9.08	-10.42	-7.29	-13.56	-14.72	0.00	0.00
dOH-	0.00	0.00	0.00	0.00	0.00	0.00	0.00	-0.87	0.00
dCO3=	0.00	0.00	0.00	0.00	0.00	0.00	0.00	0.00	0.00
dHCO3-	-1.86	-3.01	-7.90	-5.87	-8.75	16.91	17.93	-0.02	0.00

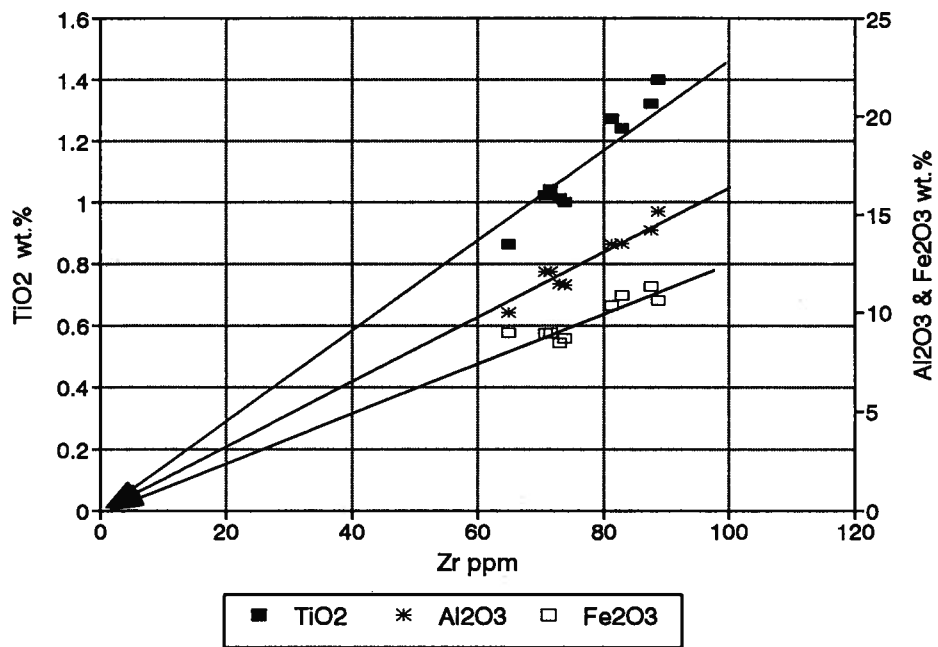


Figure 2-5. Immobility components scatter plot, Erickson gold mine, northern British Columbia

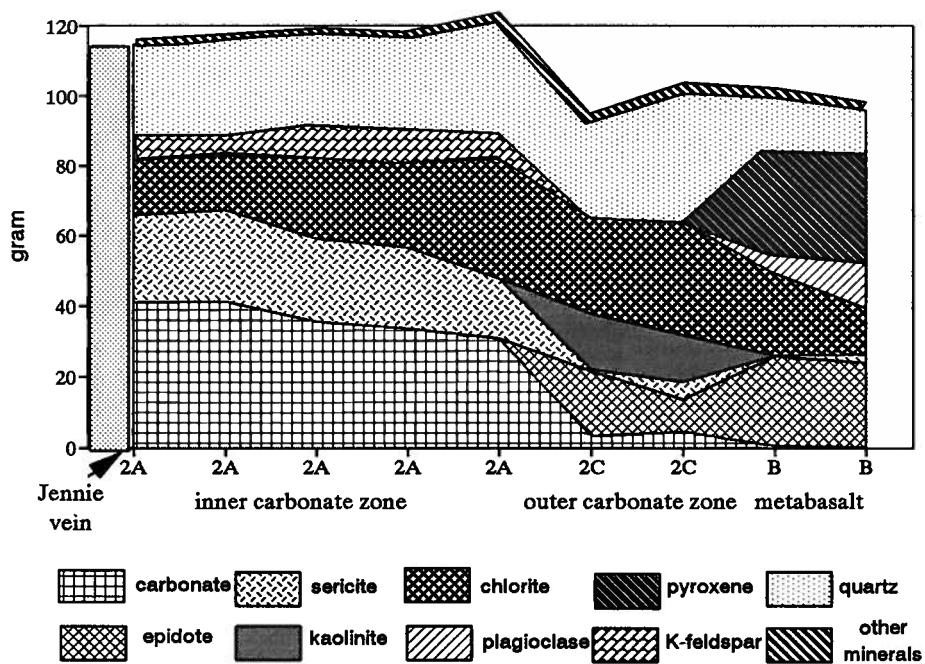
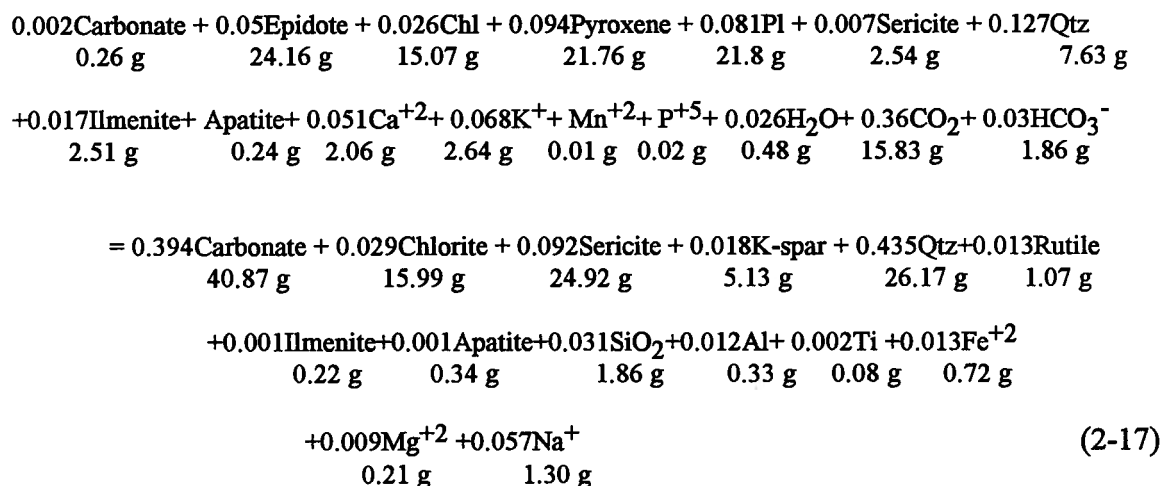


Figure 2-6. Metasomatic norm profile after closure effect removed, Erickson gold mine, northern British Columbia

provides a clear and quantitative appreciation of mineralogical differences between parent and daughter rock.

The metasomatic norms corrected for closure can be integrated with the results of the absolute loss or gain of each chemical component to illustrate the total chemico/mineralogic effect of the hydrothermal alteration process in equation form (Table 2-7a and 2-7b). For example, the hydrothermal alteration of parent rock (sample 80-88-JH-7) to altered rock (sample 80-88-JH-1) at Erickson gold mine can be illustrated in a simplified balanced equation as follows:



This equation explicitly indicates which minerals are destroyed, which minerals are formed and which components are gained and lost during the hydrothermal alteration process.

2.7. Conclusions

A metasomatic norm, particularly if constrained to approximate a mode, provides a useful tool to quantify the combined mineralogical and lithogeochemical changes affected during wallrock alteration associated with hydrothermal mineral deposits. Advantages of both mineralogical and lithogeochemical approaches to the study of such systems are inherent in the procedure. Where modes can be approximated by norms the normative procedure generally will provide results more efficiently and more optimally because of

the better representative of samples collected for lithogeochemical analysis relative to those generally used for modal analysis. Moreover, lithogeochemical analytical data generally are more objective and reproducible than are modal data.

In summary, metasomatic norms:

- (i) lead to high quality estimates of mineral abundances, and thus, provide accurate mineral distribution profiles across alteration envelopes,
- (ii) provide an objective and quantitative basis for a mineralogical classification of hydrothermally altered rock,
- (iii) give an interpretation of lithogeochemical variations in terms of mineralogical variations which are more compatible with field observations than are interpretations quantifying lithogeochemical losses and gains only,
- (iv) with the recognition of an immobile component, can be recast into the absolute masses (not percentages) of minerals relative to a specified amount of the parent rock (e.g. about 100 grams), and
- (v) can be combined with the results of calculated absolute losses and gains of lithogeochemical constituents to form comprehensive mass balanced equations (model) for a hydrothermal alteration system no matter whether it is closed or open, or in equilibrium or disequilibrium.

3.1. Introduction

In a quantitative evaluation of hydrothermal alteration, it is essential to know the quality of data so that conclusions can be derived with confidence. Thus, it is important to understand all sources of lithogeochemical variations and know how to separate the variation(s) generated by geological process(es) of interest from those generated artificially. The major causes for the variations of lithogeochemical data are listed in Table 3.1.

Table 3.1. The classification of variations of lithogeochemical data generated by different processes

Primary causes	Secondary causes	Artificial causes
Fractionation	metamorphism	sampling and sample preparation
Mixing	hydrothermal alteration	analytical measurement
Assimilation	weathering	closure effect

Ideally, variations generated by artificial processes should be eliminated. In practice, they can only be minimized through quality control, such as the estimation of the optimum sample size and the necessary fineness of the ground particle size. These variations should be evaluated by quality assessment in terms of precision, accuracy and detection limit. Among the artificial causes, closure effect has already been discussed in the foregoing chapter. Consequently, this chapter focuses on:

- (i) strategies of field sampling and sample preparation (i.e., estimation of an optimal sample size and the fineness of grain size of prepared subsample);
- (ii) determination of precision and detection limit by using a small set of duplicates, and
- (iii) the propagation of error through data evaluation procedures.

3.2. Strategies of sampling and sample preparation

Variation caused by improper strategies of sampling and sample preparation has been discussed thoroughly among analysts (Shaw, 1961; Wickman, 1962; Wilson, 1964; Kleeman, 1967; Maxwell, 1968; Ondrick and Suhr, 1969; Ingamells and Switzer, 1973; Ingamells, 1974a, 1974b, 1981; Potts, 1987) who generally agree that the error caused by sampling and sample preparation may be so large that the meaning of lithogeochemical data can be seriously distorted or obscured. The object of lithogeochemical sampling and sample preparation is to use a small amount of sample or subsample to represent a much larger geological entity. However, silicate rocks, with few exceptions, contain two or more mineral species with various grain sizes; rock powders prepared from them are heterogeneous to some extent. Consequently, it is possible that artificial variations which could significantly obscure lithogeochemical variations could arise from improper procedures of sampling and sample preparation.

The concepts of homogeneity and heterogeneity of certain elements in a sample or subsample are relative and depend on the following factors:

- (i) sample size,
- (ii) grain size of the mineral(s) containing the element of interest, and
- (iii) abundance(s) of the mineral(s) containing the element of interest.

With the variation of one of these three factors the homogeneity or heterogeneity of the element of interest in different samples can change correspondingly. From the perspective of sampling and sample preparation, the abundance of the mineral(s) containing the element of interest is an objective constant or nearly so. However, the sample size is adjustable at the sampling stage and the particle sizes of subsamples are definable at the stage of sample preparation to make the sample or subsample more representative.

Heterogeneity between the samples from the same site or subsamples from the same sample could be reduced to a minimum degree if the size (mass) of sample is large enough or the particle size of a subsample is fine enough. In general, the coarser the grain size of a

rock, the larger the sample size needed to be representative. The smaller the size (mass) of a subsample, the finer the sample must be ground in order to obtain the subsample. Regardless of the approaches of increasing the sample mass or grinding to a finer particle size prior to subsampling, the effects are the same (i.e., increasing the number of grains or particle (n) of the sample or subsample).

To estimate the optimum mass for a sample or the necessary fineness of the particle size for subsampling, the concept of a 'two-mineral mixture of uniform grain size' is helpful (e.g., Wilson, 1964; Kleeman, 1967; Ingamells and Switzer, 1973; Ingamells, 1974a, 1974b; 1981). This concept can be described through the following simplifications:

- (i) a hypothetical mixture contains only two minerals, one is rich in the element of interest and the other is poor in the element of interest;
- (ii) all the particles in a sample are of uniform volume;
- (iii) each particle consists of one mineral species only; and
- (iv) the chemical composition of each mineral species has uniform composition throughout the bulk specimen.

In reality, a sample or subsample may consist of more than two minerals and the distribution of the element of interest can be more complicated than in the simplified system above. However, the main concerns here are:

- (i) whether the element of interest is homogeneously distributed in the sample or subsample, and
- (ii) to what extent the homogeneity of the sample or subsample can be achieved.

The distribution of the element of interest in a natural and complicated system is generally more homogeneous than in a simplified 'two-mineral mixture of uniform size' system. For example, to analyze a rock consisting of quartz, K-feldspar and plagioclase as phenocrysts by using 'two-mineral mixture of uniform size' model, plagioclase will be treated as the only mineral phase containing sodium and calcium, K-feldspar as the only mineral having potassium and quartz phenocryst as the main contributor to the

heterogeneity of SiO_2 . As we know, plagioclase also can contain a minor amount of potassium, K-feldspar, similarly, can contain small amount of sodium and calcium too. Both feldspars contain significant amounts of silica. Therefore, the homogeneity of various elements as described in the simplified system is adequate in place of the more complicated real system. In brief, the simplified system is adequate for our discussion; use of real, more complicated systems may be more complicated than necessary in most cases and too complicated to deal with practically, in other cases.

With regard to the simplification of uniform grain size, the mineral rich in the element of interest contributes to both the total concentration of the element of interest and the error in determining concentration. Therefore, the grain size of the mineral rich in the element of interest is usually used as the reference of uniform grain size. The rest of the grains containing a low content of the element of interest are treated as the matrix. In reality, the grain or particle size of a sample or subsample is not commonly uniform. The assumption of a uniform grain size is acceptable if we either: (i) imagine that a coarse grain of mineral containing a negligible content of the element of interest is the equivalent of a number of grains as fine as the mineral enriched in the element of interest, or (ii) treat a few finer grains of minerals containing a negligible content of the element of interest as the equivalent of a coarser grain of the mineral enriched in the element of interest. In brief, the concept of uniform grain size always uses the grain size of the mineral rich in the element of interest as the reference.

With the above simplifications, a binomial distribution function can be used to simulate the distribution of major and trace elements during sampling and subsampling processes because:

- (i) each sample or subsample consists of n identical grains;
- (ii) each grain results in one of two outcomes, the grain is rich in the element of interest or it is poor in the element of interest;

- (iii) the probability of getting a grain rich in the element of interest on a single trial is equal to p and remains the same from grain to grain, and the probability of getting a grain poor in the element of interest is equal to $q = (1 - p)$;
- (iv) the grains are independent;
- (v) the random variable of interest is x , the number of the grains rich in the element of interest among the n grains.

For a binomial distribution we have

$$P(x) = \frac{n!}{x!(n-x)!} p^x q^{n-x} \quad (3-1)$$

where n is the total number of equant grains; x is the number of equant grains rich in the element of interest; p is the volume percentage of the grain rich in the element of interest; $(1-p)$ is the volume percentage of the grains with negligible concentration of the element of interest. Thus, the expectation (μ) of the binomial distribution is

$$\mu = np \quad (3-2)$$

and its variance (σ^2) is

$$\sigma^2 = np(1-p) = npq \quad (3-3)$$

and its coefficient of variation (R_g) is

$$R_g = \frac{\sigma}{\mu} = \frac{\sqrt{npq}}{np} = \sqrt{\frac{q}{np}} \quad (3-4)$$

Equation (3-4) given by Kleeman (1967) illustrates the relationship between the number of grains (n) of the sample or subsample and the coefficient of variation of the grain distribution (R_g) generated by sampling or stages of sample preparation. Engels and Ingamells (1970) improved Kleeman's equation through converting the coefficient of variation (R_g) generated by sampling the non-representative grain distributions to the coefficient of variation generated by lithogeochemical inhomogeneity (R_E). The reason for doing this is to take into account the minor contribution of the grains which are poor in the element of interest to the total concentration in the sample of the element of interest.

$$p_w + q_w = 1 \quad (3-5)$$

where p_w and q_w are the weight fractions of the minerals rich and poor in the element of interest, respectively. The relationship between the volume proportions and the weight proportions of the two minerals in the mixture is:

$$\frac{q}{p} = \frac{q_w d_H}{p_w d_L} \quad (3-6)$$

where d_H and d_L are the densities of the minerals rich and poor in the element of interest respectively.

$$E = Hp_w + Lq_w \quad (3-7)$$

where E represents the concentration of the element of interest in sample; H is the concentration of the element of interest in the grain population with p_w fraction; L is the concentration of the element of interest in the grain population with q_w fraction. From Kleeman's equation

$$R_H = \sqrt{\frac{q}{np}} \quad (3-8)$$

$$R_L = \sqrt{\frac{p}{nq}} \quad (3-9)$$

where R_H is the relative error due to sampling the mineral rich in the element of interest; R_L is the relative error due to sampling the mineral poor in the element of interest.

The total sampling error, ER_E is not a statistical addition of the two components LR_L and HR_H because these are not independent: as p increases, q decreases and E approaches H . The exact relation is:

$$(ER_E)^2 = (p_w HR_H - q_w LR_L)^2 \quad (3-10)$$

The physical implication of equation (3-10) is that the distribution of the element of interest will become more and more homogeneous if the contributions from both populations of grains to the total concentration of the element of interest become closer and closer to each other; thus the error from sampling and sample preparation will become

less and less significant. Furthermore, substitution of equation (3-6) in (3-8) and (3-9), and then substituting (3-8) and (3-9) in (3-10), gives

$$R_E = \sqrt{\frac{p_w q_w}{n d_H d_L}} \times \frac{H d_H - L d_L}{E} \quad (3-11)$$

Next, the relationship between the weight of the sample or subsample (w) and the coefficient of variation is derived as follows:

$$n = \frac{w p_w}{d_H v} + \frac{w q_w}{d_L v} = \frac{w (p_w d_L + q_w d_H)}{d_H d_L v} \quad (3-12)$$

where v is the grain or particle volume in cubic millimeters; w is the weight in gram of a sample or a subsample. Substitution of equation (3-12) and (3-7) in equation (3-11) gives:

$$w = \frac{p_w q_w v}{R_E^2 (p_w d_L + q_w d_H)} \times \frac{(H d_H - L d_L)^2}{(H p_w + L q_w)^2} \quad (3-13)$$

Rearranging equation (3-13) gives:

$$v = \frac{w R_E^2 (p_w d_L + q_w d_H)}{p_w q_w} \times \frac{(H p_w + L q_w)^2}{(H d_H - L d_L)^2} \quad (3-14)$$

In equations (3-13) and (3-14) the value of R_E can be predefined; the values of H , L , d_H and d_L are known when the 'two minerals' are determined, the values of p_w and q_w can be reasonably estimated by examining the hand specimen. Consequently, equation (3-13) can be used to calculate the optimum weight of the sample after the value of v is estimated through examining the grain size of the mineral containing the element of interest. For the purpose of determining the necessary fineness of the subsample, equation (3-14) can be used after the subsample weight has been defined by the analytical measuring technique. Applications of equation 3-13 and 3-14 to Silver Queen lithogeochemical data are described in Chapter 6. It is helpful to understand the significances of equation 3-13 and 3-14 by following the calculation of a realistic example.

3.3. Quality assessment of analytical measurements based on a small set of duplicates

The discussion in the foregoing section has been aimed at the improvement in quality of lithogeochemical data at the stages of sampling and sample preparation. Next, it is important to focus on the quality assessment of lithogeochemical data at the stage of analytical measurement. A similar concept, quality control, has been commonly used by chemical analysts. However, the quality of lithogeochemical data in terms of analytical precision is not in all cases under the control of the geologist, but the quality of lithogeochemical data can be assessed through the examination of different types of duplicates.

All analytical measurements are subject to error. There are two types of errors:

- (1) random errors arising from the variations inherent to any sampling or measurement process, and
- (2) non-random errors causing systematic negative or positive deviations from the true result. Bias can be recognized through repeated measurement of standards and is not considered here.

Errors are assessed in terms of either precision or accuracy. Precision is a measure of analytical repeatability. A precise analysis is one where a set of replicate analyses forms a tight cluster around the average. The degree of precision is normally measured by the standard deviation of the analyses or by the relative error (coefficient of variation). Accuracy is a measure of how close the analyzed data lie to the 'true' composition of the sample. One of the difficulties in silicate rock analysis is that the true composition, even in reference material, is in some cases poorly known (Potts, 1987). From a practical viewpoint adequate accuracy can be considered to have been achieved where different analytical methods give essentially identical results (Fletcher, 1981). Further discussion on this issue is beyond the scope of this thesis. Of practical concern is the issue of how to determine the precision by using a small set of duplicate analyses.

Thompson and Howarth (1976, 1978) demonstrate that errors in analytical determinations can vary significantly and systematically over a wide range of concentrations. Therefore, a single value of standard deviation calculated from a set of duplicates of one sample cannot properly describe the analytical precision of a particular set of geochemical data over a wide range of concentrations. Instead, quantification of the systematic relation of error to concentration is desirable. This approach leads to realistic error estimates in contrast to the usual assumption of either a constant absolute error (by using the standard deviation), or a constant relative error (by using the coefficient of variation). Thompson and Howarth (1976, 1978) approximate the variation of error as a standard deviation (S_c) as a linear function of the concentration (C):

$$S_c = S_o + kC \quad (3-15)$$

The parameters S_o (intercept) and k (slope) can be used to quantify the precision (P_c) at the 95% confidence level and at concentration C , by means of:

$$P_c = 2S_c/C \quad (3-16)$$

Substitution for S_c in equation (4-16) gives:

$$P_c = (2S_o/C + 2k) \quad (3-17)$$

In addition, the practical detection limit C_d (when $P_c = 1.0$) can also be estimated from equation (3-17) as follows:

$$C_d = 2S_o / (1-2k) \quad (3-18)$$

Equation (3-18) indicates that the detection limit C_d is proportional to S_o and k , but the value of k should not be equal to or larger than 0.5, otherwise the detection limit C will be infinite or negative and meaningless in the present context.

To calculate the precision (P_c) of a particular component in a sample at a specific concentration (C), it is necessary to know the values of S_o and k . There are two procedures utilizing duplicate analyses to estimate these values (Thompson and Howarth, 1976, 1978). Procedure 1 needs 50 or more duplicates which cover the whole range of concentration of interest in a relatively uniform pattern. These duplicates are further

divided into five or more groups (concentration ranges) with equal number of duplicates in each group; this is done easily with a data set ordered using average concentrations of pairs $[(X_1+X_2)/2]$. The mean of the concentration $[(X_1+X_2)/2]$ and the median of the difference $(|X_1-X_2|)$ for each group is then calculated. A linear regression of these values of $[(X_1+X_2)/2]$ and $(|X_1-X_2|)$ for each group is calculated or obtained graphically. The regression parameters (intercept and slope) are multiplied by a coefficient (e.g. 1.048 at 50th percentile because median values rather than mean values as the y-coordinate) to give S_o (intercept) and k (slope) of the error model (cf. Fletcher, 1981).

Procedure 2 requires only 10 to 50 duplicates. This is normally the range of lithogeochemical duplicates for a study of hydrothermally altered rocks. Therefore, a detailed discussion will be given herewith. The basic idea of this procedure is to test the available duplicate data against an empirical standard of precision to see whether the analytical duplicates can be accepted at a specific precision. The empirical equations given by Thompson and Howarth, (1976, 1978) are listed below:

$$d_{90} = 2.326(S_o + kC) \quad (3-19)$$

$$d_{99} = 3.643(S_o + kC) \quad (3-20)$$

The equations above are derived from equation (3-15) and the specific constants (2.326 and 3.643) represent specific percentiles of a one-sided normal distribution (i.e. d_{99} and d_{90} represent the 99th and 90th percentiles respectively of the absolute difference $|X_1-X_2|$ between pairs of duplicate analyses (X_1, X_2)). These absolute difference are estimators of the standard deviation (S_o) at composition C where $C = (X_1+X_2)/2$. Consider an example to illustrate this procedure. Figure 3-1 is constructed with $(X_1+X_2)/2$ as x-axis and $|X_1-X_2|$ as y-axis; eighteen pairs of Al_2O_3 duplicate data are plotted. Then assuming $S_o = 0$, two percentile lines (90th 99th respectively) are drawn on this diagram according to equation 3-17 to test whether the precision of Al_2O_3 in this set of lithogeochemical data is better than 2 % ($P_c = 0.02$). If the duplicate analytical data comply with the specification, on average 90% of the points will fall below the A_{90} line and 99 % of the points below the

A₉₉ line. If in Figure 3-1A, the precision is worse than that tested, then the value of k should be raised, a poorer precision will result. In this example, a satisfactory result is achieved by raising the value of precision to 4.2%. As a result, around 90% of the plotted points fall below the 90th percentile line and 99 % of the plotted points below the 99th percentile line in Figure 3-1B.

For general geochemical purposes a control chart (for 10% precision, i.e. with percentile lines drawn for the specification $S_c=0.05C$ on logarithmic axes) devised by Thompson and Howarth (1976,1978) has been widely used. Difficulties in the use of this control chart arise where the concentrations of some duplicates are close to the detection limit, that is, where the precision is near 100%. For example, an alteration profile cross-cutting a propylitic alteration halo and a sericitic/argillic alteration envelope are usually characterized by a high concentration of Na_2O in propylitically altered rock, but an almost complete depletion of Na_2O occurs within the sericitic/argillic alteration envelope. Using the control chart, above, the precision of Na_2O measurement tends to be largely overestimated because only the k value of the linear equations 3-19 and 3-20 is adjustable to meet the plotting requirements imposed by the 99th and 90th percentile lines (i.e. there is no point above the 99th percentile line and there are less than or equal to 10% of points above the 90th percentile line). There is an obvious discrepancy between the calculated precision and the deviation represented by the duplicates of high concentration (Figure 3-2A). The cause of this problem is that the detection limit has not been taken into account. This problem may not appear where all duplicates have concentrations far removed from the detection limit.

There is a substantial disparity between procedure 1 and 2. Procedure 1 defines error as a linear function of concentration, procedure 2 assumes a constant relative error. It seems that procedure 2 might be improved for some situations involving fewer than 50 pairs of duplicates, where data are sufficiently precise that both S_0 and k can be estimated, even if not as rigorously as in procedure 1.

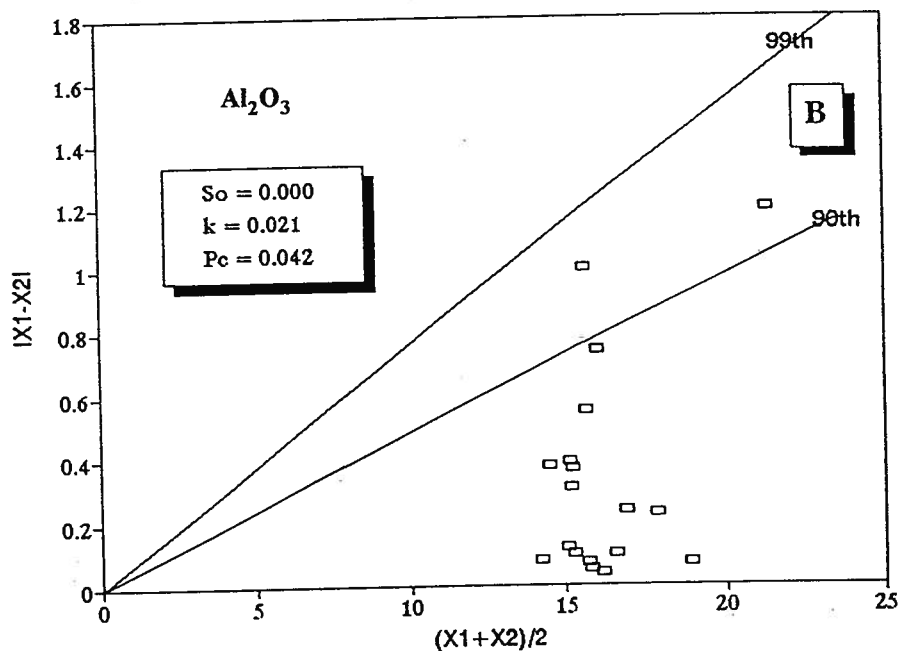
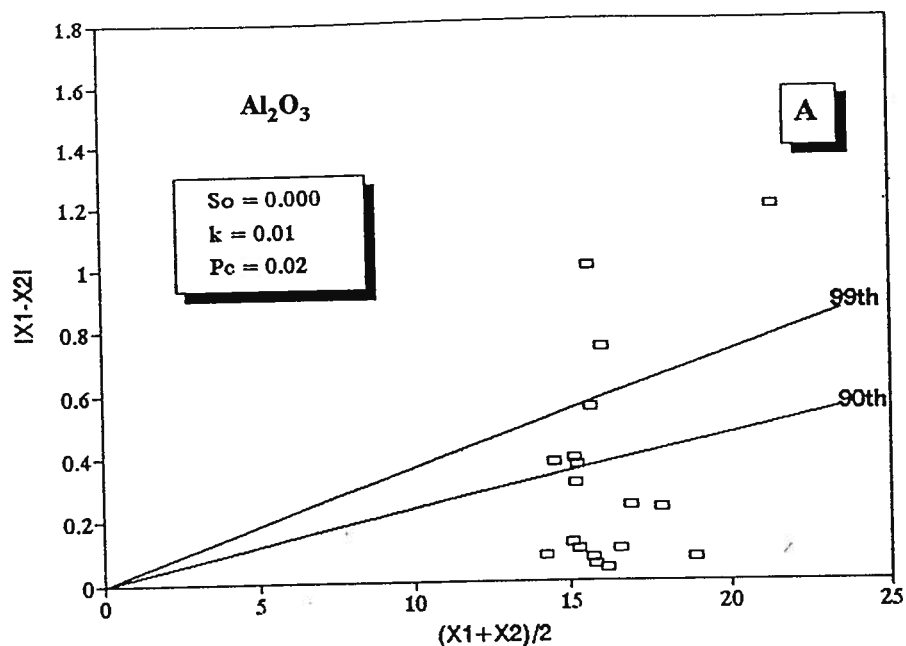


Figure 3-1. Schematic illustration of Thompson and Howarth's procedure 2 (see text) for the precision estimation of a set of lithogeochemical data. (A) The duplicate data do not comply with the 2% error test percentile lines. There are more than 10% and 1% of plots fall above the 90th and 99th percentile lines respectively. This means that the precision of Al_2O_3 in this set of data is higher than 2%. (B) After raising the precision to 4.2%, only 2 out of 18 duplicates plot between the 90th and 99th percentiles. Therefore, this precision is acceptable.

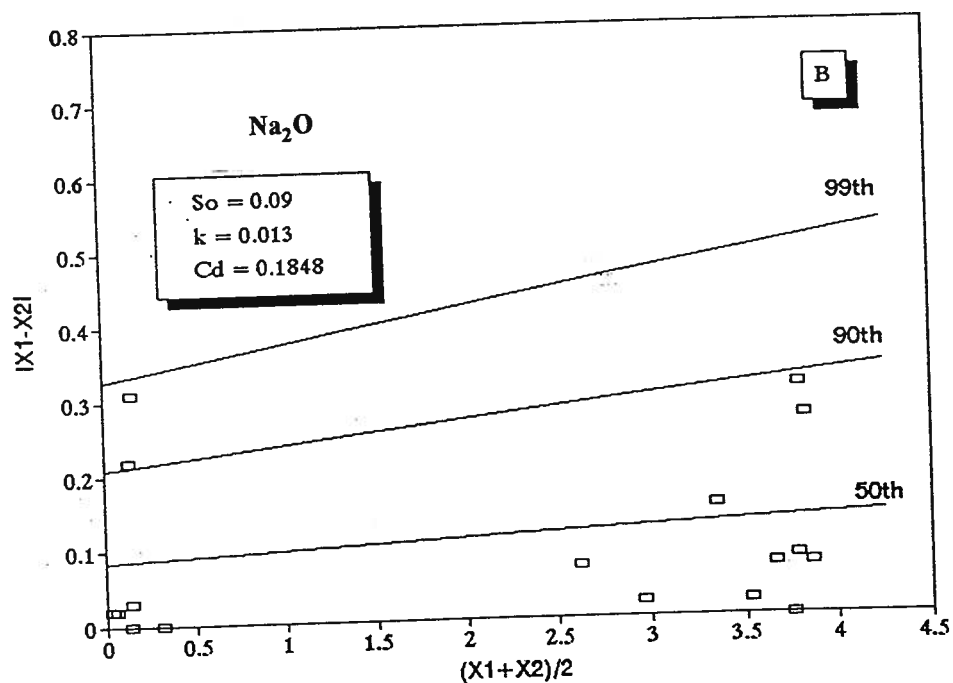
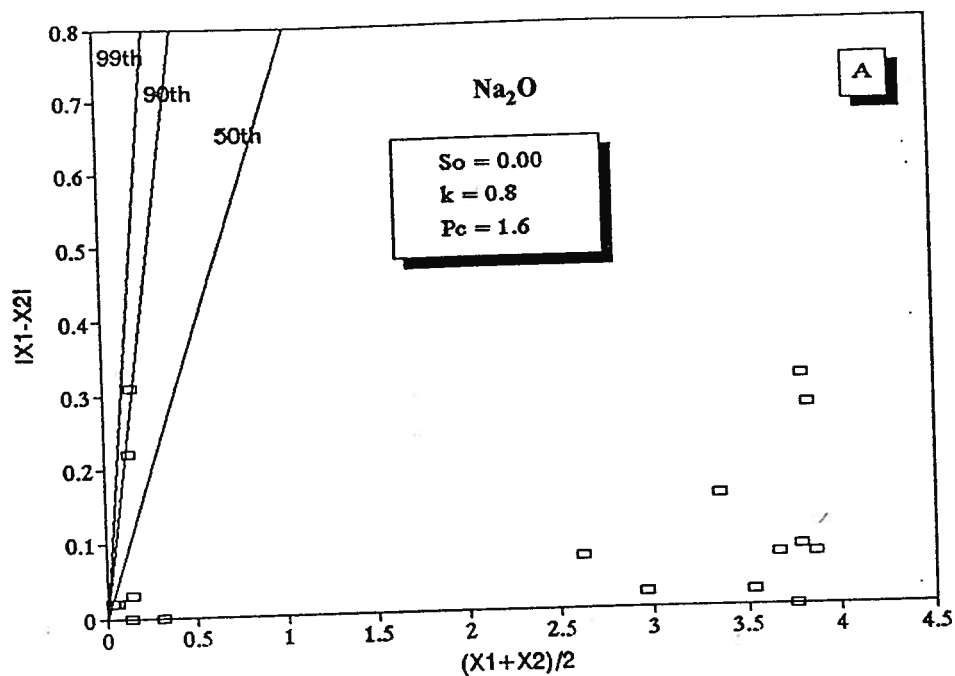


Figure 3-2. Comparison of the methods of precision estimation of lithogeochemical data by using: (A) constant precision and variable standard deviation for whole range of the concentration, and (B) variable precision and variable standard deviation. See text for detailed explanation.

One way of dealing with this problem is the introduction of the detection limit (C_d) of the element of interest to the construction of the corresponding control chart. Commonly, the values of detection limits of each analytical technique for different constituents are provided by the analyst. With the known value of detection limit (C_d), equation (3-18) can be rearranged as follows:

$$S_o = C_d (0.5 - k) \quad (3-21)$$

substitution of equation (3-21) in (3-19) and (3-20) gives:

$$d_{90} = 2.326(0.5C_d + k(C - C_d)) \quad (3-22)$$

$$d_{99} = 3.643(0.5C_d + k(C - C_d)) \quad (3-23)$$

Now only one variable (k) remains in equation (3-22) and (3-23). Following the same procedure as Thompson and Howarth (1976, 1978) one increases the value of k and moves the 99th and the 90th percentile lines up until no plotted point lies above the 99th percentile line and less than or equal to 10% of the plotted duplicates lie above the 90th percentile line. The value (k) can then be estimated. Thus, the value S_o can be calculated by using equation (3-21).

Where the information about detection limits is not available, there is another way to deal with this problem, that is, the estimation of S_o and k based on the analytical duplicates. A recommended procedure is as follows:

- (1) Introduce one more empirical precision equation to set one more constraint for taking one more variable (S_o) into account,

$$d_{50} = 0.954(S_o + kC) \quad (3-24)$$

- (2) Initially assume $S_o = 0$;
- (3) Gradually increase the value of k starting from zero in equations (3-20) until no point is above the d_{99} line (since 99% of points for a small set of duplicates 10 to 49 pair of duplicates means that all points should be below the 99th percentile line);
- (4) Construct the d_{90} line with the current values of S_o and k derived from the previous step and check whether 90% of the points are below the d_{90} line. If not, continue to

increment of k until only 10% of the points are above the d_{90} line;

- (5) Construct the d_{50} line with the current values of S_o and k derived from previous steps and check whether about 50%, or the maximum amount between 10 to 50% of the points, are above the d_{50} line. If the points above the d_{50} line are less than 50% or the maximum amount value between 10 to 50% of the total plotting points, then reject the initial assumption of S_o ;
- (6) Reassign the initial value of S_o by a small increment;
- (7) Repeat the steps (2) to (6) until the requirement for all three lines are satisfied; i.e., with certain values of S_o and k , no point is above the d_{99} line, no more than 10% of the points are above the d_{90} line and about 50% or the maximum amount between 10 to 50% of the points are above the d_{50} line (Figure 3-2B).

In brief, this approach helps obtaining reasonable estimates of S_o and k .

Consequently, the precisions of a particular set of lithogeochemical data with wide ranges of concentrations can be estimated in a form consistent with the case for more abundant paired data (i.e., duplicate pairs > 50).

3.4. Propagation of Errors in Calculation of Metasomatic Norms

Lithogeochemical data always incorporate some component of random error. Quantitative estimates of losses and gains of components during hydrothermal alteration are limited by the magnitude of these errors. Errors in analyses of individual components commonly are known. An important concern is the effect these known errors have on various calculated quantities, that is, the propagation of errors (Le Maitre, 1982; Cheng and Sinclair, 1994).

In mathematical terms, if the calculated result, z , is a function of a set of measured variables: x_1, x_2, \dots, x_n :

$$z = f(x_1, x_2, \dots, x_n) \quad (3-25)$$

The quantity z will be in error by an amount dz as a consequence of the errors in each of the measured quantities x_1, x_2, \dots, x_n . Then the error dz (as a variable) can be estimated using the approximation (e.g. Kendall, 1943):

$$S_z^2 = \sum_{i=1}^n \left(\frac{\partial f}{\partial x_i} \right)^2 S_{x_i}^2 + \sum_{j \neq i} \left(\frac{\partial^2 f}{\partial x_i \partial x_j} \right) S_{x_i x_j} \quad (3-26)$$

where x_i and x_j are the i th component and the j th component respectively, S_{x_i} is the analytical error calculated through equation (3-15) by using corresponding S_0 and k values; and $S_{x_i x_j}$ is the value of covariance between the i th and j th variable. It is reasonable to treat the error of lithogeochemical data as independent since the analytical error of one element has no obvious link to the error of the other element. Therefore, a simplified equation used to calculate error propagation is as follow:

$$S_z^2 = \sum_{i=1}^n \left(\frac{\partial f}{\partial x_i} \right)^2 S_{x_i}^2 \quad (3-27)$$

Substitution of equation (3-15) in (3-27) gives:

$$S_z^2 = \sum_{i=1}^n \left(\frac{\partial f}{\partial x_i} \right)^2 (S_0 + k_i x_i)^2 \quad (3-28)$$

Since the value of S_{x_i} is one standard deviation of a normal distribution, the value of error propagation (S_z) derived from it is at the 68% confidence level. Equation 3-27 is commonly used for calculating the variance of a function. As indicated by Le Maitre (1982), with closed data of the constant sum type, not all the covariances can be zero, and their sum must be negative. This means that if the covariance terms in equation 3-27 are ignored, the absence of their overall negative contribution will tend to give an overestimate of the variance. As this is generally more acceptable than an underestimate of the variance, the use of equation 3-27 for closed data would, therefore, seem reasonable as a first approximation.

For the calculation of loss or gain of a specific component in a single precursor system the following equation is used:

$$dx = \frac{Z_p}{Z_d} x_d - x_p \quad (3-29)$$

where dx is the value of absolute loss or gain of a component x during the hydrothermal alteration process, Z is immobile during the alteration process, x_p and x_d are the mobile element concentrations in the least altered parent rock and altered daughter rock respectively. In equation (3-29) the calculation result (dx) is derived from four analytical measurement values (i.e. Z_d , Z_p , x_d and x_p). Each of these four values has its own uncertainty. The value of dx contains the combination of the errors derived from all former dependent variables. Thus, the error propagation can be evaluated as follows:

$$S_{dx}^2 = \left(\frac{\partial}{\partial Z_p} \right)^2 (S_{oz} + k_z Z_p)^2 + \left(\frac{\partial}{\partial Z_d} \right)^2 (S_{oz} + k_z Z_d)^2 + \left(\frac{\partial}{\partial x_d} \right)^2 (S_{ox} + k_x x_d)^2 + \left(\frac{\partial}{\partial x_p} \right)^2 (S_{ox} + k_x x_p)^2 \quad (3-30)$$

$$S_{dx}^2 = \left(\frac{x_d}{Z_d} \right)^2 (S_{oz} + k_z Z_p)^2 + \left(\frac{Z_p x_d}{Z_d^2} \right)^2 (S_{oz} + k_z Z_d)^2 + \left(\frac{Z_p}{Z_d} \right)^2 (S_{ox} + k_x x_d)^2 + (S_{ox} + k_x x_p)^2 \quad (3-31)$$

By using an error determined from equation (3-31) the calculated absolute losses and gains of chemical constituents can be evaluated at an appropriate confidence level.

For the calculation of the propagated error of an specific normative mineral, it is first necessary to find the functional relationship between the amount of a specific normative mineral and related chemical constituents allotted to it. A specific normative mineral can be treated as the summation of certain portions of relevant chemical

constituents from the whole rock compositions. Therefore, the functional relationship between the percentage of normative mineral and concentration of different components used to construct it can be presented as follows:

$$z = a_1x_1 + a_2x_2 + \dots + a_nx_n \quad (3-32)$$

where z is the percentage value of the normative mineral, a_i is the proportion of the i th component used to make the normative mineral from the bulk rock compositions, and x_i is the concentration value of i th component in the rock. Substituting equation (3-32) in (3-28), we have:

$$S_{cz}^2 = \sum_{i=1}^n a_i^2 (S_{oi} + k_i x_i)^2 \quad (3-33)$$

By using equation (3-33) the uncertainty of a metasomatic norm calculation can be estimated through error propagation at the 68 % confidence level.

There are two fundamental assumptions for the calculation of propagated errors as outlined above:

- (i) the errors of lithogeochemical data are assumed to be independent of each other because the error of certain chemical constituent of the whole rock sample has no obvious link to the errors of other chemical constituents of the same rock sample;
- (ii) the error contributed by a chemical constituent is assumed to be allotted to a normative mineral in the same proportion as the chemical constituent is allotted to the normative mineral.

It is hard to prove these assumptions. Their use may lead to small overestimates of the propagated errors, and thus they provide a conservative approach.

Furthermore, the propagated errors calculated through equation (3-31) and (3-33) can be integrated with the results of the absolute losses and gains of chemical constituents, as well as the normative minerals corrected for the closure to be presented as a comprehensive mass balance equation introduced in the previous chapter. We have:

$$\begin{aligned} & \Sigma \text{Mineral}_{\text{parent rock}} \pm \text{error} + \Sigma \text{Constituent gained from solution} \pm \text{error} \\ & = \Sigma \text{Mineral}_{\text{altered rock}} \pm \text{error} + \Sigma \text{Constituent lost from wall rock} \pm \text{error} \end{aligned} \quad (3-34)$$

Propagated errors provide a basis for screening data for inclusion in the chemico-mineralogic model. Abundances less than twice the propagated error are not significantly different from zero and can be ignored.

Chapter 4. Geology of the Silver Queen Mine, Owen Lake Area, Central British Columbia

4.1. Introduction

The Silver Queen (also known as Nadina or Bradina) mine is near Owen Lake, 35 kilometres southeast of Houston, and 100 kilometres southeast of Smithers in the Bulkley Valley region of central British Columbia (Figure 4-1). The deposit has had a long history of exploration since its discovery in 1912. It has produced 3 160 oz Au, 168,000 oz Ag, 893,000 lbs Cu, 1.55 million lbs Pb, 11.1 million lbs Zn and 34,800 lbs Cd from 210,185 short tons of ore during a brief period from 1972 to 1973. Mine closure was due to overdesign of the mill and complex metallurgy (Cummings, 1987; Dawson, 1985). Geological reserves of the No. 3 vein at the Silver Queen mine presently stand at approximately 500,000 short tons grading 3 g/t Au, 200 g/t Ag, 0.23% Cu, 0.92% Pb and 6.20% Zn (Nowak, 1991). Equity Silver mine (total reserves plus production of approximately 30 million tonnes of 0.4% Cu, 110 g/t Ag, and 1 g/t Au) lies 30 km to the east-northeast.

Geological mapping of the 20 square kilometre area surrounding the deposit suggests that the stratified rocks (the Upper Cretaceous Tip Top Hill Formation: Church, 1971) hosting this epithermal gold-silver-zinc-lead-copper vein deposit may be correlated with rocks hosting the Equity Silver deposit (Wetherell et al., 1979; Cyr et al., 1984); they are lithologically similar to Kasalka Group rocks of late Early to early Late Cretaceous age (Leitch et al., 1990). Two series of igneous and volcanic rocks have been recognized by their distinctive lithogeochemical characters and K-Ar dating ages. The Silver Queen mine is hosted in the older series of igneous and volcanic rocks and is cut by dikes belonging to the younger series. Therefore, mineralization at the Silver Queen mine occurred during the period after the older series of igneous and volcanic activity, but before the younger one.

4.2. Regional Geological Setting

The study area lies within the Stikine terrane, which includes submarine calc-alkaline to alkaline immature volcanic island-arc rocks of the Late Triassic Takla Group; subaerial to submarine calc-alkaline volcanic, pyroclastic and sedimentary rocks of the Early to Middle Jurassic Hazelton Group; successor basin sedimentary rocks of the Late Jurassic and Early Cretaceous Bowser Lake, Skeena and Sustut groups; and Late Cretaceous to Tertiary calc-alkaline continental volcanic arc rocks of the Kasalka, Ootsa Lake and Endako groups (MacIntyre and Desjardins, 1988). The younger volcanic rocks occur sporadically throughout the terrane, mainly in down-thrown fault blocks and grabens. Plutonic rocks of Jurassic, Cretaceous and Tertiary ages form distinct intrusive belts (Carter, 1981), with which porphyry copper, stockwork molybdenum and mesothermal and epithermal base-precious metal veins are associated.

The Silver Queen mine lies on the caldera rim or perimeter of the Buck Creek basin, which is delineated roughly by a series of rhyolite outliers and a semicircular alignment of Upper Cretaceous and Eocene volcanic centres scattered between Francois Lake, Houston, and Burns Lake (Figure 4-1; see also Fig. 59 of Church 1985). The Buck Creek basin has been interpreted as a resurgent caldera, with the important Equity Silver mine located within a window eroded into the central uplifted area (Church, 1985; Church and Barakso, 1990). A prominent 30 km long lineament, trending east-northeasterly from the Silver Queen mine towards the central uplift hosting the Equity mine, appears to be a radial fracture coinciding with the eruptive axis of the Tip Top Hill volcanics and a line of syenomonzonite stocks and feeder dikes to an assemblage of Tertiary 'moat volcanics' (Church, 1985). Block faulting is common in the basin, locally juxtaposing volcanic rocks of various ages.

Within the basin, a Mesozoic volcanic assemblage is overlain by a Tertiary volcanic succession. The oldest rocks exposed within the basin are at the Equity Silver mine and

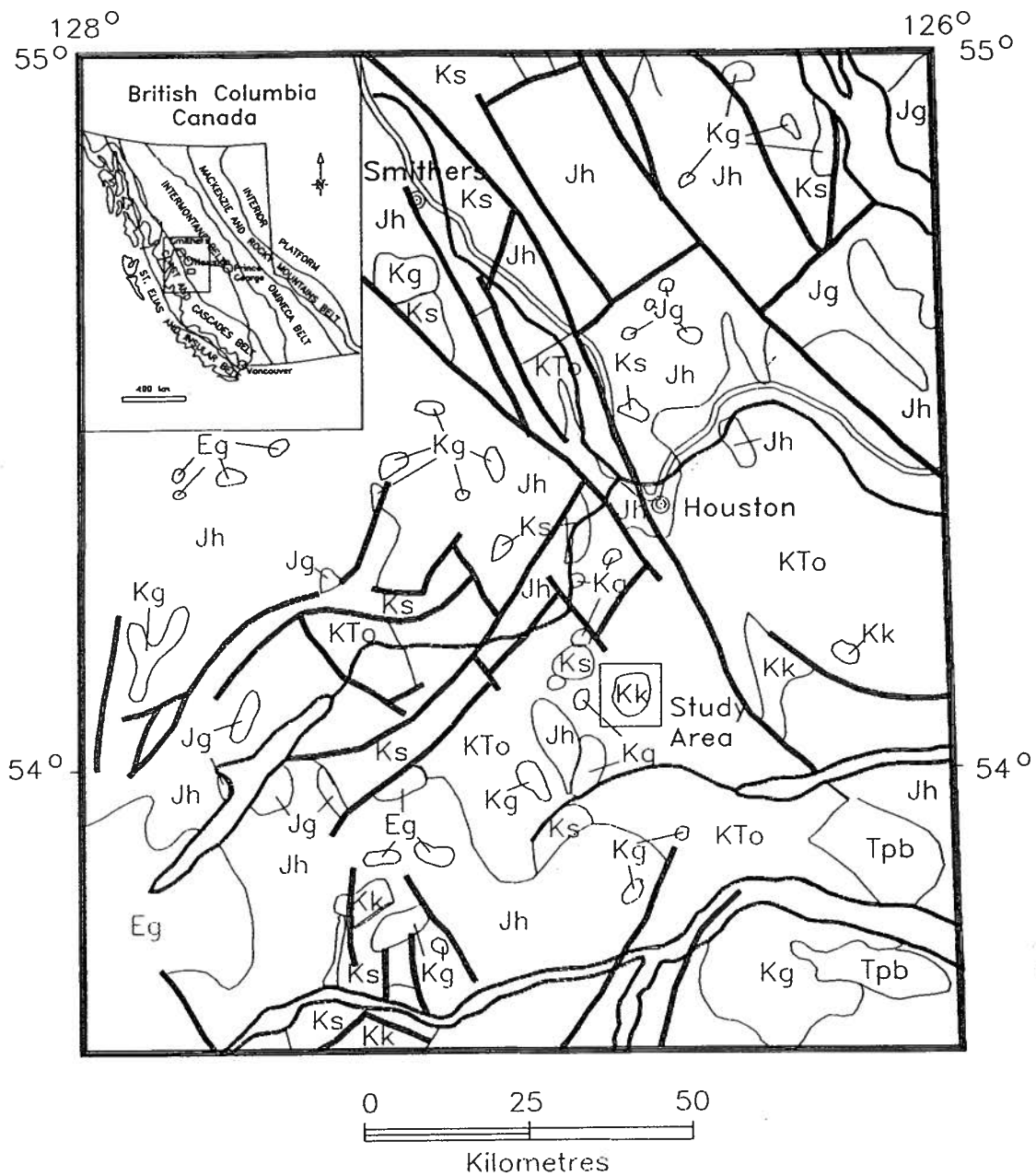


Figure 4-1. General geology of central British Columbia, showing the regional setting of the study area (after MacIntyre, 1985). Tpb - Tertiary plateau basalt; Eg - Eocene granite; KTo - Ootsa Lake Group; Kg - Cretaceous granite; Kk - Kasalka Group; Ks - Skeena Group; Jg - Jurassic granite; Jh - Hazelton Group.

the Silver Queen mine. The sequence at the Equity mine has been characterized by Church (1984) as the Lower Jurassic Telkwa Formation of the Hazelton Group, overlain with angular unconformity by Lower Cretaceous Skeena Group sedimentary rocks.

However, Wojdak and Sinclair (1984) correlate the sequence hosting the Equity mine with the Lower Cretaceous Skeena Group sediments, and Wetherell et al. (1979) and Cyr et al. (1984) correlate it with the Lower to Upper Cretaceous Kasalka Group. The Kasalka Group is considered to be a late Early Cretaceous (Armstrong, 1988) or early Late Cretaceous (MacIntyre, 1985; Leitch et al., 1991) continental volcanic succession that is predominantly porphyritic andesite and associated pyroclastic rocks. It is well exposed in the Kasalka Range type section near Tahtsa Lake.

Upper Cretaceous rocks with similarities to the Kasalka Group are exposed westwards from the Equity mine to the Owen Lake area, where they host the Silver Queen deposit (Church, 1984). These rocks, which have been dated at 75 to 80 Ma by K-Ar whole rock (Church, 1973; Leitch et al., 1991) consist of a lower felsic volcanic unit overlain by andesites and dacites of the Tip Top Hill volcanics (Church, 1984). This subdivision is based on 'rhyolitic volcanic rocks below the Tip Top Hill Formation in the Owen Lake area in extensive drill holes in the vicinity of the Silver Queen mine' (Church, 1973), which he considers to be 'lateral equivalents of quartz porphyry intrusions exposed nearby on Okusyelda Hill' (Figure 4-2). Recent mapping indicates that the lower volcanic unit exposed in the drill holes may, in part, be a strongly altered equivalent of the Tip Top Hill volcanics (Leitch et al., 1991). The quartz porphyry of Okusyelda Hill could correlate with dacitic quartz porphyry sills, dikes and laccoliths common within the type Kasalka Group section in the Tahtsa Lake area. Late quartz-feldspar porphyry dikes are also found at the Equity mine (Cyr et al., 1984; Church, 1985), although these are dated at 50 Ma and thus belong to the younger Ootsa Lake Group.

The Upper Cretaceous rocks are overlain by Eocene Ootsa Lake Group rocks, which include the Goosly Lake and Buck Creek formations of Church (1984). The Goosly

Lake andesitic to trachyandesitic volcanic rocks are dated at 48.8 ± 1.8 Ma by K-Ar on whole rock, and this is supported by similar dates of 49.6 ± 3.0 to 50.2 ± 1.5 Ma for related syenomonzonite to gabbro stocks with distinctive bladed plagioclase crystals at Goosly and Parrot Lakes between Equity and Silver Queen (Church, 1973). Andesitic to dacitic volcanic rocks of the Buck Creek formation, which directly overlie the Goosly Lake Formation, are dated at 48.1 ± 1.6 Ma by K-Ar on whole rock (Church, 1973). The Goosly Lake and Buck Creek formations correlate with Ootsa Lake Group rocks in the Whitesail Lake area south of Tahtsa Lake dated at 49.1 ± 1.7 Ma by K-Ar on biotite (Diakow and Koyanagi, 1988), but are slightly younger than dacite immediately north of Ootsa Lake, dated at 55.6 ± 2.5 Ma by K-Ar on whole rock (Woodsworth, 1982).

Basalts of the upper part of the Buck Creek formation (Swans Lake Member: Church, 1984) may correlate with the Endako Group of Eocene-Oligocene age. These rocks give dates of 41.7 ± 1.5 to 31.3 ± 1.2 Ma by K-Ar on whole rock samples from the adjacent Whitesail Lake map-area (Diakow and Koyanagi, 1988; cf. the range of 45-40 Ma reported by Woodsworth, 1982).

The youngest rocks in the Buck Creek basin are cappings of columnar olivine basalt of Miocene age, called the Poplar Buttes Formation by Church (1984). These have been dated at 21.4 ± 1.1 Ma by K-Ar on whole rock (Church, 1973) and are correlated with the Chilcotin Group.

4.3. Geology of the study area

The preliminary geology of the study area immediately surrounding the Silver Queen mine, as determined by fieldwork and petrological studies completed in 1989-1990, is shown in Figure 4-2 (units are defined in Table 4-1). Relationships between the map units are shown diagrammatically in Figure 4-3. The succession is strikingly similar to that observed in the Kasalka Range (MacIntyre 1985) and on Mount Cronin (MacIntyre and Desjardins, 1988).

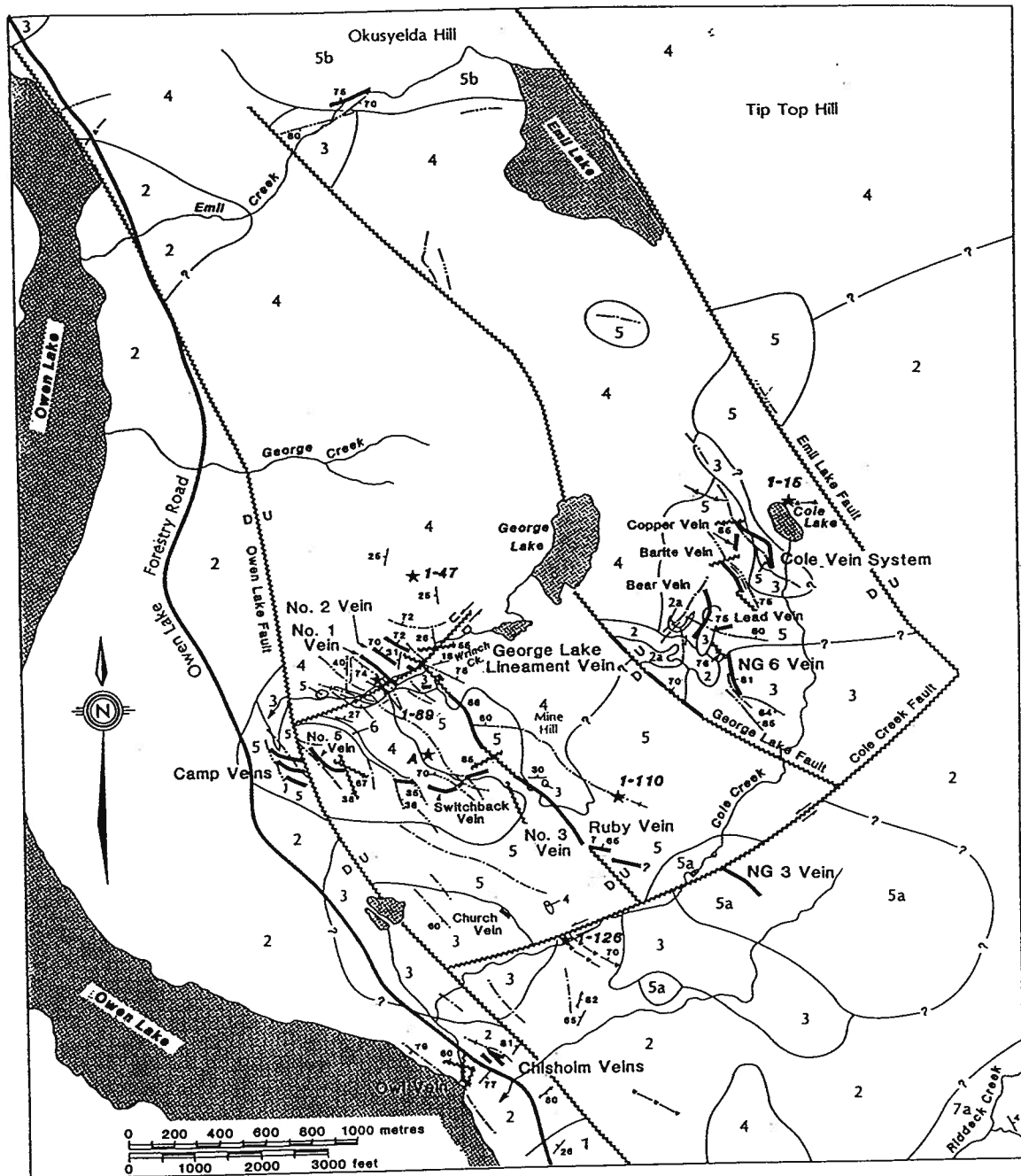


Figure 4-2. Detailed property geology of the Silver Queen mine, Owen Lake area, west-central British Columbia (from Leitch et al., 1990). Units are defined in Table 4-1.

Table 4-1. Table of formations, Owen Lake area*

Period	Epoch	Age (Ma)	Formation	Symbol	Unit	Lithology
Tertiary Cretaceous (Late)	Miocene Eocene-Oligocene Eocene	21	Poplar Buttes	M _{PBV}	8	Olivine basalt
		45-30	Endako Group	EO _{Ev}		Basalt diabase dike
		56-47	Ootsa Lake Group	E _{Ov}	7a 7	Trachyandesite basalt Bladed feldspar porphyry dike
			Mineralization	veins		
			"Okusyelda"	uKqp	6	Amygdular dikes
				uKp	5b	Quartz-eye rhyolite stock, dike
				uKud	5a	Intrusive porphyry sills, stocks
					5	"Mine Hill" microdiorite
					4a	Feldspar-biotite porphyry dike
					4	"Tip Top Hill" andesite
		85-75	"Tip Top Hill" formation	uKfp	4	
				uKb	3	Medium to coarse tuff-breccia
				uKt	2	Crystal tuff, local lapilli tuff
					2a	Fine ash tuff
				uKc	1	Polymictic basal conglomerate, sandstone and shale interbeds

*After Leitch et al., 1990

The rocks of the study area have been subdivided into five major units plus three dike types; Table 4-1 lists the map units defined to date. A basal reddish purple polymictic conglomerate (Unit 1) is overlain by fragmental rocks ranging from thick crystal tuff (Unit 2) to coarse lapilli tuff and breccia (Unit 3), and this is succeeded upwards by a thick feldspar porphyritic andesite flow unit (Unit 4), commonly grading into and locally intruded by microdiorite sills and other small intrusions (Unit 5). The stratified rocks form a gently northwest-dipping succession, with the oldest rocks exposed near Riddeck Creek to the south and the youngest exposed in Emil Creek to the north. All the units are cut by dikes that can be divided into three groups: amygdaloidal dikes (Unit 6), bladed feldspar porphyry dikes (Unit 7), and diabase dikes (Unit 8). The succession is unconformably overlain by basaltic to possibly trachyandesitic volcanics that crop out in Riddeck Creek and further south. These volcanics may be correlative with the Goosly Lake Formation

(Church, 1973). The units are described below in detail, to facilitate comparison with other possibly correlative rocks.

Basal Polymictic Conglomerate (Unit 1)

The basal member of the succession is a reddish to purple, heterolithic, poorly sorted pebble conglomerate that contains rounded to subangular small white quartz and gray-brown to less commonly maroon tuff and porphyry clasts. Local interbeds of purplish sandstone with graded bedding are found within the unit, as are rare black shaly partings. The matrix is composed of fine sand, cemented by quartz, sericite and iron oxides. The best exposure is found in a roadcut at the southern tip of Owen Lake, where the unit is about 10 m thick and dips 25° to the northwest. The base is not exposed and the unit is in presumed fault contact with the younger volcanic rocks of the Ootsa Lake Group (Goosly Lake Formation; Unit 7) exposed at higher elevations farther south along the road. In drill holes farther north, near the centre of the property, the upper contact of the conglomerate with overlying porphyry is sharp and appears conformable, but the porphyry may be an intrusion rather than a flow.

Crystal-Lithic Tuff (Unit 2)

In outcrop, the next major unit is a sequence of mainly fragmental rocks that are mostly fine crystal tuffs with thin interbeds of laminated tuff, ash tuff, lapilli tuff and less abundant breccia. The unit may be as much as 100 m thick. The most widespread rock type is a massive, gray to white, strongly quartz-sericite-pyrite altered, fine crystal tuff that grades imperceptibly into a porphyry of similar appearance and composition; the latter may be partly flow, intrusive sill, or even a welded tuff. Only the presence of broken phenocrysts and rare interbeds of laminated or coarsely fragmental material suggest that the bulk of this unit is tuffaceous. In thin section, the rock is seen to be made up of 1 to 2 mm broken, altered plagioclase relics and 0.5 mm anhedral quartz grains (that may be

partly to entirely secondary) in a fine matrix of secondary sericite, carbonate, pyrite and quartz. Drill core exposures show that the basal contact of Unit 2 with the underlying conglomerate is commonly occupied by the porphyry rather than the tuff. The best exposures of Unit 2 are in the area of Cole Creek and the Chisholm vein, where thin (10 cm) interbedded laminated tuff bands occur, many with variable dips to near-vertical, although coarser lapilli tuff lenses, up to 1 m thick, display gentle northerly dips. In drill core, sections of laminated tuffs with faint but discernible layering on a cm scale, may be up to 10 m thick; angles with the core axis suggest a gentle dip for the banding.

Outcrops on the northeast side of the George Lake fault have rare interbeds of a very fine, uniform "ash tuff" that are up to several m thick (Unit 2a). Typically they are dark gray to medium gray-green and have a siliceous appearance. Locally they contain angular fragments of either mixed origins (heterolithic clasts) or of larger blocks that are only barely distinguishable from the matrix (monolithic clasts).

Coarse Fragmental Unit (Unit 3)

A distinctive coarse fragmental unit overlies, or in some places is interlayered with, the upper part of Unit 2. It is composed of blocks and bombs(?) (cf. MacIntyre, 1985) of feldspar-porphyrific rock similar in appearance to both the underlying porphyry and the overlying porphyritic andesite. The clasts are mostly angular to subangular and about 2 to 5 cm in diameter, but some are much larger (up to 0.5 m); the matrix makes up a widely variable percentage of the rock, from almost 0 to 90 per cent. In places the rock has the appearance of an intrusive breccia with little or no rotation of fragments. In other places the fragments are clearly unrelated and "accidental" or unrelated clasts of chert or fine tuff are common, although still volumetrically minor; this has the appearance of a lahar.

In outcrop near the Cole veins, this breccia unit forms discontinuous lenses generally less than 10 m thick, with a suggestion of gentle northerly dips. The lenses appear to be conformable with the underlying or enclosing tuffs. In drill core, two

distinctly different modes of occurrence are noted for this unit: in one, it appears to be conformably overlain by Unit 4 porphyritic andesites (the total thickness of the breccia unit is up to 30 m); in the other, it appears to have subvertical contacts, implying it is an intrusive breccia. Good examples of the latter distribution are found in the Cole Lake area, the Camp vein system and around the southern end of Number 3 vein (Leitch et al., 1991). There is thus a general correlation between the subvertical breccia bodies and mineralized areas, just as there is between the microdiorite and mineralized areas.

In thin section, the clasts of the breccia are seen to be composed of highly altered andesite, fine tuff and quartz or quartzofeldspathic rocks, enclosed in a fine tuffaceous matrix. Alteration in the mine area is usually carbonate-sericite-quartz-pyrite.

Andesite (Unit 4)

The fragmental rocks appear to be conformably overlain by a thick, massive unit of porphyritic andesite that outcrops over much of Mine Hill and is best developed north of Wrinch Creek. This unit is equivalent to the Tip Top Hill volcanics of Church (1970), although in most places on the property the andesite is coarser and contains sparser phenocrysts than the exposures on Tip Top Hill. At exposures in Wrinch Creek canyon, a distinct flow lamination is developed by trachytic alignment of phenocrysts, best seen on weathered surfaces. This suggests that these andesites are mostly flows, with gentle northerly to northwesterly dips. However, some of the coarsest material probably forms intrusive sills and stocks [cf. the type sections of MacIntyre and Desjardins (1988) and MacIntyre (1985)] and in many places the andesite grades into intrusive microdiorite.

Parts of this unit, particularly in Emil Creek, west of Emil Lake, and on Tip Top Hill itself, may actually be crystal tuff. In these exposures, the feldspar phenocrysts are smaller, much more crowded and in places broken, and rare lithic fragments are visible.

Unit 4 has a Late Cretaceous K-Ar whole-rock date of 78.3 ± 2.7 Ma and 77.1 ± 2.7 Ma reported by Leitch et al. (1992) and Church (1973), respectively. Rhyolite from

Tsalit Mountain on the west side of Owen Creek valley, 10 kilometres northwest of the Silver Queen mine, gives a very similar isotopic date of 77.8 ± 3.0 Ma, also by K-Ar on whole rock. This rhyolite is correlated with the "Okusyelda" quartz porphyry by (Church, 1973).

In thin section, the andesite is seen to contain abundant 2 to 3 mm euhedral crystals of andesine. Oscillatory zoning is present, but with little overall change in composition within a given specimen, from An_{45} to An_{35} . Mafic minerals include roughly equal amounts (about 5% each) of 1-2 mm clinopyroxene and hornblende, and euhedral 1 to 2 mm biotite phenocrysts. The groundmass is an aphanitic mesh of intergrown feldspar with minor opaque grains; primary magnetite is abundant in the fresh specimens.

Biotite-feldspar porphyry dikes (Unit 4a)

Rare thin (1 m or less) dikes, similar in composition and appearance to the flows of unit 4, probably represent feeders to flows of unit 4. They are distinguished by prominent scattered books of black biotite up to 3 mm across, as well as abundant, 1-2 mm, plagioclase phenocrysts. These dikes have only been recognized near the north end of Cole Lake and on the highway at the north end of Owen Lake, but they could be more extensive (they are difficult to distinguish because of their similarity to unit 4). They are dated by K-Ar on whole rock at 70.3 ± 2.5 Ma, indicating a possible 7-8 Ma span of Tip Top Hill volcanic activity (Leitch et al., 1992).

Microdiorite (Unit 5)

Microdiorite forms subvolcanic sills, dikes, and possibly, small irregular stocks on the Silver Queen mine property. These intrusions are centrally located in the two main mineralized areas of the property, the No. 3 Vein and Cole vein areas. Contacts with the andesite are indistinct or gradational. Typically the microdiorite is a medium to fine-grained, dark greenish gray equigranular to porphyritic rock characterized by small (1 mm,

but locally glomeratic to 4 mm) plagioclase phenocrysts and 0.5 mm mafic relics in a phaneritic pink feldspathic groundmass. Primary magnetite is found in the less altered specimens. It is distinguished in outcrop by its relatively fine-grained, even-weathering texture and lacks the flow structure of the andesite. Because of the gradational relationship to the andesite, distinction is difficult in places. In thin section, the plagioclase is the same as in the andesite (oscillatory zoned andesine, An_{45-30}), and euhedral clinopyroxene phenocrysts, partly altered to carbonate, are the most abundant mafic. Apparent hornblende relics are completely altered to chlorite. No biotite is seen, but rare scattered quartz phenocrysts, displaying late-stage overgrowths of quartz, are observable ranging up to 1 mm in size (these are not visible in hand specimen). The groundmass is composed of fine (0.1 mm) quartz, plagioclase and potassium feldspar.

The microdiorite has a K-Ar whole rock age of 78.7 ± 2.7 Ma and 75.3 ± 2.0 Ma reported by Leitch et al. (1992) and Church (1973), respectively. The age of the microdiorite is indistinguishable from the age of unit 4 andesite, in agreement with the gradational contacts between these two rocks.

Porphyry (Unit 5a)

Large bodies up to 1000 m across of a coarse feldspar porphyritic rock crop out in the vicinity of Cole Creek and are also found in drill core from the south end of the No. 3 vein system, where the porphyry body usually occurs between Unit 1 and Unit 3. The rock is composed of roughly 50% plagioclase phenocrysts of up to 5 mm diameter and 10 to 20% smaller mafic minerals in a fine feldspathic groundmass. The porphyry is distinguished from the andesite, Unit 4, by its coarser texture and by the absence of flow textures. It probably represents subvolcanic or high-level intrusive bodies that were emplaced below or postdate the extrusive andesite, but are related to the same magmatic event that produced the andesite. Such subvolcanic intrusive bodies, with identical mineralogy to the extrusive porphyritic andesites, have also been noted in the Kasalka

Group near Tahtsa Lake (MacIntyre, 1985). No K-Ar whole rock age data is determined for this rock unit because no fresh sample can be found (the outcrops of this unit of rock are always variably saussuritized or sericitized).

Quartz-feldspar Porphyry (Unit 5b)

Quartz-feldspar porphyry, which appears to be part of a subvolcanic intrusive stock, crops out along Emil Creek and on Okusyelda Hill to the north of the creek. This unit was called "Okusyelda" dacite (rhyolite) by Church (1970). Although its contact relation is uncertain, it appears to intrude Unit 4 (Tip Top Hill volcanics; Leitch et al., 1992). Church (1984) correlates the quartz porphyry intrusions on Okusyelda Hill with felsic volcanic rocks in the Tchesinkut Lake and Bulkley Lake areas, and possibly with the Tsalit Mountain rhyolite of 77.8 Ma. However, in the Kasalka Range, MacIntyre (1985) found sills and dikes of quartz-porphyrific dacite and rhyolitic quartz 'eye' porphyry, commonly associated with mineralization, that cut stocks dated at approximately 76 Ma (Carter, 1981). However, the quartz porphyry cannot be significantly younger than the microdiorite-feldspar porphyry in the Owen Lake area; the 84.6 ± 0.2 Ma U-Pb date on zircon shows that it is the same age or older. It is cut by thick calcite veins and quartz-sericite-pyrite alteration on the extension of the George Lake vein and so is probably pre-mineralization.

Thin sections show the quartz porphyry consists of 10 to 15% 2 mm quartz phenocrysts and slightly smaller euhedral andesine plagioclase crystals, plus smaller relic mafic grains, in a microgranular groundmass of roughly equal amounts of quartz, plagioclase and potash feldspar. Quartz, and to a lesser extent, plagioclase also occur as angular fragments.

Amygdaloidal Dikes (Unit 6)

Units 1 to 5 are cut by a series of variably amygdaloidal dikes that are concentrated in the two main areas of mineralization (No. 3 vein and Cole vein areas). They generally trend northwesterly parallel to the mineralized veins, but north, east and northeast-trending examples are known. Dips are either subvertical to steep, or else gentle (as low as 20°). These dikes are irregular and anastomosing in some parts of the property, for example between the Camp and Switchback vein systems. Highly altered examples are commonly found adjacent to and parallel to veins; elsewhere veins cut through these dikes. These dikes have been referred to previously as 'pulaskite' at both the Silver Queen and Equity, but this is an inappropriate term, implying an alkali-rich mineralogy including soda orthoclase, alkali pyroxene or amphibole, and feldspathoids.

In underground exposures the dikes range from dark gray-green where fresh, to pale green or creamy-buff where strongly altered in underground exposures; they are purplish in weathered surface outcrops. They are typically fine grained and are characterized by amygdules filled by calcite, or less commonly, iron oxides, particularly at their chilled margins (dikes less than 1-2 m wide commonly lack amygdules). Flow orientations, generally parallel to the walls, provide an indication of attitude in surface outcrops. In the larger dikes (up to 10 m thick) the flow orientations are random.

In thin section, the most striking feature of this dike is the abundance of fine, trachytic-textured feldspar microlites that average about 0.25 mm long. Alteration to carbonate and sericite is extensive, but the texture is generally preserved. This dike has an Eocene K-Ar whole rock age of 51 ± 1.8 Ma that almost certainly reflects alteration, thus establishing a maximum but likely age of mineralization.

Bladed Feldspar Porphyry Dikes (Unit 7)

A set of trachytic-textured porphyry dikes, 1 to 5 m wide and characterized by coarse (up to 1 cm long) bladed plagioclase phenocrysts, cut and slightly offset the

amygdaloidal dikes. The complete lack of alteration in the bladed feldspar porphyry dikes, and the fact that they distinctly crosscut mineralized veins (for example, the Bear Vein, Cole Lake area), indicates that they postdate mineralization. The K-Ar whole rock age of these dikes is 51.9 ± 1.8 Ma, indistinguishable from the K-Ar whole rock isotopic age of the amygdular dikes (Unit 6). Their spatial distribution is also similar to that of the amygdaloidal dikes, with concentrations in the two main mineralized areas; orientations are similar too, but with subvertical dips only. The similarity of these post-mineral bladed feldspar porphyries to the Goosly and Parrot Lake syenomonzonite stocks, and bladed feldspar andesite dikes at Equity dated at 50.7 ± 1.8 Ma by K-Ar on whole rock, suggests that there is a genetic relation among them.

In thin section, the bladed feldspar porphyry dikes are composed of large (4-10 mm) plagioclase phenocrysts and rare to locally abundant clinopyroxene crystals up to 5 mm across, set in a dark purplish groundmass of feathery interlocking plagioclase microlites with interstitial quartz, alkali feldspar, opaque and skeletal rutile. The plagioclase forms strongly zoned, oscillatory crystals that range from cores of andesine (An_{50}) to rims of oligoclase (An_{15}). The pyroxene has a strong green color and is probably iron-rich.

Diabase Dikes (Unit 8)

Black fine-grained dikes of basaltic composition cut all other units on the property. They are much more limited in distribution than the older dikes, with subvertical dips and northwest or east-west strikes. In thin section, they lack olivine and are composed of diabasic-textured plagioclase set in clinopyroxene, with accessory opaque minerals.

The K-Ar whole rock isotopic age of these dikes is 50.4 ± 1.8 Ma, only slightly younger than the dikes of Unit 6 and Unit 7. It is likely that Unit 8 dikes are related to the basaltic Buck Creek Formation (48.1 ± 1.6 Ma; Church, 1973).

4.4 Lithogeochemical characters and two series of igneous and volcanic rocks

The various types of igneous and volcanic rocks at Owen Lake area and its peripheral region can be classified into two series according to lithogeochemical features and K-Ar ages. The first series consists of igneous and volcanic units from intermediate to felsic composition, and is characterized by having relatively low contents of TiO_2 (from 0.36 to 0.8 wt%), MgO (from 0.65 to 4.18 wt%), total iron (from 1.73 to 6.5 wt%) and P_2O_5 (from 0.09 to 0.42 wt%) as well as the older K-Ar ages (from 78.8 to 57.2 Ma). In contrast, the second series consists of the igneous and volcanic units from intermediate to mafic composition, and has higher contents of TiO_2 (from 0.95 to 1.27 wt%), MgO (from 2.11 to 7.81 wt%), total iron (from 5.14 to 8.98 wt%) and P_2O_5 (from 0.49 to 0.67 wt%) as well as younger K-Ar ages (from 48.7 to 21.4 Ma; Table 4-2). The former series predates and hosts the mineralization; the latter is post-mineralization. These two series of igneous and volcanic rocks can be distinguished by using a Zr- TiO_2 binary plot (Figure 4-4).

In Figure 4-4, the amygdaloidal dike composition plots in the middle of the older series of igneous and volcanic rock but has a young age (51.3 Ma). The tentative explanation for this apparent anomaly is that where sampled amygdaloidal dikes were 'younged' by later hydrothermal activity. It may also be noted that samples of porphyry (Unit 5a) and tuff (Unit 2) plot somewhat off the main trend of the series. These may also arise because of the effects of hydrothermal alteration; dated samples of both of these rock units were not as fresh as the others plotted in Figure 4-4.

Lithogeochemical data used to construct Figure 4-4 are selected from relatively unaltered rocks and listed in Table 4-2. Two lithogeochemical analyses with the corresponding K-Ar age known from Church and Barasko (1990) are listed in Table 4-2 to complete the illustration of the relation between the lithogeochemical compositions and the timing of igneous and volcanic activities.

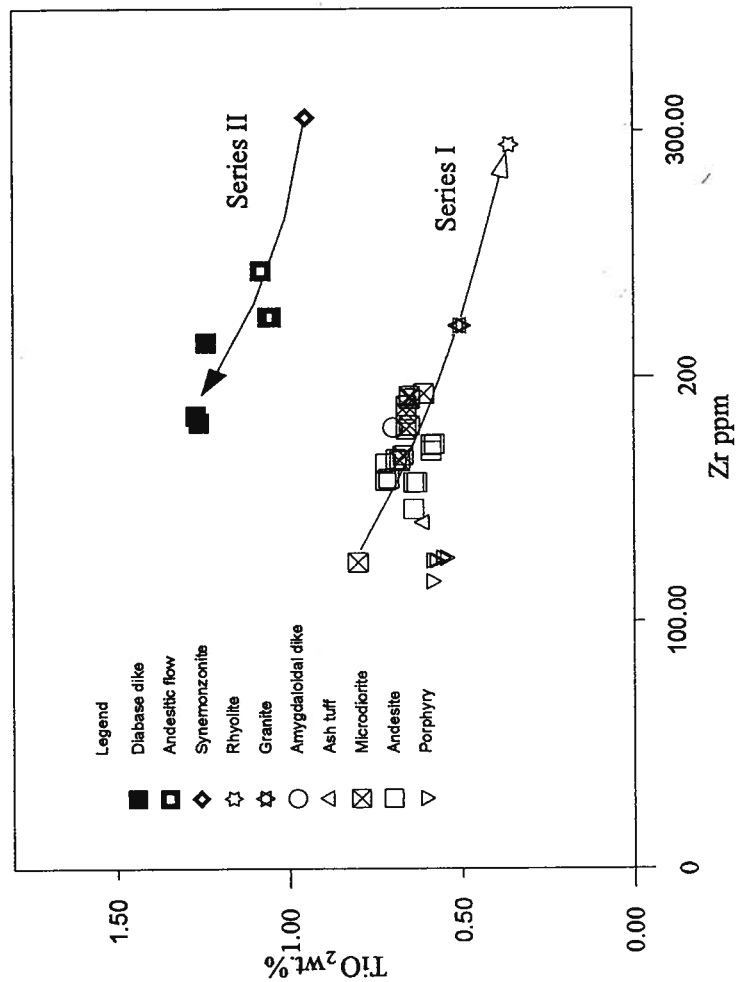


Figure 4-4. A Zr-TiO₂ binary plot distinguishes two series of igneous and volcanic rocks in Owen Lake area and its peripheral region. Series I has K-Ar age from 78-51 Ma and hosts the Silver Queen vein mineralization. Series II has K-Ar age of 50 Ma or younger and overlies or cuts the veins.

Table 4-2. Lithochemical data of various types of rock at Owen Lake area, central British Columbia

Sample ID	Church-v18	S91-9	SQ-50	S91-4	SQ-113	S91-1A	S91-3	S91-10	Church-14	DA48-13	x11-1b	x4-4
Rock Name	Basalt	Nadina dike	Diabase dike	Andesite	Andesite	Syen- monzonite	Rhyolite	Granite	Granite	Amygda- loidal dike	Microdiorite	Andesite
Location	Poplar Buttes	Nadina Mt.	Wretch Creek	E. Ridge of Owen Lake	Riddich Creek	N. Equity	N Equity	Nadina Mt.	Equity mine	Cole Lake	Jack vein	N. segment of No. 3 vein
wt%												
SiO ₂	44.00	49.64	55.20	57.26	60.39	61.38	72.11	68.03	67.00	56.05	57.05	57.86
TiO ₂	3.01	1.27	1.24	1.08	1.06	0.95	0.36	0.50	0.67	0.70	0.69	0.65
Al ₂ O ₃	15.11	15.15	15.59	15.73	15.40	15.38	13.78	14.20	16.20	15.14	15.77	15.61
Fe ₂ O ₃	5.11	3.34	3.45	6.57	4.73	3.57	1.21	1.04	2.18	2.13	2.73	3.09
FeO	7.90	5.64	4.33	0.99	1.26	1.57	0.52	1.87	1.58	2.86	3.77	2.89
MnO	0.18	0.31	0.12	0.14	0.11	0.06	0.05	0.08	0.04	0.09	0.22	0.34
MgO	8.62	7.81	4.85	2.62	3.15	2.11	0.65	1.76	1.30	2.72	4.18	2.94
CaO	9.86	6.58	6.65	5.31	4.20	4.11	1.27	2.45	3.30	4.15	5.78	6.07
Na ₂ O	4.48	2.96	3.38	3.71	4.26	3.96	4.15	3.75	4.32	2.53	3.76	3.65
K ₂ O	1.73	1.53	1.94	3.29	3.16	3.21	4.41	4.68	3.69	3.39	2.97	3.09
P ₂ O ₅	0.58	0.56	0.59	0.63	0.67	0.49	0.09	0.22	0.28	0.29	0.42	0.38
H ₂ O	3.63	1.95	0.35	0.35	0.35	0.60	0.25	0.25	1.69		0.91	0.97
CO ₂	0.01	2.88	1.89	2.03	0.90	1.36	0.48	0.36	0.08		1.25	2.03
LOI										9.33		
TOTAL	104.22	99.62	99.58	99.71	99.64	98.75	99.33	99.19	102.33	99.38	99.50	99.57
ppm												
S					30						865	33
Zr		184.40	213.90	243.34	224.29	305.64	294.32	220.68		179.31	166.44	191.07
Y		26.47	20.80	27.74	29.19	25.71	26.51	32.69		12.84	30.75	27.95
Rb		99.10	54.17	100.61	79.54	92.02	137.16	201.25		122.20	92.04	100.28
Sr		733.87	922.48	1187.57	1148.24	901.97	313.80	423.86		409.23	630.05	592.72
Age (Ma)*	21.4		50.4		48.8	48.7			57.2	51.3	78.7	78.3

* K-Ar dating age with about 2 Ma error on average.

Table 5-2. Lithochemical data of various types of rock at Owen Lake area, central British Columbia (Continuous)

Sample ID	x10-6	x10-6D	DA63-1	SQ-119	x5-6	x2-5	x3-3	x3-6	x3-7	SQ-77	S91-15
Rock Name	Microdiorite	Microdiorite	Microdiorite	Andesite	Andesite	Andesite	Andesite	Andesite	Andesite	Ash tuff	porphyry
Location	C. segment of No.3 vein	C. segment of No.3 vein	Switch Back vein	N. Owen Lake	South segment of No.3 vein	N. segment of No.3 vein	N. segment of No.3 vein	N. segment of No.3 vein	N. segment of No.3 vein	SW Cole hill	Duck Lake
wt%											
SiO ₂	61.25	59.00	57.99	56.05	56.58	57.29	57.75	57.20	57.97	61.16	63.22
TiO ₂	0.58	0.59	0.71	0.80	0.67	0.66	0.66	0.66	0.65	0.61	0.55
Al ₂ O ₃	15.11	15.98	16.53	16.09	16.04	15.70	15.85	16.03	15.87	15.53	14.81
Fe ₂ O ₃	2.30	2.52	2.22	4.45	2.36	3.08	3.02	3.12	2.86	1.07	3.00
FeO	2.86	2.85	3.76	1.74	3.38	2.92	2.86	2.70	3.05	4.76	1.82
MnO	0.14	0.18	0.16	0.13	0.22	0.25	0.31	0.23	0.20	0.15	0.12
MgO	2.78	2.18	2.63	2.78	2.50	3.33	2.87	2.61	2.64	2.71	3.40
CaO	4.92	5.16	6.25	7.45	5.11	5.67	5.75	5.97	5.66	5.29	3.03
Na ₂ O	3.93	3.63	3.43	3.22	3.05	3.39	3.96	3.55	4.09	3.81	4.20
K ₂ O	3.14	3.09	3.16	1.80	3.19	3.15	3.02	3.04	2.92	2.61	2.62
P ₂ O ₅	0.26	0.34	0.43	0.27	0.28	0.37	0.39	0.40	0.38	0.33	0.28
H ₂ O	1.39	1.22	0.93	2.35	2.16	1.04	1.14	2.18	1.27		
CO ₂	1.85	2.40	1.34	2.93	4.35	2.75	1.92	2.34	2.14		
LOI										1.32	2.45
TOTAL	100.51	99.14	99.54	100.06	99.89	99.60	99.50	100.03	99.70	99.35	99.50
ppm											
S	127	153.00	122.00	21	711	31	180	160	180	445	
Zr	172.67	169.80	158.38	124.27	168.02	178.64	185.22	188.35	192.04	140.62	126.03
Y	24.29	24.89	25.75	18.02	29.65	33.05	31.91	28.49	30.36	24.58	18.36
Rb	119.76	118.77	92.65	77.94	108.22	121.40	103.70	122.52	108.45	75.74	77.13
Sr	620.61	472.32	608.28	587.77	1071.44	573.45	597.08	566.67	607.36	524.71	562.36
Age (Ma)*											

4.5. Veins: Character and Correlation

Mineralization on the property is mainly restricted to 0.1 to 2 m thick quartz-carbonate-barite-specular hematite veins that contain disseminated to locally massive pyrite, sphalerite, galena, chalcopryite, tennantite and argentian tetrahedrite. Locally, in chalcopryite-rich samples, there is a diverse suite of Cu-Pb-Bi-Ag sulfosalts such as aikinite, matildite (in myrmekitic intergrowth with galena), pearcrite-arsenopolybasite, and possibly schirmerite (Hood, 1991). Berryite (Harris and Owens, 1973), guettardite and meneghinite (Weir, 1973), boulangerite (Marsden, 1985) and seligmannite and pyrargyrite (Bernstein, 1987) have also been reported but not yet confirmed. All the Au and much of the Ag are in the form of 60-70 fine electrum, as grains generally less than 50 microns in diameter and hosted in galena that is associated with fine grained pyrite (Hood, 1991). Paragenetically, the mineralization is divided into four distinct stages:

Stage I is characterized by fine grained pyrite, quartz and hematite in the central segment of the No. 3 vein. Barite, svanbergite, and hinsdalite become abundant towards the south end of the No. 3 vein, with marcasite more abundant towards the north.

Stage II is dominated by the presence of massive sphalerite and layered carbonate (calcite in the south, manganoan carbonates in the north).

Stage III, however, is more complex. Mineralization consists of chalcopryite, galena, fahlores (tetrahedrite-tennantite), electrum, quartz and sulfosalts. Included in the sulfosalt assemblage are the unusual Pb-Bi-Cu-Ag species berryite, matildite, gustavite and aikinite.

Stage IV is volumetrically minor and is dominated by fine grained quartz, pyrobitumen and calcite (Hood, 1991)

The veins cut the amygdaloidal, fine-grained plagioclase-rich dikes (Unit 6), and are cut by the series of dikes with bladed plagioclase crystals (Unit 7). Both these dike types are possibly correlative with the Ootsa Lake Group Goosly Lake volcanics of

Eocene (approximately 50 Ma) age, although chemically the amygdaloidal dikes appear older. The bladed feldspar porphyry dikes cut the amygdaloidal dikes, and both are cut by the diabase dikes that may correlate with Endako Group volcanism of Eocene-Oligocene (approximately 40 to 30 Ma) age.

The major veins are concentrated into two main areas on the property centered on the Mine Hill and Cole Lake areas, with an apparently less mineralized area between in which only the George Lake vein has been found to date. However, this intervening area is heavily covered by overburden and more veins may remain to be discovered here (the relatively minor Jack and Axel veins, not shown on Figure 4-2, are located west of the George Lake vein). The most important known vein on the property, both in terms of length and tonnage potential, is the No. 3 which outcrops for over 1000 m on Mine Hill. Its extension to the north appears to taper and die out, but significant potential may exist on faulted extensions to the south where exploration has been hampered by heavy overburden cover. South of Riddeck Creek post-mineralization volcanic cover may preclude further exploration.

The predominant strike direction for the main veins is northwesterly, with moderate to steep northeasterly dips. The relatively minor Church, Chisholm and Owl veins also have the dominant northwesterly trend. However, strikes in the Cole Lake, Camp, No. 5 and Switchback vein areas are more variable (see structural analysis below). Dikes and faults on the property have orientations similar to those of the veins, although one major difference is the presence of gently west-dipping dikes; no veins of this orientation are seen.

The veins are highly variable in character, ranging from simple massive or banded gangue-rich veins with well-defined walls through irregular massive sulfide veins to ill-defined stockwork zones. Note how the No. 3 vein divides into two in its upper part; further division into several sub-parallel thin veins or stringers is common, making correlation difficult even between closely spaced drill holes. In places, the vein pinches

out, with the zone of pinching (which correlates with flattening of the vein) raking moderately east in the plane of the vein. Post-mineral shearing is common along the veins, further complicating correlations by attenuating or removing (faulting out) the mineralized section. A strong bleaching alteration envelope (quartz-sericite/kaolinite-carbonate-pyrite alteration) generally accompanies the veining. True thickness of the mineralized structure is also an aid to correlation if the total thickness (e.g. of all the vein strands) is compared from hole to hole. However, the strong lateral and vertical variations make this a less useful tool over longer distances between sections. In general, the tenor of mineralization, as measured by assay composites, is the most reliable correlation tool. Although the assays are necessarily a reflection of vein mineralogy, and mineralogy is useful for correlation, the silver and gold values that have proved to be the most important correlations, cannot be seen visually.

Correlation is made more difficult by the presence of one or more hangingwall or footwall veins that are found discontinuously along the length of the major vein structures. The presence of these subsidiary structures has been well established during underground development for exploration of the No. 3 vein; however, in drill core it is difficult to be sure if a given intersection is of a hanging/footwall structure or an *en echelon* shift of the main vein. In fact, some of the 'hangingwall' and 'footwall' veins are probably *en echelon* portions of the No. 3 vein; in other places they may be splays off the No. 3 vein (Fig. 4-2).

One of the most difficult problems in making correlations is the *en echelon* character of many of the veins, both along strike and down dip. Resolution of this problem is important because of the implications it has for physical continuity of the vein, and consequently, for tonnage and grade estimations. For example, intersections of veins in the No. 3 vein, George Lake, Camp and Cole Lake areas can be interpreted either as simple tabular bodies or as *en echelon* lenses (see sections in Fig. 4-5 to 4-9); there may be no vein, or an attenuated vein, in the locations predicted by the simple tabular model.

Potential problems are: (1) an increased, non-quantifiable error in tonnage estimation, and (2) disregard for possible different grade character of two *en echelon* vein segments.

4.6. Structures and the Interpretations

The structure of the Silver Queen mine area is dominated by a gently west to northwest-dipping homocline. There is no folding apparent at the scale mapped; the sequence appears to have been tilted 20° to 30° from the horizontal by block faulting. The average bedding plane is 032/25°NW and the most prominent joint set dips steeply, roughly perpendicular to the bedding at 057/77°SE (Leitch et al., 1991).

Two prominent sets of faults displace this homoclinal sequence, cutting it into a series of fault panels: a northwest-trending (NW) set and a northeast-trending (NE) set (Fig. 4-2). The former predates or is contemporaneous with mineralization, whereas the latter is mainly post-mineral (a few veins trend east-northeast). The NW faults dip 60° to 80° to the northeast (average 315/75°NE), and the 'cross' or NE set appears to be subvertical (070/90°). There are subsidiary trends indicated at 295/85°NE and 085/90°, and a few flat-dipping faults possibly roughly parallel to bedding planes. Most of the mineralized veins and the dikes follow the northwest faults, and in places veins are cut off and displaced by the northeast set.

The sense of motion on the northwest faults is such that each successive panel to the east is upthrown, leading to successively deeper levels of exposure to the east. Thus, in the panel between the George Lake and the Emil Lake faults (Fig. 4-2), there is considerably more of the lower fragmental rocks (Unit 2 and Unit 3) exposed than in the next panel to the west, between the Owen Lake and the George Lake faults. There does not seem to be much displacement across the No. 3 vein fault; slickensides seen underground on this structure suggest a reverse sense of last movement with indeterminable horizontal component.

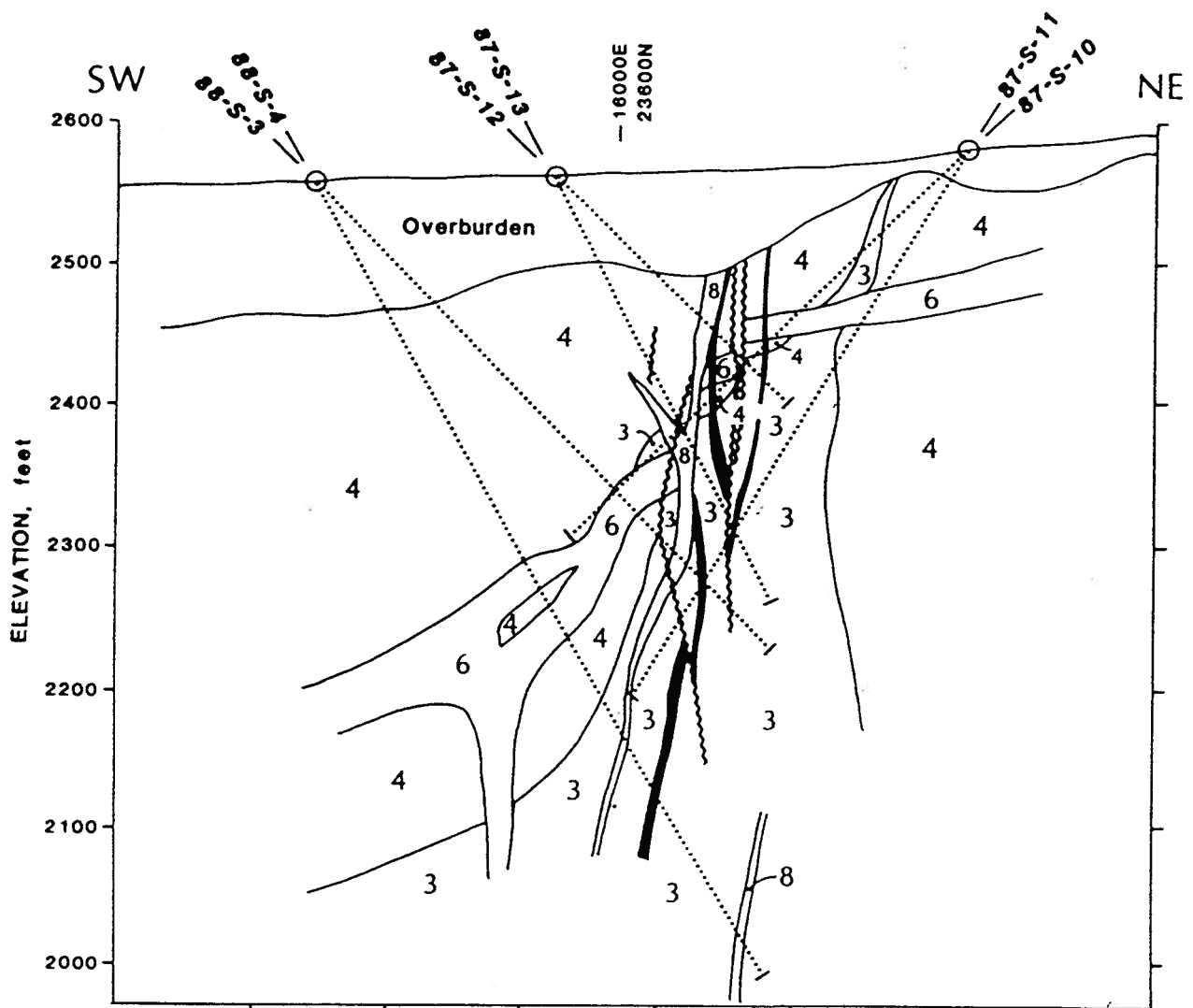


Figure 4-5. Cross-section of Camp vein shows gently dipping dike approximately perpendicular to the steeply dipping vein system. Horizontal scale equals vertical scale. Numbers represent the geological units which are defined in Table 4-1. Thick solid line - vein, thin solid line - geological contact, ripple line - fault, dash line - drill, circle - drill site.

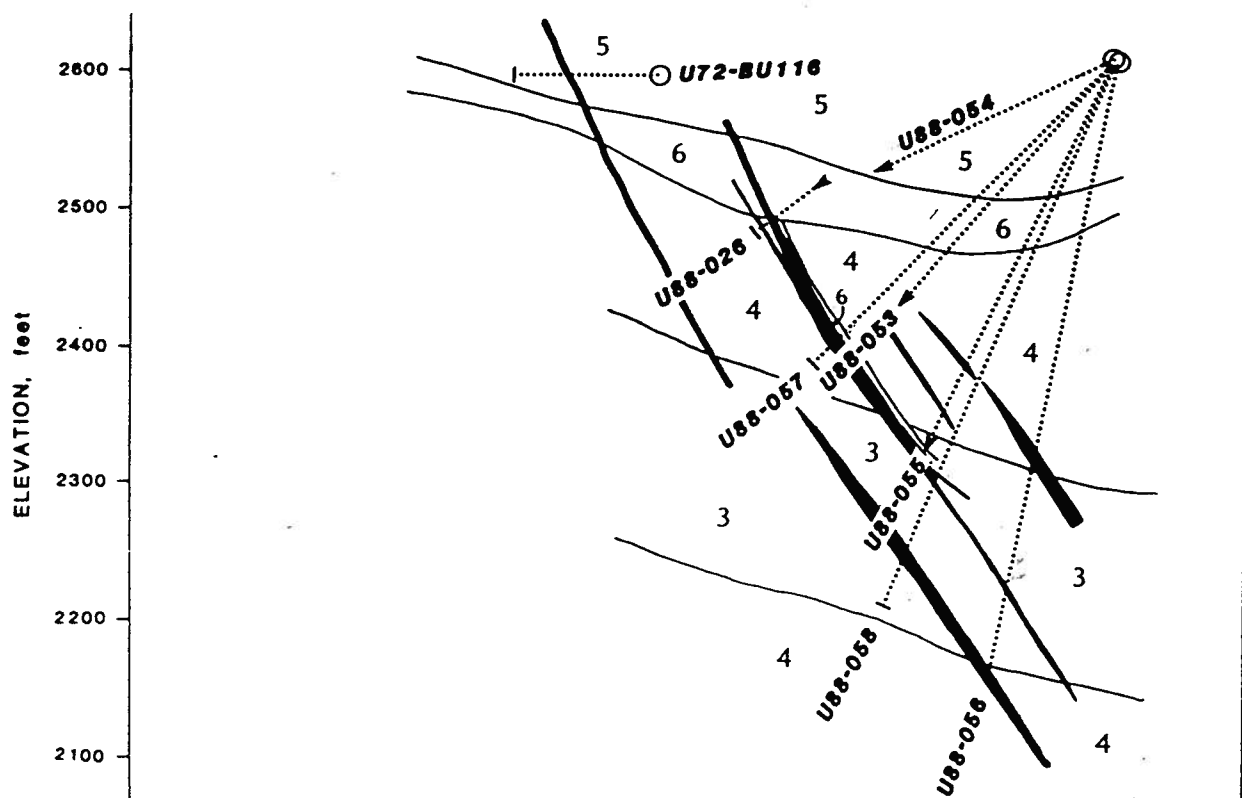


Figure 4-6. Cross-section of the southern segment of the No. 3 vein at 21000 E (BU-116) to show branching and *en echelon* character of the vein. Horizontal scale equals vertical scale. Numbers represent the geological units which are defined in Table 4-1. Thick solid line - vein, thin solid line - geological contact, dash line - drill, circle - drill site.

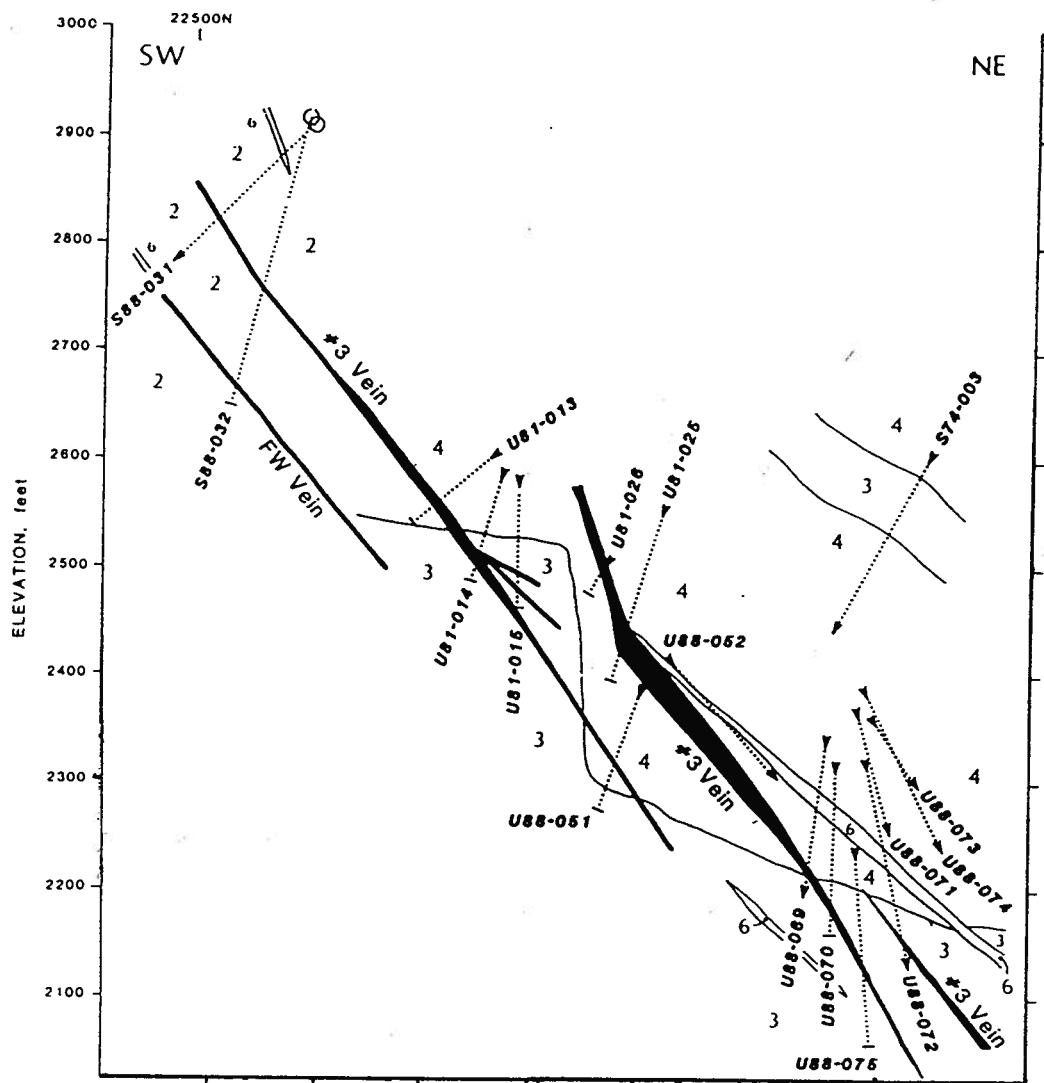


Figure 4-7. Cross-section of the southern segment of the No. 3 vein at 20,000 E (S-88-31) shows branching and *en echelon* character of the vein. Horizontal scale equals vertical scale. Numbers represent the geological units which are defined in Table 4-1. Thick solid line - vein, thin solid line - geological contact, dash line - drill, circle - drill site.

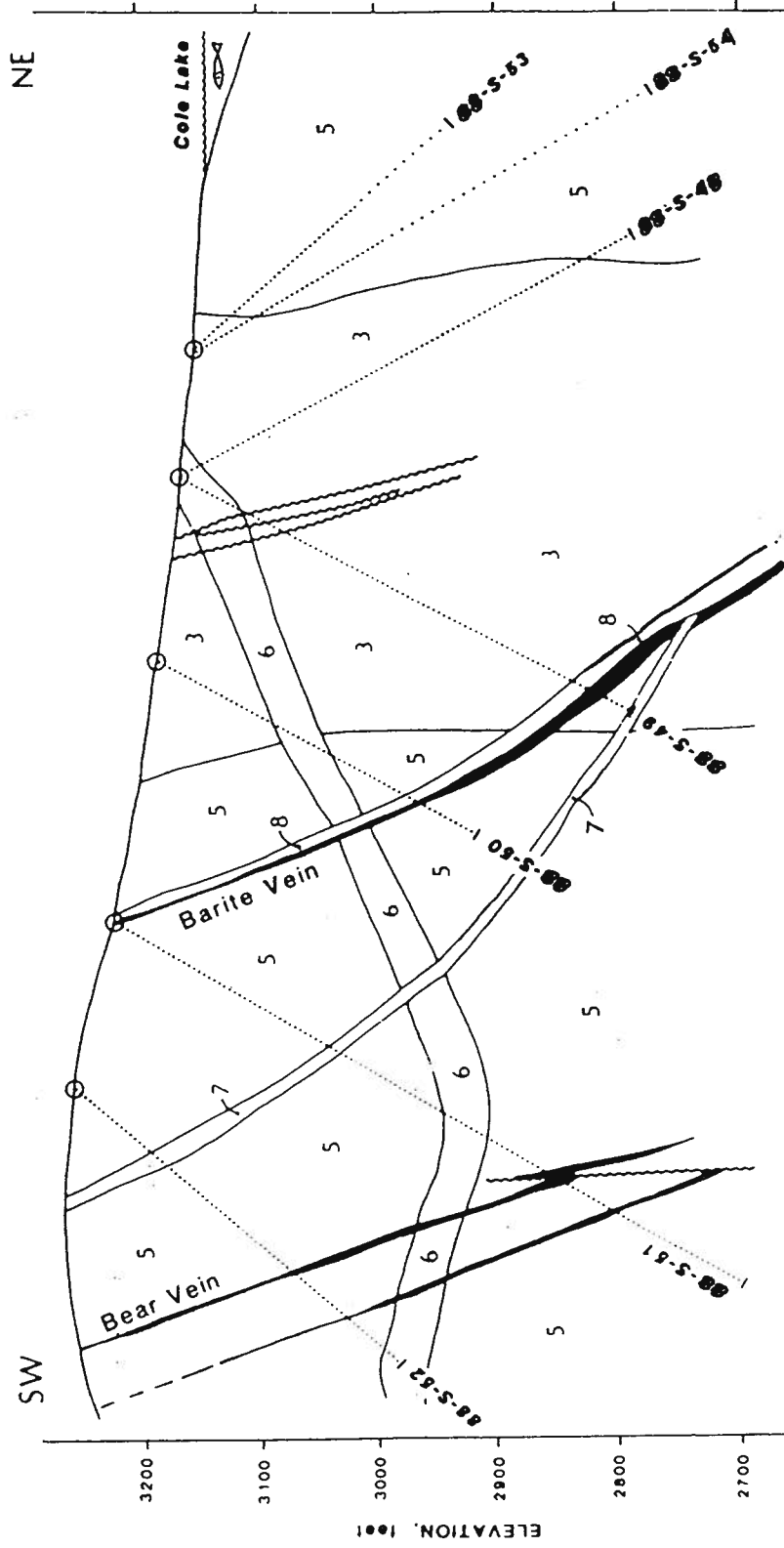


Figure 4-8. Cross-section of Cole vein shows gently dipping dike of unit 6 cut by later dikes of Units 7 and Unit 8. Horizontal scale equals vertical scale. Numbers represent the geological units which are defined in Table 4-1. Thick solid line - vein, thin solid line - geological contact, dash line - drill, circle - drill site.

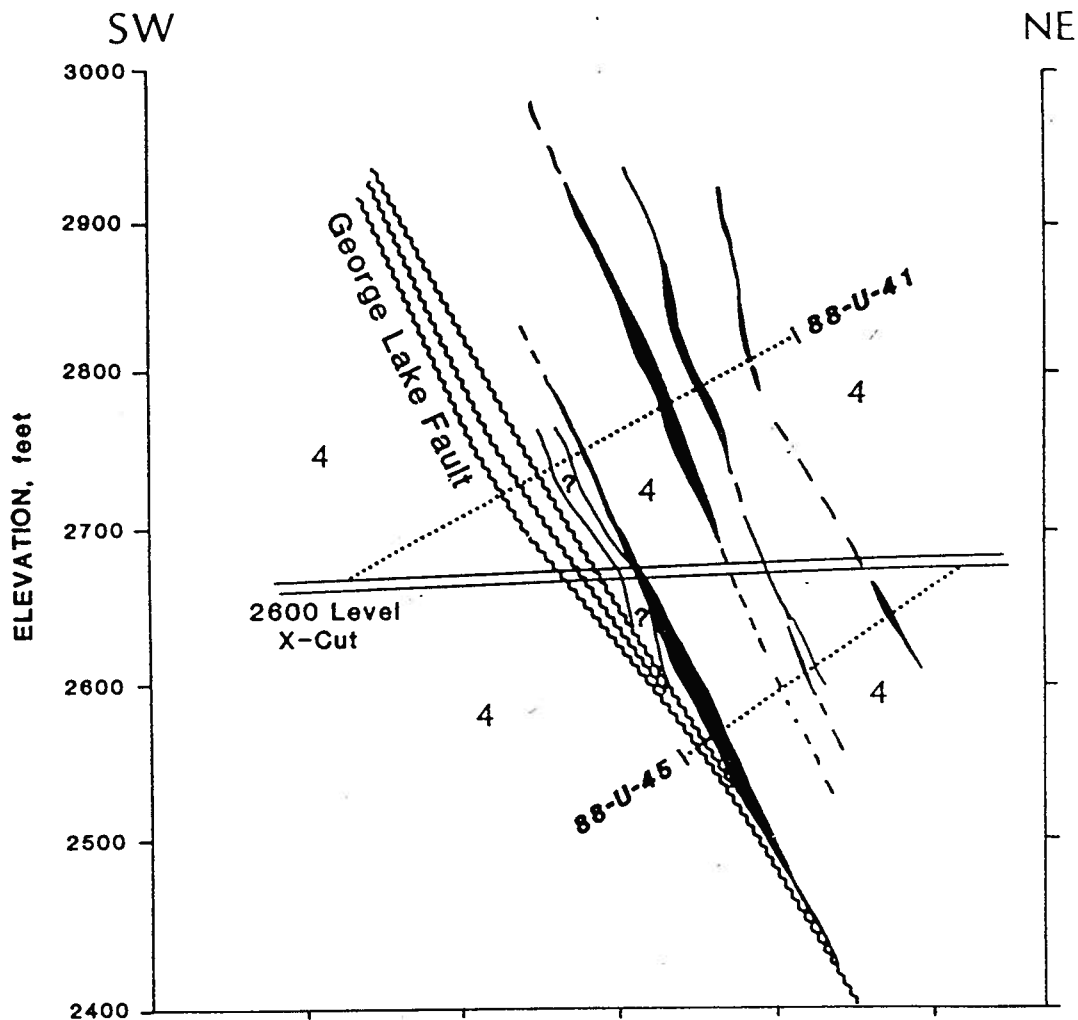


Figure 4-9. Cross-section of George vein at the 2600 foot level of the Bulkley cross-cut, with the available intersections interpreted as part of an *en echelon* system. Horizontal scale equals vertical scale. Numbers represent the geological units which are defined in Table 4-1. Thick solid line - vein, thin solid line - geological contact, dash line - drill, circle - drill site.

The sense of motion on the northeast faults appears to be south side down, with a small component of sinistral shear. Offsets of No. 1 and 2 veins across the fault along Wrinch Creek (Fig. 4-2) suggest a few m of left-lateral displacement, but the displacement of an amygdaloidal dike near the portals of the 2880 level suggests the south side must have dropped as well. The boundaries of this fault zone, and its dip, are not well constrained; in outcrops in Wrinch Creek, it appears as a vaguely defined zone up to 10 m wide, with segments that have possible shallow southerly to moderate northerly dips. The Cole Creek fault is not well exposed at surface; a splay from it may cause the change in orientation of the No. 3 vein to the Ruby vein (Fig. 4-2). A considerable left-lateral offset of as much as 200 m is suggested by drill-hole intersections of the NG3 vein, which may be a faulted extension of the No. 3 vein south of the Cole Creek fault. Underground, this fault is exposed at the southernmost extent of drifting as a northeast-trending gouge zone 1 to 2 m thick. Other examples of minor northeast faults are seen underground.

Most of the dikes show similar orientations to the veins (310-325/60-85°NE), with the pre-mineral amygdaloidal dikes commonly found parallel and adjacent to the veins. Along the No. 3 vein, one such major dike causes significant dilution problems due to the incompetent nature of some of these soft, strongly clay-altered dikes near the veins. There is one major exception to this northwest trend: a prominent gently west-dipping (323/33°SW) set of Unit 6 (pre-mineralization amygdaloidal dikes) is well-developed in both the No. 3 vein, Camp and Cole Lake areas (Fig. 4-5, 4-7, 4-8 and 4-9). This gently-dipping set is roughly orthogonal to the main, steeply northeast dipping dikes and veins, and also roughly parallel to the general gentle westerly dip of the host stratigraphy. A similar orthogonal fracture pattern, with steeply dipping fractures better mineralized and with stronger alteration surrounding them than the gently dipping fractures, is also observed in outcrops in Wrinch Creek.

4.7. SUMMARY

The sequence of rocks exposed in the Silver Queen mine area, mapped as Tip Top Hill Formation (Church, 1984) is petrographically and stratigraphically similar to the Kasalka Group as defined in the Tahtsa Lake area by MacIntyre (1985) and the Mount Cronin area by MacIntyre and Desjardins (1988). The section in all three areas comprises a sequence from a basal, reddish purple heterolithic conglomerate upwards through a sequence of fragmental volcanic rocks, to a widespread, partly intrusive porphyritic andesite, all intruded by a distinctive microdiorite. However, K-Ar dating suggests that the rocks in the Silver Queen mine area are of Late Cretaceous age; both porphyritic andesite volcanics and microdiorite are about 78 Ma. This is younger than the Kasalka Group rocks in the type section near Tahtsa Lake, which give dates of 108 to 107 Ma near the base, and are cut by intrusions dated at 87 to 84 Ma (MacIntyre, 1985). These dates actually straddle the Early to Late Cretaceous boundary (Harland et al., 1989). Thus, there may be two episodes, with the later one as young as 78 Ma (Leitch et al., 1991). Possibly the magmatic front associated with mid- to Late Cretaceous volcanic activity took longer to arrive further inland (i.e. 65 kilometres in 30 Ma gives a rate of advance of 0.22 cm per year, comparable to the rate of 0.25 cm annually suggested by Godwin, 1975; cf. Armstrong, 1988 and Leitch, 1989).

Mineralization in epithermal veins at the Silver Queen mine occurred after the time of deposition of the Late Cretaceous Kasalka Group and before the intrusion of Early Tertiary post-mineral dikes dated at about 50 Ma. Some of these dikes may correlate to the Goosly Lake trachyandesite volcanics (49 Ma) of the Ootsa Lake Group and syenomonzonite stocks (50 Ma) found at Equity Silver mine and Parrot Lakes (Church, 1973). Another dike is diabase (50 Ma), which also cuts the vein. It may correlate with the Buck Creek basaltic volcanics, dated at 48 Ma (Church, 1973). Although the main outcrop areas of Kasalka andesite and microdiorite correlate with the main areas of mineralization, and a genetic link has been postulated between two (Church, 1970), the

Late Cretaceous Kasalka andesite and microdiorite must have preceded mineralization by at least 25 Ma. So far there is no evidence at Silver Queen that the Early Tertiary dikes have remobilized older mineralization. Recognition of the fact that significant mineralization at Equity and Silver Queen is Early Tertiary in age, but is found in regionally correlative Upper Cretaceous rocks has important implications for metallogeny of the area. Since no significant mineralization has been found to date in the Early Tertiary rocks, it may be postulated that the Upper Cretaceous rocks represent a regional metallogenic province for base- and precious-metal mineralization. More significantly, it is possible that only the older (Cretaceous) rocks were sufficiently structurally prepared for ore deposition during a period of widespread magmatism during the Early Tertiary (Leitch et al., 1991).

Chapter 5. Hydrothermal Alteration at the Silver Queen mine: Field and Petrographic Characters

5.1. Introduction

The aim of this chapter is to describe petrographically the various hydrothermal alteration types, the spatial zonation of alteration associated with precious- and base-metal veins in volcanic sequences and the paragenetic sequences of the alteration mineral assemblage at the Silver Queen mine. Hydrothermal alteration at the Silver Queen mine has been examined in a preliminarily way by other workers. Most of the previous work focused mainly on the alteration types and only briefly discussed the spatial zonation of alteration. Fyles (1984) stated that clay with or without sericite is common at the Silver Queen mine, the principal clay mineral is kaolinite and the principal carbonate is siderite. Bernstein (1987) reported that alteration envelopes associated with Zn-Pb-Cu-Au-Ag sulfide-rich veins at the Silver Queen mine are characterized by silicification and argillic alteration. Church and Pettipas (1990) noted that the veins at the Silver Queen mine are commonly in an argillic envelope within a broader aureole of propylitic alteration. Cheng et al. (1991) presented field descriptions and a preliminary petrographic study of the hydrothermal alteration envelopes.

Emphasis in the present chapter is given to the qualitative identification of the alteration mineral assemblages, their spatial zonation in the wall rock, specifically andesite (Unit 4) and microdiorite (Unit 5) of the vein and their paragenetic sequences. Results are based on 20 km² field mapping, drill core logging, 72 whole rock sampling, 140 thin section examination and X-ray diffraction analysis. These investigations have defined a specific succession of related alteration and mineralization events at the Silver Queen mine and contribute to the development of a genetic model for this type of mineralization system.

5.2. Petrography of Hydrothermal Alteration Types

Six types of hydrothermal alteration have been recognized at the Silver Queen mine, viz. (i) propylitization, (ii) carbonatization, (iii) sericitization, (iv) argillization, (v) silicification and (vi) pyritization. They are further classified into three zones on which carbonatization is superimposed to various degrees: propylitic alteration halo, sericitic-argillic alteration outer envelope, and silicic-pyritic alteration inner envelope. Detailed descriptions of these hydrothermal alteration types at the Silver Queen mine are given below.

Propylitic alteration is typically a weak alteration (Cheng, et al., 1991).

Propylitically altered andesite is black or dark green in color, dense and hard. A strong magnetic character that can be tested easily in the field with a hand magnet indicates the presence of relatively abundant magnetite.

The propylitically altered andesite is typical of those with porphyritic texture. A common mineral assemblage for the propylitically altered andesite is: aphanitic groundmass (about 40%), plagioclase (35-40%), clinopyroxene (0-6%), hornblende (0-4%), biotite (0-2%), epidote (0-4%), chlorite (4-8%), carbonates (1-15%), sericite (1-8%), and accessory magnetite and ilmenite (about 5%) and apatite and zircon (trace). Of these, plagioclase, biotite, augite and hornblende are replaced by epidote, chlorite, carbonate and sericite to various degrees. Pseudomorphs of epidote, chlorite and carbonate after clinopyroxene and hornblende are commonly well preserved. The remaining minerals are not obviously affected by hydrothermal alteration (Figure 5-1).

Propylitically altered microdiorite has features roughly equivalent to those of propylitically altered andesite, except that it is paler in color and of granular or porphyroid texture. A common mineral assemblage for the propylitically altered microdiorite is: unidentified fine grain minerals (about 10%), plagioclase (25-35%), augite (0-6%), hornblende (0-4%), K-feldspar (about 10%), quartz (about 10%), epidote (0-2%), chlorite

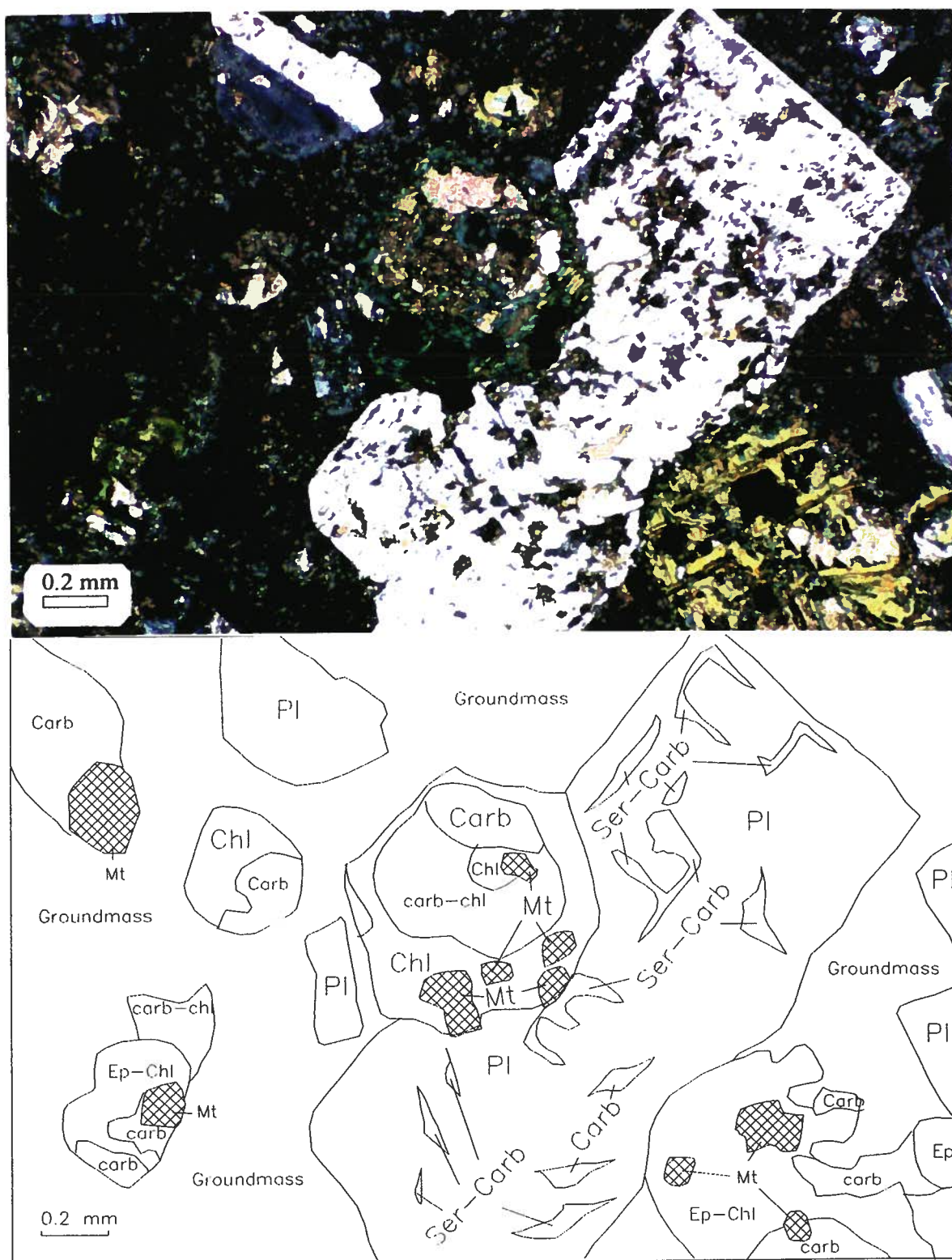


Figure 5-1. Photomicrograph (crossed nicols) of propylitically altered andesite with superimposed carbonatization (SQ-44: surface outcrop sample from the southern segment of the No. 3 vein). Plagioclase (Pl) phenocrysts are partially replaced by sericite (Ser) and carbonate (Carb). Augite phenocrysts are completely replaced by epidote (Ep), chlorite (Chl), carbonate and magnetite (mt).

(3-10%), carbonate (5-15%), sericite (2-8%), and accessory magnetite and ilmenite (about 5%) and apatite and zircon (trace). The grain sizes of plagioclase, augite and hornblende are relatively coarser. They are commonly replaced by: epidote, chlorite, carbonate and sericite to various degrees (Figure 5-2).

Sericitic-argillic alteration commonly appears as a bleached outer envelope around a vein. This type of alteration is called as 'moderate' and is more intense than propylitic alteration. Microdiorite and andesite having this type of alteration are softer and paler than their propylitic alteration equivalent. Magnetite is altered to hematite or pyrite. Biotite is unstable in this type of alteration and is progressively replaced by muscovite. Pseudomorphs of primary minerals, especially plagioclase, are remarkably well preserved. Recrystallization, especially of quartz, is obvious in the groundmass. Sericite, kaolinite and carbonates are the major dominant mineral phases and are commonly present with very fine grain size (Figure 5-3). An approximate mode of this type of altered rock is: unidentified fine grain minerals (about 25%), sericite (16-42%), kaolinite (0-28%), quartz (15-20%), hematite (2-6%), pyrite (0-5%), siderite and dolomite (4-10%) as well as trace amount of apatite, rutile and zircon.

Silicic and pyritic alteration is the most intense alteration type at the Silver Queen mine in terms of the variations of mineral composition and rock texture. It can develop particularly intensely altered zones of hard, pale apple green rock where fresh and orange-yellow on weathered surfaces. No magnetite is present. A distinctive feature of this type of alteration zone is that pseudomorphs of primary minerals are not preserved as well as they are in sericitic and argillic alteration zones. The texture of the silicification and pyritization alteration zone is mosaic or polygonal (Figure 5-4). The rock is characterized by having a simple mineral assemblage. For example, unidentified fine grain minerals (about 20%), quartz (26-30%), sericite (10-28%), kaolinite (0-24%), carbonates (10-15%) and pyrite (10-15%) as well as trace amount of apatite, rutile and zircon.

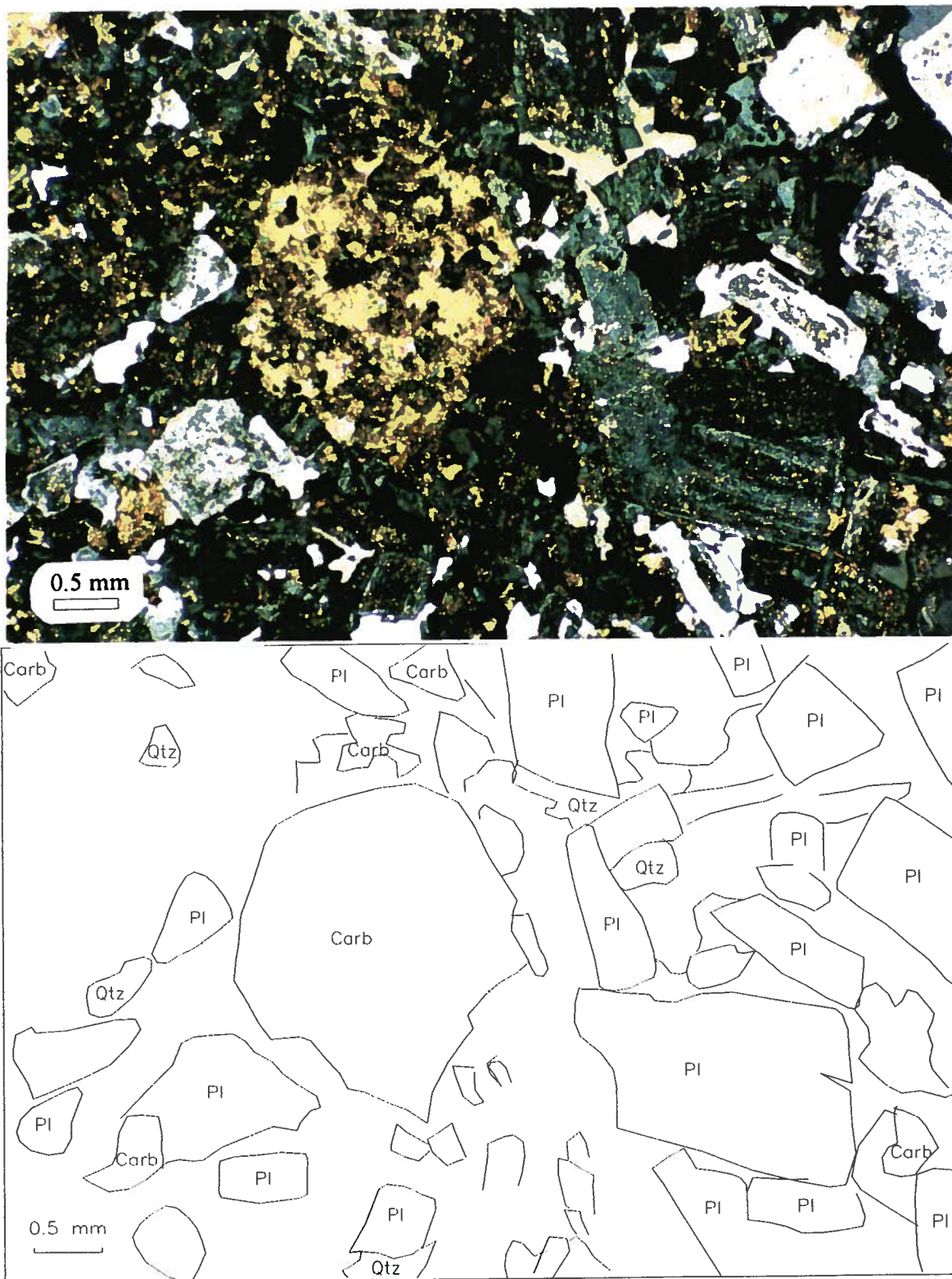


Figure 5-2. Photomicrograph (crossed nicols) of propylitically altered microdiorite with superimposed intense carbonatization (SQ-85: surface outcrop sample from the Cole lake segment). Note rock has an unequal-granular texture. Pseudomorph of carbonate after augite and some plagioclase (Pl) crystals partially replaced by carbonate (carb) and sericite (ser) are relatively coarse grained. Compare to Figure 5-1. Primary augite phenocryst is completely replaced by carbonate instead of by epidote, chlorite and carbonate.

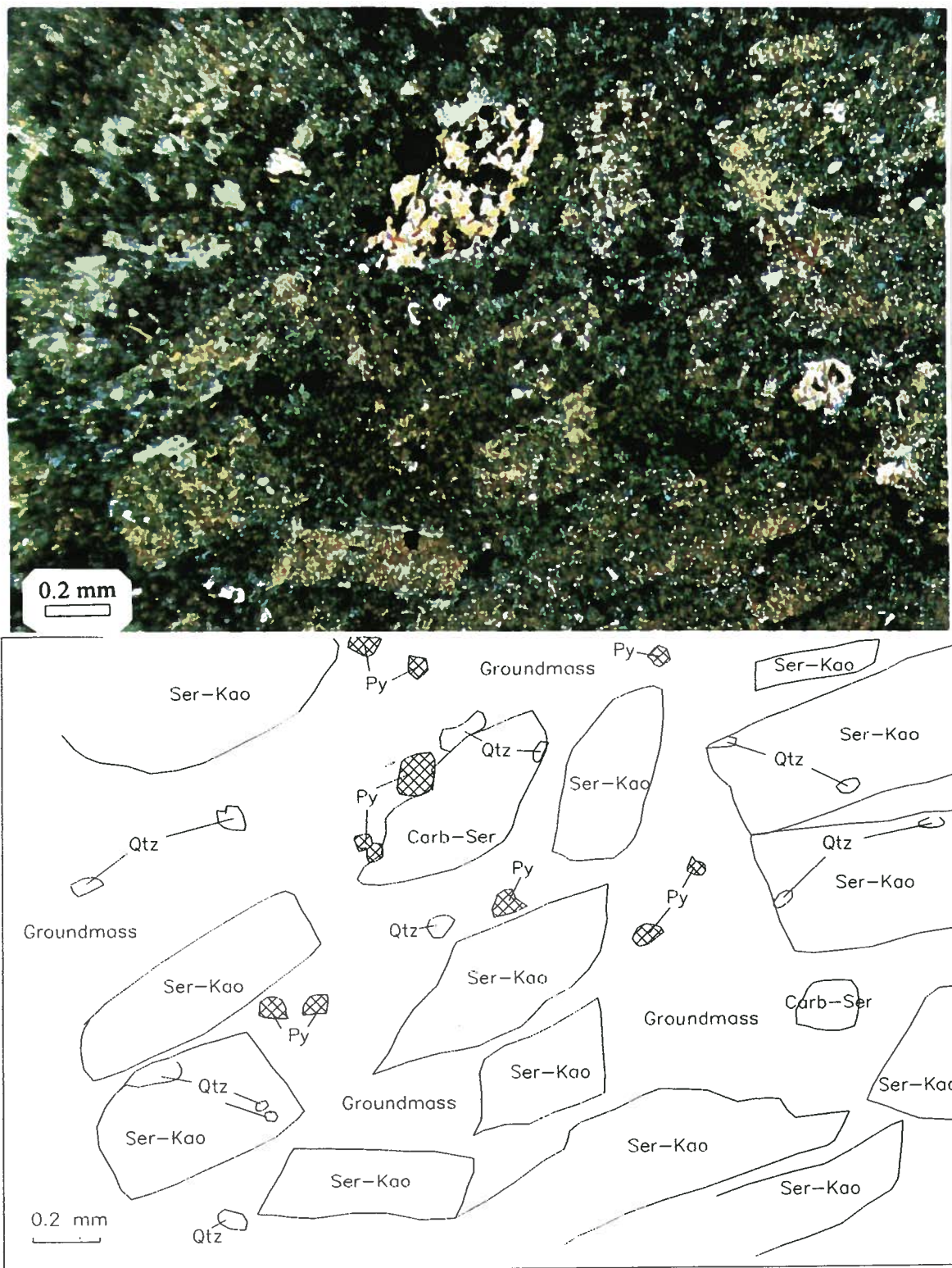


Figure 5-3. Photomicrograph (crossed nicols) of sericitized-argillized andesite (X5-3: underground sample from the southern segment of the No. 3 vein). Note pseudomorph of sericite (Ser), kaolinite (Kao) and quartz (Qtz) after plagioclase; pseudomorph of sericite and carbonate (Carb) after mafic phenocryst.

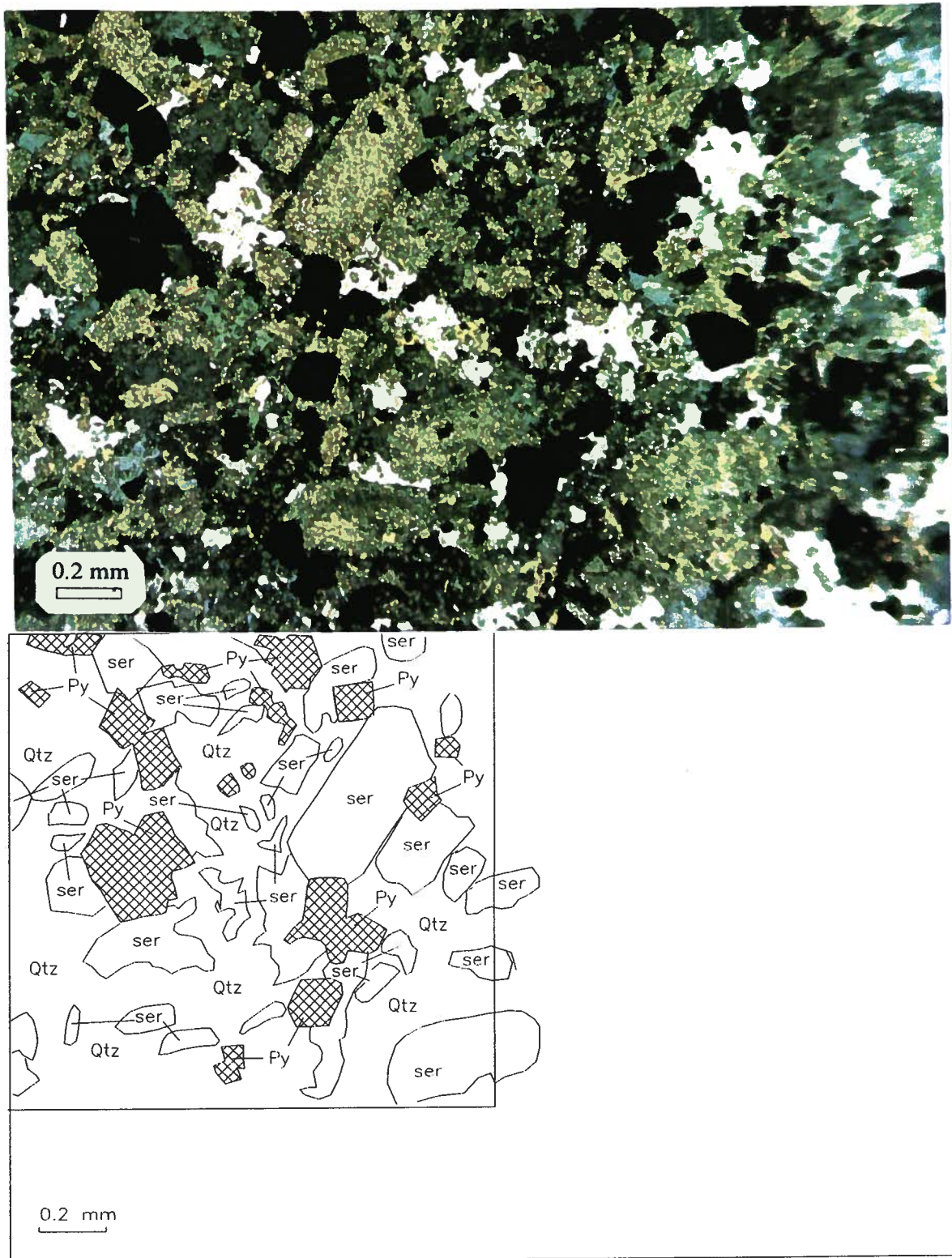


Figure 5-4. Photomicrograph (crossed nicols) of silicified-pyritized microdiorite (X5-10: underground sample from the southern segment of the No. 3 vein). Note the replacement of sericite (Ser) by abundant quartz (Qtz) and the formation of abundant pyrite (Py). The pseudomorph of sericite and kaolinite (Kao) after plagioclase is not preserved as well as those in the outer sericitic-argillic alteration envelope.

Carbonatization superposed on propylitically altered rock is characterized by the further replacements of epidote, chlorite and plagioclase by carbonates. Where the rock is intensively carbonatized, epidote and chlorite are completely replaced by carbonates which become pervasive in the rock (Figure 5-2). Of the carbonates calcite is an abundant species characterized by reacting with diluted acid fiercely. Carbonatization is also observed in the visible alteration envelope (sericitic and argillic alteration, and silicification and pyritization envelope as described below) as replacements of calcite and chlorite by Fe- and Mg-carbonates such as siderite and dolomite.

5.3. The Spatial Distribution of Hydrothermal Alteration

In general, the zonation of hydrothermally altered rocks in the Silver Queen mine district consists of a broad propylitic alteration halo which gives way as the polymetallic vein is approached to a broad bleached outer sericitic-argillic alteration envelope, which in turn gradates into a narrow inner silicic-pyritic alteration envelope (Figure 5-5).

All rocks within the study area, that are older than mineralization, have affected some degree of propylitic alteration. That is, an early stage of propylitic alteration appears to be regional in extent ($> 20 \text{ km}^2$). The least propylitized andesite and microdiorite are characterized by only slight alteration of plagioclase by sericite and partial replacement of mafic minerals (clinopyroxene and hornblende) by epidote and chlorite with very minor carbonate. A propylitically altered rock with superimposed carbonatization has been recognized at the Silver Queen mine through the examination of a total of 140 thin sections from various successive profiles cross-cutting the No. 3 vein throughout its length and rock samples altered to various degrees from different parts of the Owen Lake area. The spatial distribution of propylitically altered rocks with superimposed carbonatization is controlled by a complicated structure system, rather than by being restricted to the vein and associated mineralized structures. Samples collected a few hundred metres away from a vein commonly have intense propylitic alteration with superimposed carbonatization,

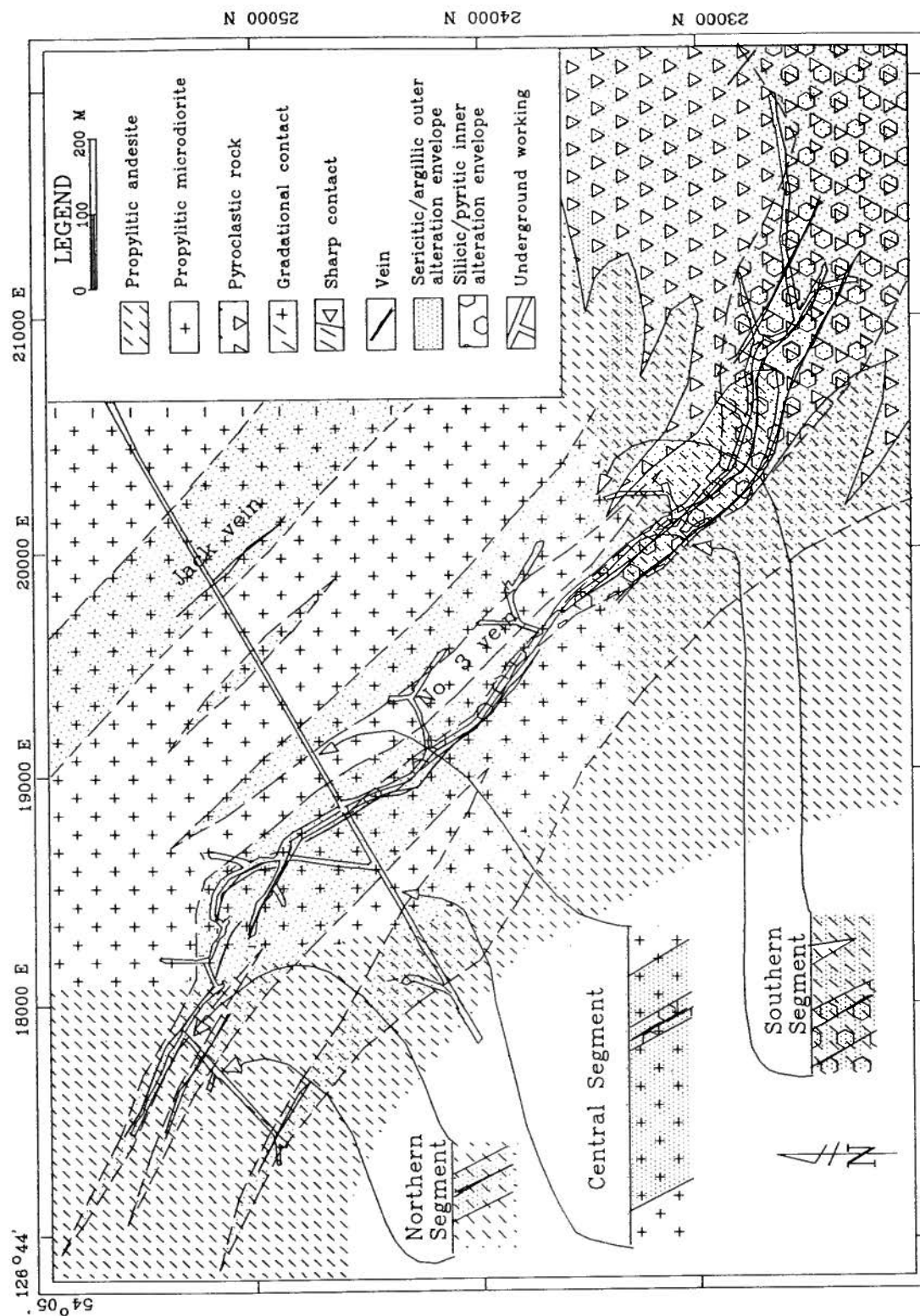


Figure 5-5. Schematic plan of hydrothermal alteration on the 2600-foot level, Silver Queen mine (modified from Cheng et al., 1991).

similar to or even stronger than those collected only a few metres from the bleached alteration envelope around the vein. In contrast, there is a tendency for the intensity of carbonatization in propylitically altered rocks at the southern segment of the No. 3 vein to be stronger than that at the northern segment of the No. 3 vein (Figures 5-6 and 5-7).

The bleached alteration envelope is characterized by having remarkable zonations both parallel and perpendicular to the vein. Three representative alteration profiles cross cutting the No. 3 vein at the 2600 foot level of the southern, the central, and the northern segments are illustrated in Figures 5-8a, 5-8b and 5-8c. In general, all alteration profiles have the following zonation parallel to the vein:

- (1) An outer sericitic and argillic alteration envelope commonly has a relative 'sharp contact' that grades from a bleached envelope into a dark colored propylitic wall rock within a few centimetres (Figure 5-9).
- (2) An inner silicification and pyritization envelope immediately adjacent to the vein has a gradational contact with the outer sericitic and argillic alteration envelope (Figure 5-10).

Zonation of alteration envelopes perpendicular to the veins are also presented. In detail, the silicic and pyritic inner envelope is almost absent at the northern segment of the No. 3 vein. Also, the alteration envelope is more argillic at the northern segment compared with the southern segment of the No. 3 vein which has more sericite than kaolinite. Silicification and pyritization are more intense at both the central and southern segments than at the northern segment of the No. 3 vein. In addition, the width of the alteration envelope is narrower along the northern segment of No. 3 vein (total width about 7 m wide) than adjacent to the central and southern segments of the No. 3 vein (total width up to 130 m wide).

Some alteration envelopes around veins are distributed asymmetrically. For example, the widths of the alteration envelopes at the northern and central cross-cuts of

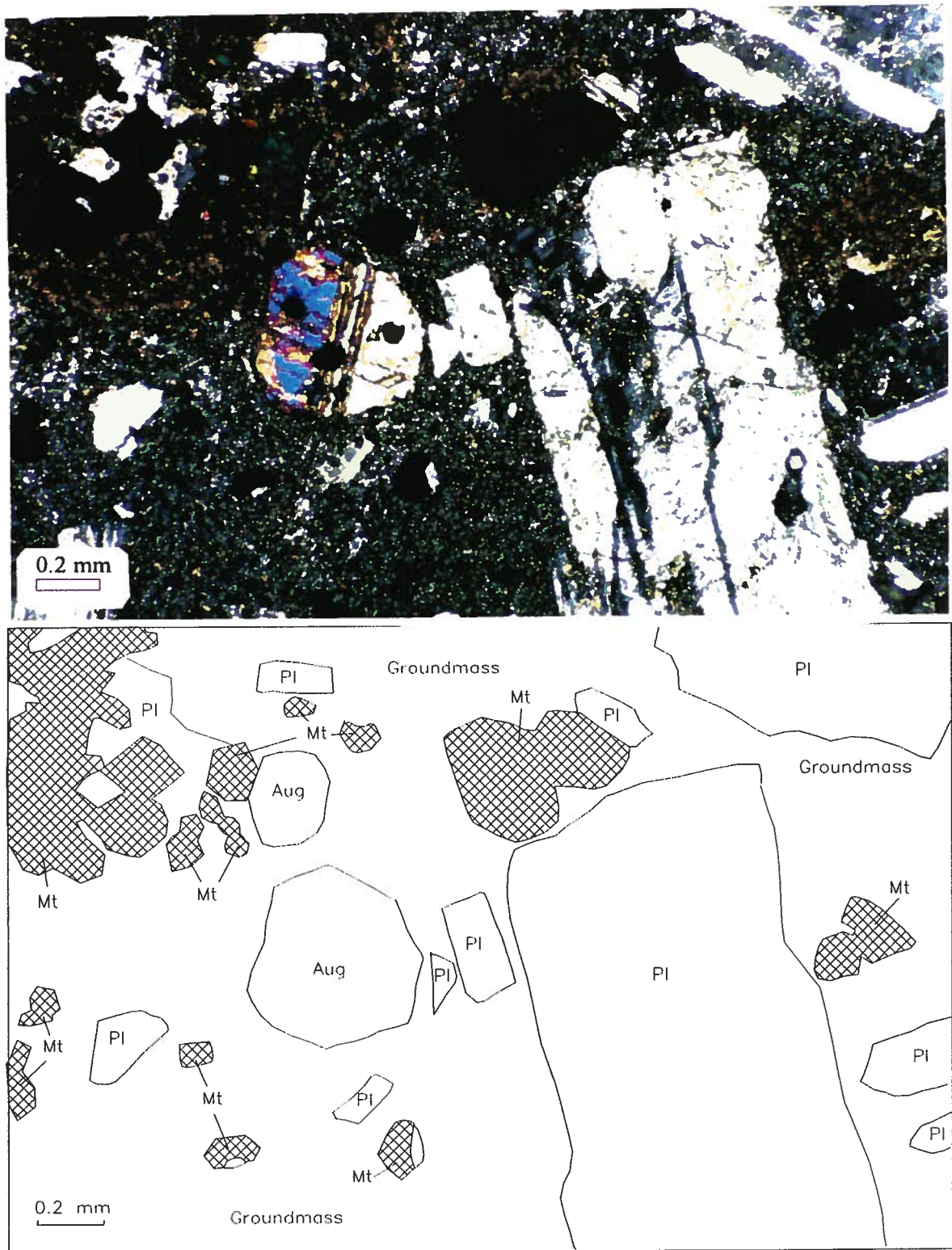


Figure 5-6. Photomicrograph (crossed nicols) of least propylitically altered andesite in the northern segment of the No. 3 vein (X3-7: underground sample from the northern segment of the No. 3 vein). Note primary phenocrysts (augite and plagioclase) are slightly altered along their margin and cleavages. Aug - augite; Pl - plagioclase, Mt - magnetite.

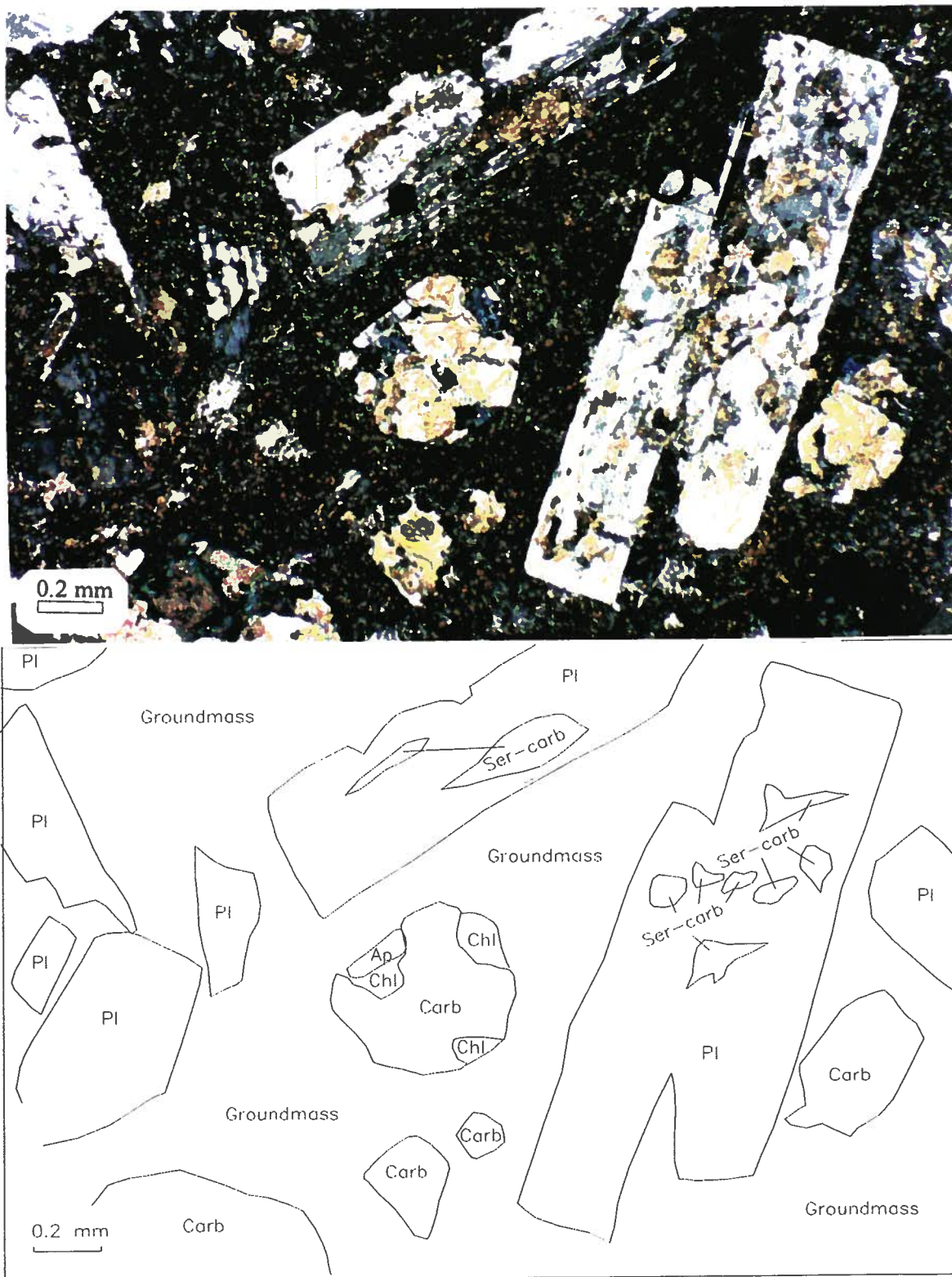


Figure 5-7. Photomicrograph (crossed nicols) of propylitically altered andesite with superimposed carbonatization in the southern segment of the No. 3 vein (SQ-44: surface outcrop sample from the southern segment of the No. 3 vein). Note pseudomorph of chlorite (Chl) and carbonate (carb) after augite, partial replacement of plagioclase (Pl) by carbonate and sericite (ser). Ap - apatite. Crossed nicols.

Tabel 5-1a. Estimated modes of alteration minerals in hydrothermally altered wall rock at the northern segment of the No. 3 vein, Silver Queen mine, central British Columbia

Mode (Volume %)	Propylitically altered andesite with superimposed carbonatization					Sericitic and argillic alteration envelope							
Distance (m)	10	9	8	7	6	5	4	3	2	1	0.5	0	
unknown*	40	40	40	40	40	25	25	25	25	25	20	20	
augite & Hb	7	9	10	7	5	0	0	0	0	0	0	0	
Epidote	1	2	2	1	0	0	0	0	0	0	0	0	
Chlorite	5	4	2	7	7	0	0	0	0	0	0	0	
Carbonate	4	3	1	3	6	4	4	4	4	5	5	6	
Magnetite	5	5	5	4	4	0	0	0	0	0	0	0	
Pyrite	0	0	0	0	0	4	4	3	3	3	4	5	
feldspar	35	36	39	35	35	0	0	0	0	0	0	0	
Muscovite	3	1	1	3	3	27	27	22	22	18	18	16	
Kaolinite	0	0	0	0	0	25	25	26	26	27	28	28	
Quartz	0	0	0	0	0	15	15	20	20	22	25	25	
Total	100	100	100	100	100	100	100	100	100	100	100	100	

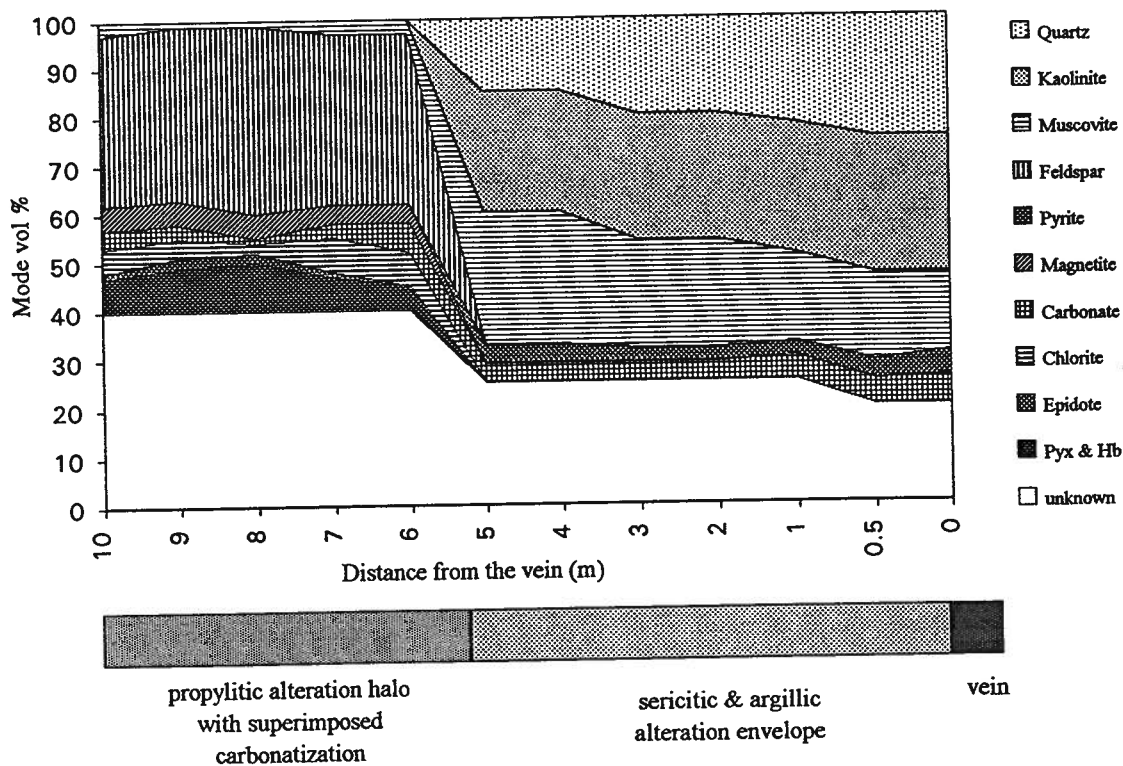


Figure 5-8a. Estimated mode of alteration minerals in hydrothermal alteration profile at northern segment of the No. 3 vein at the Silver Queen mine. Unknown - unidentifiable material including groundmass and extremely fine-grain mineral aggregates.

Tabel 5-1b. Estimated mode of alteration minerals in hydrothermally altered wall rock near the central segment of the No. 3 vein, Silver Queen mine, central British Columbia

Mode (Volume %)	Propylitic microdiorite with superposed carbonatization				Sericitic & argillic outer envelope					Silicic & pyritic inner envelope		
Distance (m)	50	45	39	38	35	30	20	10	5	4	1	0
Unknown	20	20	20	20	12	12	12	12	12	10	10	10
augite & Hb	6	7	5	4	0	0	0	0	0	0	0	0
Chl & Epi	12	9	5	12	0	0	0	0	0	0	0	0
Carbonate	5	10	15	10	5	5	8	8	10	10	12	15
Magnetite	5	5	5	5	0	0	0	0	0	0	0	0
Hematite	0	0	0	0	6	6	4	4	2	0	0	0
Pyrite	0	0	0	0	0	0	2	2	4	10	12	15
feldspar	45	38	34	38	0	0	0	0	0	0	0	0
Muscovite	2	5	8	5	42	42	32	32	26	20	15	10
Kaolinite	0	0	0	0	20	20	22	22	22	24	23	20
Quartz	5	6	8	6	15	15	20	20	24	26	28	30
Total	100	100	100	100	100	100	100	100	100	100	100	100

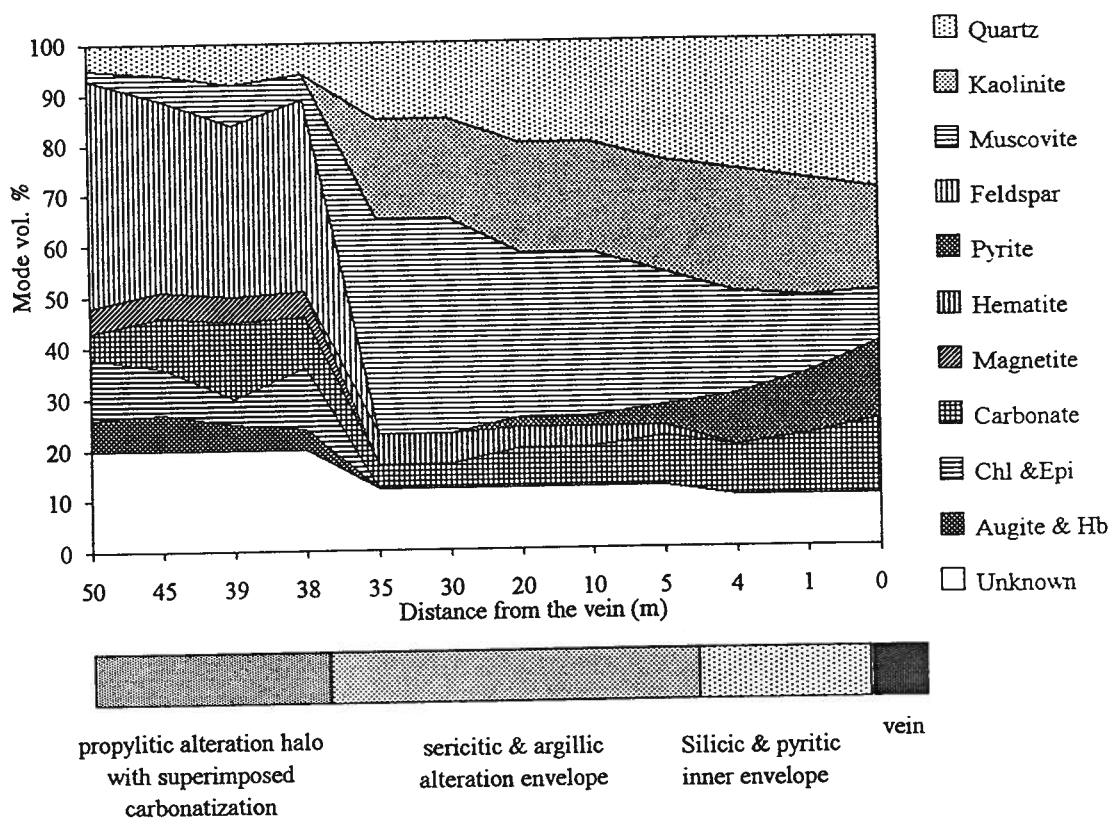


Figure 5-8b. Estimated mode of alteration minerals in hydrothermal alteration profile at central segment of the No. 3 vein at the Silver Queen mine. Unknown - unidentifiable material including groundmass and extremely fine-grain mineral aggregates.

Tabel 5-1c. Estimated mode of alteration minerals in hydrothermally altered wall rock near the southern segment of the No. 3 vein, Silver Queen mine, central British Columbia

Mode (Volume %)	Propylitic microdiorite with superposed carbonatization				Sericitic & argillic outer envelope					Silicic & pyritic inner envelope		
Distance (m)	60	55	50	48	45	35	25	20	15	10	5	0
Unknown	40	40	35	35	25	25	25	25	25	20	20	20
Augite & Hb	4	2	2	0	0	0	0	0	0	0	0	0
Chl & Epi	8	10	6	8	0	0	0	0	0	0	0	0
Carbonate	6	8	12	15	5	5	8	8	10	10	12	12
Magnetite	5	5	5	5	0	0	0	0	0	0	0	0
Hematite	0	0	0	0	5	5	3	3	2	0	0	0
Pyrite	0	0	0	0	0	0	2	2	3	10	12	12
Feldspar	35	30	30	30	0	0	0	0	0	0	0	0
Muscovite	2	5	8	5	38	38	30	32	30	28	28	26
Kaolinite	0	0	0	0	12	12	12	10	6	4	0	0
Quartz	0	0	2	2	15	15	20	20	24	28	28	30
Total	100	100	100	100	100	100	100	100	100	100	100	100

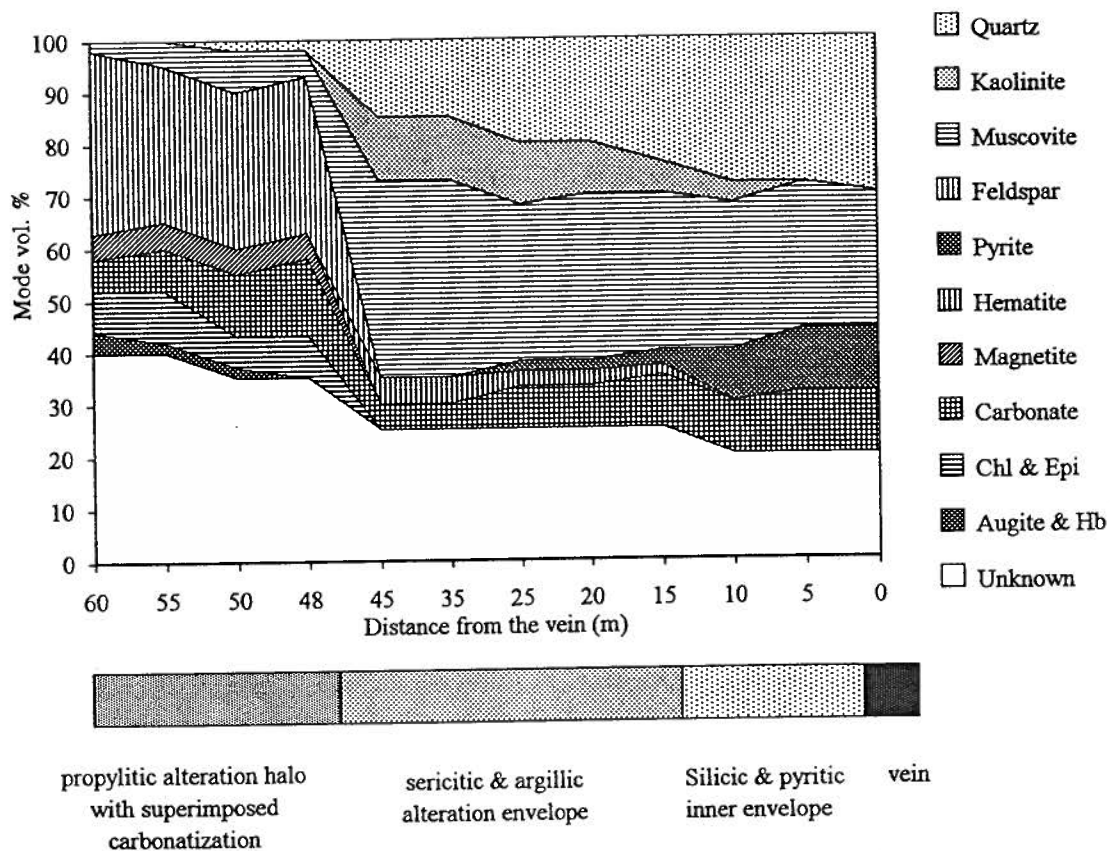


Figure 5-8c. Estimated mode of alteration minerals in hydrothermal alteration profile near the southern segment of the No. 3 vein at the Silver Queen mine. Unknown -unidentifiable material including groundmass and extremely fine-grain mineral aggregates.



Figure 5-9. The relatively sharp contact between propylitic alteration and a bleached alteration envelope (Bulkley cross-cut, 2600 foot level underground working).



Figure 5-10. Outcrop of the southern segment of the No. 3 vein and its bleached alteration envelope.

the No. 3 vein are greater on the footwall than on the hanging-wall. At the cross cuts of the Jack and George veins the situation is reversed (Figure 5-5). These asymmetrical features can be explained by *en echelon* geometry of individual veins within mineralized zones (Leitch et al., 1991). The reason for these is that the alteration envelope is developed around the structure zone centering the *en echelon* veins. Therefore, the alteration envelope may appear in different asymmetrical patterns depending upon where the cross-section cuts the upper or lower part of an individual vein (see Figure 5-11). This explanation may help exploration for hydrothermal veins developed in *en echelon* structural patterns.

5.4. Paragenetic Sequence of Hydrothermal Alteration

Propylitization, carbonatization, sericitization, argillization and silicification as well as pyritization, have all taken place in the host rock at the Silver Queen mine. Consistent, systematic sequences of alteration minerals and specific zoned distributions are observed in the host rocks. Many other textures and features in vein-wall-rock profiles strongly support the concept of a consistent sequence in the development of the hydrothermal mineral assemblages at the Silver Queen mine.

The distribution of broad propylitic alteration halos suggests that this type of alteration is the product of regional, pre-mineralization hydrothermal activity. Carbonatization controlled by the complicated fracture system developed subsequent to regional propylitic alteration and was superimposed on the propylitically altered rocks. The distribution of bleached alteration envelopes around mineralized structures suggests that the bleached alteration envelopes developed subsequent to, and superimposed on, the broad propylitic alterations referred to above. A series of schematic profiles are constructed to illustrate the spatial distribution pattern and timing sequences of these alteration types (Figure 5-12).

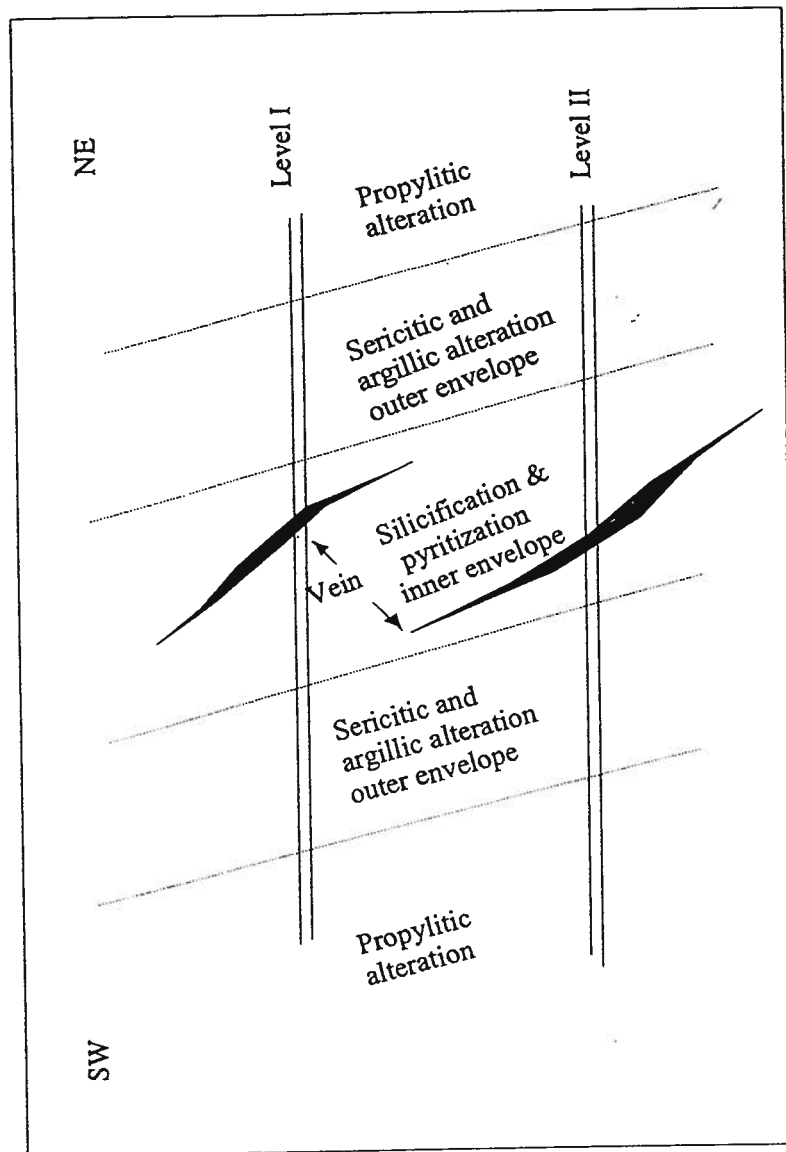


Figure 5-11. Schematic profile illustrates the asymmetrical relationship between en echelon veins and hydrothermal alteration envelopes, Silver Queen mine.

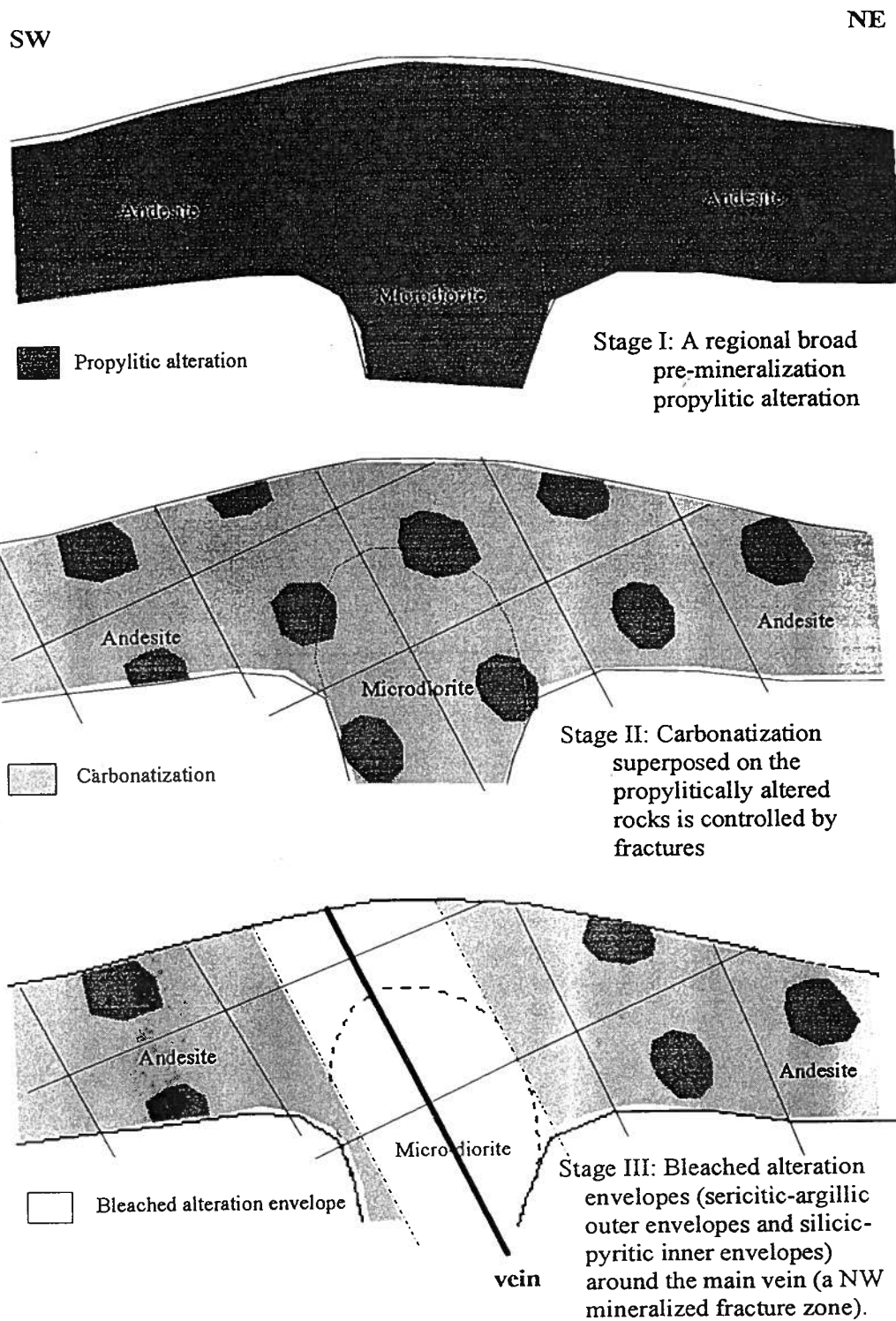


Figure 5-12. A series of schematic profiles illustrate the spatial zonation and sequence of development of various types of alteration at Silver Queen mine.

The general sequences of formation of alteration minerals has been established by the replacement relationship between mineral pairs. Microscopic observations indicate the following alteration sequences. Propylitically altered samples show that mafic minerals such as augite and hornblende and plagioclase are initially altered to epidote, chlorite, calcite and sericite along margins and cleavages (Figures 5-1, 5-2, 5-3, 5-6 and 5-7). These replacements are completed where propylitic alteration is intense with superimposed carbonatization; in such cases pseudomorphs of carbonate, mainly calcite, after primary mafic mineral occur. Early epidote and chlorite are replaced by carbonate (Figure 5-2). Biotite, magnetite, apatite and zircon remain unchanged in the propylitic alteration halo. Quartz is not significantly changed in the propylitic alteration halo.

In the bleached alteration envelope near the propylitic alteration halo, primary minerals are completely altered. In particular, plagioclase is completely replaced by sericite and kaolinite along with quartz. Clinopyroxene and hornblende are totally altered to carbonate. No epidote or chlorite pseudomorphs after primary minerals are present in the bleached alteration envelope. Therefore, it appears that epidote, chlorite and calcite pseudomorphs after primary mafic mineral, as well as biotite, are further altered to sericite and siderite. Magnetite is totally altered to hematite and pyrite. Apatite and zircon retain their euhedral forms.

Quartz increases in the outer alteration envelope largely due to the decomposition of plagioclase (Figure 5-3). Silicification in the inner envelope is characterized by the progressive replacement of sericite by quartz; eventually sericite occurs as inclusions in pervasive quartz (up to about 30 wt%). Siderite and other carbonates are abundant (up to 10 wt%). Pyrite is disseminated and locally, densely disseminated (content up to about 15 wt%) in the inner alteration envelope. Recrystallization and silicification of the matrix are intense in the inner alteration envelope (Figure 5-4).

Table 5-2. Paragenetic Sequence of Mineral Assemblages, Silver Queen mine, Owen Lake Area

Minerals	Crystallization	Propylitization	Sericitization & argillization	Silicification & pyritization
Magnetite/ilmenite	—			
Apatite	—			
Zircon	—			
Augite	—			
Hornblende	—			
Plagioclase	—			
K-feldspar	—			
Biotite	—			
Quartz	—			
Epidote	—			
Chlorite	—			
Calcite	—			
Siderite/dolomite	—			
Kaolinite	—			
Muscovite	—			
Pyrite	—			
Hematite	—			
Rutile	—			

Note: The solid line and its thickness represent the formation of a mineral and its semiquantitative abundance.
The dash line means that the minerals remain stable at certain alteration stages.

Combining all the relationships described above leads to a general paragenetic sequence for the alteration around veins at the Silver Queen mine. This sequence is summarized and illustrated in Table 5-2.

5.5 Discussion and Conclusions

Hydrothermal alteration patterns, similar to those described above, have been reported in many other deposits [e.g., Waite Amulet (Price and Bancroft, 1948), Creed and Summitville (Hayba et al., 1985), Sigma (Robert and Brown, 1984, 1986), Round Mountain (Sander and Einaudi, 1990), Erickson (Sketchley and Sinclair, 1991), Porgera (Richards et al., 1991)].

In comparison with the alteration patterns reported by Robert and Brown (1984, 1986) and Sketchley and Sinclair (1991), the propylitic alteration with superimposed carbonatization at the Silver Queen mine shares many similar features with the cryptic alteration at Sigma mine and the carbonate envelope at Erickson mine in terms of alteration mineral assemblages and the mineral paragenetic sequence. For example, primary mafic minerals initially replaced by epidote and chlorite are subsequently replaced by carbonate. However, there are significant differences in the spatial distribution patterns between the propylitic alteration with superimposed carbonatization at the Silver Queen mine and the cryptic alteration reported at the Sigma mine. The width of the cryptic alteration zone is up to 2 m into the walls of the veins at the Sigma mine (Robert and Brown, 1984). The spatial distribution of propylitically altered rock with superimposed carbonatization at the Silver Queen mine is much more widespread than the Sigma example (Figure 5-5). Propylitic rocks with intense carbonatization have also been found at Goose Lake, about 10 kilometres southwest of the Silver Queen mine, but no vein mineralization was found nearby. In short, the distribution pattern of the propylitic alteration with superimposed carbonatization at the Silver Queen mine is a wide irregular halo, unlike a restricted envelope that locally parallels the veins. In contrast, the intensity

of carbonatization, more precisely the completeness of the replacement of epidote and chlorite by carbonate, is weak in the northern segment of the No. 3 vein and stronger to the south.

In brief, the distribution pattern of propylitic alteration with superimposed carbonatization at the Silver Queen mine is likely controlled by a complicated fracture system rather than by the mineralized structure zone only. It is suggested that the propylitic alteration at the Silver Queen mine might be related to the hydrothermal activities that immediately followed the volcanic eruption and intrusion of the early Late Cretaceous Kasalka Group equivalent rocks. Carbonatization superimposed on the early propylitic alteration halo may be the product of a CO₂ degassing process. This might be related to the hydrothermal activity associated with mineralization and controlled by a complicated fracture system. Even though the propylitic alteration with superimposed carbonatization at the Silver Queen mine is not an alteration envelope, the distribution pattern of propylitic alteration with superimposed carbonatization does indicate a broad CO₂ degassing halo that may be used to delineate the hydrothermal alteration anomaly associated with mineralization.

In summary, the following conclusions about hydrothermal alteration at the Silver Queen mine can be deduced based on observations above:

- (1) Regional propylitic alteration is characterized by replacement of mainly primary mafic minerals initially by epidote and chlorite as well as minor amount of carbonate and the partial replacement of plagioclase replaced by carbonate and sericite. This type of alteration is interpreted to be the product of hydrothermal activity followed by the initial stage of volcanism, which predates the mineralization.
- (2) Carbonatization superimposed on the early propylitic alteration halo may be the product of a CO₂ degassing process, which might be related to the hydrothermal activity associated with mineralization; it is controlled by a complicated fracture

system. With increasing intensity of superimposed carbonatization on propylitic alteration at Silver Queen, more complete replacement of epidote and chlorite by abundant carbonates occurs.

- (3) Hydrothermal activity associated with mineralization forms the outer alteration envelopes marked by complete replacement of plagioclase by sericite and kaolinite, chlorite by siderite and magnetite by pyrite or hematite.
- (4) Inner alteration envelopes are interpreted as maximum stage hydrothermal alteration superimposed on the sericitic and argillic outer alteration envelope; it is marked by the replacement of sericite by quartz and direct precipitation of quartz, sulfide and carbonate. The close association between mineralization and the inner silicification envelope indicates that the ore-forming metals are transported as Si, S and C complexes, and that the precipitation of quartz, sulfide and carbonate through reaction with wall rock and hydrothermal solution might trigger ore deposition.

6.1 Introduction

The Silver Queen mine is an ideal locality to study hydrothermal alteration for the following reasons:

- (1) The major types of the rocks that host the vein at the Silver Queen mine are andesite and diorite; these are typical wall rocks in many other ore deposits of similar type.
- (2) The petrographic and timing relations among various rock types and mineralization at the Silver Queen mine are well understood through contact relations, thin section study and isotopic dating.
- (3) The young ages and short interval between the formation of wall rock and mineralization event (about 78 Ma for the wall rock and 50 Ma for mineralization, respectively) as well as the simple deformation history in the study area exclude the complexities caused by other processes superimposed, but unrelated to, deposit genesis.
- (4) The uniformity of composition of both the andesite flows and the microdiorite dome, the two host units for veins, is favorable in terms of having a single precursor.
- (5) Abundant trenches, drill cores and underground workings provide good access for the study of alteration and its spatial relationship to veins.

Silver Queen mine, thus, provides an excellent opportunity to evaluate the quantitative effects of hydrothermal alteration spatially associated with precious- and base-metal vein mineralization in volcanic sequences.

This chapter discusses a quantitative evaluation of the hydrothermal alteration at the Silver Queen mine, Owen Lake area, central British Columbia by applying the approaches described in previous chapters. I specifically address:

- (i) optimal sampling and sample preparation method,
- (ii) estimation of the precisions of lithogeochemical data,
- (iii) determination of immobile components, and the calculation of absolute losses and gains of chemical constituents during the hydrothermal alteration,
- (iv) interpretation of the lithogeochemical variations in terms of mineral variations through the use of PER diagrams,
- (v) calculation of metasomatic norms,
- (vi) calculation of the propagated errors for the quantitative evaluations of lithogeochemical data, and
- (vii) integration of the mineralogical variations corrected for closure with the absolute losses and gains of chemical components and the errors at specific confidence levels to provide a quantitative chemico-mineralogic model of hydrothermal alteration.

6.2 Sampling and Sample Preparation

The collection and preparation of samples is an often overlooked aspect of data gathering that impacts strongly on the quantitative interpretation of losses/gains in hydrothermal systems. Many published papers related to lithogeochemistry do not document sampling and sample preparation methods in detail. For example, small chips collected from limited drill core may not be of sufficient size to represent the geological unit being sampled; a small sample may not be representative of coarse grained units. As shown in Chapter 3, the larger the sample mass and the finer the sample is ground, the more homogeneous and representative the sample can be made for subsampling. However, for economic reasons it is not desirable to collect too large a sample nor to grind a subsample finer than needed. In order to minimize the artificial sampling and sample preparation errors, equations 3-13 and 3-14 have been applied to samples used to study hydrothermal alteration at the Silver Queen mine.

Rock types in study area are massive and porphyritic volcanic flows and high level intrusive rocks. Therefore, the main sources of inhomogeneities at the sampling stage are: (i) the presence of phenocrysts such as plagioclase and augite, and (ii) accessory minerals such as rutile (rich in TiO_2) and zircon (rich in Zr). The results of calculated optimal sample sizes based on equations in Chapter 3 are presented in Table 6-1. These calculations indicate that the optimal sample size depends on the coarseness of phenocrysts and inhomogeneities of the constituents of interest among the minerals. For instance, plagioclase and augite phenocrysts are the important minerals which determine the size of a field sample because they are the coarsest minerals ($v \text{ (mm}^3\text{)} = 8$ and 1.73 respectively); albite and enstatite, as end members of these two mineral series, are rich in Na_2O and MgO relative to the rest of the rock (the values of $H_{\text{Na}_2\text{O}}$ and H_{MgO} of these two end member mineral phases are 0.24 and 0.40 respectively, whereas the value of $L_{\text{Na}_2\text{O}}$ and L_{MgO} for the rest of rock are 0.00 and 0.01 , respectively). Therefore, they are the biggest contributors to inhomogeneity of the sample, and nearly 500 grams of sample is needed to reduce the sampling error to about one percent at the 68% confidence level. In contrast, another relatively coarse mineral, quartz ($v \text{ (mm}^3\text{)} = 3.38$), has a high value of $H_{\text{SiO}_2} (= 1)$ but also a high value of $L_{\text{SiO}_2} (\geq 0.4)$ for the rest of the rock. This means that SiO_2 is distributed more homogeneously in the rock than Na_2O or MgO . According to the calculation using equation 3-13 and by treating the rest of bulk rock as the equivalent of ultramafic rock or mafic rock, only 15 grams of sample are necessary to provide an adequately homogeneous sample for analysis of SiO_2 . Accessory minerals, such as apatite, may have a high value of $H (=1)$ and the rest part of rock has the low value of $L (= 0)$, but commonly accessory minerals such as apatite have much finer grain size (e.g. 0.0005 mm^3). So if the sample size is just a few grams the homogeneity of P_2O_5 in the sample will be adequate. Therefore, 500 grams is considered the optimal sample size to provide adequate homogeneity for all components of the samples. This size results in a sampling error of less than or equal to 1% (R_E) at the 68% confidence level.

Table 6-1. Estimation of Optimal Sample Size by Using Binomial Function

Component	SiO ₂	TiO ₂	FeO	MgO	Na ₂ O	P ₂ O ₅	Zr
Mineral	Quartz	Rutile	Pyrite	Enstatite	Albite	Apatite	Zircon
v (mm ³)	3.375	0.064	0.125	1.728	8.000	0.0005	0.0003
H	1.000	1.000	0.470	0.402	0.240	0.424	0.498
L	0.400	0.001	0.010	0.010	0.000	0.000	0.000
d _H (g/cm ³)	2.648	4.245	5.011	3.210	2.620	3.180	4.669
d _L (g/cm ³)	2.87	2.87	2.87	2.87	2.87	2.87	2.87
P _w	0.150	0.005	0.050	0.050	0.300	0.005	0.0003
q _w	0.850	0.995	0.950	0.950	0.700	0.995	0.9997
R _E	0.01	0.01	0.01	0.01	0.01	0.01	0.01
(Hd _H -Ld _L) ²	2.250	17.996	5.413	1.588	0.395	1.818	5.406
(Hp _w + Lq _w) ²	2.40×10 ⁻¹	3.59×10 ⁻⁵	1.09×10 ⁻³	8.75×10 ⁻⁴	5.18×10 ⁻³	4.49×10 ⁻⁶	2.28×10 ⁻⁸
w (g)	15.0	376.2	60.2	466.7	475.5	3.2	38.9

Note: the notations used are defined in Chapter 3.

The detailed descriptions of sampling strategy including: sampling locations, the length of the profile that sample represented, rock and alteration type, as well as sample size are listed in Appendix A. An example of sampling strategy along a typical profile is illustrated in Figure 6-1. The samples are collected continuously in the intensely altered zone adjacent to the vein, and discontinuously in the broad moderately and weakly altered zones away from the vein.

Using equation 3-14, the optimal fineness of subsamples have been calculated and are listed in Table 6-2. This table shows various components, their principal minerals and

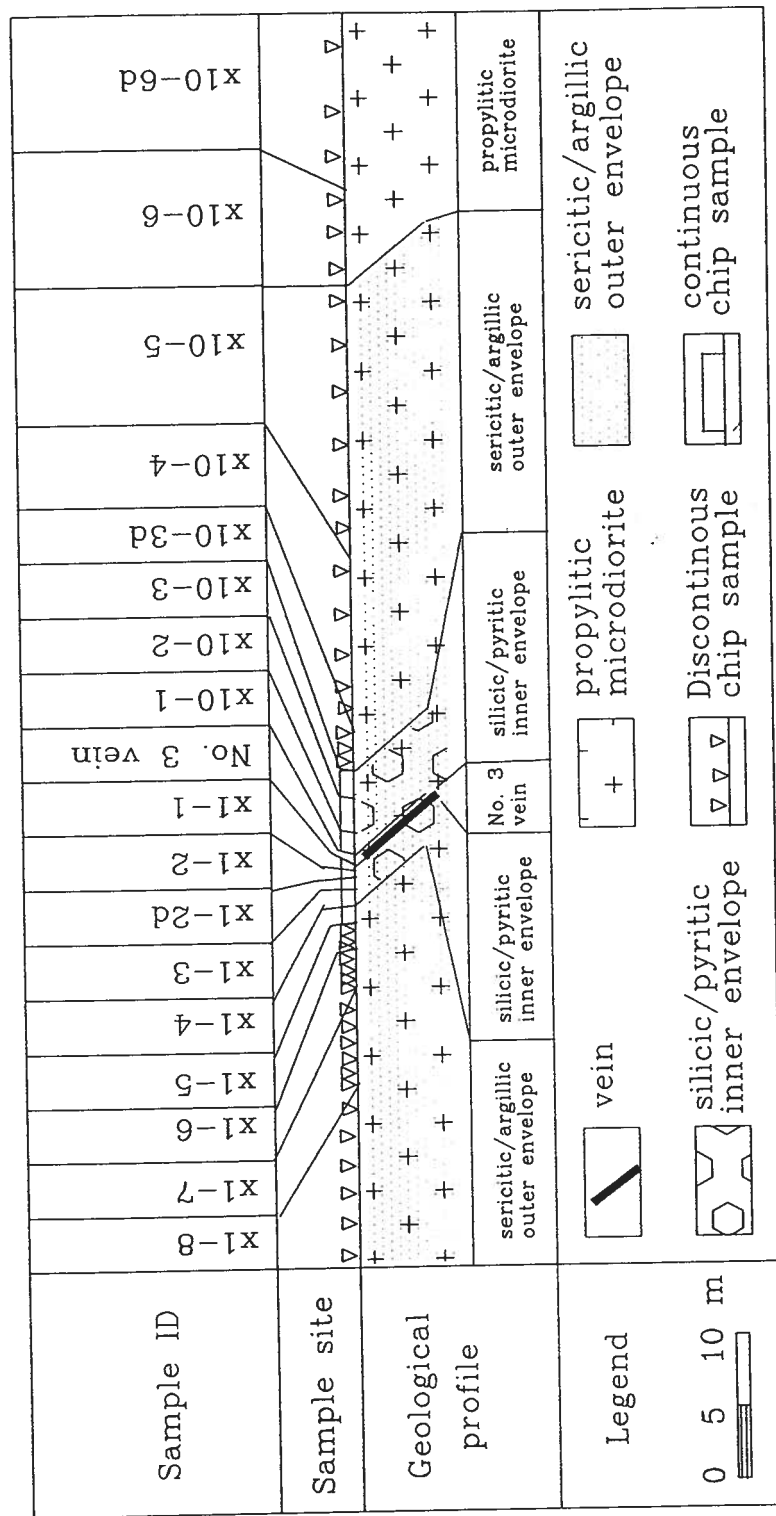


Figure 6-1. A typical sampling profile across the alteration envelope in the central segment of the No. 3 vein, Silver Queen mine.

Table 6.2. Estimated Optimal Fineness of Subsample by Using Binomial Function

Component	SiO ₂	TiO ₂	FeO	MgO	Na ₂ O	P ₂ O ₅	Zr
Mineral	Quartz	Rutile	Pyrite	Enstatite	Albite	Apatite	Zircon
H	1.000	1.000	0.470	0.402	0.240	0.424	0.498
L	0.400	0.001	0.010	0.010	0.000	0.000	0.000
d _H (g/cm ³)	2.648	4.245	5.011	3.210	2.620	3.180	4.669
d _L (g/cm ³)	2.87	2.87	2.87	2.87	2.87	2.87	2.87
p _w	0.150	0.005	0.050	0.050	0.300	0.005	0.0003
q _w	0.850	0.995	0.950	0.950	0.700	0.995	0.9997
R _E	0.01	0.01	0.01	0.01	0.01	0.01	0.04
(Hd _H -Ld _L) ²	2.250	17.996	5.413	1.588	0.395	1.818	5.406
(Hp _w + Lq _w) ²	2.40×10 ⁻¹	3.59×10 ⁻⁵	1.09×10 ⁻³	8.75×10 ⁻⁴	5.18×10 ⁻³	4.49×10 ⁻⁶	2.28×10 ⁻⁸
w (g)	4.00	4.00	4.00	4.00	4.00	4.00	4.00
v (mm ³)	0.89765	0.00068	0.00831	0.01481	0.06730	0.00063	0.00041
d (micron)	964.65	87.96	202.54	245.58	406.77	85.81	74.37
Sieve Size (mesh)	< 12	< 140	< 60	< 60	< 40	< 140	< 200

Note:	Common sieve size	Micron	Common sieve size	Micron
	12	1680	80	177
	20	841	140	105
	40	420	200	74
	60	250	400	37

the proportional abundance of each component in the principal mineral (H) and the remainder of the rock (L), as well as the weight proportion of the mineral rich in the constituent of interest (p_w). These are the key factors in determination of the optimal fineness of a subsample. For instance, the fineness of passing through 80 mesh (i.e. the diameter of grain ≤177 microns) can provide adequate homogeneity of the major components: FeO, MgO and Na₂O. It gives a subsampling error of less than or equal to 1% (R_E) at the 68% confidence level. In contrast, the homogeneities of minor constituents

such as TiO_2 and P_2O_5 require the fineness of material to be subsampled to pass through 200 mesh (i.e. the diameter of the grains are ≤ 74 microns). This provides a subsampling error of less than 1% (R_E) at the 68% confidence level. Zircon has the lowest concentration (about 0.0003 wt%) among the minerals listed in Table 6.2. It is the only common mineral containing Zr (i.e. $L = 0$), so even a subsample that has been ground to pass through 200 mesh will have a subsampling error four time larger than those of other constituents at the same confidence level. The detailed procedure of subsample preparation is documented below:

- (1) wash and saw off the mud, veinlets and weathering surface;
- (2) preserve hand specimen and select a block for thin section;
- (3) weigh the remaining sample (generally from 480 to 3000 grams);
- (4) crush sample to grains equal to, or less than, 4 mm by passing through a jaw crusher;
- (5) homogenize sample thoroughly on rag paper and randomly scoop out a 300 grams subsample;
- (6) grind this subsample in a swing mill to a particle size less than 75 microns;
- (7) check the fineness by randomly scooping out a portion of subsample and passing it through a nylon sieve (200 mesh); if not fine enough, randomly scoop out about 100 grams of sample and regrind it until all fines pass the check; and
- (8) clean the equipment to minimize carryover contamination.

In summary, the procedure outlined above minimizes the effects of artificial error arising from improper sampling and sample preparation. It is of a special significance for the determination of immobile components of interest in this study. As indicated in Table 6.1., if the size of a field sample is less than 200 grams (equivalent of a sample from a half drill core with diameter of 4 cm and length of 12 cm), the sampling error for TiO_2 could be doubled relative to the current sample size (equal to or greater than 500 g). Similarly,

if the weight of subsample is reduced from 4 gram to 2 gram, the subsampling error for Zr will increase by $\sqrt{2}$ (i.e. from $R_E = 4\%$ to $R_E = 4\% \times 1.414 = 5.7\%$). Consequently, the difficulty of recognizing and using these potentially immobile components corresponding would be increased significantly.

6.3. Errors in Lithogeochemical Data

The lithogeochemical determinations of: SiO_2 , TiO_2 , Al_2O_3 , Total Fe_2O_3 , MgO , MnO , CaO , Na_2O , K_2O , P_2O_5 , S, Rb, Sr, Y and Zr reported here were obtained by X-ray fluorescence (XRF) using 4 gram pressed rock powder pellets. This technique is suitable for the purpose here because there is neither the sample dilution problem inherent in borate bead preparation, nor the problem of incomplete solution in acid digestion methods (MacLean and Barrett, 1993). In the analytical scheme of XRF the oxidation state of iron (i.e. ferrous and ferric) cannot be distinguished. Thus, the XRF data have been supplemented by determinations for ferrous iron based on titrimetry (Potts, 1987). The determinations of structural water and carbon dioxide were conducted separately by the ignition method (Shapiro and Brannock, 1955, 1962).

The quality of lithogeochemical data is a function of various factors including the strategy of the sampling and sample preparation scheme, the skill and experience of the researcher and instrument operator, the operating condition of the instrument, the standards used to calibrate the counting values, the method of converting the counting values to meaningful lithogeochemical data and the concentrations of components/elements. Therefore, the quality of each set of lithogeochemical data should be assessed individually through the use of duplicates that are representative of the range of composition.

The duplicates selected for this study were obtained at two different stages. One was at the field sampling stage and other was at the analytical measurement stage. There are 18 sample duplicates and 20 measurement duplicates for major components analyzed

by XRF, 10 duplicates for ferrous iron, 10 duplicates for structural water, 10 duplicates for carbon dioxide, 20 duplicates for sulfur and 22 duplicates for trace elements analyzed by methods previously mentioned. The general procedure for assessing errors is presented in Appendix D (Figures 6-2a, 6-2b, 6-2c, 6-2d, 6-3a and 6-3b). The final results of error analysis of lithogeochemical data are listed in Tables 6-3 and 6-4. With the determination of the values of S_0 and k for each component or element, the standard deviation (S_c) and the precision (P_c) for each component or element at specific concentration can be calculated by using equation 3-15 and 3-16 introduced in Chapter 3.

Table 6-3. Error of lithogeochemical data estimated by using sample duplicates

	SiO ₂	TiO ₂	Al ₂ O ₃	Fe ₂ O ₃	FeO	MgO	MnO	CaO	Na ₂ O
So	0.01	0.006	0.01	0.06	0.045	0.074	0.022	0.08	0.09
k	0.012	0.008	0.021	0.018	0.018	0.03	0.007	0.011	0.013
Cd	0.02	0.012	0.021	0.124	0.093	0.157	0.045	0.164	0.185

	K ₂ O	P ₂ O ₅	CO ₂	H ₂ O	S	Zr	Y	Rb	Sr
So	0.02	0.02	0.01	0.04	18	0.01	0.3	2.00	5.00
k	0.018	0.015	0.12	0.13	0.07	0.032	0.09	0.035	0.019
Cd	0.041	0.041	0.026	0.108	41.86	0.021	0.732	4.301	10.395

Table 6-4. Error of lithogeochemical data estimated by using measurement duplicates

	SiO ₂	TiO ₂	Al ₂ O ₃	TFe	MgO	MnO	CaO	Na ₂ O	K ₂ O	P ₂ O ₅
So	0.001	0.006	0.001	0.042	0.07	0.007	0.028	0.02	0.005	0.001
k	0.002	0.008	0.007	0.025	0.008	0.01	0.012	0.003	0.009	0.04
Cd	0.002	0.012	0.002	0.088	0.142	0.014	0.057	0.04	0.01	0.002

Analytical precision for all components can be seen to be much less than field sampling precision. The reason for this is that the duplicates at the field sampling stage

contain more sources of variability, including the artificial errors caused by insufficient sample size, inhomogeneity of subsamples and inconsistent analytical measurements. On the other hand, measurement duplicates reveal only the error caused by inconsistent analytical measurements. The purpose of lithogeochemical data is to reveal lithogeochemical variations at scales larger than sample size. Therefore, the sum of all sources of variability of the samples should be known for interpretation purposes.

6.4. Lithogeochemical Data of Altered Rock and Determination of Immobile Components

The analytical results of the whole rock samples collected from four representative alteration profiles at the Silver Queen mine are listed in Appendix E (Table 6-5). A TiO_2 versus Zr binary plot (Figure 6-4) is constructed with these data and the lithogeochemical data are listed in Table 4-2. The two distinctive series of volcanic and intrusive rocks around Owen Lake area (Chapter 4) are evident in Figure 6-4. Compositions of altered rocks from four alteration profiles form linear patterns which converge toward the origin. These patterns indicate that the hydrothermally altered samples were derived from a multiple precursor system along the fractionation trend of the older series of igneous rocks at Owen Lake area. Therefore, TiO_2 and Zr are likely immobile in the hydrothermal alteration system at the Silver Queen mine.

The lithogeochemical data indicate that hydrothermally altered rocks are related to a multiple precursor system on the scale of the entire property. However, samples from each local hydrothermal alteration profile exhibit the attribute of a single precursor system that is a linear trend going through the origin of the TiO_2 -Zr binary plot. This linear pattern results from dilution or concentration of TiO_2 and Zr in proportion to the gain or loss of the total mass of the sample during the hydrothermal alteration (Figure 6-4). In other words, before wall-rock hydrothermal alteration at the Silver Queen mine, rocks that are hundreds of metres apart from each other have significant differences in their

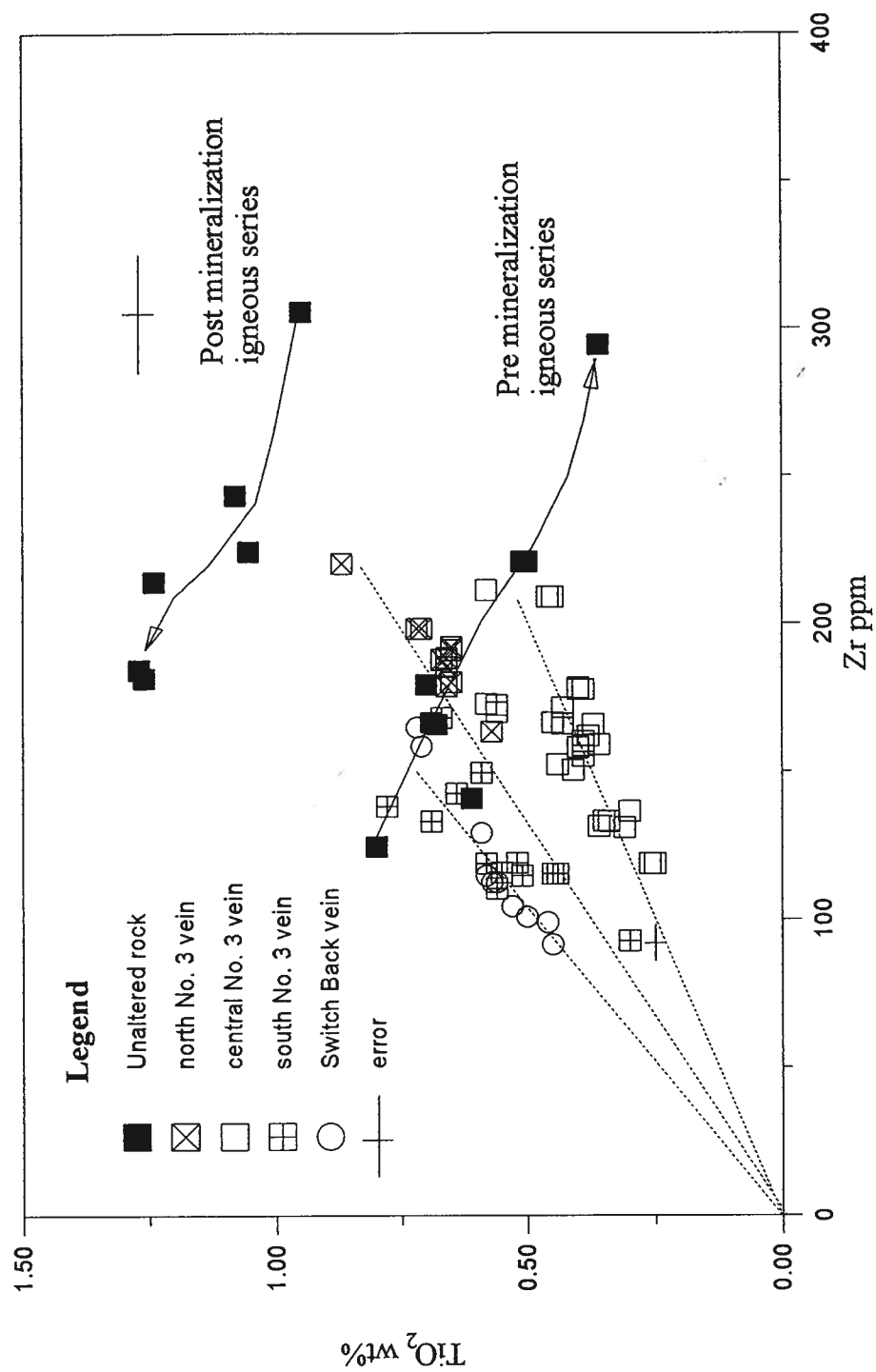


Figure 6-4. Immobile component/element scatter plot, Silver Queen mine, central British Columbia.

lithogeochemical compositions, but those within a few tens of metres from each other are not significantly different in composition. Therefore, each individual hydrothermal alteration profile can be treated as a single precursor system. Furthermore, TiO_2 and Zr are mineralogically and geochemically incompatible, hence both are used as immobile constituents with which to quantify the mobilities of other components.

Theoretically, there should be no significant difference in the recognition of mobile components using both immobile components (TiO_2 and Zr). In reality, this is not so. Thus, the question is, which should be used to correct for closure to provide the most accurate quantification of losses and gains? The sampling (+analytical) variability for TiO_2 ranges from 3 to 5.6% at 95% confidence level in the abundance range of interest (0.3 to 0.9 wt% TiO_2). Comparable variability for Zr is 6.4% or more at 95% confidence level in the abundance range of interest (120 to 220 ppm Zr). It therefore is reasonable to deduce that Zr has contributed more to the dispersion of the immobile linear trend for each profile than has TiO_2 . This conclusion is also consistent with what is expected based on the calculations of the optimal sample size and the optimal fineness of subsample (Tables 6-1 and 6-2). As a result, TiO_2 is chosen to be the preferred immobile component. It is used to remove the closure of lithogeochemical data in this study.

6.5. Calculation of Absolute Losses and Gains of Chemical Constituents and Their Spatial Variations

The total mass change of each sample can be visually and qualitatively evaluated from the TiO_2 -Zr plot (Figure 6-4) after knowing the composition of the precursor. Most of the hydrothermally altered samples at the Silver Queen mine plot between the primary Late Cretaceous fractionation trend and the origin of the plot. This means that these hydrothermally altered rocks have gained mass during alteration, so that the immobile constituents TiO_2 and Zr are diluted proportionally. For example, most of the hydrothermally altered samples from the southern and central profiles of the No. 3 vein,

and Switch Back vein plot in this fashion. In contrast, the samples that plot further from the origin reflect loss of the mass and thereby proportional concentration of the immobile constituents TiO_2 and Zr. The specific amounts lost and gained remain to be determined. Equation 1-9 is used to calculate the absolute losses and gains of individual chemical constituents. The mass of precursor is assumed to be around 100 grams and the mass loss or gain is also presented in an extensive unit (grams), which are the absolute mass change relative to the mass of the precursor (100 grams). The results are listed in Appendix E (Table 6-6). Moreover, to see what lithogeochemical variation is significant and what variation is caused by error propagation, equation 3-31 is applied to calculate the propagated error. If the variation of a constituent between two samples is obviously larger than its propagated error, then this variation is thought to be significant; otherwise, it is not significant. A selected example of these calculations are combined with the previous calculation result are present in Figure 6-5a and rest of the results in Appendix D (Figures 6-5b, -5c, -5d, -5e, -5f, -5g, -5h, -5i, -5j, -5k, -5l, -5m, -5n, -5o, -5p).

The absolute losses and gains of chemical constituents indicated by the samples from different hydrothermal alteration profiles at the Silver Queen mine have many features in common and show some systematic variations from the southern segment to the northern segment of the No. 3 vein and from different levels (from 2600-foot level to 2880-foot level). The general feature shared by all profiles may represent the common attributes of ore-forming hydrothermal solutions in this district. Whereas the differences from place to place may illustrate the spatial variations of the properties of ore-forming hydrothermal solutions. Both are important in the study of ore deposits, but the latter is of specific significance to exploration. The systematic variation in fluid/rock interaction may help to interpret the migration direction of ore-bearing hydrothermal fluid. Therefore, both the general features and the spatial variation of absolute losses and gains of each chemical constituents in various hydrothermal alteration profiles at the Silver Queen mine are described below.

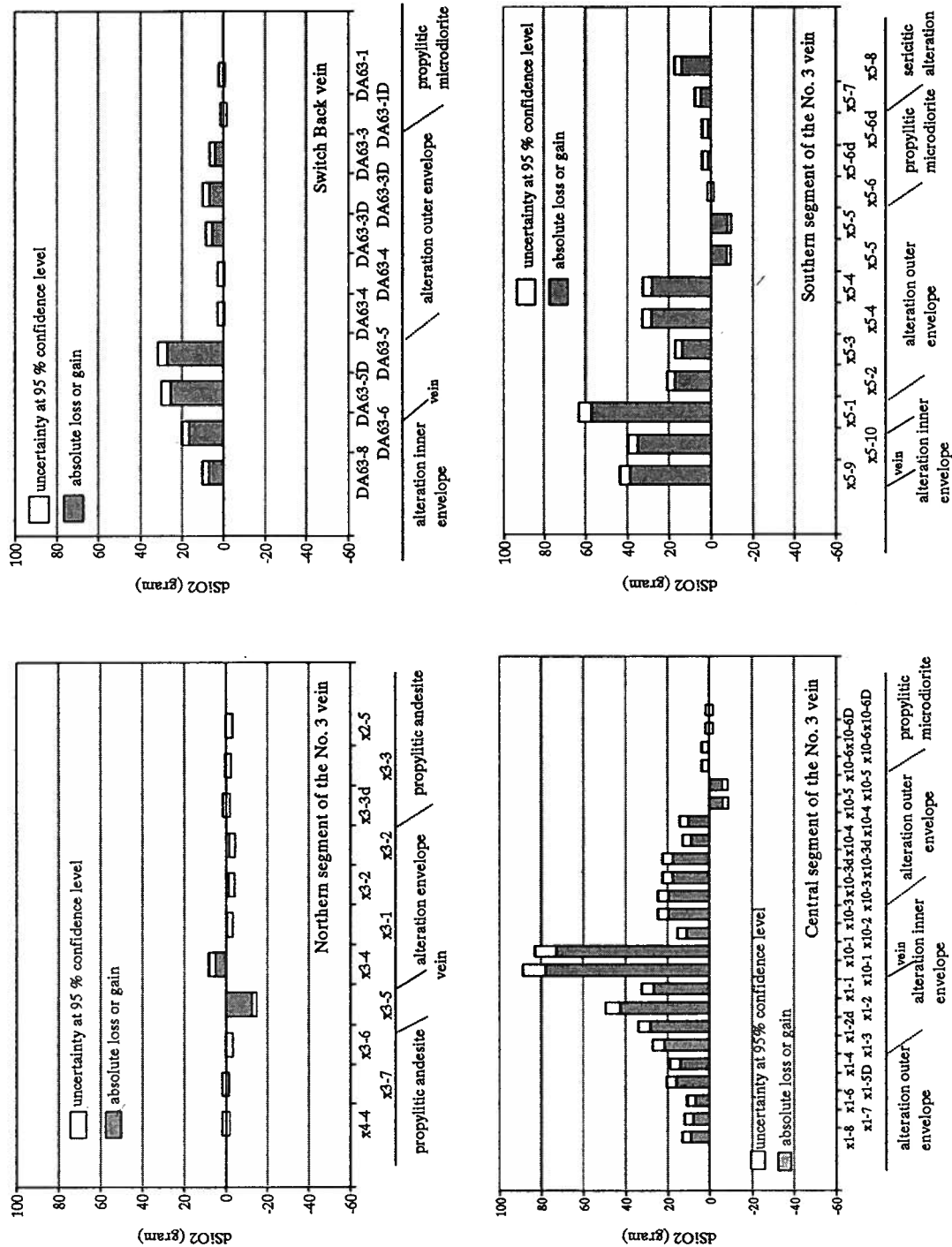


Figure 6-5a. Absolute losses and gains of SiO_2 from four alteration profiles at the Silver Queen mine, central British Columbia. The blank part of each bar includes the mean estimate (a horizontal imaginary line through the centre of the blank bar) and a range representing ± 2 standard deviations.

SiO₂: In general, this constituent is added from hydrothermal solution to wall rocks in all alteration envelopes discussed here, except in the alteration envelope of the northern segment of the No. 3 vein and in the outmost subzone of the alteration envelope at the central and southern segment of the No. 3 vein. The greatest addition of SiO₂ is at the 2600-foot level of central segment of the No. 3 vein, and the 2600-foot level of southern segment of the No. 3 vein. In turn, mildly intensive addition of SiO₂ occurs at the Switch Back vein. In contrast, a loss of SiO₂ occurs at the northern segment of the No. 3 vein and in the outmost subzone of the alteration envelope at the central and southern segments of the No. 3 vein (Figure 6-5a).

Al₂O₃: In general, Al₂O₃ has a loss-gain pattern similar to that of SiO₂, but the changes are less obvious than are those of SiO₂ (Appendix D, Figure 6-5b).

Fe₂O₃: Ferric oxide is depleted or reduced to various extents in most portions of the alteration envelopes. A moderate increase in Fe₂O₃ commonly occurs immediately adjacent to the veins, probably due to the occurrence of hematite veinlets (Appendix D, Figure 6-5c).

FeO: Ferrous oxide is 'added' (probably by reduction of ferric iron) prominently in all alteration envelopes. This 'addition' is strongly intensified at the Switch Back vein and in the central segment of the No. 3 vein (Appendix D, Figure 6-5d).

MnO: Manganese addition and depletion patterns are two-fold. Type one is characterized by a pervasive addition of MnO to the wall rocks in the alteration envelopes at the northern segment of the No. 3 vein and the Switch Back vein. Type two involves the addition of MnO to most portions of the alteration envelopes, but there is a narrow depletion 'valley' adjacent to the vein at the 2600-foot level of central segment and southern segment of the No. 3 vein (Appendix D, Figure 6-5e).

MgO: Magnesium is moderately depleted in the alteration envelopes. There is no significant systematic addition and depletion pattern in the profiles (Appendix D, Figure 6-5f).

Na₂O and CaO: Sodium and calcium depletions from the wall rocks are prominent and intense in all alteration envelopes. In particular, the depletion of Na₂O is almost complete in all alteration envelopes (Appendix D, Figures 6-5g, 6-5h).

K₂O and Rb: Potassium and rubidium additions to the wall rocks are prominent but variable in intensities from the southern segment to the northern segment of the No. 3 vein. Additions of K₂O and Rb are most intense in parts of the alteration envelopes at the 2600-foot level of the central and southern segment of the No. 3 vein, and moderately intense in the alteration envelope at the Switch Back vein. In contrast, only one sample shows a slight addition of K₂O and Rb, the rest indicate depletion or no significant mass change, of K₂O and Rb in the alteration envelope at the northern segment of the No. 3 vein. K₂O and Rb depletions occur at the outmost parts of the alteration envelopes at the central and southern segments of the No. 3 vein (Appendix D, Figures 6-5i, 6-5j).

H₂O, CO₂ and S: Volatile constituents are prominently added from hydrothermal solution to wall rocks in all alteration envelopes discussed here except the southern segment of the No. 3 vein. The spatial variation of addition of H₂O, CO₂ and S are described as follows. The additions of H₂O and CO₂ are the most intense in the alteration envelopes at the Switch Back vein and the central segment of the No. 3 vein, the second most intense in the alteration envelope at the northern segment of the No. 3 vein. There is almost no significant addition of H₂O and CO₂ in the alteration envelope at the southern segment of the No. 3 vein. In contrast to the addition of H₂O and CO₂, the addition of sulfur reaches its peak in the alteration envelope about the southern segment of the No. 3 vein, as well as at the central segment of the No. 3 vein. The addition of sulfur is minor along the Switch Back vein profile. There is very little addition of sulfur in the alteration envelope at the northern segment of the No. 3 vein (Appendix D, Figures 6-5k, 6-5l and 6-5m).

Sr: Strontium is depleted in the alteration envelopes in a pattern similar to those of Na₂O and CaO but the intensity of depletions vary from profile to profile. It appears to be

more intense at the southern segment of the No. 3 vein than at the northern segment of the No. 3 vein. In addition, the subzone adjacent to the vein in the alteration envelope at the central segment of the No. 3 vein shows strong addition of Sr (Appendix D, Figure 6-5n).

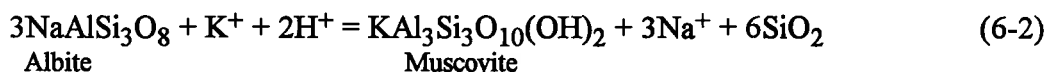
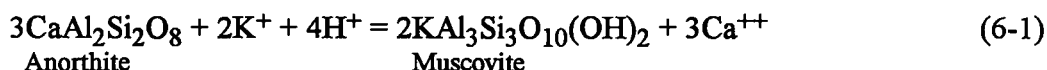
Y: Yttrium in the alteration envelope have gained a small amount of mass from the hydrothermal solution, but lost its mass in part of the alteration inner envelope in the central and southern segment of the No. 3 vein. These changes may not be significant since yttrium has a large analytical error (Appendix D, Figure 6-5o).

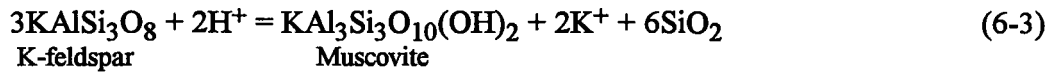
P₂O₅: Phosphorous is probably a locally immobile component during the hydrothermal alteration process because it has no significant loss or gain in the sericitic and argillic outer alteration envelope; its depletion is mild in the silicic and pyritic inner alteration envelopes at the Silver Queen mine (Appendix D, Figure 6-5p).

In brief, wall rock alteration is most intense in the alteration envelope at the central segment of No. 3 vein and least intense at the northern segment of No. 3 vein in terms of absolute losses and gains of chemical constituents according to the lithogeochemical data from the current four profiles. The total mass change of each altered sample is largely the result of the depletions of CaO and Na₂O, and the addition of SiO₂, K₂O, H₂O and CO₂.

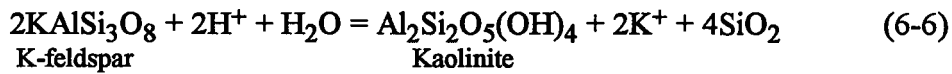
6.6. Application of PER Diagram to the Interpretation of Hydrothermal Alteration

Knowing the absolute losses and gains of chemical constituents during the hydrothermal alteration process, we can infer corresponding mineralogical changes. For example, an addition of K₂O along with the depletion of CaO and Na₂O of andesitic volcanic rock samples might be intuitively interpreted as the replacement of plagioclase or K-feldspar by muscovite. This can be illustrated by the following equations:





In another case, the depletions of K_2O , CaO and Na_2O along with no mass changes of SiO_2 might indicate the occurrence of argillic alteration. This can be represented as follows:



A previous petrographic examination documents the existences of propylitization, carbonatization, argillization, sericitization and silicification in the study area. These alteration processes lead to the replacement of primary minerals such as plagioclase, augite and hornblende by epidote, chlorite, carbonates, kaolinite and sericite, with the addition of quartz.

These processes can be tested in detail for each analysis using PER diagrams (Russell and Stanley, 1990a; Stanley and Russell, 1989a, 1989b, 1989c, 1990). There are two preconditions that must be satisfied before applying this PER diagram to the interpretation of the lithogeochemical data. The first is that the chemical composition and mineral assemblage of parent rock or precursor of alteration derivatives must be known or predictable. This has already been demonstrated in Figure 6-4 and the related discussion. The lithogeochemical composition and mineral assemblage of a propylitic rock can be treated as the precursor of the altered rocks in the superimposed alteration envelope. The second precondition is that the proportion of primary minerals converted into alteration product must be reasonably estimated. The microscope observations indicate that primary minerals are completely replaced by altered minerals including mainly sericite, kaolinite, quartz, carbonate and pyrite within the alteration envelope, and partially replaced by epidote, chlorite, carbonate and sericite in propylitic alteration halo.

The PER diagram designed previously (Figure 1) is used to test (i) whether feldspar and augite fractionations are still the main contributors to lithogeochemical variation among the propylitically altered rocks; (ii) whether either carbonatization, sericitization, argillization or silicification is the dominant alteration type at the Silver Queen mine.

The propylitically altered samples on the PER diagram are characterized by a scattered trend with a slope approximately equal to one within the error range at the 95% confidence level. This implies that the total mass of corresponding chemical constituents used to construct this PER diagram have had no significant changes during the propylitic alteration process. In other words, primary feldspar and augite crystal fractionations may be still the major causes for the lithogeochemical variations of the corresponding chemical constituents among the propylitically altered samples (Figure 6-6a). However, it is not certain whether the unchanged mass means that the mass of each constituent is unchanged or that the masses of corresponding constituents do change but the total mass remains unchanged by compensation.

In general, all the samples from the alteration envelope (not including propylitic alteration) plot far from the primary fractionation trends on this PER diagram. This implies that there are significant mass changes of the corresponding chemical constituents among these samples relative to the propylitically altered samples. Also, all the samples from the alteration envelope spread between sericitic trend and argillic trend rather than concentrating around one alteration trend, indicating that the lithogeochemical variation of altered rocks is not entirely controlled by either carbonates, sericite, kaolinite or quartz at the Silver Queen mine. Instead, the lithogeochemical variations among these samples have to be interpreted as due to the complete replacement of primary minerals as well as the 'propylitic' minerals by different proportions of sericite, kaolinite, carbonate, pyrite and quartz. According to petrographic observations one of the possible alteration paths is deduced as follows (Figure 6-6b): all primary minerals and propylitic minerals in the least

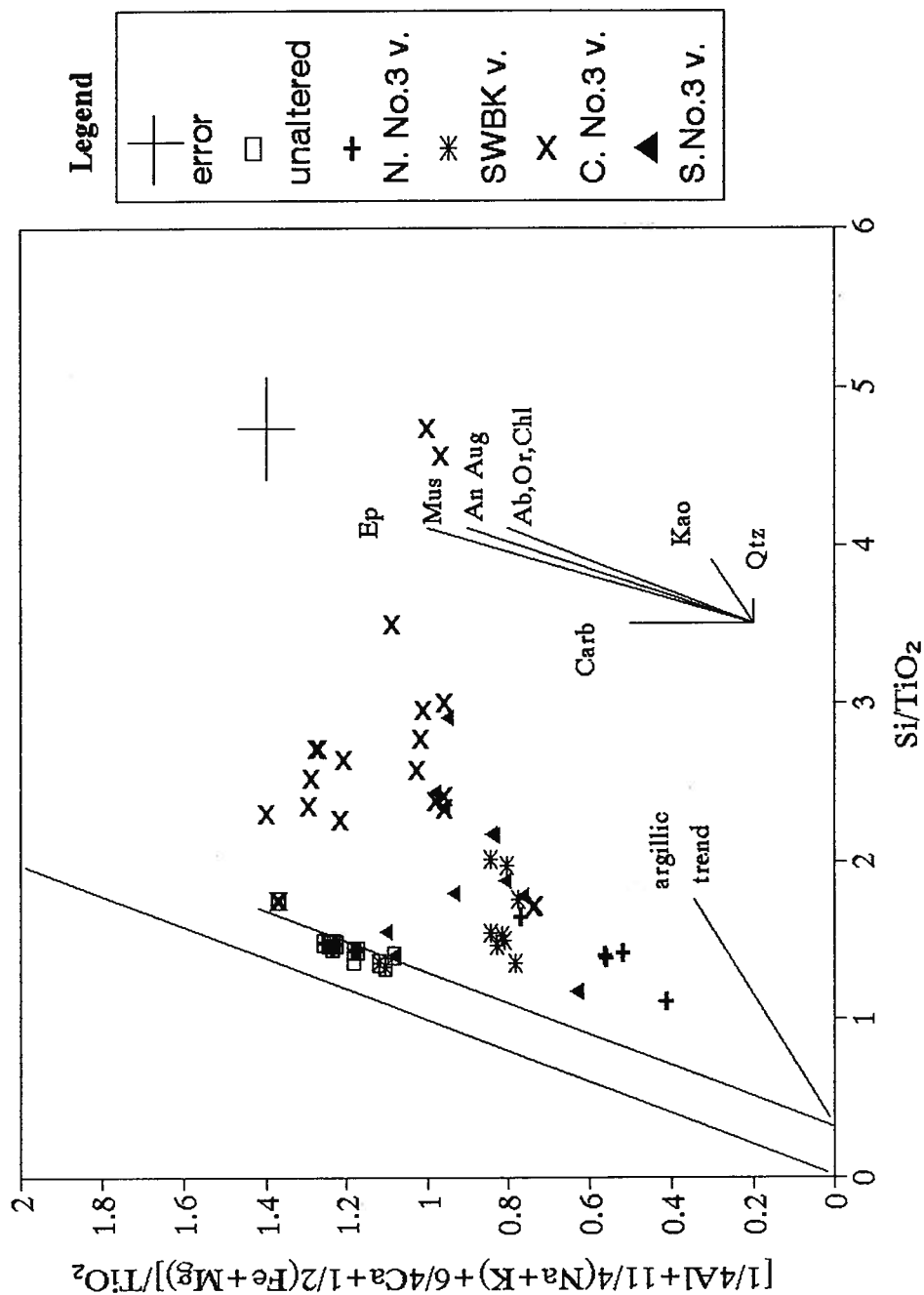


Figure 6-6a. PER plot to discriminate the alteration types associated with precious- and base-metal vein mineralization in volcanic sequences at the Silver Queen mine. Qtz - quartz, Carb - carbonates, Kao - kaolinite, An - anorthite, Ab - albite, Or, K-feldspar, Chl - chlorite, Aug - augite, Mus - muscovite, Ep - epidote, N. No. 3 v. - the northern segment of the No. 3 vein, SWBK v. - Switch Back vein, C. No. 3 v. - central segment of the No. 3 vein, S No. 3 v. - southern segment of the No. 3 vein. see text for detailed discussion.

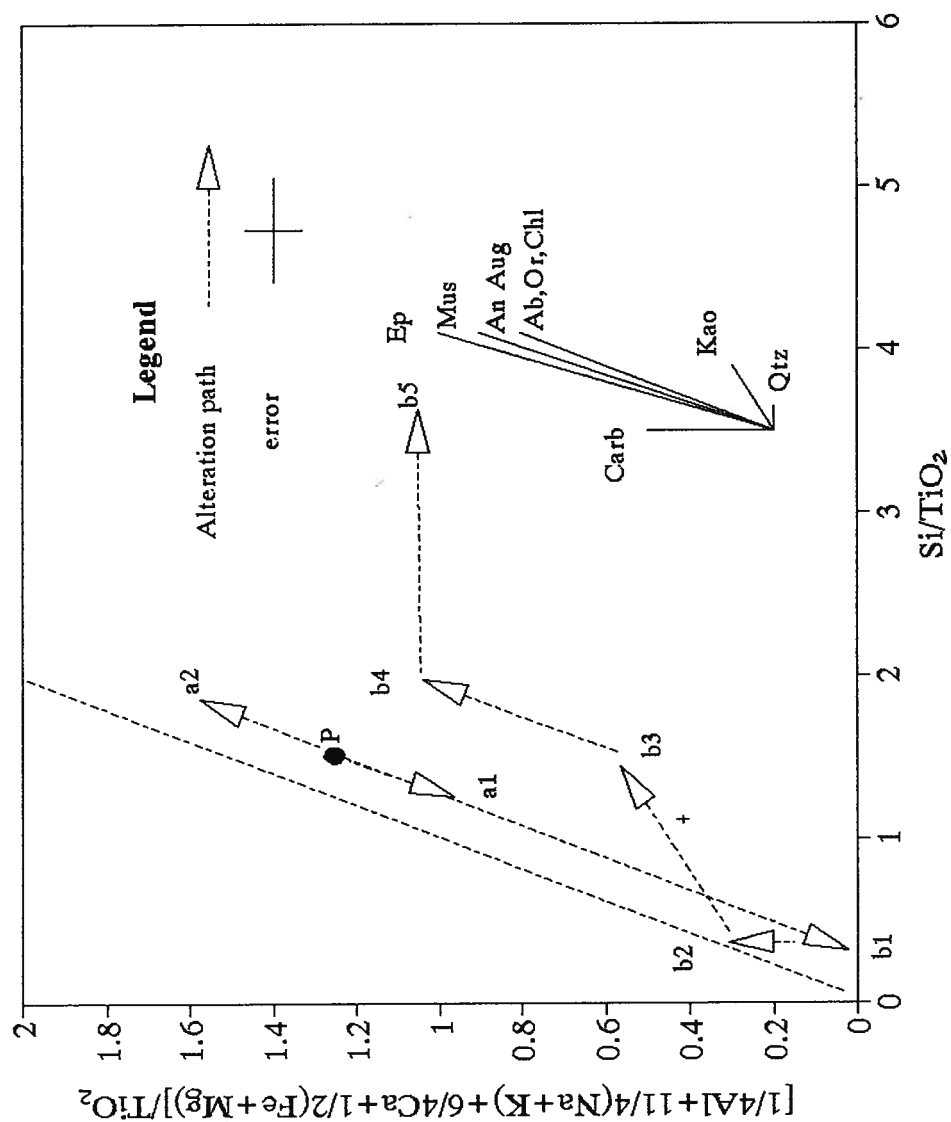


Figure 6-6b. One of the possible alteration paths on PER diagram designed to discriminate the alteration types associated with precious- and base-metal vein mineralization in volcanic sequences at the Silver Queen mine. Qtz - quartz, Carb - carbonates, Kao - kaolinite, An - anorthite, Ab - albite, Or, K-feldspar, Chl - chlorite, Aug - augite, Mus - muscovite, Ep - epidote.

or propylitically altered wall rocks are completely replaced (from P to b1) by carbonatization (from b1 to b2), argillization (from b2 to b3), sericitization (from b3 to b4) and silicification (from b4 to b5).

Another PER diagram is used to further test alteration types at the Silver Queen mine. This PER diagram has a Al/TiO_2 as x-axis and $(2\text{Ca}+\text{Na}+\text{K})/\text{TiO}_2$ as y axis (Stanley and Madeisky, 1993). The displacement vectors of primary minerals (feldspar and hornblende) are defined to have slopes equal to one, the displacement vectors of carbonates are vertical, that of kaolinite horizontal, that of muscovite has a slope equal to $1/3$, and that of quartz is perpendicular to the paper (Figure 6-6c).

The alteration samples of Silver Queen mine on this PER diagram show again that least or propylitically altered samples plot along the fractionation trend of slope equal to one within the error range (at the 95% confidence level). This means that lithgeochemical variation of least or propylitically altered wall rock is caused mainly by feldspar. The displacement vector of augite is vertical on this PER diagram (Figure 6-6d).

Compared to the previous PER diagram, this PER diagram shows a more understandable dispersion of plotted points; the alteration patterns are more distinguishable because the effect of quartz has been removed and only carbonates, muscovite and kaolinite alteration are presented on this PER diagram. In addition, a bubble plot superimposed on this PER diagram is used to investigate the effect of silicification (Figure 6-6e). With regard to the alteration intensity relative to the spatial distribution, the plots of the samples from the alteration envelopes of the northern segment of the No. 3 vein, the Switch Back vein, the southern segment of the No. 3 vein and the central segment of the No. 3 vein are presented in turn from the lowest left portion to the highest right portion of this PER diagram. This plotting pattern indicates that samples from the alteration envelope of the central segment of the No. 3 vein are affected by the most intense alteration including sericitization, carbonatization, pyritization and silicification. In contrast, the alteration intensity of the samples from alteration envelope of

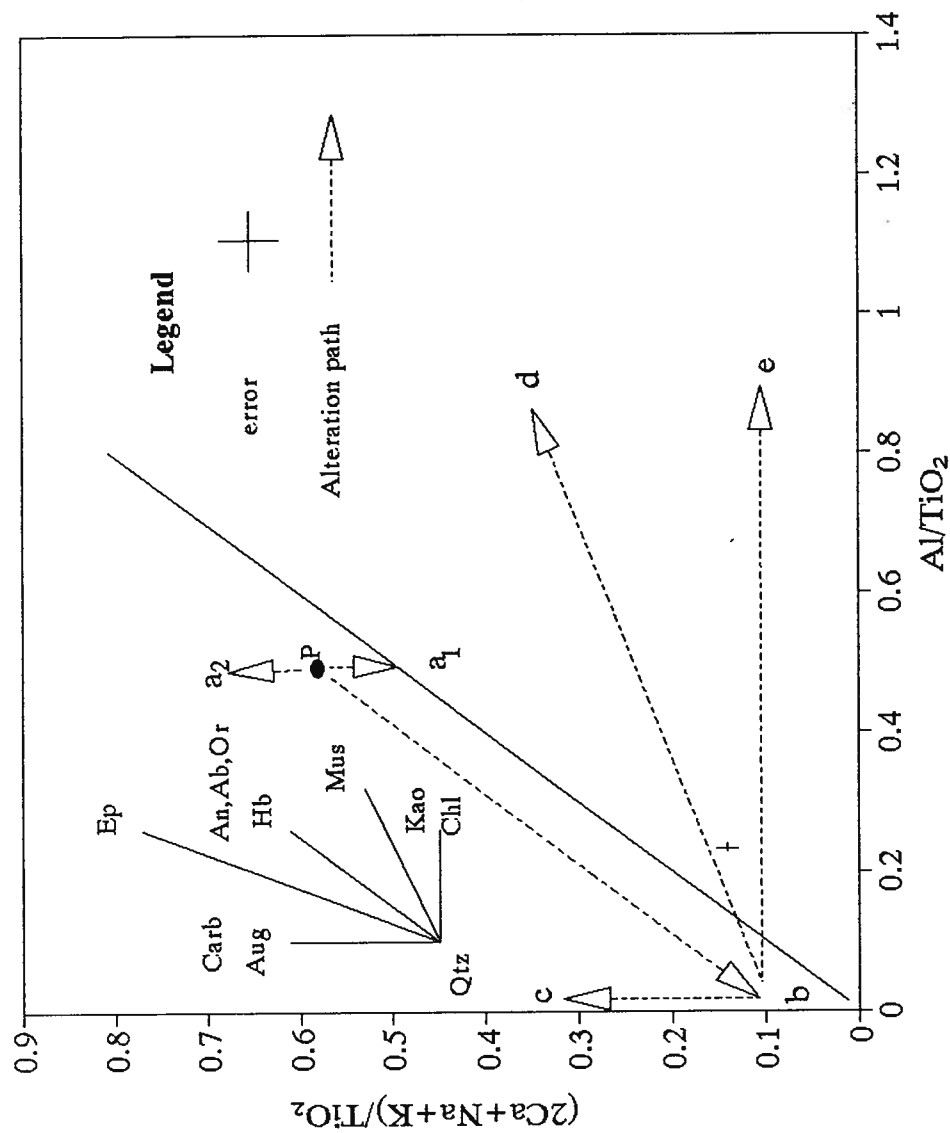
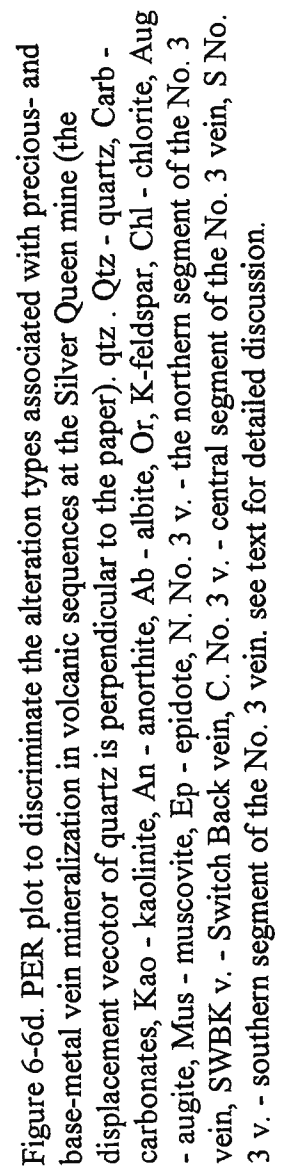


Figure 6-6c. PER diagram designed to discriminate the alteration types without considering the effect of quartz. Qtz - quartz, Carb - carbonates, Kao - kaolinite, An - anorthite, Ab - albite, Or, K-feldspar, Chl - chlorite, Aug - augite, Mus - muscovite, Ep - epidote. P - protolith; augite replaced (a1) by carbonates (a2); primary minerals are completely replaced (b) by carbonates (c), muscovite (d) or kaolinite (e).



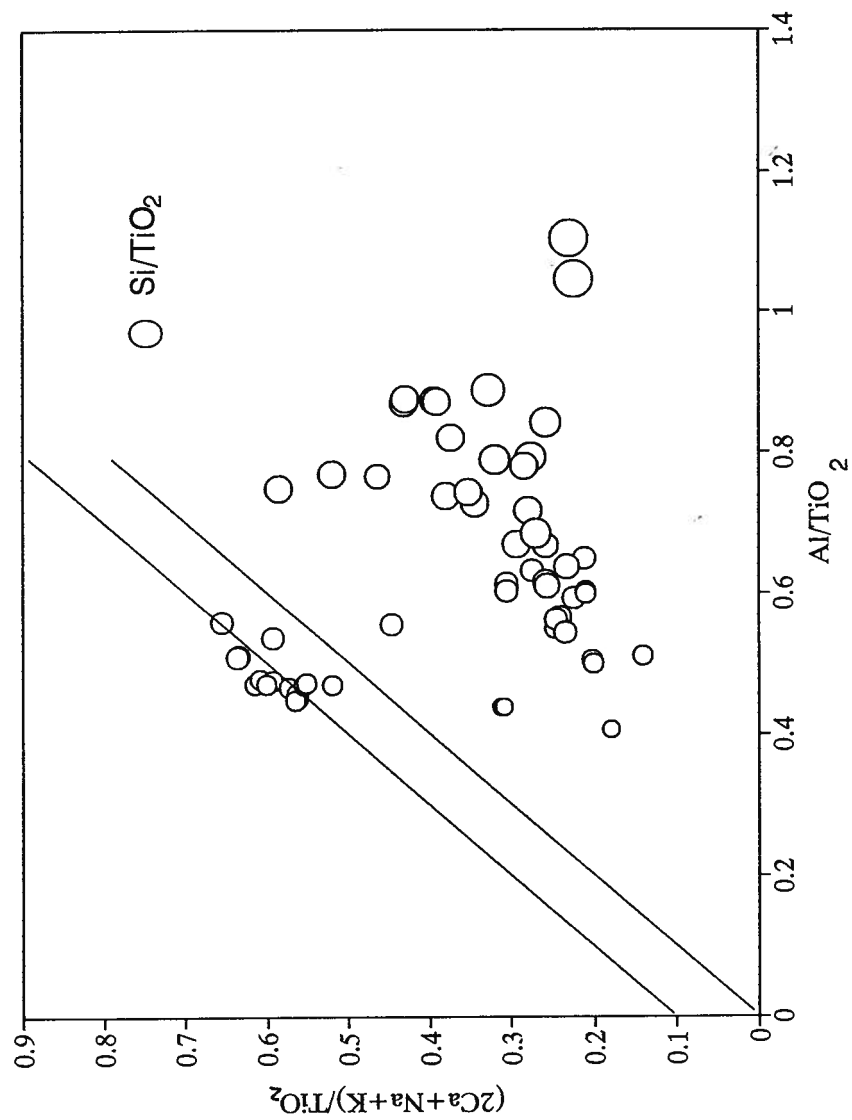


Figure 6-6e. PER diagram superimposed by Si/(immobile element) bubble plot. The size of bubble represents the relative molar amount of Si corrected for closure.

the northern segment of the No. 3 vein is the mildest relative to others. Its alteration types are mainly carbonatization and argillization plus sericitization. All these are consistent with the conclusions drawn from the calculations of absolute losses and gains of chemical constituents in the previous section.

6.7. Application of Metasomatic Norm Methodology

For the purpose of a general examination of the types and intensities of hydrothermal alteration associated with precious- and base-metal vein deposit in volcanic sequence by using the lithogeochemical data, the PER diagram, described above, is a useful tool. However, projections of multicomponents systems can be ambiguous and may not involve all variables, partly because of its 2-dimensional limitation. For example, an altered sample plotted on the PER diagram, above, could be interpreted as either the combined product of argillization, carbonatization, sericitization and silicification or simply the product of carbonatization plus intense silicification. A more complicated system has to be taken into account to reduce the ambiguities or to test other hypotheses. In the example mentioned above, the product of carbonatization plus intense silicification will lead to the content of CO₂ in the bulk rock composition being more abundant than in the case of silicification, argillization and sericitization. In contrast, the combined product of silicification, argillization, carbonatization and sericitization will contain more H₂O in the bulk rock composition than in the product of carbonatization plus intense silicification. One means of reducing these ambiguities is through use of the methodology described by Cheng and Sinclair (1994) and in Chapter 2.

The lithogeochemical data of four hydrothermal alteration profiles at the Silver Queen mine have been processed by applying the approach of metasomatic norm calculation. The minerals listed in Table 2-1 are chosen to be the standard normative minerals for the metasomatic norm calculation. These mineral occurrences are based on the petrographic observations and XRD examination of the samples (Cheng et al., 1991).

Finally, all the calculated metasomatic norm values have been corrected for closure by using TiO_2 as an immobile component and equation 1-9. The metasomatic norms corrected for the closure and the absolute loss and gain values of chemical constituents of the northern segment of the No. 3 vein profiles as the selected examples are presented in units of mole and gram in Tables 6-7a and 6-8a, respectively. The calculations of other profiles are listed in Appendix E, Table 6-7b, 6-7c and 6-7d and Tables 6-8b, 6-8c and 6-8d, respectively.

Residuals have been used to monitor how closely the masses of parent-daughter losses and gains balance. A residual is defined as $\sum \text{metasomatic norm}_{\text{altered rock}} - (\sum \text{metasomatic norm}_{\text{precursor rock}} + \Delta \text{Mass change})$. The residuals of metasomatic norm calculation after the correction for the closure range from 0.16 to -0.49 gram relative to the mass of precursor rock (about 100 gram). This indicates that the mineral assemblages chosen here represent the bulk rock composition well.

The data listed in Tables 6-8a, 6-8b, 6-8c and 6-8d are illustrated in Figures 6-7a, 6-7b, 6-7c and 6-7d. For the purpose of comparison, the scales of y-axes are uniform in Figures 6-7a, 6-7b, 6-7c and 6-7d. Thus, the type and intensity of wall-rock hydrothermal alteration in different profiles can be quantitatively evaluated and objectively compared.

The propylitic altered rock is characterized by a metasomatic normative mineral assemblage composed mainly of plagioclase, K-feldspar, pyroxene, quartz, epidote, chlorite and carbonate. There is no systematic spatial variation of the abundances of these minerals relative to the vein. This attribute is convincing evidence that propylitic alteration is related to pre-mineralization volcanic activity rather than the ore-fluid.

The carbonatization is relatively intense in hydrothermal alteration envelopes and is indicated by the increase in the content of carbonate from 5.6 gram on average in the propylitic alteration halo to about 15 gram on average in the bleached alteration envelope. Of the four profiles the alteration envelope of the Switch Back vein is the most strongly

Table 6-7a. Metasomatic norms corrected for closure and absolute losses and gains of components (in moles)
at northern segment of the No. 3 vein, Silver Queen mine, Owen Lake, central BC

Sample_id	x4-4	x3-7	x3-6	x3-5	x3-4	x3-1	x3-2	x3-2	x3-3d	x3-3	x2-5
Alteration	w-alt	w-alt	w-alt	m-alt	ms-alt	ms-alt	m-alt	m-alt	w-alt	w-alt	w-alt
mole											
Pyroxene	0.02	0.00	0.00	0.00	0.00	0.00	0.00	0.00	0.01	0.02	0.02
Plagioclase	0.14	0.16	0.10	0.00	0.00	0.00	0.00	0.00	0.11	0.15	0.15
K-feldspar	0.07	0.06	0.06	0.00	0.00	0.00	0.00	0.00	0.07	0.06	0.07
Quartz	0.20	0.22	0.26	0.46	0.68	0.59	0.58	0.58	0.23	0.19	0.24
Carbonate	0.05	0.05	0.05	0.09	0.16	0.13	0.10	0.10	0.04	0.05	0.06
Epidote	0.04	0.02	0.02	0.00	0.00	0.00	0.00	0.00	0.03	0.03	0.01
Chlorite	0.00	0.01	0.02	0.00	0.00	0.00	0.00	0.00	0.02	0.01	0.01
Sericite	0.00	0.00	0.02	0.04	0.11	0.06	0.07	0.07	0.01	0.00	0.00
Kaolinite	0.00	-0.00	0.01	0.06	0.02	0.07	0.05	0.05	-0.00	0.00	0.00
Pyrite	0.00	0.00	0.00	0.00	0.00	0.00	0.00	0.00	0.00	0.00	0.00
Hematite	0.00	0.01	0.01	0.00	0.01	0.01	0.01	0.01	0.00	0.00	0.01
Magnetite	0.00	0.00	0.00	0.00	0.00	0.00	0.00	0.00	0.00	0.00	0.00
Ilmenite	0.00	0.01	0.00	0.00	0.00	0.00	0.00	0.00	0.00	0.00	0.00
Rutile	0.01	0.00	0.01	0.01	0.01	0.01	0.01	0.01	0.01	0.01	0.01
Apatite	0.00	0.00	0.00	0.00	0.00	0.00	0.00	0.00	0.00	0.00	0.00
Total	0.53	0.55	0.56	0.67	1.00	0.87	0.83	0.82	0.52	0.52	0.58
dSiO2	0.00	0.00	-0.03	-0.24	0.11	-0.04	-0.05	-0.06	-0.00	-0.02	-0.02
dAl+3	0.00	0.01	0.00	-0.04	0.08	0.03	0.02	0.02	0.00	-0.00	-0.00
dTi+4	0.00	0.00	0.00	0.00	0.00	0.00	0.00	0.00	0.00	0.00	0.00
dFe+3	0.00	-0.00	-0.00	-0.03	-0.02	-0.02	-0.01	-0.01	-0.00	-0.00	-0.00
dFe+2	0.00	0.00	-0.00	-0.00	0.05	0.04	0.01	0.01	0.00	-0.00	-0.00
dMn+2	0.00	-0.00	-0.00	0.01	0.02	0.02	0.00	0.00	0.00	-0.00	-0.00
dMg+2	0.00	-0.01	-0.01	-0.06	-0.04	-0.05	-0.05	-0.05	0.00	-0.00	0.01
dCa+2	0.00	-0.01	-0.00	-0.07	-0.09	-0.10	-0.08	-0.08	-0.01	-0.01	-0.01
dNa+	0.00	0.01	-0.00	-0.11	-0.10	-0.11	-0.11	-0.11	0.00	0.01	-0.01
dK+	0.00	-0.00	-0.00	-0.03	0.03	-0.01	-0.00	-0.00	0.00	-0.00	0.00
dP+5	0.00	0.00	0.00	-0.00	-0.00	-0.00	-0.00	-0.00	0.00	0.00	-0.00
Sum O=	0.00	-0.01	-0.02	-0.30	-0.01	-0.15	-0.17	-0.17	-0.00	-0.01	-0.01
dH2O	0.00	0.02	0.07	0.13	0.12	0.16	0.15	0.14	0.05	0.01	0.00
dCO2	0.00	0.00	0.01	0.04	0.11	0.08	0.04	0.04	-0.01	-0.00	0.02
dS	0.00	0.00	0.00	0.00	0.00	0.00	0.00	0.00	0.00	0.00	-0.00
dTotal	0.00	0.01	0.01	-0.69	0.26	-0.15	-0.25	-0.27	0.04	-0.03	-0.03

Table 6-8a. Metasomatic norms corrected for closure and absolute losses and gains of components (in grams)
at northern segment of the No. 3 vein, Silver Queen mine, Owen Lake, central BC

Sample_id	x4-4	x3-7	x3-6	x3-5	x3-4	x3-1	x3-2	x3-2	x3-3d	x3-3	x2-5
Alteration	w-alt	w-alt	w-alt	m-alt	ms-alt	ms-alt	m-alt	m-alt	w-alt	w-alt	w-alt
gram											
Pyroxene	5.11	1.22	0.90	0.00	0.00	0.00	0.00	0.00	1.80	4.33	3.83
Plagioclase	36.01	41.63	26.19	0.25	1.12	0.53	0.89	0.08	28.51	39.58	40.72
K-feldspar	18.26	17.26	16.00	0.00	0.00	0.00	0.00	0.08	18.50	17.58	18.34
Quartz	12.02	13.40	15.88	27.38	40.90	35.35	34.72	34.76	13.87	11.17	14.21
Carbonate	4.86	5.85	5.35	9.81	17.14	14.14	10.25	10.21	3.98	5.10	5.53
Epidote	18.70	9.79	11.07	1.78	0.00	0.00	0.00	0.00	15.49	13.55	3.89
Chlorite	3.05	7.28	11.35	0.00	0.00	0.00	0.00	0.00	11.71	4.16	7.65
Sericite	0.00	0.02	7.39	17.28	44.29	25.43	28.75	29.59	3.96	0.00	0.00
Kaolinite	0.00	-0.00	1.56	16.28	6.06	17.77	13.92	12.95	-0.00	0.17	0.01
Pyrite	0.02	0.03	0.03	0.04	0.27	0.13	0.10	0.09	0.05	0.03	0.01
Hematite	0.00	1.24	1.24	0.65	1.44	1.21	2.00	2.10	0.25	0.74	2.39
Magnetite	0.00	0.00	0.00	0.00	0.00	0.00	0.00	0.00	0.00	0.00	0.00
Ilmenite	0.00	1.20	0.00	0.00	0.00	0.43	0.00	0.00	0.00	0.08	0.01
Rutile	0.65	0.02	0.65	0.65	0.65	0.42	0.65	0.65	0.65	0.61	0.64
Apatite	0.90	0.90	0.93	0.48	0.51	0.46	0.56	0.55	0.92	0.91	0.86
Total	99.58	99.83	98.53	74.60	112.38	95.86	91.83	91.06	99.69	98.01	98.09
dSiO2	0.00	0.11	-1.53	-14.19	6.76	-2.32	-2.99	-3.50	-0.27	-0.99	-1.44
dAl+3	0.00	0.14	0.09	-1.10	2.16	0.70	0.61	0.51	0.10	-0.00	-0.08
dTi+4	0.00	0.00	0.00	0.00	0.00	0.00	0.00	0.00	0.00	0.00	0.00
dFe+3	0.00	-0.16	-0.01	-1.50	-1.16	-1.31	-0.77	-0.69	-0.20	-0.08	-0.04
dFe+2	0.00	0.12	-0.18	-0.10	2.88	2.14	0.35	0.31	0.15	-0.06	-0.01
dMn+2	0.00	-0.11	-0.09	0.51	1.19	0.92	0.16	0.16	0.01	-0.03	-0.07
dMg+2	0.00	-0.18	-0.22	-1.37	-0.98	-1.14	-1.24	-1.23	0.08	-0.07	0.20
dCa+2	0.00	-0.29	-0.14	-2.90	-3.74	-3.83	-3.23	-3.22	-0.33	-0.29	-0.35
dNa+	0.00	0.33	-0.11	-2.54	-2.34	-2.50	-2.47	-2.48	0.03	0.19	-0.23
dK+	0.00	-0.14	-0.08	-1.11	1.34	-0.33	-0.00	-0.01	0.03	-0.10	0.01
dP+5	0.00	0.00	0.01	-0.08	-0.07	-0.08	-0.06	-0.06	0.00	0.00	-0.01
Sum O=	0.00	-0.10	-0.25	-4.78	-0.21	-2.40	-2.70	-2.76	-0.01	-0.17	-0.20
dH2O	0.00	0.30	1.18	2.31	2.10	2.82	2.63	2.58	0.87	0.16	0.05
dCO2	0.00	0.11	0.27	1.86	4.70	3.55	1.91	1.85	-0.38	-0.14	0.68
dS	0.00	0.00	0.00	0.01	0.13	0.06	0.04	0.03	0.01	0.00	-0.01
dTotal	0.00	0.14	-1.05	-24.98	12.76	-3.73	-7.76	-8.52	0.10	-1.57	-1.49
Residual	0.00	0.11	-0.00	0.00	0.03	0.01	0.01	0.01	0.00	0.00	-0.00

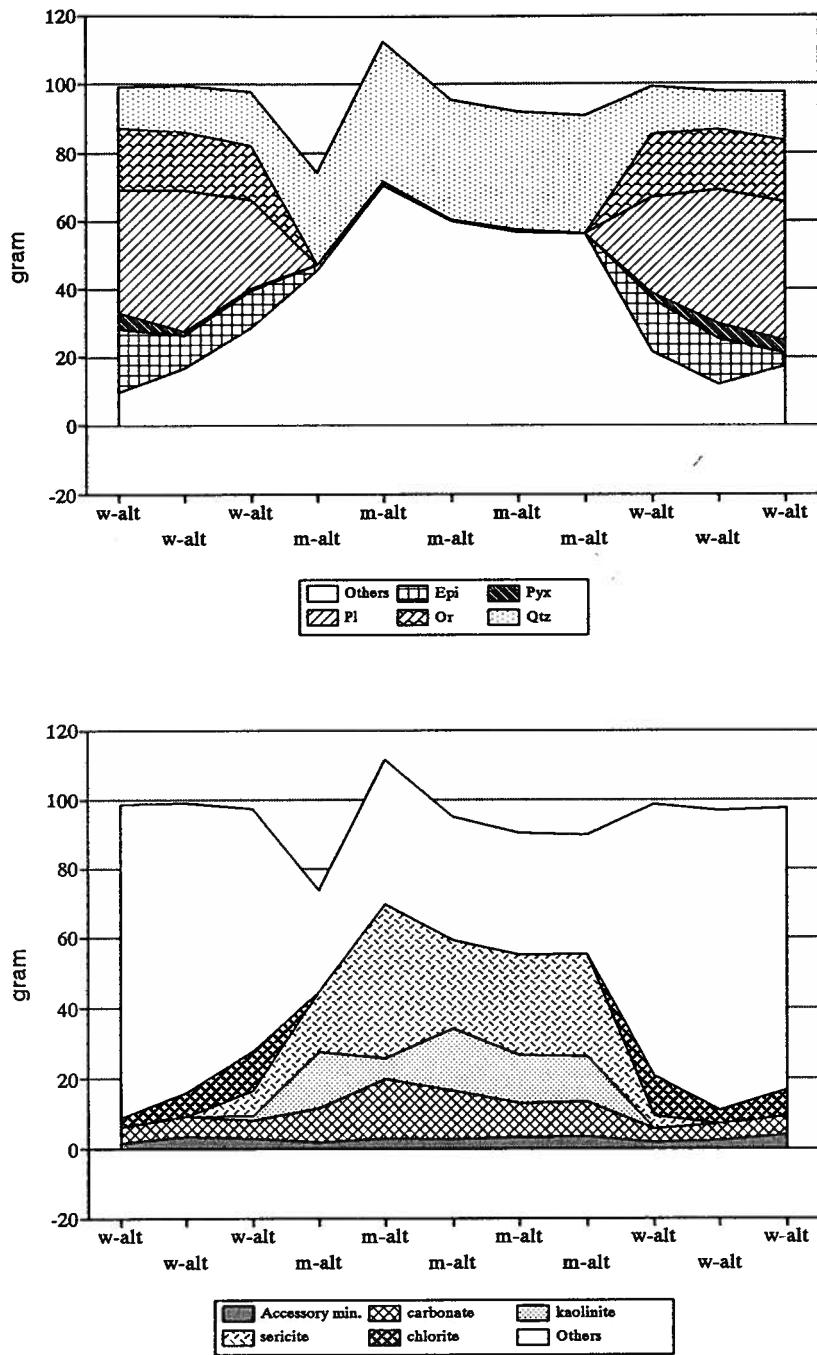


Figure 6-7a. Metasomatic norm profile (closure has been removed) at the northern segment of the No. 3 vein. w-alt., propylitic andesite; m-alt., sericitic/argillic alteration envelope.

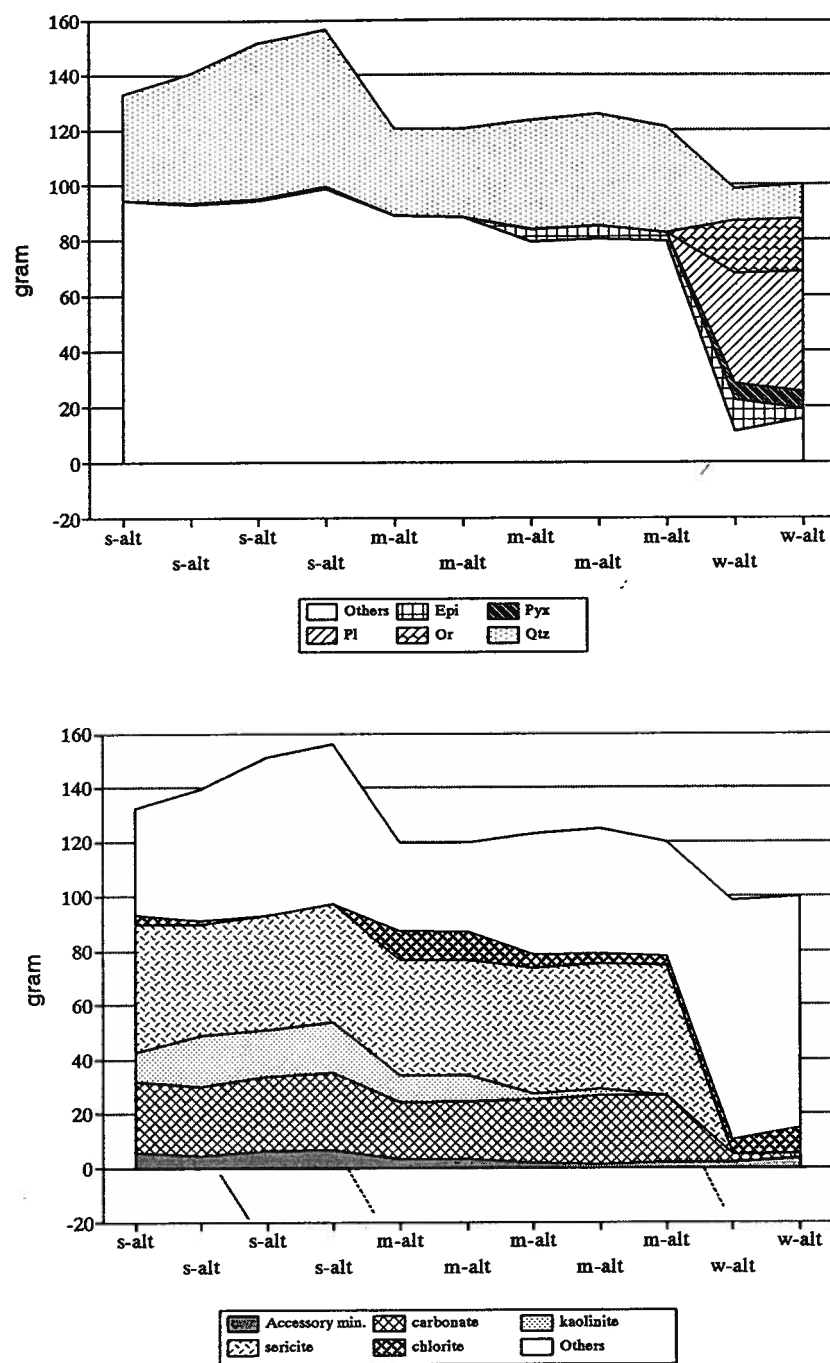


Figure 6-7b. Metasomatic norm profile (closure has been removed) at Switch Back vein
w-alt, propylitic andesite, m-alt, sericitic/argillic alteration outer envelope; s-alt, silicic
and pyritic alteration inner envelope.

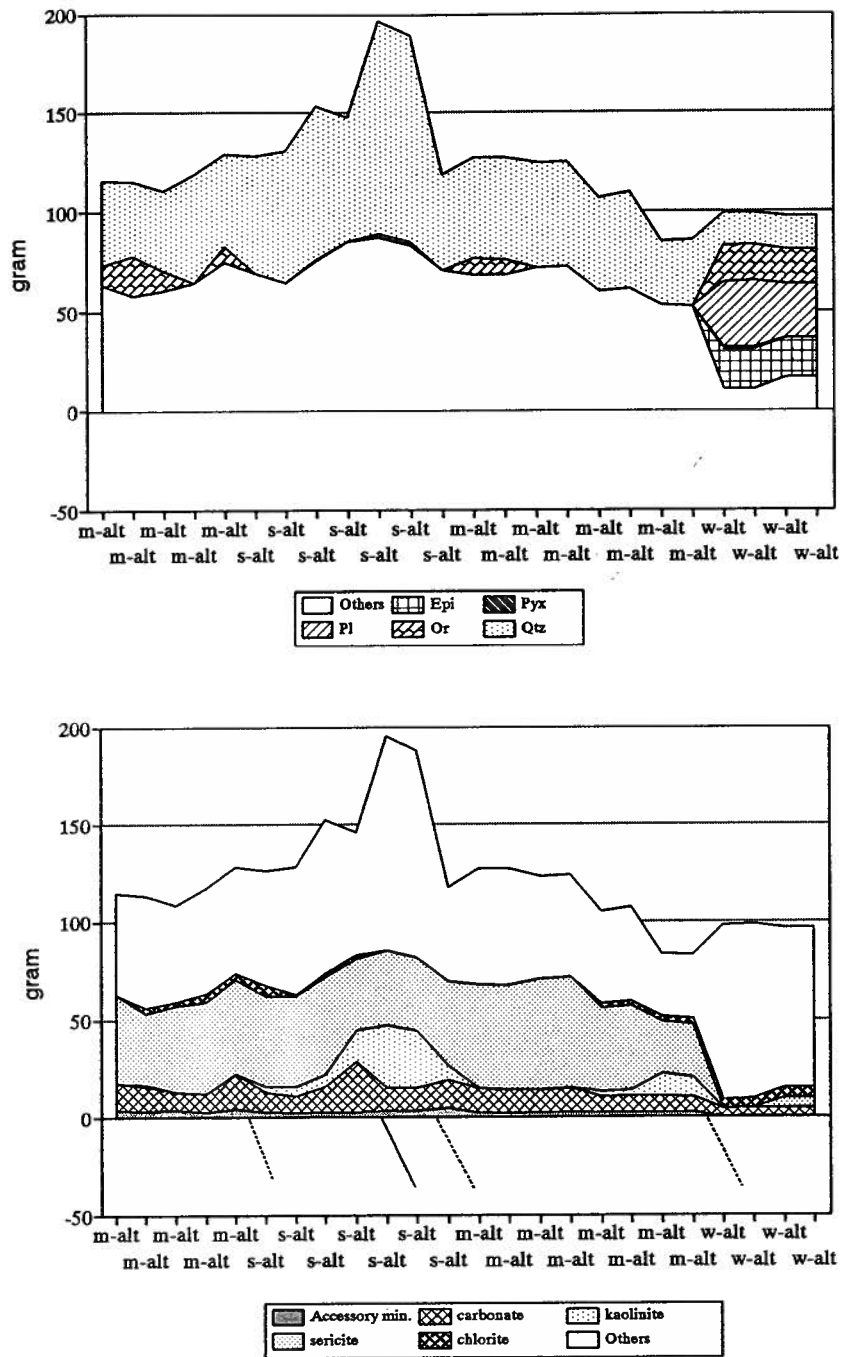


Figure 6-7c. Metasomatic norm profile (closure has been removed) at central segment of the No. 3 vein. w-alt., propylitic microdiorite; m-alt., sericitic/argillic alteration outer envelope; s-alt., silicic/pyritic alteration inner envelope.

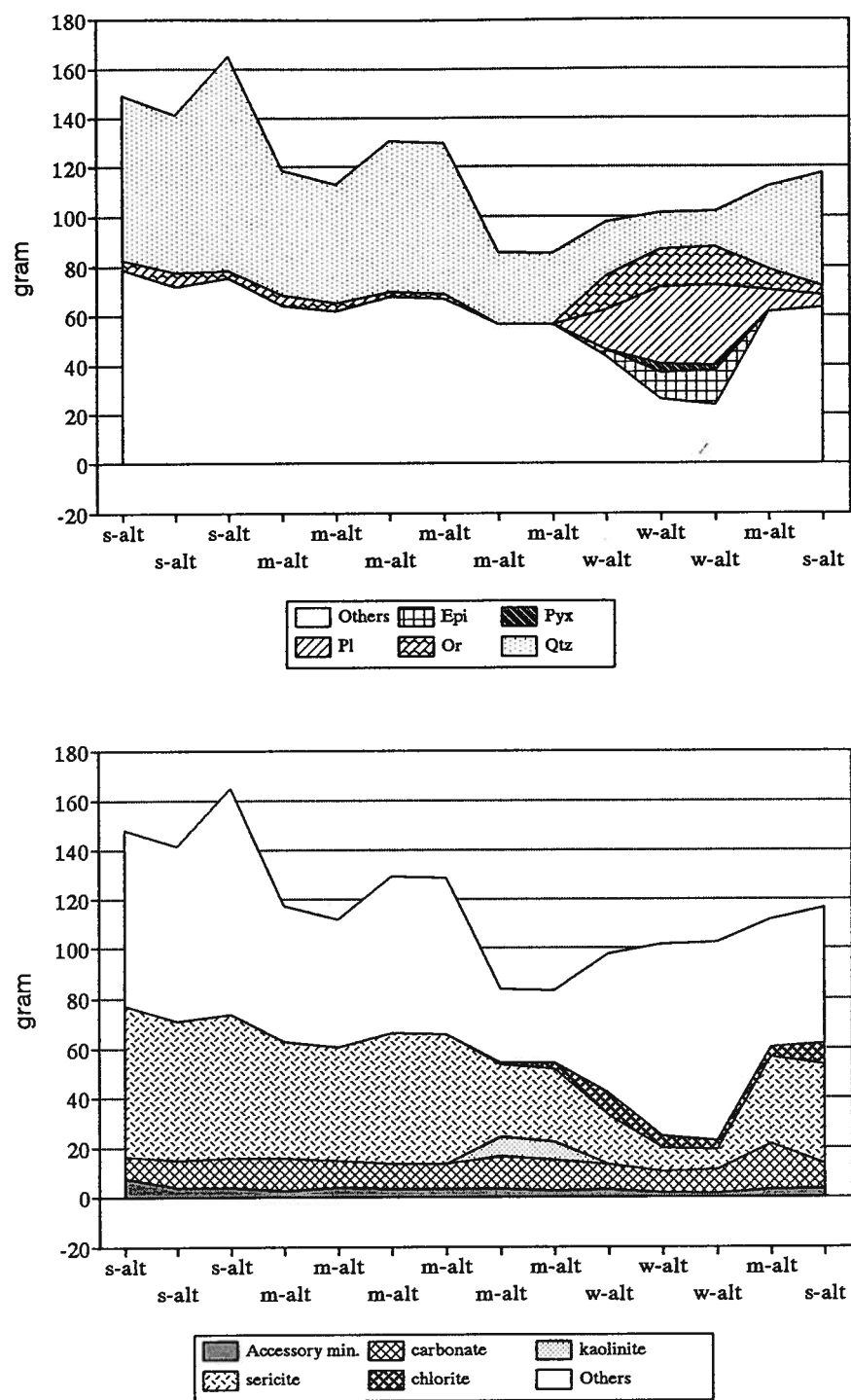


Figure 6-7d. Metasomatic norm profile (closure has been removed) at southern segment of the No. 3 vein. w-alt., propylitic andesite; m-alt., sericitic/argillic alteration outer envelope; s-alt., silicic/pyritic alteration inner envelope.

carbonatized. The carbonatization of the alteration envelope at the southern segment of the No. 3 vein is the mildest.

Argillization is extensively developed in the narrow alteration envelope at the northern segment of the No. 3 vein. The alteration envelope of the Switch Back vein is characterized by an inner extensive argillic subzone. The broad alteration envelope at the central segment of the No. 3 vein has an inner argillic subzone similar to that of the Switch Back vein but much narrower than that of the Switch Back vein. There is also an argillic alteration outer subzone adjacent to the boundary between the alteration envelope and propylitic halo at the central segment of the No. 3 vein. A similar outermost argillic subzone is present in the alteration envelope of the southern segment of the No. 3 vein too.

Sericitization is extensive in all four alteration envelopes but is strongest in the alteration envelope of the southern segment of the No. 3 vein (the content of sericite is up to about 61 gram relative to 48 gram on average). In contrast, the content of sericite in the alteration envelope of the northern segment of the No. 3 vein is relatively low (up to 44 gram and 29 gram on average, respectively).

Potassic alteration is indicated by the presence of normative K-feldspar in the alteration envelopes of the central and southern segments of the No. 3 vein. In contrast, there is no normative K-feldspar present in the alteration envelopes of the Switch Back vein and the northern segment of the No. 3 vein.

Silicification is strong in the alteration envelopes of the central and southern segments of the No. 3 vein. It is weakest in the alteration envelopes of the northern segment of the No. 3 vein and the Switch Back vein.

In brief, the results of the metasomatic norm calculations of four alteration profiles provide a comprehensive, quantitative view of mass and mineralogical changes that are associated with hydrothermal alteration at the Silver Queen mine. The ambiguities of the interpretation have been largely reduced by considering all constituents of the geochemical

system, and by using mass balance and known minerals as constraints. The metasomatic norm profiles documented in this section link the lithogeochemical variations with the mineralogical variations. They present the hydrothermal alteration associated with precious- and base-metal vein mineralization in an easily understood way.

6.8. Propagated Error Analysis and Confidence Level of the Quantitative Evaluations

To decide which chemical and mineralogical variations discussed in the previous sections are significant, the propagated errors are calculated using equations 3-31 and 3-33 and the values of S_0 and k of each chemical constituent (derived from the duplicate analyses, cf. Table 6-3). The propagated error calculation of the northern profile of the No. 3 vein are listed in Tables 6-9a as a selected example. The calculation results of other three profiles are listed in Appendix E, Table 6-9b, 6-9c and 6-9d. Only the chemical or mineralogical variations that are larger than the corresponding propagated errors can be safely considered as significant. Smaller apparent variations may be caused entirely by artificial factors. By using this technique the words 'significant' and 'insignificant' are used to describe the variations according to an objective criterion.

Based on the calculation of propagated error, the four alteration profiles can be interpreted with respect to significant chemical variations. For example, the propylitic altered samples from the alteration profile at the northern segment of the No. 3 vein have absolute losses and gains of SiO_2 ranging from -0.11 to 1.53 gram, and the propagated errors of SiO_2 for these samples range from ± 1.76 to ± 1.80 gram at 68% confidence level. Thus, SiO_2 mobility in the propylitically altered rock is not significant. In contrast, the altered samples x3-5 and x3-4 in the alteration envelope have absolute losses and gains of SiO_2 equal to -14.19 and 6.76 gram respectively. These changes in SiO_2 contents are much greater than their propagated errors (± 1.38 and ± 2.03 gram at the 68% confidence level, respectively). The other three samples (x3-1, x3-2 and x3-3d) in the alteration

Table 6-9a. Propagated errors of metasomatic norms corrected for closure and absolute losses/gains of components in grams at the 68% confidence level, the northern segment of the No. 3 vein, Silver Queen mine, central BC

Sample_id	x4-4	x3-7	x3-6	x3-5	x3-4	x3-1	x3-2	x3-2	x3-3d	x3-3	x2-5
Alteration	w-alt	w-alt	w-alt	m-alt	ms-alt	ms-alt	m-alt	m-alt	w-alt	w-alt	w-alt
gram											
Pyroxene	0.17	0.04	0.03	0.00	0.00	0.00	0.00	0.00	0.16	0.19	0.28
Plagioclase	0.95	1.10	0.69	0.01	0.04	0.02	0.04	0.00	0.75	1.04	1.08
K-feldspar	0.48	0.45	0.42	0.00	0.00	0.00	0.00	0.00	0.49	0.46	0.48
Quartz	0.33	0.36	0.43	0.71	1.15	0.96	0.93	0.93	0.38	0.30	0.39
Carbonate	0.40	0.36	0.34	0.60	1.05	0.86	0.65	0.65	0.24	0.34	0.40
Epidote	0.50	0.26	0.29	0.05	0.00	0.00	0.00	0.00	0.41	0.36	0.10
Chlorite	0.11	0.28	0.41	0.00	0.00	0.00	0.00	0.00	0.42	0.15	0.27
Sericite	0.00	0.00	0.20	0.47	1.26	0.71	0.79	0.82	0.11	0.00	0.00
Kaolinite	0.00	0.00	0.05	0.51	0.21	0.58	0.45	0.42	0.00	0.01	0.00
Pyrite	0.00	0.00	0.00	0.00	0.01	0.01	0.01	0.01	0.00	0.00	0.00
Hematite	0.00	0.06	0.06	0.04	0.10	0.09	0.10	0.10	0.01	0.03	0.11
Magnetite	0.00	0.00	0.00	0.00	0.00	0.00	0.00	0.00	0.00	0.00	0.00
Ilmenite	0.00	0.04	0.00	0.00	0.00	0.01	0.00	0.00	0.00	0.00	0.00
Rutile	0.02	0.00	0.02	0.02	0.02	0.01	0.02	0.02	0.02	0.02	0.02
Apatite	0.04	0.04	0.04	0.02	0.05	0.04	0.03	0.03	0.04	0.04	0.03
Total	2.99	2.99	2.98	2.44	3.89	3.29	3.01	2.98	3.04	2.94	3.16
dSiO2*	1.73	1.73	1.68	1.33	1.95	1.66	1.63	1.61	1.72	1.70	1.69
dAl+3	0.32	0.32	0.32	0.28	0.38	0.33	0.33	0.32	0.32	0.31	0.31
dTi+4	0.01	0.01	0.01	0.01	0.01	0.01	0.01	0.01	0.01	0.01	0.01
dFe+3	0.13	0.12	0.13	0.09	0.11	0.10	0.11	0.11	0.12	0.12	0.12
dFe+2	0.12	0.12	0.12	0.11	0.20	0.17	0.13	0.12	0.12	0.12	0.12
dMn+2	0.03	0.03	0.03	0.03	0.05	0.04	0.03	0.03	0.03	0.03	0.03
dMg+2	0.14	0.14	0.14	0.11	0.12	0.12	0.11	0.11	0.15	0.14	0.15
dCa+2	0.18	0.18	0.18	0.12	0.13	0.12	0.13	0.13	0.18	0.18	0.17
dNa+	0.16	0.16	0.16	0.11	0.13	0.12	0.12	0.12	0.16	0.16	0.15
dK+	0.11	0.11	0.11	0.08	0.15	0.10	0.11	0.11	0.11	0.11	0.11
dP+5	0.02	0.02	0.02	0.01	0.02	0.01	0.01	0.01	0.02	0.02	0.02
Sum O=	0.65	0.65	0.65	0.53	0.70	0.62	0.60	0.60	0.65	0.65	0.65
dH2O	0.24	0.27	0.36	0.49	0.48	0.56	0.54	0.53	0.33	0.25	0.24
dCO2	0.36	0.37	0.39	0.54	0.87	0.74	0.55	0.55	0.33	0.35	0.43
dS	0.00	0.00	0.00	0.00	0.01	0.01	0.01	0.01	0.00	0.00	0.00
dTotal	4.19	4.23	4.28	3.87	5.31	4.72	4.41	4.37	4.25	4.15	4.20

* prefix d stands for the absolute difference of corresponding constituent between the least altered and altered rocks.

envelope have gained SiO_2 ranging from 2.32 to 3.5 gram, respectively. This is close to their propagated errors of SiO_2 ranging from ± 1.68 to ± 1.73 gram at the 68% confidence level and is almost equal to the propagated error at the 95% confidence level (from ± 3.36 to ± 3.46 gram). Therefore, the gains of SiO_2 at the sites where these three sample were collected are very small. Similar examination of the other chemical and mineralogical variations can be carried on by comparing the data listed in Tables 6-8a, with the corresponding propagated errors listed in Tables 6-9a.

6.9. A Comprehensive Model of Hydrothermal Alteration

A comprehensive model is suggested here to illustrate the process of hydrothermal alteration at the Silver Queen mine. A set of comprehensive, mass balanced reaction equations can be constructed by combining the data listed in Tables 6-7a, 6-8a, and 6-9a. For instance, if sample x4-4 is the precursor rock of sample x3-5, the hydrothermal alteration of sample x3-5 can be interpreted as follows. The primary minerals such as pyroxene (0.023 mole or 5.11 ± 0.17 gram), plagioclase (0.136 mole or 36.01 ± 0.95 gram) and K-feldspar (0.066 mole or 18.26 ± 0.48 gram) as well as some of propylitic altered minerals including chlorite (0.004 mole or 3.05 ± 0.11 gram) and epidote (0.039 mole or 18.7 ± 0.5 gram) are mainly replaced by sericite (0.044 mole or 17.28 ± 0.47 gram), kaolinite (0.063 mole or 16.28 ± 0.51 gram), carbonate (increased from 0.053 mole or 4.86 ± 0.34 gram to 0.093 mole or 9.81 ± 0.6 gram) and quartz (increased from 0.2 mole or 12.02 ± 0.33 gram to 0.456 mole or 27.38 ± 0.71 gram). These replacements are accompanied by the mass losses of SiO_2 (-0.236 mole or -14.19 ± 1.38 gram), Al^{+3} (-0.041 mole or -1.1 ± 0.22 gram), Fe^{+3} (-0.027 mole or -1.5 ± 0.04 gram), Mg^{+2} (-0.056 mole or -1.37 ± 0.03 gram), Ca^{+2} (-0.072 mole or 2.9 ± 0.07 gram), Na^{+} (-0.110 mole or -2.54 ± 0.04 gram), K^{+} (-0.029 mole or -1.11 ± 0.06 gram) from wall rock to hydrothermal solution and the mass gains of H_2O (0.129 mole or 2.31 ± 0.1 gram) and CO_2 (0.042 mole or 1.86 ± 0.12 gram). All these exchanges can be presented as a comprehensive reaction equation as follows:

Primary minerals	0.023pyroxene + 0.136plagioclase + 0.066K-feldspar + 0.2quartz			
	5.11±0.17 g	36.01± 0.95 g	18.26±0.48 g	12.02±0.33 g
Propylitic alteration	+ 0.004chlorite + 0.039epidote + 0.053carbonate			
	3.05±0.11 g	18.7±0.5 g	4.86±0.34 g	
mass losses	- 0.236SiO ₂ - 0.041Al ⁺³ - 0.027Fe ⁺³ - 0.056Mg ⁺² - 0.072Ca ⁺² - 0.11Na ⁺ - 0.029K ⁺			
	-14.19±1.38 g	-1.1±0.22 g	-1.5±0.04 g	-1.37±0.03 g -2.9±0.07 g -2.54±0.04 g -1.11±0.06 g
mass gains	+ 0.129H ₂ O + 0.042CO ₂			
	2.31±0.1 g	1.86±0.12 g		
sericitic, argillic, carbonatized, silicified alteration	= 0.044sericite + 0.063kaolinite + 0.093carbonate + 0.456quartz			
	17.28±0.47 g	16.28±0.51 g	9.81±0.6 g	27.38±0.71 g

The chemical constituents have been converted from oxides into ionic species. There are two reasons for these conversions. One is to correct for the effect of sulfur on the value of the total weight of the sample. Analytical measurements provide the results of most constituents in the form of oxides but report sulfur in elemental form. In reality, however, sulfur is in the form of an anion combined principally with Fe. Thus, Fe⁺² may not combine with oxygen anion entirely as an oxide but may combines partly with sulfur anion as a sulfide, such as FeS₂. As a result, the total weight of the sample may be exaggerated when abundant sulfides exist in the sample and their cations are analytically reported as oxides. In contrast, calculations of a metasomatic norm allot cations to critical minerals and take corresponding required amounts of necessary anions to form each normative mineral according to the stoichiometries of the mineral. Consequently, the total value of normative minerals will not be balanced with the total value of analytical constituents when sulfur is present in an analysis. The extra oxygen will be easily taken out during the conversion of oxides to ionic species.

The other reason for converting oxides to ionic species except SiO₂ is that a mass balanced equation is commonly presented in the forms of solid mineral phases and soluble ionic species or complexes rather than oxides. SiO₂ is an exception because it exists both in a solid form as quartz and as an aqueous species. It is also possible that these species can

be further converted to any probable form of aqueous complex such as HCO_2^- , $\text{Al}(\text{OH})^{-2}$, etc., if there is sufficient evidence to support the existences of these complexes in the hydrothermal fluid.

The aim of this thesis is to extend quantitative methods in the evaluation of material exchanges during hydrothermal alteration associated with precious- and base-metal vein deposit in volcanic sequences. Of the methods currently used, Gresens' equation and Pearce element ratio diagrams are the most popular and most useful. Gresens' equation and Pearce element ratio diagrams are superficially different but are fundamentally similar in principle. That is, they both remove the closure effect in order to decipher the true chemical variations during alteration. Gresens' procedure emphasizes chemistry. Pearce element ratios provide the ability to discuss losses and gains mineralogically.

The first requirement of applying these quantitative techniques to the estimation of absolute losses and gains in a metasomatic system is to determine immobile components from lithogeochemical data. The determination of immobile components is recommended through a two-fold consideration of:

- (i) the ratio of two immobile components remains constant in a single precursor system regardless of the nature of the alteration, and
- (ii) two immobile components must not be mineralogically or geochemically compatible with each other during the hydrothermal alteration process.

In reality, there is no perfectly constant ratio of a pair of immobile components. Minor variation in ratios may result from improper sampling and sample preparation procedure as well as analytical error. Analytical error can be quantified to provide a basis for recognizing significant variation, such as ratio variability that is too large to be attributed to analytical error (thus, too large to accept the two components of the ratio as being immobile). This rule is to be used cautiously. If a PER ratio is constructed with one of the components being mobile and the other having poor analytical precision, then the latter component will contribute more to the final propagated error of the ratio, especially

where it is used as the denominator of the ratio. As a result, mobility of the former component might be obscured and the plot might lead to the incorrect conclusion that both numerator and denominator are immobile. Therefore, 'immobile' components of relatively high analytical quality should be accepted in preference to those with poor analytical precision.

The second requirement of applying these quantitative techniques for estimating losses and gains in metasomatic system is that a suite of samples for which loss/gain variations are to be evaluated, must be the alteration products of either: (i) a single parent rock characterized by chemical and mineralogical homogeneity (single precursor system), or (ii) a suite of rocks with determinable pre-alteration chemical compositions (multiple precursor system). This requirement can be met conventionally through the careful investigation of the field and petrographic relationships in the study area. Rock derivatives altered to various degrees from a common homogeneous parent rock commonly are in close spatial proximity and may show gradational contacts between each other. Primary textural and structural features may remain identifiable in least-altered to more intensively altered derivatives. To examine these types of variations rigorously it is recommended that samples be collected systematically along alteration profiles from the strongly altered rock adjacent to, or within, a mineralized zone, to the least altered rock far from the ore deposit itself. Such sampling should be done after a careful field investigation of the profile. Even though the altered rocks are our main concern, equal attention should be paid to the least altered or unaltered rocks because they provide important information about the parent rocks before hydrothermal alteration. This gives insight into the possibilities of a single precursor system versus a multiple precursor system.

The PER approach to examining a metasomatic system has an advantage over other procedures in not only removing the closure effect of lithogeochemical data by using immobile components, but also by explaining the corrected chemical variations in terms of mineralogical variation. Two specific PER diagrams have been designed to discriminate

the hydrothermal alteration types commonly associated with epithermal vein deposits in volcanic sequences. The first one is constructed with $\text{Si}/(\text{immobile component})$ as its x-axis and $[1/4\text{Al} + 11/4(\text{Na}+\text{K}) + 3/2\text{Ca} + 1/2(\text{Fe}+\text{Mg})]/(\text{immobile component})$ as its y-axis. The displacement vectors of primary minerals such as augite, anorthite, albite and K-feldspar, and alteration mineral chlorite are defined to have slopes equal to one, the displacement vectors of carbonates and pyrite are parallel to the y-axis, the slope of muscovite is $7/6$, the slope of kaolinite is $1/4$ and the slope of quartz is zero. Therefore lithogeochemical variations caused by either primary feldspar and augite fractionation, intense carbonatization, argillization, sericitization or silicification can be discriminated if either of them is the dominant contributor to the lithogeochemical variation. The second PER diagram is designed to deal with more complicated types of alteration. It has $\text{Al}/(\text{immobile component})$ as its x-axis and $(2\text{Ca}+\text{Na}+\text{K})/(\text{immobile component})$ as its y-axis. The displacement vector of quartz is designed to be perpendicular to the diagram. As a result, the discriminations of carbonatization, argillization and sericitization from primary crystal fractionations are relatively easier on this PER diagram

These specifically designed PER diagrams can be used to test the hypotheses that chemical variations are due to variations in amounts of a particular set of minerals, but the amount of each mineral can not be determined explicitly because the total displacement on a PER diagram commonly is the sum of the displacements of different minerals when a complicated multiple variable system is considered. In other words, ambiguity arises where too many variables are summarized in two dimensional space.

A metasomatic norm approach has been developed in this thesis to quantitatively and objectively evaluate material exchange in complicated hydrothermal alteration systems associated with precious- and base-metal vein deposits in volcanic sequences. A metasomatic norm is a quantitative and objective approach to estimating mineral abundances from the lithogeochemical data since the mineralogy and chemistry of a rock are intimately linked through mineral abundances and the compositions of individual

minerals. The normative approaches, originally designed principally for igneous rocks, are rigid in their application and in general, do not utilize important alteration minerals. The different approach here, to the determination of norms of hydrothermally altered rocks combines petrographic and lithogeochemical data. Metasomatic norm calculation uses the same principles as the calculation of CIPW norms, but different mineral phases including volatile component-bearing minerals are used as the normative standard minerals that represent hydrothermal alteration systems. Another distinctive difference between a metasomatic and a conventional igneous norm is that the calculation of a metasomatic norm does not proceed along a fixed hierarchical path as in the case of an igneous norm. More flexibility is necessary because of the wide range in both rock and mineral compositions. In some cases, where constrained by known mineralogy, the calculations must alternate back and forth following a loosely defined sequence in order to eventually balance or best fit a calculated mineral assemblage with the fixed chemical composition of an altered rock (i.e., to make the chemical masses and the mineral masses balance). In addition, the calculation of a metasomatic norm take into account possible incompatible mineral pairs in a hydrothermal system. A possible approach to the application of the norm concept to metasomatic rocks is to constrain the calculated normative mineralogy by *a priori* knowledge of existing minerals (i.e. to approximate the mode as closely as possible).

The selection of a set of standard minerals for metasomatic norm calculation is based on geological observations. A set of standard normative minerals based on the author's experience are given in this thesis. This set of normative minerals should not be considered exhaustive. It can be extended by the addition of new standard normative mineral(s). Other identified mineral species can be substituted to meet specific requirements.

The general procedural scheme for metasomatic norm calculation is inefficient for manual calculation. Consequently, a computer-based procedure using Quattro Pro 5.0, a

sophisticated and readily available spread sheet program, has been devised to process norm calculations. It can be easily converted to other spread sheet software (Appendix C). The procedure involves the use of a built-in module — Optimizer in the software. The general procedure of using Optimizer is to decide on the solution destination, choose the variables (standard minerals) to be included in the calculation, and set up the constraints. Then the Optimizer module can adjust the amounts of the variables and adhere to the constraints to provide a final best-fit solution. Unlike other 'black box' types of software, this calculation model is transparent. Users can easily adjust and develop it according to their own purposes.

With the recognition of an immobile component, the metasomatic norms for precursor and altered rocks, and the constituents lost or gained, can be further recast into the absolute amounts of minerals and chemical constituents relative to a given mass of parent rock by using Gresens' equation. Consequently, the calculated results can be used to construct a comprehensive mass balanced and easily understood chemico-mineralogical model to interpret a hydrothermal alteration system in terms of initial and final normative mineral assemblages (corrected for closure) plus absolute losses and gains of chemical constituents. It does not matter whether the system is closed or open, or whether it represent equilibrium or disequilibrium assemblages.

All lithogeochemical data contain errors. Therefore, errors have been propagated in this thesis to the final results of all calculations of absolute losses and gains, including metasomatic norm in intensive units (percentage) and metasomatic norm in extensive units (grams relative to a specific amount of precursor rock) after correction for closure. Such propagated errors also have been integrated with the results of the chemico-mineralogic model for material exchange (including absolute losses and gains of chemical constituents as well as the normative minerals) formulated in this work as follows:

$$\begin{aligned} & \sum \text{Mineral}_{\text{parent rock}} \pm \text{error} + \sum \text{Constituent}_{\text{gained from solution}} \pm \text{error} \\ & = \sum \text{Mineral}_{\text{altered rock}} \pm \text{error} + \sum \text{Constituent}_{\text{lost from wall rock}} \pm \text{error} \end{aligned} \quad (7-1)$$

The value of such an equation is that it provides useful, quantitative information about the hydrothermal system and limits the properties of the hydrothermal solution that effected the metasomatism, provided the equation represents a simple and unique alteration process. In reality, this type of reaction equation may more likely represent the final result of a series of sequential and/or superimposed processes. Nevertheless, the form of the equation is particularly useful because it is both quantitative and easily comprehensible. Specifically, the equation includes starting and ending rock mineralogies that may be partly evident in the field. It documents gains and losses of specific chemical constituents in space. Also it includes the uncertainties of each item at certain confidence level, which indicate what variations are significant.

In brief, this chemico-mineralogical model:

- (i) provides an objective and quantitative basis for a mineralogical classification of hydrothermally altered rock;
- (ii) maps spatial distribution of normative minerals from lithogeochemical data;
- (iii) interprets lithogeochemical variations in terms of mineralogical variations
- (iv) recasts norms to mass units relative to a specified amount of the parent rock
- (v) then combines norms with the absolute losses and gains of lithogeochemical constituents to form a comprehensive mass balanced equation;
- (vi) integrates the propagated errors to indicate what variation is significant.

The methodology for this approach is a natural extension of the use of Pearce element ratio (PER) diagrams for the study of metasomatic rocks. The metasomatic norm approach is quantitative in the same way as Pearce element ratio diagrams. The common principle is the correction for closure that provides true relative lithogeochemical and mineralogical variations between parent and daughter rocks. The normative approach is a useful supplement to PER analysis; the two procedures have much in common and contain much the same information presented in different ways. The strategy of a PER diagram is

to test whether chemical changes between two rocks can be explained purely by the variation(s) of certain mineral(s) as demonstrated by disposition of plotted points along predefined trends (slopes) according to the partial mass balance relationship. Metasomatic norms are displayed more explicitly as equations or profiles showing the spatial distributions of normative mineral assemblages, as well as the absolute losses and gains of chemical constituents based on comprehensive mass balance relationships. In brief, metasomatic norms solve the problems of multiple variables in multiple dimensional space.

In a quantitative evaluation of hydrothermal alteration, it is essential to know the quality of data so that conclusions can be derived with confidence. The major causes for the variations of lithogeochemical data are classified as primary causes (such as crystal fractionation, mixing and assimilation), secondary causes (such as metamorphism, hydrothermal alteration and weathering) and artificial causes (insufficient sample size, improper sample preparation, analytical error, etc.). Ideally, variations generated by artificial processes should be eliminated. In practice, however, they can only be minimized through quality control, such as the estimation of the optimum sample size, the necessary fineness of the ground grain size, and quality assessment of analytical results in terms of precision, accuracy and detection limit.

To estimate the optimum size for a sample or the necessary fineness of the particle size for a subsample, the model of 'two-mineral mixture of uniform grain size' and binomial distribution function are used in this thesis to simulate the distribution of major and compatible trace elements during sampling and subsampling processes. Because the rock types in the study area (Silver Queen mine) are massive and porphyritic volcanic flows and high level intrusive rocks, the inhomogeneities of various constituents at the sampling stage are mainly caused by phenocrysts, such as plagioclase and augite. Calculations indicate that the optimal sample size depends on the coarseness of phenocryst and homogeneities of the constituents of interest in the rock; 500 grams of sample are needed to reduce the sampling error to around one percent at the 68% confidence level. The

optimal particle fineness of the subsample depends on the variable being considered: both the abundance of an element in a mineral of interest and the amount of the mineral are important parameters.

The quality of lithogeochemical data is a function of various factors including: (i) strategy of sampling, (ii) the sample preparation scheme, (iii) the skill and experience of the researcher and/or instrument operator, (iv) the operating condition of the instrument, (v) the standards used to calibrate the counting values and (vi) the method of converting the counting values to meaningful lithogeochemical data as well as (vii) the concentrations of components/elements. Therefore, the quality of each set of lithogeochemical data must be assessed individually through the use of duplicates.

To assess the quality of lithogeochemical data the method of Thompson and Howarth (1976, 1978) has been used to treat precision as a function of concentration; the method has been modified slightly to deal with small sets of duplicate lithogeochemical data. Duplicates selected for the Silver Queen study are arranged at two different stages. One is at the field sample stage and the other at the analytical measurement stage. Analytical errors are consistently much lower than field sampling variability. The reason for this is that the duplicates arranged at the field sampling stage contain more sources of errors and include the artificial errors caused by insufficient sample size, inhomogeneity of subsample and inconsistent analytical measurements. Because the purpose of using lithogeochemical data is to reveal real geochemical variations it is essential to include sampling variability (i.e. using duplicates samples) as a basis for recognizing meaningful variation.

The application of the approach described in the first part of this thesis to the study of the Silver Queen mine reveals that there are two distinctive series of volcanic and intrusive rocks in Owen Lake area. The first series consists of igneous and volcanic units from intermediate to felsic composition. They are characterized by having the lower content of TiO_2 , MgO , total iron and P_2O_5 as well as the older K-Ar dating ages (range

from 78.8 to 57.2 Ma). The second series consist of igneous and volcanic units from intermediate to mafic composition. They have higher contents of TiO_2 , MgO , total iron and P_2O_5 as well as the younger K-Ar dating ages (range from 48.7 to 21.4 Ma). The former predates and hosts the mineralization. The latter is post-mineralization.

The hydrothermally altered samples at the Silver Queen mine derive from a multiple precursor system defined by the fractionation trend of the older series of igneous rocks of the Owen Lake area. However, each local, individual hydrothermal alteration profile exhibits the attributes of a single precursor system. These are characterized by a linear trend going through the origin of a TiO_2 -Zr binary plot. Furthermore, the mineralogical and geochemical incompatibility of these two potentially immobile constituents are examined to eliminate any possibility that TiO_2 and Zr could be mobile. Of these two immobile components, TiO_2 is used to remove the closure of lithogeochemical data because its lithogeochemical error is smaller than that of Zr.

Six types of hydrothermal alteration at the Silver Queen mine have been described. They are propylitic alteration, sericitic and argillic alteration, silicification, pyritization and carbonatization. In general, the wall rock alteration in the study area is composed of a widespread regional propylitic alteration which gives way as the vein is approached to an outer envelope of sericitic and argillic alteration + carbonatization and an inner envelope of silicification and pyritization + sericitic or argillic alteration + carbonatization. Widespread regional propylitic and carbonatic alteration, sericitic and argillic outer envelope and silicification and pyritization inner envelope developed sequentially in that order.

Most of the hydrothermally altered samples in alteration envelopes at the Silver Queen mine have gained mass during the hydrothermal alteration. In contrast, samples from the profile of the northern segment of the No. 3 vein have lost mass. Other spatial variations of hydrothermal alteration from the southern segment to the northern segment of the No. 3 vein and from different levels (from 2600-foot level to 2880-foot level) have

been recognized. In brief, the wall rock alteration is most intense in the alteration envelope at the central segment of the No. 3 vein and mildest at the northern segment of the No. 3 vein. The total mass change of each altered sample is largely the result of depletions of CaO and Na₂O, and additions of SiO₂, K₂O, H₂O and CO₂.

In addition, the width of the alteration envelope is very much narrower along the northern segment of the No. 3 vein (total width about 7 m wide) compared to the central and southern segments of the No. 3 vein (total width up to 130 m wide). In some places, alteration envelopes around veins are distributed asymmetrically, principally because of the presence of other veins and because the No. 3 vein is, in reality, an *en echelon* vein zone.

In brief, the hydrothermal alteration at the Silver Queen mine can be summarized as follows:

- (1) The regional propylitic alteration is characterized by the replacement of mainly primary mafic mineral initially by epidote and chlorite as well as minor amount of carbonate and the partial replacement of plagioclase replaced by carbonate and sericite. This type of alteration is interpreted to be the product of hydrothermal activity that followed the initial stage of volcanism and predates the mineralization.
- (2) Carbonatization superimposed on the early propylitic alteration may be the product of a CO₂ degassing process, which might be related to the hydrothermal activity associated with mineralization, and is controlled by complicated fracture systems. With increasing intensity of superimposed carbonatization on propylitic alteration, more complete replacements of epidote and chlorite by abundant carbonates occur.
- (3) The hydrothermal activity associated with mineralization leads to the complete replacement of plagioclase by sericite and kaolinite, chlorite by siderite and magnetite by pyrite or hematite to form the outer alteration envelope.
- (4) The inner alteration envelope is interpreted as the product of the process superimposed on sericitic and argillic alteration outer envelope at a maximum stage

of ore-forming hydrothermal activity. This is marked by the replacement of sericite by quartz and by the direct precipitation of quartz, sulfide and carbonate from the hydrothermal solution. The close association between mineralization and the inner silicification envelope is clear. This implies that ore-forming metals are transported as Si, S, C complexes, and that the precipitation of quartz, sulfide and carbonate by the reaction between wall rock and hydrothermal solutions might trigger ore deposition.

Many questions dealing with material exchange in hydrothermal systems remain unanswered. A great deal of work is required to adapt what is known to a workable system that can be used by explorationists. Further insight is required into optimizing sampling procedure. Methods such as Pearce element ratio diagrams and metasomatic norms need to be extended to a wide range of geological environments so that the methodologies can be extended and their advantages and limitations more fully appreciated.

Bibliography

- Albarede, F., and Provost, A. (1977): Petrological and geochemical mass-balance equations; an algorithm for least-square fitting and general error analysis, *Computers & Geoscience*, 3, pp. 309-326.
- Appleyard, E.C. (1980) Mass balance computations in metasomatism; metagabbro /nepheline syenite pegmatite interaction in northern Norway. *Contributions to Mineralogy and Petrology*, 73, (2), pp.131-144.
- Appleyard, E.C. and J. Guha (1991) A special issue on application of hydrothermal alteration studies to mineral exploration, Preface. *Economic Geology*, 86, (3), pp. 461-465.
- Armstrong, R.L. (1988): Mesozoic and Early Cenozoic Magmatic Evolution of the Canadian Cordillera; Geological Society of America, Special Paper 218, pp. 55-91.
- Babcock, R.S. (1973) Computational Models of Metasomatic Processes. *Lithos*, 6, pp. 279-290.
- Barrett, T.J., MacLean, W.H. (1994) Chemostratigraphy and hydrothermal alteration in exploration for VHMS deposits in Greenstones and younger volcanic rocks. in Lentz, D.R., ed., *Alteration and alteration processes associated with ore-forming systems: Geological Association of Canada, Short Course Notes*, 11, pp. 433-467.
- Barrett, T.J. and MacLean, W.H. (1991): Chemical, mass, and oxygen isotope changes during extreme hydrothermal alteration of an Archean rhyolite, Noranda, Quebec. *Economic Geology*, 86, (2), pp. 406-414.
- Barrett, T. J., MacLean, W. H. and Cattalani, S. (1993) Massive sulfide deposits of the Noranda area, Quebec. V. The Corbet mine: *Canadian Journal of Earth Sciences*, 30, pp. 1934-1954.
- Barth, T.F.W., (1959) Principles of classification and norm calculations of metamorphic rocks. *Journal of Geology*, 67: pp.135-152.
- Barth, T. F. W. (1962) *Theoretical Petrology*. Wiley, New York, 416 p.
- Bates, R. L. and Jackson, J. A, editors (1987): *Glossary of Geology*. American Geological Institute, 749 p.
- Bernier, L. R. and MacLean, W. H. (1989): Auriferous chert, banded iron formation, and related volcanogenic hydrothermal alteration, Atik Lake, Manitoba. *Canadian Journal of Earth Sciences*, 26, (12), pp. 2676-2690.
- Bernstein, L.R. (1987) Mineralogy and petrography of some ore samples from the Silver Queen mine, near Houston, British Columbia. Unpub. report to Pacific Houston

- Resources Inc. by Mineral Search, 380 Willow Road, Menlo Park, California 94025, Aug. 1, 1987, 13 p.
- Billings, M. P. and C. J. Roy (1933) Weathering of the Medford Diabase - Pre- or Postglacial? A discussion. *Journal of Geology*, XII, pp. 654-666.
- Boyle, R. W., (1979) The geochemistry of gold and its deposits (together with a chapter on geochemical prospecting for the element): Geological Survey Canada Bull. 280, 584 p.
- Bodnar, R. J., Reynolds, T. J. and Kuehn, C. A. (1985) Fluid-inclusion systematics in epithermal systems; in Berger, B. R., and Bethke, P. M. (ed.), *Geology and Geochemistry of Epithermal Systems: Society of Economic Geologists, Reviews in Economic Geology*, 2, pp. 73-98.
- Brown, T.H. and Skinner, B.J., (1974) Theoretical prediction of equilibrium phase assemblages in multicomponent systems, *American Journal of Science*, 274, pp. 961-986.
- Capitani, C. and Brown, T.H. (1987) The computation of chemical equilibrium in complex systems containing non-ideal solutions. *Geochimica et Cosmochimica Acta*, 51, pp. 2639-2652.
- Carter, N.C. (1981): *Porphyry Copper and Molybdenum Deposits West-central British Columbia*; B. C. Ministry of Energy, Mines and Petroleum Resources, Bulletin 64, 150 p.
- Cattalani, S., Barrett, T. J., MacLean, W.H., Hoy, L. Hubert, C. and Fox, J.S. (1989): The Horne massive sulfide deposit, Noranda, Quebec. *Stearn, Colin W. Geological Association of Canada, Mineralogical Association of Canada; annual meeting; program with abstracts*, 14. p. 33-34
- Cheng, X. and Sinclair, A.J. (1994) Optimizing norm calculations of metasomatic rocks. in Chung, C. F. (ed.) *Proceedings, 1994 International Association for Mathematical Geology Annual Conference*, pp. 81-86.
- Cheng, X. and Sinclair, A.J. (1991) Recognition of immobile/conserved components and its application to hydrothermal altered rocks. *Exploration Geochemistry*, 1990, ed. F. Mrna, Prague, 1991, pp. 137-143.
- Cheng, X., Sinclair, A.J., Thomson, M.L., and Zhang, Y. (1991) Hydrothermal alteration associated with Silver Queen polymetallic veins at Owen Lake, central B.C. (93L/2). B.C. Ministry of Energy, Mines and Petroleum Resources, *Geological Fieldwork 1990, Paper 1991-1*, pp. 179-183.
- Church, B.N. (1970): *Nadina (Silver Queen)*. B. C. Ministry of Mines, Energy and Petroleum Resources, *Geology, Exploration and Mining 1969*, pp. 126-139.

- Church, B.N. (1971) Geology of the Owen Lake, Parrot Lakes, and Goosly Lake Area. B. C. Ministry of Energy, Mines and Petroleum Resources, Geology, Exploration and Mining 1970, pp. 119-127.
- Church, B.N. (1973): Geology of the Buck Creek Area; B. C. Ministry of Energy, Mines and Petroleum Resources, Geology, Exploration and Mining, 1972, pp. 353-363.
- Church, B.N. (1984): Geology of the Buck Creek Tertiary Outlier; B.C. Ministry of Energy, Mines and Petroleum Resources, unpublished 1:100 000 scale map.
- Church, B.N. (1985): Update on the Geology and Mineralization in the Buck Creek Area - the Equity Silver Mine Revisited (93L/1W); B.C. Ministry of Energy, Mines and Petroleum Resources, Geological Fieldwork, 1984, Paper, 1985-1, pp. 175-187.
- Church, B.N. and Barakso, J.J. (1990): Geology, lithogeochemistry and mineralization in the Buck Creek area, British Columbia. Paper Ministry of Energy, Mines and Petroleum Resources. 95 p.
- Church, B.N. and Pettipas, A.R. (1990) Interpretation of second derivative aeromagnetic maps at the Silver Queen and Equity Silver mines, Houston, BC. Canadian Mining Metallurgy Bull., 83, no. 934, pp.69-76.
- Cox, K.G., Bell, J. D. and Pankhurst, R. J., (1979) The interpretation of igneous rocks. George Allen & Unwin Ltd. London, 450 p.
- Cross, W., Iddings, J.P., Pirsson, L. V. and Washington, H.S., (1903) Quantitative classification of igneous rocks. University of Chicago Press.
- Cross, W., Iddings, J.P., Pirsson, L. V. and Washington, H.S., (1902) A quantitative chemico-mineralogical classification and nomenclature of igneous rocks. Journal of Geology, 10: pp. 555-690.
- Cummings, W.W. (1987) Report on the Silver Queen Mine, Omineca Mining Division, British Columbia. Unpub. report for Houston Metals Corporation, March, 1987, 17 p.
- Cyr, J.B., Pease, R.B., and Schroeter, T.G. (1984) Geology and mineralization at the Equity Silver Mine. Economic Geology, 79, pp. 947-968.
- Davies, J. F., Whitehead, R. E. S., Cameron, R. A., and Duff, D. (1982) Regional and local patterns of CO₂-K-Rb-As alteration: A guide to gold in the Timmins area: Canadian Inst. Mining Metallurgy Spec., 24, pp. 130-143.
- Davis, S.R. and Ferry, J.M. (1993): Fluid infiltration during contact metamorphism of interbedded marble and calc-silicate hornfels, Twin Lakes area, central Sierra Nevada, California. Journal of Metamorphic Geology, 11. (1). pp. 71-88.

- Dawson, J.M. (1985) Report on the Owen Lake Property, Omineca Mining Division, British Columbia, for Bulkley Silver Resources Ltd. Unpub. report by Dawson Geological Consultants Ltd., Kamloops, B.C., August 1985, 30 p.
- Descarreaux, J. (1973) A petrochemical study of the Abitibi volcanic belt and its bearing on the occurrence of massive sulphide ores: *Canadian Mining Metallurgy Bull.*, 66, (730), pp. 61-69.
- Diakow, L.J. and Koyanagi, V. (1988) Stratigraphy and mineral occurrences of Chikamin Mountain and Whitesail Reach Map areas (93E/06, 10). B.C. Ministry of Energy, Mines and Petroleum Resources, Geological Fieldwork 1987, Paper 1988-1, pp. 155-168.
- Dipple, G. M., Winstch, R.P., Andrews, M.S. (1990) Identification of the scales of differential element mobility in a ductile fault zone. *Journal of Metamorphic Geology*, 8, pp. 646-661.
- Dunbar, W.R. (1948) Structural relations of the Porcupine ore deposits, in *Structural geology of Canadian ore deposits*: Montreal, Canadian Inst. Mining Metallurgy, Geology Div. Spec. Pub., pp. 442-456.
- Duffell, S. (1959): Whitesail Lake Map-area, British Columbia. Geological Survey of Canada, Memoir 299.
- Elliott-Meadows, S.R. and Appleyard, E. C. (1991): The alteration geochemistry and petrology of the Lar Cu-Zn deposit, Lynn Lake area, Manitoba, Canada. *Economic Geology*, 86. (3). pp. 486-505.
- Engels, J. C. and Ingamells, C. O. (1970) Effect of sample inhomogeneity in K-Ar dating. *Geochimica et Cosmochimica Acta*, 34, pp. 1007-1017.
- Ferry, J.M.(1985a): Hydrothermal alteration of Tertiary igneous rocks from the Isle of Skye, Northwest Scotland; 1, Gabbros. *Contributions to Mineralogy and Petrology*, 91. (3). pp. 264-282.
- Ferry, J.M. (1985b): Hydrothermal alteration of Tertiary igneous rocks from the Isle of Skye, Northwest Scotland; 2, Granites. *Contributions to Mineralogy and Petrology*, 91. (3). pp. 283-304.
- Finlow-Bates and Stumpfl (1981) The behavior of so-called immobile elements in hydrothermally altered rocks associated with volcanogenic submarine-exhalative ore deposits. *Mineralium Deposita*, 16, pp. 319-328.
- Field, C. W., and Fifarek, R. H. (1985) Light stable-isotope systematics in the epithermal environment; in Berger, B. R., and Bethke, P. M. (ed.), *Geology and Geochemistry of Epithermal Systems*: Society of Economic Geologists, Reviews in Economic Geology, 2, pp. 99-128.

- Fletcher, W.K. (1981) Analytical methods in geochemical prospecting. handbook of exploration geochemistry, editor: Govett, G. J. S. Handbook of exploration geochemistry. 1. 262 p.
- Floyd, P. A. and Winchester, J.A. (1978) Identification and discrimination of altered and metamorphosed volcanic rocks using immobile elements. *Chemical Geology*, 21, pp. 291-306.
- Fyles, J.T., (1984) Report on notes on thin sections of New Nadina DDH 84-15. unpublished report to Mr. G. Stewart. 2 p.
- Fyon, J. A., and Crocket, J. H., (1982) Gold exploration in the Timmins district using field and lithogeochemical characteristics of carbonate alteration zones: Canada Inst. Mining Metallurgy Spec., 24, pp. 113-129.
- Giggenbach, W. F. (1984) Mass transfer in hydrothermal alteration systems — A conceptual approach. *Geochimica et Cosmochimica Acta*, 48. pp. 2693-2711.
- Godwin, C.I. (1975): Imbricate Subduction Zones and their Relationship with Upper Cretaceous to Tertiary Porphyry Deposits in the Canadian Cordillera; *Canadian Journal of Earth Sciences*, 12, pp. 1362-1378.
- Golditch, S.S. (1938) A study in rock weathering, *Journal of Geology*, 46, pp. 17-58.
- Grant, J. A. (1986) The isocon diagram - A simple solution to Gresens' equation for metasomatic alteration. *Economic Geology*, 81, pp. 1976-1982.
- Gresens, R. L. (1967) Composition-volume relationships of metasomatism: *Chemical Geology*, 2, pp. 47-65.
- Guilbert, J. M. and Park, C. F. Jr. (1986): The geology of ore deposits. W.H. Freeman and Company / New York, 985 p.
- Hanor, J.S., and K. C. Duchac (1990): Isovolumetric silicification of early Archean komatiites; geochemical mass balances and constraints on origin, *Journal of Geology*, 98, pp. 863-877.
- Harland, W.B., Armstrong, R.L., Cox, A.V., Craig, L.E., Smith, A.G. and Smith, D.G. (1989): A Geologic Time Scale, 1989; Cambridge University Press, 1st Edition July, 1989.
- Harris, D.C., and Owens, D.R. (1973). Berryite, a Canadian occurrence. *Canadian Mineralogist*, 11, (5), pp. 1016-1018.
- Hashiguchi, H. and Usui, H. (1975) An approach to delimiting targets for prospecting of the Kuroko ore deposits: on the sulphur and magnetic susceptibility haloes: *Mining Geology*, 25, pp. 293-301.

- Hayba, D. O. (1983) A compilation of fluid-inclusion and stable-isotope data on selected precious- and base-metal epithermal deposits: U.S. Geological Survey, Open-File Report 83-450, 24 p.
- Hayba, D. O., Bethke, P. M. Heald, P. and Foley, N. K. (1985) Geologic, mineralogic, and geochemical characteristics of volcanic-hosted epithermal precious-metal deposits; in Berger, B. R., and Bethke, P. M. (ed.), *Geology and Geochemistry of Epithermal Systems: Society of Economic Geologists, Reviews in Economic Geology*, 2, pp. 129-168.
- Helgeson, H. C. (1979) Mass transfer among minerals and hydrothermal solutions, In *Geochemistry of hydrothermal ore deposits*. edited by H. L. Barnes, John Wiley & Sons, Inc., New York, NY, pp. 568-610.
- Hood, C.H.B. (1991) Mineralogy, paragenesis, and mineralogic zonation fo the Silver Queen vein system Owen Lake, central British Columbia, Unpublished M. Sc. thesis, The University of British Columbia, 273 p.
- Hughes, C. J., (1982) *Developments in petrology 7, Igneous petrology*, Elsevier Scientific Publishing Company, 551 p.
- Ingamells, C.O. and Switzer, P. (1973) A proposed sampling constant for use in geochemical analysis. *Talanta*, 20, pp. 547-568.
- Ingamells, C.O. (1974a) New approaches to geochemical analysis and sampling. *Talanta*, 21, pp.141-155.
- Ingamells, C.O. (1974b) Control of geochemical error through sampling and subsampling diagrams. *Geochmica et Cosmochimica Acta*, 38, pp. 1225-1237.
- Ingamells, C.O. (1981) Evaluation of skewed exploration data — the nugget effect. *Geochimica et Cosmochimica Acta*, 45, pp. 1209-1216.
- Ishikawa Y., Sawaguchi, T., Iwaya, S. and Horiuchi, M. (1976) Delineation of prospecting targets for Kuroko deposits based on modes of volcanism of underlying dacite and alteration haloes. *Mining Geology*, 26, pp. 105-117.
- Kamilli, R. J., and Ohmoto, H. (1977) Paragenesis, zoning, fluid-inclusion, and isotopic study of the Finlandia vein, Colqui district, Central Peru: *Economic Geology*, 72, pp. 950-982.
- Ke, Peiwen (1992): A new approach to mass balance modeling: Applications to igneous petrology, M. Sc. thesis, University of British Columbia, 153 p.
- Kendall, M.G. (1943) *The advanced theory of statistics*. vol. 1, Griffin & Co., London, 457 p.

- Kishida, A., and Kerrich, R. (1987) Hydrothermal alteration zoning and gold concentration at the Kerr-Addison Archean lode gold deposit, Kirkland Lake, Ontario: *Economic Geology*, 82, pp. 649-690.
- Kleeman, A.W. (1967) Sampling error in the chemical analysis of rocks. *Journal of Geological Society of Australia*, 14, pp. 43-47.
- Kranidiotis, P. and MacLean, W. H. (1987): Systematics of chlorite alteration at the Phelps Dodge massive sulfide deposit, Matagami, Quebec. *Economic Geology*, 82, (7), pp. 1898-1911.
- Krauskopf, K. B. (1967) Chemical weathering, chapter 4, *Introduction to Geochemistry*, McGraw-Hill, Inc. 721 p.
- Kwong, Y. T. J., Brown, T. H. and Greenwood, H. J. (1982) A thermodynamic approach to the understanding of the supergene alteration at the Afton copper mine, south-central British Columbia: *Canadian Journal of Earth Sciences*, 19, pp. 2378-2386.
- Le Maitre, P. W. (1982) *Numerical Petrology - Statistical Interpretation of Geochemical Data*. Developements in Petrology 8, Elsevier Scientific Publishing Company Inc. 281 p.
- Leitch, C.H.B. (1989): *Geology, Wallrock Alteration, and Characteristics of the Ore Fluids at the Bralorne Mesothermal Gold Quartz Vein Deposit, Southwestern British Columbia*; unpublished Ph.D. thesis, The University of British Columbia, Vancouver, 483 p.
- Leitch, C.H.B. and Day, S.J. (1990) Newgres: a Turbo Pascal program to solve a modified version of Gresens' hydrothermal alteration equation: *Computers & Geoscience*, 16, pp. 925-932.
- Leitch, C.H.B. and Lentz, D. R. (1994) The Gresens approach to mass balance constraints of alteration systems: Methods, Pitfalls, Examples. in Lentz, D.R., ed., *Alteration and alteration processes associated with ore-forming systems: Geological Association of Canada, Short Course Notes*, 11, pp. 161-192.
- Leitch, C.H.B., Hood, C.T., Cheng, X. and Sinclair, A.J. (1990) Geology of the Silver Queen mine area, Owen Lake, central British Columbia. B.C. Ministry of Energy, Mines and Petroleum Resources, *Geological Fieldwork 1989, Paper 1990-1*, pp. 287-295.
- Leitch, C. H. B., Cheng, X., Hood, C. T., Sinclair, A.J. (1991) Structural character of *en echelon* polymetallic veins at the Silver Queen mine, British Columbia. *CIM Bulletin*, 84, (955), pp. 57-66.
- Leitch, C.H.B., Hood, C.T., Cheng, X. and Sinclair, A.J. (1992) Tip Top Hill unit: Upper Cretaceous volcanic rocks hosting Eocene epithermal base- and precious-metal veins

- at Owen Lake, central British Columbia. *Canadian Journal of Earth Sciences*, 29, pp. 854-864.
- Lindgren, W., (1933): *Mineral Deposits*. 4th ed. New York: McGraw-Hill, 930 p.
- MacIntyre, D.G. (1985): *Geology and Mineral Deposits of the Tahtsa Lake District, West-central British Columbia*; B.C. Ministry of Energy, Mines and Petroleum Resources, Bulletin 75, 82 p.
- MacIntyre, D.G. and Desjardins, P. (1988): Babine Project (93L/15); B.C. Ministry of Energy, Mines and Petroleum Resources, *Geological Fieldwork*, 1987, Paper, 1988-1, pp. 181-193.
- MacLean, W.H. (1988) Rare earth elements mobility at constant inter-REE ratios in the alteration zone at the Phelps Dodge massive sulphide deposit, Matagami, Quebec. *Mineralium Deposita*, 23, pp. 231-238.
- MacLean, W.H. (1990): Mass change calculations in altered rock series. *Mineralium Deposita*. 25. (1). pp. 44-49.
- MacLean, W.H. and Barrett, T.J., (1993) Lithochemical techniques using immobile elements, *Journal of Geochemical Exploration*, 48, pp. 109-133.
- MacLean, W.H. and Kranidiotis, P. (1987): Immobile elements as monitors of mass transfer in hydrothermal alteration; Phelps Dodge massive sulfide deposit, Matagami, Quebec. *Economic Geology*, 82. (4). pp. 951-962.
- Madeisky, H. E. and Stanley, C. R. (1993): Identifying metasomatic zones associated with volcanic-hosted massive sulfide deposits using Pearce Element Ratio analysis, *Lithogeochemical exploration for VMS deposits. The Gangue, GAC- Mineral Deposits Division Newsletter*, issue 41, Jan. 1993, pp. 5-7.
- Margaret, G., McAfee, Jr., R., and Wolf, C. L., (1972) (eds.) *Glossary of Geology*; Amer. Geol. Inst., Washington, D. C., 805 p. plus appendix.
- Marquis, P., A. C. Brown, C. Hubert and D. M. Rigg (1990) Progressive alteration associated with auriferous massive sulfide bodies at the Dumagami mine, Abitibi greenstone belt, Quebec. *Economic Geology*, 85, pp. 746-764.
- Marsden, H.W. (1985): *Some Aspects of the Geology, Mineralization and Wallrock Alteration of the Nadina Zn-Cu-Pb-Ag-Au Vein Deposit, North-central B.C.*; Unpublished B.Sc. thesis, The University of British Columbia, 90 p.
- Maxwell, J.A. (1968) *Rock and mineral analysis*. Wiley-Interscience, new York.
- Merrill, G.P. (1897) *Rock, Rock-Weathering, and Soil*. New York, Macmillan Co., 218 p.
- Meyer, C., and Hemley, J.J. (1967) Wall rock alteration, in *Geochemistry of hydrothermal ore deposits*, ed. Barnes, H. L. : New York, Holt, Rinehart and Winston, Inc., pp. 166-235.

- Myers, J. D., and C. L. Angevine (1986): Mass balance calculations with end member compositional variability: application to petrologic problems, EOS Trans. AGU, 67, p. 404.
- Myers, J. D., C. D. Frost and C. L. Angevine (1986): A test of a quartz eclogite source for parental Aleutian magmas: a mass balance approach, Journal of Geology, 94, pp. 811-828.
- Myers, J. D., and C. L. Angevine and C. D. Frost (1987): Mass balance calculations with end member compositional variability: application to petrologic problems, Earth Planet. Sci. Lett., 81, pp.212-220.
- Morton, R.L. and Nebel, M.L. (1984): Hydrothermal alteration of felsic volcanic rocks at the Helen siderite deposit, Wawa, Ontario. Economic Geology, 79, pp. 1319-1333.
- Nicholls, J. (1988) The statistics of Pearce element diagrams and the Chayes closure problem. Contributions to Mineralogy and Petrology. 99, pp. 11-24.
- Niggli, P., (1954) Rocks and mineral deposits. San Francisco: W. H. Freeman.
- Nowak, M. (1991) Ore reserve estimation, Silver Queen vein, Owen Lake, British Columbia; Unpubl. M.A.Sc. thesis, The University of British Columbia, 204 p.
- Ondrick, C. W. and Suhr, N. H. (1969) Error and the spectrographic analysis of greywacke samples. Chemical Geology, 4, pp. 429-437.
- Pearce, T. H, (1968) A contribution to the theory of variation diagrams. Contributions to Mineralogy and Petrology, 19, pp. 142-157.
- Pearce, T.H. (1987): The identification and assessment of spurious trends in Pearce-type ratio variation diagrams; a discussion of some statistical arguments. Contributions to Mineralogy and Petrology, 97, (4), pp. 529-534.
- Philpotts, A. R. (1990) Principles of igneous and metamorphic petrology. Prentice Hall, Englewood Cliffs, New Jersey, 498 p.
- Potts, P.J.(1987) A handbook of silicate rock analysis, Blackie & Son Limited.
- Press, W. H., B. P. Flattery, S. A. Teukolsky, and W. T. Vetterling (1987): Numerical Recipes in C, Cambridge University Press, 818 p.
- Price, P., and Bancroft, W. L. (1948) Waite Amulet mine — Waite section, in Structural geology of Canadian ore deposits: Montreal, Canadian Inst. Mining metallurgy, Geology Div., Spec. Pub., pp. 748-756.
- Ribbe, P.H. (1983) Chemistry, structure and nomenclature of feldspars, Feldspar Mineralogy, ed. Ribbe, P. H., Reviews in Mineralogy, 2, Mineralogical Society of America. pp. 1-20.

- Rice, A.R. (1977): Solute banding; a possible indicator of turbulent thermal convection in magmas and a possible precursor to rollover in stratified magmas with attendant explosive volcanism. EOS (Am. Geophys. Union, Trans.). 58. (12). p. 1249
- Richards, J. P. McCulloch, M. T. Bruce, W. C. and Kerrich, R. (1991) Sources of metals in the Porgera gold deposit, Papua new Guinea: Evidence from alteration, isotope, and noble metal geochemistry. *Geochimica et Cosmochimica Acta*, 55, pp. 565-580.
- Rittmann, A., (1973) Stable mineral assemblages of igneous rocks, A method of calculation, Springer-Verlag, 262 p.
- Robert, F. and Brown, A. C. (1984): Progressive alteration associated with gold-quartz-tourmaline veins at the Sigma mine, Abitibi greenstone belt, Quebec; *Economic Geology*, 79, pp. 393-399.
- Robert, F. and Brown, A. C. (1986): Archean gold-bearing quartz veins at the Sigma mine, Abitibi Greenstone belt, Quebec: Part II. vein paragenesis and hydrothermal alteration, *Economic Geology*, 81. pp. 593-616.
- Rose, A. W. and Burt, D. M. (1979) Hydrothermal alteration, in *Geochemistry of hydrothermal ore deposits*, 2ed., ed. Barnes, H.L. New York, John Wiley and Sons, pp. 173-235
- Russell, J. K. (1986) A Fortran-77 computer program for the least squares analysis of chemical data in Pearce variation diagrams. *Computers & Geosciences*, 12, pp. 327-338.
- Russell, J. K. and Nicholls, J. (1987) Early crystallization history of alkali olivine basalts, Diamond Craters, Oregon. *Geochimica et Cosmochimica. Acta*. 51, pp. 143-154.
- Russell, J. K. and Stanley, C.R. (1989) Differentiation of the 1954-1960 lavas of Kilauea volcano. *Pacific N.W. Amer. Geoph. Union, program with abstr.*, 1, p. 10.
- Russell, J. K. and C. R. Stanley (1990a) Theory and application of Pearce Element Ratios to geochemical data analysis. *Geological Association of Canada Short Course #8*, 1989, 315 p.
- Russell, J. K. and Stanley, C. R. (1990b): Origins of the 1954-1960 lavas of Kilauea Volcano; constraints on shallow reservoir magmatic processes. *Continental magmatism; abstracts. Bulletin New Mexico Bureau of Mines and Mineral Resources*. 131. p. 230
- Saeki, Y. and Date, J. (1980) Computer application of the alteration data for the footwall dacite lava at the Ezuri Kuroko deposits, Akita Prefecture, *Mining Geology*, 30, pp. 241-250.

- Sander, M. V. and Einaudi, M. T. (1990) Epithermal deposition of gold during transition from propylitic to potassic alteration at Round Mountain, Nevada. *Economic Geology*, 85, pp. 285-311.
- Shapiro, L. and W.W. Brannock (1955) Rapid determination of water in silicate rocks. *Analytical Chemistry*. 27, pp. 560-562.
- Shapiro, L. and W.W. Brannock (1962) Rapid analysis of silicate, carbonate and phosphate rocks. *US Geological Survey Bull.* 1144-A.
- Shaw, D. M. (1961) Manipulative errors in geochemistry: a preliminary study. *Trans. Roy. Soc. Can.* LV, pp. 41-55.
- Sketchley, D.A. and Sinclair, A. J., (1987) Gains and losses of elements resulting from wall-rock alteration — a quantitative basis for evaluating lithogeochemical samples: British Columbia Ministry Energy Mines Petroleum Resources Rept. 1987-1, pp.57-63.
- Sketchley, D. A. and A. J. Sinclair (1991) Carbonate alteration in basalt, Total Erickson Gold Mine, Cassiar, Northern British Columbia, Canada, *Economic Geology*, 86, pp. 570-587.
- Spitz, G. and Darling, R. (1978) Major and minor element lithogeochemical anomalies surrounding the Louvem copper deposit, Val d'Or, Quebec. *Canadian Journal of Earth Science*, 15, pp. 1161-1169.
- Stanley, C.R. and H. E. Madeisky (1993) Pearce element ratio analysis: Applications in lithochemical exploration, MDRU short course notes: SC-13, Dept. of Geological Sciences, University of British Columbia, 542 p.
- Stanley, C.R. and H. E. Madeisky (1994) Lithogeochemical exploration for hydrothermal ore deposits using Pearce element ratio analysis. in Lentz, D.R., ed., *Alteration and alteration processes associated with ore-forming systems: Geological Association of Canada, Short Course Notes*, 11, pp. 193-211.
- Stanley, C. R. and Russell, J.K. (1989a) PEARCE.PLOT: Interactive Graphics-Supported Software for testing petrologic hypotheses with Pearce Element Ratios. *American Mineralogist*, 74, pp. 317-320.
- Stanley, C. R. and Russell, J.K. (1989b) PEARCE.PLOT: A Turbo-Pascal Program for the analysis of rock compositions with Pearce Element Ratios. *Computers & Geosciences*, 15, pp. 950-926.
- Stanley, C. R. and Russell, J.K. (1989c): Petrologic hypothesis testing with Pearce element ratio diagrams; derivation of diagram axes. *Contributions to Mineralogy and Petrology*. 103. (1). pp. 78-89.

- Stanley, C. R. and Russell, J.K. (1990): Derivation of axis coefficients for Pearce element ratio diagrams. Continental magmatism; abstracts. Bulletin New Mexico Bureau of Mines and Mineral Resources, 131. p. 252
- Stormer, J.C., and J. Nicholls (1978): XLFRAC: a program for the interactive testing of magmatic differentiation models, Computers & Geosciences, 4, pp. 143-159.
- Stout, M.Z and Nicholls, J. (1977): Mineralogy and petrology of Quaternary lavas from the Snake River plain, Idaho. Canadian Journal of Earth Science, 14. (9). pp. 2140-2156.
- Streckeisen, A.L. (1967): Classification and Nomenclature of Igneous Rocks; Neues Jahrbuch Mineralogie, Abhandlung, 107, pp. 144-214.
- Sutherland Brown, A. (1960): Geology of the Rocher Deboile Range; B.C. Ministry of Energy, Mines and Petroleum Resources, Bulletin 43, 78 p.
- Thompson, M. and Howarth, R.J., (1976) Duplicate analysis in geochemical practice, 1. Theoretical approach and estimation of analytical reproducibility. Analyst, 101: pp. 690-698.
- Thompson, M. and Howarth, R.J., (1978) A new approach to the estimation of analytical precision. Journal of Geochemical Exploration, 9: pp. 23-30.
- Tipper, H.,W. and Richards, T.A. (1976): Jurassic Stratigraphy and History of North-central British Columbia; Geological Survey of Canada, Bulletin 270, 73 p.
- Weir, B. (1973). A mineralogical and milling study of the Nadina mine. Unpub. term report for Geology 409, Univ. of British Columbia, April 1973, 31 p.
- Wetherell, D.G., (1979), Geology and ore genesis of the Sam Goosly copper-silver-antimony deposit, British Columbia. Unpub. M.Sc. thesis, Univ. of British Columbia, Vancouver, 208 p.
- Wetherell, D.G., Sinclair, A.J. and Schroeter, T.G. (1979): Preliminary Report on the Sam Goosly copper-silver Deposit; B.C. Ministry of Energy, Mines, and Petroleum Resources, Geological Fieldwork, 1978, pp. 132-137.
- Wickman, F. E. (1962) The amount of material needed for a trace element analysis. Ark. Mineral. Geol. 3, (6), pp. 131-139.
- Wilson, A.D. (1964) The sampling of silicate rock powders for chemical analysis. Analyst, 89, pp. 18-30.
- Wisser, E. (1951) Tectonic analysis of a mining district — Pachuca, Hidalgo: Economic Geology, 46, pp. 459-477.
- Winchester, T.A. and Floyd, P.A. (1977) Geochemical discrimination of different magma series and their differentiation products using immobile elements. Chemical Geology, 20, pp. 325-347.

- Wojdak, P.J. and Sinclair, A.J. (1984): Equity Ag-Cu-Au Deposit: Alteration and Fluid Inclusion Study; *Economic Geology*, 79, pp. 969-990.
- Woods, T. L., Bethke, P. M., and Roedder, E. (1982) Fluid-inclusion data at Creede, Colorado in relation to mineral paragenesis: U. S. Geological Survey, Open-File Report 82-313, 61 p.
- Woodsworth, G.J. (1982): Age Determinations and Geological Studies, K-Ar Isotopic Ages, Report 15; Geological Survey of Canada, Paper 81-2, pp. 8-9.
- Wright, T.L. and P.C. Doherty (1970) A linear programming and least square computer method for solving petrologic mixing problems, *Geol. Soc. America. Bull.*, 81, pp. 1995-2008.

Appendix A.

Megascopic Description of Altered Samples, Silver Queen Mine

Table A-1. Megascopic Description of Altered Samples, Silver Queen Mine

Sample No.	Description	Weight* (g)
X1-1	the main cross-cut (also named Bulkley cross-cut) of 2600 foot level of underground working; 0-0.3 m from the footwall of the No. 3 vein (1.2 m wide, 325/NE/47°) to wallrock; strongly silicified and pyritized microdiorite; pale apple green, not magnetic, fine grain porphyroid texture, quartz, clay minerals and abundant disseminated pyrite.	610
X1-2	same location as above; 0.3-0.6 m from the footwall of the No. 3 vein to wallrock; strongly silicified and pyritized microdiorite; petrographic features are same as above except containing less pyrite.	1260
X1-2d	same location as above; 0.6-0.8 m from the footwall of the No. 3 vein to wallrock; moderately silicified microdiorite, petrographic features are same as above.	645
X1-3	same location as above; 0.8-1.6 m from the footwall of the No. 3 vein to wallrock; sericitic-argillic altered microdiorite, it is getting away from the vein, the intensity of alteration seems weaker than above samples; the color of the rock looks pale white to grey white or yellowish grey, the rock has more clay (can be tasted) and less quartz and pyrite than the above samples.	1196
X1-4	same location as above; 1.6 - 2.4 m from the footwall of the No. 3 vein to wallrock; sericitic-argillic altered microdiorite; its petrographic features are similar to the above sample.	1085
X1-5.	same location as above; 2.4- 3.2 m from the footwall of the No. 3 vein to wallrock; sericitic-argillic altered microdiorite; its petrographic features are similar to the above sample.	1522
X1-6.	same location as above; 5-7 m from the footwall of the No. 3 vein to wallrock (inaccessible for sampling between 3.2-5m); sericitic-argillic altered microdiorite; its petrographic features are similar to the above sample.	2143
X1-7.	same location as above; 7-14 m from the footwall of the No. 3 vein to wallrock; sericitic-argillic microdiorite; it seems having more sericitic and less clays. Primary texture is well preserved.	2216
X1-8.	same location as above; 14-27 m from the footwall of the No. 3 vein to wallrock; moderate sericitic-argillic microdiorite; the alteration intensity looks obviously weaker than the samples above; there is a post-mineralization structure zone at the place of 27 m.	3051

X2-1	the northern cross-cut of 2600 foot level underground working; 6.4-8.9 m from the hanging-wall of the No. 1 vein to wall-rock (at the footwall side of the No. 2 vein), propylitic andesite, black or dark grey, massive and dense, detectable magnetism, reacting with diluted acid, porphyritic and flow texture, feldspar, hornblende and augite are identifiable phenocrysts, their sizes range from 0.5 to 2 mm, there are about 40% of aphanitic groundmass.	880
X3-1	the northern cross-cut of 2600 foot level underground working; 1 m of horse rock between two veins (belong to No. 2 vein system), strong sericitic-argillic andesite; pale green, no magnetic, not reacts with diluted acid, alteration is relatively strong characterized by intense fracture and poorly preserved primary texture; disseminated pyrite and other sphalerite are observed; all primary minerals are altered to clay minerals (stick tongue).	920
X3-2	same location as above; 0-2.5 m from the footwall of the No. 2 vein to wall rock; moderate sericitic-argillic andesite; petrographic features are similar to the above sample.	580
X3-2d	same location as above; 2.5-6 m from the footwall of the No. 2 vein to wall rock; moderate sericitic-argillic andesite; pale white or grey white, no magnetic, no reaction with diluted acid, primary porphyritic and flow texture is well preserved, primary minerals such as feldspar, hornblende and augite are all altered to clay minerals.	840
X3-3	same location as above; 6-8 m from the footwall of the No. 2 vein to wallrock; propylitic andesite, its petrographic features are similar to those of sample X2-1.	1380
X3-3d	same location as above; 8-16 m from the footwall of the No. 2 vein to wallrock; propylitic andesite, its petrographic features are similar to those of sample X2-1.	995
X3-4.	same location as above; 0-0.4 m from the hanging-wall of the No. 2 vein to wallrock; strong sericitic-argillic andesite; its petrographic features are similar to sample X3-1.	990
X3-5.	same location as above; 0.4-1.4 m from the hanging-wall of the No. 2 vein to wallrock; moderate sericitic-argillic andesite. Its petrographic features are similar to X3-2d.	770
X3-6.	same location as above; 1.4 - 4.4 m from the hanging-wall of the No. 2 vein to wallrock; propylitic andesite. Its petrographic features are similar to X3-2d.	860
X3-7.	same location as above; 4.4-15 m from the hanging-wall of the No. 2 vein to wallrock; propylitic andesite. Its petrographic features are similar to X2-1.	967

X4-4	same location as above; 3-12 m from the footwall of the No. 3 vein to wall rock, propylitica andesite. Its petrographic features are similar to X2-1.	980
X5-1	the southern cross-cut of 2600 foot level underground working; 0-0.3 m from the hanging-wall of the No. 3 vein to wallrock, silicic and pyritic andesite. It is intensely fractured and altered.	1350
X5-2.	same location as above; 0.3-1.1 m from the hanging-wall of the No. 3 vein to wall rock, moderate silicic and pyritic andesite, similar to the sample above but less intensely fractured.	1320
X5-3.	same location as above; 1.1-1.6 m from the hanging-wall of the No. 3 vein to wallrock, sericitic and argillic andesite, pale brown, massive, primary texture well preserved, no magnetic and no reaction with diluted acide.	1110
X5-4.	same location as above; 1.6-3.1 m from the hanging-wall of the No. 3 vein to wallrock, sericitic and argillic andesite,	1615
X5-5.	same location as above; 3.1-14 m from the hanging-wall of the No. 3 vein to wallrock, sericitic and argillic andesite.	1058
X5-5d	same location as above; 14-33 m from the hanging-wall of the No. 3 vein to wallrock, sericitic and argillic andesite.	908
X5-6.	same location as above; 33-36 m. from the hanging-wall of the No. 3 vein to wallrock, propylitic andesite.	893
X5-6d.	same location as above; 36-38 m. from the hanging-wall of the No. 3 vein to wallrock, propylitic andesite.	860
X5-7.	same location as above; 38-56 m from the hanging-wall of the No. 3 vein to wall-rock, sericitic and argillic andesite. This alteration envelope may be related to a non-mineralized breccia zone (see the description below).	956
X5-8	same location as above; 56-70 m from the hanging-wall of the No. 3 vein to wall-rock, sericitic and argillic andesite. The rock at the working face (70 m) is intensely fractured (breccia zone).	1512
X5-9	same location as above; 0-0.5 m from the hanging-wall of the Footwall vein to wall-rock, silicic and pyritic andesite, pale apple green, abundant disseminated pyrite.	1528
X5-10	same location as above; 0.5-6.5 m from the hanging-wall of the Footwall vein to the footwall of the No. 3 vein, silicic and pyritic andesite, similar to the sample above but less abundant disseminated pyrite.	1715

X10-1	the main cross-cut (also named Bulkley cross cut) of 2600 foot level of underground working; 0-1.2 m from the hanging-wall of the No. 3 vein to wall-rock, silicic and pyritic microdiorite, pale apple green, abundant hematite veinlets cut pyrite veinlets and altered wallrock with abundant disseminated pyrite. It is also intensely fractured.	487
X10-2	same location as above; 1.2-4 m from the hanging-wall of the No. 3 vein to wall-rock, moderate silicic and argillic microdiorite. Its petrographic features are similar to the above but less abundant of veinlets, disseminated pyrite and not intensely fractured.	950
X10-3	same location as above; 4-5.5 m from the hanging-wall of the No. 3 vein to wall-rock, sericitic and argillic microdiorite. Its petrographic features are similar to above but there is much less veinlets than above sample.	830
X10-3d	same location as above; 5.5-7.5 m from the hanging-wall of the No. 3 vein to wall-rock, sericitic and argillic microdiorite, buffer brown. There is no veinlets.	815
X10-4.	same location as above; 7.5-20 m from the hanging-wall of the No. 3 vein to wall-rock, sericitic and argillic microdiorite, similar to the sample above.	803
X10-5.	same location as above; 20-38 m from the hanging-wall of the No. 3 vein to wall-rock, moderate sericitic and argillic microdiorite, similar to the sample above.	847
X10-6	same location as above; 38-44 m from the hanging-wall of the No. 3 vein to wall-rock, propylitic microdiorite, black, dark grey, magnetic. It has a 'sharp contact' (gradational contact in the range of 2 cm) with the sample above.	651
X10-6d	same location as above; 44-56 m from the hanging-wall of the No. 3 vein to wall-rock, propylitic microdiorite, similar to the sample above.	545
DA63-1	Switch back vein, 32- 44 ft of drill 87-S-04, propylitic andesite contacts with a post-mineralization dike (DA63-2).	488
DA63-3	same location as above, 460-469 ft of drill 87-S-04, sericitic and argillic andesite	720
DA63-4	same location as above, 472-496 ft of drill 87-S-04, sericitic and argillic andesite,	610
DA63-5	same location as above, 497-499 ft of drill 87-S-04, silicic andesite	620
DA63-6	same location as above, 500-504 ft of drill 87-S-04, silicic andesite. There is hanging-wall sphalerite-galena-pyrite-barite vein (DA63-7) between sample DA63-6 and DA63-8.	720
DA63-8	same location as above, 506-514 ft of drill 87-S-04, silicic andesite contacts the hanging-wall of the main vein at 514 ft.	770

* sample weight after sawing out the weathering surface and veinlets.

Appendix B.
Lithogeochemical Duplicate Analyses,
Silver Queen Mine

Table B-1. Sample Duplicates of Major Components at Silver Queen mine, central British Columbia

SAMPLE ID	ROCK TYPE	ALTERATION	LOCATION	SiO ₂	Al ₂ O ₃	Fe ₂ O ₃	FeO	MgO	CaO	Na ₂ O	K ₂ O	TiO ₂	MnO	P ₂ O ₅
x10-6d	m. di.*	w-alt	main x-cut	59.05	15.43	2.64	2.89	2.69	5.10	3.70	3.15	0.59	0.18	0.28
DA63-3	m. di.	m-alt	Switch bk v. 87-S-4	51.19	16.24	0.66	11.24	1.35	1.25	0.25	4.27	0.58	0.98	0.28
DA8-3	and.	s-alt	Camp v. 88-S-29	58.11	15.69	2.73	3.49	0.38	1.00	0.03	3.57	0.54	4.09	0.30
DA63-5	m. di.	s-alt	Switch bk v. 87-S-4	54.41	15.34	2.15	9.14	0.80	1.24	0.04	3.34	0.45	0.69	0.31
DA63-1	m. di.	w-alt	Switch bk v. 87-S-4	57.99	16.53	2.22	3.76	2.63	6.25	3.43	3.16	0.71	0.16	0.43
DA48-2	m. di.	m-alt	Cole lk v. 88-S-5	52.68	18.88	0.81	6.43	1.16	2.16	0.14	6.39	0.61	1.16	0.32
S91-15D	porphyry	wm-alt	Duck lake	60.05	15.34	2.59	2.42	2.76	5.02	3.83	2.37	0.59	0.41	0.29
DA48-5	m. di.	wm-alt	Cole lk v. 88-S-5	54.71	16.81	2.46	3.20	2.14	5.67	2.66	4.34	0.58	0.21	0.41
DA48-4	m. di.	m-alt	Cole lk v. 88-S-5	52.77	21.94	2.02	3.60	0.92	4.95	0.13	3.05	0.51	0.31	0.31
x3-3	and.	w-alt	N No3 v. x-cut	57.75	15.85	3.02	2.86	2.87	5.75	3.96	3.02	0.66	0.31	0.39
x11-1	m. di.	w-alt	FW Jack v.	57.01	15.70	2.69	3.77	4.29	5.80	3.76	2.98	0.68	0.21	0.42
S91-9	Nadian dk	w-alt	Nadina Mt. E. slo	49.64	15.15	3.34	5.64	7.81	6.58	2.96	1.53	1.27	0.31	0.56
S91-10	Nd granite	w-alt	Nadina Mt. E. slo	68.03	14.20	1.04	1.87	1.76	2.45	3.75	4.68	0.50	0.08	0.22
x10-6	m. di.	w-alt	main x-cut	61.20	15.06	2.36	2.86	2.81	4.90	3.96	3.15	0.58	0.14	0.27
x10-3d	m. di.	w-alt	main x-cut	63.27	17.76	0.99	3.11	1.05	1.60	0.32	4.98	0.40	0.49	0.13
x1-1	m. di.	s-alt	main x-cut	59.10	14.67	0.51	9.11	0.85	0.66	0.05	2.75	0.34	1.08	0.17
x1-90	m. di.	w-alt	main x-cut	61.89	15.33	1.99	2.44	2.25	4.09	3.52	3.69	0.43	0.16	0.23
x1-5	m. di.	m-alt	main x-cut	63.85	16.15	1.33	3.33	1.22	1.56	0.31	4.55	0.41	1.06	0.12
x10-6D	m. di.	w-alt	main x-cut	59.00	15.98	2.52	2.85	2.18	5.16	3.63	3.09	0.56	0.18	0.34
DA63-3D	m. di.	m-alt	Switch bk v. 87-S-4	51.68	16.20	0.41	11.24	1.34	1.24	0.03	4.24	0.56	0.98	0.25
DA8-3D	and.	s-alt	Camp v. 88-S-29	55.69	16.43	2.81	3.49	0.39	1.55	0.05	3.78	0.55	4.27	0.30
DA63-5D	m. di.	s-alt	Switch bk v. 87-S-4	54.59	14.95	2.02	9.13	0.87	1.04	0.02	3.29	0.46	0.63	0.29
DA63-1D	m. di.	w-alt	Switch bk v. 87-S-4	57.72	16.63	2.32	3.76	2.62	6.45	3.28	3.26	0.72	0.16	0.43
DA48-2D	m. di.	m-alt	Cole lk v. 88-S-5	52.63	18.95	0.81	6.43	1.16	2.04	0.14	6.37	0.60	1.18	0.32
S91-15Dd	porphyry	wm-alt	Duck lake	60.64	15.24	2.54	2.42	2.62	4.98	3.90	2.36	0.59	0.36	0.29
DA48-5D	m. di.	wm-alt	Cole lk v. 88-S-5	54.20	17.05	2.41	3.20	2.15	5.68	2.59	4.42	0.57	0.21	0.41
DA48-4D	m. di.	m-alt	Cole lk v. 88-S-5	53.82	20.75	2.02	3.60	0.84	4.65	0.16	3.05	0.53	0.31	0.33
x3-3d	and.	w-alt	N No3 v. x-cut	57.59	15.80	2.81	3.08	3.07	5.61	3.69	3.13	0.65	0.35	0.39
x11-1b	m. di.	w-alt	FW Jack v.	57.05	15.77	2.73	3.77	4.18	5.78	3.76	2.97	0.69	0.22	0.42
S91-9D	Nadian dk	w-alt	Nadina Mt. E. slo	49.82	15.03	3.23	5.64	7.64	6.50	2.98	1.51	1.26	0.31	0.56
S91-10D	Nd granite	w-alt	Nadina Mt. E. slo	67.46	14.28	1.05	1.87	1.86	2.44	3.83	4.69	0.51	0.08	0.21
x10-6d	m. di.	w-alt	main x-cut	59.00	15.98	2.52	2.85	2.18	5.16	3.63	3.09	0.56	0.18	0.34
x10-3D	m. di.	w-alt	main x-cut	63.52	17.99	1.02	3.11	1.06	1.62	0.32	5.03	0.40	0.49	0.14
X1-1D	m. di.	s-alt	main x-cut	59.20	14.29	0.67	9.17	0.83	0.68	0.07	2.78	0.35	1.06	0.17
x1-90d	m. di.	w-alt	main x-cut	61.87	15.02	1.83	2.61	2.47	3.97	3.54	3.72	0.43	0.19	0.22
X1-5D	m. di.	m-alt	main x-cut	64.51	15.15	1.52	3.19	0.86	1.81	0.00	4.19	0.44	1.14	0.20

* m. di. - microdiorite; and. - andesite; w-alt. - weakly altered; m-alt. - moderately altered; s-alt. - strongly altered; x-cut - cross cut; lk - lake; v. - vein.

Table B-2. Measurement Duplicates of Major Components at Silver Queen mine, central British Columbia

SAMPLE ID	ROCK TYPE	ALTERATION	LOCATION	SiO ₂	Al ₂ O ₃	Fe ₂ O ₃	FeO	MgO	CaO	Na ₂ O	K ₂ O	TiO ₂	MnO	P ₂ O ₅
x5-9	and.	s-alt	S No3 v. x-cut	64.10	16.00	2.23	3.35	1.10	0.35	0.33	4.73	0.45	0.08	0.19
S91-15	porphyry	w-m-alt	Duck lake	63.22	14.81	3.00	1.82	3.40	3.03	4.20	2.62	0.55	0.12	0.28
x10-3	m. dl.	m-alt	main x-cut	63.27	17.41	0.88	3.52	1.01	0.66	0.31	5.67	0.39	0.95	0.12
x10-2	m. dl.	s-alt	main x-cut	60.43	15.71	2.45	5.40	1.28	0.63	0.29	4.45	0.39	1.41	0.10
x10-5	m. dl.	m-alt	main x-cut	59.71	18.16	1.43	3.43	1.48	2.71	0.31	3.34	0.58	0.31	0.19
x10-4	m. dl.	m-alt	main x-cut	64.19	17.08	1.22	2.75	1.25	1.60	0.28	4.36	0.46	0.36	0.15
x1-3	m. dl.	s-alt	main x-cut	64.23	15.50	1.35	4.70	0.92	0.95	0.14	4.02	0.39	0.81	0.15
DA48-5	m. dl.	w-m-alt	Cole lk v. 88-S-5	54.61	16.77	2.41	3.20	2.12	5.73	2.69	4.31	0.58	0.21	0.42
DA48-4D	m. dl.	m-alt	Cole lk v. 88-S-5	53.82	20.75	2.02	3.60	0.84	4.65	0.16	3.05	0.53	0.31	0.33
DA63-4	m. dl.	m-alt	Swrch bk v. 87-S-	48.40	18.16	0.86	12.79	1.21	1.02	0.06	4.04	0.59	0.90	0.29
DA63-3D	m. dl.	m-alt	Swrch bk v. 87-S-	51.68	16.20	0.41	11.24	1.34	1.24	0.03	4.24	0.56	0.98	0.25
x5-5d	and.	m-alt	S No3 v. x-cut	53.53	16.58	1.81	3.60	1.93	6.42	0.81	3.93	0.69	0.47	0.28
x5-5	and.	m-alt	S No3 v. x-cut	55.24	17.51	1.57	4.26	1.71	4.34	0.33	3.58	0.78	0.67	0.26
x5-6d	and.	w-alt	S No3 v. x-cut	56.68	15.34	2.22	3.58	3.42	4.56	4.19	2.70	0.64	0.19	0.26
x5-6	and.	w-alt	S No3 v. x-cut	56.54	15.94	2.40	3.38	2.49	5.31	3.00	3.15	0.67	0.22	0.25
x5-4	and.	m-alt	S No3 v. x-cut	66.30	15.90	1.48	2.62	1.26	0.66	0.33	4.56	0.51	0.37	0.20
x2-5	and.	w-alt	N No3 v. x-cut	57.18	15.76	3.09	2.92	3.23	5.91	3.36	3.09	0.66	0.26	0.37
x10-6	m. dl.	w-alt	main x-cut	61.25	15.11	2.30	2.86	2.78	4.92	3.93	3.14	0.58	0.14	0.26
x3-7	and.	w-alt	N No3 v. x-cut	57.91	15.82	2.89	3.05	2.57	5.85	4.10	2.83	0.65	0.20	0.38
x3-2	and.	m-alt	N No3 v. x-cut	59.94	18.30	2.18	3.65	0.97	1.70	0.35	3.37	0.71	0.59	0.26
x5-9	and.	s-alt	S No3 v. x-cut	64.31	16.09	2.20	3.35	1.14	0.35	0.35	4.69	0.44	0.08	0.19
S91-15	porphyry	w-m-alt	Duck lake	63.00	14.89	3.01	1.82	3.40	3.07	4.26	2.64	0.56	0.12	0.28
x10-3	m. dl.	m-alt	main x-cut	63.39	17.37	0.85	3.52	1.00	0.67	0.31	5.61	0.39	0.96	0.11
x10-2	m. dl.	s-alt	main x-cut	59.19	16.35	2.93	4.20	0.93	0.70	0.03	1.29	0.41	1.66	0.19
x10-5	m. dl.	m-alt	main x-cut	59.90	17.87	1.44	3.43	1.47	2.72	0.29	3.38	0.58	0.30	0.19
x10-4	m. dl.	m-alt	main x-cut	64.27	17.07	1.19	2.75	1.25	1.60	0.27	4.37	0.45	0.37	0.14
x1-3	m. dl.	s-alt	main x-cut	64.14	15.68	1.24	4.68	0.78	1.00	0.20	3.96	0.40	0.83	0.19
DA48-5	m. dl.	w-m-alt	Cole lk v. 88-S-5	54.71	16.81	2.46	3.20	2.14	5.67	2.66	4.34	0.58	0.21	0.41
DA48-4D	m. dl.	m-alt	Cole lk v. 88-S-5	53.44	20.81	2.09	3.60	0.85	4.69	0.15	3.06	0.54	0.31	0.34
DA63-4	m. dl.	m-alt	Swrch bk v. 87-S-	48.43	18.07	1.01	12.68	1.21	1.02	0.06	4.05	0.59	0.90	0.29
DA63-3D	m. dl.	m-alt	Swrch bk v. 87-S-	51.36	16.29	0.59	11.24	1.36	1.24	0.05	4.26	0.57	0.98	0.26
x5-5d	and.	m-alt	S No3 v. x-cut	53.63	16.87	1.85	3.60	2.13	6.23	0.82	3.94	0.69	0.48	0.28
x5-5	and.	m-alt	S No3 v. x-cut	55.40	17.50	1.86	4.00	1.86	4.38	0.33	3.62	0.78	0.69	0.26
x5-6d	and.	w-alt	S No3 v. x-cut	56.64	15.42	2.23	3.58	3.43	4.44	4.22	2.75	0.64	0.19	0.30
x5-6	and.	w-alt	S No3 v. x-cut	56.58	16.04	2.36	3.38	2.50	5.11	3.05	2.75	0.67	0.22	0.28
x5-4	and.	m-alt	S No3 v. x-cut	66.43	16.05	1.49	2.62	1.24	0.66	0.34	4.59	0.51	0.36	0.20
x2-5	and.	w-alt	N No3 v. x-cut	57.29	15.70	3.08	2.92	3.33	5.67	3.39	3.15	0.66	0.25	0.37
x10-6	m. dl.	w-alt	main x-cut	61.20	15.06	2.36	2.86	2.81	4.90	3.96	3.15	0.58	0.14	0.27
x3-7	and.	w-alt	N No3 v. x-cut	57.97	15.87	2.86	3.05	2.64	5.66	4.09	2.92	0.65	0.20	0.38
x3-2	and.	m-alt	N No3 v. x-cut	60.21	18.35	2.33	3.65	0.99	1.73	0.34	3.41	0.72	0.60	0.26

Table B-3. Duplicates of CO₂, H₂O & S at Silver Queen mine, central British Columbia

SAMPLE ID	CO ₂	H ₂ O	S (ppm)	SAMPLE ID	CO ₂	H ₂ O	S (ppm)
x10-2	3.64		898	x10-2	4.69		867
x1-2	3.75	1.95	800	x1-2d	3.26	1.90	732
x1-90	2.35		128	x1-90d	2.40		124
x10-3	4.15	1.86	458	x10-3d	4.04	2.27	659
x10-6	1.85	1.39	127	x10-6d	2.40	1.22	154
x10-4			421	x10-4			423
x10-5			357	x10-5			349
x5-4	3.30	2.12	1635	x5-4	3.40	2.02	1610
x5-5			751	x5-5			720
x11-1		0.90	970	x11-1b		0.91	865
x3-3	1.92	1.14	181	x3-3d	1.85	1.64	250
x5-6	4.35	2.16	711	x5-6d	4.15	1.28	1056
S91-10	0.25	0.36		S91-10D	0.35	0.58	
S91-9		2.88		S91-9D		3.19	
SQ-119		2.93	21	SQ119D		3.19	5
x1-2			800	x1-2			768
x3-2			559	x3-2			504

Table B-4. Duplicates of Trace Elements at Silver Queen mine, central British Columbia

SAMPLE ID	ZR	Y	RB	SR	SAMPLE ID	ZR	Y	RB	SR
DA48-4D	127	29	116	217	DA48-4D	145	30	116	220
x1-1	133	20	110	35	x1-1	131	20	105	42
x1-2	135	18	148	201	x1-2d	159	21	165	219
x1-2D	159	22	166	220	x1-2d	159	21	165	216
x1-3	158	21	172	208	x1-3	162	26	169	209
x10-2	150	19	199	69	x10-2	155	21	204	79
x10-3	177	26	206	179	x10-3d	178	27	177	172
x10-3D	178	26	206	179	x10-3d	178	27	177	172
x10-6	172	24	120	511	x10-6d	172	27	121	462
x10-6D	170	25	119	472	x10-6d	172	27	121	462
x3-2	198	27	123	376	x3-2	198	27	123	376
S91-15Dd	125	17	82	397	S91-15D	116	17	77	398
DA48-2D	135	30	260	196	DA48-2	142	31	265	200
DA48-4D	127	30	116	220	DA48-4	127	30	116	220
DA48-5D	124	28	179	446	DA48-5	138	28	188	454
DA63-1D	165	25	104	636	DA63-1	158	26	93	608
DA63-3D	112	24	179	143	DA63-3	114	25	173	141
DA63-5D	99	20	120	87	DA63-5	91	21	123	74
DA8-2D	152	31	177	23	DA8-2	152	31	177	23
DA8-3D	163	31	127	182	DA8-3	164	30	121	176
X1-1D	133	18	113	32	x1-1	132	19	110	32
x1-2D	159	22	166	220	x1-2	135	18	148	201
X1-5D	156	24	177	111	x1-5	160	25	179	114
x1-90d	167	21	136	421	x1-90	165	24	135	422
x11-1b	166	31	92	630	x11-1	166	28	90	595
x3-3d	180	24	117	606	x3-3	185	32	104	597
S91-9D	182	25	99	732	S91-9	184	26	99	734
SQ119D	124	18	71	557	SQ-119	145	18	78	588

Appendix C

Metasomatic Norm Calculation

Using Quattro Pro for DOS 5.0

Instruction of using Quattro Pro for DOS 5.0 to calculate metasomatic norm

Page A.

This is the title page of metasomatic norm calculation using Quattro Pro for DOS 5.0

Page B.

The first block of this page contains lithogeochemical raw data. For example, the block B: B3..I26 contains the raw data in following page.

The second block of page B converts the lithogeochemical raw data into their corresponding molar amounts. For example, the content of SiO₂ of sample x4-4 in cell C7, 57.86, divided by the molar weight of SiO₂, 60.09 g/mole in cell A32 gives its molar amount of 0.962889 in cell C32.

Page C.

Absolute losses and gains of lithogeochemical constituents are calculated in the first notebook block of this page using TiO₂ as immobile component and sample x4-4 as equivalent of least altered parent rock. For example, the value in cell C:D6 is calculated by Gresens' equation (cf. equation 1-9. in chapter 1):

$$dX = \frac{z}{z_o} x_o - x \quad (C-1)$$

In detail, dX is the value of absolute loss or gain of SiO₂ of sample x3-5, z_o is the immobile component TiO₂ of sample x3-5 (B:E9), z the immobile component TiO₂ of sample x4-4 (B:C9), x_o (B:E7) and x (B:C7) are SiO₂ wt.% of the altered sample x3-5 and the least altered sample x4-4 respectively.

The second block of page C presents lithogeochemical data corrected for closure using the equation as follows:

$$X = \frac{z}{z_o} x_o \quad (\text{C-2})$$

Clearly, the equation above is derived from equation (C-1). It converts the intensive value of x_o (wt.%) to X with an extensive unit (such as gram).

Page D and E

Page D and E contain the formulas to calculate metasomatic norms using Optimizer, one of the powerful tools provided in Quattro Pro for DOS 5.0. In general, Optimizer can (i) evaluate more than one formula; (ii) solve sets of linear and nonlinear equations and inequalities; (iii) find a minimum or maximum solution instead of an exact target; (iv) find values that satisfy limits.

To use Optimizer, a notebook model is created. It contains the realistic estimates and define the elements of metasomatic norm calculation as follows:

1. The results of calculated metasomatic norms, which are given on page E. The formulas in this notebook block are based on equations introduced in Chapter 2;
2. A set of variables Optimizer can change to produce the results above, which is listed in the block of Adjust Factor Matrix on page D; and
3. The constraints, or limitations, the solution must accommodate, which are listed in the block of Constraint Matrix on page D. For example, $d\text{Total} = 0$, $d\text{H}_2\text{O} < 0.3$ and > -0.3 , $d\text{CO}_2 < 0.3$ and > -0.3 etc.

All formulas in these notebook blocks are based on the equations introduced in Chapter 2 and attached on the pages following page D and E. After the problem is properly defined, Optimizer can adjust the variables, recalculates the notebook, and then, based on the new results, continues these adjustments until it finds a solution that meets the requirements.

Page F

This page contains the notebook blocks calculating propagated error. The formulas in each notebook blocks on this page are based on the equations introduced in Chapter 3 and attached on the pages following page F for reference.

Page G

This is the last notebook page of this program. It presents the final results of metasomatic norm calculation in units of mole and gram respectively. A set of comprehensive, mass balanced reaction equations can be constructed by combining the results listed on page F and G. For example, sample x4-4 is the least altered precursor rock of altered sample x3-5, the hydrothermal alteration of sample x3-5 can be presented as follows:

Primary minerals	0.023pyroxene + 0.136plagioclase + 0.066K-feldspar + 0.2quartz			
	5.11±0.17 g	36.01±0.95 g	18.26±0.48 g	12.02±0.33 g
Propylitic alteration	+ 0.004chlorite + 0.039epidote + 0.053carbonate			
	3.05±0.11 g	18.7±0.5 g	4.86±0.34 g	
mass losses	- 0.236SiO ₂ - 0.041Al ⁺³ - 0.027Fe ⁺³ - 0.056Mg ⁺² - 0.072Ca ⁺² - 0.11Na ⁺ - 0.029K ⁺			
	-14.19±1.38 g	-1.1±0.22 g	-1.5±0.04 g	-1.37±0.03 g -2.9±0.07 g -2.54±0.04 g -1.11±0.06 g
mass gains	+ 0.129H ₂ O + 0.042CO ₂			
	2.31±0.1 g	1.86±0.12 g		
sericitic, argillic, carbonatized, silicified alteration	= 0.044sericite + 0.063kaolinite + 0.093carbonate + 0.456quartz			
	17.28±0.47 g	16.28±0.51 g	9.81±0.6 g	27.38±0.71 g

Unlike other 'black box' types of software, this Quattro Pro program is transparent. User can easily adjust and develop it according to his own purpose, such as add or replace some standard norm minerals, set different constrains. In addition, user should keep in mind when using Optimizer that calculations of metasomatic norms are complex nonlinear problems and could have many different solutions. Depending on the values user start

with, Optimizer's recommended solutions vary. User should use his knowledge to well constrain the problem and treat his negative results as a case that his hypothesis is rejected and his positive results as the case that his hypothesis is not rejected rather than approved.

Notebook page A.

METASOMATIC NORM

By

Xiaolin Cheng and A. J. Sinclair

Dept. of Geological Sciences

University of British Columbia

1995

Notebook page B.

A	B	C	D	E	F	G	H	I	
Lithogeochemical Raw Data									2
Sample_id	x4-4	x3-7	x3-5	x3-4	x3-1	x3-3d	x2-5		3
Alteration	w-alt	w-alt	m-alt	ms-alt	ms-alt	w-alt	w-alt		4
rock	and.	and.	and.	and.	and.	and.	and.		5
location	N No3 v. x	N No3 v. x	N No3 v. x	N No3 v. x	N No3 v. x	N No3 v. x	N No3 v. x		6
SiO2	57.86	57.97	58.45	56.67	57.25	57.59	57.29		7
Al2O3	15.61	15.87	18.11	17.27	17.45	15.80	15.70		8
TiO2	0.65	0.65	0.87	0.57	0.67	0.65	0.66		9
Fe2O3	3.09	2.86	1.26	1.26	1.25	2.81	3.08		10
FeO	2.89	3.05	3.69	5.78	5.82	3.08	2.92		11
MnO	0.34	0.20	1.34	1.65	1.57	0.35	0.25		12
MgO	2.94	2.64	0.90	1.15	1.09	3.07	3.33		13
CaO	6.07	5.66	2.69	0.73	0.73	5.61	5.67		14
Na2O	3.65	4.09	0.31	0.44	0.29	3.69	3.39		15
K2O	3.09	2.92	2.34	4.12	2.77	3.13	3.15		16
P2O5	0.38	0.38	0.27	0.19	0.20	0.39	0.37		17
H2O	0.97	1.27	4.39	2.69	3.9	1.84	1.04		18
CO2	2.03	2.14	5.2	5.9	5.75	1.65	2.75		19
S	0.013	0.018	0.029	0.127	0.073	0.025	0.003		20
LOI	3.01	3.43	9.62	8.72	9.72	3.52	3.79		21
Total	99.58	99.72	99.85	98.55	98.81	99.69	99.60		22
Zr	191	192	220	163	188	180.19	178.64		23
Y	28	30	32	12	23	23.62	33.05		24
Rb	100	108	96	172	114	117.16	121.40		25
Sr	593	607	238	231	630	605.75	573.45		26
									27
									28
									29
Conversion of wt% to molar amount									30
Sample_id	x4-4	x3-7	x3-5	x3-4	x3-1	x3-3d	x2-5		31
Alteration	w-alt	w-alt	m-alt	ms-alt	ms-alt	w-alt	w-alt		32
Molar wt									33
60.09	Si	0.962889	0.96472	0.972708	0.943085	0.952738	0.958396	0.953403	34
101.96	Al	0.306199	0.311299	0.355237	0.33876	0.342291	0.309925	0.307964	35
79.90	Ti	0.008135	0.008135	0.010889	0.007134	0.008385	0.008135	0.00826	36
159.70	Fe+3	0.038698	0.035817	0.01578	0.01578	0.015654	0.035191	0.038572	37
71.85	Fe+2	0.040223	0.04245	0.051357	0.080445	0.081002	0.042867	0.04064	38
70.94	Mn	0.004793	0.002819	0.018889	0.023259	0.022131	0.004934	0.003524	39
40.31	Mg	0.072935	0.065492	0.022327	0.028529	0.02704	0.07616	0.08261	40
56.08	Ca	0.108238	0.100927	0.047967	0.013017	0.013017	0.100036	0.101106	41
61.98	Na	0.11778	0.131978	0.010003	0.014198	0.009358	0.119071	0.10939	42
94.18	K	0.065619	0.062009	0.049692	0.087492	0.058824	0.066468	0.066893	43
141.94	P	0.005354	0.005354	0.003804	0.002677	0.002818	0.005495	0.005213	44
18.00	OH-	0.107411	0.141111	0.487778	0.298889	0.433333	0.204444	0.115211	45
44.01	CO3=	0.046126	0.048625	0.118155	0.13406	0.130652	0.037491	0.062486	46
32.06	S	0.000415	0.000549	0.000895	0.003949	0.002283	0.000780	0.000097	
90.03	Zr	2.122293	2.133067	2.445851	1.813284	2.086082	2.001444	1.984227	

A	B	C	D	E	F	G	H	
Absolute loss or gain calculation								2
(by using Gresens's/MacLean's Equation)								3
Sample_id	x4-4	x3-7	x3-5	x3-4	x3-1	x3-3d	x2-5	4
Alteration	w-alt	w-alt	m-alt	ms-alt	ms-alt	w-alt	w-alt	5
dSiO2	0.00	0.11	-14.19	6.76	-2.32	-0.27	-1.44	6
dAl2O3	0.00	0.26	-2.08	4.08	1.32	0.19	-0.15	7
dTiO2	0.00	0.00	0.00	0.00	0.00	0.00	0.00	8
dFe2O3	0.00	-0.23	-2.15	-1.65	-1.88	-0.28	-0.06	9
dFeO	0.00	0.16	-0.13	3.70	2.76	0.19	-0.01	10
dMnO	0.00	-0.14	0.66	1.54	1.18	0.01	-0.09	11
dMgO	0.00	-0.30	-2.27	-1.63	-1.88	0.13	0.34	12
dCaO	0.00	-0.41	-4.06	-5.24	-5.36	-0.46	-0.49	13
dNa2O	0.00	0.44	-3.42	-3.15	-3.37	0.04	-0.31	14
dK2O	0.00	-0.17	-1.34	1.61	-0.40	0.04	0.01	15
dP2O5	0.00	0.00	-0.18	-0.16	-0.19	0.01	-0.02	16
dH2O	0.00	0.30	2.31	2.10	2.82	0.87	0.05	17
dCO2	0.00	0.11	1.86	4.70	3.55	-0.38	0.68	18
dS	0.00	0.00	0.01	0.13	0.06	0.01	-0.01	19
dLOI	0.00	0.42	4.18	6.93	6.42	0.51	0.72	20
dTotal	0.00	0.14	-24.98	12.80	-3.72	0.11	-1.49	21
dZr	0.00	0.97	-26.55	-4.91	-8.87	-10.88	-15.14	22
dY	0.00	2.41	-3.88	-14.29	-5.69	-4.33	4.60	23
dRb	0.00	8.17	-28.33	95.59	10.33	16.88	19.28	24
dSr	0.00	14.64	-414.58	-328.93	18.37	13.03	-27.96	25
								26
Lithogeochemical Data Corrected for Closure								27
Sample_id	x4-4	x3-7	x3-5	x3-4	x3-1	x3-3d	x2-5	28
Alteration	w-alt	w-alt	m-alt	ms-alt	ms-alt	w-alt	w-alt	29
dSiO2	57.86	57.97	43.67	64.62	55.54	57.59	56.42	30
dAl2O3	15.61	15.87	13.53	19.69	16.93	15.80	15.46	31
dTiO2	0.65	0.65	0.65	0.65	0.65	0.65	0.65	32
dFe2O3	3.09	2.86	0.94	1.44	1.21	2.81	3.03	33
dFeO	2.89	3.05	2.76	6.59	5.65	3.08	2.88	34
dMnO	0.34	0.20	1.00	1.88	1.52	0.35	0.25	35
dMgO	2.94	2.64	0.67	1.31	1.06	3.07	3.28	36
dCaO	6.07	5.66	2.01	0.83	0.71	5.61	5.58	37
dNa2O	3.65	4.09	0.23	0.50	0.28	3.69	3.34	38
dK2O	3.09	2.92	1.75	4.70	2.69	3.13	3.10	39
dP2O5	0.38	0.38	0.20	0.22	0.19	0.39	0.36	40
dH2O	0.97	1.27	3.28	3.07	3.78	1.84	1.02	41
dCO2	2.03	2.14	3.89	6.73	5.58	1.65	2.71	42
dS	0.01	0.02	0.02	0.14	0.07	0.03	0.00	43
dLOI	3.01	3.43	7.19	9.94	9.43	3.52	3.73	44
dTotal	99.58	99.72	74.60	112.38	95.86	99.69	98.09	45
dZr	191.07	192.04	164.52	186.16	182.20	180.19	175.93	46
dY	27.95	30.36	24.07	13.66	22.26	23.62	32.55	47
dRb	100.28	108.45	71.95	195.87	110.61	117.16	119.56	48
dSr	592.72	607.36	178.14	263.79	611.09	605.75	564.76	49

A	B	C	D	E	F	G	H	
Adjust factor matrix								2
Sample_id	x4-4	x3-7	x3-5	x3-4	x3-1	x3-3d	x2-5	3
Alteration	w-alt	w-alt	m-alt	ms-alt	ms-alt	w-alt	w-alt	4
Calcite	0.043	0.393	0.763	1.000	1.000	0.149	0.271	5
Mg-chl	0.000	1.000	0.000	0.000	0.000	1.000	0.339	6
Mg-pyx	0.472	0.000	0.000	0.000	0.000	0.000	0.000	7
Fe-chl	0.535	0.000	0.000	0.000	0.000	0.535	0.805	8
Fe-pyx	0.312	0.270	0.000	0.000	0.000	0.000	0.195	9
Or	1.000	1.000	0.000	0.000	0.000	1.000	1.000	10
An	0.156	0.191	0.000	0.000	0.000	0.000	0.416	11
Ab	1.000	1.000	0.127	0.265	0.221	0.913	1.000	12
ilmenite	0.000	0.969	0.000	0.000	0.349	0.000	0.011	13
Ca-pyx	0.000	0.000	0.000	0.000	0.000	0.171	0.522	14
magnetite	0.000	0.000	0.000	0.000	0.000	0.000	0.000	15
Mg-chl+p	0.472389	1	0.000479	0	0	1	0.339311	16
Fe-chl+py	0.846492	0.270079	0	0	0	0.535345	1	17
Residual Matrix								18
Sample_id	x4-4	x3-7	x3-5	x3-4	x3-1	x3-3d	x2-5	19
Alteration	w-alt	w-alt	m-alt	ms-alt	ms-alt	w-alt	w-alt	20
dSiO2	0.00000	0.00000	0.00000	0.00000	0.00000	0.00000	0.00000	21
dAl2O3	0.00000	0.00000	0.00000	0.00000	0.00000	0.00000	0.00000	22
dTiO2	0.00000	0.00000	0.00000	0.00000	0.00000	0.00000	0.00000	23
dFe2O3	0.00000	0.00000	0.00000	0.00000	0.00000	0.00000	0.00000	24
dFeO	0.00000	0.00000	0.00000	0.00000	0.00000	0.00000	0.00000	25
dMnO	0.00000	0.00000	0.00000	0.00000	0.00000	0.00000	0.00000	26
dMgO	0.00000	0.00000	0.00000	0.00000	0.00000	0.00000	0.00000	27
dCaO	0.00000	0.00000	0.00000	0.00000	0.00000	0.00000	0.00000	28
dNa2O	0.00000	0.00000	0.00000	0.00000	0.00000	0.00000	0.00000	29
dK2O	0.00000	0.00000	0.00000	0.00000	0.00000	0.00000	0.00000	30
dP2O5	0.00000	0.00000	0.00000	0.00000	0.00000	0.00000	0.00000	31
Constraint matrix								32
dH2O	0.294	0.128	0.244	0.178	0.148	-0.076	0.073	33
dCO2	-0.299	-0.240	-0.251	-0.209	-0.166	0.069	-0.075	34
dS	0.000	0.000	0.000	0.000	0.000	0.000	0.000	35
dLOI	0.004	0.112	0.007	0.032	0.018	0.007	0.001	36
dTotal	0.001	0.108	0.000	0.000	0.000	0.000	0.000	37
Carbnate	4.857	5.850	13.129	15.027	14.570	3.981	5.615	38
Epidote	18.700	9.787	2.388	0.000	0.000	15.489	3.952	39
Sericite	0.000	0.016	23.128	38.839	26.216	3.961	0.000	40
Kaol	0.000	-0.000	21.789	5.318	18.313	-0.000	0.008	41
Chl	3.052	7.280	0.001	0.000	0.000	11.711	7.771	42
Pyx	5.106	1.222	0.000	0.000	0.000	1.802	3.884	43
Or	18.264	17.260	0.000	0.000	0.000	18.501	18.619	44
Pl	36.013	41.628	0.334	0.985	0.542	28.508	41.346	45
Pyrite	0.025	0.033	0.054	0.237	0.137	0.047	0.006	46
Qtz	12.017	13.395	36.654	35.863	36.433	13.867	14.434	47

A	B	C	D	E	F	G	H	I	
Metasomatic Norms (closed)									2
	Sample_id	x4-4	x3-7	x3-5	x3-4	x3-1	x3-3d	x2-5	3
Molar wt	Alteration	w-alt	w-alt	m-alt	ms-alt	ms-alt	w-alt	w-alt	4
100.09	Calcite	0.350	2.626	3.177	0.856	0.833	1.127	0.608	5
483.24	Epidote	18.700	9.787	2.388	0.000	0.000	15.489	3.952	6
232.34	Ca-pyx	0.000	0.000	0.000	0.000	0.000	1.802	2.844	7
278.22	An	5.126	7.029	0.000	0.000	0.000	0.000	12.659	8
84.32	Mg-carb	3.245	0.000	1.882	2.406	2.280	0.000	4.602	9
555.78	Mg-chl	0.000	7.280	0.001	0.000	0.000	8.466	3.116	10
200.80	Mg-pyx	3.459	0.000	0.000	0.000	0.000	0.000	0.000	11
115.86	Fe-carb	0.712	2.900	5.898	9.092	8.913	2.287	-0.000	12
713.48	Fe-chl	3.052	0.000	0.000	0.000	0.000	3.245	4.656	13
263.88	Fe-pyx	1.647	1.222	0.000	0.000	0.000	0.000	1.039	14
398.30	Muscovite	0.000	0.000	19.792	34.848	23.429	0.000	0.000	15
278.34	Or	18.264	17.260	0.000	0.000	0.000	18.501	18.619	16
382.20	Na-mica	0.000	0.016	3.336	3.991	2.786	3.961	0.000	17
262.24	Ab	30.887	34.599	0.334	0.985	0.542	28.508	28.686	18
151.75	ilmenite	0.000	1.196	0.000	0.000	0.444	0.000	0.013	19
79.90	rutile	0.650	0.020	0.870	0.570	0.436	0.650	0.653	20
258.14	Kaol	0.000	-0.000	21.789	5.318	18.313	-0.000	0.008	21
60.09	qtz	12.017	13.395	36.654	35.863	36.433	13.867	14.434	22
114.95	Mn-carb	0.551	0.324	2.171	2.674	2.544	0.567	0.405	23
502.21	apatite	0.896	0.896	0.637	0.448	0.472	0.920	0.873	24
119.97	pyrite	0.025	0.033	0.054	0.237	0.137	0.047	0.006	25
159.70	hemtite	0.000	1.243	0.865	1.260	1.250	0.251	2.427	26
231.55	magnetite	0.000	0.000	0.000	0.000	0.000	0.000	0.000	27
	total	99.581	99.825	99.849	98.547	98.813	99.685	99.600	28
									29
Final Metasomatic Norms (Closed)									30
	Sample_id	x4-4	x3-7	x3-5	x3-4	x3-1	x3-3d	x2-5	31
	Alteration	w-alt	w-alt	m-alt	ms-alt	ms-alt	w-alt	w-alt	32
	apatite	0.896	0.896	0.637	0.448	0.472	0.920	0.873	33
	ilmenite	0.000	1.196	0.000	0.000	0.444	0.000	0.013	34
	magnetite	0.000	0.000	0.000	0.000	0.000	0.000	0.000	35
	pyroxene	5.106	1.222	0.000	0.000	0.000	1.802	3.884	36
	plagioclase	36.013	41.628	0.334	0.985	0.542	28.508	41.346	37
	orthoclase	18.264	17.260	0.000	0.000	0.000	18.501	18.619	38
	quartz	12.017	13.395	36.654	35.863	36.433	13.867	14.434	39
	epidote	18.700	9.787	2.388	0.000	0.000	15.489	3.952	40
	chlorite	3.052	7.280	0.001	0.000	0.000	11.711	7.771	41
	sericite	0.000	0.016	23.128	38.839	26.216	3.961	0.000	42
	kaolinite	0.000	-0.000	21.789	5.318	18.313	-0.000	0.008	43
	carbonate	4.857	5.850	13.129	15.027	14.570	3.981	5.615	44
	rutile	0.650	0.020	0.870	0.570	0.436	0.650	0.653	45
	hemtite	0.000	1.243	0.865	1.260	1.250	0.251	2.427	46
	pyrite	0.025	0.033	0.054	0.237	0.137	0.047	0.006	47
	total	99.581	99.825	99.849	98.547	98.813	99.685	99.600	48

A	B	C	D	E	F	G	H	I	
Error Propagation									2
	So	k	Cd			So	k	Cd	3
SiO2	0.010	0.012	0.020		K2O	0.020	0.018	0.041	4
Al2O3	0.012	0.020	0.025		P2O5	0.020	0.015	0.041	5
TiO2	0.006	0.008	0.012		H2O	0.040	0.130	0.108	6
Fe2O3	0.060	0.018	0.124		CO2	0.010	0.120	0.026	7
FeO	0.045	0.018	0.093		S	0.002	0.070	0.004	8
MnO	0.022	0.007	0.045		Zr(ppm)	0.010	0.032	0.021	9
MgO	0.074	0.030	0.157		Y(ppm)	0.300	0.090	0.732	10
CaO	0.080	0.011	0.164		Rb(ppm)	2.000	0.035	4.301	11
Na2O	0.090	0.013	0.185		Sr(ppm)	5.000	0.019	1.395	12
Standard Deviation at 68% confidence level									13
Sample_id	x4-4	x3-7	x3-5	x3-4	x3-1	x3-3d	x2-5		14
Calcite	0.0000	0.1706	0.2657	0.1037	0.1008	0.0784	0.0416		15
Epidote	0.0025	0.2544	0.0358	0.0000	0.0000	0.3735	0.0952		16
Ca-pyx	0.0937	0.0000	0.0061	0.0000	0.0000	0.0333	0.0524		17
An	0.2666	0.1186	0.0013	0.0000	0.0000	0.0000	0.2270		18
Mg-carb	0.4208	0.0000	0.2144	0.2613	0.2516	0.0000	0.4119		19
Mg-chl	0.1024	0.3620	0.0000	0.0000	0.0000	0.3982	0.1512		20
Mg-pyx	0.0000	0.0000	0.0034	0.0000	0.0000	0.0000	0.0000		21
Fe-carb	0.0039	0.1864	0.3591	0.5657	0.5544	0.1557	-0.0000		22
Fe-chl	0.0000	0.0000	0.0000	0.0000	0.0000	0.1226	0.1857		23
Fe-pyx	0.0821	0.0323	0.0094	0.0000	0.0000	0.0000	0.0247		24
Muscovite	0.0000	0.0000	0.3479	0.6067	0.4095	0.0000	0.0000		25
Or	0.2891	0.2742	0.0000	0.0000	0.0000	0.2926	0.2943		26
Na-mica	0.0174	0.0003	0.1516	0.1316	0.1152	0.0740	0.0000		27
Ab	0.5104	0.5722	0.0000	0.0375	0.0274	0.4796	0.4899		28
ilmenite	0.0153	0.0296	0.0000	0.0000	0.0094	0.0000	0.0003		29
rutile	0.0057	0.0003	0.0130	0.0106	0.0074	0.0112	0.0112		30
Kaol	0.0113	-0.0000	0.7336	0.1811	0.6116	-0.0000	0.0003		31
qtz	0.1607	0.1611	0.4456	0.4367	0.4436	0.1688	0.1757		32
Mn-carb	0.0507	0.0389	0.1327	0.1581	0.1516	0.0518	0.0429		33
apatite	0.0406	0.0409	0.0401	0.0542	0.0559	0.0413	0.0404		34
pyrite	0.0005	0.0006	0.0010	0.0037	0.0021	0.0009	0.0001		35
hemtite	0.0589	0.0438	0.0704	0.0827	0.0825	0.0099	0.0910		36
magnetite	0.0788	0.0000	0.0000	0.0000	0.0000	0.0000	0.0000		37
Sc_SiO2	0.704	0.706	0.711	0.690	0.697	0.701	0.697		38
Sc_Al2O3	0.324	0.329	0.374	0.357	0.361	0.328	0.326		39
Sc_TiO2	0.011	0.011	0.013	0.011	0.011	0.011	0.011		40
Sc_Fe2O3	0.116	0.111	0.083	0.083	0.083	0.111	0.115		41
Sc_FeO	0.097	0.100	0.111	0.149	0.150	0.100	0.098		42
Sc_MnO	0.024	0.023	0.031	0.034	0.033	0.024	0.024		43
Sc_MgO	0.162	0.153	0.101	0.109	0.107	0.166	0.174		44
Sc_CaO	0.147	0.142	0.110	0.088	0.088	0.142	0.142		45
Sc_Na2O	0.137	0.143	0.094	0.096	0.094	0.138	0.134		46
Sc_K2O	0.076	0.073	0.062	0.094	0.070	0.076	0.077		47
Sc_P2O5	0.026	0.026	0.024	0.023	0.023	0.026	0.026		48
Sc_H2O	0.166	0.205	0.611	0.390	0.547	0.279	0.175		49
Sc_CO2	0.254	0.267	0.634	0.718	0.700	0.208	0.340		50
Sc_S	0.003	0.003	0.004	0.011	0.007	0.004	0.002		51
Sc_Zr	6.124	6.155	7.056	5.234	6.020	5.776	5.726		52

Notebook page F.

A	B	C	D	E	F	G	H	I	53
Table 7- . Error propagation of norms corrected for closure in gram(SD at 68% confidence level)									54
at northern segment of No.3 vein, Silver Queen mine, Owen Lake, central BC									55
Sample_id	x4-4	x3-7	x3-5	x3-4	x3-1	x3-3d	x2-5		56
Calcite	0.025	0.192	0.189	0.121	0.100	0.083	0.043		57
Epidote	0.638	0.336	0.070	0.000	0.000	0.531	0.133		58
Ca-pyx	0.000	0.000	0.000	0.000	0.000	0.055	0.085		59
An	0.155	0.213	0.000	0.000	0.000	0.000	0.376		60
Mg-carb	0.307	0.000	0.168	0.306	0.250	0.000	0.420		61
Mg-chl	0.000	0.403	0.000	0.000	0.000	0.448	0.167		62
Mg-pyx	0.132	0.000	0.000	0.000	0.000	0.000	0.000		63
Fe-carb	0.052	0.209	0.304	0.696	0.577	0.165	0.000		64
Fe-chl	0.144	0.000	0.000	0.000	0.000	0.146	0.214		65
Fe-pyx	0.056	0.041	0.000	0.000	0.000	0.000	0.035		66
Muscovite	0.000	0.000	0.425	1.220	0.678	0.000	0.000		67
Or	0.531	0.502	0.000	0.000	0.000	0.537	0.531		68
Na-mica	0.000	0.000	0.114	0.189	0.129	0.122	0.000		69
Ab	0.915	1.019	0.013	0.051	0.029	0.844	0.838		70
ilmenite	0.000	0.041	0.000	0.000	0.014	0.000	0.000		71
rutile	0.019	0.001	0.018	0.020	0.012	0.019	0.019		72
Kaol	0.000	0.000	0.656	0.257	0.732	0.000	0.000		73
qtz	0.327	0.365	0.707	1.148	0.957	0.378	0.386		74
Mn-carb	0.052	0.040	0.106	0.196	0.159	0.054	0.043		75
apatite	0.046	0.046	0.032	0.063	0.055	0.047	0.045		76
pyrite	0.001	0.001	0.001	0.008	0.004	0.001	0.000		77
hemtite	0.000	0.057	0.045	0.101	0.085	0.012	0.107		78
magnetite	0.000	0.000	0.000	0.000	0.000	0.000	0.000		79
Total	3.4013	3.4662	2.8480	4.3782	3.7823	3.4430	3.4443		80
Table 7- . Error propagation of absolute losses & gains in gram (SD at 68% confidence level)									81
at northern segment of No.3 vein, Silver Queen mine, Owen Lake, central BC									82
Sample_id	x4-4	x3-7	x3-5	x3-4	x3-1	x3-3d	x2-5		83
dSiO2	1.726	1.729	1.330	1.946	1.660	1.720	1.686	1.000	84
dAl+3	0.315	0.319	0.279	0.381	0.333	0.318	0.313	0.529	85
dTi+2	0.013	0.013	0.013	0.014	0.013	0.013	0.013	0.599	86
dFe+3	0.126	0.122	0.093	0.107	0.100	0.122	0.125	0.699	87
dFe+2	0.120	0.123	0.111	0.200	0.172	0.123	0.119	0.777	88
dMn+2	0.027	0.026	0.032	0.051	0.042	0.028	0.027	0.774	89
dMg+2	0.145	0.140	0.108	0.125	0.117	0.147	0.150	0.603	90
dCa+2	0.182	0.176	0.124	0.128	0.122	0.176	0.174	0.715	91
dNa+	0.159	0.165	0.115	0.131	0.122	0.159	0.154	0.742	92
dK+	0.109	0.105	0.081	0.147	0.100	0.109	0.109	0.830	93
dP+5	0.016	0.016	0.014	0.016	0.015	0.016	0.016	0.436	94
dH2O	0.235	0.265	0.491	0.481	0.563	0.328	0.240	1.000	95
dCO2	0.362	0.372	0.545	0.874	0.737	0.330	0.425	1.000	96
dS	0.004	0.004	0.004	0.013	0.007	0.005	0.003	1.000	97
dO=	0.652	0.650	0.533	0.696	0.618	0.653	0.647	1.000	98
									99

Notebook page G.

A	B	C	D	E	F	G	H	
Table 7a. Metasomatic norms corrected for closure & absolute losses and gains								2
at northern segment of No. 3 vein, Silver Queen mine, Owen Lake, central BC								3
Sample_id	x4-4	x3-7	x3-5	x3-4	x3-1	x3-3d	x2-5	4
Alteration	w-alt	w-alt	m-alt	ms-alt	ms-alt	w-alt	w-alt	5
mole								6
Calcite	0.0035	0.0262	0.0237	0.0098	0.0081	0.0113	0.0060	7
Epidote	0.0387	0.0203	0.0037	0.0000	0.0000	0.0321	0.0081	8
Ca-pyx	0.0000	0.0000	0.0000	0.0000	0.0000	0.0078	0.0121	9
An	0.0184	0.0253	0.0000	0.0000	0.0000	0.0000	0.0448	10
Mg-carb	0.0385	0.0000	0.0167	0.0325	0.0262	0.0000	0.0538	11
Mg-chl	0.0000	0.0131	0.0000	0.0000	0.0000	0.0152	0.0055	12
Mg-pyx	0.0172	0.0000	0.0000	0.0000	0.0000	0.0000	0.0000	13
Fe-carb	0.0061	0.0250	0.0380	0.0895	0.0746	0.0197	-0.0000	14
Fe-chl	0.0043	0.0000	0.0000	0.0000	0.0000	0.0045	0.0064	15
Fe-pyx	0.0062	0.0046	0.0000	0.0000	0.0000	0.0000	0.0039	16
Muscovite	0.0000	0.0000	0.0371	0.0998	0.0571	0.0000	0.0000	17
Or	0.0656	0.0620	0.0000	0.0000	0.0000	0.0665	0.0659	18
Na-mica	0.0000	0.0000	0.0065	0.0119	0.0071	0.0104	0.0000	19
Ab	0.1178	0.1319	0.0010	0.0043	0.0020	0.1087	0.1077	20
ilmenite	0.0000	0.0079	0.0000	0.0000	0.0028	0.0000	0.0001	21
rutile	0.0081	0.0003	0.0081	0.0081	0.0053	0.0081	0.0080	22
Kaol	0.0000	-0.0000	0.0631	0.0235	0.0688	-0.0000	0.0000	23
qtz	0.2000	0.2229	0.4557	0.6806	0.5882	0.2308	0.2366	24
Mn-carb	0.0048	0.0028	0.0141	0.0265	0.0215	0.0049	0.0035	25
apatite	0.0018	0.0018	0.0009	0.0010	0.0009	0.0018	0.0017	26
pyrite	0.0002	0.0003	0.0003	0.0023	0.0011	0.0004	0.0000	27
hemtite	0.0000	0.0078	0.0040	0.0090	0.0076	0.0016	0.0150	28
magnetite	0.0000	0.0000	0.0000	0.0000	0.0000	0.0000	0.0000	29
Total	0.5313	0.5522	0.6731	0.9987	0.8713	0.5238	0.5790	30
dSiO2	0.0000	0.0018	-0.2362	0.1126	-0.0386	-0.0045	-0.0239	31
dAl+3	0.0000	0.0051	-0.0408	0.0801	0.0259	0.0037	-0.0029	32
dTi+4	0.0000	0.0000	0.0000	0.0000	0.0000	0.0000	0.0000	33
dFe+3	0.0000	-0.0029	-0.0269	-0.0207	-0.0235	-0.0035	-0.0007	34
dFe+2	0.0000	0.0022	-0.0019	0.0515	0.0384	0.0026	-0.0002	35
dMn+2	0.0000	-0.0020	0.0093	0.0217	0.0167	0.0001	-0.0013	36
dMg+2	0.0000	-0.0074	-0.0563	-0.0404	-0.0467	0.0032	0.0084	37
dCa+2	0.0000	-0.0073	-0.0724	-0.0934	-0.0956	-0.0082	-0.0087	38
dNa+	0.0000	0.0142	-0.1103	-0.1016	-0.1087	0.0013	-0.0100	39
dK+	0.0000	-0.0036	-0.0285	0.0342	-0.0086	0.0008	0.0003	40
dP+5	0.0000	0.0000	-0.0025	-0.0023	-0.0026	0.0001	-0.0002	41
Sum O=	0.000	-0.006	-0.299	-0.013	-0.150	-0.001	-0.012	42
dH2O	0.000	0.017	0.129	0.117	0.156	0.049	0.003	43
dCO2	0.000	0.002	0.042	0.107	0.081	-0.009	0.015	44
dS	0.000	0.000	0.000	0.004	0.002	0.000	-0.000	45
dTotal	0.000	0.014	-0.694	0.256	-0.154	0.035	-0.034	46
								47
								48
								49

Notebook page G.

A	B	C	D	E	F	G	H	50
Table 7b. Metasomatic norms corrected for closure & absolute losses and gains								51
at northern segment of No. 3 vein, Silver Queen mine, Owen Lake, central BC								52
Sample_id	x4-4	x3-7	x3-5	x3-4	x3-1	x3-3d	x2-5	53
Alteration	w-alt	w-alt	m-alt	ms-alt	ms-alt	w-alt	w-alt	54
gram								55
Calcite	0.3499	2.6257	2.3738	0.9765	0.8079	1.1268	0.5989	56
Epidote	18.6998	9.7869	1.7840	0.0000	0.0000	15.4890	3.8918	57
Ca-pyx	0.0000	0.0000	0.0000	0.0000	0.0000	1.8023	2.8013	58
An	5.1260	7.0290	0.0000	0.0000	0.0000	0.0000	12.4674	59
Mg-carb	3.2447	0.0000	1.4059	2.7432	2.2120	0.0000	4.5324	60
Mg-chl	0.0000	7.2799	0.0009	0.0000	0.0000	8.4656	3.0685	61
Mg-pyx	3.4591	0.0000	0.0000	0.0000	0.0000	0.0000	0.0000	62
Fe-carb	0.7117	2.9001	4.4068	10.3677	8.6472	2.2868	-0.0000	63
Fe-chl	3.0522	0.0000	0.0000	0.0000	0.0000	3.2449	4.5852	64
Fe-pyx	1.6470	1.2220	0.0000	0.0000	0.0000	0.0000	1.0237	65
Muscovite	0.0000	0.0000	14.7874	39.7390	22.7300	0.0000	0.0000	66
Or	18.2644	17.2596	0.0000	0.0000	0.0000	18.5008	18.3369	67
Na-mica	0.0000	0.0156	2.4924	4.5513	2.7033	3.9605	0.0000	68
Ab	30.8866	34.5992	0.2498	1.1231	0.5259	28.5076	28.2518	69
ilmenite	0.0000	1.1961	0.0000	0.0000	0.4312	0.0000	0.0130	70
rutile	0.6500	0.0202	0.6500	0.6500	0.4230	0.6500	0.6432	71
Kaol	0.0002	-0.0001	16.2790	6.0642	17.7660	-0.0004	0.0078	72
qtz	12.0169	13.3950	27.3848	40.8959	35.3457	13.8670	14.2150	73
Mn-carb	0.5509	0.3241	1.6222	3.0489	2.4681	0.5671	0.3990	74
apatite	0.8963	0.8963	0.4758	0.5111	0.4577	0.9199	0.8595	75
pyrite	0.0249	0.0329	0.0401	0.2701	0.1329	0.0468	0.0057	76
hemtite	0.0001	1.2428	0.6466	1.4368	1.2127	0.2506	2.3903	77
magnetite	0.0000	0.0000	0.0000	0.0000	0.0000	0.0000	0.0000	78
total	99.5809	99.8254	74.5996	112.3777	95.8636	99.6854	98.0914	79
dSiO2	0.0000	0.1100	-14.1905	6.7637	-2.3190	-0.2700	-1.4380	80
dAl+3	0.0000	0.1376	-1.1005	2.1613	0.6981	0.1006	-0.0783	81
dTi+4	0.0000	0.0000	0.0000	0.0000	0.0000	0.0000	0.0000	82
dFe+3	0.0000	-0.1609	-1.5028	-1.1563	-1.3131	-0.1958	-0.0396	83
dFe+2	0.0000	0.1244	-0.1035	2.8770	2.1425	0.1477	-0.0111	84
dMn+2	0.0000	-0.1084	0.5120	1.1939	0.9163	0.0077	-0.0726	85
dMg+2	0.0000	-0.1809	-1.3675	-0.9822	-1.1353	0.0784	0.2048	86
dCa+2	0.0000	-0.2930	-2.9018	-3.7432	-3.8320	-0.3288	-0.3473	87
dNa+	0.0000	0.3264	-2.5359	-2.3355	-2.4990	0.0297	-0.2310	88
dK+	0.0000	-0.1411	-1.1138	1.3350	-0.3343	0.0332	0.0102	89
dP+5	0.0000	0.0000	-0.0778	-0.0713	-0.0812	0.0044	-0.0068	90
Sum O=	0.000	-0.095	-4.777	-0.207	-2.397	-0.010	-0.199	91
dH2O	0.000	0.303	2.313	2.101	2.817	0.873	0.054	92
dCO2	0.000	0.110	1.855	4.698	3.548	-0.380	0.678	93
dS	0.000	0.004	0.008	0.131	0.058	0.012	-0.010	94
dTotal	0.000	0.137	-24.982	12.765	-3.731	0.102	-1.487	95
Residual	0.000	0.108	0.001	0.032	0.014	0.002	-0.003	96
								97
								98

D:B34: 'Constaint matrix

D:A35: ^ dH2O

D:B35: (F3) @ROUND(B:C18-B:\$A\$18*(E:C6/E:\$A\$6+E:C10*8/E:\$A\$10+E:C13*8/E:\$A\$13+E:C15*2/E:\$A\$15+E:C17*2/E:\$A\$17+E:C21*4/E:\$A\$21+E:C24/E:\$A\$24)/2,5)

D:C35: (F3) @ROUND(B:D18-B:\$A\$18*(E:D6/E:\$A\$6+E:D10*8/E:\$A\$10+E:D13*8/E:\$A\$13+E:D15*2/E:\$A\$15+E:D17*2/E:\$A\$17+E:D21*4/E:\$A\$21+E:D24/E:\$A\$24)/2,5)

D:D35: (F3) @ROUND(B:E18-B:\$A\$18*(E:E6/E:\$A\$6+E:E10*8/E:\$A\$10+E:E13*8/E:\$A\$13+E:E15*2/E:\$A\$15+E:E17*2/E:\$A\$17+E:E21*4/E:\$A\$21+E:E24/E:\$A\$24)/2,5)

D:E35: (F3) @ROUND(B:F18-B:\$A\$18*(E:F6/E:\$A\$6+E:F10*8/E:\$A\$10+E:F13*8/E:\$A\$13+E:F15*2/E:\$A\$15+E:F17*2/E:\$A\$17+E:F21*4/E:\$A\$21+E:F24/E:\$A\$24)/2,5)

D:F35: (F3) @ROUND(B:G18-B:\$A\$18*(E:G6/E:\$A\$6+E:G10*8/E:\$A\$10+E:G13*8/E:\$A\$13+E:G15*2/E:\$A\$15+E:G17*2/E:\$A\$17+E:G21*4/E:\$A\$21+E:G24/E:\$A\$24)/2,5)

D:G35: (F3) @ROUND(B:H18-B:\$A\$18*(E:H6/E:\$A\$6+E:H10*8/E:\$A\$10+E:H13*8/E:\$A\$13+E:H15*2/E:\$A\$15+E:H17*2/E:\$A\$17+E:H21*4/E:\$A\$21+E:H24/E:\$A\$24)/2,5)

D:H35: (F3) @ROUND(B:I18-B:\$A\$18*(E:I6/E:\$A\$6+E:I10*8/E:\$A\$10+E:I13*8/E:\$A\$13+E:I15*2/E:\$A\$15+E:I17*2/E:\$A\$17+E:I21*4/E:\$A\$21+E:I24/E:\$A\$24)/2,5)

D:A36: ^ dCO2

D:B36: (F3) @ROUND(B:C19-B:\$A\$19*(E:C5/E:\$A\$5+E:C9/E:\$A\$9+E:C12/E:\$A\$12+E:C23/E:\$A\$23),5)

D:C36: (F3) @ROUND(B:D19-B:\$A\$19*(E:D5/E:\$A\$5+E:D9/E:\$A\$9+E:D12/E:\$A\$12+E:D23/E:\$A\$23),5)

D:D36: (F3) @ROUND(B:E19-B:\$A\$19*(E:E5/E:\$A\$5+E:E9/E:\$A\$9+E:E12/E:\$A\$12+E:E23/E:\$A\$23),5)

D:E36: (F3) @ROUND(B:F19-B:\$A\$19*(E:F5/E:\$A\$5+E:F9/E:\$A\$9+E:F12/E:\$A\$12+E:F23/E:\$A\$23),5)

D:F36: (F3) @ROUND(B:G19-B:\$A\$19*(E:G5/E:\$A\$5+E:G9/E:\$A\$9+E:G12/E:\$A\$12+E:G23/E:\$A\$23),5)

D:G36: (F3) @ROUND(B:H19-B:\$A\$19*(E:H5/E:\$A\$5+E:H9/E:\$A\$9+E:H12/E:\$A\$12+E:H23/E:\$A\$23),5)

D:H36: (F3) @ROUND(B:I19-B:\$A\$19*(E:I5/E:\$A\$5+E:I9/E:\$A\$9+E:I12/E:\$A\$12+E:I23/E:\$A\$23),5)

D:A37: ^ dS

D:B37: (F3) @ROUND(B:C20-B:\$A\$20*E:C25*2/E:\$A\$25,5)

D:C37: (F3) @ROUND(B:D20-B:\$A\$20*E:D25*2/E:\$A\$25,5)

D:D37: (F3) @ROUND(B:E20-B:\$A\$20*E:E25*2/E:\$A\$25,5)

D:E37: (F3) @ROUND(B:F20-B:\$A\$20*E:F25*2/E:\$A\$25,5)

D:F37: (F3) @ROUND(B:G20-B:\$A\$20*E:G25*2/E:\$A\$25,5)

D:G37: (F3) @ROUND(B:H20-B:\$A\$20*E:H25*2/E:\$A\$25,5)

D:H37: (F3) @ROUND(B:I20-B:\$A\$20*E:I25*2/E:\$A\$25,5)

D:A38: ^ dLOI

D:B38: (F3) + B:C21-@SUM(B:C18..C20)-@SUM(B35..B37)

D:C38: (F3) + B:D21-@SUM(B:D18..D20)-@SUM(C35..C37)

D:D38: (F3) + B:E21-@SUM(B:E18..E20)-@SUM(D35..D37)

D:E38: (F3) + B:F21-@SUM(B:F18..F20)-@SUM(E35..E37)

D:F38: (F3) + B:G21-@SUM(B:G18..G20)-@SUM(F35..F37)

D:G38: (F3) + B:H21 @SUM(B:H18..H20) @SUM(G35..G37)
D:H38: (F3) + B:I21 @SUM(B:I18..I20) @SUM(H35..H37)
D:A39: ^ dTotal
D:B39: (F3) @ABS(+B:C22-E:C28)
D:C39: (F3) @ABS(+B:D22-E:D28)
D:D39: (F3) @ABS(+B:E22-E:E28)
D:E39: (F3) @ABS(+B:F22-E:F28)
D:F39: (F3) @ABS(+B:G22-E:G28)
D:G39: (F3) @ABS(+B:H22-E:H28)
D:H39: (F3) @ABS(+B:I22-E:I28)
D:A40: ^ Carbrate
D:B40: (F3) + E:C5+E:C9+E:C12+E:C23
D:C40: (F3) + E:D6+E:D9+E:D12+E:D23
D:D40: (F3) + E:E5+E:E9+E:E12+E:E23
D:E40: (F3) + E:F5+E:F9+E:F12+E:F23
D:F40: (F3) + E:G5+E:G9+E:G12+E:G23
D:G40: (F3) + E:H5+E:H9+E:H12+E:H23
D:H40: (F3) + E:I5+E:I9+E:I12+E:I23
D:A41: ^ Epidote
D:B41: (F3) + E:C6
D:C41: (F3) + E:D6
D:D41: (F3) + E:E6
D:E41: (F3) + E:F6
D:F41: (F3) + E:G6
D:G41: (F3) + E:H6
D:H41: (F3) + E:I6
D:A42: (F3) ^ Sericite
D:B42: (F3) + E:C15+E:C17
D:C42: (F3) + E:D15+E:D17
D:D42: (F3) + E:E15+E:E17
D:E42: (F3) + E:F15+E:F17
D:F42: (F3) + E:G15+E:G17
D:G42: (F3) + E:H15+E:H17
D:H42: (F3) + E:I15+E:I17
D:A43: ^ Kaol
D:B43: (F3) + E:C21
D:C43: (F3) + E:D21
D:D43: (F3) + E:E21
D:E43: (F3) + E:F21
D:F43: (F3) + E:G21
D:G43: (F3) + E:H21
D:H43: (F3) + E:I21
D:A44: ^ Chl
D:B44: (F3) + E:C10+E:C13
D:C44: (F3) + E:D10+E:D13
D:D44: (F3) + E:E10+E:E13
D:E44: (F3) + E:F10+E:F13
D:F44: (F3) + E:G10+E:G13
D:G44: (F3) + E:H10+E:H13
D:H44: (F3) + E:I10+E:I13
D:A45: ^ Pyx
D:B45: (F3) + E:C7+E:C11+E:C14
D:C45: (F3) + E:D7+E:D11+E:D14
D:D45: (F3) + E:E7+E:E11+E:E14
D:E45: (F3) + E:F7+E:F11+E:F14
D:F45: (F3) + E:G7+E:G11+E:G14
D:G45: (F3) + E:H7+E:H11+E:H14
D:H45: (F3) + E:I7+E:I11+E:I14
D:A46: ^ Or
D:B46: (F3) + E:C16
D:C46: (F3) + E:D16
D:D46: (F3) + E:E16
D:E46: (F3) + E:F16
D:F46: (F3) + E:G16
D:G46: (F3) + E:H16
D:H46: (F3) + E:I16
D:A47: ^ Pl
D:B47: (F3) + E:C8+E:C18
D:C47: (F3) + E:D8+E:D18
D:D47: (F3) + E:E8+E:E18
D:E47: (F3) + E:F8+E:F18
D:F47: (F3) + E:G8+E:G18
D:G47: (F3) + E:H8+E:H18
D:H47: (F3) + E:I8+E:I18
D:A48: ^ Pyrite
D:B48: (F3) + E:C25
D:C48: (F3) + E:D25
D:D48: (F3) + E:E25
D:E48: (F3) + E:F25
D:F48: (F3) + E:G25
D:G48: (F3) + E:H25
D:H48: (F3) + E:I25
D:A49: ^ Qiz
D:B49: (F3) + E:C22
D:C49: (F3) + E:D22
D:D49: (F3) + E:E22
D:E49: (F3) + E:F22
D:F49: (F3) + E:G22
D:G49: (F3) + E:H22
D:H49: (F3) + E:I22

E.C2: 'Metasomatic Norms (closed)

E.B3: [W10] ^ Sample_id

E.C3: (F0) U ^ x4-4

E.D3: (F0) U ^ x3-7

E.E3: (F0) U ^ x3-5

E.F3: (F0) U ^ x3-4

E.G3: (F0) U ^ x3-1

E.H3: (F0) U ^ x3-3d

E.I3: (F0) U ^ x2-5

E.A4: ' Molar wt%

E.B4: [W10] ^ Alteration

E.C4: (F0) U ^ w-alt

E.D4: (F0) U ^ w-alt

E.E4: (F0) U ^ m-alt

E.F4: (F0) U ^ ms-alt

E.G4: (F0) U ^ ms-alt

E.H4: (F0) U ^ w-alt

E.I4: (F0) U ^ w-alt

E.A5: (F2) 40.08+12.01+16*3

E.B5: [W10] ^ Calcite

E.C5: (F3) + D:B5*(B:C39-C7*2/\$A\$7-C8/\$A\$8-C24*5/\$A\$24)*\$A\$5

E.D5: (F3) + D:C5*(B:D39-D7*2/\$A\$7-D8/\$A\$8-D24*5/\$A\$24)*\$A\$5

E.E5: (F3) + D:D5*(B:E39-E7*2/\$A\$7-E8/\$A\$8-E24*5/\$A\$24)*\$A\$5

E.F5: (F3) + D:E5*(B:F39-F7*2/\$A\$7-F8/\$A\$8-F24*5/\$A\$24)*\$A\$5

E.G5: (F3) + D:F5*(B:G39-G7*2/\$A\$7-G8/\$A\$8-G24*5/\$A\$24)*\$A\$5

E.H5: (F3) + D:H5*(B:H39-H7*2/\$A\$7-H8/\$A\$8-H24*5/\$A\$24)*\$A\$5

E.I5: (F3) + D:I5*(B:I39-I7*2/\$A\$7-I8/\$A\$8-I24*5/\$A\$24)*\$A\$5

E.A6: (F2) 40.08*2+55.85+26.98*2+28.09*3+16*12+17

E.B6: [W10] ^ Epidote

E.C6: (F3) (1-D:B5)*(B:C39-C7*2/\$A\$7-C8/\$A\$8-C24*5/\$A\$24)*\$A\$6/2

E.D6: (F3) (1-D:C5)*(B:D39-D7*2/\$A\$7-D8/\$A\$8-D24*5/\$A\$24)*\$A\$6/2

E.E6: (F3) (1-D:D5)*(B:E39-E7*2/\$A\$7-E8/\$A\$8-E24*5/\$A\$24)*\$A\$6/2

E.F6: (F3) (1-D:E5)*(B:F39-F7*2/\$A\$7-F8/\$A\$8-F24*5/\$A\$24)*\$A\$6/2

E.G6: (F3) (1-D:F5)*(B:G39-G7*2/\$A\$7-G8/\$A\$8-G24*5/\$A\$24)*\$A\$6/2

E.H6: (F3) (1-D:H5)*(B:H39-H7*2/\$A\$7-H8/\$A\$8-H24*5/\$A\$24)*\$A\$6/2

E.I6: (F3) (1-D:I5)*(B:I39-I7*2/\$A\$7-I8/\$A\$8-I24*5/\$A\$24)*\$A\$6/2

E.A7: (F2) 40.08*2+28.09*2+16*6

E.B7: [W10] ^ Ca-pyx

E.C7: (F3) + D:B14*(B:C39-C8/\$A\$8-C24*5/\$A\$24)*\$A\$7/2

E.D7: (F3) + D:C14*(B:D39-D8/\$A\$8-D24*5/\$A\$24)*\$A\$7/2

E.E7: (F3) + D:D14*(B:E39-E8/\$A\$8-E24*5/\$A\$24)*\$A\$7/2

E.F7: (F3) + D:E14*(B:F39-F8/\$A\$8-F24*5/\$A\$24)*\$A\$7/2

E.G7: (F3) + D:F14*(B:G39-G8/\$A\$8-G24*5/\$A\$24)*\$A\$7/2

E.H7: (F3) + D:H14*(B:H39-H8/\$A\$8-H24*5/\$A\$24)*\$A\$7/2

E.I7: (F3) + D:I14*(B:I39-I8/\$A\$8-I24*5/\$A\$24)*\$A\$7/2

E.A8: (F2) 40.08+26.98*2+28.09*2+16*8

E.B8: [W10] ^ An

E.C8: (F3) + D:B11*(B:C40*\$A\$8

E.D8: (F3) + D:C11*(B:D40*\$A\$8

E.E8: (F3) + D:D11*(B:E40*\$A\$8

E.F8: (F3) + D:E11*(B:F40*\$A\$8

E.G8: (F3) + D:F11*(B:G40*\$A\$8

E.H8: (F3) + D:H11*(B:H40*\$A\$8

E.I8: (F3) + D:I11*(B:I40*\$A\$8

E.A9: (F2) 24.31+60.01

E.B9: [W10] ^ Mg-carb

E.C9: (F3) (1-D:B6-D:B7)*B:C38*\$A\$9

E.D9: (F3) (1-D:C6-D:C7)*B:D38*\$A\$9

E.E9: (F3) (1-D:D6-D:D7)*B:E38*\$A\$9

E.F9: (F3) (1-D:E6-D:E7)*B:F38*\$A\$9

E.G9: (F3) (1-D:F6-D:F7)*B:G38*\$A\$9

E.H9: (F3) (1-D:H6-D:H7)*B:H38*\$A\$9

E:I9: (F3) (1-D:H6-D:H7)*B:I38*\$A\$9
 E:A10: (F2) 24.31*5+26.98*2+28.09*3+16*10+17*8
 E:B10: [W10] ^ Mg-chl
 E:C10: (F3) + D:B6*B:C38/5*\$A\$10
 E:D10: (F3) + D:C6*B:D38/5*\$A\$10
 E:E10: (F3) + D:D6*B:E38/5*\$A\$10
 E:F10: (F3) + D:E6*B:F38/5*\$A\$10
 E:G10: (F3) + D:F6*B:G38/5*\$A\$10
 E:H10: (F3) + D:G6*B:H38/5*\$A\$10
 E:I10: (F3) + D:H6*B:I38/5*\$A\$10
 E:A11: (F2) 24.31*2+28.09*2+16*6
 E:B11: [W10] ^ Mg-pyx
 E:C11: (F3) + D:B7*B:C38/2*\$A\$11
 E:D11: (F3) + D:C7*B:D38/2*\$A\$11
 E:E11: (F3) + D:D7*B:E38/2*\$A\$11
 E:F11: (F3) + D:E7*B:F38/2*\$A\$11
 E:G11: (F3) + D:F7*B:G38/2*\$A\$11
 E:H11: (F3) + D:G7*B:H38/2*\$A\$11
 E:I11: (F3) + D:H7*B:I38/2*\$A\$11
 E:A12: (F2) 55.85+60.01
 E:B12: [W10] ^ Fe-carb
 E:C12: (F3) (1-D:B8-D:B9)*(B:C36-C19/\$A\$19-C25/\$A\$25-C27/\$A\$27)*\$A\$12
 E:D12: (F3) (1-D:C8-D:C9)*(B:D36-D19/\$A\$19-D25/\$A\$25-D27/\$A\$27)*\$A\$12
 E:E12: (F3) (1-D:D8-D:D9)*(B:E36-E19/\$A\$19-E25/\$A\$25-E27/\$A\$27)*\$A\$12
 E:F12: (F3) (1-D:E8-D:E9)*(B:F36-F19/\$A\$19-F25/\$A\$25-F27/\$A\$27)*\$A\$12
 E:G12: (F3) (1-D:F8-D:F9)*(B:G36-G19/\$A\$19-G25/\$A\$25-G27/\$A\$27)*\$A\$12
 E:H12: (F3) (1-D:G8-D:G9)*(B:H36-H19/\$A\$19-H25/\$A\$25-H27/\$A\$27)*\$A\$12
 E:I12: (F3) (1-D:H8-D:H9)*(B:I36-I19/\$A\$19-I25/\$A\$25-I27/\$A\$27)*\$A\$12
 E:A13: (F2) 55.85*5+26.98*2+28.09*3+16*10+17*8
 E:B13: [W10] ^ Fe-chl
 E:C13: (F3) + D:B8*(B:C36-C19/\$A\$19-C25/\$A\$25-C27/\$A\$27/5*\$A\$13
 E:D13: (F3) + D:C8*(B:D36-D19/\$A\$19-D25/\$A\$25-D27/\$A\$27/5*\$A\$13
 E:E13: (F3) + D:D8*(B:E36-E19/\$A\$19-E25/\$A\$25-E27/\$A\$27/5*\$A\$13
 E:F13: (F3) + D:E8*(B:F36-F19/\$A\$19-F25/\$A\$25-F27/\$A\$27/5*\$A\$13
 E:G13: (F3) + D:F8*(B:G36-G19/\$A\$19-G25/\$A\$25-G27/\$A\$27/5*\$A\$13
 E:H13: (F3) + D:G8*(B:H36-H19/\$A\$19-H25/\$A\$25-H27/\$A\$27/5*\$A\$13
 E:I13: (F3) + D:H8*(B:I36-I19/\$A\$19-I25/\$A\$25-I27/\$A\$27/5*\$A\$13
 E:A14: (F2) 55.85*2+28.09*2+16*6
 E:B14: [W10] ^ Fe-pyx
 E:C14: (F3) + D:B9*(B:C36-C19/\$A\$19-C25/\$A\$25-C27/\$A\$27/2*\$A\$14
 E:D14: (F3) + D:C9*(B:D36-D19/\$A\$19-D25/\$A\$25-D27/\$A\$27/2*\$A\$14
 E:E14: (F3) + D:D9*(B:E36-E19/\$A\$19-E25/\$A\$25-E27/\$A\$27/2*\$A\$14
 E:F14: (F3) + D:E9*(B:F36-F19/\$A\$19-F25/\$A\$25-F27/\$A\$27/2*\$A\$14
 E:G14: (F3) + D:F9*(B:G36-G19/\$A\$19-G25/\$A\$25-G27/\$A\$27/2*\$A\$14
 E:H14: (F3) + D:G9*(B:H36-H19/\$A\$19-H25/\$A\$25-H27/\$A\$27/2*\$A\$14
 E:I14: (F3) + D:H9*(B:I36-I19/\$A\$19-I25/\$A\$25-I27/\$A\$27/2*\$A\$14
 E:A15: (F2) 39.09+26.98*3+28.09*3+16*10+17*2
 E:B15: [W10] ^ Muscovite
 E:C15: (F3) (1-D:B10)*B:C41*\$A\$15
 E:D15: (F3) (1-D:C10)*B:D41*\$A\$15
 E:E15: (F3) (1-D:D10)*B:E41*\$A\$15
 E:F15: (F3) (1-D:E10)*B:F41*\$A\$15
 E:G15: (F3) (1-D:F10)*B:G41*\$A\$15
 E:H15: (F3) (1-D:G10)*B:H41*\$A\$15
 E:I15: (F3) (1-D:H10)*B:I41*\$A\$15
 E:A16: (F2) 39.09+26.98+28.09*3+16*8
 E:B16: [W10] ^ Or
 E:C16: (F3) + D:B10*B:C41*\$A\$16
 E:D16: (F3) + D:C10*B:D41*\$A\$16
 E:E16: (F3) + D:D10*B:E41*\$A\$16
 E:F16: (F3) + D:E10*B:F41*\$A\$16
 E:G16: (F3) + D:F10*B:G41*\$A\$16

E:C20: (F3) (1-D:B13)*B:C34*\$A\$20
 E:D20: (F3) (1-D:C13)*B:D34*\$A\$20
 E:E20: (F3) (1-D:D13)*B:E34*\$A\$20
 E:F20: (F3) (1-D:E13)*B:F34*\$A\$20
 E:G20: (F3) (1-D:F13)*B:G34*\$A\$20
 E:H20: (F3) (1-D:G13)*B:H34*\$A\$20
 E:I20: (F3) (1-D:H13)*B:I34*\$A\$20
 E:A21: (F2) 26.98*2+28.09*2+16*5+17*4
 E:B21: [W10] ^ Kad
 E:C21: (F3) (B:C33-C6*2/\$A\$6-C8*2/\$A\$6-C10*2/\$A\$10-C13*2/\$A\$13-C15*3/\$A\$15-C16/\$A\$16-C17*3/\$A\$17-C18/\$A\$18)/2*\$A\$21
 E:D21: (F3) (B:D33-D6*2/\$A\$6-D8*2/\$A\$8-D10*2/\$A\$10-D13*2/\$A\$13-D15*3/\$A\$15-D16/\$A\$16-D17*3/\$A\$17-D18/\$A\$18)/2*\$A\$21
 E:E21: (F3) (B:E33-E6*2/\$A\$6-E8*2/\$A\$8-E10*2/\$A\$10-E13*2/\$A\$13-E15*3/\$A\$15-E16/\$A\$16-E17*3/\$A\$17-E18/\$A\$18)/2*\$A\$21
 E:F21: (F3) (B:F33-F6*2/\$A\$6-F8*2/\$A\$8-F10*2/\$A\$10-F13*2/\$A\$13-F15*3/\$A\$15-F16/\$A\$16-F17*3/\$A\$17-F18/\$A\$18)/2*\$A\$21
 E:G21: (F3) (B:G33-G6*2/\$A\$6-G8*2/\$A\$8-G10*2/\$A\$10-G13*2/\$A\$13-G15*3/\$A\$15-G16/\$A\$16-G17*3/\$A\$17-G18/\$A\$18)/2*\$A\$21
 E:H21: (F3) (B:H33-H6*2/\$A\$6-H8*2/\$A\$8-H10*2/\$A\$10-H13*2/\$A\$13-H15*3/\$A\$15-H16/\$A\$16-H17*3/\$A\$17-H18/\$A\$18)/2*\$A\$21
 E:I21: (F3) (B:I33-I6*2/\$A\$6-I8*2/\$A\$8-I10*2/\$A\$10-I13*2/\$A\$13-I15*3/\$A\$15-I16/\$A\$16-I17*3/\$A\$17-I18/\$A\$18)/2*\$A\$21
 E:A22: (F2) 28.09+16*2
 E:B22: [W10] ^ qiz
 E:C22: (F3) (+B:C32-C6*3/\$A\$6-C7*2/\$A\$7-C8*2/\$A\$8-C10*3/\$A\$10-C11*2/\$A\$11-C13*3/\$A\$13-C14*2/\$A\$14-C15*3/\$A\$15-C16*3/\$A\$16-C17*3/\$A\$17-C18*3/\$A\$18-C21*2/\$A\$21)*\$A\$22
 E:D22: (F3) (+B:D32-D6*3/\$A\$6-D7*2/\$A\$7-D8*2/\$A\$8-D10*3/\$A\$10-D11*2/\$A\$11-D13*3/\$A\$13-D14*2/\$A\$14-D15*3/\$A\$15-D16*3/\$A\$16-D17*3/\$A\$17-D18*3/\$A\$18-D21*2/\$A\$21)*\$A\$22
 E:E22: (F3) (+B:E32-E6*3/\$A\$6-E7*2/\$A\$7-E8*2/\$A\$8-E10*3/\$A\$10-E11*2/\$A\$11-E13*3/\$A\$13-E14*2/\$A\$14-E15*3/\$A\$15-E16*3/\$A\$16-E17*3/\$A\$17-E18*3/\$A\$18-E21*2/\$A\$21)*\$A\$22
 E:F22: (F3) (+B:F32-F6*3/\$A\$6-F7*2/\$A\$7-F8*2/\$A\$8-F10*3/\$A\$10-F11*2/\$A\$11-F13*3/\$A\$13-F14*2/\$A\$14-F15*3/\$A\$15-F16*3/\$A\$16-F17*3/\$A\$17-F18*3/\$A\$18-F21*2/\$A\$21)*\$A\$22
 E:G22: (F3) (+B:G32-G6*3/\$A\$6-G7*2/\$A\$7-G8*2/\$A\$8-G10*3/\$A\$10-G11*2/\$A\$11-G13*3/\$A\$13-G14*2/\$A\$14-G15*3/\$A\$15-G16*3/\$A\$16-G17*3/\$A\$17-G18*3/\$A\$18-G21*2/\$A\$21)*\$A\$22
 E:H22: (F3) (+B:H32-H6*3/\$A\$6-H7*2/\$A\$7-H8*2/\$A\$8-H10*3/\$A\$10-H11*2/\$A\$11-H13*3/\$A\$13-H14*2/\$A\$14-H15*3/\$A\$15-H16*3/\$A\$16-H17*3/\$A\$17-H18*3/\$A\$18-H21*2/\$A\$21)*\$A\$22
 E:I22: (F3) (+B:I32-I6*3/\$A\$6-I7*2/\$A\$7-I8*2/\$A\$8-I10*3/\$A\$10-I11*2/\$A\$11-I13*3/\$A\$13-I14*2/\$A\$14-I15*3/\$A\$15-I16*3/\$A\$16-I17*3/\$A\$17-I18*3/\$A\$18-I21*2/\$A\$21)*\$A\$22
 E:A23: (F2) 54.94+12.01+16*3
 E:B23: [W10] ^ Mn-carb
 E:C23: (F3) +B:C37*\$A\$23
 E:D23: (F3) +B:D37*\$A\$23
 E:E23: (F3) +B:E37*\$A\$23
 E:F23: (F3) +B:F37*\$A\$23

E:H16: (F3) + D:G10*B:H41*\$A\$16
 E:I16: (F3) + D:H10*B:I41*\$A\$16
 E:A17: (F2) 22.99+26.98*3+28.09*3+16*10+17*2
 E:B17: [W10] ^Na-mica
 E:C17: (F3) (1-D:B12)*B:C40*\$A\$17
 E:D17: (F3) (1-D:C12)*B:D40*\$A\$17
 E:E17: (F3) (1-D:D12)*B:E40*\$A\$17
 E:F17: (F3) (1-D:E12)*B:F40*\$A\$17
 E:G17: (F3) (1-D:F12)*B:G40*\$A\$17
 E:H17: (F3) (1-D:G12)*B:H40*\$A\$17
 E:I17: (F3) (1-D:H12)*B:I40*\$A\$17
 E:A18: (F2) 22.99+26.98+28.09*3+16*8
 E:B18: [W10] ^Ab
 E:C18: (F3) + D:B12*B:C40*\$A\$18
 E:D18: (F3) + D:C12*B:D40*\$A\$18
 E:E18: (F3) + D:D12*B:E40*\$A\$18
 E:F18: (F3) + D:E12*B:F40*\$A\$18
 E:G18: (F3) + D:F12*B:G40*\$A\$18
 E:H18: (F3) + D:G12*B:H40*\$A\$18
 E:I18: (F3) + D:H12*B:I40*\$A\$18
 E:A19: (F2) 55.85+47.9+16*3
 E:B19: [W10] ^Ilmenite
 E:C19: (F3) + D:B13*B:C34*\$A\$19
 E:D19: (F3) + D:C13*B:D34*\$A\$19
 E:E19: (F3) + D:D13*B:E34*\$A\$19
 E:F19: (F3) + D:E13*B:F34*\$A\$19
 E:G19: (F3) + D:F13*B:G34*\$A\$19
 E:H19: (F3) + D:G13*B:H34*\$A\$19
 E:I19: (F3) + D:H13*B:I34*\$A\$19
 E:A20: (F2) 47.9+16*2
 E:B20: (F3) [W10] ^Tullite
 E:C23: (F3) + B:G37*\$A\$23
 E:H23: (F3) + B:H37*\$A\$23
 E:I23: (F3) + B:I37*\$A\$23
 E:A24: (F2) 40.06*5+30.97*3+16*12+17
 E:B24: [W10] ^apatite
 E:C24: (F3) + B:C42/3*\$A\$24
 E:D24: (F3) + B:D42/3*\$A\$24
 E:E24: (F3) + B:E42/3*\$A\$24
 E:F24: (F3) + B:F42/3*\$A\$24
 E:G24: (F3) + B:G42/3*\$A\$24
 E:H24: (F3) + B:H42/3*\$A\$24
 E:I24: (F3) + B:I42/3*\$A\$24
 E:A25: (F2) 55.85+2*32.06
 E:B25: [W10] ^pyrite
 E:C25: (F3) + B:C45/2*\$A\$25
 E:D25: (F3) + B:D45/2*\$A\$25
 E:E25: (F3) + B:E45/2*\$A\$25
 E:F25: (F3) + B:F45/2*\$A\$25
 E:G25: (F3) + B:G45/2*\$A\$25
 E:H25: (F3) + B:H45/2*\$A\$25
 E:I25: (F3) + B:I45/2*\$A\$25
 E:A26: (F2) 55.85*2+16*3
 E:B26: [W10] ^hemite
 E:C26: (F3) (1-D:B15)*(+B:C35-C6/\$A\$6)*\$A\$26/2
 E:D26: (F3) (1-D:C15)*(+B:D35-D6/\$A\$6)*\$A\$26/2
 E:E26: (F3) (1-D:D15)*(+B:E35-E6/\$A\$6)*\$A\$26/2
 E:F26: (F3) (1-D:E15)*(+B:F35-F6/\$A\$6)*\$A\$26/2
 E:G26: (F3) (1-D:F15)*(+B:G35-G6/\$A\$6)*\$A\$26/2
 E:H26: (F3) (1-D:G15)*(+B:H35-H6/\$A\$6)*\$A\$26/2
 E:I26: (F3) (1-D:H15)*(+B:I35-I6/\$A\$6)*\$A\$26/2
 E:A27: 55.85*3+16*4

E:B27: [W10] ^magnetite
 E:C27: (F3) + D:B15*(+B:C35-C6/\$A\$6)*\$A\$27/2
 E:D27: (F3) + D:C15*(+B:D35-D6/\$A\$6)*\$A\$27/2
 E:E27: (F3) + D:D15*(+B:E35-E6/\$A\$6)*\$A\$27/2
 E:F27: (F3) + D:E15*(+B:F35-F6/\$A\$6)*\$A\$27/2
 E:G27: (F3) + D:F15*(+B:G35-G6/\$A\$6)*\$A\$27/2
 E:H27: (F3) + D:G15*(+B:H35-H6/\$A\$6)*\$A\$27/2
 E:I27: (F3) + D:H15*(+B:I35-I6/\$A\$6)*\$A\$27/2
 E:B28: [W10] ^total
 E:C28: (F3) @SUM(C5..C27)
 E:D28: (F3) @SUM(D5..D27)
 E:E28: (F3) @SUM(E5..E27)
 E:F28: (F3) @SUM(F5..F27)
 E:G28: (F3) @SUM(G5..G27)
 E:H28: (F3) @SUM(H5..H27)
 E:I28: (F3) @SUM(I5..I27)

F:B13: 'Standard Deviation at 68% confidence level

F:A14: 'Sample_id

F:B14: (F0) ^ x4-4

F:C14: (F0) ^ x3-7

F:D14: (F0) ^ x3-5

F:E14: (F0) ^ x3-4

F:F14: (F0) ^ x3-1

F:G14: (F0) ^ x3-3d

F:H14: (F0) ^ x2-5

F:A15: ^ Calcite

F:B15: (F4) + E:C5/E:\$A5*(B:\$A14/B:C14*B45 + B:\$A19/B:C19*B50)

F:C15: (F4) + E:D5/E:\$A5*(B:\$A14/B:D14*C45 + B:\$A19/B:D19*C50)

F:D15: (F4) + E:E5/E:\$A5*(B:\$A14/B:E14*D45 + B:\$A19/B:E19*D50)

F:E15: (F4) + E:F5/E:\$A5*(B:\$A14/B:F14*E45 + B:\$A19/B:F19*E50)

F:F15: (F4) + E:G5/E:\$A5*(B:\$A14/B:G14*F45 + B:\$A19/B:G19*F50)

F:G15: (F4) + E:H5/E:\$A5*(B:\$A14/B:H14*G45 + B:\$A19/B:H19*G50)

F:H15: (F4) + E:I5/E:\$A5*(B:\$A14/B:I14*H45 + B:\$A19/B:I19*H50)

F:A16: ^ Epidote

F:B16: (F4) + E:C6/E:\$A6*(2*B:\$A14*B45/B:C14 + 0.5*B:\$A10*B41/B:C10 + B:\$A8*B39/B:C8 + 3*B:\$A7*B38/B:C7 + 0.5*B:\$A18*B49/B:C18)

F:C16: (F4) + E:D6/E:\$A6*(2*B:\$A14*C45/B:D14 + 0.5*B:\$A10*C41/B:D10 + B:\$A8*C39/B:D8 + 3*B:\$A7*C38/B:D7 + 0.5*B:\$A18*C49/B:D18)

F:D16: (F4) + E:E6/E:\$A6*(2*B:\$A14*D45/B:E14 + 0.5*B:\$A10*D41/B:E10 + B:\$A8*D39/B:E8 + 3*B:\$A7*D38/B:E7 + 0.5*B:\$A18*D49/B:E18)

F:E16: (F4) + E:F6/E:\$A6*(2*B:\$A14*E45/B:F14 + 0.5*B:\$A10*E41/B:F10 + B:\$A8*E39/B:F8 + 3*B:\$A7*E38/B:F7 + 0.5*B:\$A18*E49/B:F18)

F:F16: (F4) + E:G6/E:\$A6*(2*B:\$A14*F45/B:G14 + 0.5*B:\$A10*F41/B:G10 + B:\$A8*F39/B:G8 + 3*B:\$A7*F38/B:G7 + 0.5*B:\$A18*F49/B:G18)

F:G16: (F4) + E:H6/E:\$A6*(2*B:\$A14*G45/B:H14 + 0.5*B:\$A10*G41/B:H10 + B:\$A8*G39/B:H8 + 3*B:\$A7*G38/B:H7 + 0.5*B:\$A18*G49/B:H18)

F:H16: (F4) + E:I6/E:\$A6*(2*B:\$A14*H45/B:I14 + 0.5*B:\$A10*H41/B:I10 + B:\$A8*H39/B:I8 + 3*B:\$A7*H38/B:I7 + 0.5*B:\$A18*H49/B:I18)

F:A17: ^ Ca-pyx

F:B17: (F4) + E:C7/E:\$A7*2*(B:\$A14/B:C14*B45 + B:\$A7/B:C7*B38)

F:C17: (F4) + E:D7/E:\$A7*2*(B:\$A14/B:D14*C45 + B:\$A7/B:D7*C38)

F:D17: (F4) + E:E7/E:\$A7*2*(B:\$A14/B:E14*D45 + B:\$A7/B:E7*D38)

F:E17: (F4) + E:F7/E:\$A7*2*(B:\$A14/B:F14*E45 + B:\$A7/B:F7*E38)

F: F17: (F4) + E: G7/E: \$A7*2*(B: \$A14/B: G14*F45 + B: \$A7/B: G7*F38)
 F: G17: (F4) + E: H7/E: \$A7*2*(B: \$A14/B: H14*G45 + B: \$A7/B: H7*G38)
 F: H17: (F4) + E: I7/E: \$A7*2*(B: \$A14/B: I14*H45 + B: \$A7/B: I7*H38)
 F: A18: \sim A_n
 F: B18: (F4) + E: C8/E: \$A8*(B: \$A14/B: C14*B45 + B: \$A8/B: C8*B39 + 2*B: \$A7/B: C7*B38)
 F: C18: (F4) + E: D8/E: \$A8*(B: \$A14/B: D14*C45 + B: \$A8/B: D8*C39 + 2*B: \$A7/B: D7*C38)
 F: D18: (F4) + E: E8/E: \$A8*(B: \$A14/B: E14*D45 + B: \$A8/B: E8*D39 + 2*B: \$A7/B: E7*D38)
 F: E18: (F4) + E: F8/E: \$A8*(B: \$A14/B: F14*E45 + B: \$A8/B: F8*E39 + 2*B: \$A7/B: F7*E38)
 F: F18: (F4) + E: G8/E: \$A8*(B: \$A14/B: G14*F45 + B: \$A8/B: G8*F39 + 2*B: \$A7/B: G7*F38)
 F: G18: (F4) + E: H8/E: \$A8*(B: \$A14/B: H14*G45 + B: \$A8/B: H8*G39 + 2*B: \$A7/B: H7*G38)
 F: H18: (F4) + E: I8/E: \$A8*(B: \$A14/B: I14*H45 + B: \$A8/B: I8*H39 + 2*B: \$A7/B: I7*H38)
 F: A19: \sim Mg-carb
 F: B19: (F4) + E: C9/E: \$A9*(B: \$A13/B: C13*B44 + B: \$A19/B: C19*B50)
 F: C19: (F4) + E: D9/E: \$A9*(B: \$A13/B: D13*C44 + B: \$A19/B: D19*C50)
 F: D19: (F4) + E: E9/E: \$A9*(B: \$A13/B: E13*D44 + B: \$A19/B: E19*D50)
 F: E19: (F4) + E: F9/E: \$A9*(B: \$A13/B: F13*E44 + B: \$A19/B: F19*E50)
 F: F19: (F4) + E: G9/E: \$A9*(B: \$A13/B: G13*F44 + B: \$A19/B: G19*F50)
 F: G19: (F4) + E: H9/E: \$A9*(B: \$A13/B: H13*G44 + B: \$A19/B: H19*G50)
 F: H19: (F4) + E: I9/E: \$A9*(B: \$A13/B: I13*H44 + B: \$A19/B: I19*H50)
 F: A20: \sim Mg-chl
 F: B20: (F4) + E: C10/E: \$A10*(5*B: \$A13/B: C13*B44 + B: \$A8/B: C8*B39 + 3*B: \$A7/B: C7*B38 + 4*B: \$A19/B: C18*B49)
 F: C20: (F4) + E: D10/E: \$A10*(5*B: \$A13/B: D13*C44 + B: \$A8/B: D8*C39 + 3*B: \$A7/B: D7*C38 + 4*B: \$A18/B: D18*C49)
 F: D20: (F4) + E: E10/E: \$A10*(5*B: \$A13/B: E13*D44 + B: \$A8/B: E8*D39 + 3*B: \$A7/B: E7*D38 + 4*B: \$A18/B: E18*D49)
 F: E20: (F4) + E: F10/E: \$A10*(5*B: \$A13/B: F13*E44 + B: \$A8/B: F8*E39 + 3*B: \$A7/B: F7*E38 + 4*B: \$A18/B: F18*E49)
 F: F20: (F4) + E: G10/E: \$A10*(5*B: \$A13/B: G13*F44 + B: \$A8/B: G8*F39 + 3*B: \$A7/B: G7*F38 + 4*B: \$A18/B: G18*F49)
 F: G20: (F4) + E: H10/E: \$A10*(5*B: \$A13/B: H13*G44 + B: \$A8/B: H8*G39 + 3*B: \$A7/B: H7*G38 + 4*B: \$A18/B: H18*G49)
 F: H20: (F4) + E: I10/E: \$A10*(5*B: \$A13/B: I13*H44 + B: \$A8/B: I8*H39 + 3*B: \$A7/B: I7*H38 + 4*B: \$A18/B: I18*H49)
 F: A21: \sim Mg-pyx
 F: B21: (F4) + E: C11*2/E: \$A11*(B: \$A13/B: C13*B44 + B: \$A7/B: C7*B38)
 F: C21: (F4) + E: D11*2/E: \$A11*(B: \$A13/B: D13*C44 + B: \$A7/B: D7*C38)

F:D21: (F4) + E:E11*2/E:\$A11*(B:\$A13/B:E13*D44+B:\$A7/B:E7*D38)
 F:E21: (F4) + E:F11*2/E:\$A11*(B:\$A13/B:F13*E44+B:\$A7/B:F7*E38)
 F:F21: (F4) + E:G11*2/E:\$A11*(B:\$A13/B:G13*F44+B:\$A7/B:G7*F38)
 F:G21: (F4) + E:H11*2/E:\$A11*(B:\$A13/B:H13*G44+B:\$A7/B:H7*G38)
 F:H21: (F4) + E:I11*2/E:\$A11*(B:\$A13/B:I13*H44+B:\$A7/B:I7*H38)
 F:A22: ^ Fe-carb
 F:B22: (F4) + E:C12/E:\$A12*(B:\$A11/B:C11*B42+B:\$A19/B:C19*B50)
 F:C22: (F4) + E:D12/E:\$A12*(B:\$A11/B:D11*C42+B:\$A19/B:D19*C50)
 F:D22: (F4) + E:E12/E:\$A12*(B:\$A11/B:E11*D42+B:\$A19/B:E19*D50)
 F:E22: (F4) + E:F12/E:\$A12*(B:\$A11/B:F11*E42+B:\$A19/B:F19*E50)
 F:F22: (F4) + E:G12/E:\$A12*(B:\$A11/B:G11*F42+B:\$A19/B:G19*F50)
 F:G22: (F4) + E:H12/E:\$A12*(B:\$A11/B:H11*G42+B:\$A19/B:H19*G50)
 F:H22: (F4) + E:I12/E:\$A12*(B:\$A11/B:I11*H42+B:\$A19/B:I19*H50)
 F:A23: ^ Fe-chl
 F:B23: (F4) + E:C13/E:\$A13*(B:\$A11*5/B:C11*B42+B:\$A8/B:C8*B39+3*B:\$A7/B:C7*B38+4*B:\$A18/B:C18*B49)
 F:C23: (F4) + E:D13/E:\$A13*(B:\$A11*5/B:D11*C42+B:\$A8/B:D8*C39+3*B:\$A7/B:D7*C38+4*B:\$A18/B:D18*C49)
 F:D23: (F4) + E:E13/E:\$A13*(B:\$A11*5/B:E11*D42+B:\$A8/B:E8*D39+3*B:\$A7/B:E7*D38+4*B:\$A18/B:E18*D49)
 F:E23: (F4) + E:F13/E:\$A13*(B:\$A11*5/B:F11*E42+B:\$A8/B:F8*E39+3*B:\$A7/B:F7*E38+4*B:\$A18/B:F18*E49)
 F:F23: (F4) + E:G13/E:\$A13*(B:\$A11*5/B:G11*F42+B:\$A8/B:G8*F39+3*B:\$A7/B:G7*F38+4*B:\$A18/B:G18*F49)
 F:G23: (F4) + E:H13/E:\$A13*(B:\$A11*5/B:H11*G42+B:\$A8/B:H8*G39+3*B:\$A7/B:H7*G38+4*B:\$A18/B:H18*G49)
 F:H23: (F4) + E:I13/E:\$A13*(B:\$A11*5/B:I11*H42+B:\$A8/B:I8*H39+3*B:\$A7/B:I7*H38+4*B:\$A18/B:I18*H49)
 F:A24: ^ Fe-pyx
 F:B24: (F4) + E:C14*2/E:\$A14*(B:\$A11/B:C11*B42+B:\$A7/B:C7*B38)
 F:C24: (F4) + E:D14*2/E:\$A14*(B:\$A11/B:D11*C42+B:\$A7/B:D7*C38)
 F:D24: (F4) + E:E14*2/E:\$A14*(B:\$A11/B:E11*D42+B:\$A7/B:E7*D38)
 F:E24: (F4) + E:F14*2/E:\$A14*(B:\$A11/B:F11*E42+B:\$A7/B:F7*E38)
 F:F24: (F4) + E:G14*2/E:\$A14*(B:\$A11/B:G11*F42+B:\$A7/B:G7*F38)
 F:G24: (F4) + E:H14*2/E:\$A14*(B:\$A11/B:H11*G42+B:\$A7/B:H7*G38)
 F:H24: (F4) + E:I14*2/E:\$A14*(B:\$A11/B:I11*H42+B:\$A7/B:I7*H38)
 F:A25: ^ Muscovite

F:B25: (F4) + E:C15/E:\$A15*(0.5*B:\$A16/B:C16*B47 + 0.5*B:\$A8/B:C8*B39 + 3*B:\$A7/B:C7*B38 + B:\$A18/B:C18*B49)
 F:C25: (F4) + E:D15/E:\$A15*(0.5*B:\$A16/B:D16*C47 + 0.5*B:\$A8/B:D8*C39 + 3*B:\$A7/B:D7*C38 + B:\$A18/B:D18*C49)
 F:D25: (F4) + E:E15/E:\$A15*(0.5*B:\$A16/B:E16*D47 + 0.5*B:\$A9/B:E9*D39 + 3*B:\$A7/B:E7*D38 + B:\$A18/B:E18*D49)
 F:E25: (F4) + E:F15/E:\$A15*(0.5*B:\$A16/B:F16*E47 + 0.5*B:\$A8/B:F8*E39 + 3*B:\$A7/B:F7*E38 + B:\$A18/B:F18*E49)
 F:F25: (F4) + E:G15/E:\$A15*(0.5*B:\$A16/B:G16*F47 + 0.5*B:\$A8/B:G8*F39 + 3*B:\$A7/B:G7*F38 + B:\$A18/B:G18*F49)
 F:G25: (F4) + E:H15/E:\$A15*(0.5*B:\$A16/B:H16*G47 + 0.5*B:\$A8/B:H8*G39 + 3*B:\$A7/B:H7*G38 + B:\$A18/B:H18*G49)
 F:H25: (F4) + E:I15/E:\$A15*(0.5*B:\$A16/B:I16*H47 + 0.5*B:\$A8/B:I8*H39 + 3*B:\$A7/B:I7*H38 + B:\$A18/B:I18*H49)
 F:A26: ^ Or
 F:B26: (F4) + E:C16/E:\$A16*(0.5*B:\$A16/B:C16*B47 + 0.5*B:\$A8/B:C8*B39 + 3*B:\$A7/B:C7*B38)
 F:C26: (F4) + E:D16/E:\$A16*(0.5*B:\$A16/B:D16*C47 + 0.5*B:\$A8/B:D8*C39 + 3*B:\$A7/B:D7*C38)
 F:D26: (F4) + E:E16/E:\$A16*(0.5*B:\$A16/B:E16*D47 + 0.5*B:\$A8/B:E8*D39 + 3*B:\$A7/B:E7*D38)
 F:E26: (F4) + E:F16/E:\$A16*(0.5*B:\$A16/B:F16*E47 + 0.5*B:\$A8/B:F8*E39 + 3*B:\$A7/B:F7*E38)
 F:F26: (F4) + E:G16/E:\$A16*(0.5*B:\$A16/B:G16*F47 + 0.5*B:\$A8/B:G8*F39 + 3*B:\$A7/B:G7*F38)
 F:G26: (F4) + E:H16/E:\$A16*(0.5*B:\$A16/B:H16*G47 + 0.5*B:\$A8/B:H8*G39 + 3*B:\$A7/B:H7*G38)
 F:H26: (F4) + E:I16/E:\$A16*(0.5*B:\$A16/B:I16*H47 + 0.5*B:\$A8/B:I8*H39 + 3*B:\$A7/B:I7*H38)
 F:A27: ^ Na-mica
 F:B27: (F4) + E:C17/E:\$A17*(0.5*B:\$A15/B:C15*B46 + 0.5*B:\$A8/B:C8*B39 + 3*B:\$A7/B:C7*B38 + B:\$A18/B:C18*B49)
 F:C27: (F4) + E:D17/E:\$A17*(0.5*B:\$A15/B:D15*C46 + 0.5*B:\$A8/B:D8*C39 + 3*B:\$A7/B:D7*C38 + B:\$A18/B:D18*C49)
 F:D27: (F4) + E:E17/E:\$A17*(0.5*B:\$A15/B:E15*D46 + 0.5*B:\$A8/B:E8*D39 + 3*B:\$A7/B:E7*D38 + B:\$A18/B:E18*D49)
 F:E27: (F4) + E:F17/E:\$A17*(0.5*B:\$A15/B:F15*E46 + 0.5*B:\$A8/B:F8*E39 + 3*B:\$A7/B:F7*E38 + B:\$A18/B:F18*E49)
 F:F27: (F4) + E:G17/E:\$A17*(0.5*B:\$A15/B:G15*F46 + 0.5*B:\$A8/B:G8*F39 + 3*B:\$A7/B:G7*F38 + B:\$A18/B:G18*F49)
 F:G27: (F4) + E:H17/E:\$A17*(0.5*B:\$A15/B:H15*G46 + 0.5*B:\$A8/B:H8*G39 + 3*B:\$A7/B:H7*G38 + B:\$A18/B:H18*G49)
 F:H27: (F4) + E:I17/E:\$A17*(0.5*B:\$A15/B:I15*H46 + 0.5*B:\$A8/B:I8*H39 + 3*B:\$A7/B:I7*H38 + B:\$A18/B:I18*H49)
 F:A28: ^ Ab
 F:B28: (F4) + E:C18/E:\$A18*(0.5*B:\$A15/B:C15*B46 + 0.5*B:\$A8/B:C8*B39 + 3*B:\$A7/B:C7*B38)
 F:C28: (F4) + E:D18/E:\$A18*(0.5*B:\$A15/B:D15*C46 + 0.5*B:\$A8/B:D8*C39 + 3*B:\$A7/B:D7*C38)
 F:D28: (F4) + E:E18/E:\$A18*(0.5*B:\$A15/B:E15*D46 + 0.5*B:\$A8/B:E8*D39 + 3*B:\$A7/B:E7*D38)
 F:E28: (F4) + E:F18/E:\$A18*(0.5*B:\$A15/B:F15*E46 + 0.5*B:\$A8/B:F8*E39 + 3*B:\$A7/B:F7*E38)
 F:F28: (F4) + E:G18/E:\$A18*(0.5*B:\$A15/B:G15*F46 + 0.5*B:\$A8/B:G8*F39 + 3*B:\$A7/B:G7*F38)
 F:G28: (F4) + E:H18/E:\$A18*(0.5*B:\$A15/B:H15*G46 + 0.5*B:\$A8/B:H8*G39 + 3*B:\$A7/B:H7*G38)

F:H28: (F4) + E:I18/E:\$A18*(0.5*B:\$A15/B:I15*H46 + 0.5*B:\$A8/B:I8*H39 + 3*B:\$A7/B:I7*H38)
 F:A29: ^ ilmenite
 F:B29: (F4) + E:C19/E:\$A19*(B:\$A9/B:C9*B40 + B:\$A11/B:C11*B42)
 F:C29: (F4) + E:D19/E:\$A19*(B:\$A9/B:D9*C40 + B:\$A11/B:D11*C42)
 F:D29: (F4) + E:E19/E:\$A19*(B:\$A9/B:E9*D40 + B:\$A11/B:E11*D42)
 F:E29: (F4) + E:F19/E:\$A19*(B:\$A9/B:F9*E40 + B:\$A11/B:F11*E42)
 F:F29: (F4) + E:G19/E:\$A19*(B:\$A9/B:G9*F40 + B:\$A11/B:G11*F42)
 F:G29: (F4) + E:H19/E:\$A19*(B:\$A9/B:H9*G40 + B:\$A11/B:H11*G42)
 F:H29: (F4) + E:I19/E:\$A19*(B:\$A9/B:I9*H40 + B:\$A11/B:I11*H42)
 F:A30: (F3) ^ rutile
 F:B30: (F4) + E:C20/E:\$A20*B:\$A9/B:C9*B40
 F:C30: (F4) + E:D20/E:\$A20*B:\$A9/B:D9*C40
 F:D30: (F4) + E:E20/E:\$A20*B:\$A9/B:E9*D40
 F:E30: (F4) + E:F20/E:\$A20*B:\$A9/B:F9*E40
 F:F30: (F4) + E:G20/E:\$A20*B:\$A9/B:G9*F40
 F:G30: (F4) + E:H20/E:\$A20*B:\$A9/B:H9*G40
 F:H30: (F4) + E:I20/E:\$A20*B:\$A9/B:I9*H40
 F:A31: ^ Kaol
 F:B31: (F4) + E:C21/E:\$A21*(B:\$A8/B:C8*B39 + 2*B:\$A7/B:C7*B38 + 2*B:\$A18/B:C18*B49)
 F:C31: (F4) + E:D21/E:\$A21*(B:\$A8/B:D8*C39 + 2*B:\$A7/B:D7*C38 + 2*B:\$A18/B:D18*C49)
 F:D31: (F4) + E:E21/E:\$A21*(B:\$A8/B:E8*D39 + 2*B:\$A7/B:E7*D38 + 2*B:\$A18/B:E18*D49)
 F:E31: (F4) + E:F21/E:\$A21*(B:\$A8/B:F8*E39 + 2*B:\$A7/B:F7*E38 + 2*B:\$A18/B:F18*E49)
 F:F31: (F4) + E:G21/E:\$A21*(B:\$A8/B:G8*F39 + 2*B:\$A7/B:G7*F38 + 2*B:\$A18/B:G18*F49)
 F:G31: (F4) + E:H21/E:\$A21*(B:\$A8/B:H8*G39 + 2*B:\$A7/B:H7*G38 + 2*B:\$A18/B:H18*G49)
 F:H31: (F4) + E:I21/E:\$A21*(B:\$A8/B:I8*H39 + 2*B:\$A7/B:I7*H38 + 2*B:\$A18/B:I18*H49)
 F:A32: ^ qtz
 F:B32: (F4) + E:C22/B:C7*B38
 F:C32: (F4) + E:D22/B:D7*C38
 F:D32: (F4) + E:E22/B:E7*D38
 F:E32: (F4) + E:F22/B:F7*E38

F:F32: (F4) + E:G22/B:G7*F38
 F:G32: (F4) + E:H22/B:H7*G38
 F:H32: (F4) + E:I22/B:I7*H38
 F:A33: ^ Mn-carb
 F:B33: (F4) + E:C23/E:\$A23*(B:\$A12/B:C12*B43 + B:\$A19/B:C19*B50)
 F:C33: (F4) + E:D23/E:\$A23*(B:\$A12/B:D12*C43 + B:\$A19/B:D19*C50)
 F:D33: (F4) + E:E23/E:\$A23*(B:\$A12/B:E12*D43 + B:\$A19/B:E19*D50)
 F:E33: (F4) + E:F23/E:\$A23*(B:\$A12/B:F12*E43 + B:\$A19/B:F19*E50)
 F:F33: (F4) + E:G23/E:\$A23*(B:\$A12/B:G12*F43 + B:\$A19/B:G19*F50)
 F:G33: (F4) + E:H23/E:\$A23*(B:\$A12/B:H12*G43 + B:\$A19/B:H19*G50)
 F:H33: (F4) + E:I23/E:\$A23*(B:\$A12/B:I12*H43 + B:\$A19/B:I19*H50)
 F:A34: ^ apatite
 F:B34: (F4) + E:C24/E:\$A24*(5*B:\$A14/B:C14*B45 + 1.5*B:\$A17/B:C17*B48 + 0.5*B:\$A18/B:C18*B49)
 F:C34: (F4) + E:D24/E:\$A24*(5*B:\$A14/B:D14*C45 + 1.5*B:\$A17/B:D17*C48 + 0.5*B:\$A18/B:D18*C49)
 F:D34: (F4) + E:E24/E:\$A24*(5*B:\$A14/B:E14*D45 + 1.5*B:\$A17/B:E17*D48 + 0.5*B:\$A18/B:E18*D49)
 F:E34: (F4) + E:F24/E:\$A24*(5*B:\$A14/B:F14*E45 + 1.5*B:\$A17/B:F17*E48 + 0.5*B:\$A18/B:F18*E49)
 F:F34: (F4) + E:G24/E:\$A24*(5*B:\$A14/B:G14*F45 + 1.5*B:\$A17/B:G17*F48 + 0.5*B:\$A18/B:G18*F49)
 F:G34: (F4) + E:H24/E:\$A24*(5*B:\$A14/B:H14*G45 + 1.5*B:\$A17/B:H17*G48 + 0.5*B:\$A18/B:H18*G49)
 F:H34: (F4) + E:I24/E:\$A24*(5*B:\$A14/B:I14*H45 + 1.5*B:\$A17/B:I17*H48 + 0.5*B:\$A18/B:I18*H49)
 F:A35: ^ pyrite
 F:B35: (F4) + E:C25/E:\$A25*(B:\$A11/B:C11*B42 + 2*B:\$A20/(B:C20*10000)*B51)
 F:C35: (F4) + E:D25/E:\$A25*(B:\$A11/B:D11*C42 + 2*B:\$A20/(B:D20*10000)*C51)
 F:D35: (F4) + E:E25/E:\$A25*(B:\$A11/B:E11*D42 + 2*B:\$A20/(B:E20*10000)*D51)
 F:E35: (F4) + E:F25/E:\$A25*(B:\$A11/B:F11*E42 + 2*B:\$A20/(B:F20*10000)*E51)
 F:F35: (F4) + E:G25/E:\$A25*(B:\$A11/B:G11*F42 + 2*B:\$A20/(B:G20*10000)*F51)
 F:G35: (F4) + E:H25/E:\$A25*(B:\$A11/B:H11*G42 + 2*B:\$A20/(B:H20*10000)*G51)
 F:H35: (F4) + E:I25/E:\$A25*(B:\$A11/B:I11*H42 + 2*B:\$A20/(B:I20*10000)*H51)
 F:A36: ^ hematite
 F:B36: (F4) + E:C26/B:C10*B41
 F:C36: (F4) + E:D26/B:D10*C41

F:D36: (F4) + E:E26/B:E10*D41
 F:E36: (F4) + E:F26/B:F10*E41
 F:F36: (F4) + E:G26/B:G10*F41
 F:G36: (F4) + E:H26/B:H10*G41
 F:H36: (F4) + E:I26/B:I10*H41
 F:A37: ^ magnetite
 F:B37: (F4) + E:C27/E:\$A27*(B:\$A10/B:C10*B41+B:\$A11/B:C11*B42)
 F:C37: (F4) + E:D27/E:\$A27*(B:\$A10/B:D10*C41+B:\$A11/B:D11*C42)
 F:D37: (F4) + E:E27/E:\$A27*(B:\$A10/B:E10*D41+B:\$A11/B:E11*D42)
 F:E37: (F4) + E:F27/E:\$A27*(B:\$A10/B:F10*E41+B:\$A11/B:F11*E42)
 F:F37: (F4) + E:G27/E:\$A27*(B:\$A10/B:G10*F41+B:\$A11/B:G11*F42)
 F:G37: (F4) + E:H27/E:\$A27*(B:\$A10/B:H10*G41+B:\$A11/B:H11*G42)
 F:H37: (F4) + E:I27/E:\$A27*(B:\$A10/B:I10*H41+B:\$A11/B:I11*H42)

F:A38: 'Sc_SiO2
 F:B38: (F3) + \$B4 + B:C7*\$C4
 F:C38: (F3) + \$B4 + B:D7*\$C4
 F:D38: (F3) + \$B4 + B:E7*\$C4
 F:E38: (F3) + \$B4 + B:F7*\$C4
 F:F38: (F3) + \$B4 + B:G7*\$C4
 F:G38: (F3) + \$B4 + B:H7*\$C4
 F:H38: (F3) + \$B4 + B:I7*\$C4
 F:A39: 'Sc_Al2O3
 F:B39: (F3) + \$B5 + B:C8*\$C5
 F:C39: (F3) + \$B5 + B:D8*\$C5
 F:D39: (F3) + \$B5 + B:E8*\$C5
 F:E39: (F3) + \$B5 + B:F8*\$C5
 F:F39: (F3) + \$B5 + B:G8*\$C5
 F:G39: (F3) + \$B5 + B:H8*\$C5
 F:H39: (F3) + \$B5 + B:I8*\$C5
 F:A40: 'Sc_TiO2
 F:B40: (F3) + \$B6 + B:C9*\$C6
 F:C40: (F3) + \$B6 + B:D9*\$C6
 F:D40: (F3) + \$B6 + B:E9*\$C6
 F:E40: (F3) + \$B6 + B:F9*\$C6
 F:F40: (F3) + \$B6 + B:G9*\$C6
 F:G40: (F3) + \$B6 + B:H9*\$C6
 F:H40: (F3) + \$B6 + B:I9*\$C6
 F:A41: 'Sc_Fe2O3
 F:B41: (F3) + \$B7 + B:C10*\$C7
 F:C41: (F3) + \$B7 + B:D10*\$C7
 F:D41: (F3) + \$B7 + B:E10*\$C7
 F:E41: (F3) + \$B7 + B:F10*\$C7
 F:F41: (F3) + \$B7 + B:G10*\$C7
 F:G41: (F3) + \$B7 + B:H10*\$C7
 F:H41: (F3) + \$B7 + B:I10*\$C7
 F:A42: 'Sc_FeO
 F:B42: (F3) + \$B8 + B:C11*\$C8
 F:C42: (F3) + \$B8 + B:D11*\$C8
 F:D42: (F3) + \$B8 + B:E11*\$C8
 F:E42: (F3) + \$B8 + B:F11*\$C8
 F:F42: (F3) + \$B8 + B:G11*\$C8
 F:G42: (F3) + \$B8 + B:H11*\$C8
 F:H42: (F3) + \$B8 + B:I11*\$C8
 F:A43: 'Sc_MnO
 F:B43: (F3) + \$B9 + B:C12*\$C9
 F:C43: (F3) + \$B9 + B:D12*\$C9
 F:D43: (F3) + \$B9 + B:E12*\$C9
 F:E43: (F3) + \$B9 + B:F12*\$C9
 F:F43: (F3) + \$B9 + B:G12*\$C9
 F:G43: (F3) + \$B9 + B:H12*\$C9
 F:H43: (F3) + \$B9 + B:I12*\$C9
 F:A44: 'Sc_MgO
 F:B44: (F3) + \$B10 + B:C13*\$C10
 F:C44: (F3) + \$B10 + B:D13*\$C10
 F:D44: (F3) + \$B10 + B:E13*\$C10
 F:E44: (F3) + \$B10 + B:F13*\$C10
 F:F44: (F3) + \$B10 + B:G13*\$C10
 F:G44: (F3) + \$B10 + B:H13*\$C10
 F:H44: (F3) + \$B10 + B:I13*\$C10
 F:A45: 'Sc_CaO
 F:B45: (F3) + \$B11 + B:C14*\$C11
 F:C45: (F3) + \$B11 + B:D14*\$C11
 F:D45: (F3) + \$B11 + B:E14*\$C11
 F:E45: (F3) + \$B11 + B:F14*\$C11
 F:F45: (F3) + \$B11 + B:G14*\$C11
 F:G45: (F3) + \$B11 + B:H14*\$C11
 F:H45: (F3) + \$B11 + B:I14*\$C11
 F:A46: 'Sc_Na2O
 F:B46: (F3) + \$B12 + B:C15*\$C12
 F:C46: (F3) + \$B12 + B:D15*\$C12
 F:D46: (F3) + \$B12 + B:E15*\$C12
 F:E46: (F3) + \$B12 + B:F15*\$C12
 F:F46: (F3) + \$B12 + B:G15*\$C12
 F:G46: (F3) + \$B12 + B:H15*\$C12
 F:H46: (F3) + \$B12 + B:I15*\$C12

F:A47: 'Sc_K2O	F:A50: 'Sc_CO2
F:B47: (F3) + \$G4+B:C16*\$H4	F:B50: (F3) + \$G7+B:C19*\$H7
F:C47: (F3) + \$G4+B:D16*\$H4	F:C50: (F3) + \$G7+B:D19*\$H7
F:D47: (F3) + \$G4+B:E16*\$H4	F:D50: (F3) + \$G7+B:E19*\$H7
F:E47: (F3) + \$G4+B:F16*\$H4	F:E50: (F3) + \$G7+B:F19*\$H7
F:F47: (F3) + \$G4+B:G16*\$H4	F:F50: (F3) + \$G7+B:G19*\$H7
F:G47: (F3) + \$G4+B:H16*\$H4	F:G50: (F3) + \$G7+B:H19*\$H7
F:H47: (F3) + \$G4+B:I16*\$H4	F:H50: (F3) + \$G7+B:I19*\$H7
F:A48: 'Sc_P2O5	F:A51: 'Sc_S
F:B48: (F3) + \$G5+B:C17*\$H5	F:B51: (F3) + \$G8+B:C20*\$H8
F:C48: (F3) + \$G5+B:D17*\$H5	F:C51: (F3) + \$G8+B:D20*\$H8
F:D48: (F3) + \$G5+B:E17*\$H5	F:D51: (F3) + \$G8+B:E20*\$H8
F:E48: (F3) + \$G5+B:F17*\$H5	F:E51: (F3) + \$G8+B:F20*\$H8
F:F48: (F3) + \$G5+B:G17*\$H5	F:F51: (F3) + \$G8+B:G20*\$H8
F:G48: (F3) + \$G5+B:H17*\$H5	F:G51: (F3) + \$G8+B:H20*\$H8
F:H48: (F3) + \$G5+B:I17*\$H5	F:H51: (F3) + \$G8+B:I20*\$H8
F:A49: 'Sc_H2O	F:A52: 'Sc_Zr
F:B49: (F3) + \$G6+B:C18*\$H6	F:B52: (F3) + \$G9+B:C23*\$H9
F:C49: (F3) + \$G6+B:D18*\$H6	F:C52: (F3) + \$G9+B:D23*\$H9
F:D49: (F3) + \$G6+B:E18*\$H6	F:D52: (F3) + \$G9+B:E23*\$H9
F:E49: (F3) + \$G6+B:F18*\$H6	F:E52: (F3) + \$G9+B:F23*\$H9
F:F49: (F3) + \$G6+B:G18*\$H6	F:F52: (F3) + \$G9+B:G23*\$H9
F:G49: (F3) + \$G6+B:H18*\$H6	F:G52: (F3) + \$G9+B:H23*\$H9
F:H49: (F3) + \$G6+B:I18*\$H6	F:H52: (F3) + \$G9+B:I23*\$H9

F:A54: 'Table 7- .

F:B54: 'Error propagation of norms corrected for closure in gram(SD at 68% confidence level)

F:B55: ' at northern segment of No.3 vein, Silver Queen mine, Owen Lake, central BC

F:A56: 'Sample_id

F:B56: ^ x4-4

F:C56: ^ x3-7

F:D56: ^ x3-5

F:E56: ^ x3-4

F:F56: ^ x3-1

F:G56: ^ x3-3d

F:H56: ^ x2-5

F:A57: ^ Calcite

F:B57: (F3) @ SQRT(+ E:C5 ^ 2/B:C\$9 ^ 2*\$B\$40 ^ 2 + B:\$C\$9 ^ 2*E:C5 ^ 2/B:C\$9 ^ 4*B40 ^ 2 + B:\$C\$9 ^ 2/B:C\$9 ^ 2*B15 ^ 2)

F:C57: (F3) @ SQRT(+ E:D5 ^ 2/B:D\$9 ^ 2*\$B\$40 ^ 2 + B:\$C\$9 ^ 2*E:D5 ^ 2/B:D\$9 ^ 4*C40 ^ 2 + B:\$C\$9 ^ 2/B:D\$9 ^ 2*C15 ^ 2)

F:D57: (F3) @ SQRT(+ E:E5 ^ 2/B:E\$9 ^ 2*\$B\$40 ^ 2 + B:\$C\$9 ^ 2*E:E5 ^ 2/B:E\$9 ^ 4*D40 ^ 2 + B:\$C\$9 ^ 2/B:E\$9 ^ 2*D15 ^ 2)

F:E57: (F3) @ SQRT(+ E:F5 ^ 2/B:F\$9 ^ 2*\$B\$40 ^ 2 + B:\$C\$9 ^ 2*E:F5 ^ 2/B:F\$9 ^ 4*E40 ^ 2 + B:\$C\$9 ^ 2/B:F\$9 ^ 2*E15 ^ 2)

F:F57: (F3) @ SQRT(+ E:G5 ^ 2/B:G\$9 ^ 2*\$B\$40 ^ 2 + B:\$C\$9 ^ 2*E:G5 ^ 2/B:G\$9 ^ 4*F40 ^ 2 + B:\$C\$9 ^ 2/B:G\$9 ^ 2*F15 ^ 2)

F:G57: (F3) @ SQRT(+ E:H5 ^ 2/B:H\$9 ^ 2*\$B\$40 ^ 2 + B:\$C\$9 ^ 2*E:H5 ^ 2/B:H\$9 ^ 4*G40 ^ 2 + B:\$C\$9 ^ 2/B:H\$9 ^ 2*G15 ^ 2)

F:H57: (F3) @ SQRT(+ E:I5 ^ 2/B:I\$9 ^ 2*\$B\$40 ^ 2 + B:\$C\$9 ^ 2*E:I5 ^ 2/B:I\$9 ^ 4*H40 ^ 2 + B:\$C\$9 ^ 2/B:I\$9 ^ 2*H15 ^ 2)

F:A58: ^ Epidote

F:B58: (F3) @ SQRT(+ E:C6 ^ 2/B:C\$9 ^ 2*\$B\$40 ^ 2 + B:\$C\$9 ^ 2*E:C6 ^ 2/B:C\$9 ^ 4*B\$40 ^ 2 + B:\$C\$9 ^ 2/B:C\$9 ^ 2*B16 ^ 2)

F:C58: (F3) @ SQRT(+ E:D6 ^ 2/B:D\$9 ^ 2*\$B\$40 ^ 2 + B:\$C\$9 ^ 2*E:D6 ^ 2/B:D\$9 ^ 4*C\$40 ^ 2 + B:\$C\$9 ^ 2/B:D\$9 ^ 2*C16 ^ 2)

F:D58: (F3) @ SQRT(+ E:E6 ^ 2/B:E\$9 ^ 2*\$B\$40 ^ 2 + B:\$C\$9 ^ 2*E:E6 ^ 2/B:E\$9 ^ 4*D\$40 ^ 2 + B:\$C\$9 ^ 2/B:E\$9 ^ 2*D16 ^ 2)

F:E58: (F3) @ SQRT(+ E:F6 ^ 2/B:F\$9 ^ 2*\$B\$40 ^ 2 + B:\$C\$9 ^ 2*E:F6 ^ 2/B:F\$9 ^ 4*E\$40 ^ 2 + B:\$C\$9 ^ 2/B:F\$9 ^ 2*E16 ^ 2)

F:F58: (F3) @ SQRT(+ E:G6 ^ 2/B:G\$9 ^ 2*\$B\$40 ^ 2 + B:\$C\$9 ^ 2*E:G6 ^ 2/B:G\$9 ^ 4*F\$40 ^ 2 + B:\$C\$9 ^ 2/B:G\$9 ^ 2*F16 ^ 2)

F:G58: (F3) @ SQRT(+ E:H6 ^ 2/B:H\$9 ^ 2*\$B\$40 ^ 2 + B:\$C\$9 ^ 2*E:H6 ^ 2/B:H\$9 ^ 4*G\$40 ^ 2 + B:\$C\$9 ^ 2/B:H\$9 ^ 2*G16 ^ 2)

F:H58: (F3) @ SQRT(+ E:I6 ^ 2/B:I\$9 ^ 2*\$B\$40 ^ 2 + B:\$C\$9 ^ 2*E:I6 ^ 2/B:I\$9 ^ 4*H\$40 ^ 2 + B:\$C\$9 ^ 2/B:I\$9 ^ 2*H16 ^ 2)

F:A59: ^ Ca-pyx

F:B59: (F3) @ SQRT(+ E:C7 ^ 2/B:C\$9 ^ 2*\$B\$40 ^ 2 + B:\$C\$9 ^ 2*E:C7 ^ 2/B:C\$9 ^ 4*B\$40 ^ 2 + B:\$C\$9 ^ 2/B:C\$9 ^ 2*B17 ^ 2)

F:C59: (F3) @ SQRT(+ E:D7 ^ 2/B:D\$9 ^ 2*\$B\$40 ^ 2 + B:\$C\$9 ^ 2*E:D7 ^ 2/B:D\$9 ^ 4*C\$40 ^ 2 + B:\$C\$9 ^ 2/B:D\$9 ^ 2*C17 ^ 2)

F:D59: (F3) @SQRT(+E:E7^2/B:ES9^2*\$B\$40^2+B:\$C\$9^2*E:E7^2/B:ES9^4*D\$40^2+B:\$C\$9^2/B:ES9^2*D17^2)
F:E59: (F3) @SQRT(+E:F7^2/B:FS9^2*\$B\$40^2+B:\$C\$9^2*E:F7^2/B:FS9^4*E\$40^2+B:\$C\$9^2/B:FS9^2*E17^2)
F:F59: (F3) @SQRT(+E:G7^2/B:GS9^2*\$B\$40^2+B:\$C\$9^2*E:G7^2/B:GS9^4*F\$40^2+B:\$C\$9^2/B:GS9^2*F17^2)
F:G59: (F3) @SQRT(+E:H7^2/B:HS9^2*\$B\$40^2+B:\$C\$9^2*E:H7^2/B:HS9^4*G\$40^2+B:\$C\$9^2/B:HS9^2*G17^2)
F:H59: (F3) @SQRT(+E:I7^2/B:IS9^2*\$B\$40^2+B:\$C\$9^2*E:I7^2/B:IS9^4*H\$40^2+B:\$C\$9^2/B:IS9^2*H17^2)
F:A60: ^An
F:B60: (F3) @SQRT(+E:C8^2/B:C\$9^2*\$B\$40^2+B:\$C\$9^2*E:C8^2/B:C\$9^4*B\$40^2+B:\$C\$9^2/B:C\$9^2*B18^2)
F:C60: (F3) @SQRT(+E:D8^2/B:D\$9^2*\$B\$40^2+B:\$C\$9^2*E:D8^2/B:D\$9^4*C\$40^2+B:\$C\$9^2/B:D\$9^2*C18^2)
F:D60: (F3) @SQRT(+E:E8^2/B:ES9^2*\$B\$40^2+B:\$C\$9^2*E:E8^2/B:ES9^4*D\$40^2+B:\$C\$9^2/B:ES9^2*D18^2)
F:E60: (F3) @SQRT(+E:F8^2/B:FS9^2*\$B\$40^2+B:\$C\$9^2*E:F8^2/B:FS9^4*E\$40^2+B:\$C\$9^2/B:FS9^2*E18^2)
F:F60: (F3) @SQRT(+E:G8^2/B:GS9^2*\$B\$40^2+B:\$C\$9^2*E:G8^2/B:GS9^4*F\$40^2+B:\$C\$9^2/B:GS9^2*F18^2)
F:G60: (F3) @SQRT(+E:H8^2/B:HS9^2*\$B\$40^2+B:\$C\$9^2*E:H8^2/B:HS9^4*G\$40^2+B:\$C\$9^2/B:HS9^2*G18^2)
F:H60: (F3) @SQRT(+E:I8^2/B:IS9^2*\$B\$40^2+B:\$C\$9^2*E:I8^2/B:IS9^4*H\$40^2+B:\$C\$9^2/B:IS9^2*H18^2)
F:A61: ^Mg-carb
F:B61: (F3) @SQRT(+E:C9^2/B:C\$9^2*\$B\$40^2+B:\$C\$9^2*E:C9^2/B:C\$9^4*B\$40^2+B:\$C\$9^2/B:C\$9^2*B19^2)
F:C61: (F3) @SQRT(+E:D9^2/B:D\$9^2*\$B\$40^2+B:\$C\$9^2*E:D9^2/B:D\$9^4*C\$40^2+B:\$C\$9^2/B:D\$9^2*C19^2)
F:D61: (F3) @SQRT(+E:E9^2/B:ES9^2*\$B\$40^2+B:\$C\$9^2*E:E9^2/B:ES9^4*D\$40^2+B:\$C\$9^2/B:ES9^2*D19^2)
F:E61: (F3) @SQRT(+E:F9^2/B:FS9^2*\$B\$40^2+B:\$C\$9^2*E:F9^2/B:FS9^4*E\$40^2+B:\$C\$9^2/B:FS9^2*E19^2)
F:F61: (F3) @SQRT(+E:G9^2/B:GS9^2*\$B\$40^2+B:\$C\$9^2*E:G9^2/B:GS9^4*F\$40^2+B:\$C\$9^2/B:GS9^2*F19^2)
F:G61: (F3) @SQRT(+E:H9^2/B:HS9^2*\$B\$40^2+B:\$C\$9^2*E:H9^2/B:HS9^4*G\$40^2+B:\$C\$9^2/B:HS9^2*G19^2)
F:H61: (F3) @SQRT(+E:I9^2/B:IS9^2*\$B\$40^2+B:\$C\$9^2*E:I9^2/B:IS9^4*H\$40^2+B:\$C\$9^2/B:IS9^2*H19^2)
F:A62: ^Mg-chl
F:B62: (F3) @SQRT(+E:C10^2/B:C\$9^2*\$B\$40^2+B:\$C\$9^2*E:C10^2/B:C\$9^4*B\$40^2+B:\$C\$9^2/B:C\$9^2*B20^2)
F:C62: (F3) @SQRT(+E:D10^2/B:D\$9^2*\$B\$40^2+B:\$C\$9^2*E:D10^2/B:D\$9^4*C\$40^2+B:\$C\$9^2/B:D\$9^2*C20^2)
F:D62: (F3) @SQRT(+E:E10^2/B:ES9^2*\$B\$40^2+B:\$C\$9^2*E:E10^2/B:ES9^4*D\$40^2+B:\$C\$9^2/B:ES9^2*D20^2)
F:E62: (F3) @SQRT(+E:F10^2/B:FS9^2*\$B\$40^2+B:\$C\$9^2*E:F10^2/B:FS9^4*E\$40^2+B:\$C\$9^2/B:FS9^2*E20^2)
F:F62: (F3) @SQRT(+E:G10^2/B:GS9^2*\$B\$40^2+B:\$C\$9^2*E:G10^2/B:GS9^4*F\$40^2+B:\$C\$9^2/B:GS9^2*F20^2)
F:G62: (F3) @SQRT(+E:H10^2/B:HS9^2*\$B\$40^2+B:\$C\$9^2*E:H10^2/B:HS9^4*G\$40^2+B:\$C\$9^2/B:HS9^2*G20^2)
F:H62: (F3) @SQRT(+E:I10^2/B:IS9^2*\$B\$40^2+B:\$C\$9^2*E:I10^2/B:IS9^4*H\$40^2+B:\$C\$9^2/B:IS9^2*H20^2)
F:A63: ^Mg-pyx

F:B63: (F3) @SQRT(+E:C11 ^ 2/B:C\$9 ^ 2*\$B\$40 ^ 2 + B:\$C\$9 ^ 2*E:C11 ^ 2/B:C\$9 ^ 4*B\$40 ^ 2 + B:\$C\$9 ^ 2/B:C\$9 ^ 2*B21 ^ 2)
 F:C63: (F3) @SQRT(+E:D11 ^ 2/B:D\$9 ^ 2*\$B\$40 ^ 2 + B:\$C\$9 ^ 2*E:D11 ^ 2/B:D\$9 ^ 4*C\$40 ^ 2 + B:\$C\$9 ^ 2/B:D\$9 ^ 2*C21 ^ 2)
 F:D63: (F3) @SQRT(+E:E11 ^ 2/B:E\$9 ^ 2*\$B\$40 ^ 2 + B:\$C\$9 ^ 2*E:E11 ^ 2/B:E\$9 ^ 4*D\$40 ^ 2 + B:\$C\$9 ^ 2/B:E\$9 ^ 2*D21 ^ 2)
 F:E63: (F3) @SQRT(+E:F11 ^ 2/B:F\$9 ^ 2*\$B\$40 ^ 2 + B:\$C\$9 ^ 2*E:F11 ^ 2/B:F\$9 ^ 4*E\$40 ^ 2 + B:\$C\$9 ^ 2/B:F\$9 ^ 2*E21 ^ 2)
 F:F63: (F3) @SQRT(+E:G11 ^ 2/B:G\$9 ^ 2*\$B\$40 ^ 2 + B:\$C\$9 ^ 2*E:G11 ^ 2/B:G\$9 ^ 4*F\$40 ^ 2 + B:\$C\$9 ^ 2/B:G\$9 ^ 2*F21 ^ 2)
 F:G63: (F3) @SQRT(+E:H11 ^ 2/B:H\$9 ^ 2*\$B\$40 ^ 2 + B:\$C\$9 ^ 2*E:H11 ^ 2/B:H\$9 ^ 4*G\$40 ^ 2 + B:\$C\$9 ^ 2/B:H\$9 ^ 2*G21 ^ 2)
 F:H63: (F3) @SQRT(+E:I11 ^ 2/B:I\$9 ^ 2*\$B\$40 ^ 2 + B:\$C\$9 ^ 2*E:I11 ^ 2/B:I\$9 ^ 4*H\$40 ^ 2 + B:\$C\$9 ^ 2/B:I\$9 ^ 2*H21 ^ 2)
 F:A64: ^ Fe-carb
 F:B64: (F3) @SQRT(+E:C12 ^ 2/B:C\$9 ^ 2*\$B\$40 ^ 2 + B:\$C\$9 ^ 2*E:C12 ^ 2/B:C\$9 ^ 4*B\$40 ^ 2 + B:\$C\$9 ^ 2/B:C\$9 ^ 2*B22 ^ 2)
 F:C64: (F3) @SQRT(+E:D12 ^ 2/B:D\$9 ^ 2*\$B\$40 ^ 2 + B:\$C\$9 ^ 2*E:D12 ^ 2/B:D\$9 ^ 4*C\$40 ^ 2 + B:\$C\$9 ^ 2/B:D\$9 ^ 2*C22 ^ 2)
 F:D64: (F3) @SQRT(+E:E12 ^ 2/B:E\$9 ^ 2*\$B\$40 ^ 2 + B:\$C\$9 ^ 2*E:E12 ^ 2/B:E\$9 ^ 4*D\$40 ^ 2 + B:\$C\$9 ^ 2/B:E\$9 ^ 2*D22 ^ 2)
 F:E64: (F3) @SQRT(+E:F12 ^ 2/B:F\$9 ^ 2*\$B\$40 ^ 2 + B:\$C\$9 ^ 2*E:F12 ^ 2/B:F\$9 ^ 4*E\$40 ^ 2 + B:\$C\$9 ^ 2/B:F\$9 ^ 2*E22 ^ 2)
 F:F64: (F3) @SQRT(+E:G12 ^ 2/B:G\$9 ^ 2*\$B\$40 ^ 2 + B:\$C\$9 ^ 2*E:G12 ^ 2/B:G\$9 ^ 4*F\$40 ^ 2 + B:\$C\$9 ^ 2/B:G\$9 ^ 2*F22 ^ 2)
 F:G64: (F3) @SQRT(+E:H12 ^ 2/B:H\$9 ^ 2*\$B\$40 ^ 2 + B:\$C\$9 ^ 2*E:H12 ^ 2/B:H\$9 ^ 4*G\$40 ^ 2 + B:\$C\$9 ^ 2/B:H\$9 ^ 2*G22 ^ 2)
 F:H64: (F3) @SQRT(+E:I12 ^ 2/B:I\$9 ^ 2*\$B\$40 ^ 2 + B:\$C\$9 ^ 2*E:I12 ^ 2/B:I\$9 ^ 4*H\$40 ^ 2 + B:\$C\$9 ^ 2/B:I\$9 ^ 2*H22 ^ 2)
 F:A65: ^ Fe-chl
 F:B65: (F3) @SQRT(+E:C13 ^ 2/B:C\$9 ^ 2*\$B\$40 ^ 2 + B:\$C\$9 ^ 2*E:C13 ^ 2/B:C\$9 ^ 4*B\$40 ^ 2 + B:\$C\$9 ^ 2/B:C\$9 ^ 2*B23 ^ 2)
 F:C65: (F3) @SQRT(+E:D13 ^ 2/B:D\$9 ^ 2*\$B\$40 ^ 2 + B:\$C\$9 ^ 2*E:D13 ^ 2/B:D\$9 ^ 4*C\$40 ^ 2 + B:\$C\$9 ^ 2/B:D\$9 ^ 2*C23 ^ 2)
 F:D65: (F3) @SQRT(+E:E13 ^ 2/B:E\$9 ^ 2*\$B\$40 ^ 2 + B:\$C\$9 ^ 2*E:E13 ^ 2/B:E\$9 ^ 4*D\$40 ^ 2 + B:\$C\$9 ^ 2/B:E\$9 ^ 2*D23 ^ 2)
 F:E65: (F3) @SQRT(+E:F13 ^ 2/B:F\$9 ^ 2*\$B\$40 ^ 2 + B:\$C\$9 ^ 2*E:F13 ^ 2/B:F\$9 ^ 4*E\$40 ^ 2 + B:\$C\$9 ^ 2/B:F\$9 ^ 2*E23 ^ 2)
 F:F65: (F3) @SQRT(+E:G13 ^ 2/B:G\$9 ^ 2*\$B\$40 ^ 2 + B:\$C\$9 ^ 2*E:G13 ^ 2/B:G\$9 ^ 4*F\$40 ^ 2 + B:\$C\$9 ^ 2/B:G\$9 ^ 2*F23 ^ 2)
 F:G65: (F3) @SQRT(+E:H13 ^ 2/B:H\$9 ^ 2*\$B\$40 ^ 2 + B:\$C\$9 ^ 2*E:H13 ^ 2/B:H\$9 ^ 4*G\$40 ^ 2 + B:\$C\$9 ^ 2/B:H\$9 ^ 2*G23 ^ 2)
 F:H65: (F3) @SQRT(+E:I13 ^ 2/B:I\$9 ^ 2*\$B\$40 ^ 2 + B:\$C\$9 ^ 2*E:I13 ^ 2/B:I\$9 ^ 4*H\$40 ^ 2 + B:\$C\$9 ^ 2/B:I\$9 ^ 2*H23 ^ 2)
 F:A66: ^ Fe-pyx
 F:B66: (F3) @SQRT(+E:C14 ^ 2/B:C\$9 ^ 2*\$B\$40 ^ 2 + B:\$C\$9 ^ 2*E:C14 ^ 2/B:C\$9 ^ 4*B\$40 ^ 2 + B:\$C\$9 ^ 2/B:C\$9 ^ 2*B24 ^ 2)
 F:C66: (F3) @SQRT(+E:D14 ^ 2/B:D\$9 ^ 2*\$B\$40 ^ 2 + B:\$C\$9 ^ 2*E:D14 ^ 2/B:D\$9 ^ 4*C\$40 ^ 2 + B:\$C\$9 ^ 2/B:D\$9 ^ 2*C24 ^ 2)
 F:D66: (F3) @SQRT(+E:E14 ^ 2/B:E\$9 ^ 2*\$B\$40 ^ 2 + B:\$C\$9 ^ 2*E:E14 ^ 2/B:E\$9 ^ 4*D\$40 ^ 2 + B:\$C\$9 ^ 2/B:E\$9 ^ 2*D24 ^ 2)
 F:E66: (F3) @SQRT(+E:F14 ^ 2/B:F\$9 ^ 2*\$B\$40 ^ 2 + B:\$C\$9 ^ 2*E:F14 ^ 2/B:F\$9 ^ 4*E\$40 ^ 2 + B:\$C\$9 ^ 2/B:F\$9 ^ 2*E24 ^ 2)
 F:F66: (F3) @SQRT(+E:G14 ^ 2/B:G\$9 ^ 2*\$B\$40 ^ 2 + B:\$C\$9 ^ 2*E:G14 ^ 2/B:G\$9 ^ 4*F\$40 ^ 2 + B:\$C\$9 ^ 2/B:G\$9 ^ 2*F24 ^ 2)
 F:G66: (F3) @SQRT(+E:H14 ^ 2/B:H\$9 ^ 2*\$B\$40 ^ 2 + B:\$C\$9 ^ 2*E:H14 ^ 2/B:H\$9 ^ 4*G\$40 ^ 2 + B:\$C\$9 ^ 2/B:H\$9 ^ 2*G24 ^ 2)

F:H66: (F3) @ SQRT(+E:I14 ^ 2/B:I\$9 ^ 2*\$B\$40 ^ 2 + B:\$C\$9 ^ 2*E:I14 ^ 2/B:I\$9 ^ 4*H\$40 ^ 2 + B:\$C\$9 ^ 2/B:I\$9 ^ 2*H24 ^ 2)
 F:A67: ^ Muscovite
 F:B67: (F3) @ SQRT(+E:C15 ^ 2/B:C\$9 ^ 2*\$B\$40 ^ 2 + B:\$C\$9 ^ 2*E:C15 ^ 2/B:C\$9 ^ 4*B\$40 ^ 2 + B:\$C\$9 ^ 2/B:B:C\$9 ^ 2*B25 ^ 2)
 F:C67: (F3) @ SQRT(+E:D15 ^ 2/B:D\$9 ^ 2*\$B\$40 ^ 2 + B:\$C\$9 ^ 2*E:D15 ^ 2/B:D\$9 ^ 4*C\$40 ^ 2 + B:\$C\$9 ^ 2/B:B:D\$9 ^ 2*C25 ^ 2)
 F:D67: (F3) @ SQRT(+E:E15 ^ 2/B:E\$9 ^ 2*\$B\$40 ^ 2 + B:\$C\$9 ^ 2*E:E15 ^ 2/B:E\$9 ^ 4*D\$40 ^ 2 + B:\$C\$9 ^ 2/B:B:E\$9 ^ 2*D25 ^ 2)
 F:E67: (F3) @ SQRT(+E:F15 ^ 2/B:F\$9 ^ 2*\$B\$40 ^ 2 + B:\$C\$9 ^ 2*E:F15 ^ 2/B:F\$9 ^ 4*E\$40 ^ 2 + B:\$C\$9 ^ 2/B:B:F\$9 ^ 2*E25 ^ 2)
 F:F67: (F3) @ SQRT(+E:G15 ^ 2/B:G\$9 ^ 2*\$B\$40 ^ 2 + B:\$C\$9 ^ 2*E:G15 ^ 2/B:G\$9 ^ 4*F\$40 ^ 2 + B:\$C\$9 ^ 2/B:B:G\$9 ^ 2*F25 ^ 2)
 F:G67: (F3) @ SQRT(+E:H15 ^ 2/B:H\$9 ^ 2*\$B\$40 ^ 2 + B:\$C\$9 ^ 2*E:H15 ^ 2/B:H\$9 ^ 4*G\$40 ^ 2 + B:\$C\$9 ^ 2/B:B:H\$9 ^ 2*G25 ^ 2)
 F:H67: (F3) @ SQRT(+E:I15 ^ 2/B:I\$9 ^ 2*\$B\$40 ^ 2 + B:\$C\$9 ^ 2*E:I15 ^ 2/B:I\$9 ^ 4*H\$40 ^ 2 + B:\$C\$9 ^ 2/B:B:I\$9 ^ 2*H25 ^ 2)
 F:A68: ^ Or
 F:B68: (F3) @ SQRT(+E:C16 ^ 2/B:C\$9 ^ 2*\$B\$40 ^ 2 + B:\$C\$9 ^ 2*E:C16 ^ 2/B:C\$9 ^ 4*B\$40 ^ 2 + B:\$C\$9 ^ 2/B:B:C\$9 ^ 2*B26 ^ 2)
 F:C68: (F3) @ SQRT(+E:D16 ^ 2/B:D\$9 ^ 2*\$B\$40 ^ 2 + B:\$C\$9 ^ 2*E:D16 ^ 2/B:D\$9 ^ 4*C\$40 ^ 2 + B:\$C\$9 ^ 2/B:B:D\$9 ^ 2*C26 ^ 2)
 F:D68: (F3) @ SQRT(+E:E16 ^ 2/B:E\$9 ^ 2*\$B\$40 ^ 2 + B:\$C\$9 ^ 2*E:E16 ^ 2/B:E\$9 ^ 4*D\$40 ^ 2 + B:\$C\$9 ^ 2/B:B:E\$9 ^ 2*D26 ^ 2)
 F:E68: (F3) @ SQRT(+E:F16 ^ 2/B:F\$9 ^ 2*\$B\$40 ^ 2 + B:\$C\$9 ^ 2*E:F16 ^ 2/B:F\$9 ^ 4*E\$40 ^ 2 + B:\$C\$9 ^ 2/B:B:F\$9 ^ 2*E26 ^ 2)
 F:F68: (F3) @ SQRT(+E:G16 ^ 2/B:G\$9 ^ 2*\$B\$40 ^ 2 + B:\$C\$9 ^ 2*E:G16 ^ 2/B:G\$9 ^ 4*F\$40 ^ 2 + B:\$C\$9 ^ 2/B:B:G\$9 ^ 2*F26 ^ 2)
 F:G68: (F3) @ SQRT(+E:H16 ^ 2/B:H\$9 ^ 2*\$B\$40 ^ 2 + B:\$C\$9 ^ 2*E:H16 ^ 2/B:H\$9 ^ 4*G\$40 ^ 2 + B:\$C\$9 ^ 2/B:B:H\$9 ^ 2*G26 ^ 2)
 F:H68: (F3) @ SQRT(+E:I16 ^ 2/B:I\$9 ^ 2*\$B\$40 ^ 2 + B:\$C\$9 ^ 2*E:I16 ^ 2/B:I\$9 ^ 4*H\$40 ^ 2 + B:\$C\$9 ^ 2/B:B:I\$9 ^ 2*H26 ^ 2)
 F:A69: ^ Na-mica
 F:B69: (F3) @ SQRT(+E:C17 ^ 2/B:C\$9 ^ 2*\$B\$40 ^ 2 + B:\$C\$9 ^ 2*E:C17 ^ 2/B:C\$9 ^ 4*B\$40 ^ 2 + B:\$C\$9 ^ 2/B:B:C\$9 ^ 2*B27 ^ 2)
 F:C69: (F3) @ SQRT(+E:D17 ^ 2/B:D\$9 ^ 2*\$B\$40 ^ 2 + B:\$C\$9 ^ 2*E:D17 ^ 2/B:D\$9 ^ 4*C\$40 ^ 2 + B:\$C\$9 ^ 2/B:B:D\$9 ^ 2*C27 ^ 2)
 F:D69: (F3) @ SQRT(+E:E17 ^ 2/B:E\$9 ^ 2*\$B\$40 ^ 2 + B:\$C\$9 ^ 2*E:E17 ^ 2/B:E\$9 ^ 4*D\$40 ^ 2 + B:\$C\$9 ^ 2/B:B:E\$9 ^ 2*D27 ^ 2)
 F:E69: (F3) @ SQRT(+E:F17 ^ 2/B:F\$9 ^ 2*\$B\$40 ^ 2 + B:\$C\$9 ^ 2*E:F17 ^ 2/B:F\$9 ^ 4*E\$40 ^ 2 + B:\$C\$9 ^ 2/B:B:F\$9 ^ 2*E27 ^ 2)
 F:F69: (F3) @ SQRT(+E:G17 ^ 2/B:G\$9 ^ 2*\$B\$40 ^ 2 + B:\$C\$9 ^ 2*E:G17 ^ 2/B:G\$9 ^ 4*F\$40 ^ 2 + B:\$C\$9 ^ 2/B:B:G\$9 ^ 2*F27 ^ 2)
 F:G69: (F3) @ SQRT(+E:H17 ^ 2/B:H\$9 ^ 2*\$B\$40 ^ 2 + B:\$C\$9 ^ 2*E:H17 ^ 2/B:H\$9 ^ 4*G\$40 ^ 2 + B:\$C\$9 ^ 2/B:B:H\$9 ^ 2*G27 ^ 2)
 F:H69: (F3) @ SQRT(+E:I17 ^ 2/B:I\$9 ^ 2*\$B\$40 ^ 2 + B:\$C\$9 ^ 2*E:I17 ^ 2/B:I\$9 ^ 4*H\$40 ^ 2 + B:\$C\$9 ^ 2/B:B:I\$9 ^ 2*H27 ^ 2)
 F:A70: ^ Ab
 F:B70: (F3) @ SQRT(+E:C18 ^ 2/B:C\$9 ^ 2*\$B\$40 ^ 2 + B:\$C\$9 ^ 2*E:C18 ^ 2/B:C\$9 ^ 4*B\$40 ^ 2 + B:\$C\$9 ^ 2/B:B:C\$9 ^ 2*B28 ^ 2)
 F:C70: (F3) @ SQRT(+E:D18 ^ 2/B:D\$9 ^ 2*\$B\$40 ^ 2 + B:\$C\$9 ^ 2*E:D18 ^ 2/B:D\$9 ^ 4*C\$40 ^ 2 + B:\$C\$9 ^ 2/B:B:D\$9 ^ 2*C28 ^ 2)
 F:D70: (F3) @ SQRT(+E:E18 ^ 2/B:E\$9 ^ 2*\$B\$40 ^ 2 + B:\$C\$9 ^ 2*E:E18 ^ 2/B:E\$9 ^ 4*D\$40 ^ 2 + B:\$C\$9 ^ 2/B:B:E\$9 ^ 2*D28 ^ 2)
 F:E70: (F3) @ SQRT(+E:F18 ^ 2/B:F\$9 ^ 2*\$B\$40 ^ 2 + B:\$C\$9 ^ 2*E:F18 ^ 2/B:F\$9 ^ 4*E\$40 ^ 2 + B:\$C\$9 ^ 2/B:B:F\$9 ^ 2*E28 ^ 2)

F:F70: (F3) @ Sqrt(+E:G18 ^ 2/B:G\$9 ^ 2*\$B\$40 ^ 2 + B:\$C\$9 ^ 2*E:G18 ^ 2/B:G\$9 ^ 4*F\$40 ^ 2 + B:\$C\$9 ^ 2/B:G\$9 ^ 2*F28 ^ 2)
 F:G70: (F3) @ Sqrt(+E:H18 ^ 2/B:H\$9 ^ 2*\$B\$40 ^ 2 + B:\$C\$9 ^ 2*E:H18 ^ 2/B:H\$9 ^ 4*G\$40 ^ 2 + B:\$C\$9 ^ 2/B:H\$9 ^ 2*G28 ^ 2)
 F:H70: (F3) @ Sqrt(+E:I18 ^ 2/B:I\$9 ^ 2*\$B\$40 ^ 2 + B:\$C\$9 ^ 2*E:I18 ^ 2/B:I\$9 ^ 4*H\$40 ^ 2 + B:\$C\$9 ^ 2/B:I\$9 ^ 2*H28 ^ 2)
 F:A71: ^ ilmenite
 F:B71: (F3) @ Sqrt(+E:C19 ^ 2/B:C\$9 ^ 2*\$B\$40 ^ 2 + B:\$C\$9 ^ 2*E:C19 ^ 2/B:C\$9 ^ 4*B\$40 ^ 2 + B:\$C\$9 ^ 2/B:C\$9 ^ 2*B29 ^ 2)
 F:C71: (F3) @ Sqrt(+E:D19 ^ 2/B:D\$9 ^ 2*\$B\$40 ^ 2 + B:\$C\$9 ^ 2*E:D19 ^ 2/B:D\$9 ^ 4*C\$40 ^ 2 + B:\$C\$9 ^ 2/B:D\$9 ^ 2*C29 ^ 2)
 F:D71: (F3) @ Sqrt(+E:E19 ^ 2/B:E\$9 ^ 2*\$B\$40 ^ 2 + B:\$C\$9 ^ 2*E:E19 ^ 2/B:E\$9 ^ 4*D\$40 ^ 2 + B:\$C\$9 ^ 2/B:E\$9 ^ 2*D29 ^ 2)
 F:E71: (F3) @ Sqrt(+E:F19 ^ 2/B:F\$9 ^ 2*\$B\$40 ^ 2 + B:\$C\$9 ^ 2*E:F19 ^ 2/B:F\$9 ^ 4*E\$40 ^ 2 + B:\$C\$9 ^ 2/B:F\$9 ^ 2*E29 ^ 2)
 F:F71: (F3) @ Sqrt(+E:G19 ^ 2/B:G\$9 ^ 2*\$B\$40 ^ 2 + B:\$C\$9 ^ 2*E:G19 ^ 2/B:G\$9 ^ 4*F\$40 ^ 2 + B:\$C\$9 ^ 2/B:G\$9 ^ 2*F29 ^ 2)
 F:G71: (F3) @ Sqrt(+E:H19 ^ 2/B:H\$9 ^ 2*\$B\$40 ^ 2 + B:\$C\$9 ^ 2*E:H19 ^ 2/B:H\$9 ^ 4*G\$40 ^ 2 + B:\$C\$9 ^ 2/B:H\$9 ^ 2*G29 ^ 2)
 F:H71: (F3) @ Sqrt(+E:I19 ^ 2/B:I\$9 ^ 2*\$B\$40 ^ 2 + B:\$C\$9 ^ 2*E:I19 ^ 2/B:I\$9 ^ 4*H\$40 ^ 2 + B:\$C\$9 ^ 2/B:I\$9 ^ 2*H29 ^ 2)
 F:A72: (F3) ^ rutile
 F:B72: (F3) @ Sqrt(+E:C20 ^ 2/B:C\$9 ^ 2*\$B\$40 ^ 2 + B:\$C\$9 ^ 2*E:C20 ^ 2/B:C\$9 ^ 4*B\$40 ^ 2 + B:\$C\$9 ^ 2/B:C\$9 ^ 2*B30 ^ 2)
 F:C72: (F3) @ Sqrt(+E:D20 ^ 2/B:D\$9 ^ 2*\$B\$40 ^ 2 + B:\$C\$9 ^ 2*E:D20 ^ 2/B:D\$9 ^ 4*C\$40 ^ 2 + B:\$C\$9 ^ 2/B:D\$9 ^ 2*C30 ^ 2)
 F:D72: (F3) @ Sqrt(+E:E20 ^ 2/B:E\$9 ^ 2*\$B\$40 ^ 2 + B:\$C\$9 ^ 2*E:E20 ^ 2/B:E\$9 ^ 4*D\$40 ^ 2 + B:\$C\$9 ^ 2/B:E\$9 ^ 2*D30 ^ 2)
 F:E72: (F3) @ Sqrt(+E:F20 ^ 2/B:F\$9 ^ 2*\$B\$40 ^ 2 + B:\$C\$9 ^ 2*E:F20 ^ 2/B:F\$9 ^ 4*E\$40 ^ 2 + B:\$C\$9 ^ 2/B:F\$9 ^ 2*E30 ^ 2)
 F:F72: (F3) @ Sqrt(+E:G20 ^ 2/B:G\$9 ^ 2*\$B\$40 ^ 2 + B:\$C\$9 ^ 2*E:G20 ^ 2/B:G\$9 ^ 4*F\$40 ^ 2 + B:\$C\$9 ^ 2/B:G\$9 ^ 2*F30 ^ 2)
 F:G72: (F3) @ Sqrt(+E:H20 ^ 2/B:H\$9 ^ 2*\$B\$40 ^ 2 + B:\$C\$9 ^ 2*E:H20 ^ 2/B:H\$9 ^ 4*G\$40 ^ 2 + B:\$C\$9 ^ 2/B:H\$9 ^ 2*G30 ^ 2)
 F:H72: (F3) @ Sqrt(+E:I20 ^ 2/B:I\$9 ^ 2*\$B\$40 ^ 2 + B:\$C\$9 ^ 2*E:I20 ^ 2/B:I\$9 ^ 4*H\$40 ^ 2 + B:\$C\$9 ^ 2/B:I\$9 ^ 2*H30 ^ 2)
 F:A73: ^ Kaol
 F:B73: (F3) @ Sqrt(+E:C21 ^ 2/B:C\$9 ^ 2*\$B\$40 ^ 2 + B:\$C\$9 ^ 2*E:C21 ^ 2/B:C\$9 ^ 4*B\$40 ^ 2 + B:\$C\$9 ^ 2/B:C\$9 ^ 2*B31 ^ 2)
 F:C73: (F3) @ Sqrt(+E:D21 ^ 2/B:D\$9 ^ 2*\$B\$40 ^ 2 + B:\$C\$9 ^ 2*E:D21 ^ 2/B:D\$9 ^ 4*C\$40 ^ 2 + B:\$C\$9 ^ 2/B:D\$9 ^ 2*C31 ^ 2)
 F:D73: (F3) @ Sqrt(+E:E21 ^ 2/B:E\$9 ^ 2*\$B\$40 ^ 2 + B:\$C\$9 ^ 2*E:E21 ^ 2/B:E\$9 ^ 4*D\$40 ^ 2 + B:\$C\$9 ^ 2/B:E\$9 ^ 2*D31 ^ 2)
 F:E73: (F3) @ Sqrt(+E:F21 ^ 2/B:F\$9 ^ 2*\$B\$40 ^ 2 + B:\$C\$9 ^ 2*E:F21 ^ 2/B:F\$9 ^ 4*E\$40 ^ 2 + B:\$C\$9 ^ 2/B:F\$9 ^ 2*E31 ^ 2)
 F:F73: (F3) @ Sqrt(+E:G21 ^ 2/B:G\$9 ^ 2*\$B\$40 ^ 2 + B:\$C\$9 ^ 2*E:G21 ^ 2/B:G\$9 ^ 4*F\$40 ^ 2 + B:\$C\$9 ^ 2/B:G\$9 ^ 2*F31 ^ 2)
 F:G73: (F3) @ Sqrt(+E:H21 ^ 2/B:H\$9 ^ 2*\$B\$40 ^ 2 + B:\$C\$9 ^ 2*E:H21 ^ 2/B:H\$9 ^ 4*G\$40 ^ 2 + B:\$C\$9 ^ 2/B:H\$9 ^ 2*G31 ^ 2)
 F:H73: (F3) @ Sqrt(+E:I21 ^ 2/B:I\$9 ^ 2*\$B\$40 ^ 2 + B:\$C\$9 ^ 2*E:I21 ^ 2/B:I\$9 ^ 4*H\$40 ^ 2 + B:\$C\$9 ^ 2/B:I\$9 ^ 2*H31 ^ 2)
 F:A74: ^ qtz
 F:B74: (F3) @ Sqrt(+E:C22 ^ 2/B:C\$9 ^ 2*\$B\$40 ^ 2 + B:\$C\$9 ^ 2*E:C22 ^ 2/B:C\$9 ^ 4*B\$40 ^ 2 + B:\$C\$9 ^ 2/B:C\$9 ^ 2*B32 ^ 2)
 F:C74: (F3) @ Sqrt(+E:D22 ^ 2/B:D\$9 ^ 2*\$B\$40 ^ 2 + B:\$C\$9 ^ 2*E:D22 ^ 2/B:D\$9 ^ 4*C\$40 ^ 2 + B:\$C\$9 ^ 2/B:D\$9 ^ 2*C32 ^ 2)

F:D74: (F3) @ SQRT(+E:E22 ^ 2/B:ES\$9 ^ 2*\$B\$40 ^ 2 + B:\$C\$9 ^ 2*E:E22 ^ 2/B:ES\$9 ^ 4*D\$40 ^ 2 + B:\$C\$9 ^ 2/B:ES\$9 ^ 2*D32 ^ 2)
 F:E74: (F3) @ SQRT(+E:F22 ^ 2/B:FS\$9 ^ 2*\$B\$40 ^ 2 + B:\$C\$9 ^ 2*E:F22 ^ 2/B:FS\$9 ^ 4*E\$40 ^ 2 + B:\$C\$9 ^ 2/B:FS\$9 ^ 2*E32 ^ 2)
 F:F74: (F3) @ SQRT(+E:G22 ^ 2/B:GS\$9 ^ 2*\$B\$40 ^ 2 + B:\$C\$9 ^ 2*E:G22 ^ 2/B:GS\$9 ^ 4*F\$40 ^ 2 + B:\$C\$9 ^ 2/B:GS\$9 ^ 2*F32 ^ 2)
 F:G74: (F3) @ SQRT(+E:H22 ^ 2/B:HS\$9 ^ 2*\$B\$40 ^ 2 + B:\$C\$9 ^ 2*E:H22 ^ 2/B:HS\$9 ^ 4*G\$40 ^ 2 + B:\$C\$9 ^ 2/B:HS\$9 ^ 2*G32 ^ 2)
 F:H74: (F3) @ SQRT(+E:I22 ^ 2/B:IS\$9 ^ 2*\$B\$40 ^ 2 + B:\$C\$9 ^ 2*E:I22 ^ 2/B:IS\$9 ^ 4*H\$40 ^ 2 + B:\$C\$9 ^ 2/B:IS\$9 ^ 2*H32 ^ 2)
 F:A75: ^ Mn-carb
 F:B75: (F3) @ SQRT(+E:C23 ^ 2/B:CS\$9 ^ 2*\$B\$40 ^ 2 + B:\$C\$9 ^ 2*E:C23 ^ 2/B:CS\$9 ^ 4*B\$40 ^ 2 + B:\$C\$9 ^ 2/B:CS\$9 ^ 2*B33 ^ 2)
 F:C75: (F3) @ SQRT(+E:D23 ^ 2/B:DS\$9 ^ 2*\$B\$40 ^ 2 + B:\$C\$9 ^ 2*E:D23 ^ 2/B:DS\$9 ^ 4*C\$40 ^ 2 + B:\$C\$9 ^ 2/B:DS\$9 ^ 2*C33 ^ 2)
 F:D75: (F3) @ SQRT(+E:E23 ^ 2/B:ES\$9 ^ 2*\$B\$40 ^ 2 + B:\$C\$9 ^ 2*E:E23 ^ 2/B:ES\$9 ^ 4*D\$40 ^ 2 + B:\$C\$9 ^ 2/B:ES\$9 ^ 2*D33 ^ 2)
 F:E75: (F3) @ SQRT(+E:F23 ^ 2/B:FS\$9 ^ 2*\$B\$40 ^ 2 + B:\$C\$9 ^ 2*E:F23 ^ 2/B:FS\$9 ^ 4*E\$40 ^ 2 + B:\$C\$9 ^ 2/B:FS\$9 ^ 2*E33 ^ 2)
 F:F75: (F3) @ SQRT(+E:G23 ^ 2/B:GS\$9 ^ 2*\$B\$40 ^ 2 + B:\$C\$9 ^ 2*E:G23 ^ 2/B:GS\$9 ^ 4*F\$40 ^ 2 + B:\$C\$9 ^ 2/B:GS\$9 ^ 2*F33 ^ 2)
 F:G75: (F3) @ SQRT(+E:H23 ^ 2/B:HS\$9 ^ 2*\$B\$40 ^ 2 + B:\$C\$9 ^ 2*E:H23 ^ 2/B:HS\$9 ^ 4*G\$40 ^ 2 + B:\$C\$9 ^ 2/B:HS\$9 ^ 2*G33 ^ 2)
 F:H75: (F3) @ SQRT(+E:I23 ^ 2/B:IS\$9 ^ 2*\$B\$40 ^ 2 + B:\$C\$9 ^ 2*E:I23 ^ 2/B:IS\$9 ^ 4*H\$40 ^ 2 + B:\$C\$9 ^ 2/B:IS\$9 ^ 2*H33 ^ 2)
 F:A76: ^ apatite
 F:B76: (F3) @ SQRT(+E:C24 ^ 2/B:CS\$9 ^ 2*\$B\$40 ^ 2 + B:\$C\$9 ^ 2*E:C24 ^ 2/B:CS\$9 ^ 4*B\$40 ^ 2 + B:\$C\$9 ^ 2/B:CS\$9 ^ 2*B34 ^ 2)
 F:C76: (F3) @ SQRT(+E:D24 ^ 2/B:DS\$9 ^ 2*\$B\$40 ^ 2 + B:\$C\$9 ^ 2*E:D24 ^ 2/B:DS\$9 ^ 4*C\$40 ^ 2 + B:\$C\$9 ^ 2/B:DS\$9 ^ 2*C34 ^ 2)
 F:D76: (F3) @ SQRT(+E:E24 ^ 2/B:ES\$9 ^ 2*\$B\$40 ^ 2 + B:\$C\$9 ^ 2*E:E24 ^ 2/B:ES\$9 ^ 4*D\$40 ^ 2 + B:\$C\$9 ^ 2/B:ES\$9 ^ 2*D34 ^ 2)
 F:E76: (F3) @ SQRT(+E:F24 ^ 2/B:FS\$9 ^ 2*\$B\$40 ^ 2 + B:\$C\$9 ^ 2*E:F24 ^ 2/B:FS\$9 ^ 4*E\$40 ^ 2 + B:\$C\$9 ^ 2/B:FS\$9 ^ 2*E34 ^ 2)
 F:F76: (F3) @ SQRT(+E:G24 ^ 2/B:GS\$9 ^ 2*\$B\$40 ^ 2 + B:\$C\$9 ^ 2*E:G24 ^ 2/B:GS\$9 ^ 4*F\$40 ^ 2 + B:\$C\$9 ^ 2/B:GS\$9 ^ 2*F34 ^ 2)
 F:G76: (F3) @ SQRT(+E:H24 ^ 2/B:HS\$9 ^ 2*\$B\$40 ^ 2 + B:\$C\$9 ^ 2*E:H24 ^ 2/B:HS\$9 ^ 4*G\$40 ^ 2 + B:\$C\$9 ^ 2/B:HS\$9 ^ 2*G34 ^ 2)
 F:H76: (F3) @ SQRT(+E:I24 ^ 2/B:IS\$9 ^ 2*\$B\$40 ^ 2 + B:\$C\$9 ^ 2*E:I24 ^ 2/B:IS\$9 ^ 4*H\$40 ^ 2 + B:\$C\$9 ^ 2/B:IS\$9 ^ 2*H34 ^ 2)
 F:A77: ^ pyrite
 F:B77: (F3) @ SQRT(+E:C25 ^ 2/B:CS\$9 ^ 2*\$B\$40 ^ 2 + B:\$C\$9 ^ 2*E:C25 ^ 2/B:CS\$9 ^ 4*B\$40 ^ 2 + B:\$C\$9 ^ 2/B:CS\$9 ^ 2*B35 ^ 2)
 F:C77: (F3) @ SQRT(+E:D25 ^ 2/B:DS\$9 ^ 2*\$B\$40 ^ 2 + B:\$C\$9 ^ 2*E:D25 ^ 2/B:DS\$9 ^ 4*C\$40 ^ 2 + B:\$C\$9 ^ 2/B:DS\$9 ^ 2*C35 ^ 2)
 F:D77: (F3) @ SQRT(+E:E25 ^ 2/B:ES\$9 ^ 2*\$B\$40 ^ 2 + B:\$C\$9 ^ 2*E:E25 ^ 2/B:ES\$9 ^ 4*D\$40 ^ 2 + B:\$C\$9 ^ 2/B:ES\$9 ^ 2*D35 ^ 2)
 F:E77: (F3) @ SQRT(+E:F25 ^ 2/B:FS\$9 ^ 2*\$B\$40 ^ 2 + B:\$C\$9 ^ 2*E:F25 ^ 2/B:FS\$9 ^ 4*E\$40 ^ 2 + B:\$C\$9 ^ 2/B:FS\$9 ^ 2*E35 ^ 2)
 F:F77: (F3) @ SQRT(+E:G25 ^ 2/B:GS\$9 ^ 2*\$B\$40 ^ 2 + B:\$C\$9 ^ 2*E:G25 ^ 2/B:GS\$9 ^ 4*F\$40 ^ 2 + B:\$C\$9 ^ 2/B:GS\$9 ^ 2*F35 ^ 2)
 F:G77: (F3) @ SQRT(+E:H25 ^ 2/B:HS\$9 ^ 2*\$B\$40 ^ 2 + B:\$C\$9 ^ 2*E:H25 ^ 2/B:HS\$9 ^ 4*G\$40 ^ 2 + B:\$C\$9 ^ 2/B:HS\$9 ^ 2*G35 ^ 2)
 F:H77: (F3) @ SQRT(+E:I25 ^ 2/B:IS\$9 ^ 2*\$B\$40 ^ 2 + B:\$C\$9 ^ 2*E:I25 ^ 2/B:IS\$9 ^ 4*H\$40 ^ 2 + B:\$C\$9 ^ 2/B:IS\$9 ^ 2*H35 ^ 2)
 F:A78: ^ hematite

F:B78: (F3) @ SQRT(+E:C26 ^ 2/B:C\$9 ^ 2*\$B\$40 ^ 2 + B:\$C\$9 ^ 2*E:C26 ^ 2/B:C\$9 ^ 4*B\$40 ^ 2 + B:\$C\$9 ^ 2/B:C\$9 ^ 2*B36 ^ 2)
 F:C78: (F3) @ SQRT(+E:D26 ^ 2/B:D\$9 ^ 2*\$B\$40 ^ 2 + B:\$C\$9 ^ 2*E:D26 ^ 2/B:D\$9 ^ 4*C\$40 ^ 2 + B:\$C\$9 ^ 2/B:D\$9 ^ 2*C36 ^ 2)
 F:D78: (F3) @ SQRT(+E:E26 ^ 2/B:E\$9 ^ 2*\$B\$40 ^ 2 + B:\$C\$9 ^ 2*E:E26 ^ 2/B:E\$9 ^ 4*D\$40 ^ 2 + B:\$C\$9 ^ 2/B:E\$9 ^ 2*D36 ^ 2)
 F:E78: (F3) @ SQRT(+E:F26 ^ 2/B:F\$9 ^ 2*\$B\$40 ^ 2 + B:\$C\$9 ^ 2*E:F26 ^ 2/B:F\$9 ^ 4*E\$40 ^ 2 + B:\$C\$9 ^ 2/B:F\$9 ^ 2*E36 ^ 2)
 F:F78: (F3) @ SQRT(+E:G26 ^ 2/B:G\$9 ^ 2*\$B\$40 ^ 2 + B:\$C\$9 ^ 2*E:G26 ^ 2/B:G\$9 ^ 4*F\$40 ^ 2 + B:\$C\$9 ^ 2/B:G\$9 ^ 2*F36 ^ 2)
 F:G78: (F3) @ SQRT(+E:H26 ^ 2/B:H\$9 ^ 2*\$B\$40 ^ 2 + B:\$C\$9 ^ 2*E:H26 ^ 2/B:H\$9 ^ 4*G\$40 ^ 2 + B:\$C\$9 ^ 2/B:H\$9 ^ 2*G36 ^ 2)
 F:H78: (F3) @ SQRT(+E:I26 ^ 2/B:I\$9 ^ 2*\$B\$40 ^ 2 + B:\$C\$9 ^ 2*E:I26 ^ 2/B:I\$9 ^ 4*H\$40 ^ 2 + B:\$C\$9 ^ 2/B:I\$9 ^ 2*H36 ^ 2)
 F:A79: ^ magnetite
 F:B79: (F3) @ SQRT(+E:C27 ^ 2/B:C\$9 ^ 2*\$B\$40 ^ 2 + B:\$C\$9 ^ 2*E:C27 ^ 2/B:C\$9 ^ 4*B\$40 ^ 2 + B:\$C\$9 ^ 2/B:C\$9 ^ 2*B37 ^ 2)
 F:C79: (F3) @ SQRT(+E:D27 ^ 2/B:D\$9 ^ 2*\$B\$40 ^ 2 + B:\$C\$9 ^ 2*E:D27 ^ 2/B:D\$9 ^ 4*C\$40 ^ 2 + B:\$C\$9 ^ 2/B:D\$9 ^ 2*C37 ^ 2)
 F:D79: (F3) @ SQRT(+E:E27 ^ 2/B:E\$9 ^ 2*\$B\$40 ^ 2 + B:\$C\$9 ^ 2*E:E27 ^ 2/B:E\$9 ^ 4*D\$40 ^ 2 + B:\$C\$9 ^ 2/B:E\$9 ^ 2*D37 ^ 2)
 F:E79: (F3) @ SQRT(+E:F27 ^ 2/B:F\$9 ^ 2*\$B\$40 ^ 2 + B:\$C\$9 ^ 2*E:F27 ^ 2/B:F\$9 ^ 4*E\$40 ^ 2 + B:\$C\$9 ^ 2/B:F\$9 ^ 2*E37 ^ 2)
 F:F79: (F3) @ SQRT(+E:G27 ^ 2/B:G\$9 ^ 2*\$B\$40 ^ 2 + B:\$C\$9 ^ 2*E:G27 ^ 2/B:G\$9 ^ 4*F\$40 ^ 2 + B:\$C\$9 ^ 2/B:G\$9 ^ 2*F37 ^ 2)
 F:G79: (F3) @ SQRT(+E:H27 ^ 2/B:H\$9 ^ 2*\$B\$40 ^ 2 + B:\$C\$9 ^ 2*E:H27 ^ 2/B:H\$9 ^ 4*G\$40 ^ 2 + B:\$C\$9 ^ 2/B:H\$9 ^ 2*G37 ^ 2)
 F:H79: (F3) @ SQRT(+E:I27 ^ 2/B:I\$9 ^ 2*\$B\$40 ^ 2 + B:\$C\$9 ^ 2*E:I27 ^ 2/B:I\$9 ^ 4*H\$40 ^ 2 + B:\$C\$9 ^ 2/B:I\$9 ^ 2*H37 ^ 2)
 F:A80: (F4) 'Total
 F:B80: (F4) @ SUM(B57..B79)
 F:C80: (F4) @ SUM(C57..C79)
 F:D80: (F4) @ SUM(D57..D79)
 F:E80: (F4) @ SUM(E57..E79)
 F:F80: (F4) @ SUM(F57..F79)
 F:G80: (F4) @ SUM(G57..G79)
 F:H80: (F4) @ SUM(H57..H79)

F:A82: 'Table 7- .

F:B82: ' Error propagation of absolute losses & gains in gram (SD at 68% confidence level)

F:B83: ' at northern segment of No.3 vein, Silver Queen mine, Owen Lake, central BC

F:A84: 'Sample_id

F:B84: (F0) ^ x4-4

F:C84: (F0) ^ x3-7

F:D84: (F0) ^ x3-5

F:E84: (F0) ^ x3-4

F:F84: (F0) ^ x3-1

F:G84: (F0) ^ x3-3d

F:H84: (F0) ^ x2-5

F:A85: ^ dSiO2

F:B85: (F3) + \$185*@SQRT((B:C7/B:C\$9*\$B\$40) ^ 2 + (B:\$C\$9*B:C7/B:C\$9 ^ 2*B\$40) ^ 2 + (B:\$C\$9/B:C\$9*B38) ^ 2 + \$B38 ^ 2)

F:C85: (F3) + \$185*@SQRT((B:D7/B:D\$9*\$B\$40) ^ 2 + (B:\$C\$9*B:D7/B:D\$9 ^ 2*C\$40) ^ 2 + (B:\$C\$9/B:D\$9*C38) ^ 2 + \$B38 ^ 2)

F:D85: (F3) + \$185*@SQRT((B:E7/B:E\$9*\$B\$40) ^ 2 + (B:\$C\$9*B:E7/B:E\$9 ^ 2*D\$40) ^ 2 + (B:\$C\$9/B:E\$9*D38) ^ 2 + \$B38 ^ 2)

F:E85: (F3) + \$185*@SQRT((B:F7/B:F\$9*\$B\$40) ^ 2 + (B:\$C\$9*B:F7/B:F\$9 ^ 2*E\$40) ^ 2 + (B:\$C\$9/B:F\$9*E38) ^ 2 + \$B38 ^ 2)

F:F85: (F3) + \$185*@SQRT((B:G7/B:G\$9*\$B\$40) ^ 2 + (B:\$C\$9*B:G7/B:G\$9 ^ 2*F\$40) ^ 2 + (B:\$C\$9/B:G\$9*F38) ^ 2 + \$B38 ^ 2)

F:G85: (F3) + \$185*@SQRT((B:H7/B:H\$9*\$B\$40) ^ 2 + (B:\$C\$9*B:H7/B:H\$9 ^ 2*G\$40) ^ 2 + (B:\$C\$9/B:H\$9*G38) ^ 2 + \$B38 ^ 2)

F:H85: (F3) + \$185*@SQRT((B:I7/B:I\$9*\$B\$40) ^ 2 + (B:\$C\$9*B:I7/B:I\$9 ^ 2*H\$40) ^ 2 + (B:\$C\$9/B:I\$9*H38) ^ 2 + \$B38 ^ 2)

F:I85: (F3) 1

F:A86: ^ dAl+3

F:B86: (F3) + \$186*@SQRT((B:C8/B:C\$9*\$B\$40) ^ 2 + (B:\$C\$9*B:C8/B:C\$9 ^ 2*B\$40) ^ 2 + (B:\$C\$9/B:C\$9*B39) ^ 2 + \$B39 ^ 2)

F:C86: (F3) + \$186*@SQRT((B:D8/B:D\$9*\$B\$40) ^ 2 + (B:\$C\$9*B:D8/B:D\$9 ^ 2*C\$40) ^ 2 + (B:\$C\$9/B:D\$9*C39) ^ 2 + \$B39 ^ 2)

F:D86: (F3) + \$186*@SQRT((B:E8/B:E\$9*\$B\$40) ^ 2 + (B:\$C\$9*B:E8/B:E\$9 ^ 2*D\$40) ^ 2 + (B:\$C\$9/B:E\$9*D39) ^ 2 + \$B39 ^ 2)

F:E86: (F3) + \$186*@SQRT((B:F8/B:F\$9*\$B\$40) ^ 2 + (B:\$C\$9*B:F8/B:F\$9 ^ 2*E\$40) ^ 2 + (B:\$C\$9/B:F\$9*E39) ^ 2 + \$B39 ^ 2)

F:F86: (F3) + \$186*@SQRT((B:G8/B:G\$9*\$B\$40) ^ 2 + (B:\$C\$9*B:G8/B:G\$9 ^ 2*F\$40) ^ 2 + (B:\$C\$9/B:G\$9*F39) ^ 2 + \$B39 ^ 2)

F:G86: (F3) + \$186*@SQRT((B:H8/B:H\$9*\$B\$40) ^ 2 + (B:\$C\$9*B:H8/B:H\$9 ^ 2*G\$40) ^ 2 + (B:\$C\$9/B:H\$9*G39) ^ 2 + \$B39 ^ 2)

F:H86: (F3) + \$186*@SQRT((B:I8/B:I\$9*\$B\$40) ^ 2 + (B:\$C\$9*B:I8/B:I\$9 ^ 2*H\$40) ^ 2 + (B:\$C\$9/B:I\$9*H39) ^ 2 + \$B39 ^ 2)

F:I86: (F3) 26.98*2/B:\$A\$8

F:A87: ^ dTi+2

F:B87: (F3) + \$I87* @ SQRT((B:C9/B:C\$9*\$B\$40) ^ 2 + (B:\$C\$9*B:C9/B:C\$9 ^ 2*\$B\$40) ^ 2 + (B:\$C\$9/B:C\$9*\$B40) ^ 2 + \$B40 ^ 2)
F:C87: (F3) + \$I87* @ SQRT((B:D9/B:D\$9*\$B\$40) ^ 2 + (B:\$C\$9*B:D9/B:D\$9 ^ 2*\$C\$40) ^ 2 + (B:\$C\$9/B:D\$9*\$C40) ^ 2 + \$B40 ^ 2)
F:D87: (F3) + \$I87* @ SQRT((B:E9/B:E\$9*\$B\$40) ^ 2 + (B:\$C\$9*B:E9/B:E\$9 ^ 2*\$D\$40) ^ 2 + (B:\$C\$9/B:E\$9*\$D40) ^ 2 + \$B40 ^ 2)
F:E87: (F3) + \$I87* @ SQRT((B:F9/B:F\$9*\$B\$40) ^ 2 + (B:\$C\$9*B:F9/B:F\$9 ^ 2*\$E\$40) ^ 2 + (B:\$C\$9/B:F\$9*\$E40) ^ 2 + \$B40 ^ 2)
F:F87: (F3) + \$I87* @ SQRT((B:G9/B:G\$9*\$B\$40) ^ 2 + (B:\$C\$9*B:G9/B:G\$9 ^ 2*\$F\$40) ^ 2 + (B:\$C\$9/B:G\$9*\$F40) ^ 2 + \$B40 ^ 2)
F:G87: (F3) + \$I87* @ SQRT((B:H9/B:H\$9*\$B\$40) ^ 2 + (B:\$C\$9*B:H9/B:H\$9 ^ 2*\$G\$40) ^ 2 + (B:\$C\$9/B:H\$9*\$G40) ^ 2 + \$B40 ^ 2)
F:H87: (F3) + \$I87* @ SQRT((B:I9/B:I\$9*\$B\$40) ^ 2 + (B:\$C\$9*B:I9/B:I\$9 ^ 2*\$H\$40) ^ 2 + (B:\$C\$9/B:I\$9*\$H40) ^ 2 + \$B40 ^ 2)
F:I87: (F3) 47.9/B:\$A\$9
F:A88: ^ dFe + 3
F:B88: (F3) + \$I88* @ SQRT((B:C10/B:C\$9*\$B\$40) ^ 2 + (B:\$C\$9*B:C10/B:C\$9 ^ 2*\$B\$40) ^ 2 + (B:\$C\$9/B:C\$9*\$B41) ^ 2 + \$B41 ^ 2)
F:C88: (F3) + \$I88* @ SQRT((B:D10/B:D\$9*\$B\$40) ^ 2 + (B:\$C\$9*B:D10/B:D\$9 ^ 2*\$C\$40) ^ 2 + (B:\$C\$9/B:D\$9*\$C41) ^ 2 + \$B41 ^ 2)
F:D88: (F3) + \$I88* @ SQRT((B:E10/B:E\$9*\$B\$40) ^ 2 + (B:\$C\$9*B:E10/B:E\$9 ^ 2*\$D\$40) ^ 2 + (B:\$C\$9/B:E\$9*\$D41) ^ 2 + \$B41 ^ 2)
F:E88: (F3) + \$I88* @ SQRT((B:F10/B:F\$9*\$B\$40) ^ 2 + (B:\$C\$9*B:F10/B:F\$9 ^ 2*\$E\$40) ^ 2 + (B:\$C\$9/B:F\$9*\$E41) ^ 2 + \$B41 ^ 2)
F:F88: (F3) + \$I88* @ SQRT((B:G10/B:G\$9*\$B\$40) ^ 2 + (B:\$C\$9*B:G10/B:G\$9 ^ 2*\$F\$40) ^ 2 + (B:\$C\$9/B:G\$9*\$F41) ^ 2 + \$B41 ^ 2)
F:G88: (F3) + \$I88* @ SQRT((B:H10/B:H\$9*\$B\$40) ^ 2 + (B:\$C\$9*B:H10/B:H\$9 ^ 2*\$G\$40) ^ 2 + (B:\$C\$9/B:H\$9*\$G41) ^ 2 + \$B41 ^ 2)
F:H88: (F3) + \$I88* @ SQRT((B:I10/B:I\$9*\$B\$40) ^ 2 + (B:\$C\$9*B:I10/B:I\$9 ^ 2*\$H\$40) ^ 2 + (B:\$C\$9/B:I\$9*\$H41) ^ 2 + \$B41 ^ 2)
F:I88: (F3) 55.85*2/B:\$A\$10
F:A89: ^ dFe + 2
F:B89: (F3) + \$I89* @ SQRT((B:C11/B:C\$9*\$B\$40) ^ 2 + (B:\$C\$9*B:C11/B:C\$9 ^ 2*\$B\$40) ^ 2 + (B:\$C\$9/B:C\$9*\$B42) ^ 2 + \$B42 ^ 2)
F:C89: (F3) + \$I89* @ SQRT((B:D11/B:D\$9*\$B\$40) ^ 2 + (B:\$C\$9*B:D11/B:D\$9 ^ 2*\$C\$40) ^ 2 + (B:\$C\$9/B:D\$9*\$C42) ^ 2 + \$B42 ^ 2)
F:D89: (F3) + \$I89* @ SQRT((B:E11/B:E\$9*\$B\$40) ^ 2 + (B:\$C\$9*B:E11/B:E\$9 ^ 2*\$D\$40) ^ 2 + (B:\$C\$9/B:E\$9*\$D42) ^ 2 + \$B42 ^ 2)
F:E89: (F3) + \$I89* @ SQRT((B:F11/B:F\$9*\$B\$40) ^ 2 + (B:\$C\$9*B:F11/B:F\$9 ^ 2*\$E\$40) ^ 2 + (B:\$C\$9/B:F\$9*\$E42) ^ 2 + \$B42 ^ 2)
F:F89: (F3) + \$I89* @ SQRT((B:G11/B:G\$9*\$B\$40) ^ 2 + (B:\$C\$9*B:G11/B:G\$9 ^ 2*\$F\$40) ^ 2 + (B:\$C\$9/B:G\$9*\$F42) ^ 2 + \$B42 ^ 2)
F:G89: (F3) + \$I89* @ SQRT((B:H11/B:H\$9*\$B\$40) ^ 2 + (B:\$C\$9*B:H11/B:H\$9 ^ 2*\$G\$40) ^ 2 + (B:\$C\$9/B:H\$9*\$G42) ^ 2 + \$B42 ^ 2)
F:H89: (F3) + \$I89* @ SQRT((B:I11/B:I\$9*\$B\$40) ^ 2 + (B:\$C\$9*B:I11/B:I\$9 ^ 2*\$H\$40) ^ 2 + (B:\$C\$9/B:I\$9*\$H42) ^ 2 + \$B42 ^ 2)
F:I89: (F3) 55.85/B:\$A\$11
F:A90: ^ dMn + 2
F:B90: (F3) + \$I90* @ SQRT((B:C12/B:C\$9*\$B\$40) ^ 2 + (B:\$C\$9*B:C12/B:C\$9 ^ 2*\$B\$40) ^ 2 + (B:\$C\$9/B:C\$9*\$B43) ^ 2 + \$B43 ^ 2)
F:C90: (F3) + \$I90* @ SQRT((B:D12/B:D\$9*\$B\$40) ^ 2 + (B:\$C\$9*B:D12/B:D\$9 ^ 2*\$C\$40) ^ 2 + (B:\$C\$9/B:D\$9*\$C43) ^ 2 + \$B43 ^ 2)
F:D90: (F3) + \$I90* @ SQRT((B:E12/B:E\$9*\$B\$40) ^ 2 + (B:\$C\$9*B:E12/B:E\$9 ^ 2*\$D\$40) ^ 2 + (B:\$C\$9/B:E\$9*\$D43) ^ 2 + \$B43 ^ 2)

F:E90: (F3) + \$I90* @ Sqrt((B:F12/B:F\$9*\$B\$40) ^ 2 + (B:\$C\$9*B:F12/B:F\$9 ^ 2*E\$40) ^ 2 + (B:\$C\$9/B:F\$9*E43) ^ 2 + \$B43 ^ 2)
F:F90: (F3) + \$I90* @ Sqrt((B:G12/B:G\$9*\$B\$40) ^ 2 + (B:\$C\$9*B:G12/B:G\$9 ^ 2*F\$40) ^ 2 + (B:\$C\$9/B:G\$9*F43) ^ 2 + \$B43 ^ 2)
F:G90: (F3) + \$I90* @ Sqrt((B:H12/B:H\$9*\$B\$40) ^ 2 + (B:\$C\$9*B:H12/B:H\$9 ^ 2*G\$40) ^ 2 + (B:\$C\$9/B:H\$9*G43) ^ 2 + \$B43 ^ 2)
F:H90: (F3) + \$I90* @ Sqrt((B:I12/B:I\$9*\$B\$40) ^ 2 + (B:\$C\$9*B:I12/B:I\$9 ^ 2*H\$40) ^ 2 + (B:\$C\$9/B:I\$9*H43) ^ 2 + \$B43 ^ 2)
F:I90: (F3) 54.94/B:\$A\$12
F:A91: ^ dMg + 2
F:B91: (F3) + \$I91* @ Sqrt((B:C13/B:C\$9*\$B\$40) ^ 2 + (B:\$C\$9*B:C13/B:C\$9 ^ 2*B\$40) ^ 2 + (B:\$C\$9/B:C\$9*B44) ^ 2 + \$B44 ^ 2)
F:C91: (F3) + \$I91* @ Sqrt((B:D13/B:D\$9*\$B\$40) ^ 2 + (B:\$C\$9*B:D13/B:D\$9 ^ 2*C\$40) ^ 2 + (B:\$C\$9/B:D\$9*C44) ^ 2 + \$B44 ^ 2)
F:D91: (F3) + \$I91* @ Sqrt((B:E13/B:E\$9*\$B\$40) ^ 2 + (B:\$C\$9*B:E13/B:E\$9 ^ 2*D\$40) ^ 2 + (B:\$C\$9/B:E\$9*D44) ^ 2 + \$B44 ^ 2)
F:E91: (F3) + \$I91* @ Sqrt((B:F13/B:F\$9*\$B\$40) ^ 2 + (B:\$C\$9*B:F13/B:F\$9 ^ 2*E\$40) ^ 2 + (B:\$C\$9/B:F\$9*E44) ^ 2 + \$B44 ^ 2)
F:F91: (F3) + \$I91* @ Sqrt((B:G13/B:G\$9*\$B\$40) ^ 2 + (B:\$C\$9*B:G13/B:G\$9 ^ 2*F\$40) ^ 2 + (B:\$C\$9/B:G\$9*F44) ^ 2 + \$B44 ^ 2)
F:G91: (F3) + \$I91* @ Sqrt((B:H13/B:H\$9*\$B\$40) ^ 2 + (B:\$C\$9*B:H13/B:H\$9 ^ 2*G\$40) ^ 2 + (B:\$C\$9/B:H\$9*G44) ^ 2 + \$B44 ^ 2)
F:H91: (F3) + \$I91* @ Sqrt((B:I13/B:I\$9*\$B\$40) ^ 2 + (B:\$C\$9*B:I13/B:I\$9 ^ 2*H\$40) ^ 2 + (B:\$C\$9/B:I\$9*H44) ^ 2 + \$B44 ^ 2)
F:I91: (F3) 24.31/B:\$A\$13
F:A92: ^ dCa + 2
F:B92: (F3) + \$I92* @ Sqrt((B:C14/B:C\$9*\$B\$40) ^ 2 + (B:\$C\$9*B:C14/B:C\$9 ^ 2*B\$40) ^ 2 + (B:\$C\$9/B:C\$9*B45) ^ 2 + \$B45 ^ 2)
F:C92: (F3) + \$I92* @ Sqrt((B:D14/B:D\$9*\$B\$40) ^ 2 + (B:\$C\$9*B:D14/B:D\$9 ^ 2*C\$40) ^ 2 + (B:\$C\$9/B:D\$9*C45) ^ 2 + \$B45 ^ 2)
F:D92: (F3) + \$I92* @ Sqrt((B:E14/B:E\$9*\$B\$40) ^ 2 + (B:\$C\$9*B:E14/B:E\$9 ^ 2*D\$40) ^ 2 + (B:\$C\$9/B:E\$9*D45) ^ 2 + \$B45 ^ 2)
F:E92: (F3) + \$I92* @ Sqrt((B:F14/B:F\$9*\$B\$40) ^ 2 + (B:\$C\$9*B:F14/B:F\$9 ^ 2*E\$40) ^ 2 + (B:\$C\$9/B:F\$9*E45) ^ 2 + \$B45 ^ 2)
F:F92: (F3) + \$I92* @ Sqrt((B:G14/B:G\$9*\$B\$40) ^ 2 + (B:\$C\$9*B:G14/B:G\$9 ^ 2*F\$40) ^ 2 + (B:\$C\$9/B:G\$9*F45) ^ 2 + \$B45 ^ 2)
F:G92: (F3) + \$I92* @ Sqrt((B:H14/B:H\$9*\$B\$40) ^ 2 + (B:\$C\$9*B:H14/B:H\$9 ^ 2*G\$40) ^ 2 + (B:\$C\$9/B:H\$9*G45) ^ 2 + \$B45 ^ 2)
F:H92: (F3) + \$I92* @ Sqrt((B:I14/B:I\$9*\$B\$40) ^ 2 + (B:\$C\$9*B:I14/B:I\$9 ^ 2*H\$40) ^ 2 + (B:\$C\$9/B:I\$9*H45) ^ 2 + \$B45 ^ 2)
F:I92: (F3) 40.08/B:\$A\$14
F:A93: ^ dNa +
F:B93: (F3) + \$I93* @ Sqrt((B:C15/B:C\$9*\$B\$40) ^ 2 + (B:\$C\$9*B:C15/B:C\$9 ^ 2*B\$40) ^ 2 + (B:\$C\$9/B:C\$9*B46) ^ 2 + \$B46 ^ 2)
F:C93: (F3) + \$I93* @ Sqrt((B:D15/B:D\$9*\$B\$40) ^ 2 + (B:\$C\$9*B:D15/B:D\$9 ^ 2*C\$40) ^ 2 + (B:\$C\$9/B:D\$9*C46) ^ 2 + \$B46 ^ 2)
F:D93: (F3) + \$I93* @ Sqrt((B:E15/B:E\$9*\$B\$40) ^ 2 + (B:\$C\$9*B:E15/B:E\$9 ^ 2*D\$40) ^ 2 + (B:\$C\$9/B:E\$9*D46) ^ 2 + \$B46 ^ 2)
F:E93: (F3) + \$I93* @ Sqrt((B:F15/B:F\$9*\$B\$40) ^ 2 + (B:\$C\$9*B:F15/B:F\$9 ^ 2*E\$40) ^ 2 + (B:\$C\$9/B:F\$9*E46) ^ 2 + \$B46 ^ 2)
F:F93: (F3) + \$I93* @ Sqrt((B:G15/B:G\$9*\$B\$40) ^ 2 + (B:\$C\$9*B:G15/B:G\$9 ^ 2*F\$40) ^ 2 + (B:\$C\$9/B:G\$9*F46) ^ 2 + \$B46 ^ 2)
F:G93: (F3) + \$I93* @ Sqrt((B:H15/B:H\$9*\$B\$40) ^ 2 + (B:\$C\$9*B:H15/B:H\$9 ^ 2*G\$40) ^ 2 + (B:\$C\$9/B:H\$9*G46) ^ 2 + \$B46 ^ 2)

F:H93: (F3) + \$I93*@SQRT((B:I15/B:\$I9*\$B\$40) ^ 2 + (B:\$C\$9*B:I15/B:\$I9 ^ 2*H\$40) ^ 2 + (B:\$C\$9/B:\$I9*H46) ^ 2 + \$B46 ^ 2)
 F:I93: (F3) 22.99*2/B:\$A\$15
 F:A94: ^ dK +
 F:B94: (F3) + \$I94*@SQRT((B:C16/B:C\$9*\$B\$40) ^ 2 + (B:\$C\$9*B:C16/B:C\$9 ^ 2*B\$40) ^ 2 + (B:\$C\$9/B:C\$9*B47) ^ 2 + \$B47 ^ 2)
 F:C94: (F3) + \$I94*@SQRT((B:D16/B:D\$9*\$B\$40) ^ 2 + (B:\$C\$9*B:D16/B:D\$9 ^ 2*C\$40) ^ 2 + (B:\$C\$9/B:D\$9*C47) ^ 2 + \$B47 ^ 2)
 F:D94: (F3) + \$I94*@SQRT((B:E16/B:E\$9*\$B\$40) ^ 2 + (B:\$C\$9*B:E16/B:E\$9 ^ 2*D\$40) ^ 2 + (B:\$C\$9/B:E\$9*D47) ^ 2 + \$B47 ^ 2)
 F:E94: (F3) + \$I94*@SQRT((B:F16/B:F\$9*\$B\$40) ^ 2 + (B:\$C\$9*B:F16/B:F\$9 ^ 2*E\$40) ^ 2 + (B:\$C\$9/B:F\$9*E47) ^ 2 + \$B47 ^ 2)
 F:F94: (F3) + \$I94*@SQRT((B:G16/B:G\$9*\$B\$40) ^ 2 + (B:\$C\$9*B:G16/B:G\$9 ^ 2*F\$40) ^ 2 + (B:\$C\$9/B:G\$9*F47) ^ 2 + \$B47 ^ 2)
 F:G94: (F3) + \$I94*@SQRT((B:H16/B:H\$9*\$B\$40) ^ 2 + (B:\$C\$9*B:H16/B:H\$9 ^ 2*G\$40) ^ 2 + (B:\$C\$9/B:H\$9*G47) ^ 2 + \$B47 ^ 2)
 F:H94: (F3) + \$I94*@SQRT((B:I16/B:\$I9*\$B\$40) ^ 2 + (B:\$C\$9*B:I16/B:\$I9 ^ 2*H\$40) ^ 2 + (B:\$C\$9/B:\$I9*H47) ^ 2 + \$B47 ^ 2)
 F:I94: (F3) 39.09*2/B:\$A\$16
 F:A95: ^ dP + 5
 F:B95: (F3) + \$I95*@SQRT((B:C17/B:C\$9*\$B\$40) ^ 2 + (B:\$C\$9*B:C17/B:C\$9 ^ 2*B\$40) ^ 2 + (B:\$C\$9/B:C\$9*B48) ^ 2 + \$B48 ^ 2)
 F:C95: (F3) + \$I95*@SQRT((B:D17/B:D\$9*\$B\$40) ^ 2 + (B:\$C\$9*B:D17/B:D\$9 ^ 2*C\$40) ^ 2 + (B:\$C\$9/B:D\$9*C48) ^ 2 + \$B48 ^ 2)
 F:D95: (F3) + \$I95*@SQRT((B:E17/B:E\$9*\$B\$40) ^ 2 + (B:\$C\$9*B:E17/B:E\$9 ^ 2*D\$40) ^ 2 + (B:\$C\$9/B:E\$9*D48) ^ 2 + \$B48 ^ 2)
 F:E95: (F3) + \$I95*@SQRT((B:F17/B:F\$9*\$B\$40) ^ 2 + (B:\$C\$9*B:F17/B:F\$9 ^ 2*E\$40) ^ 2 + (B:\$C\$9/B:F\$9*E48) ^ 2 + \$B48 ^ 2)
 F:F95: (F3) + \$I95*@SQRT((B:G17/B:G\$9*\$B\$40) ^ 2 + (B:\$C\$9*B:G17/B:G\$9 ^ 2*F\$40) ^ 2 + (B:\$C\$9/B:G\$9*F48) ^ 2 + \$B48 ^ 2)
 F:G95: (F3) + \$I95*@SQRT((B:H17/B:H\$9*\$B\$40) ^ 2 + (B:\$C\$9*B:H17/B:H\$9 ^ 2*G\$40) ^ 2 + (B:\$C\$9/B:H\$9*G48) ^ 2 + \$B48 ^ 2)
 F:H95: (F3) + \$I95*@SQRT((B:I17/B:\$I9*\$B\$40) ^ 2 + (B:\$C\$9*B:I17/B:\$I9 ^ 2*H\$40) ^ 2 + (B:\$C\$9/B:\$I9*H48) ^ 2 + \$B48 ^ 2)
 F:I95: (F3) 30.97*2/B:\$A\$17
 F:A96: ^ dH2O
 F:B96: (F3) + \$I96*@SQRT((B:C18/B:C\$9*\$B\$40) ^ 2 + (B:\$C\$9*B:C18/B:C\$9 ^ 2*B\$40) ^ 2 + (B:\$C\$9/B:C\$9*B49) ^ 2 + \$B49 ^ 2)
 F:C96: (F3) + \$I96*@SQRT((B:D18/B:D\$9*\$B\$40) ^ 2 + (B:\$C\$9*B:D18/B:D\$9 ^ 2*C\$40) ^ 2 + (B:\$C\$9/B:D\$9*C49) ^ 2 + \$B49 ^ 2)
 F:D96: (F3) + \$I96*@SQRT((B:E18/B:E\$9*\$B\$40) ^ 2 + (B:\$C\$9*B:E18/B:E\$9 ^ 2*D\$40) ^ 2 + (B:\$C\$9/B:E\$9*D49) ^ 2 + \$B49 ^ 2)
 F:E96: (F3) + \$I96*@SQRT((B:F18/B:F\$9*\$B\$40) ^ 2 + (B:\$C\$9*B:F18/B:F\$9 ^ 2*E\$40) ^ 2 + (B:\$C\$9/B:F\$9*E49) ^ 2 + \$B49 ^ 2)
 F:F96: (F3) + \$I96*@SQRT((B:G18/B:G\$9*\$B\$40) ^ 2 + (B:\$C\$9*B:G18/B:G\$9 ^ 2*F\$40) ^ 2 + (B:\$C\$9/B:G\$9*F49) ^ 2 + \$B49 ^ 2)
 F:G96: (F3) + \$I96*@SQRT((B:H18/B:H\$9*\$B\$40) ^ 2 + (B:\$C\$9*B:H18/B:H\$9 ^ 2*G\$40) ^ 2 + (B:\$C\$9/B:H\$9*G49) ^ 2 + \$B49 ^ 2)
 F:H96: (F3) + \$I96*@SQRT((B:I18/B:\$I9*\$B\$40) ^ 2 + (B:\$C\$9*B:I18/B:\$I9 ^ 2*H\$40) ^ 2 + (B:\$C\$9/B:\$I9*H49) ^ 2 + \$B49 ^ 2)
 F:I96: (F3) 1
 F:A97: ^ dCO2

F:B97: (F3) + \$I97* @SQRT((B:C19/B:C\$9*\$B\$40) ^ 2 + (B:\$C\$9*B:C19/B:C\$9 ^ 2*\$B\$40) ^ 2 + (B:\$C\$9/B:C\$9*B50) ^ 2 + \$B50 ^ 2)
 F:C97: (F3) + \$I97* @SQRT((B:D19/B:D\$9*\$B\$40) ^ 2 + (B:\$C\$9*B:D19/B:D\$9 ^ 2*\$C\$40) ^ 2 + (B:\$C\$9/B:D\$9*C50) ^ 2 + \$B50 ^ 2)
 F:D97: (F3) + \$I97* @SQRT((B:E19/B:E\$9*\$B\$40) ^ 2 + (B:\$C\$9*B:E19/B:E\$9 ^ 2*\$D\$40) ^ 2 + (B:\$C\$9/B:E\$9*D50) ^ 2 + \$B50 ^ 2)
 F:E97: (F3) + \$I97* @SQRT((B:F19/B:F\$9*\$B\$40) ^ 2 + (B:\$C\$9*B:F19/B:F\$9 ^ 2*\$E\$40) ^ 2 + (B:\$C\$9/B:F\$9*E50) ^ 2 + \$B50 ^ 2)
 F:F97: (F3) + \$I97* @SQRT((B:G19/B:G\$9*\$B\$40) ^ 2 + (B:\$C\$9*B:G19/B:G\$9 ^ 2*\$F\$40) ^ 2 + (B:\$C\$9/B:G\$9*F50) ^ 2 + \$B50 ^ 2)
 F:G97: (F3) + \$I97* @SQRT((B:H19/B:H\$9*\$B\$40) ^ 2 + (B:\$C\$9*B:H19/B:H\$9 ^ 2*\$G\$40) ^ 2 + (B:\$C\$9/B:H\$9*G50) ^ 2 + \$B50 ^ 2)
 F:H97: (F3) + \$I97* @SQRT((B:I19/B:I\$9*\$B\$40) ^ 2 + (B:\$C\$9*B:I19/B:I\$9 ^ 2*\$H\$40) ^ 2 + (B:\$C\$9/B:I\$9*H50) ^ 2 + \$B50 ^ 2)
 F:I97: (F3) 1
 F:A98: ^ dS
 F:B98: (F3) @SQRT((B:C20/B:C\$9*\$B\$40) ^ 2 + (B:\$C\$9*B:C20/B:C\$9 ^ 2*\$B\$40) ^ 2 + (B:\$C\$9/B:C\$9*B51) ^ 2 + \$B51 ^ 2)
 F:C98: (F3) @SQRT((B:D20/B:D\$9*\$B\$40) ^ 2 + (B:\$C\$9*B:D20/B:D\$9 ^ 2*\$C\$40) ^ 2 + (B:\$C\$9/B:D\$9*C51) ^ 2 + \$B51 ^ 2)
 F:D98: (F3) @SQRT((B:E20/B:E\$9*\$B\$40) ^ 2 + (B:\$C\$9*B:E20/B:E\$9 ^ 2*\$D\$40) ^ 2 + (B:\$C\$9/B:E\$9*D51) ^ 2 + \$B51 ^ 2)
 F:E98: (F3) @SQRT((B:F20/B:F\$9*\$B\$40) ^ 2 + (B:\$C\$9*B:F20/B:F\$9 ^ 2*\$E\$40) ^ 2 + (B:\$C\$9/B:F\$9*E51) ^ 2 + \$B51 ^ 2)
 F:F98: (F3) @SQRT((B:G20/B:G\$9*\$B\$40) ^ 2 + (B:\$C\$9*B:G20/B:G\$9 ^ 2*\$F\$40) ^ 2 + (B:\$C\$9/B:G\$9*F51) ^ 2 + \$B51 ^ 2)
 F:G98: (F3) @SQRT((B:H20/B:H\$9*\$B\$40) ^ 2 + (B:\$C\$9*B:H20/B:H\$9 ^ 2*\$G\$40) ^ 2 + (B:\$C\$9/B:H\$9*G51) ^ 2 + \$B51 ^ 2)
 F:H98: (F3) @SQRT((B:I20/B:I\$9*\$B\$40) ^ 2 + (B:\$C\$9*B:I20/B:I\$9 ^ 2*\$H\$40) ^ 2 + (B:\$C\$9/B:I\$9*H51) ^ 2 + \$B51 ^ 2)
 F:I98: (F3) 1
 F:A99: ^ dO =
 F:B99: (F3) 16*(3/54*B86 + 2/47.9*B87 + 3/111.7*B88 + B89/55.85 + B90/54.94 + B91/24.31 + B92/40.08 + B93/46 + B94/78.17 + 5/62*B95)
 F:C99: (F3) 16*(3/54*C86 + 2/47.9*C87 + 3/111.7*C88 + C89/55.85 + C90/54.94 + C91/24.31 + C92/40.08 + C93/46 + C94/78.17 + 5/62*C95)
 F:D99: (F3) 16*(3/54*D86 + 2/47.9*D87 + 3/111.7*D88 + D89/55.85 + D90/54.94 + D91/24.31 + D92/40.08 + D93/46 + D94/78.17 + 5/62*D95)
 F:E99: (F3) 16*(3/54*E86 + 2/47.9*E87 + 3/111.7*E88 + E89/55.85 + E90/54.94 + E91/24.31 + E92/40.08 + E93/46 + E94/78.17 + 5/62*E95)
 F:F99: (F3) 16*(3/54*F86 + 2/47.9*F87 + 3/111.7*F88 + F89/55.85 + F90/54.94 + F91/24.31 + F92/40.08 + F93/46 + F94/78.17 + 5/62*F95)
 F:G99: (F3) 16*(3/54*G86 + 2/47.9*G87 + 3/111.7*G88 + G89/55.85 + G90/54.94 + G91/24.31 + G92/40.08 + G93/46 + G94/78.17 + 5/62*G95)
 F:H99: (F3) 16*(3/54*H86 + 2/47.9*H87 + 3/111.7*H88 + H89/55.85 + H90/54.94 + H91/24.31 + H92/40.08 + H93/46 + H94/78.17 + 5/62*H95)
 F:I99: (F3) 1

Appendix D.

Diagrams of Alteration Evaluation, Silver Queen Mine

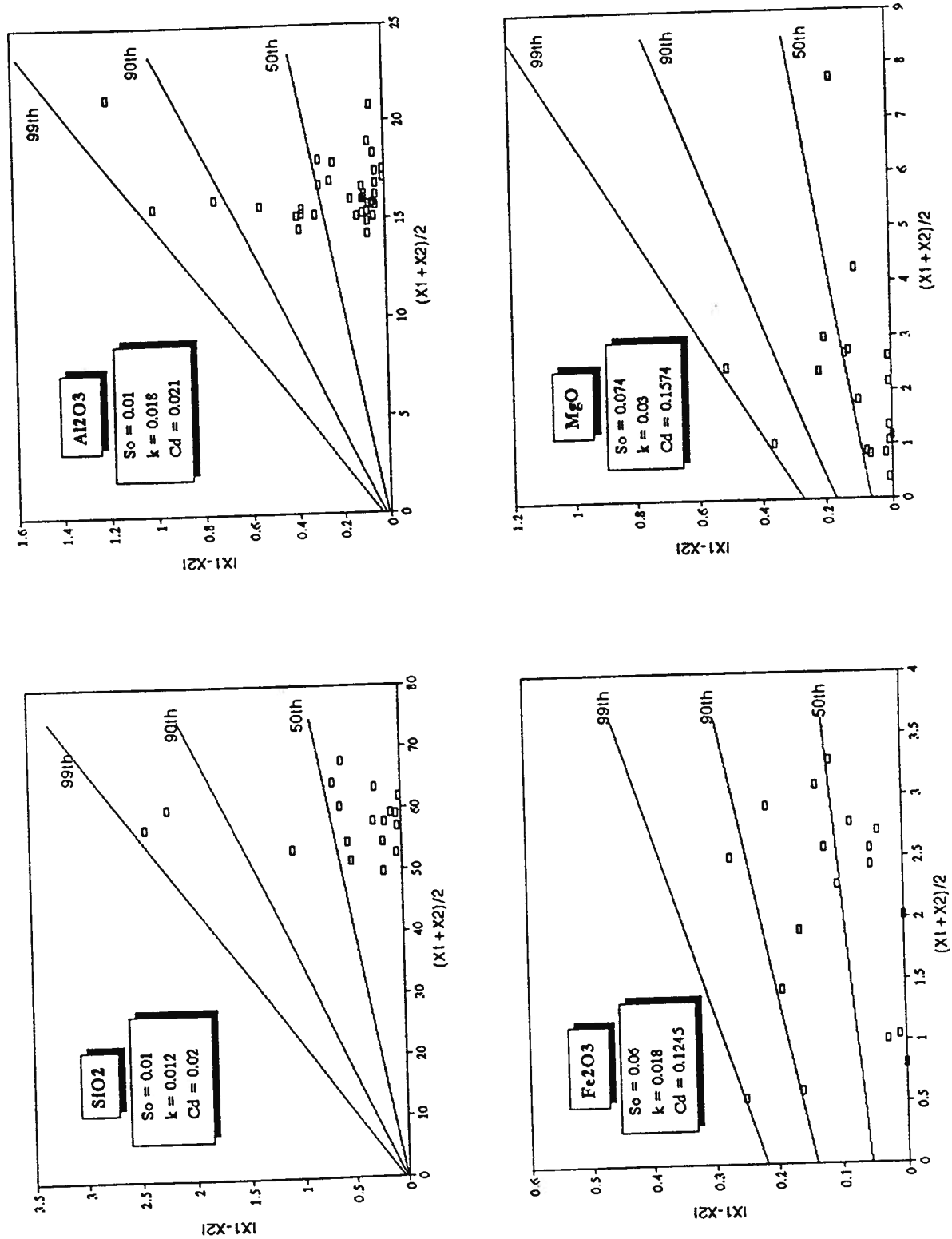


Figure 6-2a. Error of major components estimated by sample duplicates of XRF analyses.

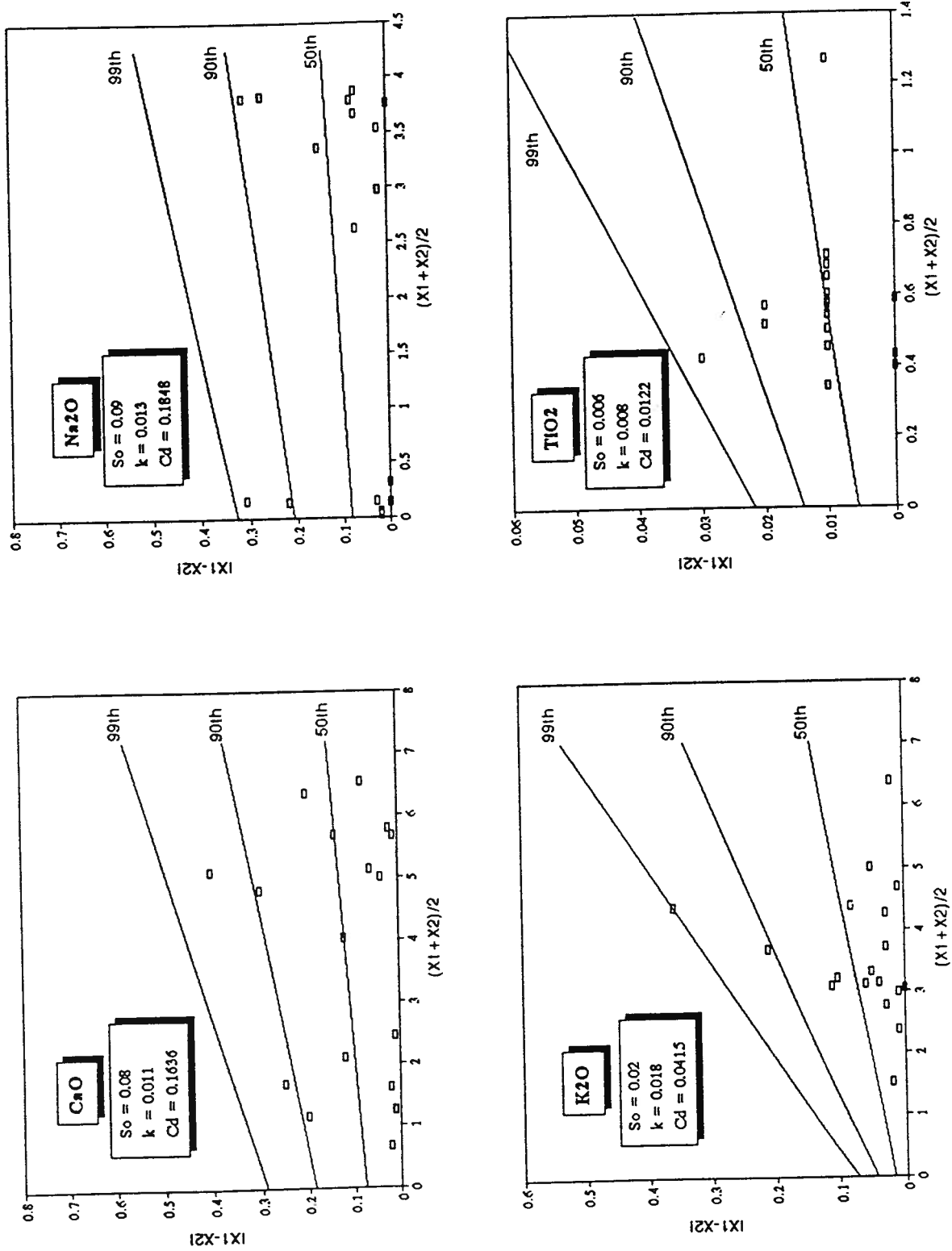


Figure 6-2b. Error of major components estimated by sample duplicates of XRF analyses.

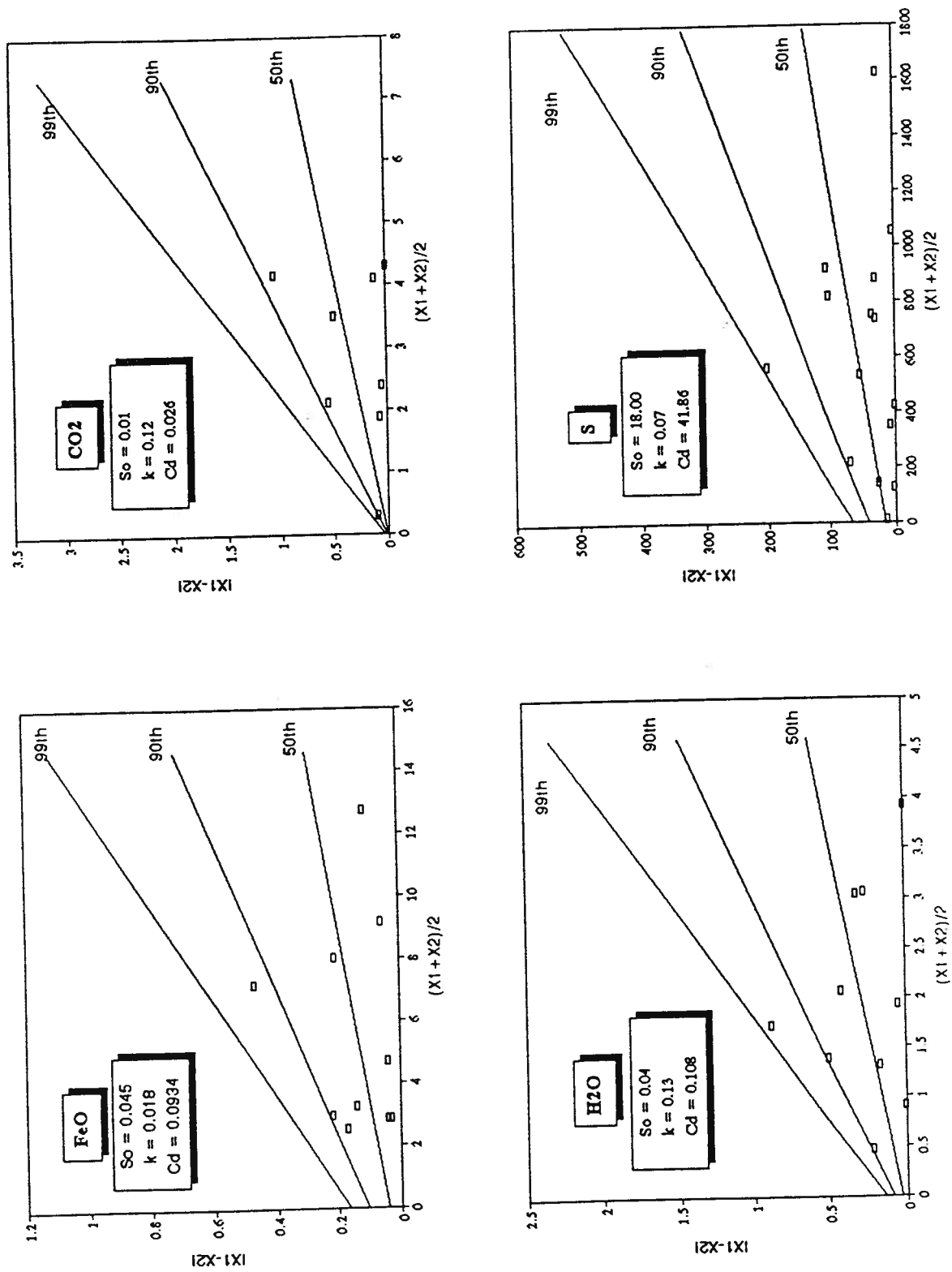


Figure 6-2c. Error of ferrous iron and volatile components estimated by measurement duplicates.

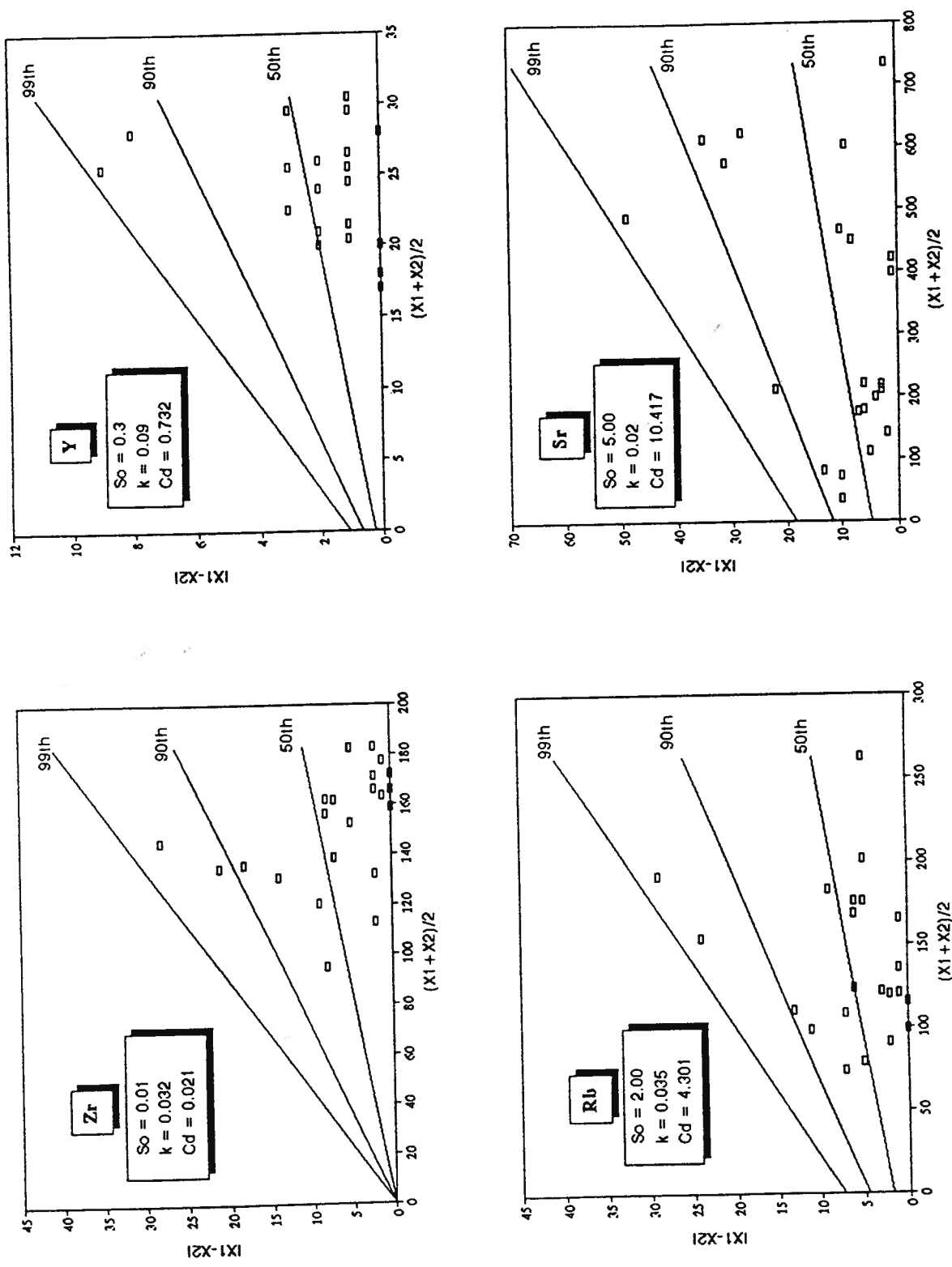


Figure 6-2d. Error of trace elements estimated by duplicates of XRF analyses.

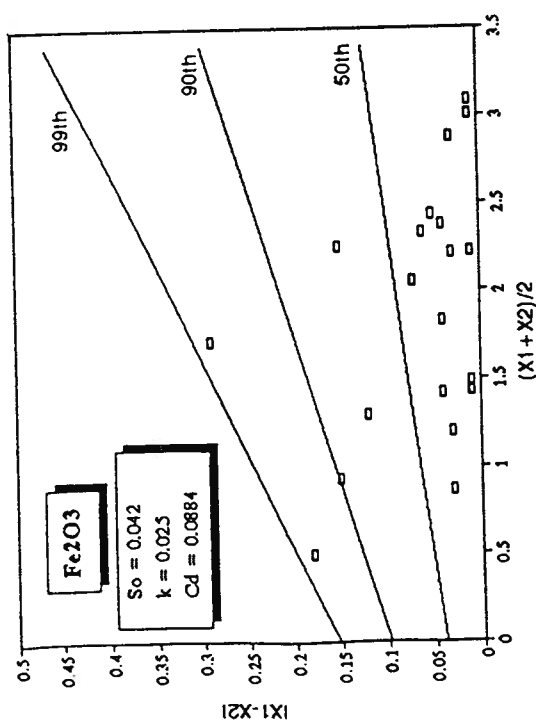
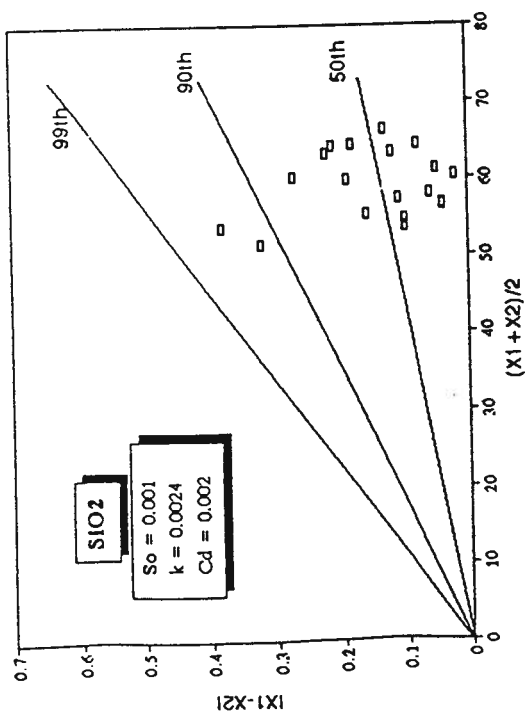
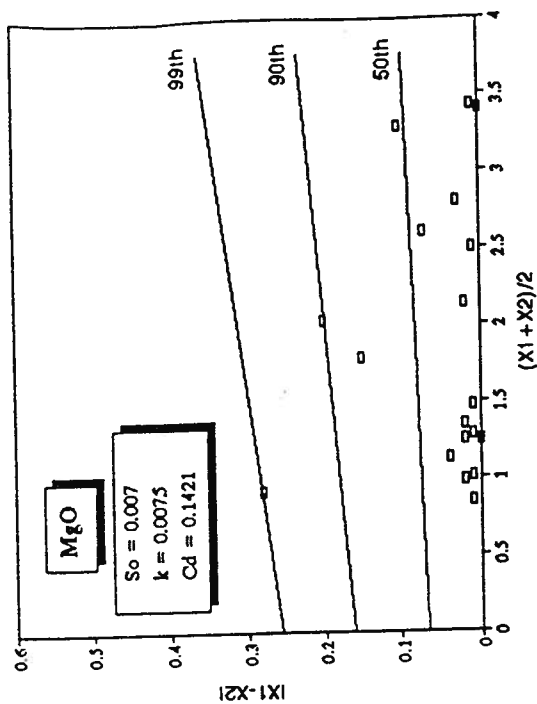
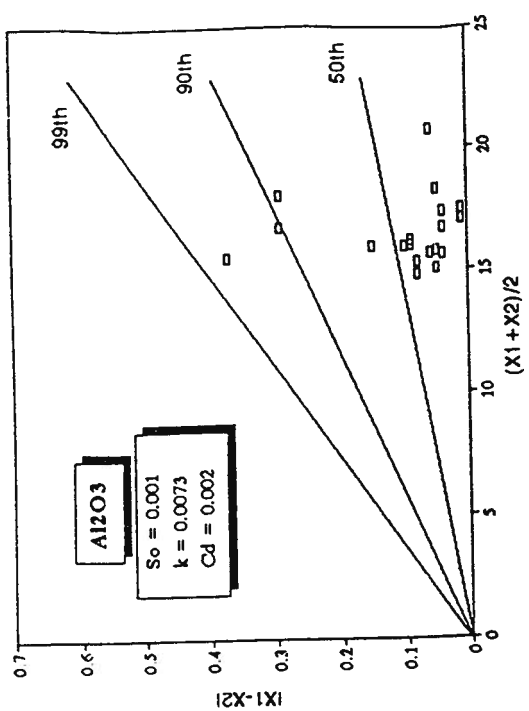


Figure 6-3a. Error of major components estimated by measurement duplicates of XRF analyses.

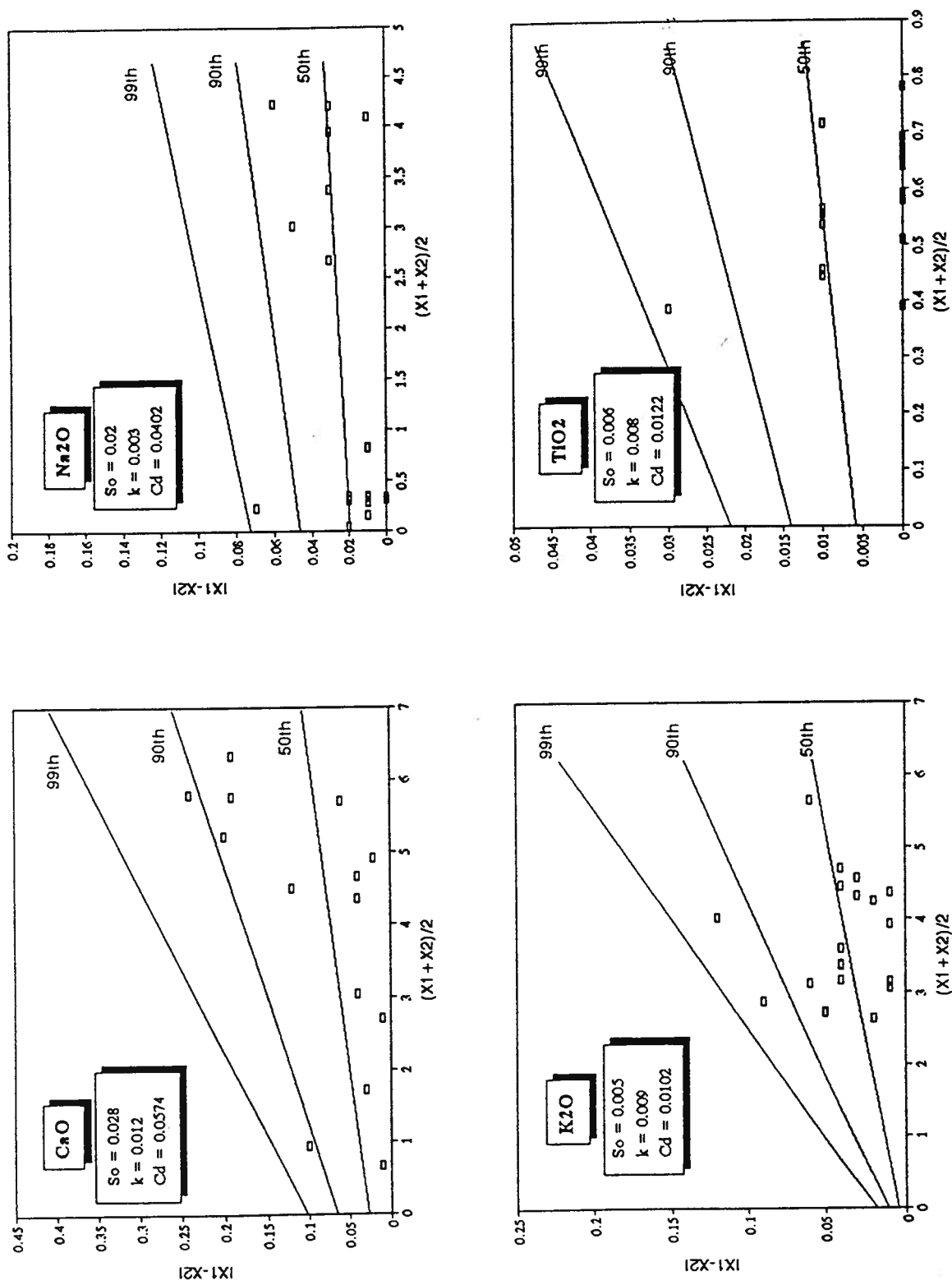


Figure 6-3b. Error of major components estimated by measurement duplicates of XRF analyses.

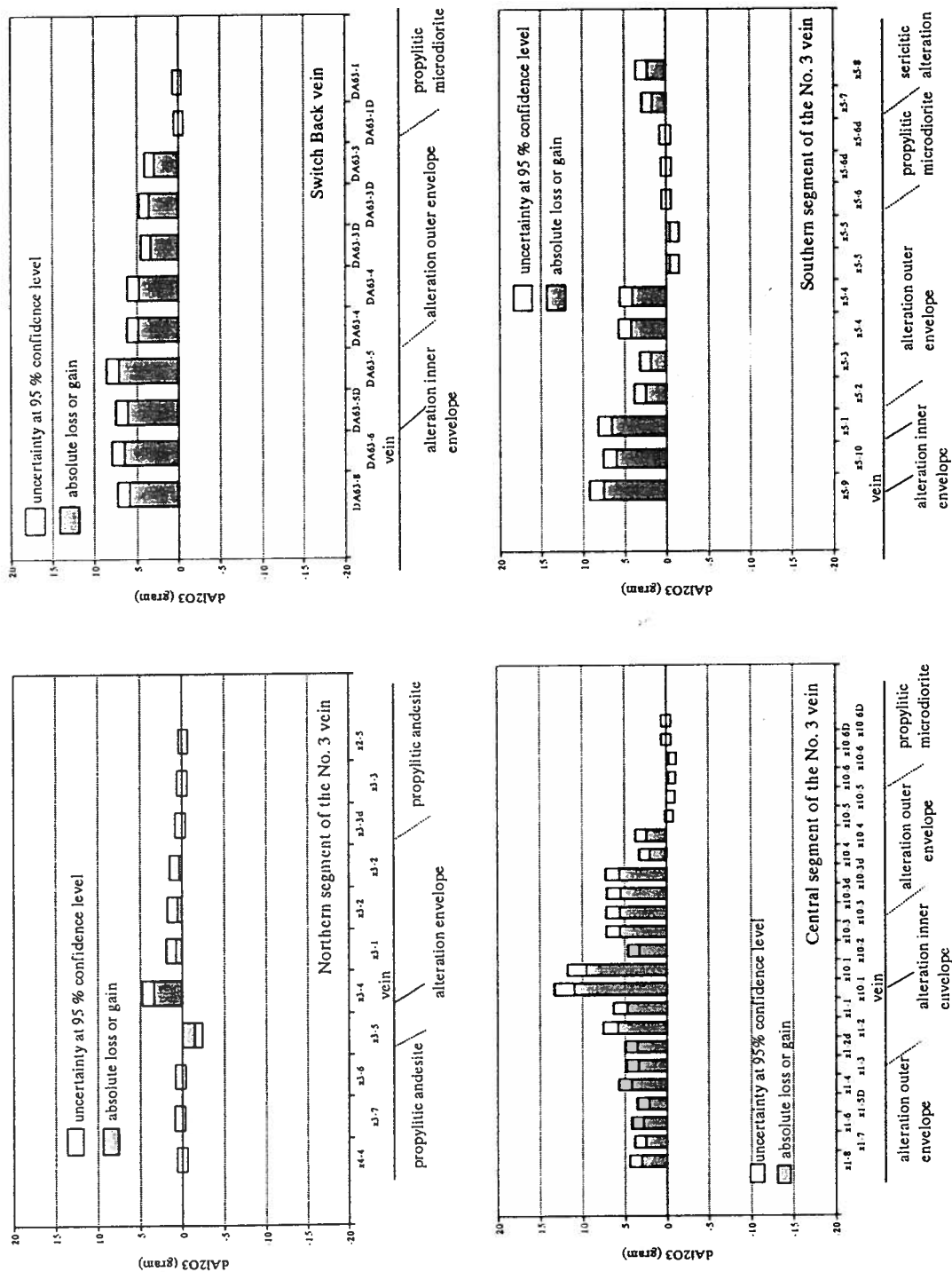


Figure 6-5b. Absolute losses and gains of Al_2O_3 from four alteration profiles at the Silver Queen mine, central British Columbia. The blank part of each bar includes the mean estimate (a horizontal imaginary line through the centre of the blank bar) and a range representing ± 2 standard deviations.

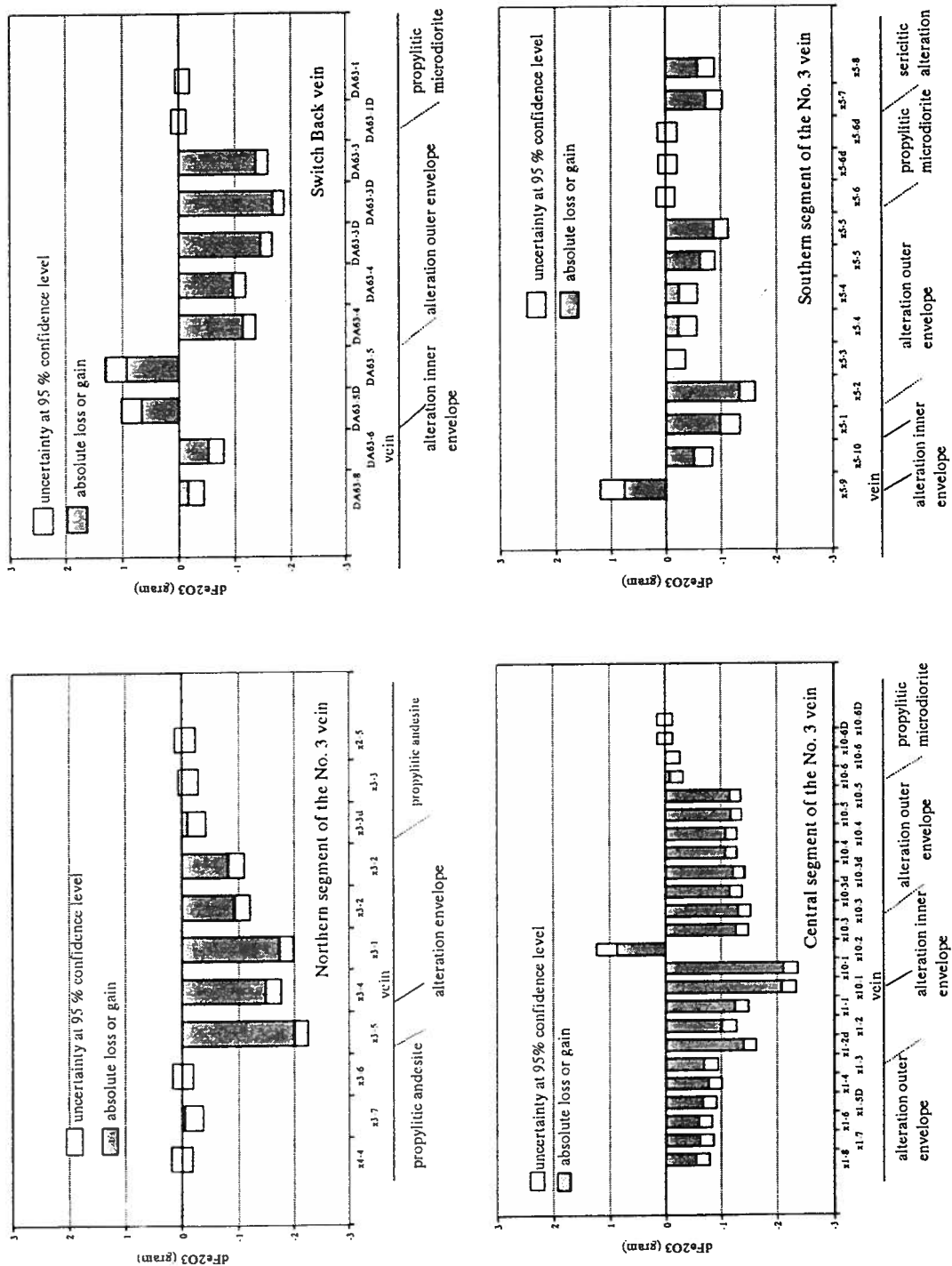


Figure 6-5c. Absolute losses and gains of Fe_2O_3 from four alteration profiles at the Silver Queen mine, central British Columbia. The blank part of each bar includes the mean estimate (a horizontal imaginary line through the centre of the blank bar) and a range representing ± 2 standard deviations.

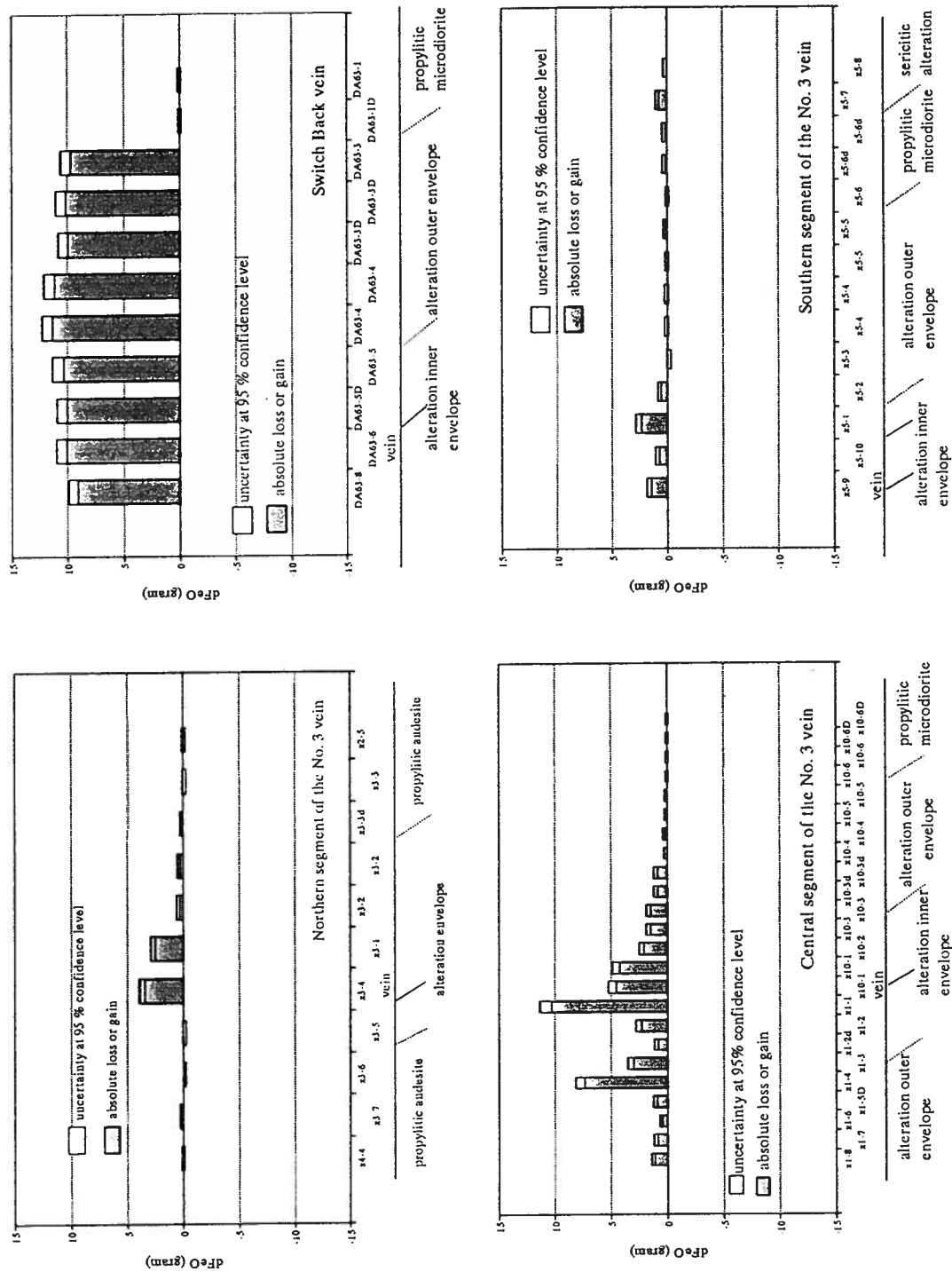


Figure 6-5d. Absolute losses and gains of FeO from four alteration profiles at the Silver Queen mine, central British Columbia. The blank part of each bar includes the mean estimate (a horizontal imaginary line through the centre of the blank bar) and a range representing ± 2 standard deviations.

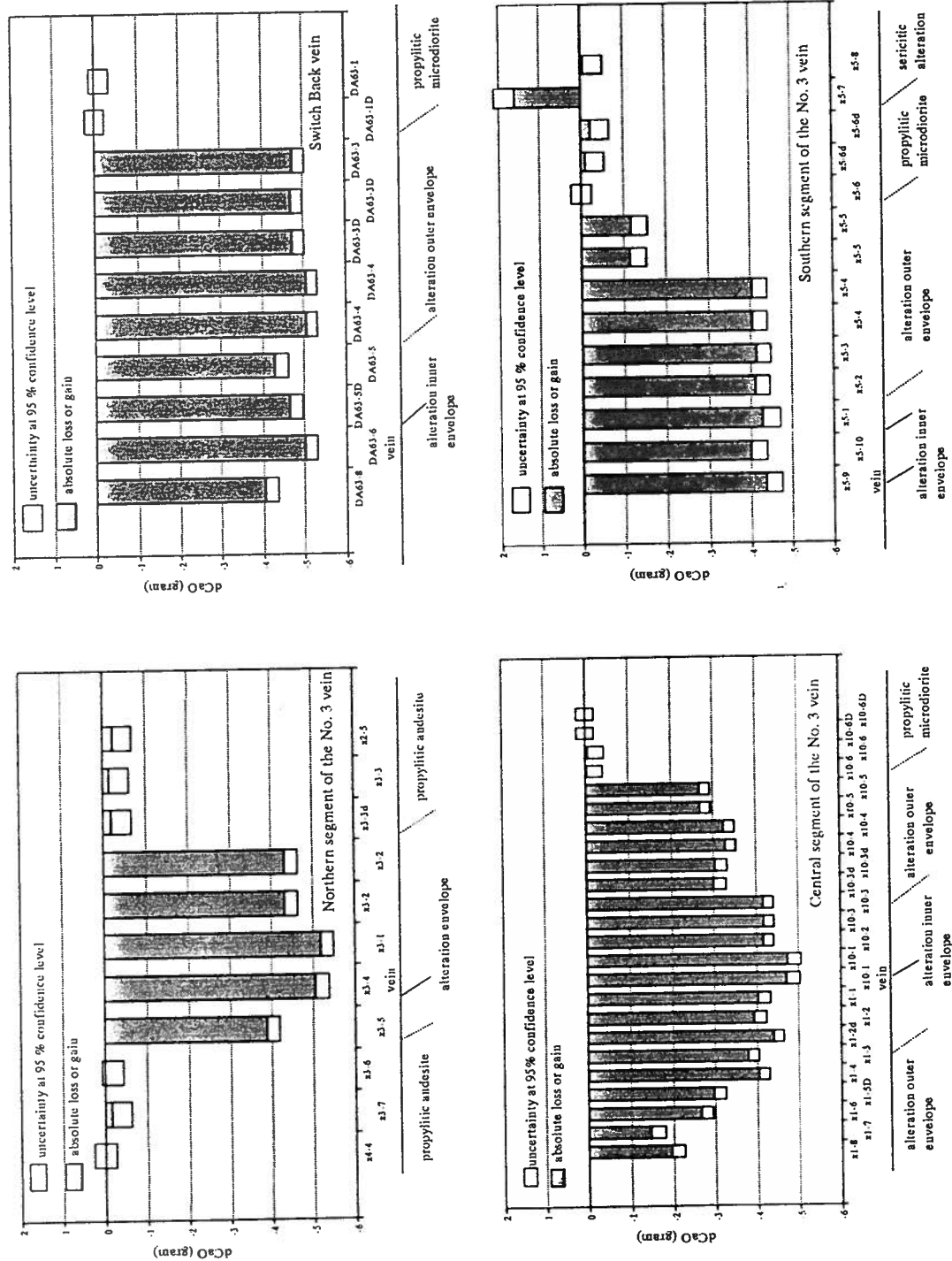


Figure 6-5g. Absolute losses and gains of CaO from four alteration profiles at the Silver Queen mine, central British Columbia. The blank part of each bar includes the mean estimate (a horizontal imaginary line through the centre of the blank bar) and a range representing ± 2 standard deviations.

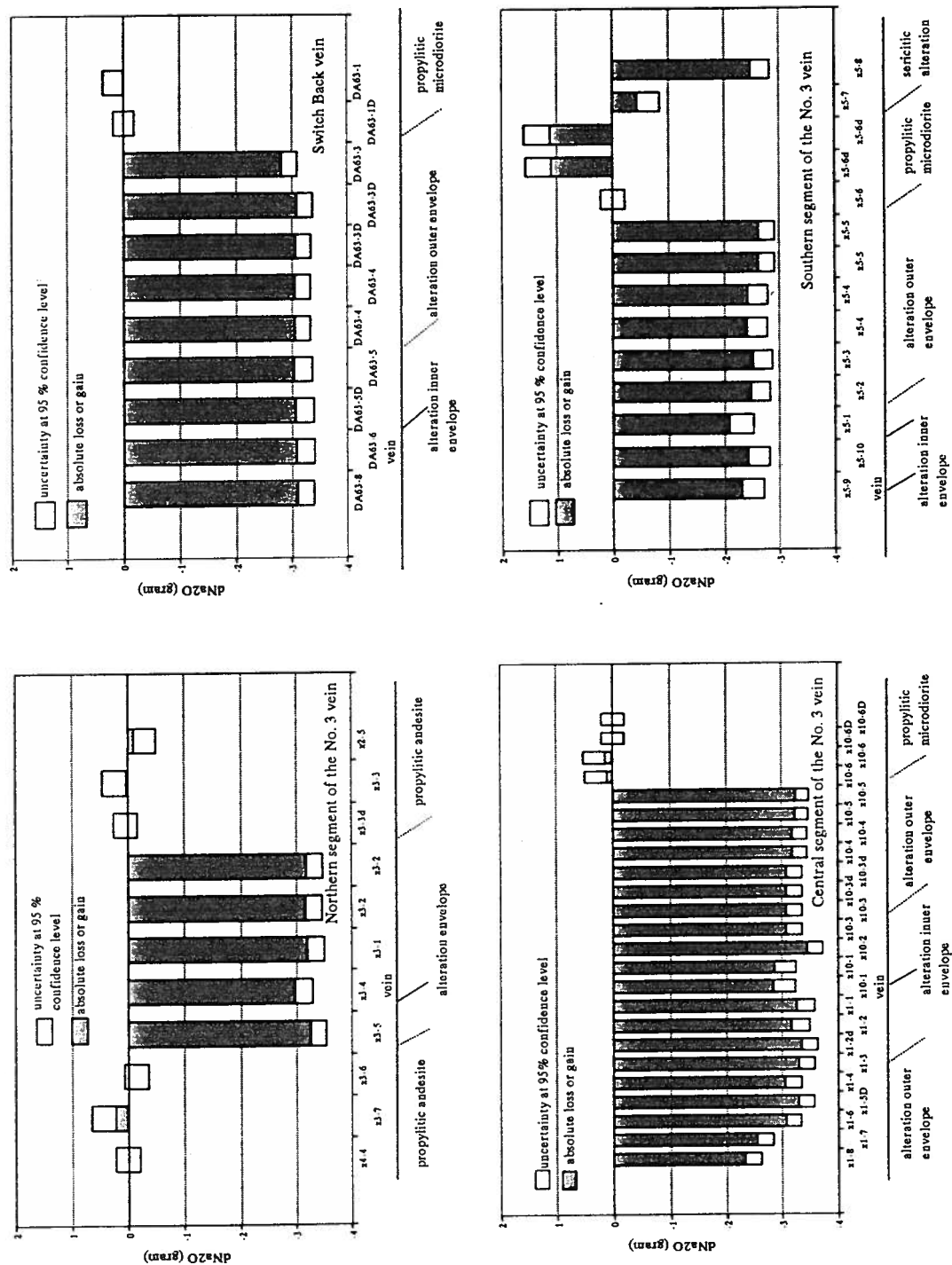


Figure 6-5h. Absolute losses and gains of Na_2O from four alteration profiles at the Silver Queen mine, central British Columbia. The blank part of each bar includes the mean estimate (a horizontal imaginary line through the centre of the blank bar) and a range representing ± 2 standard deviations.

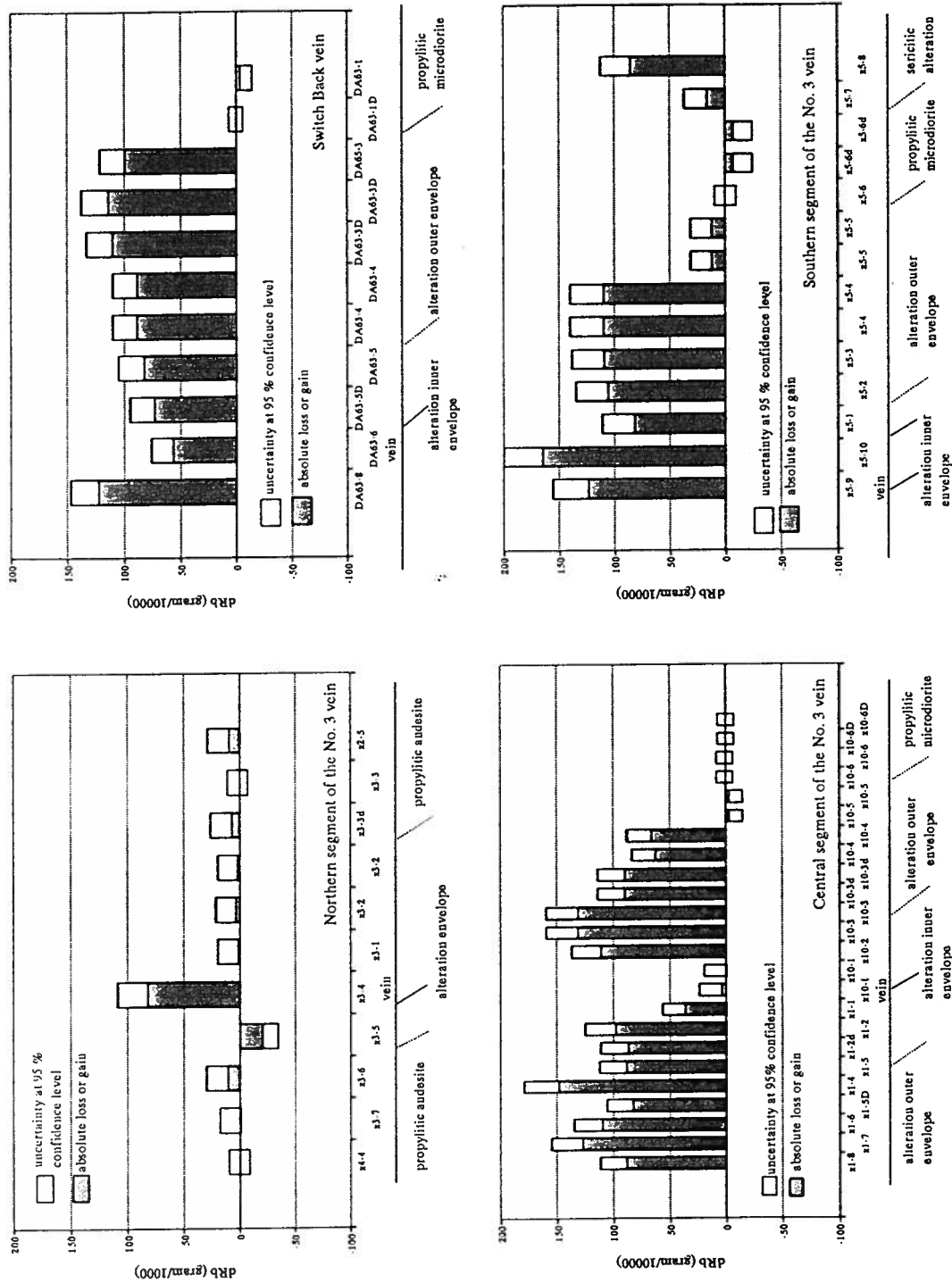


Figure 6-5j. Absolute losses and gains of Rb from four alteration profiles at the Silver Queen mine, central British Columbia. The blank part of each bar includes the mean estimate (a horizontal imaginary line through the centre of the blank bar) and a range representing ± 2 standard deviations.

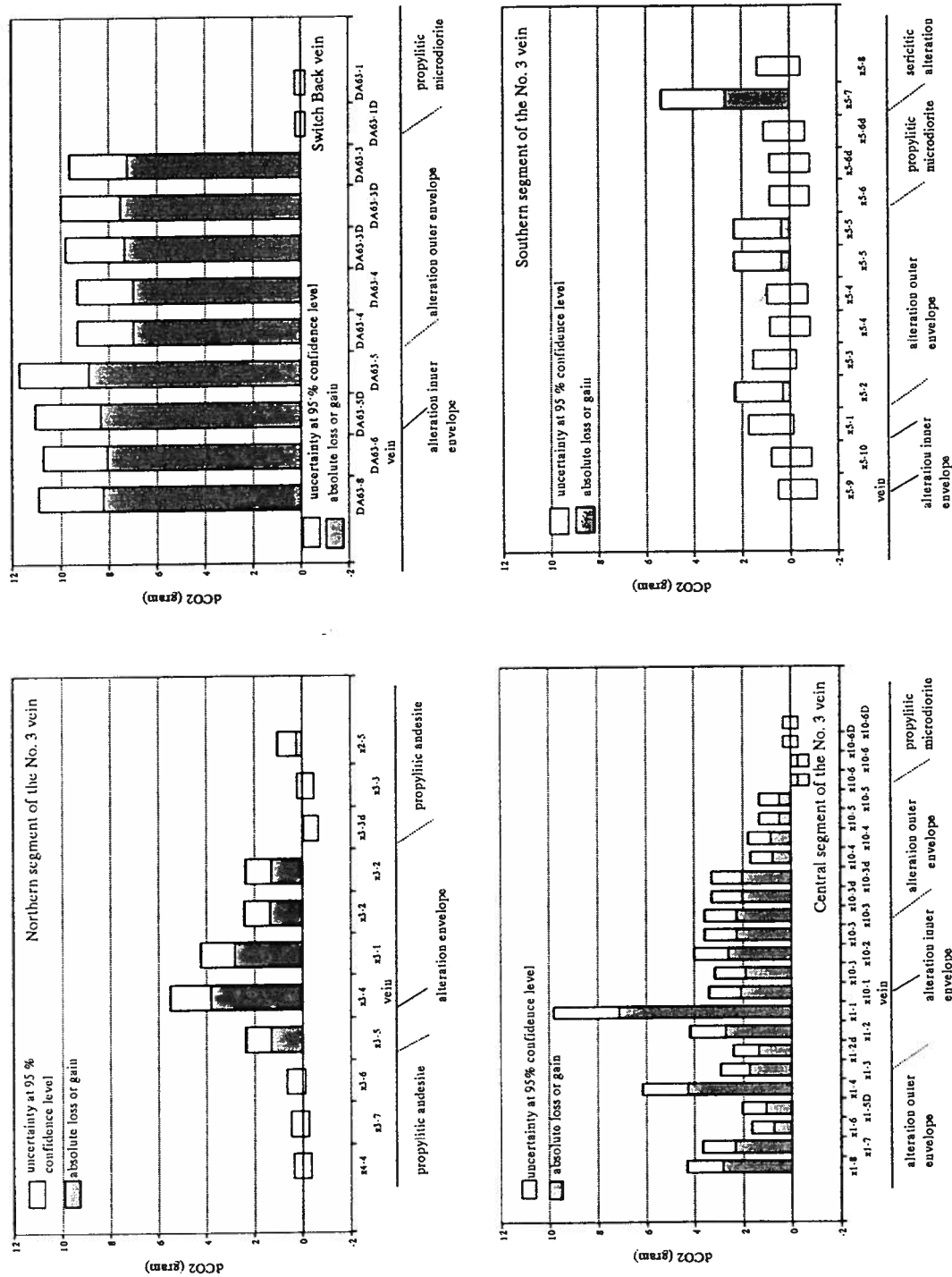


Figure 6-51. Absolute losses and gains of CO_2 from four alteration profiles at the Silver Queen mine, central British Columbia. The blank part of each bar includes the mean estimate (a horizontal imaginary line through the centre of the blank bar) and a range representing ± 2 standard deviations.

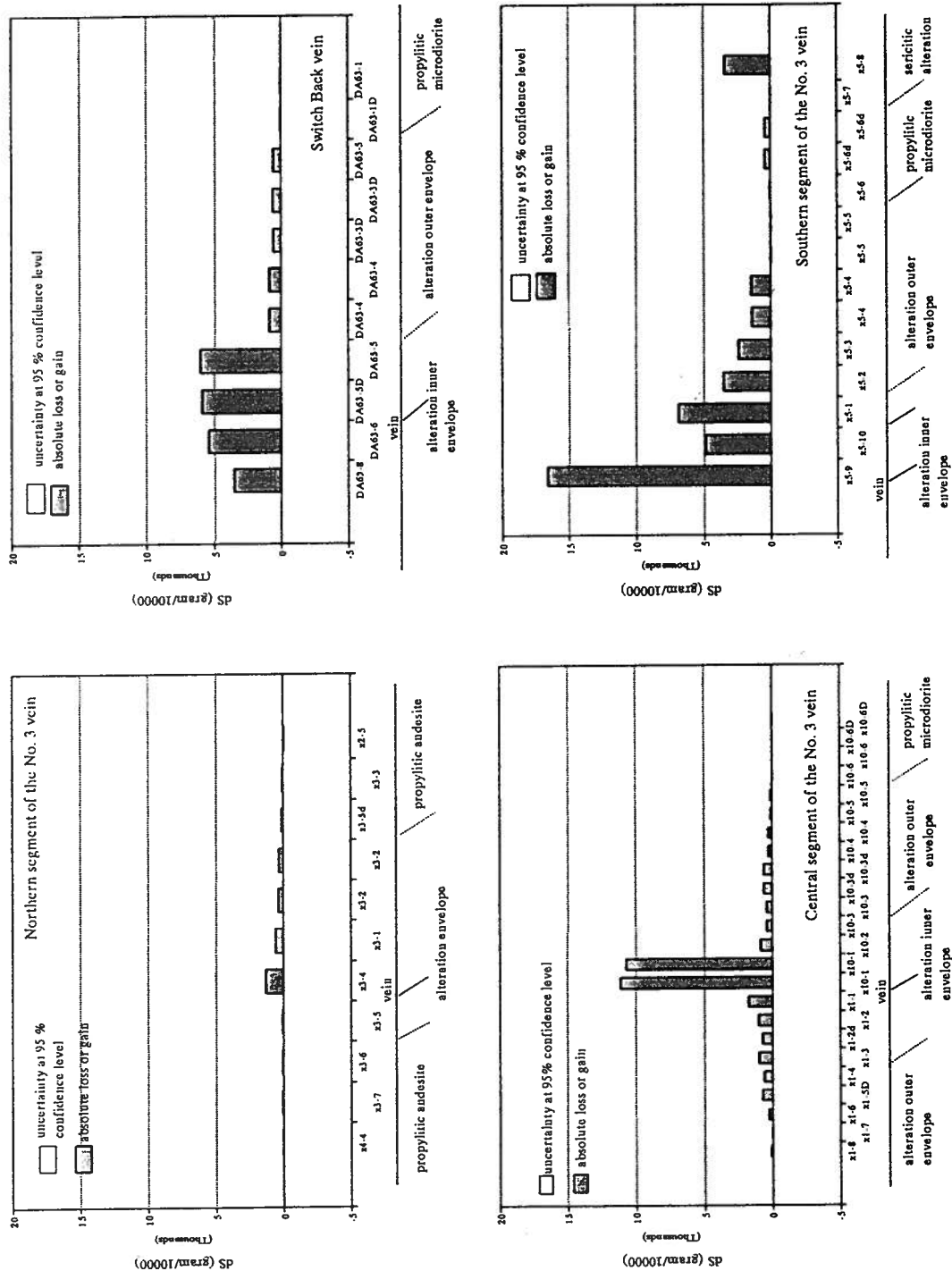


Figure 6-5m. Absolute losses and gains of S from four alteration profiles at the Silver Queen mine, central British Columbia. The blank part of each bar includes the mean estimate (a horizontal imaginary line through the centre of the blank bar) and a range representing ± 2 standard deviations.

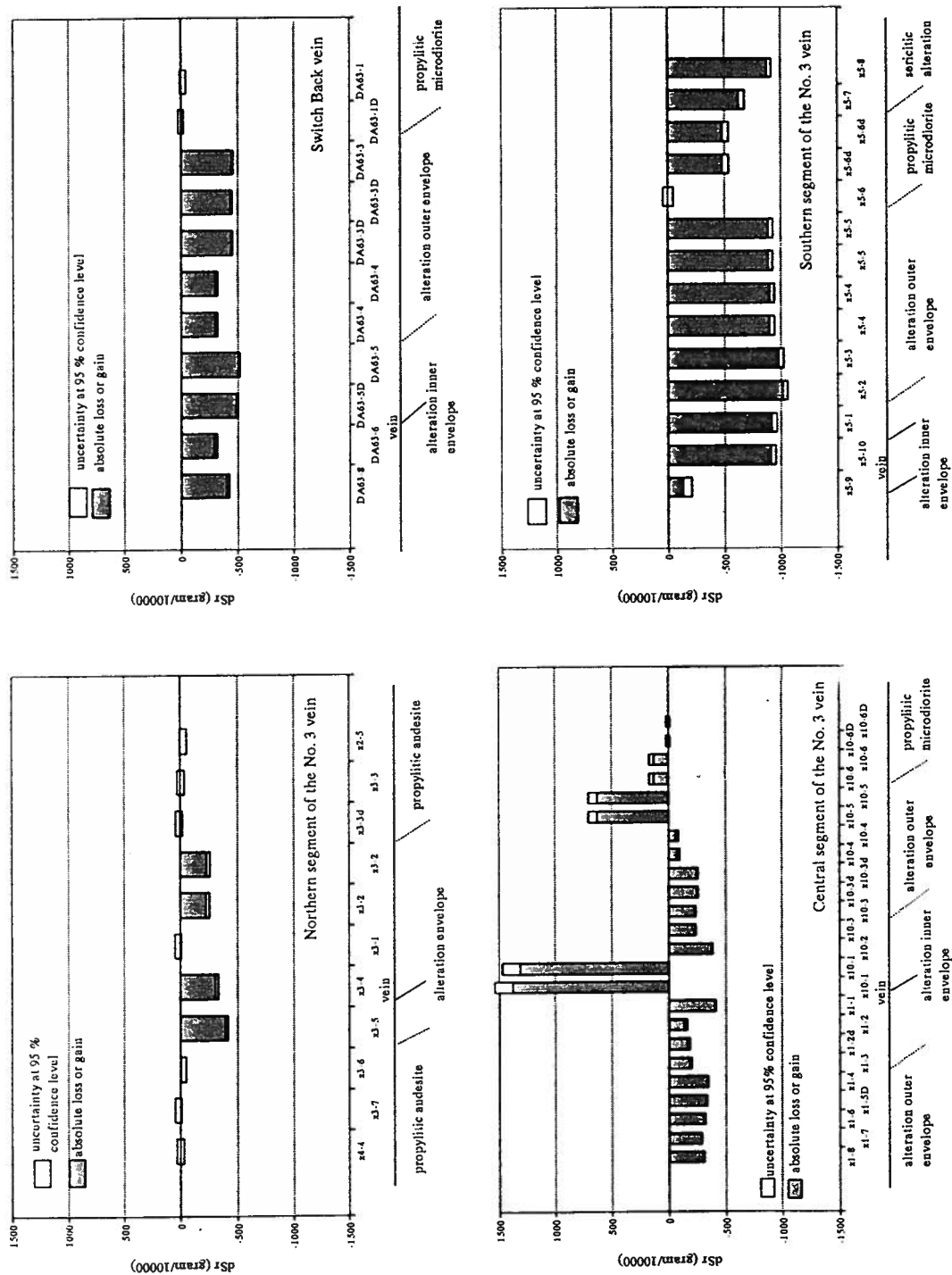


Figure 6-5n. Absolute losses and gains of Sr from four alteration profiles at the Silver Queen mine, central British Columbia. The blank part of each bar includes the mean estimate (a horizontal imaginary line through the centre of the blank bar) and a range representing ± 2 standard deviations.

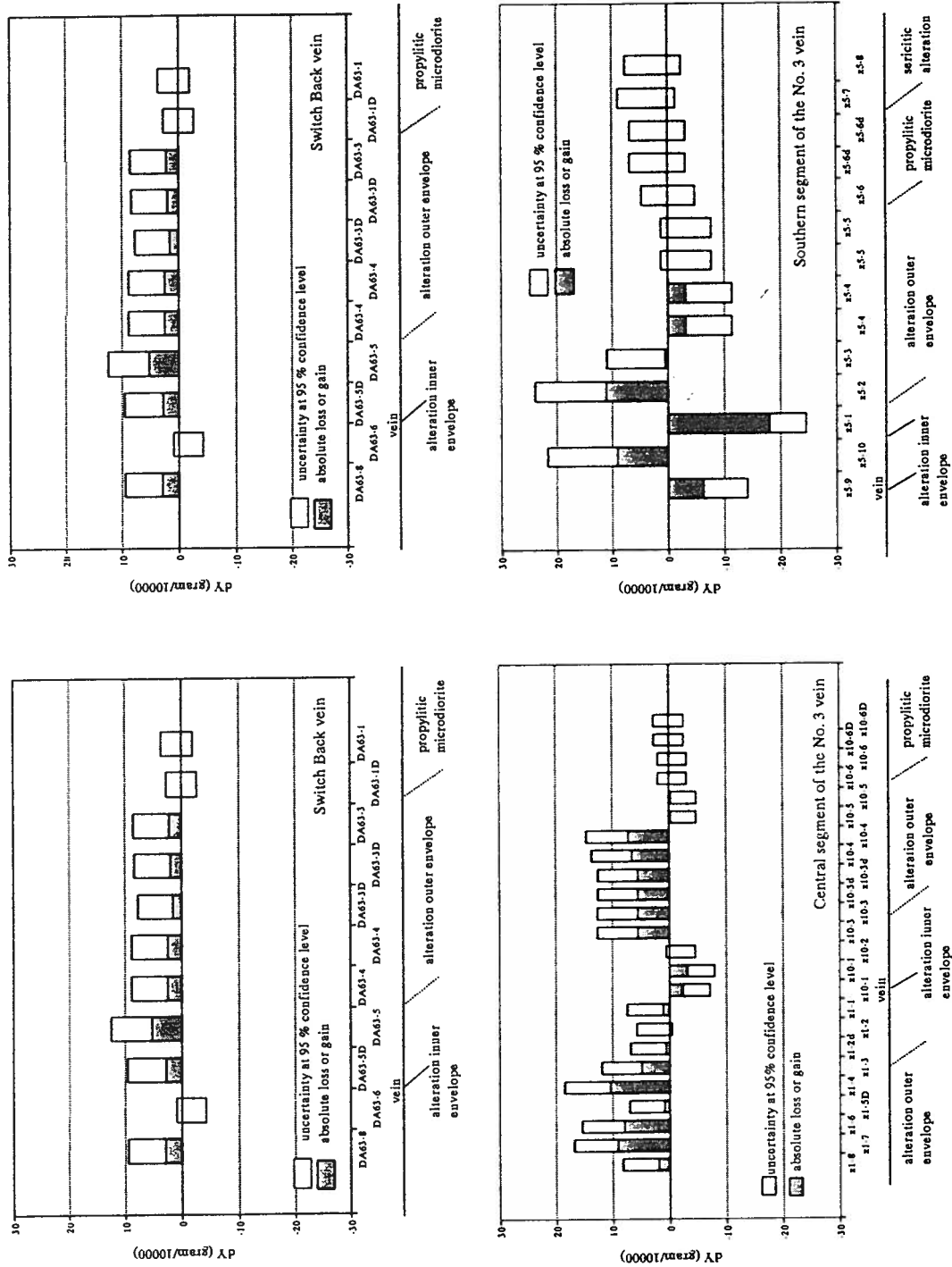


Figure 6-50. Absolute losses and gains of Y from four alteration profiles at the Silver Queen mine, central British Columbia. The blank part of each bar includes the mean estimate (a horizontal imaginary line through the centre of the blank bar) and a range representing ± 2 standard deviations.



Figure 6-5p. Absolute losses and gains of P_2O_5 from four alteration profiles at the Silver Queen mine, central British Columbia. The blank part of each bar includes the mean estimate (a horizontal imaginary line through the centre of the blank bar) and a range representing ± 2 standard deviations.

Appendix E.
Tables of Alteration Evaluation, Silver Queen Mine

Table 6-5. Lithogeochemical data of altered rocks at the Silver Queen mine, central British Columbia

Sample Alteration* Rock type	x4-4 prop. andesite	x3-7 prop. andesite	x3-6 prop. andesite	x3-5 ser-arg andesite	x3-4 ser-arg andesite	x3-1 arg andesite	x3-2 ser-arg andesite	x3-2 ser-arg andesite	x3-3d prop. andesite	x3-3 prop. andesite
Location	North segmen of No.3 vein	North segmen of No.3 vein	North segmen of No.3 vein	North segmen of No.3 vein	North segmen of No.3 vein	North segmen of No.3 vein	North segmen of No.3 vein	North segmen of No.3 vein	North segmen of No.3 vein	North segmen of No.3 vein
wt %										
SiO ₂	57.86	57.97	57.20	58.45	56.67	57.25	59.94	59.94	57.59	57.75
Al ₂ O ₃	15.61	15.87	16.03	18.11	17.27	17.45	18.30	18.30	15.80	15.85
TiO ₂	0.65	0.65	0.66	0.87	0.57	0.67	0.71	0.71	0.65	0.66
Fe ₂ O ₃	3.09	2.86	3.12	1.26	1.26	1.25	2.18	2.18	2.81	3.02
FeO	2.89	3.05	2.70	3.69	5.78	5.82	3.65	3.65	3.08	2.86
MnO	0.34	0.20	0.23	1.34	1.65	1.57	0.59	0.59	0.35	0.31
MgO	2.94	2.64	2.61	0.90	1.15	1.09	0.97	0.97	3.07	2.87
CaO	6.07	5.66	5.97	2.69	0.73	0.73	1.70	1.70	5.61	5.75
Na ₂ O	3.65	4.09	3.55	0.31	0.44	0.29	0.35	0.35	3.69	3.96
K ₂ O	3.09	2.92	3.04	2.34	4.12	2.77	3.37	3.37	3.13	3.02
P ₂ O ₅	0.38	0.38	0.40	0.27	0.19	0.20	0.26	0.26	0.39	0.39
H ₂ O	0.97	1.27	2.18	4.39	2.69	3.9	3.93	3.93	1.84	1.14
CO ₂	2.03	2.14	2.34	5.2	5.9	5.75	4.3	4.3	1.65	1.92
S	0.013	0.018	0.016	0.029	0.127	0.073	0.056	0.056	0.025	0.018
Total	99.58	99.72	100.05	99.85	98.55	98.81	100.31	100.31	99.69	99.52
ppm										
ZR	191	192	188	220	163	188	198	198	180.19	185.22
Y	28	30	28	32	12	23	27	27	23.62	31.91
Rb	100	108	123	96	172	114	123	123	117.16	103.70
Sr	593	607	567	238	231	630	376	376	605.75	597.08
Distance**	25.0	15.0	4.9	1.9	0.9	0.5	-2.5	-2.5	-16.0	-8.0
Density	2.80	2.68	2.76	2.62	2.84	2.76			2.74	2.66

* prop - propylitization; ser-arg - sericitization and argillization; silicic - silicification and pyritization.

** distance from the vein in metres, + in hanging-wall side and - in footwall side.

Table 6-5 (continued-1) Lithogeochemical data of altered rocks at Silver Queen mine, central British Columbia

Sample Alteration Rock type	x2-5 prop. andesite	DA63-8 s-salt m. diorite*	DA63-6 s-salt m. diorite	DA63-5D silicic m. diorite	DA63-5 silicic m. diorite	DA63-4 ser-arg m. diorite	DA63-4 ser-arg m. diorite	DA63-3D ser-arg m. diorite	DA63-3D ser-arg m. diorite	DA63-3 ser-arg m. diorite
Location	North segmen of No.3 vein	Switch back Vein	Switch back Vein	Switch back Vein	Switch back Vein	Switch back Vein	Switch back Vein	Switch back Vein	Switch back Vein	Switch back Vein
wt %										
SiO ₂	57.29	49.14	53.00	54.59	54.41	48.40	48.43	51.36	51.68	51.19
Al ₂ O ₃	15.70	17.09	16.59	14.95	15.34	18.16	18.07	16.29	16.20	16.24
TiO ₂	0.66	0.53	0.50	0.46	0.45	0.59	0.59	0.57	0.56	0.58
Fe ₂ O ₃	3.08	1.48	1.15	2.02	2.15	0.86	1.01	0.59	0.41	0.66
FeO	2.92	9.83	9.94	9.13	9.14	12.79	12.68	11.24	11.24	11.24
MnO	0.25	2.46	0.81	0.63	0.69	0.90	0.90	0.98	0.98	0.98
MgO	3.33	0.90	0.69	0.87	0.80	1.21	1.21	1.36	1.34	1.35
CaO	5.67	1.64	0.89	1.04	1.24	1.02	1.02	1.24	1.24	1.25
Na ₂ O	3.39	0.01	0.02	0.02	0.04	0.06	0.06	0.05	0.03	0.25
K ₂ O	3.15	4.11	3.48	3.29	3.34	4.04	4.05	4.26	4.24	4.27
P ₂ O ₅	0.37	0.21	0.28	0.29	0.31	0.29	0.29	0.26	0.25	0.28
H ₂ O	1.04	2.83	2.93	2.88	2.88	3.01	3.01	2.14	2.14	2.14
CO ₂	2.75	8.04	7.45	7.05	7.25	7.79	7.79	7.85	7.85	7.85
S	0.003	0.2673	0.3849	0.3815	0.3815	0.0825	0.0825	0.0566	0.0566	0.0566
Total	99.60	98.54	98.11	97.60	98.42	99.20	99.19	98.25	98.22	98.34
ppm										
Zr	178.64	104.20	100.64	98.78	91.49	128.98	128.98	112.23	112.23	114.43
Y	33.05	23.18	16.39	20.10	21.35	25.39	25.39	23.69	23.69	24.75
Rb	121.40	175.61	118.44	120.07	123.33	166.47	166.47	178.76	178.76	173.06
Sr	573.45	160.12	225.10	86.99	73.83	260.16	260.16	142.96	142.96	141.19
Distance	-26.0	-1.0	-1.0	1.0	1.0	2.0	2.0	4.0	4.0	4.0
Density		2.89	2.95			2.85				2.78

* m.diorite - microdiorite

Table 6-5 (continued-2) Lithogeochemical data of altered rocks at the Silver Queen mine, central British Columbia

Sample Alteration Rock type	DA63-1D w-alt m. di.	DA63-1 prop. m.diorite	x1-8 ser-arg m.diorite	x1-7 ser-arg m.diorite	x1-6 ser-arg m.diorite	x1-5D ser-arg m.diorite	x1-4 ser-arg m.diorite	x1-3 silicic m.diorite	x1-2d silicic m.diorite	x1-2 silicic m.diorite
Location	Switch back Vein	Switch back Vein	Central segme of No.3 vein	Central segme of No.3 vein	Central segme of No.3 vein	Central segme of No.3 vein	Central segme of No.3 vein	Central segme of No.3 vein	Central segme of No.3 vein	Central segme of No.3 vein
wt %										
SiO ₂	57.72	57.99	60.43	59.43	61.11	64.18	57.46	64.23	68.44	67.14
Al ₂ O ₃	16.63	16.53	16.90	16.44	17.60	15.65	15.93	15.50	15.38	14.51
TiO ₂	0.72	0.71	0.43	0.43	0.45	0.42	0.38	0.39	0.38	0.32
Fe ₂ O ₃	2.32	2.22	1.58	1.51	1.61	1.43	1.23	1.30	0.76	0.87
FeO	3.76	3.76	3.53	3.36	3.07	3.26	8.05	4.70	2.93	3.46
MnO	0.16	0.16	0.42	0.81	0.65	1.10	0.98	0.81	0.68	1.36
MgO	2.62	2.63	1.52	1.54	1.36	1.04	1.38	0.92	0.93	1.06
CaO	6.45	6.25	2.61	3.01	2.11	1.69	0.74	0.95	0.47	0.68
Na ₂ O	3.28	3.43	0.99	0.79	0.37	0.16	0.32	0.14	0.09	0.19
K ₂ O	3.26	3.16	4.69	5.61	5.73	4.37	4.98	4.02	4.04	3.53
P ₂ O ₅	0.43	0.43	0.16	0.15	0.15	0.16	0.11	0.15	0.16	0.12
H ₂ O	0.93	0.93	2.03	2.25	2.51	2.43	1.63	2.14	1.90	1.95
CO ₂	1.34	1.34	5.16	4.66	3.24	3.30	5.80	3.65	3.26	3.75
S	0.0122	0.0122	0.028	0.019	0.041	0.080	0.062	0.091	0.073	0.080
Total	99.63	99.55	100.45	100.01	99.99	99.25	99.03	98.97	99.50	99.01
ppm										
ZR	164.70	158.38	171.40	165.87	166.25	156.04	161.74	161.90	158.67	134.75
Y	25.23	25.75	25.86	32.51	32.94	23.94	29.89	25.59	21.74	17.61
Rb	103.70	92.65	187.90	223.70	217.03	176.68	214.85	168.89	165.81	147.60
Sr	636.30	608.28	137.58	157.42	132.04	111.36	90.54	209.32	219.70	201.17
Distance	6.0	6.0	-27.0	-14.0	-7.0	-3.2	-2.4	-1.6	-0.8	-0.6
Density		2.7	2.7	2.68				2.72		2.65

Table 6-5 (continued-3) Lithochemochemical data of altered rocks at the Silver Queen mine, central British Columbia

Sample Alteration Rock type	x1-1 silicic m.diorite	x10-1 silicic m.diorite	x10-1 silicic m.diorite	x10-2 silicic m.diorite	x10-3 ser-arg m.diorite	x10-3 ser-arg m.diorite	x10-3d ser-arg m.diorite	x10-3d ser-arg m.diorite	x10-4 ser-arg m.diorite	x10-4 ser-arg m.diorite
Location	Central segme of No.3 vein	Central segme of No.3 vein	Central segme of No.3 vein	Central segme of No.3 vein	Central segme of No.3 vein	Central segme of No.3 vein	Central segme of No.3 vein	Central segme of No.3 vein	Central segme of No.3 vein	Central segme of No.3 vein
wt %										
SiO ₂	59.05	71.11	71.21	59.19	63.27	63.39	63.27	63.24	64.19	64.27
Al ₂ O ₃	14.32	14.09	13.87	16.35	17.41	17.37	17.76	17.88	17.08	17.07
TiO ₂	0.33	0.25	0.26	0.41	0.39	0.39	0.40	0.40	0.46	0.45
Fe ₂ O ₃	0.76	0.15	0.14	2.93	0.88	0.85	0.99	0.95	1.22	1.19
FeO	9.14	3.86	3.86	4.20	3.52	3.52	3.11	3.11	2.75	2.75
MnO	1.04	0.08	0.09	1.66	0.95	0.96	0.49	0.49	0.36	0.37
MgO	0.97	0.44	0.46	0.93	1.01	1.00	1.05	1.02	1.25	1.25
CaO	0.64	0.13	0.13	0.70	0.66	0.67	1.60	1.58	1.60	1.60
Na ₂ O	0.13	0.29	0.29	0.03	0.31	0.31	0.32	0.32	0.28	0.27
K ₂ O	2.77	2.06	2.09	4.29	5.67	5.61	4.98	4.98	4.36	4.37
P ₂ O ₅	0.14	0.08	0.08	0.19	0.12	0.11	0.13	0.14	0.15	0.14
H ₂ O	2.37	3.14	3.14	2.76	1.86	1.86	2.27	2.27	2.51	2.51
CO ₂	7.25	2.58	2.58	4.69	4.15	4.15	4.04	4.04	3.35	3.35
S	0.132	0.565	0.565	0.0867	0.0458	0.0458	0.0659	0.0659	0.0421	0.0423
Total	99.04	98.83	98.77	98.42	100.25	100.24	100.48	100.49	99.60	99.63
ppm										
Zr	132.35	118.57	118.57	150.32	177.68	177.68	178.24	178.24	208.88	208.88
Y	19.48	10.00	10.00	18.75	26.48	26.48	27.14	27.14	32.22	32.22
Rb	110.08	66.37	66.37	198.96	206.06	206.06	176.79	176.79	176.58	176.58
Sr	35.37	968.62	968.62	69.07	179.10	179.10	171.81	171.81	346.02	346.02
Distance	-0.3	1.2	1.2	4.0	5.5	5.5	7.5	7.5	20.0	20.0
Density	2.81	2.87			2.58				2.9	

Table 6-5 (continued-4) Lithogeochemical data of altered rocks at the Silver Queen mine, central British Columbia

Sample Alteration Rock type	x10-5 ser-arg m.diorite	x10-5 ser-arg m.diorite	x10-6 prop. m.diorite	x10-6 prop m.diorite	x10-6D prop m.diorite	x11-1b w-alt m. di.	x5-9 silicic andesite	x5-10 silicic andesite	x5-1 silicic andesite	x5-2 ser-arg andesite
Location	Central segme of No.3 vein	Central segme of No.3 vein	Central segme of No.3 vein	Central segme of No.3 vein	Central segme of No.3 vein	Bulkley cross cut of No.3 vei	South segment of No.3 vein	South segment of No.3 vein	South segment of No.3 vein	South segment of No.3 vein
wt %										
SiO ₂	59.71	59.90	61.25	61.20	59.00	57.05	64.31	65.91	69.72	62.02
Al ₂ O ₃	18.16	17.87	15.11	15.06	15.98	15.77	16.09	16.06	14.00	15.83
TiO ₂	0.58	0.58	0.58	0.58	0.56	0.69	0.44	0.47	0.40	0.55
Fe ₂ O ₃	1.43	1.44	2.30	2.36	2.52	2.73	2.20	1.18	0.71	0.73
FeO	3.43	3.43	2.86	2.86	2.85	3.77	3.35	3.03	3.60	3.42
MnO	0.31	0.30	0.14	0.14	0.18	0.22	0.08	0.61	0.17	1.55
MgO	1.48	1.47	2.78	2.81	2.18	4.18	1.14	1.22	1.01	1.37
CaO	2.71	2.72	4.92	4.90	5.16	5.78	0.35	0.63	0.36	0.67
Na ₂ O	0.31	0.29	3.93	3.96	3.63	3.76	0.35	0.29	0.44	0.32
K ₂ O	3.34	3.38	3.14	3.15	3.09	2.97	4.69	5.01	3.84	4.76
P ₂ O ₅	0.19	0.19	0.26	0.27	0.34	0.42	0.19	0.16	0.16	0.20
H ₂ O	4.18	4.18	1.39	1.39	1.22	0.91	2.04	2.29	1.86	1.94
CO ₂	3.85	3.85	1.85	1.85	2.4	1.25	2.65	3.01	3.07	4.66
S	0.0357	0.0349	0.0127	0.0127	0.0153	0.0865	1.1367	0.3919	0.4512	0.3487
Total	99.72	99.63	100.52	100.54	99.13	99.59	99.02	100.26	99.79	98.37
ppm										
ZR	211.06	211.06	172.67	172.67	169.80	166.44	115.13	118.69	92.72	115.54
Y	25.66	25.66	24.29	24.29	24.89	30.75	12.80	31.63	5.00	38.76
Rb	126.72	126.72	119.76	119.76	118.77	92.04	162.75	204.09	122.29	187.75
Sr	1322.73	1322.73	510.61	510.61	472.32	630.05	590.47	98.06	75.55	29.55
Distance	38.0	38.0	44.0	44.0	56.0	6.5	-6.5	-6.0	0.3	1.1
Density	2.85		2.83				2.80	2.80	2.80	2.80

Table 6-5 (continued-5) Lithogeochemical data of altered rocks at the Silver Queen mine, central British Columbia

Sample Alteration Rock type	x5-3 ser-arg andesite	x5-4 ser-arg andesite	x5-4 ser-arg andesite	x5-5 ser-arg andesite	x5-5 ser-arg andesite	x5-6 prop andesite	x5-6d prop andesite	x5-6d prop andesite	x5-7 ser-arg andesite
Location	South segment of No.3 vein	South segment of No.3 vein	South segment of No.3 vein	South segment of No.3 vein	South segment of No.3 vein	South segment of No.3 vein	South segment of No.3 vein	South segment of No.3 vein	South segment of No.3 vein
wt %									
SiO ₂	62.18	66.43	66.30	55.40	55.24	56.58	56.68	56.64	55.21
Al ₂ O ₃	16.11	16.05	15.90	17.50	17.51	16.04	15.34	15.42	16.16
TiO ₂	0.58	0.51	0.51	0.78	0.78	0.67	0.64	0.64	0.59
Fe ₂ O ₃	1.89	1.49	1.48	1.86	1.57	2.36	2.22	2.23	1.30
FeO	2.82	2.62	2.62	4.00	4.26	3.38	3.58	3.58	3.80
MnO	1.31	0.36	0.37	0.69	0.67	0.22	0.19	0.19	0.44
MgO	1.42	1.24	1.26	1.86	1.71	2.50	3.42	3.43	1.72
CaO	0.68	0.66	0.66	4.38	4.34	5.11	4.56	4.44	6.16
Na ₂ O	0.30	0.34	0.33	0.33	0.33	3.05	4.19	4.22	2.11
K ₂ O	4.81	4.59	4.56	3.62	3.58	3.19	2.70	2.75	2.92
P ₂ O ₅	0.21	0.20	0.20	0.26	0.26	0.28	0.26	0.30	0.28
H ₂ O	2.21	2.12	2.02	3.12	3.12	2.16	1.28	1.08	2.15
CO ₂	4.31	3.3	3.4	6.65	6.65	4.35	4.15	4.35	7.39
S	0.2676	0.161	0.1635	0.072	0.0751	0.0711	0.1056	0.1052	0.0593
Total	99.10	100.07	99.77	100.52	100.10	99.96	99.32	99.38	100.29
ppm									
ZR	118.48	114.52	114.52	138.14	138.14	168.02	142.24	142.24	149.39
Y	30.72	17.00	17.00	30.79	30.79	29.65	30.05	30.05	29.39
Rb	201.45	177.65	177.65	151.87	151.87	108.22	88.12	88.12	119.23
Sr	61.24	115.26	115.26	191.55	191.55	1071.44	535.92	535.92	369.35
Distance	1.6	3.1	3.1	14.0	14.0	36.0	38.0	38.0	56.0
Density	2.68	2.71	2.76	2.62	2.84	2.74	2.78	2.66	2.71

Table 6-6. Absolute loss or gain of lithochemical constituents caused by hydrothermal alteration

Sample_id	x4-4	x3-7	x3-6	x3-5	x3-4	x3-1	x3-2	x3-2	x3-3d	x3-3	x2-5	DA63-8
gram*												
dSiO2	0.00	0.11	-1.53	-14.19	6.76	-2.32	-2.99	-3.50	-0.27	-0.99	-1.44	9.04
dAl2O3	0.00	0.26	0.18	-2.08	4.08	1.32	1.14	0.96	0.19	-0.00	-0.15	6.59
dTiO2	0.00	0.00	0.00	0.00	0.00	0.00	0.00	0.00	0.00	0.00	0.00	0.00
dFe2O3	0.00	-0.23	-0.02	-2.15	-1.65	-1.88	-1.09	-0.99	-0.28	-0.12	-0.06	-0.31
dFeO	0.00	0.16	-0.23	-0.13	3.70	2.76	0.45	0.41	0.19	-0.07	-0.01	9.59
dMnO	0.00	-0.14	-0.11	0.66	1.54	1.18	0.20	0.20	0.01	-0.03	-0.09	3.18
dMgO	0.00	-0.30	-0.37	-2.27	-1.63	-1.88	-2.05	-2.05	0.13	-0.11	0.34	-1.40
dCaO	0.00	-0.41	-0.19	-4.06	-5.24	-5.36	-4.51	-4.51	-0.46	-0.41	-0.49	-4.22
dNa2O	0.00	0.44	-0.15	-3.42	-3.15	-3.37	-3.33	-3.34	0.04	0.25	-0.31	-3.27
dK2O	0.00	-0.17	-0.10	-1.34	1.61	-0.40	-0.00	-0.01	0.04	-0.12	0.01	2.32
dP2O5	0.00	0.00	0.01	-0.18	-0.16	-0.19	-0.14	-0.15	0.01	0.00	-0.02	-0.14
dH2O	0.00	0.30	1.18	2.31	2.10	2.82	2.63	2.58	0.87	0.16	0.05	2.91
dCO2	0.00	0.11	0.27	1.86	4.70	3.55	1.91	1.85	-0.38	-0.14	0.68	9.58
dTotal	0.00	0.14	-1.05	-24.98	12.80	-3.72	-7.75	-8.52	0.11	-1.57	-1.49	34.23
gram/10000*												
dS	0.00	43.00	27.53	81.43	1310.68	577.15	378.76	322.00	117.00	45.26	-102.47	3509.25
dZr	0.00	0.97	-5.57	-26.55	-4.91	-8.87	-9.60	-12.12	-10.88	-8.66	-15.14	-23.15
dY	0.00	2.41	0.11	-3.88	-14.29	-5.69	-2.95	-3.30	-4.33	3.48	4.60	6.26
dRb	0.00	8.17	20.38	-28.33	95.59	10.33	12.24	10.68	16.88	1.85	19.28	134.86
dSr	0.00	14.64	-34.64	-414.58	-328.93	18.37	-248.08	-252.87	13.03	-4.69	-27.96	-418.78

* The values in this table are in the mass unit (gram or gram/10000) by assuming the mass of the precursor as 100 gram.

Table 6-6. (continued-1) Absolute loss or gain of lithochemical constituents caused by hydrothermal alteration

Sample_id	DA63-6	DA63-5D	DA63-5	DA63-4	DA63-4	DA63-3D	DA63-3D	DA63-3	DA63-1D	DA63-1	x1-8	x1-7
gram*												
dSiO2	18.60	27.73	29.34	1.34	1.38	7.16	8.73	5.83	0.00	1.09	11.27	10.10
dAl2O3	7.26	6.77	7.91	5.53	5.42	3.95	4.20	3.53	0.00	0.13	3.67	3.14
dTiO2	0.00	0.00	0.00	0.00	0.00	0.00	0.00	0.00	0.00	0.00	-0.06	-0.06
dFe2O3	-0.66	0.84	1.12	-1.27	-1.09	-1.57	-1.79	-1.50	0.00	-0.07	-0.69	-0.76
dFeO	10.55	10.53	10.86	11.85	11.71	10.44	10.69	10.19	0.00	0.05	1.25	1.06
dMnO	1.01	0.83	0.94	0.94	0.94	1.08	1.10	1.06	0.00	0.00	0.31	0.76
dMgO	-1.63	-1.26	-1.34	-1.14	-1.14	-0.90	-0.90	-0.94	0.00	0.05	-0.42	-0.39
dCaO	-5.17	-4.82	-4.47	-5.21	-5.21	-4.88	-4.86	-4.90	0.00	-0.11	-2.13	-1.66
dNa2O	-3.25	-3.25	-3.22	-3.21	-3.21	-3.22	-3.24	-2.97	0.00	0.20	-2.48	-2.71
dK2O	1.75	1.89	2.08	1.67	1.68	2.12	2.19	2.04	0.00	-0.06	2.36	3.43
dP2O5	-0.03	0.02	0.07	-0.08	-0.08	-0.10	-0.11	-0.08	0.00	0.01	-0.15	-0.17
dH2O	3.29	3.58	3.68	2.74	2.74	1.77	1.82	1.73	0.00	0.01	1.14	1.40
dCO2	9.39	9.69	10.26	8.17	8.17	8.58	8.75	8.40	0.00	0.02	3.60	3.02
dTotal	41.65	53.14	57.84	21.43	21.42	24.47	26.65	22.44	0.00	1.32	17.68	17.16
gram/10000*												
dS	5420.56	5849.30	5982.00	884.78	884.78	592.95	605.71	580.62	0.00	1.72	177.23	62.12
dZr	-19.78	-10.09	-18.32	-7.30	-7.30	-22.94	-20.40	-22.65	0.00	-4.09	29.50	23.07
dY	-1.63	6.23	8.93	5.75	5.75	4.69	5.23	5.49	0.00	0.88	5.18	12.91
dRb	66.85	84.24	93.63	99.45	99.45	122.10	126.13	111.13	0.00	-9.75	99.72	141.35
dSr	-312.16	-500.14	-518.17	-318.82	-318.82	-455.72	-452.49	-461.03	0.00	-19.45	-312.34	-289.27

Table 6-6. (continued-2) Absolute loss or gain of lithochemical constituents caused by hydrothermal alteration

Sample_id	x1-6	x1-5D	x1-4	x1-3	x1-2d	x1-2	x1-1	x10-1	x10-1	x10-2	x10-3	x10-3
gram*												
dSiO2	8.89	18.33	16.61	24.42	31.05	45.91	29.57	83.22	77.94	13.18	22.12	22.27
dAl2O3	3.58	2.88	4.97	4.14	4.25	6.69	5.50	12.20	10.69	3.96	6.34	6.29
dTiO2	-0.06	-0.06	-0.06	-0.06	-0.06	-0.06	-0.06	-0.06	-0.06	-0.06	-0.06	-0.06
dFe2O3	-0.74	-0.80	-0.91	-0.83	-1.52	-1.16	-1.39	-2.22	-2.25	1.05	-1.39	-1.43
dFeO	0.56	1.08	7.74	3.25	1.01	2.56	10.86	4.87	4.57	2.27	1.66	1.66
dMnO	0.54	1.15	1.11	0.87	0.72	1.95	1.38	-0.02	-0.01	1.84	1.04	1.05
dMgO	-0.67	-0.93	-0.37	-0.99	-0.95	-0.52	-0.73	-1.30	-1.30	-1.05	-0.89	-0.90
dCaO	-2.82	-3.13	-4.19	-3.93	-4.55	-4.10	-4.20	-4.90	-4.91	-4.31	-4.31	-4.30
dNa2O	-3.22	-3.44	-3.21	-3.45	-3.51	-3.33	-3.43	-3.05	-3.07	-3.59	-3.23	-3.23
dK2O	3.28	2.18	3.46	2.13	2.22	2.42	1.06	1.03	0.93	2.14	4.18	4.10
dP2O5	-0.17	-0.15	-0.20	-0.15	-0.13	-0.16	-0.13	-0.18	-0.19	-0.11	-0.19	-0.20
dH2O	1.57	1.71	0.92	1.56	1.28	1.83	2.34	5.06	4.82	2.15	1.16	1.16
dCO2	1.20	1.58	5.23	2.34	1.89	3.46	8.48	2.76	2.56	3.32	2.92	2.92
dTotal	11.98	20.45	31.17	29.40	31.79	55.58	49.43	98.52	90.81	20.89	29.39	29.38
gram/10000*												
dS	300.33	815.67	668.05	1034.01	810.16	1099.08	1827.00	11147.00	10712.38	904.32	434.18	434.18
dZr	14.92	18.19	43.02	40.45	38.98	40.75	28.72	67.34	58.22	13.52	57.99	57.99
dY	11.71	3.95	14.44	8.34	3.71	2.63	4.33	-4.89	-5.66	-2.02	9.06	9.06
dRb	122.37	94.09	163.93	100.57	99.41	111.85	46.35	13.97	8.86	123.86	145.41	145.41
dSr	-325.61	-338.15	-353.19	-200.48	-183.24	-158.00	-419.26	1464.92	1390.41	-388.09	-242.70	-242.70

Table 6-6. (continued-3) Absolute loss or gain of lithochemical constituents caused by hydrothermal alteration

Sample_id	x10-3d	x10-3d	x10-4	x10-4	x10-5	x10-5	x10-6	x10-6D	x10-6D	x5-9	x5-10
gram*											
dSiO2	20.09	20.05	10.77	12.41	-7.53	-7.36	2.25	2.20	0.00	41.35	37.38
dAl2O3	6.22	6.37	2.59	2.99	-0.32	-0.57	-0.87	-0.92	0.00	8.46	6.85
dTiO2	-0.06	-0.06	-0.06	-0.06	-0.06	-0.06	0.02	0.02	0.00	-0.00	0.00
dFe2O3	-1.28	-1.33	-1.19	-1.20	-1.29	-1.28	-0.22	-0.16	0.00	0.99	-0.68
dFeO	1.04	1.04	0.14	0.21	0.11	0.11	0.01	0.01	0.00	1.72	0.94
dMnO	0.43	0.43	0.21	0.23	0.09	0.08	-0.04	-0.04	0.00	-0.10	0.65
dMgO	-0.87	-0.91	-0.82	-0.79	-0.90	-0.91	0.60	0.63	0.00	-0.76	-0.76
dCaO	-3.16	-3.19	-3.42	-3.38	-2.82	-2.82	-0.24	-0.26	0.00	-4.58	-4.21
dNa2O	-3.23	-3.23	-3.33	-3.33	-3.36	-3.38	0.30	0.33	0.00	-2.52	-2.64
dK2O	3.14	3.14	1.65	1.77	-0.21	-0.18	0.05	0.06	0.00	3.95	3.95
dP2O5	-0.18	-0.17	-0.18	-0.18	-0.18	-0.18	-0.08	-0.07	0.00	0.01	-0.05
dH2O	1.62	1.62	1.51	1.57	2.38	2.38	0.17	0.17	0.00	0.95	1.10
dCO2	2.65	2.65	1.24	1.32	0.92	0.92	-0.55	-0.55	0.00	-0.31	-0.06
dTotal	26.47	26.48	9.14	11.58	-13.16	-13.23	1.40	1.42	0.00	50.38	42.83
gram/10000*											
dS	670.75	670.75	304.61	317.00	154.76	147.86	-26.00	-26.00	0.00	16597.84	4875.66
dZr	53.00	53.00	57.24	62.29	12.15	12.15	2.87	2.87	0.00	7.29	1.18
dY	9.04	9.04	10.13	10.91	-2.77	-2.77	-0.60	-0.60	0.00	-10.16	15.44
dRb	102.22	102.22	73.16	77.43	-9.53	-9.53	0.99	0.99	0.00	139.60	182.72
dSr	-257.56	-257.56	-96.21	-87.85	667.96	667.96	148.29	148.29	0.00	-172.32	-931.65

Table 6-6. (continued-4) Absolute loss or gain of lithochemical constituents caused by hydrothermal alteration

Sample_id gram*	x5-1	x5-2	x5-3	x5-4	x5-4	x5-5	x5-5	x5-6	x5-6d	x5-6d	x5-7	x5-8
dSiO2	60.20	18.97	15.25	30.69	30.52	-8.99	-9.13	0.00	2.76	2.72	6.12	15.78
dAl2O3	7.41	3.24	2.57	5.05	4.85	-1.01	-1.00	0.00	0.02	0.10	2.31	2.98
dTiO2	0.00	0.00	0.00	0.00	0.00	0.00	0.00	0.00	0.00	0.00	0.00	0.00
dFe2O3	-1.17	-1.47	-0.18	-0.40	-0.42	-0.76	-1.01	0.00	-0.04	-0.03	-0.88	-0.74
dFeO	2.65	0.79	-0.12	0.06	0.06	0.06	0.28	0.00	0.37	0.37	0.94	0.19
dMnO	0.06	1.67	1.29	0.25	0.27	0.37	0.36	0.00	-0.02	-0.02	0.28	0.21
dMgO	-0.81	-0.83	-0.86	-0.87	-0.84	-0.90	-1.03	0.00	1.08	1.09	-0.55	-0.30
dCaO	-4.51	-4.29	-4.32	-4.24	-4.24	-1.35	-1.38	0.00	-0.34	-0.46	1.89	-0.30
dNa2O	-2.31	-2.66	-2.70	-2.60	-2.62	-2.77	-2.77	0.00	1.34	1.37	-0.65	-2.66
dK2O	3.24	2.61	2.37	2.84	2.80	-0.08	-0.11	0.00	-0.36	-0.31	0.13	2.24
dP2O5	-0.01	-0.04	-0.04	-0.02	-0.02	-0.06	-0.06	0.00	-0.01	0.03	0.04	-0.00
dH2O	0.96	0.20	0.39	0.63	0.49	0.52	0.52	0.00	-0.82	-1.02	0.28	0.58
dCO2	0.79	1.33	0.63	-0.01	0.12	1.36	1.36	0.00	-0.01	0.20	4.04	0.44
dTotal	67.00	19.76	14.44	31.45	31.06	-13.63	-14.00	0.00	3.99	4.05	13.91	18.65
gram/10000*												
dS	6846.60	3536.80	2380.24	1404.10	1436.94	-92.54	-65.91	0.00	394.50	390.31	-37.59	3372.41
dZr	-12.71	-27.27	-31.16	-17.57	-17.57	-49.36	-49.36	0.00	-19.11	-19.11	1.63	-36.33
dY	-21.28	17.57	5.84	-7.32	-7.32	-3.20	-3.20	0.00	1.81	1.81	3.73	2.65
dRb	96.62	120.49	124.49	125.16	125.16	22.23	22.23	0.00	-15.97	-15.97	27.18	99.29
dSr	-944.89	-1035.44	-1000.70	-920.02	-920.02	-906.90	-906.90	0.00	-510.40	-510.40	-652.01	-897.34

Table 6-7b. Metasomatic norms corrected for closure and absolute losses and gains of components (in moles)
at Switch Back vein, Silver Queen mine, Owen Lake, central BC

Sample_id	DA63-8	DA63-6	DA63-5D	DA63-5	DA63-4	DA63-4	DA63-3D	DA63-3D	DA63-3	DA63-1D	DA63-1
Alteration	s-alt	s-alt	s-alt	s-alt	m-alt	m-alt	m-alt	m-alt	m-alt	w-alt	w-alt
mole											
Pyroxene	0.00	0.00	0.00	0.00	0.00	0.00	0.00	0.00	0.00	0.03	0.03
Plagioclase	0.00	0.00	0.00	0.00	0.00	0.00	0.00	0.00	0.00	0.15	0.16
K-feldspar	0.00	0.00	0.00	0.00	0.00	0.00	0.00	0.00	0.00	0.07	0.07
Quartz	0.65	0.79	0.95	0.96	0.53	0.53	0.66	0.68	0.64	0.19	0.21
Carbonate	0.24	0.23	0.25	0.26	0.20	0.20	0.22	0.22	0.22	0.03	0.02
Epidote	0.00	0.00	0.00	0.00	0.00	0.00	0.01	0.01	0.01	0.02	0.01
Chlorite	0.01	0.00	0.00	0.00	0.02	0.02	0.01	0.01	0.01	0.01	0.02
Sericite	0.12	0.10	0.11	0.11	0.11	0.11	0.12	0.12	0.12	0.00	0.00
Kaolinite	0.04	0.07	0.07	0.07	0.04	0.04	0.01	0.01	0.00	-0.00	-0.00
Pyrite	0.01	0.00	0.00	0.00	0.00	0.00	0.00	-0.00	0.00	0.00	0.00
Hematite	0.00	0.00	0.00	0.00	0.00	0.00	0.00	0.00	0.00	0.00	0.00
Magnetite	0.01	0.01	0.01	0.01	0.00	0.00	0.00	0.00	0.00	0.00	0.00
Ilmenite	0.01	0.00	0.00	0.00	0.00	0.00	0.00	0.00	0.00	0.00	0.00
Rutile	0.00	0.01	0.01	0.01	0.01	0.01	0.01	0.01	0.01	0.01	0.01
Apatite	0.00	0.01	0.02	0.02	0.01	0.01	0.00	-0.00	0.00	0.00	0.01
Total	1.09	1.24	1.43	1.45	0.91	0.92	1.03	1.06	1.01	0.52	0.54
dSiO2	0.15	0.31	0.46	0.49	0.02	0.02	0.12	0.15	0.10	0.00	0.02
dAl+3	0.13	0.14	0.13	0.16	0.11	0.11	0.08	0.08	0.07	0.00	0.00
dTi+4	0.00	0.00	0.00	0.00	0.00	0.00	0.00	0.00	0.00	0.00	0.00
dFe+3	-0.00	-0.01	0.01	0.01	-0.02	-0.01	-0.02	-0.02	-0.02	0.00	-0.00
dFe+2	0.13	0.15	0.15	0.15	0.16	0.16	0.15	0.15	0.14	0.00	0.00
dMn+2	0.04	0.01	0.01	0.01	0.01	0.01	0.02	0.02	0.01	0.00	0.00
dMg+2	-0.03	-0.04	-0.03	-0.03	-0.03	-0.03	-0.02	-0.02	-0.02	0.00	0.00
dCa+2	-0.08	-0.09	-0.09	-0.08	-0.09	-0.09	-0.09	-0.09	-0.09	0.00	-0.00
dNa+	-0.11	-0.10	-0.10	-0.10	-0.10	-0.10	-0.10	-0.10	-0.10	0.00	0.01
dK+	0.05	0.04	0.04	0.04	0.04	0.04	0.05	0.05	0.04	0.00	-0.00
dP+5	-0.00	-0.00	0.00	0.00	-0.00	-0.00	-0.00	-0.00	-0.00	0.00	0.00
Sum O=	0.22	0.19	0.22	0.27	0.16	0.16	0.10	0.11	0.09	0.00	0.01
dH2O	0.16	0.18	0.20	0.20	0.15	0.15	0.10	0.10	0.10	0.00	0.00
dCO2	0.22	0.21	0.22	0.23	0.19	0.19	0.19	0.20	0.19	0.00	0.00
dS	0.01	0.02	0.02	0.02	0.00	0.00	0.00	0.00	0.00	0.00	0.00
dTotal	0.89	1.00	1.23	1.38	0.60	0.60	0.57	0.61	0.52	0.00	0.03

Table 6-7c. Metasomatic norms corrected for closure and absolute losses and gains of components (in moles)
at the central segment of the No. 3 vein, Silver Queen mine, central BC

Sample_id	x1-8	x1-7	x1-6	x1-5D	x1-4	x1-3	x1-2d	x1-2
Alteration	m-alt	m-alt	m-alt	m-alt	m-alt	s-alt	s-alt	s-alt
mole								
Pyroxene	-0.00	0.00	0.00	0.00	0.00	0.00	0.00	0.00
Plagioclase	0.00	0.00	0.00	0.00	0.00	0.00	0.00	0.00
K-feldspar	0.04	0.07	0.04	0.00	0.03	0.00	0.00	0.00
Quartz	0.71	0.62	0.67	0.91	0.78	0.98	1.10	1.29
Carbonate	0.14	0.13	0.09	0.10	0.16	0.10	0.09	0.12
Epidote	0.00	0.00	0.00	-0.00	0.00	0.00	0.00	0.00
Chlorite	0.00	0.01	0.00	0.01	0.01	0.01	0.00	0.00
Sericite	0.12	0.09	0.11	0.12	0.12	0.12	0.12	0.13
Kaolinite	-0.00	0.00	-0.00	0.00	-0.00	0.01	0.02	0.03
Pyrite	0.01	0.01	0.01	0.00	0.02	0.00	0.00	0.00
Hematite	0.00	0.00	0.00	0.00	0.00	0.00	0.00	0.00
Magnetite	0.00	0.00	0.00	0.00	0.00	0.00	0.00	0.00
Ilmenite	0.00	0.00	0.01	0.00	0.01	0.00	0.00	0.00
Rutile	0.00	0.00	-0.00	0.01	-0.00	0.01	0.01	0.00
Apatite	0.00	0.00	-0.00	0.01	-0.01	0.01	0.01	0.01
Total	1.03	0.95	0.93	1.15	1.12	1.24	1.34	1.59
dSiO2	0.19	0.17	0.15	0.30	0.28	0.41	0.52	0.76
dAl+3	0.07	0.06	0.07	0.06	0.10	0.08	0.08	0.13
dTi+4	-0.00	-0.00	-0.00	-0.00	-0.00	-0.00	-0.00	-0.00
dFe+3	-0.01	-0.01	-0.01	-0.01	-0.01	-0.01	-0.02	-0.01
dFe+2	0.02	0.01	0.01	0.01	0.11	0.05	0.01	0.04
dMn+2	0.00	0.01	0.01	0.02	0.02	0.01	0.01	0.03
dMg+2	-0.01	-0.01	-0.02	-0.02	-0.01	-0.02	-0.02	-0.01
dCa+2	-0.04	-0.03	-0.05	-0.06	-0.07	-0.07	-0.08	-0.07
dNa+	-0.08	-0.09	-0.10	-0.11	-0.10	-0.11	-0.11	-0.11
dK+	0.05	0.07	0.07	0.05	0.07	0.05	0.05	0.05
dP+5	-0.00	-0.00	-0.00	-0.00	-0.00	-0.00	-0.00	-0.00
Sum O=	0.05	0.05	0.01	-0.02	0.14	0.03	-0.02	0.11
dH2O	0.06	0.08	0.09	0.09	0.05	0.09	0.07	0.10
dCO2	0.08	0.07	0.03	0.04	0.12	0.05	0.04	0.08
dS	0.00	0.00	0.00	0.00	0.00	0.00	0.00	0.00
dTotal	0.38	0.38	0.25	0.35	0.68	0.54	0.52	1.10

Table 6-7c. (continued-1) Metasomatic norms corrected for closure and absolute losses and gains of components
(in moles) at the central segment of the No. 3 vein, Silver Queen mine, central BC

Sample_id	x1-1	x10-1	x10-1	x10-2	x10-3	x10-3	x10-3d	x10-3d
Alteration	s-alt	s-alt	s-alt	s-alt	m-alt	m-alt	m-alt	m-alt
mole								
Pyroxene	0.00	0.00	0.00	0.00	0.00	0.00	0.00	0.00
Plagioclase	0.00	0.00	0.00	0.00	0.00	0.00	0.00	0.00
K-feldspar	-0.00	0.01	0.01	0.00	0.03	0.03	0.00	0.00
Quartz	1.04	1.80	1.74	0.80	0.85	0.85	0.88	0.87
Carbonate	0.23	0.11	0.11	0.14	0.12	0.12	0.12	0.12
Epidote	0.00	0.00	0.00	0.00	0.00	0.00	0.00	0.00
Chlorite	0.00	0.00	0.00	0.00	0.00	0.00	0.00	0.00
Sericite	0.09	0.10	0.10	0.11	0.14	0.14	0.14	0.14
Kaolinite	0.06	0.12	0.11	0.03	0.00	0.00	0.00	0.00
Pyrite	0.00	0.00	0.00	0.00	0.00	0.00	0.00	0.00
Hematite	0.00	0.00	0.00	0.00	0.00	0.00	0.00	0.00
Magnetite	0.00	0.02	0.02	0.00	0.00	0.00	0.00	0.00
Ilmenite	0.00	0.00	0.00	0.00	0.00	0.00	0.00	0.00
Rutile	0.00	0.01	0.01	0.01	0.01	0.01	0.00	0.00
Apatite	0.01	0.00	0.00	0.02	0.00	0.01	0.00	0.00
Total	1.46	2.17	2.10	1.11	1.15	1.15	1.16	1.16
dSiO2	0.49	1.38	1.30	0.22	0.37	0.37	0.33	0.33
dAl+3	0.11	0.24	0.21	0.08	0.12	0.12	0.12	0.12
dTi+4	-0.00	-0.00	-0.00	-0.00	-0.00	-0.00	-0.00	-0.00
dFe+3	-0.02	-0.03	-0.03	0.01	-0.02	-0.02	-0.02	-0.02
dFe+2	0.15	0.07	0.06	0.03	0.02	0.02	0.01	0.01
dMn+2	0.02	-0.00	-0.00	0.03	0.01	0.01	0.01	0.01
dMg+2	-0.02	-0.03	-0.03	-0.03	-0.02	-0.02	-0.02	-0.02
dCa+2	-0.07	-0.09	-0.09	-0.08	-0.08	-0.08	-0.06	-0.06
dNa+	-0.11	-0.10	-0.10	-0.12	-0.10	-0.10	-0.10	-0.10
dK+	0.02	0.02	0.02	0.05	0.09	0.09	0.07	0.07
dP+5	-0.00	-0.00	-0.00	-0.00	-0.00	-0.00	-0.00	-0.00
Sum O=	0.16	0.20	0.15	0.05	0.08	0.08	0.07	0.08
dH2O	0.13	0.28	0.27	0.12	0.06	0.06	0.09	0.09
dCO2	0.19	0.06	0.06	0.08	0.07	0.07	0.06	0.06
dS	0.01	0.03	0.03	0.00	0.00	0.00	0.00	0.00
dTotal	1.06	2.04	1.85	0.44	0.61	0.61	0.57	0.57

Table 6-7c.(continued-2) Metasomatic norms corrected for closure and absolute losses and gains of components
(in moles) at the central segment of the No. 3 vein, Silver Queen mine, central BC

Sample_id	x10-4	x10-4	x10-5	x10-5	x10-6	x10-6	x10-6D	x10-6D
Alteration	m-alt	m-alt	m-alt	m-alt	w-alt	w-alt	w-alt	w-alt
mole								
Pyroxene	0.00	0.00	0.00	0.00	0.01	0.01	0.00	0.00
Plagioclase	0.00	0.00	0.00	0.00	0.13	0.13	0.10	0.10
K-feldspar	0.00	0.00	0.00	0.00	0.07	0.07	0.06	0.06
Quartz	0.79	0.81	0.54	0.55	0.27	0.27	0.28	0.28
Carbonate	0.08	0.08	0.08	0.09	0.05	0.05	0.05	0.05
Epidote	0.00	0.00	0.00	0.00	0.04	0.04	0.04	0.04
Chlorite	0.01	0.01	0.00	0.00	0.01	0.01	0.01	0.01
Sericite	0.11	0.11	0.07	0.07	0.00	0.00	0.02	0.02
Kaolinite	0.01	0.01	0.05	0.04	0.00	-0.00	-0.00	-0.00
Pyrite	0.00	0.00	0.00	0.00	-0.00	-0.00	-0.00	-0.00
Hematite	0.00	0.00	0.00	0.00	0.00	0.00	0.00	0.00
Magnetite	0.00	0.00	0.00	0.00	0.00	0.00	0.00	0.00
Ilmenite	0.00	0.00	0.00	0.00	0.00	0.00	0.00	0.00
Rutile	0.01	0.01	0.00	0.01	0.01	0.01	0.01	0.01
Apatite	0.01	0.01	0.00	0.01	-0.01	-0.01	-0.01	-0.01
Total	1.01	1.04	0.76	0.77	0.57	0.57	0.57	0.57
dSiO2	0.18	0.21	-0.13	-0.12	0.04	0.04	0.00	0.00
dAl+3	0.05	0.06	-0.01	-0.01	-0.02	-0.02	0.00	0.00
dTi+4	-0.00	-0.00	-0.00	-0.00	0.00	0.00	0.00	0.00
dFe+3	-0.01	-0.02	-0.02	-0.02	-0.00	-0.00	0.00	0.00
dFe+2	0.00	0.00	0.00	0.00	0.00	0.00	0.00	0.00
dMn+2	0.00	0.00	0.00	0.00	-0.00	-0.00	0.00	0.00
dMg+2	-0.02	-0.02	-0.02	-0.02	0.01	0.02	0.00	0.00
dCa+2	-0.06	-0.06	-0.05	-0.05	-0.00	-0.00	0.00	0.00
dNa+	-0.11	-0.11	-0.11	-0.11	0.01	0.01	0.00	0.00
dK+	0.04	0.04	-0.00	-0.00	0.00	0.00	0.00	0.00
dP+5	-0.00	-0.00	-0.00	-0.00	-0.00	-0.00	0.00	0.00
Sum O=	-0.07	-0.05	-0.17	-0.18	-0.02	-0.02	0.00	0.00
dH2O	0.08	0.09	0.13	0.13	0.01	0.01	0.00	0.00
dCO2	0.03	0.03	0.02	0.02	-0.01	-0.01	0.00	0.00
dS	0.00	0.00	0.00	0.00	-0.00	-0.00	0.00	0.00
dTotal	0.11	0.17	-0.35	-0.36	0.02	0.02	0.00	0.00

Table 6-7d. Metasomatic norms corrected for closure and absolute losses and gains of components (in moles)
at the southern segment of the No. 3 vein, Silver Queen mine, central BC

Sample_id	x5-9	x5-10	x5-1	x5-2	x5-3	x5-4	x5-4
Alteration	s-alt	s-alt	s-alt	m-alt	m-alt	m-alt	m-alt
mole							
Pyroxene	0.00	0.00	0.00	-0.00	-0.00	-0.00	0.00
Plagioclase	0.00	0.00	0.00	0.00	0.00	0.00	0.00
K-feldspar	0.02	0.02	0.01	0.02	0.01	0.01	0.01
Quartz	1.12	1.06	1.45	0.85	0.80	1.02	1.02
Carbonate	0.09	0.11	0.12	0.13	0.11	0.10	0.10
Epidote	0.00	0.00	-0.00	0.00	0.00	0.00	0.00
Chlorite	0.00	0.00	0.00	-0.00	0.00	0.00	0.00
Sericite	0.15	0.14	0.15	0.12	0.12	0.13	0.13
Kaolinite	0.00	-0.00	0.00	0.00	0.00	0.00	0.00
Pyrite	0.00	0.00	0.00	0.00	0.00	0.00	0.00
Hematite	0.00	0.00	0.00	0.00	0.00	0.00	0.00
Magnetite	0.03	0.01	0.01	0.01	0.00	0.00	0.00
Ilmenite	0.00	0.00	0.00	0.00	0.00	0.00	0.00
Rutile	0.01	0.01	0.01	0.01	0.01	0.01	0.01
Apatite	0.02	0.01	0.01	0.01	0.01	0.01	0.01
Total	1.44	1.37	1.76	1.13	1.07	1.29	1.29
dSiO ₂	0.69	0.62	1.00	0.32	0.25	0.51	0.51
dAl+3	0.17	0.13	0.15	0.06	0.05	0.10	0.10
dTi+4	-0.00	0.00	0.00	0.00	0.00	0.00	0.00
dFe+3	0.01	-0.01	-0.01	-0.02	-0.00	-0.01	-0.01
dFe+2	0.02	0.01	0.04	0.01	-0.00	0.00	0.00
dMn+2	-0.00	0.01	0.00	0.02	0.02	0.00	0.00
dMg+2	-0.02	-0.02	-0.02	-0.02	-0.02	-0.02	-0.02
dCa+2	-0.08	-0.08	-0.08	-0.08	-0.08	-0.08	-0.08
dNa+	-0.08	-0.09	-0.07	-0.09	-0.09	-0.08	-0.08
dK+	0.08	0.08	0.07	0.06	0.05	0.06	0.06
dP+5	0.00	-0.00	-0.00	-0.00	-0.00	-0.00	-0.00
Sum O=	0.17	0.11	0.12	-0.02	-0.03	0.03	0.03
dH ₂ O	0.05	0.06	0.05	0.01	0.02	0.03	0.03
dCO ₂	-0.01	-0.00	0.02	0.03	0.01	-0.00	0.00
dS	0.05	0.02	0.02	0.01	0.01	0.00	0.00
dTotal	1.05	0.86	1.28	0.30	0.19	0.56	0.54

Table 6-7d. (continued) Metasomatic norms corrected for closure and absolute losses and gains of components
(in moles) at the southern segment of the No. 3 vein, Silver Queen mine, central BC

Sample_id	x5-5	x5-5	x5-6	x5-6d	x5-6d	x5-7	x5-8
Alteration	m-alt	m-alt	w-alt	w-alt	w-alt	m-alt	s-alt
mole							
Pyroxene	0.00	0.00	0.00	0.02	0.01	0.00	0.00
Plagioclase	0.00	0.00	0.06	0.12	0.12	0.03	0.02
K-feldspar	0.00	0.00	0.05	0.06	0.06	0.03	0.01
Quartz	0.49	0.49	0.37	0.26	0.25	0.56	0.76
Carbonate	0.13	0.13	0.10	0.10	0.11	0.19	0.11
Epidote	0.00	0.00	0.01	0.02	0.03	0.00	0.00
Chlorite	0.00	0.00	0.02	0.01	0.01	0.01	0.01
Sericite	0.08	0.07	0.05	0.03	0.02	0.09	0.10
Kaolinite	0.03	0.03	-0.00	-0.00	0.00	-0.00	-0.00
Pyrite	0.00	0.00	0.00	0.00	0.00	0.00	0.00
Hematite	0.00	0.00	0.00	0.00	0.00	0.00	0.00
Magnetite	0.00	0.00	0.00	0.00	0.00	0.00	0.01
Ilmenite	0.01	0.00	0.00	0.00	0.00	0.00	0.00
Rutile	0.00	0.01	0.01	0.01	0.01	0.01	0.01
Apatite	0.01	0.01	0.01	0.00	0.00	0.01	0.01
Total	0.75	0.74	0.68	0.62	0.61	0.94	1.05
dSiO2	-0.15	-0.15	0.00	0.05	0.05	0.10	0.26
dAl+3	-0.02	-0.02	0.00	0.00	0.00	0.05	0.06
dTi+4	0.00	0.00	0.00	0.00	0.00	0.00	0.00
dFe+3	-0.01	-0.01	0.00	-0.00	-0.00	-0.01	-0.01
dFe+2	0.00	0.00	0.00	0.01	0.01	0.01	0.00
dMn+2	0.01	0.01	-0.00	-0.00	-0.00	0.00	0.00
dMg+2	-0.02	-0.03	0.00	0.03	0.03	-0.01	-0.01
dCa+2	-0.02	-0.02	0.00	-0.01	-0.01	0.03	-0.01
dNa+	-0.09	-0.09	0.00	0.04	0.04	-0.02	-0.09
dK+	-0.00	-0.00	0.00	-0.01	-0.01	0.00	0.05
dP+5	-0.00	-0.00	0.00	-0.00	0.00	0.00	-0.00
Sum O=	-0.13	-0.14	0.00	0.04	0.05	0.08	0.04
dH2O	0.03	0.03	0.00	-0.05	-0.06	0.02	0.03
dCO2	0.03	0.03	0.00	-0.00	0.00	0.09	0.01
dS	-0.00	-0.00	0.00	0.00	0.00	-0.00	0.01
dTotal	-0.38	-0.40	0.00	0.10	0.10	0.34	0.36

Table 6-8b. Metasomatic norms corrected for closure and absolute losses and gains of components (in grams)
at Switch Back vein, Silver Queen mine, Owen Lake, central BC

Sample_id	DA63-8	DA63-6	DA63-5D	DA63-5	DA63-4	DA63-4	DA63-3D	DA63-3D	DA63-3	DA63-1D	DA63-1
Alteration	s-alt	s-alt	s-alt	s-alt	m-alt	m-alt	m-alt	m-alt	m-alt	w-alt	w-alt
gram											
Pyroxene	0.00	0.00	0.00	0.00	0.00	0.02	0.11	0.00	0.18	6.37	6.54
Plagioclase	0.12	0.24	0.26	0.48	0.34	0.25	0.46	0.35	0.27	39.85	43.59
K-feldspar	0.00	0.72	0.94	0.96	0.00	0.00	0.00	0.00	0.00	19.26	18.94
Quartz	39.07	47.58	57.31	57.47	31.98	32.14	39.54	40.85	38.74	11.62	12.74
Carbonate	26.65	25.87	27.96	29.08	21.58	21.76	23.86	25.43	24.96	2.91	2.13
Epidote	0.14	0.02	0.01	0.01	0.00	0.29	4.49	4.74	3.32	11.49	3.58
Chlorite	3.60	1.85	0.35	0.29	11.31	10.82	5.38	4.20	3.82	5.92	9.99
Sericite	47.39	41.36	42.21	43.92	42.60	42.71	46.29	46.59	48.27	0.01	0.00
Kaolinite	11.19	19.14	17.51	18.65	10.19	9.94	2.29	2.62	0.29	-0.01	-0.01
Pyrite	2.88	0.01	0.01	0.01	0.24	0.17	0.00	-0.00	0.22	0.00	0.00
Hematite	0.67	0.95	1.07	1.17	0.83	0.83	0.77	0.76	0.82	1.01	1.03
Magnetite	0.68	1.04	1.12	1.14	0.19	0.19	0.13	0.14	0.13	0.02	0.02
Ilmenite	1.37	0.01	0.00	0.00	0.35	0.26	0.06	0.26	0.39	0.03	0.04
Rutile	0.00	0.72	0.72	0.72	0.53	0.58	0.69	0.58	0.51	0.70	0.70
Apatite	0.00	1.64	3.16	3.43	0.88	1.07	0.00	-0.26	0.12	0.42	1.66
Total	133.77	141.15	152.62	157.32	121.04	121.02	124.08	126.26	122.06	99.63	100.95
dSiO2	9.04	18.60	27.73	29.34	1.34	1.38	7.16	8.73	5.83	0.00	1.09
dAl+3	3.49	3.84	3.58	4.19	2.93	2.87	2.09	2.22	1.87	0.00	0.07
dTi+4	0.00	0.00	0.00	0.00	0.00	0.00	0.00	0.00	0.00	0.00	0.00
dFe+3	-0.22	-0.46	0.59	0.78	-0.89	-0.76	-1.10	-1.25	-1.05	0.00	-0.05
dFe+2	7.46	8.20	8.19	8.44	9.21	9.11	8.11	8.31	7.92	0.00	0.04
dMn+2	2.46	0.78	0.64	0.73	0.73	0.73	0.83	0.85	0.82	0.00	0.00
dMg+2	-0.84	-0.98	-0.76	-0.81	-0.69	-0.69	-0.54	-0.54	-0.57	0.00	0.03
dCa+2	-3.02	-3.69	-3.45	-3.19	-3.72	-3.72	-3.49	-3.47	-3.50	0.00	-0.08
dNa+	-2.42	-2.41	-2.41	-2.39	-2.38	-2.38	-2.39	-2.40	-2.20	0.00	0.15
dK+	1.93	1.45	1.57	1.73	1.39	1.40	1.76	1.82	1.69	0.00	-0.05
dP+5	-0.06	-0.01	0.01	0.03	-0.03	-0.03	-0.04	-0.05	-0.04	0.00	0.00
Sum O=	3.49	2.98	3.45	4.30	2.52	2.50	1.66	1.78	1.47	0.00	0.09
dH2O	2.91	3.29	3.58	3.68	2.74	2.74	1.77	1.82	1.73	0.00	0.01
dCO2	9.58	9.39	9.69	10.26	8.17	8.17	8.58	8.75	8.40	0.00	0.02
dS	0.35	0.54	0.58	0.60	0.09	0.09	0.06	0.06	0.06	0.00	0.00
dTotal	34.14	41.52	52.99	57.69	21.41	21.39	24.45	26.63	22.43	0.00	1.32
Residual	-0.00	-0.00	-0.00	-0.00	-0.00	-0.00	-0.00	-0.00	-0.00	0.00	0.00

Table 6-8c. Metasomatic norms corrected for closure and absolute losses and gains of components (in grams)
at the central segment of the No. 3 vein, Silver Queen mine, central BC

Sample_id	x1-8	x1-7	x1-6	x1-5D	x1-4	x1-3	x1-2d	x1-2
Alteration	m-alt	m-alt	m-alt	m-alt	m-alt	s-alt	s-alt	s-alt
gram								
Pyroxene	-0.00	0.00	0.00	0.00	0.00	0.00	0.00	0.75
Plagioclase	0.00	0.00	0.00	0.00	0.00	0.00	0.00	0.56
K-feldspar	10.10	20.47	9.87	0.00	8.41	0.00	0.00	0.00
Quartz	42.75	37.42	40.31	54.63	46.87	59.14	66.06	77.48
Carbonate	14.31	13.51	9.51	10.22	18.47	10.52	9.29	13.38
Epidote	0.00	0.00	0.00	-0.00	0.00	0.00	0.00	0.45
Chlorite	0.00	3.18	2.53	4.92	3.79	6.30	1.62	2.61
Sericite	45.75	37.21	44.80	46.84	48.53	46.32	46.44	50.27
Kaolinite	-0.00	0.93	-0.00	0.09	-0.00	3.44	5.39	6.46
Pyrite	2.60	2.23	2.72	0.00	3.51	0.00	0.07	0.10
Hematite	0.44	0.41	0.39	0.45	0.34	0.44	0.50	0.43
Magnetite	0.06	0.04	0.08	0.18	0.15	0.22	0.18	0.23
Ilmenite	0.52	0.35	0.98	0.00	1.42	0.00	0.08	0.51
Rutile	0.23	0.32	-0.02	0.50	-0.25	0.50	0.46	0.23
Apatite	0.04	0.22	-0.09	1.72	-0.81	1.69	0.95	1.21
Total	116.79	116.28	111.09	119.55	130.44	128.58	131.03	154.67
dSiO2	11.27	10.10	8.89	18.33	16.61	24.42	31.05	45.91
dAl+3	1.94	1.66	1.89	1.52	2.63	2.19	2.25	3.54
dTi+4	-0.04	-0.04	-0.04	-0.04	-0.04	-0.04	-0.04	-0.04
dFe+3	-0.48	-0.53	-0.52	-0.56	-0.64	-0.58	-1.06	-0.81
dFe+2	0.98	0.82	0.44	0.84	6.02	2.53	0.78	1.99
dMn+2	0.24	0.59	0.42	0.89	0.86	0.67	0.56	1.51
dMg+2	-0.25	-0.23	-0.40	-0.56	-0.22	-0.59	-0.57	-0.32
dCa+2	-1.52	-1.19	-2.01	-2.24	-3.00	-2.81	-3.25	-2.93
dNa+	-1.84	-2.01	-2.39	-2.55	-2.38	-2.56	-2.60	-2.47
dK+	1.96	2.85	2.72	1.81	2.87	1.77	1.84	2.01
dP+5	-0.07	-0.07	-0.08	-0.06	-0.09	-0.07	-0.06	-0.07
Sum O=	0.74	0.79	0.24	-0.30	2.31	0.44	-0.39	1.84
dH2O	1.14	1.40	1.57	1.71	0.92	1.56	1.28	1.83
dCO2	3.60	3.02	1.20	1.58	5.23	2.34	1.89	3.46
dS	0.02	0.01	0.03	0.08	0.07	0.10	0.08	0.11
dTotal	17.67	17.16	11.97	20.43	31.16	29.38	31.77	55.55
Residual	0.00	0.00	-0.00	-0.00	0.16	0.08	0.14	0.00

Table 6-8c. (continued-1) Metasomatic norms corrected for closure and absolute losses and gains of components
(in grams) at the central segment of the No. 3 vein, Silver Queen mine, central BC

Sample_id	x1-1	x10-1	x10-1	x10-2	x10-3	x10-3	x10-3d	x10-3d
Alteration	s-alt	s-alt	s-alt	s-alt	m-alt	m-alt	m-alt	m-alt
gram								
Pyroxene	0.25	0.00	0.00	0.00	0.00	0.38	0.00	0.00
Plagioclase	0.23	0.60	0.58	0.31	0.00	0.38	0.00	0.38
K-feldspar	-0.01	1.57	1.54	0.49	8.87	8.05	0.37	0.00
Quartz	62.74	108.05	104.57	48.33	50.98	51.20	52.73	52.53
Carbonate	25.93	12.59	12.22	14.70	12.65	12.67	12.32	12.16
Epidote	0.14	0.00	0.00	0.00	0.00	0.03	0.25	0.00
Chlorite	2.52	0.00	0.00	0.00	0.00	0.00	0.00	0.00
Sericite	37.25	38.88	37.83	43.55	53.69	53.73	57.05	57.04
Kaolinite	16.72	32.27	29.51	7.76	0.00	0.00	0.24	0.77
Pyrite	0.10	0.00	0.00	0.00	0.50	0.01	0.60	0.72
Hematite	0.50	0.38	0.36	0.55	0.36	0.33	0.38	0.41
Magnetite	0.37	2.11	2.03	0.20	0.11	0.11	0.15	0.15
Ilmenite	0.49	0.00	0.00	0.00	0.14	0.00	0.43	0.49
Rutile	0.24	0.50	0.50	0.50	0.43	0.50	0.27	0.24
Apatite	1.04	0.30	0.27	3.57	0.78	1.08	0.78	0.69
Total	148.50	197.26	189.42	119.96	128.51	128.49	125.57	125.59
dSiO2	29.57	83.22	77.94	13.18	22.12	22.27	20.09	20.05
dAl+3	2.91	6.46	5.66	2.10	3.36	3.33	3.29	3.37
dTi+4	-0.04	-0.04	-0.04	-0.04	-0.04	-0.04	-0.04	-0.04
dFe+3	-0.97	-1.55	-1.57	0.74	-0.97	-1.00	-0.90	-0.93
dFe+2	8.44	3.79	3.55	1.77	1.29	1.29	0.81	0.81
dMn+2	1.07	-0.02	-0.01	1.43	0.80	0.81	0.33	0.33
dMg+2	-0.44	-0.78	-0.78	-0.63	-0.53	-0.54	-0.52	-0.55
dCa+2	-3.00	-3.50	-3.51	-3.08	-3.08	-3.07	-2.26	-2.28
dNa+	-2.54	-2.26	-2.28	-2.67	-2.40	-2.40	-2.40	-2.40
dK+	0.88	0.86	0.77	1.78	3.47	3.41	2.60	2.60
dP+5	-0.06	-0.08	-0.08	-0.05	-0.08	-0.09	-0.08	-0.07
Sum O=	2.57	3.23	2.43	0.79	1.32	1.27	1.18	1.22
dH2O	2.34	5.06	4.82	2.15	1.16	1.16	1.62	1.62
dCO2	8.48	2.76	2.56	3.32	2.92	2.92	2.65	2.65
dS	0.18	1.11	1.07	0.09	0.04	0.04	0.07	0.07
dTotal	49.38	98.25	90.54	20.87	29.38	29.37	26.45	26.47
Residual	-0.00	-0.11	-0.25	-0.04	-0.00	-0.00	-0.00	-0.00

Table 6-8c. (continued-2) Metasomatic norms corrected for closure and absolute losses and gains of components
(in grams) at the central segment of the No. 3 vein, Silver Queen mine, central BC

Sample_id	x10-4	x10-4	x10-5	x10-5	x10-6	x10-6	x10-6D	x10-6D
Alteration	m-alt	m-alt	m-alt	m-alt	w-alt	w-alt	w-alt	w-alt
gram								
Pyroxene	0.00	0.00	0.00	0.26	1.74	1.72	0.25	0.25
Plagioclase	0.33	0.33	0.41	0.00	33.26	33.51	27.48	27.48
K-feldspar	0.33	0.33	0.00	0.00	18.56	18.62	17.41	17.41
Quartz	47.27	48.43	32.54	33.05	16.35	16.24	16.91	16.91
Carbonate	8.66	8.88	8.90	8.49	4.96	5.02	4.64	4.64
Epidote	0.00	0.00	0.00	0.00	19.72	19.58	20.30	20.30
Chlorite	3.00	3.08	2.67	3.54	5.46	5.48	5.63	5.63
Sericite	42.90	43.81	27.05	27.73	0.00	0.00	5.95	5.95
Kaolinite	3.46	3.55	11.79	10.64	0.21	-0.00	-0.00	-0.00
Pyrite	0.00	0.00	0.82	0.00	-0.00	-0.00	-0.01	-0.01
Hematite	0.38	0.37	0.39	0.39	0.61	0.64	0.80	0.80
Magnetite	0.09	0.09	0.06	0.06	0.02	0.02	0.03	0.03
Ilmenite	0.00	0.00	0.35	0.00	0.00	0.00	0.00	0.00
Rutile	0.50	0.50	0.31	0.50	0.58	0.58	0.56	0.56
Apatite	1.33	1.32	0.67	1.24	-0.96	-0.88	-0.83	-0.83
Total	108.24	110.69	85.95	85.88	100.52	100.54	99.12	99.12
dSiO2	10.77	12.41	-7.53	-7.36	2.25	2.20	0.00	0.00
dAl+3	1.37	1.58	-0.17	-0.30	-0.46	-0.49	0.00	0.00
dTi+4	-0.04	-0.04	-0.04	-0.04	0.01	0.01	0.00	0.00
dFe+3	-0.84	-0.84	-0.90	-0.89	-0.15	-0.11	0.00	0.00
dFe+2	0.11	0.16	0.08	0.08	0.01	0.01	0.00	0.00
dMn+2	0.16	0.18	0.07	0.06	-0.03	-0.03	0.00	0.00
dMg+2	-0.50	-0.48	-0.55	-0.55	0.36	0.38	0.00	0.00
dCa+2	-2.44	-2.42	-2.02	-2.01	-0.17	-0.19	0.00	0.00
dNa+	-2.47	-2.47	-2.49	-2.51	0.22	0.24	0.00	0.00
dK+	1.37	1.47	-0.17	-0.15	0.04	0.05	0.00	0.00
dP+5	-0.08	-0.08	-0.08	-0.08	-0.03	-0.03	0.00	0.00
Sum O=	-1.07	-0.83	-2.69	-2.81	-0.26	-0.25	0.00	0.00
dH2O	1.51	1.57	2.38	2.38	0.17	0.17	0.00	0.00
dCO2	1.24	1.32	0.92	0.92	-0.55	-0.55	0.00	0.00
dS	0.03	0.03	0.02	0.01	-0.00	-0.00	0.00	0.00
dTotal	9.13	11.57	-13.17	-13.24	1.40	1.42	0.00	0.00
Residual	-0.01	-0.00	0.00	0.00	0.00	0.00	0.00	0.00

Table 6-8d. Metasomatic norms corrected for closure and absolute losses and gains of components (in grams)
at southern segment of No. 3 vein, Silver Queen mine, Owen Lake, central BC

Sample_id	x5-9	x5-10	x5-1	x5-2	x5-3	x5-4	x5-4
Alteration	s-alt	s-alt	s-alt	m-alt	m-alt	m-alt	m-alt
gram							
Pyroxene	0.00	0.43	0.50	-0.00	-0.00	-0.00	0.00
Plagioclase	0.00	0.01	0.04	0.00	0.05	0.00	0.00
K-feldspar	4.27	6.43	3.70	4.54	3.57	2.49	2.50
Quartz	67.20	63.97	87.28	50.86	48.33	61.34	61.40
Carbonate	9.20	11.65	12.36	13.39	11.41	10.27	10.34
Epidote	0.00	0.00	-0.00	0.00	0.00	0.00	0.00
Chlorite	0.00	0.06	0.00	-0.00	0.00	0.00	0.00
Sericite	60.87	56.31	58.20	47.35	46.08	52.95	52.44
Kaolinite	0.61	-0.00	0.67	0.49	0.46	0.53	0.53
Pyrite	0.00	0.00	0.00	0.00	0.00	0.00	0.00
Hematite	0.68	0.54	0.63	0.57	0.57	0.62	0.62
Magnetite	3.24	1.05	1.41	0.79	0.58	0.40	0.40
Ilmenite	0.00	0.00	0.00	0.00	0.00	0.00	0.00
Rutile	0.67	0.67	0.67	0.67	0.67	0.67	0.67
Apatite	3.35	1.68	1.19	0.89	2.18	1.96	1.94
Total	150.09	142.79	166.65	119.56	113.91	131.22	130.84
dSiO ₂	41.35	37.38	60.20	18.97	15.25	30.69	30.52
dAl+3	4.48	3.63	3.92	1.72	1.36	2.67	2.57
dTi+4	-0.00	0.00	0.00	0.00	0.00	0.00	0.00
dFe+3	0.69	-0.47	-0.82	-1.03	-0.12	-0.28	-0.29
dFe+2	1.34	0.73	2.06	0.61	-0.10	0.05	0.05
dMn+2	-0.08	0.50	0.05	1.29	1.00	0.20	0.21
dMg+2	-0.46	-0.46	-0.49	-0.50	-0.52	-0.53	-0.51
dCa+2	-3.27	-3.01	-3.22	-3.07	-3.09	-3.03	-3.03
dNa+	-1.87	-1.96	-1.72	-1.97	-2.01	-1.93	-1.94
dK+	3.28	3.28	2.69	2.17	1.96	2.36	2.32
dP+5	0.00	-0.02	-0.01	-0.02	-0.02	-0.01	-0.01
Sum O=	2.65	1.71	1.91	-0.27	-0.53	0.53	0.44
dH ₂ O	0.95	1.10	0.96	0.20	0.39	0.63	0.49
dCO ₂	-0.31	-0.06	0.79	1.33	0.63	-0.01	0.12
dS	1.66	0.49	0.68	0.35	0.24	0.14	0.14
dTotal	50.40	42.84	67.02	19.78	14.45	31.47	31.08
Residual	-0.25	-0.00	-0.31	-0.17	-0.49	-0.19	-0.18

Table 6-8d. (continued) Metasomatic norms corrected for closure and absolute losses and gains of components
(in grams) at the southern segment of the No. 3 vein, Silver Queen mine, central BC

Sample_id	x5-5	x5-5	x5-6	x5-6d	x5-6d	x5-7	x5-8
Alteration	m-alt	m-alt	w-alt	w-alt	w-alt	m-alt	s-alt
gram							
Pyroxene	0.26	0.21	0.50	3.83	2.75	0.00	0.00
Plagioclase	0.26	0.18	16.51	31.50	32.56	9.19	5.34
K-feldspar	0.00	0.00	14.24	15.64	16.07	8.97	3.85
Quartz	29.56	29.30	22.37	15.35	14.73	33.80	45.91
Carbonate	13.34	12.94	10.33	9.05	9.91	19.05	10.38
Epidote	0.00	0.00	2.99	11.27	14.12	0.00	0.00
Chlorite	1.45	3.31	9.51	5.61	3.84	4.32	8.98
Sericite	29.80	29.51	20.16	9.72	8.38	35.17	40.43
Kaolinite	8.03	7.80	-0.00	-0.00	0.00	-0.00	-0.00
Pyrite	0.41	0.10	0.00	0.00	0.00	0.01	0.00
Hematite	0.53	0.53	0.66	0.64	0.74	0.75	0.65
Magnetite	0.12	0.12	0.13	0.21	0.21	0.13	0.76
Ilmenite	1.27	0.07	0.00	0.00	0.07	0.01	0.04
Rutile	0.00	0.63	0.67	0.67	0.63	0.67	0.65
Apatite	1.32	1.28	1.87	0.46	0.00	1.47	1.62
Total	86.33	85.96	99.94	103.95	104.01	113.53	118.61
dSiO ₂	-8.99	-9.13	0.00	2.76	2.72	6.12	15.78
dAl+3	-0.53	-0.53	0.00	0.01	0.05	1.22	1.58
dTi+4	0.00	0.00	0.00	0.00	0.00	0.00	0.00
dFe+3	-0.53	-0.71	0.00	-0.03	-0.02	-0.62	-0.52
dFe+2	0.04	0.22	0.00	0.29	0.29	0.73	0.14
dMn+2	0.29	0.28	-0.00	-0.02	-0.02	0.22	0.16
dMg+2	-0.54	-0.62	0.00	0.65	0.66	-0.33	-0.18
dCa+2	-0.96	-0.99	0.00	-0.24	-0.33	1.35	-0.21
dNa+	-2.05	-2.05	0.00	0.99	1.01	-0.49	-1.97
dK+	-0.07	-0.10	0.00	-0.30	-0.26	0.10	1.86
dP+5	-0.02	-0.02	0.00	-0.00	0.01	0.02	-0.00
Sum O=	-2.11	-2.20	0.00	0.68	0.73	1.29	0.67
dH ₂ O	0.52	0.52	0.00	-0.82	-1.02	0.28	0.58
dCO ₂	1.36	1.36	0.00	-0.01	0.20	4.04	0.44
dS	-0.01	-0.01	0.00	0.04	0.04	-0.00	0.34
dTotal	-13.61	-13.98	0.00	4.00	4.07	13.93	18.67
Residual	0.00	0.00	0.00	0.00	0.00	-0.35	-0.00

Table 6-9b. Propagated errors of metasomatic norms corrected for closure and absolute losses/gains of components in grams the at 68% confidence level, Switch Back vein, Silver Queen mine, central BC

Sample_id	DA63-8	DA63-6	DA63-5	DA63-5	DA63-4	DA63-4	DA63-3	DA63-3	DA63-3	DA63-1	DA63-1
Alteration	s-alt	s-alt	s-alt	s-alt	m-alt	m-alt	m-alt	m-alt	m-alt	w-alt	w-alt
gram											
Pyroxene	0.00	0.00	0.00	0.00	0.00	0.00	0.00	0.00	0.01	0.20	0.18
Plagioclase	0.00	0.13	0.14	0.13	0.01	0.01	0.01	0.01	0.01	1.01	1.11
K-feldspar	0.00	0.02	0.03	0.03	0.00	0.00	0.00	0.00	0.00	0.48	0.48
Quartz	1.10	1.36	1.68	1.70	0.87	0.88	1.09	1.13	1.06	0.30	0.33
Carbonate	1.57	1.54	1.68	1.75	1.27	1.28	1.38	1.39	1.37	0.22	0.17
Epidote	0.00	0.00	0.00	0.00	0.00	0.01	0.16	0.20	0.12	0.29	0.09
Chlorite	0.12	0.06	0.01	0.01	0.35	0.34	0.17	0.19	0.17	0.19	0.36
Sericite	1.44	1.18	1.23	1.31	1.25	1.25	1.37	1.39	1.37	0.00	0.00
Kaolinite	0.38	0.65	0.61	0.65	0.34	0.33	0.08	0.09	0.01	0.00	0.00
Pyrite	0.09	0.00	0.00	0.00	0.01	0.01	0.00	0.00	0.01	0.00	0.00
Hematite	0.04	0.07	0.06	0.06	0.08	0.07	0.09	0.13	0.09	0.05	0.05
Magnetite	0.06	0.10	0.08	0.08	0.02	0.02	0.02	0.03	0.02	0.00	0.00
Ilmenite	0.04	0.00	0.00	0.00	0.01	0.01	0.00	0.01	0.01	0.00	0.00
Rutile	0.00	0.02	0.02	0.02	0.02	0.02	0.02	0.02	0.02	0.02	0.02
Apatite	0.00	0.35	0.61	0.59	0.17	0.21	0.00	0.05	0.02	0.04	0.16
Total	4.85	5.48	6.15	6.33	4.39	4.42	4.41	4.62	4.29	2.82	2.95
dSiO2*	1.88	2.18	2.50	2.57	1.61	1.61	1.79	1.84	1.74	1.51	1.54
dAl+3	0.40	0.42	0.42	0.44	0.38	0.37	0.35	0.36	0.34	0.27	0.28
dTi+4	0.02	0.02	0.02	0.02	0.01	0.01	0.02	0.02	0.01	0.01	0.01
dFe+3	0.10	0.10	0.13	0.14	0.08	0.09	0.08	0.08	0.08	0.10	0.09
dFe+2	0.35	0.38	0.39	0.40	0.40	0.39	0.37	0.38	0.36	0.12	0.12
dMn+2	0.08	0.04	0.04	0.05	0.04	0.04	0.04	0.04	0.04	0.03	0.03
dMg+2	0.10	0.10	0.11	0.11	0.10	0.10	0.11	0.11	0.11	0.11	0.12
dCa+2	0.12	0.11	0.12	0.13	0.10	0.10	0.11	0.11	0.11	0.16	0.16
dNa+	0.12	0.12	0.13	0.13	0.11	0.11	0.11	0.11	0.11	0.14	0.14
dK+	0.16	0.15	0.16	0.16	0.14	0.14	0.15	0.15	0.15	0.09	0.09
dP+5	0.02	0.02	0.02	0.02	0.02	0.02	0.02	0.02	0.02	0.02	0.02
Sum O=	1.11	1.13	1.17	1.22	1.04	1.04	1.00	1.01	0.98	0.81	0.82
dH2O	0.58	0.63	0.67	0.69	0.55	0.55	0.43	0.44	0.42	0.21	0.21
dCO2	1.36	1.33	1.38	1.45	1.18	1.18	1.23	1.25	1.21	0.20	0.20
dS	0.09	0.10	0.10	0.10	0.07	0.07	0.07	0.07	0.07	0.07	0.07
dTotal	6.48	6.84	7.36	7.62	5.84	5.84	5.88	5.99	5.77	3.85	3.90

* prefix d stands for the absolute difference of corresponding constituent between the least altered and altered rocks.

Table 6-9c. Propagated errors of norms corrected for closure and losses and gains of constituents in grams at the 68% confidence level, the central segment of the No. 3 vein, Silver Queen mine, central BC

Sample_id	x1-8	x1-7	x1-6	x1-5D	x1-4	x1-3	x1-2d	x1-2
Alteration	m-alt	m-alt	m-alt	m-alt	m-alt	s-alt	s-alt	s-alt
gram								
Pyroxene	0.00	0.00	0.00	0.00	0.00	0.00	0.00	0.05
Plagioclase	0.00	0.00	0.00	0.00	0.00	0.00	0.00	0.02
K-feldspar	0.32	0.64	0.30	0.00	0.27	0.00	0.00	0.00
Quartz	1.37	1.20	1.28	1.77	1.56	1.97	2.20	2.75
Carbonate	0.96	0.88	0.62	0.66	1.14	0.71	0.66	0.87
Epidote	0.00	0.00	0.00	0.00	0.00	0.00	0.00	0.02
Chlorite	0.00	0.13	0.12	0.22	0.18	0.25	0.07	0.13
Sericite	1.48	1.21	1.45	1.58	1.66	1.61	1.63	1.85
Kaolinite	0.00	0.03	0.00	0.00	0.00	0.13	0.21	0.26
Pyrite	0.00	0.00	0.01	0.01	0.01	0.01	0.01	0.01
Hematite	0.00	0.01	0.01	0.12	0.06	0.12	0.10	0.11
Magnetite	0.13	0.11	0.13	0.00	0.20	0.00	0.01	0.01
Ilmenite	0.02	0.01	0.03	0.00	0.05	0.00	0.00	0.02
Rutile	0.01	0.01	0.00	0.02	0.01	0.02	0.02	0.01
Apatite	0.03	0.03	0.03	0.03	0.04	0.04	0.06	0.05
Total	4.32	4.28	3.98	4.41	5.18	4.86	4.97	6.18
dSiO2	2.26	2.22	2.15	2.51	2.52	2.77	3.00	3.73
dAl+3	0.34	0.33	0.33	0.33	0.37	0.36	0.36	0.43
dTi+4	0.02	0.02	0.02	0.02	0.02	0.02	0.02	0.02
dFe+3	0.05	0.04	0.04	0.04	0.04	0.04	0.03	0.04
dFe+2	0.11	0.10	0.09	0.10	0.28	0.16	0.10	0.15
dMn+2	0.02	0.03	0.03	0.04	0.04	0.03	0.03	0.06
dMg+2	0.04	0.04	0.03	0.03	0.04	0.03	0.03	0.04
dCa+2	0.07	0.08	0.06	0.05	0.03	0.04	0.02	0.03
dNa+	0.03	0.03	0.02	0.02	0.02	0.02	0.02	0.02
dK+	0.15	0.18	0.17	0.15	0.19	0.15	0.15	0.17
dP+5	0.01	0.01	0.01	0.01	0.01	0.01	0.01	0.01
Sum O=	0.77	0.77	0.75	0.74	0.88	0.80	0.78	0.95
dH2O	0.08	0.09	0.09	0.10	0.08	0.10	0.09	0.12
dCO2	0.20	0.18	0.12	0.13	0.26	0.16	0.15	0.21
dS	0.02	0.02	0.02	0.02	0.02	0.02	0.02	0.02
dTotal	4.16	4.13	3.93	4.29	4.80	4.71	4.82	6.01

Table 6-9c.(continued-1) Propagated errors of norms corrected for closure and losses and gains of constituents in grams at the 68% confidence level, the central segment of the No. 3 vein, Silver Queen mine, central BC

Sample_id	x1-1	x10-1	x10-1	x10-2	x10-3	x10-3	x10-3d	x10-3d
Alteration	s-alt	s-alt	s-alt	s-alt	m-alt	m-alt	m-alt	m-alt
gram								
Pyroxene	0.02	0.00	0.00	0.00	0.00	0.02	0.00	0.00
Plagioclase	0.02	0.03	0.03	0.11	0.00	0.02	0.00	0.02
K-feldspar	0.00	0.06	0.06	0.02	0.29	0.26	0.01	0.00
Quartz	2.20	4.28	4.07	1.57	1.69	1.69	1.73	1.72
Carbonate	1.59	0.96	0.92	0.96	0.86	0.86	0.84	0.83
Epidote	0.01	0.00	0.00	0.00	0.00	0.00	0.01	0.00
Chlorite	0.14	0.00	0.00	0.00	0.00	0.00	0.00	0.00
Sericite	1.37	1.59	1.52	1.42	1.82	1.81	1.91	1.90
Kaolinite	0.67	1.41	1.27	0.29	0.00	0.00	0.01	0.03
Pyrite	0.02	0.12	0.12	0.01	0.01	0.01	0.01	0.01
Hematite	0.11	0.13	0.12	0.17	0.07	0.10	0.07	0.06
Magnetite	0.01	0.00	0.00	0.00	0.03	0.00	0.04	0.05
Ilmenite	0.02	0.00	0.00	0.00	0.00	0.00	0.02	0.02
Rutile	0.01	0.02	0.02	0.02	0.02	0.02	0.01	0.01
Apatite	0.05	0.14	0.13	0.05	0.04	0.04	0.03	0.03
Total	6.22	8.75	8.27	4.62	4.83	4.83	4.68	4.68
dSiO2	3.10	5.64	5.33	2.35	2.68	2.69	2.60	2.59
dAl+3	0.40	0.59	0.55	0.35	0.39	0.39	0.39	0.39
dTi+4	0.02	0.02	0.02	0.02	0.02	0.02	0.02	0.02
dFe+3	0.03	0.02	0.02	0.09	0.03	0.03	0.03	0.03
dFe+2	0.38	0.24	0.23	0.13	0.12	0.12	0.10	0.10
dMn+2	0.05	0.02	0.02	0.06	0.04	0.04	0.02	0.02
dMg+2	0.04	0.03	0.03	0.03	0.03	0.03	0.03	0.03
dCa+2	0.03	0.02	0.02	0.03	0.03	0.03	0.05	0.05
dNa+	0.02	0.03	0.03	0.02	0.02	0.02	0.02	0.02
dK+	0.13	0.14	0.14	0.15	0.20	0.20	0.17	0.17
dP+5	0.01	0.01	0.01	0.01	0.01	0.01	0.01	0.01
Sum O=	0.94	1.24	1.16	0.79	0.86	0.86	0.85	0.85
dH2O	0.13	0.26	0.24	0.12	0.09	0.09	0.10	0.10
dCO2	0.39	0.21	0.20	0.19	0.18	0.18	0.17	0.17
dS	0.02	0.06	0.05	0.02	0.02	0.02	0.02	0.02
dTotal	5.68	8.53	8.05	4.34	4.73	4.73	4.59	4.59

Table 6-9c. (continued-2) Propagated errors of norms corrected for closure and losses and gains of constituents in grams at the 68% confidence level, the central segment of the No. 3 vein, Silver Queen mine, central BC

Sample_id	x10-4	x10-4	x10-5	x10-5	x10-6	x10-6	x10-6D	x10-6D
Alteration	m-alt	m-alt	m-alt	m-alt	w-alt	w-alt	w-alt	w-alt
gram								
Pyroxene	0.00	0.00	0.00	0.01	0.06	0.06	0.01	0.01
Plagioclase	0.02	0.02	0.02	0.00	0.93	0.93	0.78	0.78
K-feldspar	0.01	0.01	0.00	0.00	0.51	0.52	0.49	0.49
Quartz	1.49	1.53	0.97	0.98	0.47	0.47	0.49	0.49
Carbonate	0.56	0.58	0.56	0.58	0.33	0.33	0.36	0.36
Epidote	0.00	0.00	0.00	0.00	0.56	0.56	0.58	0.58
Chlorite	0.14	0.15	0.12	0.12	0.21	0.22	0.20	0.20
Sericite	1.38	1.42	0.83	0.85	0.00	0.00	0.18	0.18
Kaolinite	0.13	0.13	0.41	0.37	0.01	0.00	0.00	0.00
Pyrite	0.01	0.01	0.00	0.00	0.00	0.00	0.00	0.00
Hematite	0.10	0.10	0.04	0.08	0.05	0.04	0.04	0.04
Magnetite	0.00	0.00	0.04	0.00	0.00	0.00	0.00	0.00
Ilmenite	0.00	0.00	0.01	0.00	0.00	0.00	0.00	0.00
Rutile	0.02	0.02	0.01	0.02	0.02	0.02	0.02	0.02
Apatite	0.03	0.03	0.02	0.02	0.03	0.03	0.04	0.04
Total	3.88	3.99	3.03	3.04	3.18	3.17	3.19	3.19
dSiO2	2.20	2.26	1.53	1.54	1.76	1.75	1.72	1.72
dAl+3	0.31	0.32	0.25	0.24	0.23	0.23	0.25	0.25
dTi+4	0.02	0.02	0.02	0.02	0.02	0.02	0.02	0.02
dFe+3	0.03	0.03	0.03	0.03	0.05	0.05	0.06	0.06
dFe+2	0.08	0.08	0.07	0.07	0.07	0.07	0.07	0.07
dMn+2	0.02	0.02	0.02	0.02	0.02	0.02	0.02	0.02
dMg+2	0.03	0.03	0.03	0.03	0.05	0.05	0.04	0.04
dCa+2	0.04	0.05	0.05	0.05	0.10	0.10	0.11	0.11
dNa+	0.02	0.02	0.02	0.02	0.09	0.09	0.08	0.08
dK+	0.13	0.13	0.08	0.08	0.08	0.08	0.08	0.08
dP+5	0.01	0.01	0.01	0.01	0.01	0.01	0.01	0.01
Sum O=	0.69	0.71	0.56	0.55	0.60	0.60	0.63	0.63
dH2O	0.09	0.09	0.11	0.11	0.05	0.05	0.04	0.04
dCO2	0.12	0.12	0.10	0.10	0.06	0.06	0.08	0.08
dS	0.02	0.02	0.02	0.02	0.02	0.02	0.02	0.02
dTotal	3.80	3.91	2.89	2.88	3.20	3.20	3.22	3.22

Table 6-9d. Propagated errors of metasomatic norms corrected for closure and absolute losses/gains of components in grams at the 68% confidence level, the southern segment of the No. 3 vein, Silver Queen mine, central BC

Sample_id	x5-9	x5-10	x5-1	x5-2	x5-3	x5-4	x5-4
Alteration	s-alt	s-alt	s-alt	m-alt	m-alt	m-alt	m-alt
gram							
Pyroxene	0.00	0.01	0.02	0.00	0.00	0.00	0.00
Plagioclase	0.00	0.00	0.00	0.00	0.00	0.00	0.00
K-feldspar	0.09	0.14	0.08	0.10	0.08	0.05	0.05
Quartz	1.54	1.47	1.99	1.19	1.13	1.42	1.42
Carbonate	0.65	0.76	0.79	0.84	0.73	0.69	0.70
Epidote	0.00	0.00	0.00	0.00	0.00	0.00	0.00
Chlorite	0.00	0.00	0.00	0.00	0.00	0.00	0.00
Sericite	1.45	1.35	1.38	1.15	1.12	1.28	1.27
Kaolinite	0.02	0.00	0.02	0.01	0.01	0.02	0.02
Pyrite	0.14	0.04	0.06	0.03	0.02	0.02	0.02
Hematite	0.15	0.12	0.12	0.09	0.11	0.11	0.11
Magnetite	0.06	0.02	0.03	0.02	0.01	0.01	0.01
Ilmenite	0.00	0.00	0.00	0.00	0.00	0.00	0.00
Rutile	0.02	0.02	0.02	0.02	0.02	0.02	0.02
Apatite	0.12	0.06	0.09	0.05	0.07	0.07	0.07
Total	4.24	4.01	4.61	3.50	3.31	3.69	3.68
dSiO2*	2.70	2.57	3.24	2.06	1.96	2.37	2.37
dAl+3	0.47	0.44	0.46	0.38	0.37	0.41	0.41
dTi+4	0.02	0.02	0.02	0.01	0.01	0.01	0.01
dFe+3	0.16	0.12	0.13	0.11	0.12	0.12	0.12
dFe+2	0.19	0.17	0.22	0.16	0.14	0.15	0.15
dMn+2	0.04	0.04	0.04	0.05	0.05	0.04	0.04
dMg+2	0.15	0.15	0.16	0.14	0.14	0.14	0.14
dCa+2	0.15	0.15	0.16	0.14	0.13	0.14	0.14
dNa+	0.16	0.15	0.17	0.14	0.14	0.15	0.15
dK+	0.22	0.21	0.20	0.18	0.17	0.19	0.18
dP+5	0.02	0.02	0.02	0.02	0.02	0.02	0.02
Sum O=	1.27	1.19	1.26	1.05	1.02	1.11	1.10
dH2O	0.66	0.67	0.66	0.54	0.56	0.60	0.58
dCO2	0.81	0.84	0.95	1.01	0.92	0.85	0.86
dS	0.19	0.08	0.11	0.07	0.06	0.05	0.05
dTotal	7.20	6.84	7.80	6.05	5.81	6.36	6.34

* prefix d stands for the absolute difference of corresponding constituent between the least altered and altered rocks.

Table 6-9d. (continued)

Sample_id	x5-5	x5-5	x5-6	x5-6d	x5-6d	x5-7	x5-8
Alteration	m-alt	m-alt	w-alt	w-alt	w-alt	m-alt	s-alt
gram							
Pyroxene	0.01	0.01	0.01	0.14	0.09	0.00	0.00
Plagioclase	0.01	0.00	0.38	0.71	0.74	0.21	0.18
K-feldspar	0.00	0.00	0.32	0.35	0.36	0.20	0.09
Quartz	0.72	0.71	0.53	0.36	0.35	0.79	1.07
Carbonate	0.80	0.78	0.61	0.62	0.65	1.16	0.66
Epidote	0.00	0.00	0.07	0.27	0.33	0.00	0.00
Chlorite	0.06	0.11	0.32	0.17	0.12	0.13	0.30
Sericite	0.75	0.74	0.48	0.23	0.20	0.83	0.94
Kaolinite	0.25	0.24	0.00	0.00	0.00	0.00	0.00
Pyrite	0.01	0.01	0.01	0.01	0.01	0.01	0.03
Hematite	0.07	0.07	0.08	0.02	0.02	0.10	0.10
Magnetite	0.01	0.00	0.00	0.00	0.00	0.00	0.02
Ilmenite	0.03	0.00	0.00	0.00	0.00	0.00	0.00
Rutile	0.00	0.02	0.02	0.02	0.02	0.02	0.02
Apatite	0.04	0.03	0.05	0.03	0.03	0.04	0.04
Total	2.74	2.73	2.89	2.95	2.92	3.49	3.45
dSiO2	1.37	1.36	1.58	1.65	1.65	1.74	1.98
dAl+3	0.31	0.31	0.33	0.33	0.33	0.36	0.38
dTi+4	0.01	0.01	0.01	0.01	0.01	0.01	0.01
dFe+3	0.10	0.10	0.12	0.12	0.12	0.11	0.11
dFe+2	0.14	0.14	0.14	0.15	0.15	0.16	0.15
dMn+2	0.03	0.03	0.03	0.03	0.03	0.03	0.03
dMg+2	0.12	0.12	0.15	0.17	0.17	0.14	0.15
dCa+2	0.15	0.15	0.17	0.17	0.17	0.20	0.18
dNa+	0.12	0.12	0.16	0.18	0.18	0.16	0.14
dK+	0.11	0.11	0.11	0.11	0.11	0.12	0.17
dP+5	0.02	0.02	0.02	0.02	0.02	0.02	0.02
Sum O=	0.88	0.88	0.95	0.98	0.98	1.04	1.05
dH2O	0.57	0.57	0.51	0.42	0.40	0.55	0.59
dCO2	1.01	1.01	0.84	0.84	0.87	1.36	0.90
dS	0.03	0.03	0.04	0.04	0.04	0.04	0.07
dTotal	4.96	4.96	5.16	5.22	5.22	6.06	5.93